

VOL. **632**, NOS. **1 + 2** FEBRUARY 19, 1993

ISSN

Period.

COMPLETE IN ONE ISSUE

**16th International Symposium
on Column Liquid Chromatography
Baltimore, MD, June 14-19, 1992
Part II**

JOURNAL OF

CHROMATOGRAPHY

INCLUDING ELECTROPHORESIS AND OTHER SEPARATION METHODS



SYMPOSIUM VOLUMES

EDITORS

E. Heftmann (Orinda, CA)
Z. Deyl (Prague)

EDITORIAL BOARD

E. Bayer (Tübingen)
S. R. Binder (Hercules, CA)
S. C. Churms (Rondebosch)
J. C. Fetzer (Richmond, CA)
E. Gelpi (Barcelona)
K. M. Gooding (Lafayette, IN)
S. Hara (Tokyo)
P. Helboe (Brønshøj)
W. Lindner (Graz)
T. M. Phillips (Washington, DC)
S. Terabe (Hyogo)
H. F. Walton (Boulder, CO)
M. Wilchek (Rehovot)

ELSEVIER

JOURNAL OF CHROMATOGRAPHY

INCLUDING ELECTROPHORESIS AND OTHER SEPARATION METHODS

Scope. The *Journal of Chromatography* publishes papers on all aspects of **chromatography, electrophoresis** and related methods. Contributions consist mainly of research papers dealing with chromatographic theory, instrumental developments and their applications. The section *Biomedical Applications*, which is under separate editorship, deals with the following aspects: developments in and applications of chromatographic and electrophoretic techniques related to clinical diagnosis or alterations during medical treatment; screening and profiling of body fluids or tissues related to the analysis of active substances and to metabolic disorders; drug level monitoring and pharmacokinetic studies; clinical toxicology; forensic medicine; veterinary medicine; occupational medicine; results from basic medical research with direct consequences in clinical practice. In *Symposium volumes*, which are under separate editorship, proceedings of symposia on chromatography, electrophoresis and related methods are published.

Submission of Papers. The preferred medium of submission is on disk with accompanying manuscript (see *Electronic manuscripts* in the Instructions to Authors, which can be obtained from the publisher, Elsevier Science Publishers B.V., P.O. Box 330, 1000 AH Amsterdam, Netherlands). Manuscripts (in English; *four* copies are required) should be submitted to: Editorial Office of *Journal of Chromatography*, P.O. Box 681, 1000 AR Amsterdam, Netherlands, Telefax (+31-20) 5862 304, or to: The Editor of *Journal of Chromatography, Biomedical Applications*, P.O. Box 681, 1000 AR Amsterdam, Netherlands. Review articles are invited or proposed in writing to the Editors who welcome suggestions for subjects. An outline of the proposed review should first be forwarded to the Editors for preliminary discussion prior to preparation. Submission of an article is understood to imply that the article is original and unpublished and is not being considered for publication elsewhere. For copyright regulations, see below.

Publication. The *Journal of Chromatography* (incl. *Biomedical Applications*) has 40 volumes in 1993. The subscription prices for 1993 are:

J. Chromatogr. (incl. *Cum. Indexes, Vols. 601-650*) + *Biomed. Appl.* (Vols. 612-651):
Dfl. 8520.00 plus Dfl. 1320.00 (p.p.h.) (total ca. US\$ 5622.75)

J. Chromatogr. (incl. *Cum. Indexes, Vols. 601-650*) only (Vols. 623-651):

Dfl. 7047.00 plus Dfl. 957.00 (p.p.h.) (total ca. US\$ 4573.75)

Biomed. Appl. only (Vols. 612-622):

Dfl. 2783.00 plus Dfl. 363.00 (p.p.h.) (total ca. US\$ 1797.75).

Subscription Orders. The Dutch guildner price is definitive. The US\$ price is subject to exchange-rate fluctuations and is given as a guide. Subscriptions are accepted on a prepaid basis only, unless different terms have been previously agreed upon. Subscription orders can be entered only by calendar year (Jan.-Dec.) and should be sent to Elsevier Science Publishers, Journal Department, P.O. Box 211, 1000 AE Amsterdam, Netherlands, Tel. (+31-20) 5803 642, Telefax (+31-20) 5803 598, or to your usual subscription agent. Postage and handling charges include surface delivery except to the following countries where air delivery via SAL (Surface Air Lift) mail is ensured: Argentina, Australia, Brazil, Canada, China, Hong Kong, India, Israel, Japan*, Malaysia, Mexico, New Zealand, Pakistan, Singapore, South Africa, South Korea, Taiwan, Thailand, USA. *For Japan air delivery (SAL) requires 25% additional charge of the normal postage and handling charge. For all other countries airmail rates are available upon request. Claims for missing issues must be made within six months of our publication (mailing) date, otherwise such claims cannot be honoured free of charge. Back volumes of the *Journal of Chromatography* (Vols. 1-611) are available at Dfl. 230.00 (plus postage). Customers in the USA and Canada wishing information on this and other Elsevier journals, please contact Journal Information Center, Elsevier Science Publishing Co. Inc., 655 Avenue of the Americas, New York, NY 10010, USA, Tel. (+1-212) 633 3750, Telefax (+1-212) 633 3764.

Abstracts/Contents Lists published in Analytical Abstracts, Biochemical Abstracts, Biological Abstracts, Chemical Abstracts, Chemical Titles, Chromatography Abstracts, Clinical Chemistry Lookout, Current Awareness in Biological Sciences (CABS), Current Contents/Life Sciences, Current Contents/Physical, Chemical & Earth Sciences, Deep-Sea Research/Part B: Oceanographic Literature Review, Excerpta Medica, Index Medicus, Mass Spectrometry Bulletin, PASCAL-CNRS, Pharmaceutical Abstracts, Referativnyi Zhurnal, Research Alert, Science Citation Index and Trends in Biotechnology.

US Mailing Notice. *Journal of Chromatography* (ISSN 0021-9673) is published weekly (total 58 issues) by Elsevier Science Publishers (Sara Burgerhartstraat 25, P.O. Box 211, 1000 AE Amsterdam, Netherlands). Annual subscription price in the USA US\$ 5622.75 (subject to change), including air speed delivery. Application to mail at second class postage rate is pending at Jamaica, NY 11431. **USA POSTMASTERS:** Send address changes to *Journal of Chromatography*, Publications Expediting, Inc., 200 Meacham Avenue, Elmont, NY 11003. Airfreight and mailing in the USA by Publication Expediting.

See inside back cover for Publication Schedule, Information for Authors and information on Advertisements.

© 1993 ELSEVIER SCIENCE PUBLISHERS B.V. All rights reserved.

0021-9673/93/\$06.00

No part of this publication may be reproduced, stored in a retrieval system or transmitted in any form or by any means, electronic, mechanical, photocopying, recording or otherwise, without the prior written permission of the publisher, Elsevier Science Publishers B.V., Copyright and Permissions Department, P.O. Box 521, 1000 AM Amsterdam, Netherlands.

Upon acceptance of an article by the journal, the author(s) will be asked to transfer copyright of the article to the publisher. The transfer will ensure the widest possible dissemination of information.

Special regulations for readers in the USA. This journal has been registered with the Copyright Clearance Center, Inc. Consent is given for copying of articles for personal or internal use, or for the personal use of specific clients. This consent is given on the condition that the copier pays through the Center the per-copy fee stated in the code on the first page of each article for copying beyond that permitted by Sections 107 or 108 of the US Copyright Law. The appropriate fee should be forwarded with a copy of the first page of the article to the Copyright Clearance Center, Inc., 27 Congress Street, Salem, MA 01970, USA. If no code appears in an article, the author has not given broad consent to copy and permission to copy must be obtained directly from the author. All articles published prior to 1980 may be copied for a per-copy fee of US\$ 2.25, also payable through the Center. This consent does not extend to other kinds of copying, such as for general distribution, resale, advertising and promotion purposes, or for creating new collective works. Special written permission must be obtained from the publisher for such copying.

No responsibility is assumed by the Publisher for any injury and/or damage to persons or property as a matter of products liability, negligence or otherwise, or from any use or operation of any methods, products, instructions or ideas contained in the materials herein. Because of rapid advances in the medical sciences, the Publisher recommends that independent verification of diagnoses and drug dosages should be made.

Although all advertising material is expected to conform to ethical (medical) standards, inclusion in this publication does not constitute a guarantee or endorsement of the quality or value of such product or of the claims made of it by its manufacturer.

This issue is printed on acid-free paper.

Printed in the Netherlands

For Contents, see p. VII

JOURNAL OF CHROMATOGRAPHY

VOL. 632 (1993)

JOURNAL of CHROMATOGRAPHY

INCLUDING ELECTROPHORESIS AND OTHER SEPARATION METHODS

SYMPOSIUM VOLUMES

EDITORS

E. HEFTMANN (Orinda, CA), Z. DEYL (Prague)

EDITORIAL BOARD

E. Bayer (Tübingen), S. R. Binder (Hercules, CA), S. C. Churms (Rondebosch), J. C. Fetzer (Richmond, CA), E. Gelpí (Barcelona), K. M. Gooding (Lafayette, IN), S. Hara (Tokyo), P. Helboe (Brønshøj), W. Lindner (Graz), T. M. Phillips (Washington, DC), S. Terabe (Hyogo), H. F. Walton (Boulder, CO), M. Wilchek (Rehovot)



ELSEVIER
AMSTERDAM — LONDON — NEW YORK — TOKYO

J. Chromatogr., Vol. 632 (1993)

© 1993 ELSEVIER SCIENCE PUBLISHERS B.V. All rights reserved.

0021-9673/93/\$06.00

No part of this publication may be reproduced, stored in a retrieval system or transmitted in any form or by any means, electronic, mechanical, photocopying, recording or otherwise, without the prior written permission of the publisher, Elsevier Science Publishers B.V., Copyright and Permissions Department, P.O. Box 521, 1000 AM Amsterdam, Netherlands.

Upon acceptance of an article by the journal, the author(s) will be asked to transfer copyright of the article to the publisher. The transfer will ensure the widest possible dissemination of information.

Special regulations for readers in the USA. This journal has been registered with the Copyright Clearance Center, Inc. Consent is given for copying of articles for personal or internal use, or for the personal use of specific clients. This consent is given on the condition that the copier pays through the Center the per-copy fee stated in the code on the first page of each article for copying beyond that permitted by Sections 107 or 108 of the US Copyright Law. The appropriate fee should be forwarded with a copy of the first page of the article to the Copyright Clearance Center, Inc., 27 Congress Street, Salem, MA 01970, USA. If no code appears in an article, the author has not given broad consent to copy and permission to copy must be obtained directly from the author. All articles published prior to 1980 may be copied for a per-copy fee of US\$ 2.25, also payable through the Center. This consent does not extend to other kinds of copying, such as for general distribution, resale, advertising and promotion purposes, or for creating new collective works. Special written permission must be obtained from the publisher for such copying.

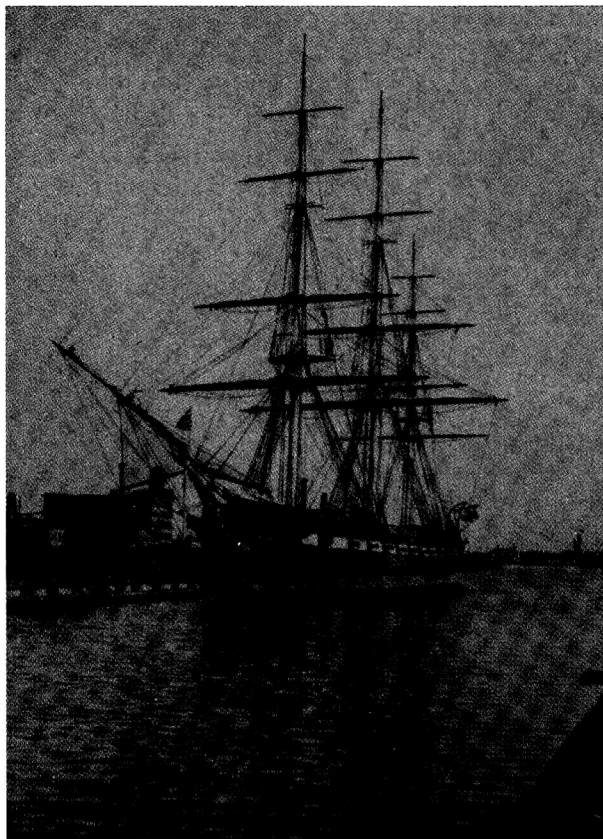
No responsibility is assumed by the Publisher for any injury and/or damage to persons or property as a matter of products liability, negligence or otherwise, or from any use or operation of any methods, products, instructions or ideas contained in the materials herein. Because of rapid advances in the medical sciences, the Publisher recommends that independent verification of diagnoses and drug dosages should be made.

Although all advertising material is expected to conform to ethical (medical) standards, inclusion in this publication does not constitute a guarantee or endorsement of the quality or value of such product or of the claims made of it by its manufacturer.

This issue is printed on acid-free paper.

Printed in the Netherlands

SYMPOSIUM VOLUME



**16TH INTERNATIONAL SYMPOSIUM
ON
COLUMN LIQUID CHROMATOGRAPHY**

PART II

Baltimore, MD (USA), June 14-19, 1992

The proceedings of the *16th International Symposium on Column Liquid Chromatography, Baltimore, MD, June 14–19, 1992*, are published in two consecutive volumes of the *Journal of Chromatography*:

Vols. 631 and 632 (1993). A combined Author Index to both Vols. 631 and 632 only appears in Vol. 632.

CONTENTS

16TH INTERNATIONAL SYMPOSIUM ON COLUMN LIQUID CHROMATOGRAPHY, BALTIMORE, MD, JUNE 14-19, 1992, PART II

Applications: proteins and their constituents (continued)

| | |
|---|----|
| Isolation of plasma proteins from the clotting cascade by heparin affinity chromatography by D. Josić, F. Bal and H. Schwinn (Vienna, Austria) | 1 |
| High-performance liquid chromatography of amino acids, peptides and proteins. CXXII. Application of experimentally derived retention coefficients to the prediction of peptide retention times: studies with myohemerythrin by M. C. J. Wilce, M. I. Aguilar and M. T. W. Hearn (Clayton, Australia) | 11 |
| High-performance liquid chromatographic analysis of carbohydrate mass composition in glycoproteins by M. Kunitani and L. Kresin (Emmeryville, CA, USA) | 19 |
| Conformational changes of brain-derived neurotrophic factor during reversed-phase high-performance liquid chromatography by R. Rosenfeld and K. Benedek (Thousand Oaks, CA, USA) | 29 |
| Immunochemical analysis of proteins. Identification, characterization and purity determination by A. Riggin and J. R. Sportsman (Indianapolis, IN, USA) and F. E. Regnier (West Lafayette, IN, USA) | 37 |
| Structural characterization of glycoprotein digests by microcolumn liquid chromatography-ionspray tandem mass spectrometry by J. Liu, K. J. Volk, E. H. Kerns, S. E. Klohr, M. S. Lee and I. E. Rosenberg (Wallingford, CT, USA) | 45 |
| High-performance liquid chromatography of tryptophan and other amino acids in hydrochloric acid hydrolysates by I. Molnár-Perl, M. Pintér-Szakács and M. Khalifa (Budapest, Hungary) | 57 |

Biochemical applications

| | |
|---|-----|
| High-performance liquid chromatographic quantitation of phenylthiocarbonyl muramic acid and glucosamine from bacterial cell walls by S. R. Hagen (Hamilton, MT, USA) | 63 |
| Detection of alkaloids in foods with a multi-detector high-performance liquid chromatographic system by L. A. Lin (Cincinnati, OH, USA) | 69 |
| Comparison of columns of chemically modified porous glass and silica in reversed-phase high-performance liquid chromatography of ginsenosides by H. Kanazawa, Y. Nagata, E. Kurosaki, Y. Matsushima and N. Takai (Tokyo, Japan) | 79 |
| Carbohydrate analysis of fermentation broth by high-performance liquid chromatography utilizing solid-phase extraction by R. G. Bell and K. L. Newman (Chicago Heights, IL, USA) | 87 |
| High-performance liquid chromatography with ion pairing and electrochemical detection for the determination of the stability of two forms of vitamin C by K. M. De Antonis, P. R. Brown and Z. Yi (Kingston, RI, USA) and P. D. Maugle (Norwich, CT, USA) | 91 |
| Estimation of the extent of lipid peroxidation in the ischemic and reperfused heart by monitoring lipid metabolic products with the aid of high-performance liquid chromatography by G. A. Cordis and N. Maulik (Farmington, CT, USA), D. Bagchi (Omaha, NE, USA) and R. M. Engelman and D. K. Das (Farmington, CT, USA) | 97 |
| Size-exclusion chromatographic determination of β -glucan with postcolumn reaction detection by T. Suortti (Espoo, Finland) | 105 |
| Identification and determination of phenolic constituents in natural beverages and plant extracts by means of a coulometric electrode array system by G. Achilli, G. P. Cellerino and P. H. Gamache (Bedford, MA, USA) and G. V. Melzi d'Eril (Pavia, Italy) | 111 |
| Supercritical fluid extraction of synthetic organochlorine compounds in submerged aquatic plants by P. R. McEachern and G. D. Foster (Fairfax, VA, USA) | 119 |

Electrophoresis

| | |
|--|-----|
| Separation of metallothionein isoforms by capillary zone electrophoresis by J. H. Beattie (Aberdeen, UK), M. P. Richards (Beltsville, MD, USA) and R. Self (Aberdeen, UK) | 127 |
| Temperature-programmed capillary affinity gel electrophoresis for the sensitive base-specific separation of oligodeoxynucleotides by Y. Baba and M. Tshako (Kobe, Japan) and T. Sawa and M. Akashi (Kagoshima, Japan) | 137 |
| Determination of ten β -blockers in urine by micellar electrokinetic capillary chromatography by P. Lukkari, H. Sirén, M. Pantsar and M.-L. Riekkola (Helsinki, Finland) | 143 |
| Voltage programming in capillary zone electrophoresis by H.-T. Chang and E. S. Yeung (Ames, IA, USA) | 149 |
| Fundamental and practical aspects of coupled capillaries for the control of electroosmotic flow in capillary zone electrophoresis of proteins by W. Nashabeh and Z. El Rassi (Stillwater, OK, USA) | 157 |
| Determination of sulphonamides in pharmaceuticals by capillary electrophoresis by C. L. Ng, H. K. Lee and S. F. Y. Li (Singapore, Singapore) | 165 |
| Capillary sodium dodecyl sulfate gel electrophoresis of proteins by A. Guttman, J. A. Noland and N. Cooke (Fullerton, CA, USA) | 171 |
| Prediction of the migration behavior of organic acids in micellar electrokinetic chromatography by S. C. Smith and M. G. Khaledi (Raleigh, NC, USA) | 177 |
| Polymer- and surfactant-coated capillaries for isoelectric focusing by X.-W. Yao and F. E. Regnier (West Lafayette, IN, USA) | 185 |
| Capillary electrophoresis of glycoconjugates in alkaline media by M. Stefansson and D. Westerlund (Uppsala, Sweden) | 195 |
| Observation of flow profiles in electroosmosis in a rectangular capillary by T. Tsuda and M. Ikedo (Nagoya, Japan) and G. Jones, R. Dadoo and R. N. Zare (Stanford, CA, USA) | 201 |
| On-line sample preconcentration on a packed-inlet capillary for improving the sensitivity of capillary electrophoretic analysis of pharmaceuticals by M. E. Swartz and M. Merion (Milford, MA, USA) | 209 |
| OTHER SEPARATION METHODS | |
| Screening of β -blockers in human serum by ion-pair chromatography and their identification as methyl or acetyl derivatives by gas chromatography–mass spectrometry by H. Sirén, M. Saarinen, S. Hainari, P. Lukkari and M.-L. Riekkola (Helsinki, Finland) | 215 |
| Isoelectric focusing field-flow fractionation and capillary isoelectric focusing with electroosmotic zone displacement. Two approaches to protein analysis in flowing streams by J. Chmelík (Brno, Czechoslovakia) and W. Thormann (Berne, Switzerland) | 229 |
| <i>Author Index Vols. 631 and 632</i> | 235 |

Isolation of plasma proteins from the clotting cascade by heparin affinity chromatography

Djuro Josić, Frederic Bal and Horst Schwinn

Octapharma Pharmazeutika Produktionsgesellschaft mbH, Oberlaaer Str. 249A, A-1100 Vienna (Austria)

ABSTRACT

The use of heparin affinity chromatography for the isolation of plasma proteins from the clotting cascade is described. The separation is carried out with heparin agarose and, in parallel operations, with different rigid gels on a polymer base. The quality of the separation and the reproducibility of the results were investigated and the stability of the materials at high pH was tested. The affinity supports were used for the isolation of antithrombin III from human plasma and for the separation of factor IX from factor X, after partial purification by anion-exchange chromatography. The isolation of antithrombin III from human plasma served as a model. The non-specific bindings were investigated, together with the resistance of the support when treated with 0.2 and 0.5 *M* sodium hydroxide. Heparin agarose has low non-specific bindings, but it cannot be exposed to high pH. The supports on a polymer base are resistant to high pH, up to 13.7. However, they may remain slightly hydrophobic, and the hydrophobicity of the matrix leads to an increase in non-specific bindings. When antithrombin III is isolated, the non-specific bindings result in contamination of the final product. The lack of resistance of the matrix at high pH causes a weaker binding of antithrombin III, and the product is eluted at lower and lower sodium chloride concentrations. The results can be indicative of the behaviour of the support in the separation of factor IX from factor X. High non-specific bindings will lead to contamination of the factor IX product and consequently to low specific activity. Insufficient resistance of the support at high pH will result in failure to separate the two clotting factors satisfactorily. The separation can be monitored by heparin high-performance membrane affinity chromatography (HPMAC). Contamination of the sample, which occur in sodium dodecyl sulphate–polyacrylamide gel electrophoresis are detected within minutes by fast heparin HPMAC.

INTRODUCTION

Heparin has been used for some time in the isolation of plasma and membrane proteins, having been immobilized first to soft gels and later also to rigid gels [1,2]. The most frequent use of heparin affinity chromatography (AC) involves the isolation of antithrombin III from human plasma [1,3]. Recently this method has been used as the last step in the isolation process of human blood clotting factor IX [4].

Agarose-based supports with immobilized heparin have also been used successfully for the above-mentioned purification process. The column lasts a long time and non-specific binding is low [5], and

therefore reproducible separations are achieved. An important disadvantage is that the soft gels cannot be treated with 0.2–0.5 *M* sodium hydroxide. This in turn creates a risk of pyrogenic substances accumulating on the column and contaminating the product after several runs.

This paper deals with applications of AC, using heparin on soft, agarose-based gels and heparin immobilized to hard, polymer-based gels and to membranes. The hard gels allow higher flow-rates and consequently shorter purification times. Their chemical stability is much greater than that of the soft gels, and they can be treated with 0.5 *M* sodium hydroxide.

The isolation of antithrombin III serves as a model investigation for determining the non-specific bindings of the gel and its behaviour after treatment with sodium hydroxide. These model investigations indicate whether or not the gel can also be

Correspondence to: D. Josić, Octapharma Pharmazeutika Produktionsgesellschaft mbH, Oberlaaer Str. 249A, A-1100 Vienna, Austria.

used in the last step of factor IX purification, namely the separation of factor IX from factor X from the concentrate resulting from the previous step, partial purification by preparative anion-exchange HPLC. The option of fast process monitoring by heparin high-performance membrane AC (HPMAC) was also investigated.

EXPERIMENTAL

Chemicals

Human plasma of blood group A + was provided by Octapharma (Hurdal, Norway) as fresh frozen plasma. Virus-inactivated plasma after treatment with 1% (w/v) Triton X-100, 1% (w/v) tri-*n*-butyl phosphate at 30°C [6] was applied to the column for the isolation of antithrombin III.

Chemicals of analytical-reagent grade were purchased from Merck (Darmstadt, Germany), Serva (Heidelberg, Germany) and Sigma (Munich, Germany).

Clotting assays, solvent, detergent and protein determination

A one-stage coagulation assay for factor IX was performed by mixing the corresponding clotting plasma with the diluted sample and incubating it in an activator (lipid extract and kaolin). After incubation, coagulation was stopped by adding calcium chloride solution. The time required for the clot to form was measured. Each test was calibrated against factor IX concentrate (Octapharma, Vienna, Austria), which in turn was calibrated against the latest WHO standard.

For the factor X assay, the plasma that is deficient of the corresponding clotting factor was mixed with the diluted sample and incubated. After incubation, clotting was terminated by adding calcium thromboplastin. The time required for the clot to form was measured. Each test was calibrated against standard human plasma, which in turn was calibrated against the latest WHO standard.

Factor IX, X-deficient plasma and all other reagents were purchased from Behring (Marburg, Germany). Coagulation tests were carried out with an Amelung (Lemgo, Germany) koagulometer.

Tri-*n*-butyl phosphate and Triton X-100 were determined by the methods described by Horowitz *et al.* [6]. The protein in the samples was determined

according to the procedure of Lowry *et al.* [7] or according to Smith *et al.* [8], using a protein determination kit manufactured by Pierce (Rodgau, Germany). Bovine serum albumin was used as a standard.

Factor IX purification

The initial steps for the enrichment of factor IX were carried out with the method described by Brummelhuis [9]. The only modification was the replacement of DEAE-Sephadex with DEAE-Sepharose Fast Flow (Pharmacia, Vienna, Austria) in the second run of anion-exchange chromatography. The amount used in our large-scale production process was 1000 kg of plasma per run.

The samples for heparin affinity chromatography were taken from our production process, after partial purification by two anion-exchange steps [9].

Chromatographic equipment

The iron(III) ion-free HPLC system consisted of two pumps, a programmer, a spectrophotometer with a deuterium lamp and a Rheodyne loop injection valve (all from Knauer, Berlin, Germany). A BioPilot system (Pharmacia) was used for semi-preparative and preparative chromatography. The salt gradient in heparin affinity chromatography was controlled by measuring the osmotic pressure (Osmomat 030 cryoscopic osmometer; Gonotec, Berlin, Germany).

Supports and buffers for affinity chromatography

For fast heparin HPMAC, a QuickDisc separation unit with immobilized heparin was used (Säulentechnik Knauer, Berlin, Germany).

The following supports were used for semi-preparative and preparative heparin AC: Heparin Sepharose (Pharmacia), Bio-Gel Heparin (Bio-Rad, Vienna, Austria) Eupergit Heparin (Röhm Pharma, Weiterstadt, Germany) and Toyopearl Heparin 650 M (TosoHaas, Stuttgart, Germany). The supports were packed into glass columns of different dimensions (Säulentechnik Knauer or Pharmacia).

A 10–20 mM sodium citrate buffer (pH 7.4) was used for sample application and equilibration. Sodium chloride was added to both the washing buffer (about 0.25 mol/l) and the elution buffer (about 0.45 mol/l) until the desired osmolarity was reached at 500 and 900 mOsmol.

Sodium dodecyl sulphate–polyacrylamide gel electrophoresis (SDS-PAGE)

The dialysed and freeze-dried samples were dissolved in 62.5 mM Tris–HCl buffer (pH 6.8) containing 3% (w/v) of SDS, 5% (v/v) of mercaptoethanol, 10% (v/v) of glycerol and 0.001% (w/v) of bromophenol blue. In other experiments, 10–30 μ l of sample were taken from the collected fractions after chromatographic separation and mixed with buffer containing five times higher concentrations of the above-mentioned substances. The amount of the buffer taken for the experiments was measured in such a way as to yield the original concentration after dilution with the sample. SDS-PAGE was carried out by the Laemmli method [10] using a mini system (Protean, Bio-Rad) or in the case of larger gels, 15 cm long, a Hoefer system (Hoefer Scientific Instruments, Vienna, Austria); 10% minigels or 5–15% large gradient gels were used. The staining of the gels was performed with 0.1% Coomassie Brilliant Blue. The amount of applied protein was between 2 and 20 μ g per lane when a mini system was used and between 5 and 50 μ g for large gels.

RESULTS

Isolation of antithrombin III

Antithrombin III can be isolated directly from the plasma by heparin HPAC. A step gradient with buffers of 500 or 900 mOsmol is used to remove the non-specifically bound proteins and the weakly bound proteins, respectively. The antithrombin III is subsequently eluted by a step gradient with 2 M sodium chloride.

Fig. 1 shows the isolation of antithrombin III from human plasma by means of heparin HPAC. The plasma is first virus inactivated with solvent–detergent (see Experimental) and then applied to a column with immobilized heparin. The weakly bound proteins are washed out by two step gradients at 500 and 900 mOsmol. The antithrombin III is subsequently eluted with 2 M sodium chloride and tri-*n*-butyl phosphate. The solvent tri-*n*-butyl phosphate and the non-ionic detergent Triton X-100 do not bind to the column. Any remnants of solvent or detergent are removed by the first washing. The amount of Triton X-100 and tri-*n*-butyl phosphate in the final product was always less than 1 ppm. The multiple treatment with sodium hy-

droxide, to which the support Toyopearl Heparin is exposed in the experiments, does not impair the chromatographic performance of the column. A similar behaviour towards the exposure to sodium hydroxide is observed with the Eupergit Heparin support (Fig. 1, right-hand side, only SDS-PAGE is shown). When Toyopearl Heparin is used, only antithrombin III is eluted. However, with Eupergit Heparin additional bands appear in the eluate with 2 M sodium chloride. They represent mainly a polypeptide with an apparent relative molecular mass (M_r) of 220 000, and another polypeptide slightly larger than antithrombin III and a smaller polypeptide with an apparent M_r of about 35 000 (see SDS-PAGE in Fig. 1). The contaminants can be removed by chromatography with Toyopearl Heparin, when washed with diluted sodium chloride solution. The column with heparin agarose has lost to a great extent its binding capacity to antithrombin III after being treated only twice with 0.2 M sodium hydroxide for 2 h. This leads to a shift in the elution of this protein. Antithrombin III is eluted already in the second peak, that is, by the buffer with 900 mOsmol (see SDS-PAGE in Fig. 1).

Separation of clotting factor IX from factor X

The separation of the clotting factor IX from factor X is the last step in the isolation process of factor IX from human plasma (see Experimental and ref. 4). By anion-exchange chromatography an enriched factor IX fraction is obtained. Virus inactivation using the solvent–detergent method is carried out after elution from the anion-exchange column. Factor X is the main contaminant still present in the sample after anion-exchange HPLC. As can be seen in Table I, the sample contains almost identical activities of both factor IX and factor X after partial purification by anion-exchange HPLC.

Factor X is separated from factor IX by heparin AC. Either factor X does not bind at all to the column, or it is washed out in the washing step, using the buffer of 500 mOsmol (see Fig. 2 and Table I). Neither solvent nor detergent binds to the heparin column, and any remnants of these substances are removed in the subsequent washing step with the application buffer. Factor IX is subsequently eluted in a second step, using a step gradient at 900 mOsmol (see Fig. 2). All the investigated supports perform in a way similar to that shown in Fig. 2. Dif-

ferences between the supports exist with regard to yield and specific activity or enrichment (see Table I).

Of the four supports listed in Table I, three were investigated further. Bio-Gel Heparin was excluded

from subsequent studies, as the first experiments showed that neither the yield of factor IX nor its enrichment was satisfactory (see Table I).

Table II shows the performance of the heparin affinity supports, after undergoing five treatments

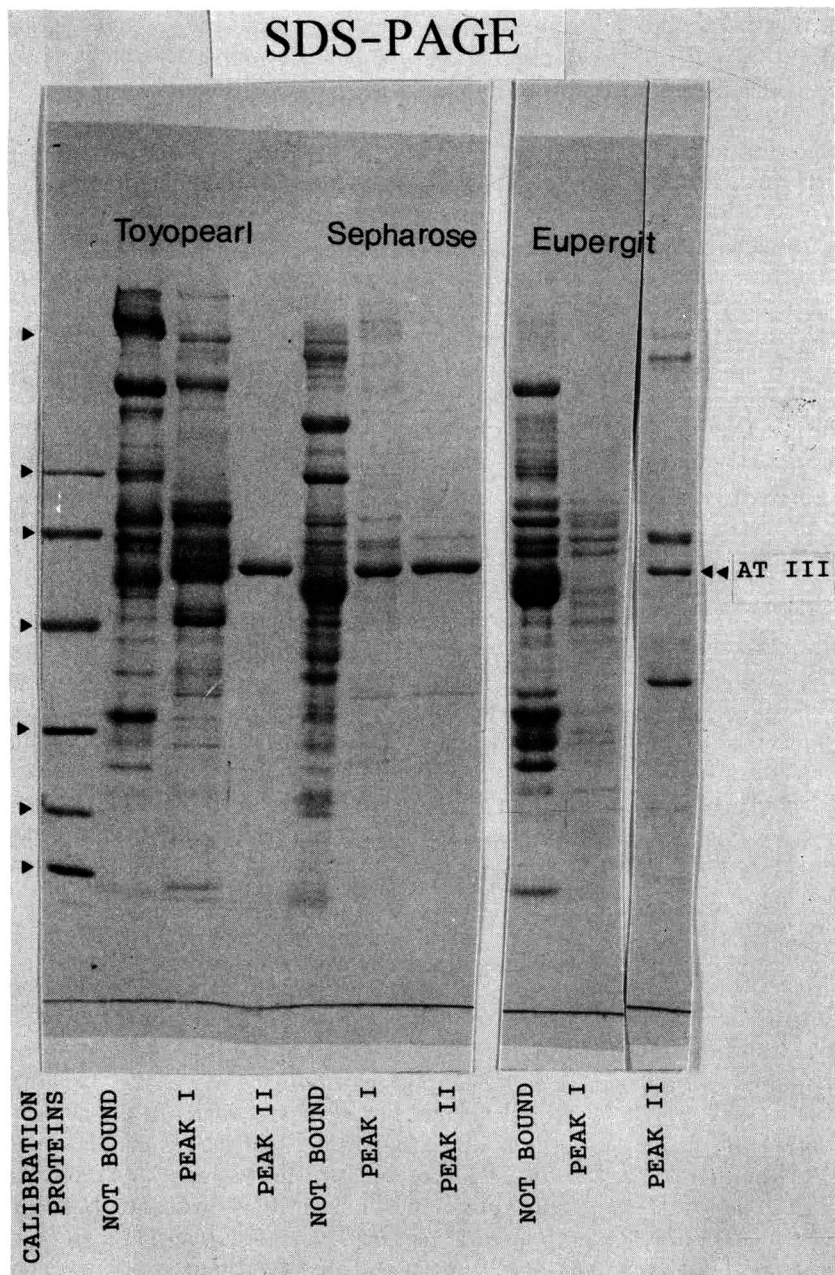


Fig. 1.

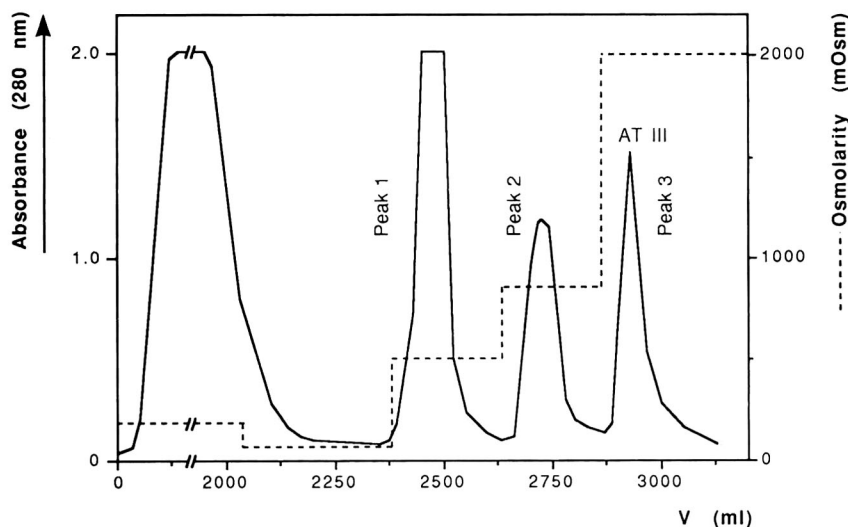


Fig. 1. Isolation of antithrombin III from human plasma by heparin HPAC. Virus-inactivated human plasma (1500 ml, *ca.* 90 g of protein) was applied to a column with immobilized heparin. The bound proteins were eluted with the step gradient shown. The resulting peaks were pooled and electrophoretically represented. Chromatographic conditions: column dimensions, 200 × 20 mm I.D.; support, Toyopearl Heparin, Eupergit Heparin or Heparin Sepharose CL6B; flow-rate, 20 ml/min (10 ml/min with Heparin Sepharose); pressure, 2–3 bar; room temperature. Previous page: SDS-PAGE of the fractions that were separated on Toyopearl Heparin, Eupergit Heparin or Heparin Sepharose. Calibration proteins (from top to bottom): M_r 211 000, 94 000, 67 000, 49 000, 30 000, 20 000, 14 400. A gradient gel between 5 and 15% was used. The amount of sample loaded was *ca.* 40 μ g (peaks 1 and 2) and *ca.* 5 μ g (peak 3, purified antithrombin III).

with 0.2 and 0.5 M sodium hydroxide for 2 h each time. Although the shape of the chromatogram remains the same (not shown here), the composition of single fractions and the yield of factor IX are significantly different. The most remarkable change

in this context is the mixing of factor IX and factor X in the washing step with the buffer of 500 mOsmol. A conspicuous development takes place in the column with Heparin Sepharose. After only two treatments for 2 h each with 0.5 M sodium hydrox-

TABLE I

SEPARATION OF FACTOR IX AND FACTOR X BY HEPARIN AFFINITY CHROMATOGRAPHY: COMPARISON OF THE SUPPORTS USED IN THE EXPERIMENTS

After preparative anion-exchange HPLC the sample contains almost identical activities of factors IX and X: the concentration of factor IX is 29–31 U/ml and that of factor X is about 27–30 U/ml.

| Support | Factor X in flow-through (%) | Factor X in peak I (%) | Factor X in peak II (%) | Factor IX yield (%) | Factor IX, specific activity (U/ml) | Factor IX in peak I (%) (loss) | Factor IX enrichment |
|-------------------|------------------------------|------------------------|-------------------------|---------------------|-------------------------------------|--------------------------------|----------------------|
| Heparin Sepharose | 5 | 93 | 2 | 50–65 | 80 | 5 | 21.3 × |
| BioGel Heparin | 3 | 90 | 7 | 30–40 | 62 | 8 | 16.5 × |
| Eupergit Heparin | 8 | 90 | 2 | 60–85 | 82 | 6 | 21.9 × |
| Toyopearl Heparin | 80 | 19 | 0 | 80–92 | 122 | 2 | 32.5 × |

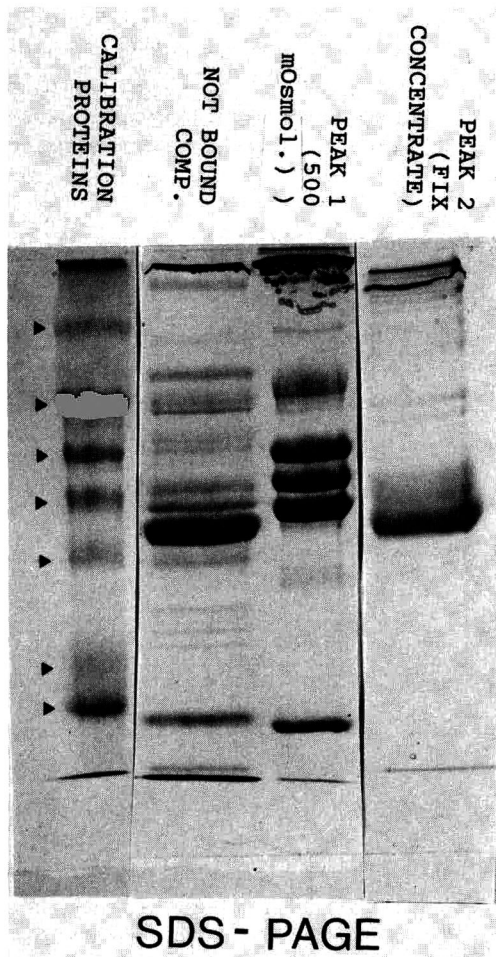
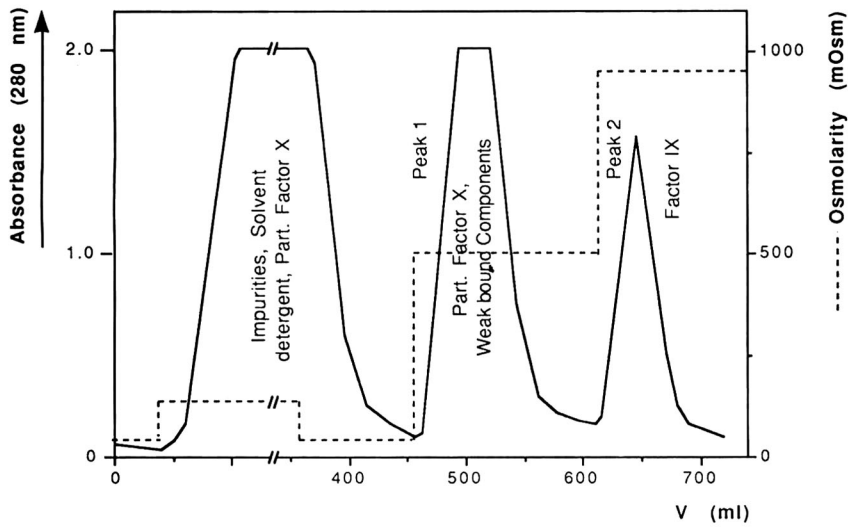


Fig. 2. Separation of clotting factor IX from clotting factor X by heparin HPAC. Eluate from anion-exchange HPLC (150 ml, with about 3000 units each of factor IX and factor X) was dialysed, virus inactivated by the solvent-detergent method and applied to a heparin column. The column was washed with 20 mM citrate buffer (pH 7.4) (at ca. 50 mOsmol). Factor X and factor IX were subsequently eluted with a step gradient of sodium chloride. The respective activities of factor IX and factor X in each peak were determined in clotting assays. The separated peaks were represented electrophoretically, using a mini gel system. Factor X does not bind at all or only weakly to the heparin column, and appears either in the flow-through fraction or in the first peak, eluted by a buffer of 500 mOsmol. The highly enriched factor IX is eluted in the second peak by a buffer of 900 mOsmol. Chromatographic conditions: column dimensions, 100 × 20 mm I.D.; support, Toyopearl Heparin; flow-rate, 10 ml/min; pressure, 1–2 bar; room temperature. SDS-PAGE; calibration proteins (from top to bottom): M_r 211 000, 119 000, 98 000, 80 600, 64 400, 44 600, 38 900. A mini gel (10%) was used. The amount of sample loaded was 15 μ g (peak 1) or 10 μ g (peak 2, factor IX concentrate).

TABLE II

SEPARATION OF FACTOR IX AND FACTOR X BY HEPARIN AFFINITY CHROMATOGRAPHY: COMPARISON OF THE SUPPORTS AFTER REPEATED TREATMENT WITH SODIUM HYDROXIDE

| Support | Factor X in flow-through (%) | Factor X in peak I (%) | Factor X in peak II (%) | Factor IX yield (%) | Factor IX specific activity (U/ml) | Factor IX in peak I (%) (loss) | Factor IX enrichment (peak II) |
|--------------------------------|------------------------------|------------------------|-------------------------|---------------------|------------------------------------|--------------------------------|--------------------------------|
| Eupergit Heparin ^a | 3 | 93 | 3 | 50–70 | 65 | 10 | 17.3 × |
| Toyopearl Heparin ^a | 16 | 82 | 1 | 65–80 | 92 | 5–7 | 24.5 × |
| Heparin Sepharose ^b | 20 | 75 | 2 | 20–30 | 50 | 60–70 | — ^b |

^a Treated five times, each time 2 h, with 0.5 M sodium hydroxide.

^b Treated twice, each time for 2 h, with 0.2 M sodium hydroxide; factor IX was chiefly eluted in the first peak, mixed with factor X.

ide, the material binds factor IX only weakly and loses almost all of its selectivity between the factors IX and X (see Table II).

Heparin high-performance membrane affinity chromatography

Fig. 3 illustrates an option for fast process monitoring by means of heparin HPMAC. The eluate

from the last peak of the HPAC column, containing purified antithrombin III (*cf.* Fig. 1), is diluted, applied to the Quick Disk Heparin separation unit and analysed with the same step gradient as used in the experiment shown in Fig. 1 (antithrombin III purification). The contamination in the antithrombin III preparation after using the Eupergit Heparin column, as detected by SDS-PAGE (see Fig. 1), ap-

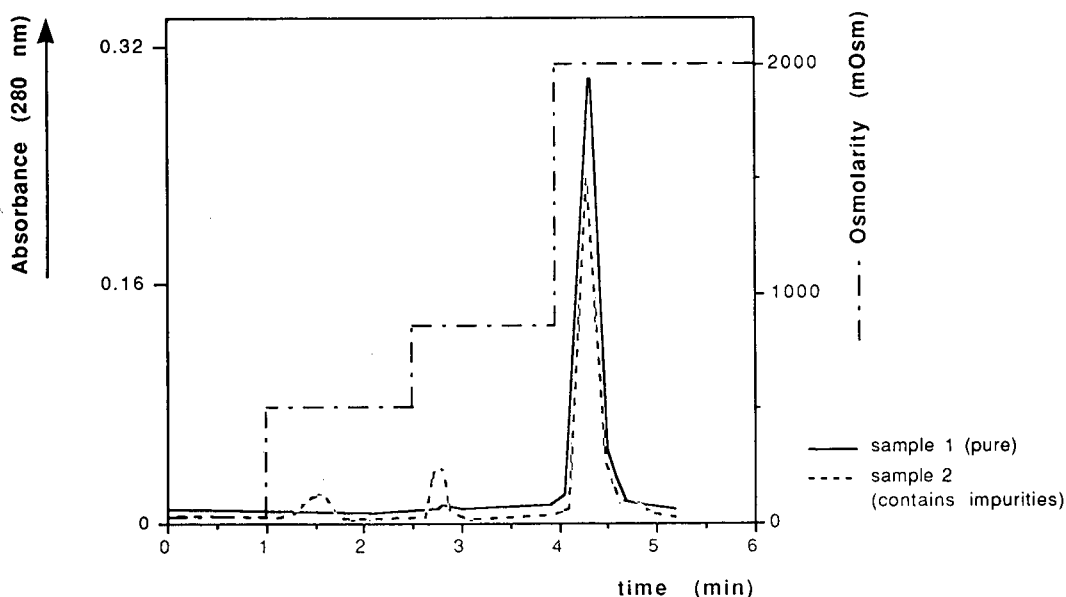


Fig. 3. Process monitoring of the isolation of antithrombin III by fast heparin HPMAC. Sample 1, antithrombin III, obtained by separation with Toyopearl Heparin (solid line); sample 2, obtained by separation with Eupergit Heparin (broken line). A 50- μ l volume of sample (*ca.* 20 μ g of protein) was diluted to 500 μ l with 10 mM citrate buffer (pH 7.4) and applied to the separation unit. Chromatographic conditions: separation unit, QuickDisk Heparin, 25 mm diameter, 3 mm thickness; flow-rate, 3 ml/min; pressure, 2 bar; room temperature.

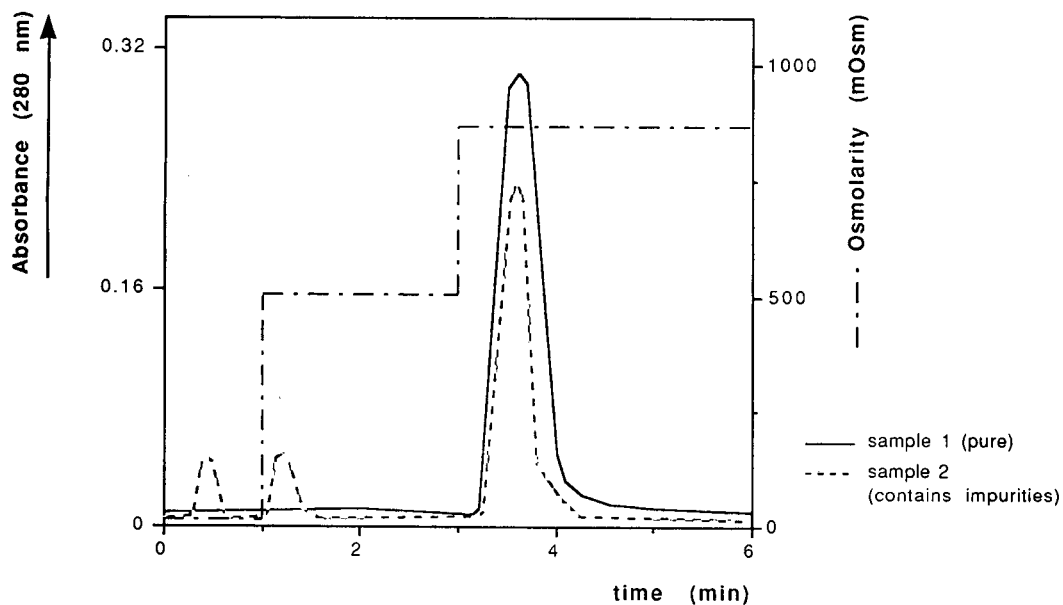


Fig. 4. Process monitoring of the isolation of factor IX by fast heparin HPMAC. Sample 1, factor IX without contamination by factor X (full line); sample 2, containing minimal factor X activity apart from factor IX (broken line). A 50- μ l volume of sample (ca. 75 μ g of protein) was diluted with 10 mM citrate buffer (pH 7.4) and applied to a QuickDisk Heparin separation unit. Chromatographic conditions as in Fig. 3.

pears in the chromatogram resulting from the heparin HPMAC unit as an additional peak eluted in the second step with a 900 mOsmol buffer.

Fig. 4 shows fast affinity HPMAC using a disc with immobilized heparin, similar to Fig. 3. A sample without contamination by factor X (full line) is compared with a sample with about 5% of contamination by factor X (broken line). The contamination is the result of an impaired performance of the column, resulting from repeated treatment with 0.5 M sodium hydroxide. It can be detected at once through the analytical QuickDisk unit.

DISCUSSION

Heparin AC has considerable advantages over other affinity chromatographic methods when used for the separation of biopolymers. The binding between ligand and ligate is easily dissociated by increasing the salt concentration in the elution buffer. This ensures the stability of the separation medium, and the sample usually retains its biological activity.

The isolation of antithrombin III from human

plasma by heparin AC has been carried out for some time even on an industrial scale, in order to produce this therapeutically important protein [1,3]. Antithrombin III binds strongly to heparin and is eluted from the column only at very high salt concentrations. In the experiments carried out here, the method was used chiefly to evaluate heparin affinity supports. The model investigations with the isolation of antithrombin III should help to develop further guidelines for choosing appropriate supports for the separation of the clotting factor IX from factor X. Heparin AC is the last and probably the most difficult step in the isolation process of factor IX. Apart from its selectivity requirements, the support has to be resistant at high pH. Treatment with 0.2–0.5 M sodium hydroxide is still the most frequently used and easiest way for column sanitizing, that is, chiefly the removal of bacterial endotoxins. Consequently, the buffers used in the separation of factor IX from factor X, namely sodium chloride of 500 and 900 mOsmol, were also chosen for the removal of the weakly bound proteins in the isolation of antithrombin III.

As in other affinity chromatographic methods,

the matrix used for immobilization plays an important part in heparin AC. The silica gel-based supports were excluded straightaway from these investigations, as they have a low stability even in weakly basic media. Consequently, supports based on natural polymers (agarose) or synthetic polymers were investigated further. The remaining hydrophobicity of the synthetic support is again an important factor. The non-specific bindings in the case of Eupergit Heparin and the poor recovery after separation on Bio-Gel Heparin probably originate in the relatively hydrophobic matrix. Although all the plasma proteins with the exception of antithrombin III are supposed to be washed out by the two previous step gradients, several additional lines appear in the elution peak when this support is used. These polypeptides are seen also in the second washing step, but they cannot be removed completely (see Fig. 1, SDS-PAGE).

When the Toyopearl Heparin support is used (see Fig. 1), non-specific bindings are much reduced. Apart from the antithrombin III, no other bands are seen in SDS-PAGE. A disadvantage of the Heparin Sepharose support is its low stability at high pH. This results in increasingly weak binding of antithrombin III after only the second treatment with 0.2 M sodium hydroxide (*cf.*, SDS-PAGE in Fig. 1). New, untreated Heparin Sepharose binds antithrombin III very strongly, similarly to Toyopearl and Eupergit Heparin. Non-specific bindings are low, so that the protein is eluted in a virtually pure state in the third step with 2 M sodium chloride. After treatment with sodium hydroxide, however, part of the antithrombin III is eluted earlier, along with several other proteins, by the buffer of 500 mOsmol (*cf.*, SDS-PAGE in Fig. 1).

On the one hand, the other agarose-based supports survive treatment with 0.5 M sodium hydroxide without difficulty, *e.g.*, DEAE-Sepharose Fast Flow, which was used for the prepurification of factor IX (see Experimental). On the other hand, heparin for its part, if bound to other supports, can also be treated with sodium hydroxide without adverse effects (see above). This indicates strongly that the binding itself that exists between heparin and agarose with this support is unstable at high pH.

Heparin HPAC, when used as the final step in the purification of clotting factor IX from human plasma, cannot be regarded as affinity chromatography

in the original sense. The precise nature of the interaction between the heparin and the sample components is not clearly defined. It has to be assumed that ionic interactions are the most important element. Also in this step the solvent-detergent mixture from the virus inactivation is removed from the sample (see Fig. 2 and Results). With such a sophisticated separation, the reproducibility of the results is of utmost importance. Even very small changes in the binding characteristics of the support can have an adverse effect on the separation. Besides, sanitizing of the gel with 0.5 M sodium hydroxide is necessary after each separation in order to remove any pyrogenic substances that may have formed. Heparin agarose and heparin bound to silica gel matrices are less suited for these applications, as they lack stability in basic media (*cf.*, Fig. 1 and Tables I and II). In contrast, other media such as Eupergit Heparin, Toyopearl Heparin and QuickDisk membranes with immobilized heparin withstand repeated treatment with sodium hydroxide. Heparin, immobilized to compact, porous discs, can be used successfully for preparative purification of factor IX (not shown here). However, this separation technique has so far been used only on an experimental scale and is described elsewhere [11]. The treatment with sodium hydroxide leads to a deterioration in the separation of factor IX from factor X. This applies to all supports, but the phenomenon is least noticeable in the case of Toyopearl Heparin (see Tables I and II). However, the separation performance of all three synthetic supports that were investigated stabilizes after the first contact with 0.5 M sodium hydroxide, and subsequent separations and yields are reproducible.

The performance of the supports in the isolation of antithrombin III from plasma is also indicative of their effectiveness in the separation of factor IX from factor X. If the support concerned shows higher non-specific binding in the isolation process of antithrombin III, as was the case here with Eupergit Heparin (see Fig. 1), the amount of other proteins in the factor IX product will also be higher, and its specific activity will be lower (*cf.*, Table I). The increasingly weak binding of antithrombin III to the support after treatment with sodium hydroxide indicates that under these conditions the separation between factor IX and factor X will be insufficient, *e.g.*, in the case of Heparin Sepharose (*cf.*, Fig. 1

and Tables I and II). Preliminary model investigations help in choosing the likely supports. Subsequent experiments can then be carried out specifically, with a reduced number of supports, cutting the cost of the expensive factor IX samples.

The use of heparin HPMAC for fast analyses of the samples can serve as process monitoring during isolation of both antithrombin III and factor IX. Any contamination that may occur is quickly detected as additional peaks (see Figs. 3 and 4). The results obtained in this way agree with those from other analytical methods. When the antithrombin III is contaminated (broken line in Fig. 3), the substances appear as bands in SDS-PAGE.

Contaminants in the factor IX product caused by factor X (broken line in Fig. 4) are also detected in the clotting test. However, both analyses, SDS-PAGE and the clotting test, take much longer to carry out, and the necessary information is available only much later. Using QuickDisk Heparin HPMAC the results are obtained within minutes. This allows an almost immediate response, e.g., modifications of the production process or possibly corrections in the fractioning. Similar proposals for process monitoring exist in connection with other materials that allow fast chromatographic analyses, e.g., ion-exchange chromatography or immunoaffinity chromatography, using perfusion chromatographic supports.[12].

REFERENCES

- 1 Y. L. Hao, K. C. Ingham and M. Wickerhauser, in J. M. Curling (Editor), *Methods of Plasma Protein Fractionation*, Academic Press, London, Orlando, 1980, p. 57.
- 2 Dj. Josić, J. Reusch, K. Löster, O. Baum and W. Reutter, *J. Chromatogr.*, 590 (1992) 59.
- 3 Dj. Josić, W. Reutter and D. M. Krämer, *Angew. Makromol. Chem.*, 166/167 (1989) 249.
- 4 R. Eketorp, in M. Perrut (Editor), *Proceeding of the 9th International Symposium on Preparative and Industrial Chromatography*, Nancy, Société Française de Chimie, Vandœuvre, 1992, p. 319.
- 5 S. C. March, J. Parikh and P. A. Cuatrecasas, *Anal. Biochem.*, 60 (1974) 149.
- 6 B. Horowitz, R. Bonomo, A. M. Prince, S. N. Chin, B. Brotman and R. W. Shulman, *Blood*, 79 (1992) 826.
- 7 D. H. Lowry, N. J. Rosenbrough, A. L. Farrand and R. J. Rendall, *J. Biol. Chem.*, 193 (1951) 265.
- 8 P. K. Smith, R. I. Krohn, G. T. Hermanson, A. K. Malla, F. H. Gartner, M. C. Provenzano, E. K. Fujimoto, N. M. Goeke, B. J. Olson and D. C. Klenk, *Anal. Biochem.*, 150 (1985) 76.
- 9 H. G. J. Brummelhuis, in J. M. Curling (Editor), *Methods of Plasma Protein Fractionation*, Academic Press, London, Orlando, 1980, p. 117.
- 10 U. K. Laemmli, *Nature (London)*, 227 (1970) 680.
- 11 Dj. Josić, O. Baum, K. Löster, W. Reutter and J. Reusch, in M. Perrut (Editor), *Proceedings of the 9th International Symposium on Preparative and Industrial Chromatography*, Nancy, Société Française de Chimie, Vandœuvre, 1992, p. 113.
- 12 N. B. Afeyan, B. Dorval and L. Khatchaturian, presented at the 16th International Symposium on Column Liquid Chromatography, Baltimore, MD, 1992, paper 135.

High-performance liquid chromatography of amino acids, peptides and proteins

CXXII[☆]. Application of experimentally derived retention coefficients to the prediction of peptide retention times: studies with myohemerythrin

M. C. J. Wilce, M. I. Aguilar and M. T. W. Hearn

Department of Biochemistry and Centre for Bioprocess Technology, Monash University, Clayton, Victoria 3168 (Australia)

ABSTRACT

Amino acid retention coefficients were derived from the experimental retention data of 118 overlapping peptide heptamers related to the primary amino acid sequence of myohemerythrin. Individual retention coefficient values for each amino acid were derived by a multiple linear regression matrix approach. Retention data were derived for five different experimental conditions including different organic modifiers (acetonitrile, methanol or 2-propanol), different mobile phase additives (trifluoroacetic acid or potassium phosphate) and different silica-based stationary phase ligands (octadecyl or phenyl groups). A high degree of correlation was observed between these experimentally derived amino acid coefficients (EXP) and the coefficients (LIT) which we recently reported derived from the retention data of over 2000 peptides [M. C. J. Wilce *et al.*, *J. Chromatogr.*, 536 (1991) 165 and 548 (1991) 105]. These results demonstrated that the LIT and EXP coefficients can be used for the prediction of the retention of any peptide set. The effect of peptide length was also further investigated and the correlation results demonstrated the importance of peptide flexibility on the final value of the amino acid coefficient.

INTRODUCTION

Reversed-phase high-performance liquid chromatography (RP-HPLC) continues to provide a very powerful technique for the analysis and purification of peptides and proteins. In addition, significant information on the physicochemical basis of the interaction between peptides and proteins and the stationary phase ligand has been derived using RP-HPLC [1–5]. However, fully developed mecha-

nistic models are not yet available to describe, in molecular terms, the interactive processes that occur between the stationary phase, the mobile phase and the peptide or protein solute. The development of such models requires large and systematic data bases and associated structure–retention relationships to be determined. In addition, the influence of chromatographic parameters on the secondary and tertiary structure of the solutes also needs to be addressed. As part of our on-going studies into the mechanism of peptides and protein retention in RP-HPLC, we have previously derived individual amino acid group retention coefficients (GRCs) using a multiple linear regression analysis approach [6]. Several sets of retention coefficients have been re-

Correspondence to: Professor M. T. W. Hearn, Department of Biochemistry and Centre for Bioprocess Technology, Monash University, Clayton, Victoria 3168, Australia.

[☆] For part CXXI, see ref. 15

purchased from BDH (Kilsyth, Australia). All mobile phases were filtered prior to use with a Millipore Durapore filter and then further degassed by helium sparging for 10 min.

Apparatus

Peptide retention times were measured using a Hewlett-Packard 1090 liquid chromatograph consisting of a DR5 solvent delivery system, a thermostatically controlled oven set at 37°C, an autosampler and a diode-array detector with an HP79994A workstation coupled to a Thinkjet printer and an HP7470 plotter. All data were stored on the HP computer before transfer to either an IBM PC or the Monash University VAX computer for further analysis.

Four different mobile phase systems were used for the derivation of the experimental retention data base. These included: solvent 1: A, 0.1% TFA; B, 0.09% TFA–50% acetonitrile; solvent 2: A, 0.1% TFA; B, 0.09% TFA–50% methanol; solvent 3: A, 0.1% TFA; B, 0.09% TFA–50% 2-propanol; solvent 4: A, 25 mM KH₂PO₄; B, 35 mM KH₂PO₄–50% acetonitrile. The flow-rate was 1 ml/min except for solvent 3 where 0.7 ml/min was used due to a high pressure drop. Two different alkyl ligand types were used: column 1: *n*-octadecylsilane (RP-C₁₈, 15 cm × 4.6 mm I.D., 5 μm, 75 nm pore size, DuPont Zorbax); column 2: phenylsilane (RP-phenyl, 15 cm × 4.6 mm I.D., 5 μm, 75 nm pore size, DuPont Zorbax). Table I lists the codes and chromatographic conditions used for the derivation of the GRCs.

TABLE I
CODES AND CHROMATOGRAPHIC CONDITIONS
USED TO DERIVE THE EXP COEFFICIENT SET

| Code | Chromatographic conditions |
|--------------------|--|
| C ₁₈ TA | RP-C ₁₈ sorbent, TFA–acetonitrile mobile phase |
| C ₁₈ KP | RP-C ₁₈ sorbent, KH ₂ PO ₄ –acetonitrile mobile phase |
| C ₁₈ TM | RP-C ₁₈ sorbent, TFA–methanol mobile phase |
| C ₁₈ TP | RP-C ₁₈ sorbent, TFA–2-propanol mobile phase |
| PHETA | RP-phenyl sorbent, TFA–acetonitrile mobile phase |

RESULTS AND DISCUSSION

Influence of ligand type and mobile phase on five sets of experimental retention coefficients

According to the solvophobic theory [12], peptide retention in RP-HPLC is largely caused by entropic expulsion of the peptide from the polar mobile phase, accompanied by their adsorption onto the non-polar stationary phase. A practical consequence of this phenomenon is that, in the absence of significant conformational effects, peptide retention can be correlated with the hydrophobicity of the peptide contact area as revealed by the GRCs of the constituent amino acids. These observations thus have important consequences in the development of protocols for the optimisation of retention times for peptides of known composition. To extend the observations based on our recently derived literature retention coefficient (LIT) sets [6,10], 112 heptapeptides which represent the entire group of overlapping peptide heptamers derived from the amino acid sequence of myohemerythrin were eluted under five different chromatographic conditions as described in the Experimental section. Myohemerythrin is the subject of related studies on epitope mapping and protein surface analysis and seven amino acid residues represent the minimum sequence required for epitope recognition by antibodies. Table II lists the values for each of the five experimental (EXP) GRCs and the correlation coefficients for the statistical comparisons of these scales are listed in Table III. It is evident that all five of the scale exhibited a high degree of similarity. The highest correlation ($R=1.00$) was observed for the comparison between the C₁₈TA and the C₁₈TP sets while the poorest correlation ($R=0.80$) was observed between the C₁₈KP and the C₁₈TM sets. With 18 degrees of freedom, the probability of observing $R > 0.80$ is less than 0.05% ($P < 0.001$). The similarity of the five EXP GRC scales is in contrast to the results observed for the previously published LIT GRCs [6]. It was found that a C₁₈ or a C₈ ligand and a TFA–acetonitrile mobile phase resulted in GRCs that were very similar but which were both significantly different to GRCs derived using a C₄ ligand with the same solvent or a C₁₈ ligand with a TFA–acetonitrile–propanol-based mobile phase. In the present study the experimental parameters that were systematically changed were the nature of the

TABLE II
EXPERIMENTALLY DERIVED AMINO ACID GRCs (min)

| Amino acid | C ₁₈ TA | C ₁₈ KP | C ₁₈ TM | C ₁₈ TP | PHETA |
|---------------|--------------------|--------------------|--------------------|--------------------|-------|
| Alanine | 1.70 | 2.91 | 1.76 | 1.36 | 1.24 |
| Cysteine | 0.49 | 0.19 | 1.66 | 0.33 | -1.41 |
| Aspartic acid | 1.10 | -1.47 | 0.31 | 0.71 | 1.01 |
| Glutamic acid | 0.79 | 0.00 | 0.03 | 0.24 | 0.69 |
| Phenylalanine | 8.79 | 9.14 | 10.66 | 7.21 | 9.18 |
| Glycine | 0.39 | 0.36 | 0.00 | 0.00 | 0.00 |
| Histidine | 0.62 | 2.21 | -0.46 | 0.12 | 0.23 |
| Isoleucine | 8.35 | 9.80 | 11.76 | 6.97 | 8.29 |
| Lysine | 0.00 | 3.36 | -1.41 | -0.54 | -0.24 |
| Leucine | 9.51 | 7.88 | 14.69 | 7.56 | 8.88 |
| Methionine | 2.60 | 3.90 | 1.63 | 1.92 | 2.31 |
| Asparagine | -0.02 | 1.31 | -2.01 | -0.40 | -0.26 |
| Proline | 2.79 | 3.50 | 4.21 | 2.08 | 2.09 |
| Glutamine | -0.66 | 3.09 | -7.52 | -0.76 | -1.28 |
| Arginine | 2.36 | 4.67 | 1.62 | 1.66 | 3.19 |
| Serine | 0.27 | 1.66 | 2.64 | -0.41 | 0.10 |
| Threonine | 1.80 | 2.40 | 2.10 | 0.97 | 1.40 |
| Valine | 4.93 | 4.97 | 6.03 | 3.80 | 4.72 |
| Tryptophan | 9.75 | 9.99 | 13.30 | 7.47 | 10.54 |
| Tyrosine | 6.14 | 4.93 | 9.01 | 4.06 | 5.95 |

organic modifier, the pH of the mobile phase and the nature of the stationary phase ligand which all exerted little effect on the experimentally measured GRCs for each amino acid residue.

There are a number of explanations for the differences in the statistical comparisons of the LIT GRCs and the similarity of the EXP GRCs. Firstly, large differences in the frequency distribution of the amino acids within the respective data base of peptides shown for the LIT GRC set (Fig. 2) and the EXP GRC set (Fig. 3) can strongly influence the outcome of the multiple linear regression used to calculate the GRCs. However, comparison of the relative frequency distribution for the LIT GRCs shown in Fig. 2 demonstrated that the frequency of

each amino acid residue is not significantly different in the four data bases (Table IV). As a consequence, the amino acid frequency distribution would therefore not contribute to the differences between the LIT GRCs. The second parameter which may affect the calculation of the GRCs is the sample size of the experimental peptide data set. It has been previously established [6] that a minimum of 100 peptide retention times are required to establish statistically consistent sets of GRCs. The experimental peptide data set for the myohemerythrin heptamers consisted of 112 peptides which thus satisfies the sample size requirements. The third parameter which may also influence the resultant GRC values is the specific sequences of the respective peptide data bases.

The origin of the peptides represents the most significant differences between the 2 data sets. The LIT peptides were derived from enzymatic and chemical cleavage of a large range of proteins while the EXP peptides of the present study were derived from a single protein and were synthesised as overlapping peptides as depicted in Fig. 4. Peptide 1 consisted of the first seven residues of the myohemerythrin sequence while peptide 2 comprised residues 2–8. The remaining peptides were composed in a similar manner by proceeding along the sequence 1

TABLE III
CORRELATION COEFFICIENTS FOR LINEAR REGRESSION ANALYSIS OF 5 EXP GRC SETS ($n=18$, $r_{95\%}=0.44$)

| | C ₁₈ KP | C ₁₈ TM | C ₁₈ TP | PHETA |
|--------------------|--------------------|--------------------|--------------------|-------|
| C ₁₈ TA | 0.90 | 0.97 | 1.00 | 0.99 |
| C ₁₈ KP | | 0.80 | 0.90 | 0.91 |
| C ₁₈ TM | | | 0.96 | 0.94 |
| C ₁₈ TP | | | | 0.98 |

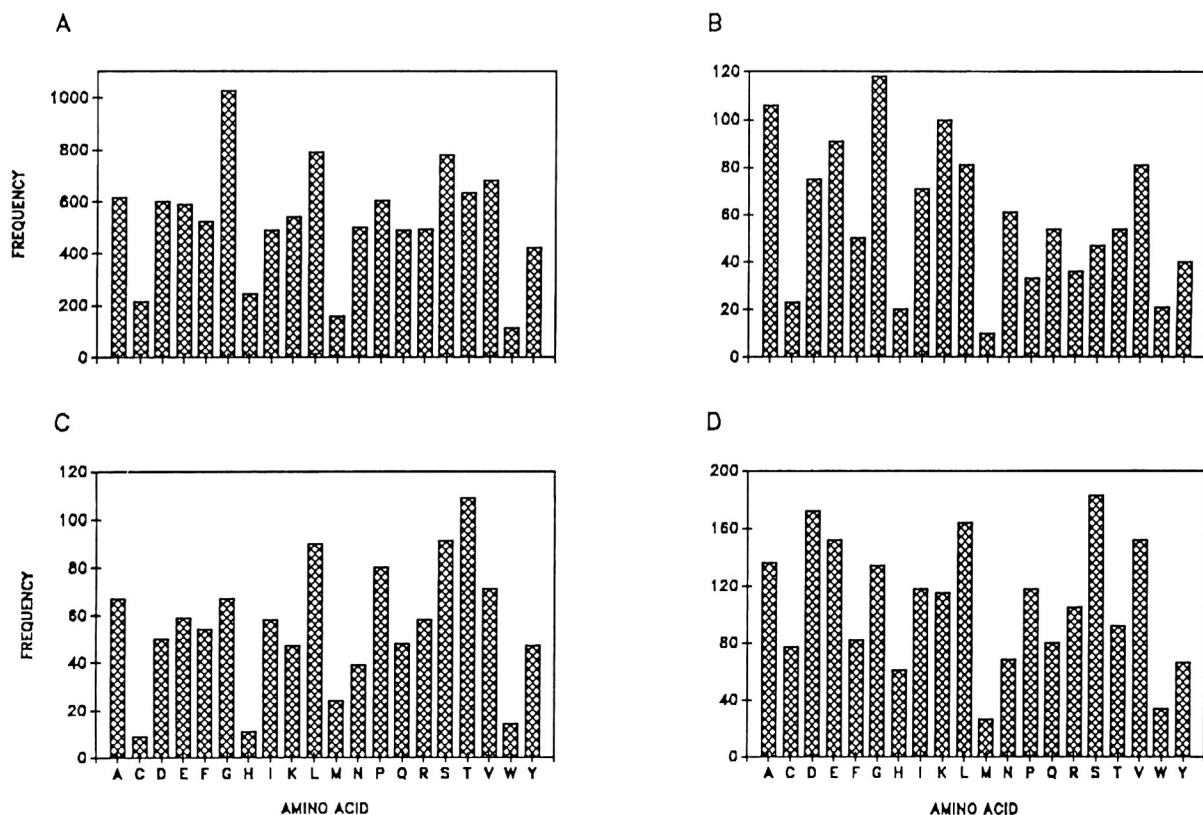


Fig. 2. Amino acid frequency distribution in each of the four LIT peptide data sets. The correlation coefficients for linear comparison between each data set are listed in Table IV.

residue at a time. While there are a large number of peptides generated with this procedure the variations in the molecular environment surrounding

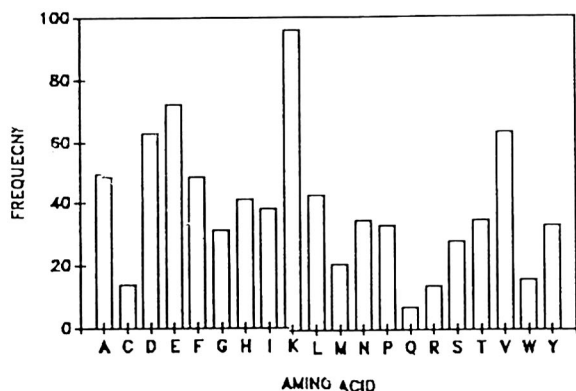


Fig. 3. Amino acid frequency distribution in the EXP peptide data sets.

each amino acid residue is greatly reduced. For example, as illustrated in Fig. 4, glutamic acid-6 is flanked by 2 proline residues in 6 peptides. Thus, while there are more than 100 peptides in the data set, the number of amino acid environmental categories sampled by the non-polar ligands is reduced by a factor of 6 compared to the peptides selected from random sequences. The chromatographic results suggest that the range of amino acid environments associated with the synthetic heptapeptides does not allow differentiation of the molecular dynamics of each peptide during interaction with the stationary phase ligands in each of the 5 different chromatographic conditions.

Influence of peptide length on experimental coefficients

It is well established that peptides larger than 15-20 residues are often eluted with retention times

TABLE IV

CORRELATION COEFFICIENTS FOR THE LINEAR COMPARISON OF THE AMINO ACID FREQUENCIES IN EACH OF THE LIT PEPTIDE DATA SETS ($n=18$, $r_{95\%}=0.44$)

| | C ₁₈ TA | C ₈ TA | C ₄ TA |
|---------------------|--------------------|-------------------|-------------------|
| C ₈ TA | 0.65 | | |
| C ₄ TA | 0.75 | 0.44 | |
| C ₁₈ TPA | 0.69 | 0.66 | 0.66 |

which are different to the predicted times based on the summation of their GRCs. The differences in the chain lengths of the peptides used for the LIT and EXP data bases may therefore represent an additional factor which contributes to the similarity of the 5 EXP coefficient sets. The EXP peptides were all 7 residues in length while the LIT peptides ranged in length from 2 to 30 amino acids. It is generally considered that as peptide length increases, there is a greater probability for chromatographic ligands to induce transitions from a disorganised random coil structure to a stabilised secondary structure. Conformational rearrangements of peptides have been monitored in RP-HPLC through measurements of the change in chromatographic contact areas and affinity and also through changes in the enthalpy and entropy associated with the binding of the peptide to the stationary phase ligands [1,2]. Thus, the hydrophobic nature of the reversed-phase ligands can induce the formation of secondary structure, such as an amphipathic α -helix [13] and this process will prevent the amino acid residues which are oriented away from the stationary phase surface to contribute to the peptide retention. The extent of conformational flexibility of the peptides

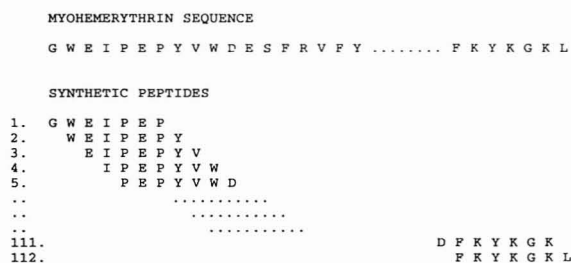


Fig. 4. Diagram illustrating the method used to generate overlapping heptamers of the amino acid sequence of myohemerythrin.

used for the retention data base will thus strongly influence the calculation of the GRCs.

The effect of peptide length on the GRCs was therefore assessed by performing additional linear regression analysis between the EXP-C₁₈TA and LIT-C₁₈TA GRC scales according to various peptide length criteria. In the first instance, 8 groups of peptides of different chain lengths were established using the LIT-C₁₈TA GRC scale which included peptides containing 2–30, 2–20, 2–15, 2–10, 2–8, 2–7, 2–5 and 2–4 amino acid residues in length. The correlation coefficient from the linear regression analysis of these restricted LIT GRCs with the EXP-C₁₈TA scales are shown in Fig. 5. The highest correlation for these comparisons was obtained for the LIT sub-group containing peptides up to 15 amino acid residues. The average length of the LIT peptides in the group of peptides with 2–15 residues was 7.2 residues. It can therefore be anticipated that the LIT peptide group with 2–15 amino acid residues should exhibit a high degree of correlation with the EXP-C₁₈TA scale which were derived from peptides of 7 amino acid residues. The LIT peptide groups consisting of shorter peptides, *i.e.* 2–10, 2–8, 2–7, 2–5 and 2–4 amino acid residues, exhibited lower correlation with the EXP-C₁₈TA scale. This divergence may be due to exaggerated N- and C-terminal effects associated with the LIT peptide sets due to their origin. For example, many peptides were tryptic peptides which contain a basic amino acid residue (arginine or lysine) at the C-terminal

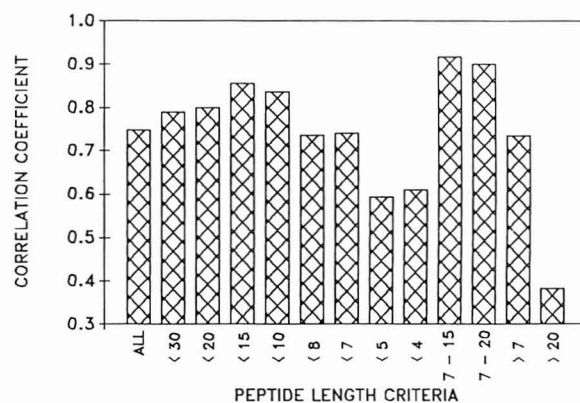


Fig. 5. Correlation coefficients generated for the comparison of the EXP C₁₈TA GRCs and LIT GRCs with specified peptide length criteria.

position. Similar sequence-dependent retention behaviour has been noted by Guo *et al.* [7]. However, in the derivation of both the LIT and EXP GRCs, the influence of the end-groups was minimised through the calculation of separate coefficients for the N- and C-terminal end-groups. Comparison of the correlation coefficients for the peptide groups consisting of longer peptides, *i.e.* peptides containing 2–20 or 2–30 residues, revealed that the r value for these groups was similar to that of the peptide group containing only 1–15 amino acid residues. In these cases, a large number of smaller peptides which are common to the sub-groups with 2–15, 2–20 and 2–30 amino acid residues will exert the dominant influence on the final GRC values.

Three further cluster groups were also defined with the LIT peptides comprising 7–15 residues and all peptides with more than 7 or more than 20 amino acid residues. The maximum correlation with the EXP GRC sets was found for the LIT group derived from peptides between 7 and 15 residues in length and thus represented the highest correlation observed for the comparisons of all peptide sub-groups. The low correlation coefficient (0.38) for the comparison of the LIT group containing peptides greater than 19 residues in length with the EXP-C₁₈TA set clearly demonstrates the influence of the peptide length on the GRCs. Overall, the results of the linear regressions of the peptide sub-groups indicates that peptide length is an important factor controlling the differences within LIT GRCs and the constancy of the EXP GRCs. It should thus be possible to selectively improve the degree of linear correlation by restricting the length of the peptides in the original calculation of the LIT GRCs. This was performed using the LIT-C₁₈TA and the LIT-C₁₈TPA GRC scales. The original correlation coefficient between both scales has been calculated as 0.44 [6]. If the LIT-C₁₈TA data base is restricted to include only peptides containing up to 7 residues in length the correlation increases to 0.82. It can be concluded from these results that selectivity changes and reversals which are observed in the elution of peptides in RP-HPLC under different chromatographic conditions are not only due to changes in the intrinsic hydrophobicity of each amino acid. The relative retention of a peptide will also be strongly influenced by the conformational flexibility of the peptide which in turn controls the portion of

the peptide that interacts with the stationary phase surface.

Prediction of peptide retention times

The ability of the EXP and the LIT scales to predict the retention times of the 112 peptides was examined. Fig. 6 shows the retention time profile predicted according to the summation of the LIT-C₁₈TA coefficient scale (A), the EXP-C₁₈TA coefficient scale (B) and the experimentally observed retention times for these peptides under the same experimental conditions (*i.e.* TFA–acetonitrile) (C). A correlation coefficient of 0.98 was observed from linear regression comparison between the EXP-C₁₈TA GRCs and the experimentally observed retention times for the 118 synthetic peptides. Comparison of the retention times predicted by the LIT-C₁₈TA coefficient scale and the experimentally ob-

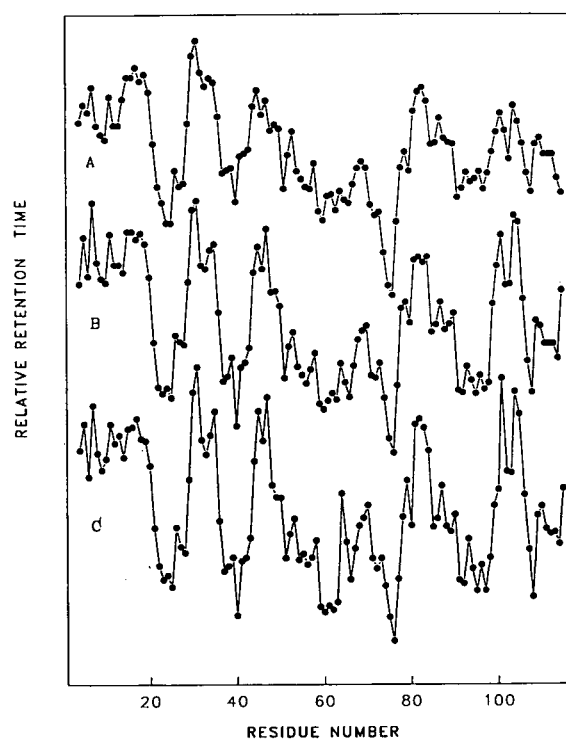


Fig. 6. Retention profile of overlapping heptamers derived from the amino acid sequence of myohemerythrin. (A) Retention times (min) predicted with the LIT GRCs; (B) retention times predicted with the EXP GRCs; (C) experimentally observed retention times, which ranged between 10 and 45 min. The linear relationship between panel A and panel C is given by eqn. 1.

served times gave a correlation coefficient of 0.91 for the same 118 synthetic peptides. In order to accommodate differences in column configuration and experimental parameters, the retention times predicted by the LIT-C₁₈TA scale required linear adjustment to correlate in magnitude with the experimentally observed retention times according to the following relationship:

$$\text{observed retention time} = (\text{LIT predicted retention time}) \times 1.46 + 14.02 \quad (1)$$

The high degree of linear correlation between the retention times predicted using the LIT GRCs and the experimentally observed retention times demonstrates the general utility of the LIT GRCs for the prediction of relative retention times of peptide solutes not originally used as part of the data base for the derivation of the GRCs. The ability of both the LIT GRCs and the EXP GRCs to predict the hydrophobic surface accessibilities of unrelated sets of peptides and proteins is documented elsewhere [14].

ACKNOWLEDGEMENTS

These investigations were supported by grants from the Australian Research Council and the National Health and Medical Research Council.

REFERENCES

- 1 A. W. Purcell, M. I. Aguilar and M. T. W. Hearn, *J. Chromatogr.*, 476 (1989) 125.
- 2 A. W. Purcell, M. I. Aguilar and M. T. W. Hearn, *J. Chromatogr.*, 593 (1992) 103.
- 3 M. Kunitani, D. Johnson and L. R. Snyder, *J. Chromatogr.*, 371 (1986) 313.
- 4 M. L. Heinitz, E. Flanigan, R. C. Orłowski and F. E. Regnier, *J. Chromatogr.*, 443 (1988) 229.
- 5 M. T. W. Hearn and M. I. Aguilar, *J. Chromatogr.*, 392 (1987) 33.
- 6 M. C. J. Wilce, M. I. Aguilar and M. T. W. Hearn, *J. Chromatogr.*, 536 (1991) 165.
- 7 D. Guo, C. T. Mant, A. K. Taneja, J. M. R. Parker and R. S. Hodges, *J. Chromatogr.*, 359 (1986) 499.
- 8 J. L. Meek and Z. L. Rosetti, *J. Chromatogr.*, 211 (1981) 15.
- 9 C. Chabanet and M. Yvon, *J. Chromatogr.*, 599 (1992) 211.
- 10 M. C. J. Wilce, M. I. Aguilar and M. T. W. Hearn, *J. Chromatogr.*, 548 (1991) 105.
- 11 N. J. Macji, A. M. Bray and H. M. Geysen, *J. Immunol. Methods.*, 134, (1990) 23.
- 12 Cs. Horvath, W. R. Melander and I. Molnar, *J. Chromatogr.*, 125 (1976) 129.
- 13 N. E. Zhou, C. T. Mant and R. S. Hodges, *Peptide Res.*, 3 (1990) 8.
- 14 K. L. Spiers, M. I. Aguilar and M. T. W. Hearn, in preparation.
- 15 M. Zacheriou and M. T. W. Hearn, *J. Chromatogr.*, 599 (1992) 171.

High-performance liquid chromatographic analysis of carbohydrate mass composition in glycoproteins

M. Kunitani and L. Kresin

Department of Analytical Chemistry, Chiron Corporation, 4560 Horton Street, Emeryville, CA 94608 (USA)

ABSTRACT

A method has been developed which characterizes the carbohydrate portion of glycoproteins by its mass composition (mass carbohydrate per mass protein). This size-exclusion HPLC method uses both UV and refractive index detectors in series and requires only a single injection of intact glycoprotein. It has been shown that for calibration purposes any carbohydrate or protein which chromatographs well on the sizing system can be substituted for the carbohydrate or protein moiety of the glycoprotein of interest. The accuracy of this method was demonstrated for RNase B and fetuin. Mass compositions of various monoclonal IgMs were determined with an average intraday precision of approximately 6%; the limit of lot-to-lot resolution. Thus, the primary utility of this simple HPLC method is to identify substantial changes in the carbohydrate moiety among various glycoprotein preparations.

INTRODUCTION

It is known that glycosylation of pharmaceutical proteins can be influenced by many factors, including cell type and cell culture environment, and can result in changes in distribution of glycoforms [1,2]. The carbohydrate moiety can have a significant effect on physical, immunological and biological properties of glycoproteins, including solubility, specific activity and clearance rate from the circulatory system [3,4].

Determination of the exact amount of carbohydrate in a glycoprotein still remains a significant challenge in spite of recent advances in methodology [5]. It usually consists of a difficult series of enzymatic and/or chemical cleavages followed by chromatographic quantitation of the various monosaccharides. The lack of quantitative cleavage of carbohydrate from the protein and chemical degradation of some monosaccharides during oligosaccharide hydrolysis leads to uncertainty as to the

accuracy of the final result. Mass spectrometry and enzymatic techniques are used to yield sequencing information but the precise distribution of the various glycoforms is not determined. In fact, rigorous validation of accuracy for carbohydrate analysis of any complex glycoprotein containing a variety of glycoforms remains unsettled. This paper presents a simple size-exclusion HPLC (SEC) method which determines the carbohydrate mass composition (mass carbohydrate/mass protein) for intact glycoproteins, thus circumventing the potential for incomplete deglycosylation and monosaccharide degradation, weaknesses of traditional compositional analysis. This analysis is not designed to be comprehensive, as the single value of mass composition does not provide detailed characterization of glycoprotein structure. However, it does provide a simple and useful method of comparing the degree of glycosylation in glycoprotein pharmaceuticals.

THEORY

This method is identical to that developed for characterization of polyethylene glycol (PEG)-proteins [6], which uses SEC with UV and refractive

Correspondence to: M. Kunitani, Department of Analytical Chemistry, Chiron Corporation, 4560 Horton Street, Emeryville, CA 94608, USA.

index (RI) detectors in series. The UV detector at 280 nm selectively detects only the aromatic residues in the protein moiety of a glycoprotein, as sugars do not absorb at this wavelength. The RI detector responds to the mass of protein and of the carbohydrate. The protein contribution to the RI signal is calculated from the protein concentration calibration derived from the UV detector data; the remaining RI response is due to the carbohydrate. The fundamental assumption is that the refractive index of the glycoprotein solution (N_{GP}), can be expressed as the sum of the refractive indices of its components, P (protein) and G (carbohydrate):

$$N_{GP} = N_0 + C_P \left(\frac{dn}{dc} \right)_P + C_G \left(\frac{dn}{dc} \right)_G \quad (1)$$

where N_0 is the refractive index of pure solvent; $(dn/dc)_P$ and $(dn/dc)_G$ are the specific refractive index increments of protein and carbohydrate, respectively, and C_P and C_G are their mass concentrations. Since the protein and oligosaccharide moieties are relatively large polymers linked with a single covalent bond, the assumption of eqn. 1 should be accurate. Eqn. 1 can be rearranged to give the working eqn. 2. The detail for this derivation is presented in ref. 6.

$$\frac{W_G}{W_P} = \frac{\frac{\text{RI area glycoprotein}}{\left(\frac{\text{UV area glycoprotein}}{\text{UV area/mg protein}} \right)} - \text{RI area/mg protein}}{\text{RI area/mg carbohydrate}} \quad (2)$$

Determination of glycoprotein mass composition requires calibration of the SEC system with the protein and carbohydrate moieties separately, which will yield the RI and UV peak area/mg terms (calibration slopes). A single injection of the intact glycoprotein will give the UV and RI area for the glycoprotein and allow calculation of the mass composition (W_G/W_P). There are many instances when it is not possible nor practical to calibrate this mass composition analysis with the deglycosylated portion of the glycoprotein. In these instances another non-glycosylated protein can be used as a calibrator. Eqn. 2 then becomes:

$$\frac{W_G}{W_P} = \frac{\frac{\text{RI area glycoprotein}}{\left(\frac{\text{UV area glycoprotein}}{\text{UV area/mg calib. protein} \cdot K} \right)} - \text{RI area/mg calib. protein} \cdot K'}{\text{RI area/mg carbohydrate}} \quad (3)$$

The K and K' in eqn. 3 represent the respective correction factors for differences in UV 280 nm and RI response between the glycoprotein of interest and the calibration protein.

$$K = \frac{E^{0.1\%} \text{ glycoprotein}}{E^{0.1\%} \text{ calib. protein}}$$

and

$$K' = \frac{\left(\frac{dn}{dc} \right)_{\text{glycoprotein}}}{\left(\frac{dn}{dc} \right)_{\text{calib. protein}}} \cong 1 \quad (4)$$

where K is the ratio of extinction coefficients and K' is the ratio the refractive index increment for the glycoprotein of interest to that of the calibration protein. The assumption that $K' \cong 1$ will be evaluated in this paper. The purpose of this work is to establish the validity of the RI/UV method for compositional analysis of glycoproteins and to establish its precision for typical glycoproteins.

EXPERIMENTAL

Materials

Sialic acid, N-acetylglucosamine (GlcNAc), maltose, maltotriose, maltotetraose, ribonuclease A (RNase A), and ribonuclease B (RNase B) from bovine pancreas were obtained from Sigma (St. Louis, MO, USA). Glucose and galactose were from Applied Science Labs. (State College, PA, USA). Fucose was from United States Biochemical Corp. (Cleveland, OH, USA). The dextran 1000 ($M_n = 1010$, $M_w = 1270$) and dextran 6000 ($M_n = 6100$, $M_w = 6700$) were obtained from American Polymer Standards Corp. (Mentor, OH, USA). Bovine serum albumin (BSA) was from National Institute of Standards and Technology (Gaithersburg, MD, USA). IgM samples were from Chiron (Emeryville, CA, USA) and Rockland (Gilbertsville, PA, USA). The source of bovine fetuin was from Gibco Labs. (Grand Island, NY, USA) and was obtained as a gift from the laboratory of Professor R. Townsend [7]. Interleukin-2, a human recombinant protein was produced in *E. coli* (Chiron) and contains no carbohydrate.

Chromatography was performed with system consisting of a SP 8700 pump (Spectra-Physics, San Jose, CA, USA), a WISP 710 B injector (Millipore-Waters, MA, USA), an ERC-7510 RI detector (Erma, Tokyo, Japan), a LC135 UV detector (Perkin-Elmer, Norwalk, CT, USA) set at 280 nm, and a Nelson Analytical 6000 data system (Perkin-Elmer/Nelson, Cupertino, CA, USA). Due to pressure limitations on most RI detector flow cells, the UV detector always proceeds the RI detector in a series configuration.

Methods

Carbohydrates were run on two different HPLC columns based upon their selectivity. Monosaccharide chromatography was performed on an Aminex HPX-87H (300 × 7.8 mm I.D.) column (Bio-Rad, Richmond, CA, USA) with an RI detector. The eluent was 0.005 M H₂SO₄ at a flow-rate of 0.6 ml/min. The column temperature was 45°C and the injection volume was 20 μl. Oligosaccharides were separated from each other and from monosaccharides using an Aminex HPX-42A column (Bio-Rad). The eluent was water at a flow-rate of 0.6 ml/min. The column temperature was 85°C and injection volume was 20 μl.

For the protein and glycoprotein separations, the SEC columns were chosen on their ability to achieve adequate resolution of the analyte proteins from RI system peaks at the included or excluded volume of the column. A Superose 12 column (Pharmacia LKB, Piscataway, NJ, USA) was used to compare the RI response of various proteins. The eluent was 0.1 M sodium sulphate and 0.01 M sodium phosphate (pH 7.0) at flow-rate of 0.5 ml/min. Literature extinction coefficients were used to determine protein concentrations and 100 μl of each protein were injected separately [8–10]. The chromatographic system used for mass composition analysis of RNase B consisted of two Zorbax GF-250 (25 cm × 9.4 mm I.D.) columns (DuPont, Wilmington, DE, USA) at room temperature using 0.5 M Na₂SO₄, 0.01 M phosphate buffer, pH 7.0, at a flow-rate of 0.5 ml/min. Calibration curves were run for dextran 1000 (as a carbohydrate calibrator) and for RNase A (as a deglycosylated protein calibrator). Repurified RNase B as well as each standard were run in triplicate. The injection volume was 100 μl. A Superose 6 (Pharmacia) column was used for analy-

sis of IgMs using 50 mM (NH₄)₂SO₄, 50 mM phosphate buffer (pH 7.5) at an eluent of a flow-rate of 0.4 ml/min at room temperature. Fetuin was analyzed with a Zorbax GF-250 column using the same eluent at 0.8 ml/min. The injection volume was 100 μl. Dextran 6000 was used as a carbohydrate calibrator and BSA as a protein calibrator for both IgM and fetuin analyses. A generic extinction coefficient of $E^{0.1\%} = 1.4$ was used for IgM analyses while a theoretical value of $E^{0.1\%} = 1.67$ was used for fetuin [5].

RNase B was purified by chromatography at room temperature on a Con A-Sepharose column (4 cm × 2.6 cm I.D.) (Pharmacia, Uppsala, Sweden) equilibrated in 0.1 M Tris-HCl, pH 7.4, containing 1 M NaCl, 1 mM CaCl₂, 1 mM MgCl₂, and 1 mM MnCl₂ [11]. The column was loaded with 40 mg of RNase B dissolved in 3.0 ml of eluent, which was eluted at 0.1 ml/min. Following collection of the unretained material (RNase A), a step elution was performed with 10% α-methyl-D-mannopyranoside in the same eluent. The collected peaks were dialyzed against 50 mM phosphate buffer, pH 6.8. Commercial RNase B and the two peaks collected from the Con-A Sepharose column were analyzed on a pre-cast 10–20% gradient gel (Daiichi, Tokyo, Japan) stained with Coomassie Blue.

For a detailed description of the UV-RI SEC calibration and a analyses procedure see ref. 6. Linear regression analyses were performed on the calibration data (0.2–1.0 mg/ml BSA and dextran 6000) generated daily with each set of samples. If encountered, aggregate shoulders on glycoprotein peaks were included in the integration of analyte peak area.

RESULTS AND DISCUSSION

Carbohydrate calibration

The carbohydrate moiety of any glycoprotein consists of various monosaccharides linked together to form one or more oligosaccharides. Hence the RI response of monosaccharides, oligosaccharides and proteins were independently investigated. The RI increment (dn/dc) is a measure of electron density of a molecule and is not affected by molecular conformation [12]. Since carbohydrates are largely composed of repeating hydroxymethylene (CHOH) functionality, all carbohydrates should have identi-

in carbohydrate chemistry that the RI response of carbohydrates is a measure of mass concentration and varies little among monosaccharides or with the carbohydrate size [13,14]. Phosphorylated or sulfonated carbohydrates have been excluded from consideration in this report. Thus, any carbohydrate with an appropriate retention time can be used as a calibration substitute for the carbohydrate moiety in the UV-RI SEC mass composition analysis of a glycoprotein. This report utilizes commercially available dextran samples as carbohydrate calibrators which are chosen to be baseline resolved from included or excluded volume RI system peaks.

Protein calibration

The most accurate method of protein calibration is to use the deglycosylated protein of interest. However, there are some potential complications with this approach, such as possible insolubility of the deglycosylated protein or lack of complete deglycosylation. For proteins, the main source of electron density and hence the RI response is the amide peptide bond, which is proportional to the number of amino acid residues in the protein. Except for proteins of highly unusual amino acid composition, as a first approximation the number of amino

acid residues is proportional to the protein's molecular mass. Thus, most proteins should have similar RI response per mass [15]. Table III shows RI standard curves for several unglycosylated proteins. The correlation coefficients of the standard curves establish linearity and the slopes are similar, with an R.S.D. of 2.3%, validating the assumption that the RI response of proteins is largely independent of composition and molecular mass, and that $K' \cong 1$ in eqn. 4. Thus, any convenient protein whose extinction coefficient is known may be used for calibration with only a small uncertainty in accuracy. This approach to calibration does not affect assay precision.

Validity of compositional analysis

In order to test the validity of the UV-RI SEC method, the model proteins RNase A and RNase B were used. Both proteins are very well characterized [16]. They have identical amino acid sequences. RNase B contains a single oligosaccharide chain at Asn 35, composed of six mannose and two GlcNAc residues per molecule. RNase A does not have any carbohydrate and represents unglycosylated RNase B. Thus, RNase A can be used as a protein calibrator for RNase B. By this approach the deglycosylation

TABLE III
RI RESPONSE OF PROTEINS

| Protein | MW | Concentration (mg/ml) | Peak area · 10 ⁶ | R.S.D. (%) (n = 3) | Slope (area/mg · 10 ⁶) | r ² |
|---------------|--------|--------------------------|--------------------------------|-----------------------|---------------------------------------|----------------|
| RNase | 13 700 | 0.16 | 1.1 | — | 7.4 | 0.999 |
| | | 0.41 | 2.9 | 0.6 | | |
| | | 0.81 | 6.0 | — | | |
| BSA | 67 500 | 0.18 | 1.1 | — | 7.3 | 0.999 |
| | | 0.43 | 3.0 | 0.7 | | |
| | | 0.93 | 6.7 | — | | |
| Myoglobin | 16 900 | 0.16 | 1.0 | — | 7.5 | 0.999 |
| | | 0.40 | 2.9 | 1.3 | | |
| | | 0.81 | 6.0 | — | | |
| Interleukin-2 | 15 300 | 0.22 | 1.4 | — | 7.7 | 0.999 |
| | | 0.56 | 4.1 | — | | |
| | | 1.12 | 8.5 | — | | |
| Average | | | | | 7.5 | |
| R.S.D. | | | | | 2.3% | |

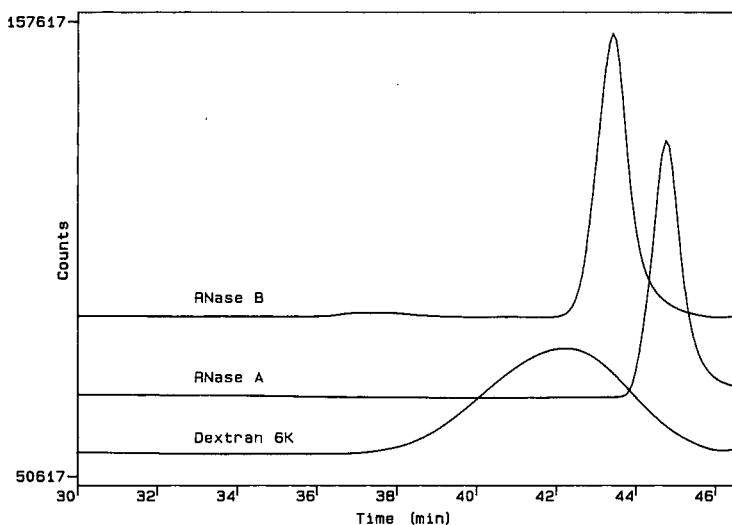


Fig. 3. Refractive index chromatograms for the mass composition analysis of RNase B. RNase A calibration 80 μg , dextran 6000 (6K) calibration 80 μg , purified RNase B analysis 50 μg . HPLC conditions are described in Experimental.

of RNase B and resulting validation of complete carbohydrate cleavage and potential monosaccharide degradation during hydrolysis can be avoided.

Commercial preparations of RNase B contain substantial amounts of RNase A although RNase A preparations are free of RNase B. Thus RNase B was repurified on a Con-A Sepharose affinity column. The RNase A passed through the column, while RNase B was selectively bound by lectin, and was eluted with 10% α -methyl-D-mannopyranoside. The purity of the RNase A and RNase B preparations were verified by sodium dodecyl sulphate-polyacrylamide gel electrophoresis (SDS-PAGE) (not shown). In order to fully separate the relatively small RNase proteins from the included volume, two GF-250 columns in series were used as a sizing system to determine W_G/W_P of RNase B. RNase A and dextran 6000 were used as the protein and the carbohydrate calibrators of the SEC system (Fig. 3). After injection of purified RNase B, its mass composition was determined using eqn. 2. The mass composition (W_G/W_P) was experimentally determined to be 0.11 (R.S.D. = 13%, $n = 3$), which is comparable to the literature value of 0.10 [15], demonstrating the accuracy of the UV-RI SEC method in measuring the carbohydrate/protein mass ratio of a glycoprotein.

A problem for the validation of the mass composition method for large, more complex glycoproteins is the lack of a well characterized standard. The same glycoprotein from different sources is likely to contain different types and proportions of oligosaccharide structures, making comparative analyses difficult [5]. Bovine fetuin is one of the most frequently studied glycoproteins with complex oligosaccharide structures and, in spite of the variability of glycosylation in different preparations, it was chosen for study by the UV-RI SEC mass composition method. Mass spectral studies have characterized fetuin as containing three triantennary N-linked and three O-linked oligosaccharides resulting in a theoretical mass composition of 0.29 [17–19]. BSA and dextran 6000 were used as calibrators for the UV-RI SEC mass composition analysis of fetuin, which was found to be 0.18 ± 0.02 ($n = 8$) (Fig. 4). Chemical hydrolysis on the identical lot of fetuin followed by high-pH anion-exchange chromatography (HPAEC)-pulsed amperometric detection (PAD) monosaccharide analysis yielded a weight composition of 0.18, comparable to the UV-RI SEC approach [7]. This result is consistent with other HPLC-derived monosaccharide analyses of fetuin, although sialic acid quantitation is generally not reported, making comparable weight com-

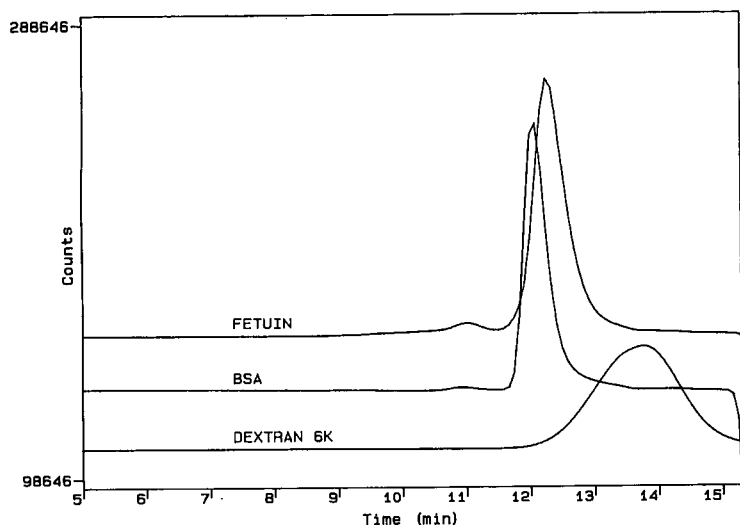


Fig. 4. Refractive index chromatograms for the mass composition analysis of fetuin. BSA protein calibration 48 μg , dextran 6000 calibration 80 μg , fetuin analysis 100 μg . HPLC conditions are described in Experimental.

position calculations impossible [5]. The causes for the discrepancy between theoretical and reported monosaccharide compositions in complex glycoproteins are unknown and are further complicated by variation in glycoprotein preparations and differences among various monosaccharide methods.

Mass composition of IgM

It has been shown that changes in fermentation conditions can alter the distribution and levels of carbohydrates on a glycoprotein produced by mammalian cell culture [1,4]. The UV-RI SEC mass composition analysis was one method which was

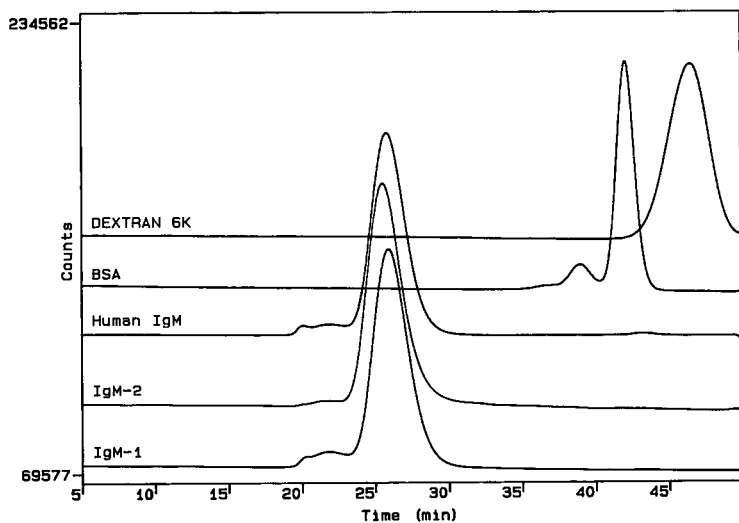


Fig. 5. Refractive index chromatograms for the mass composition analysis of three different IgM antibodies. BSA protein calibration 40 μg , dextran 6000 calibration 70 μg , IgM-1 analysis 90 μg , IgM-2 analysis 100 μg , human IgM analysis 100 μg . HPLC conditions are described in Experimental.

applied to unrelated IgMs produced from cell culture and another from human serum, in order to characterize potential changes in these complex glycoproteins. Calibration of the SEC system was done with dextran 6000 and BSA while a generic $E^{0.1\%}$ for IgM was used with eqn. 3. Although this calibration approach has uncertainties as to the accuracy of the final value, the precision is not affected. The large-pore Superose 6 column was used to chromatograph the large IgM (MW \approx 900 000) glycoprotein between the included and excluded volume of the SEC column (Fig. 5). The results in Table IV shows that the three different IgM antibodies, IgM-1, IgM-2 and commercial human IgM, could easily be distinguished from each other. The higher mass composition IgM-1 over that of IgM-2 correlate with observations such as the lower clearance rate and higher aqueous solubility of IgM-1 compared to that IgM-2 [3]. These results

also show that analyses of different fermentation/purification lots of these IgMs were indistinguishable from each other by the mass composition criteria. Samples 5 and 6 of IgM-1 in Table IV represent, respectively, a 10-fold change in fermentation scale and a different clone, establishing constancy in overall carbohydrate content during these process changes. The average intraday R.S.D. for IgM-1 was 4%, which probably represents the limit of sample-to-sample resolution of the technique. The average intraday R.S.D. for IgM-2 was higher (7%) showing that the method has poorer precision at lower mass composition values. The sensitivity of the mass composition analysis is affected by many factors including the mass composition value, the SEC glycoprotein recovery, the protein extinction coefficient, the SEC column efficiency and RI noise of the HPLC system. Using IgM-1 and IgM-2 as glycoproteins of representative mass composition, the sensitivity was approximately 4 μ g antibody with a limiting RI signal-to-noise ratio of 10. The method is not designed to detect monosaccharide substitution, nor is it precise enough to determine subtle alterations in glycosylation patterns. However, it is precise enough to identify significant changes in mass fraction carbohydrate.

TABLE IV

MASS COMPOSITION OF THREE DIFFERENT IgM ANTIBODIES

Lots 1–6 and 11–16 represent independent fermentation and purification preparations of IgM-1 and IgM-2, respectively. For HPLC conditions, see Experimental.

| Fermentation lot | Mass composition W_G/W_P | R.S.D. (%) | <i>n</i> |
|------------------|----------------------------|------------|----------|
| <i>IgM-1</i> | | | |
| 1 | 0.28 | 11 | 3 |
| 2 | 0.27 | 6 | 3 |
| 3 | 0.28 | 2 | 4 |
| 4 | 0.26 | 4 | 6 |
| 5 | 0.26 | 0 | 3 |
| 6 | 0.26 | 2 | 3 |
| Average | 0.26 | 4 | — |
| <i>IgM-2</i> | | | |
| 11 | 0.10 | 10 | 3 |
| 12 | 0.12 | 13 | 4 |
| 13 | 0.11 | 5 | 3 |
| 14 | 0.10 | 6 | 3 |
| 15 | 0.10 | 6 | 3 |
| 16 | 0.13 | 4 | 3 |
| Average | 0.11 | 7 | — |
| <i>Human IgM</i> | 0.33 | — | — |

CONCLUSIONS

The UV-RI SEC mass composition method for characterizing glycoproteins has been validated for accuracy with ribonuclease and fetuin, two highly studied glycoproteins. The primary utility of this method is to identify substantial changes in the carbohydrate moiety of various glycoprotein preparations. The precision of the method is reasonable, but complications in accuracy may arise in the protein calibration when using the deglycosylated protein moiety. In addition, inaccuracies in the glycoprotein extinction coefficient will cause ambiguity as to the absolute value of carbohydrate mass composition. An asset to this method is its simplicity; requiring only the addition of an RI detector to the usual SEC system. It is not meant to replace monosaccharide analysis, oligosaccharide mapping or mass spectral identification of glycopeptides. However, it will be a useful analysis to complement the sizing information generated on SEC.

ACKNOWLEDGEMENTS

We wish to thank Ira Krull for his suggestions, which initiated work on this application, Gavin Dollinger for helpful discussions and R. Townsend for the fetuin samples and analysis.

REFERENCES

- 1 C. F. Goochee, M. J. Gramer, D. C. Andersen, J. B. Bahr and J. R. Rasmussen, *Bio/Technology*, 9 (1991) 1347.
- 2 R. B. Parekh, R. A. Dwek, J. R. Thomas, G. Opdenakker, T. W. Rademacher, A. J. Wittwer, S. C. Howard, R. Nelson, N. R. Siegel, M. G. Jennings, N. K. Harakas and J. Feder, *Biochemistry*, 28 (1989) 7644.
- 3 S. S. Gauny, J. Andya, J. Thomson, J. D. Young and J. L. Winkelhake, *Hum. Antibod. Hybridomas*, 2 (1991) 33.
- 4 M. Takeuchi, S. Takasaki, M. Shimada and A. Kobata, *J. Biol. Chem.*, 265 (1990) 12127.
- 5 R. R. Townsend, in L. Ettre and Cs. Horváth (Editors), *HPLC of Glycoconjugates and Preparative/Process Chromatography of Biopolymers*, American Chemical Society, Washington, DC, in press.
- 6 M. Kunitani, G. Dollinger, D. Johnson and L. Kresin, *J. Chromatogr.*, 588 (1991) 125.
- 7 R. R. Townsend, personal communication.
- 8 T. A. Bewley, *Anal. Biochem.*, 123 (1982) 55.
- 9 C. M. Harris and R. L. Hill, *J. Biol. Chem.*, 244 (1969) 2195.
- 10 T. Arakawa, T. Boone, J. M. Davis and W. C. Kenny, *Biochemistry*, 25 (1986) 8274.
- 11 J. Baynes and F. Wold, *J. Biol. Chem.*, 251 (1976) 6016.
- 12 C. Tanford, *Physical Chemistry of Macromolecules*, New York, 1961, p. 116.
- 13 F. Stolle, *Z. Ver. Dtsch. Zucker Ind.*, 51 (1901) 469.
- 14 L. Tolman and W. Smith, *J. Am. Chem. Soc.*, 28 (1906) 1476.
- 15 P. Kratochvíl, *Classical Light Scattering from Polymer Solutions*, Elsevier, Amsterdam, 1987, p. 314.
- 16 T. Plummer and C. Hirs, *J. Biol. Chem.*, 239 (1964) 2530.
- 17 R. G. Spiro, *J. Biol. Chem.*, 237 (1962) 382.
- 18 R. R. Townsend, M. R. Hardy, T. C. Wong and Y. C. Lee, *Biochemistry*, 25 (1986) 5725.
- 19 R. R. Townsend, M. R. Hardy, D. Cumming, J. P. Carver and B. Bendiak, *Anal. Biochem.*, 182 (1989) 1.

Conformational changes of brain-derived neurotrophic factor during reversed-phase high-performance liquid chromatography

Robert Rosenfeld and Kálmán Benedek

AMGEN, Inc., Amgen Center, Thousand Oaks, CA 91320-1789 (USA)

ABSTRACT

Recombinant human brain-derived neurotrophic factor (r-HuBDNF) is eluted as two peaks under reversed-phase liquid chromatographic conditions with gradient elution. Sodium dodecyl sulfate polyacrylamide gel electrophoresis confirmed identical molecular weights in the two peaks, while rechromatography of the separated peaks showed interconvertibility. The two peaks are identified as the monomeric forms of the parent molecules. The molecular weight of the components in the peaks was determined by on-line 90° light scattering using a fluorescence detector as a scatterograph. The early eluted peak is a folded form of the r-HuBDNF monomer, while the later eluted peak is an unfolded form of the BDNF monomer. The conformational states were established using a fluorescence detector both at a fixed wavelength and in the scanning mode.

INTRODUCTION

The discovery of a diffusible factor(s) responsible for the survival and enhanced growth of sympathetic sensory ganglia was demonstrated in the early 1950s [1]. The first discovered protein in this family to be purified and sequenced was nerve growth factor (NGF) [2].

Brain-derived neurotrophic factor (BDNF), the second member in the NGF family to be discovered, is a protein containing 119 amino acids. It has a molecular weight of 13.5 kD and a pI of 10.3 [3–5]. This molecule is 55% homologous to NGF. Both NGF and BDNF support the survival of distinct neuronal populations *in vivo*. NGF supports sympathetic and sensory neurons in the peripheral nervous system as well as cholinergic neurons in the basal forebrain [6,7]. BDNF also supports sensory neurons from embryonic peripheral sensory ganglia *in*

vitro, just like NGF, but has activities on neurons that are unresponsive to NGF, such as neurons originating from the neural crest, ectodermal placoid and retinal ganglion [8].

A third member of the NGF family, neurotrophin-3 (NT-3), was discovered utilizing primer sequences constructed from conserved regions of BDNF and NGF by means of polymerase chain reaction (PCR) techniques [9,10]. NT-3 is 58% homologous with BDNF and 57% homologous with NGF. Recently, a fourth member of this family has been identified and named neurotrophin-4 (NT-4) [11]. With the help of genetic engineering techniques some of these factors are now cloned, expressed, and purified in sufficient quantities for their analytical and biochemical characterization as well as their potential pharmaceutical application.

In this study r-HuBDNF, derived from Chinese Hamster Ovary cells (CHO) was examined. r-HuBDNF shows one band by sodium dodecyl sulfate polyacrylamide gel electrophoresis (SDS-PAGE) analysis and one peak in size-exclusion and ion-exchange chromatography. The same sample exhib-

Correspondence to: Dr. K. Benedek, AMGEN, Inc., Amgen Center, Thousand Oaks, CA 91320-1789, USA.

ited two peaks in reversed-phase high-performance liquid chromatographic (RP-HPLC) analyses. The peaks were of identical molecular weight when analyzed by SDS-PAGE. The early eluted peak converts into later eluted peak as shallower gradients were applied. Similar chromatographic behavior has been reported before and was attributed to conformational changes induced by RP-HPLC conditions [12–14]. This publication describes an experimental pathway for peak identification and describes the relationship between the observed peaks.

EXPERIMENTAL

Materials and methods

r-HuBDNF expressed in CHO cells was purified as described previously [15]. Ribonuclease (RNase), lysozyme (LYS), ovalbumin (OVA) and bovine serum albumin (BSA) were from Sigma (St. Louis, MO, USA). HPLC solvents were purchased from Fisher. Two different VYDAC Protein C4 reversed-phase columns (Separation Groups, Hesperia, CA, USA) were used in this work. The column parameters will be specified in the figure captions.

HPLC instrumentation and conditions

The basic HPLC system consisted of a gradient pump, UV detector, integrator and data station (Spectra Physics, San Jose, CA, USA). The temperature control of chromatography was provided by immersing the column in a thermostated water bath (Neslab Instruments). The temperature was kept at 25°C in all experiments reported here. In general a 1 ml/min flow-rate has been used, unless it is stated otherwise. The mobile phase system used is as follows: mobile phase A, 0.1% trifluoroacetic acid (TFA)–distilled water (0.1:99.9); mobile phase B, TFA–acetonitrile (0.1:99.9) or TFA–acetonitrile–water (0.1:90:9.9). The descriptions of the gradients are provided in the text.

Fluorescence detection

Two Shimadzu fluorescence detectors were used, a Model RF-551 scanning fluorescence monitor for the on-line scanning experiments and a Model RF-535 fluorescence detector for the light scattering experiments.

In the scanning mode the fluorescence emission spectra between 300 and 400 nm were collected at

the apex of the peaks at an excitation wavelength of 276 nm. A Shimadzu RF-551 fluorescence detector was used to follow the fluorescence trace of the r-HuBDNF elution. The excitation wavelength was 276 nm and the emission wavelength was 385 nm.

Light scattering

The 90° light scattering was measured using a Shimadzu RF-535 fluorescence detector according to the method of Dollinger *et al.* [16]. In essence, the method is based on the fact that selecting a wavelength where no excitation and emission of the sample or buffer can be observed, a fluorescence detector can be used as a 90° scatterometer. Using calibration curves obtained with standard proteins the molecular weight of proteins can be calculated from on line data collection. In this study the excitation and emission wavelength was 465 nm. The elution of proteins was followed by a UV detector at 280 nm and by a scatterometer. The peak areas from both signals were integrated. The molecular weight calculations using the corresponding peak areas and were performed according to Dollinger *et al.* [16]. The extinction coefficients of the standard proteins were obtained from the literature [16], and for r-HuBDNF a value of 1.7 was applied.

SDS-PAGE analysis

SDS-PAGE analysis of r-HuBDNF was performed according to Laemmli [17] using 10–20% (w/v) acrylamide gel. The visualization of the bands was performed by Coomassie Brilliant Blue staining. Under non-reducing conditions, r-HuBDNF migrates as a monomer with an apparent molecular weight of 14.3 kD. Under reduced conditions, the mobility of the r-HuBDNF is slightly decreased, an observation which is characteristic with intramolecular disulphide bonds.

RESULTS AND DISCUSSION

After the purification of r-HuBDNF it was observed that an electrophoretically homogeneous protein sample eluted in two peaks under reversed-phase chromatographic conditions. Fig. 1 displays the reversed-phase chromatographic separation of an r-HuBDNF sample using gradient elution. The chromatogram contains two peaks, which are labeled peak I and peak II.

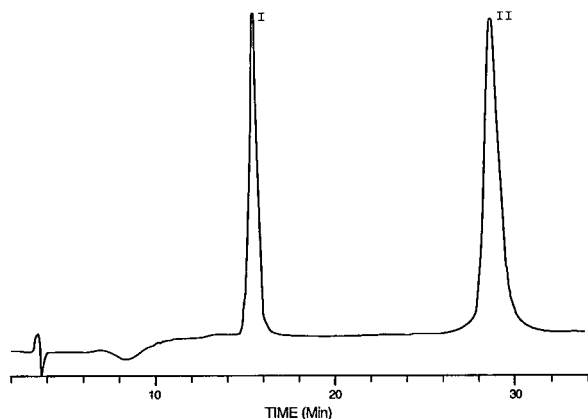


Fig. 1. Reversed-phase chromatographic analysis of r-HuBDNF. Chromatographic conditions: column, 25 cm \times 4.6 mm I.D. Vydac Protein C4; mobile phases, A: 0.1% TFA–water (0.1:99.9), B: TFA–acetonitrile–water (0.1:90:9.9); gradient, 20–27% B solvent in 7 min, 10 min hold at 27% B, 27–33% B in 24 min, 3 min hold at 34% B; detection, 214 nm; temperature, 25°C.

Off-line peak characterization

The resolved peaks were collected and SDS-PAGE of reduced and non-reduced samples revealed that the molecular weights of the proteins in peaks I and II were identical to each other and to the r-HuBDNF standard, confirming that the peaks were r-HuBDNF. Amino terminal sequence analysis showed the first 15 residues to be identical in both peaks (data not shown).

The biological activity of r-HuBDNF from the peaks (I, II) was also measured and the two peaks were equally active. The activity measurement is a biological assay in which the survival of neurons from chick dorsal root ganglia are measured after a 24-h period.

The isolated peaks were rechromatographed and analyzed under the original reversed-phase conditions. Fig. 2A shows the chromatogram of the r-HuBDNF standard. Fig. 2B is the rechromatography of peak I displaying two peaks with retention times matching the original peaks I and II. The rechromatography of peak II, shown in Fig. 2C gave two peaks with retention times matching the original peak I and II. These experiments illustrate that peak I converts into peak II and some portion of peak II converts into peak I. The fact that the peak I/II ratio is significantly smaller than in the original sample indicates that the refolding of peak II in the

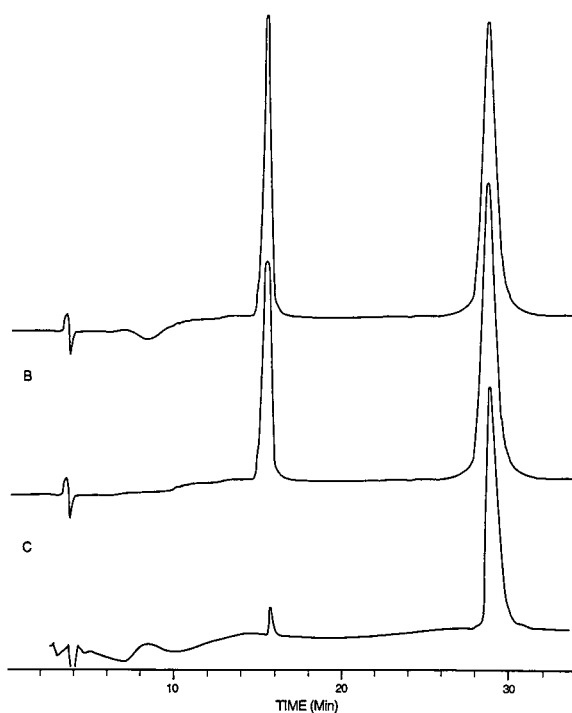


Fig. 2. Reinjection experiments. Peaks I and II were collected and analyzed with the same elution method. (A) Chromatogram of r-HuBDNF, (B) peak I, (C) peak II. Chromatographic conditions: see Fig. 1.

collection media (TFA–acetonitrile–water) is a slow process, and possibly the equilibrium distribution of the folded and unfolded species is also different as compared to the neutral condition. Nevertheless the appearance of peak I in the chromatogram of peak II is indicative of a reversible conversion mechanism. It has to be mentioned, that protein recovery was always above 95%, based on peak area analysis and the experiments were reproducible.

Because the reversibility of the peaks could be an important factor in explaining their nature, other collection conditions for peak II were explored. Peak II was collected, lyophilized, reconstituted in PBS and then analyzed by RP-HPLC. The chromatograms of the lyophilized peak showed peak I and a second peak with retention times corresponding to peak II. The reversibility hypothesis was further strengthened by an experiment where peak II was collected in PBS, followed by RP-HPLC analysis. Again two peaks appeared in the chromatogram.

Since the peak I/II ratio in all of these refolding experiments was identical, it can be assumed that the conformational state after refolding in PBS is identical or very similar to the original conformation.

Since the amino acid sequence of peak I and peak II is the same, and the biological activity equal in both peaks, we focused our attention on the biophysical characterization of peaks I and II.

Peak conversion

Gradient optimization experiments also revealed that the peak I to peak II ratio decreased with shallower gradients. This observation suggested that the more time r-HuBDNF molecule spent on the reversed-phase column the greater the conversion of peak I to peak II.

The importance of the on-column residence time of r-HuBDNF was substantiated by injecting the sample into the reversed-phase column and washing for 60 min with the starting mobile phase prior to gradient elution. The result of this extended on-column incubation is shown in Fig. 3B, which demonstrated that peak I had almost completely disappeared. This experiment was repeated several times, with incubation times ranging from 0 to 20 min and identical elution gradients. Plotting the logarithm of

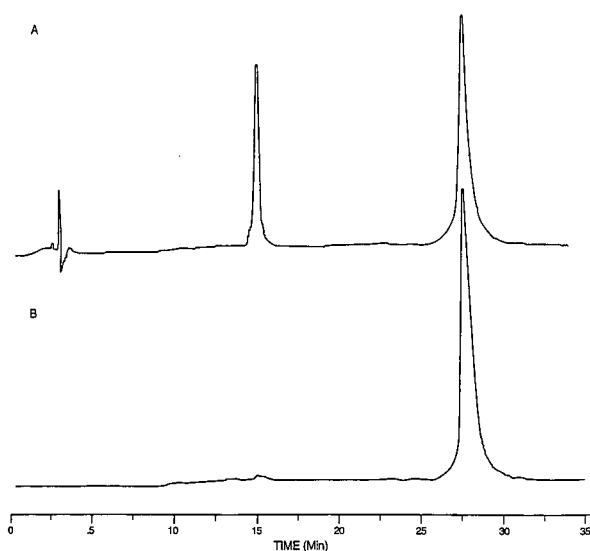


Fig. 3. On-column incubation of r-HuBDNF. The injected sample was incubated for 0 (A) and 60 min (B) on the reversed-phase column prior elution. Chromatographic conditions: see Fig. 1.

the area of peak I as a function of incubation time, shown in Fig. 4, we established that the peak disappearance fits to a first-order kinetic model [18]. The rate constant of conversion at room temperature was calculated as $2.13 \cdot 10^{-3} \text{ s}^{-1}$, which corresponds to a 5.4-min half-life.

Based on the above described experimental results it was established, that (a) peaks I and II represent r-HuBDNF; (b) peak I can be converted into peak II, by varying the RP-HPLC parameters; (c) under appropriate conditions the conversion is reversible.

Peaks I and II showed the same monomeric

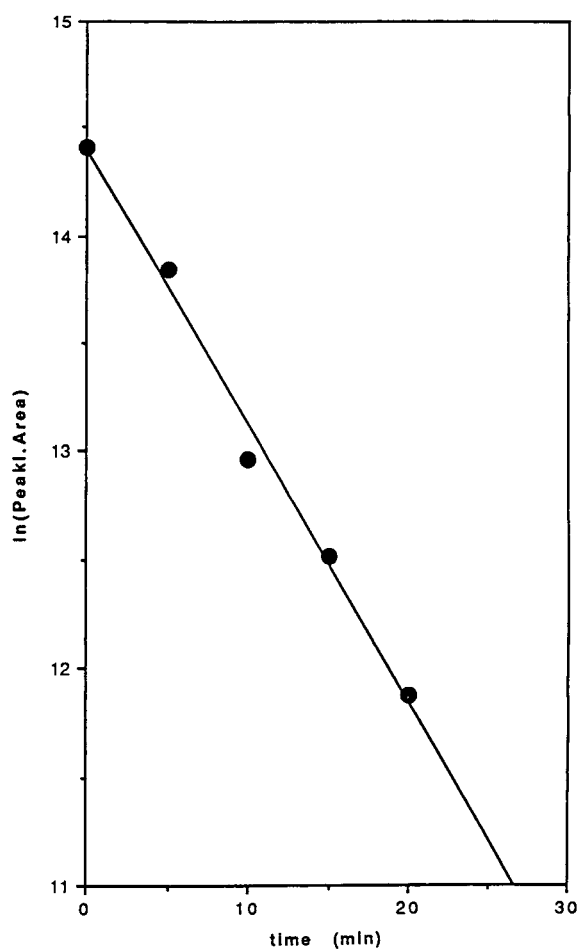


Fig. 4. r-HuBDNF peak conversion kinetics. r-HuBDNF samples were injected onto a reversed-phase column and incubated for 0, 5, 10, 15 and 20 min at constant temperature (25°C) prior elution. $y = 14.400 - 0.12805x$; $R^2 = 0.992$.

molecular weight under reducing and non-reducing SDS-PAGE. It is known that r-HuBDNF exists as a non disulphide linked dimer in PBS, as shown by size exclusion chromatography and sedimentation equilibrium [19], and has been reported for NGF [2]. The question remains whether peaks I and II, observed under RP-HPLC conditions represent a dimer and monomer distribution or both peaks are in the same dimeric or monomeric form. Because of the reversibility and short time scale of conversion the utilization of off-line methods was excluded and instead we employed on-line analytical techniques suitable for detecting size and conformational changes of proteins.

On-line peak characterization by light scattering

An on-line light scattering method, developed by Dollinger *et al.* was selected for characterizing the molecular weight of r-HuBDNF in peak I and II [16]. This novel method based on the Takagi approach [20] but utilizes a fluorescence detector as a 90° scatterometer and a UV detector for concentration determination. The detector signals were calibrated against well defined protein standards such as RNase, LYS, OVA, and BSA. The molecular weight is proportional to the two signals as follows:

$$M_w = \frac{I_s \varepsilon}{k A}$$

where k is an empirical constant, I_s and A are the light scattering and ultraviolet signals, respectively, and ε is the extinction coefficient at the UV absorption wavelength. Using standard proteins with known molecular weight (M_w^k) the molecular weight (M_w^u) of unknown proteins can be calculated according to the following equation:

$$M_w^u = M_w^k \frac{I_s^u A^k \varepsilon^u}{I_s^k A^u \varepsilon^k}$$

Fig. 5 displays the UV trace (A) and the scatterogram (B) of r-HuBDNF under reversed-phase elution conditions. In both chromatograms the ratio of peak I to peak II is similar and close to one, implying that the molecules constituting both peaks have very similar mass. The results of the calculations using 4 different standard proteins are listed in Table I. The calculated average molecular weights for peak I and peak II are 14.8 kD and 12.4 kD, respectively. These

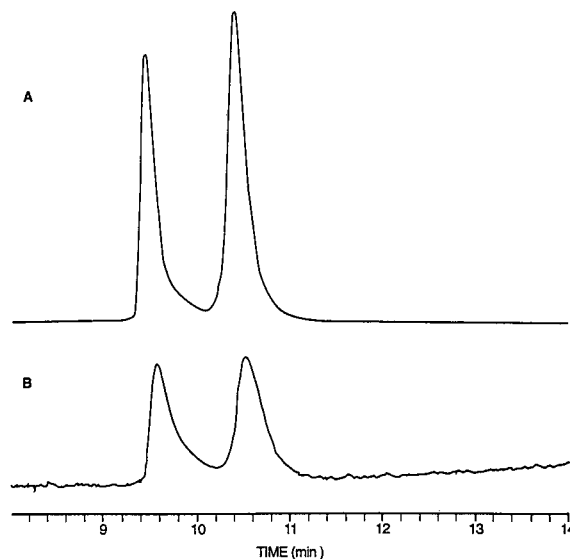


Fig. 5. Molecular weight determination of r-HuBDNF using 90° light scattering. (A) UV; (B) scatterogram. Column, 15 cm × 4.6 mm I.D. Vydac Protein C4; mobile phases, A: TFA–water (0.1:99.9), B: TFA–acetonitrile–water (0.1:90:9.9); gradient, 5–45% B solvent in 30 min; UV detection, 280 nm; light scattering detection, 465 nm; temperature, 25°C.

values are consistent with the monomeric molecular mass of 13.5 kD calculated from the amino acid composition of r-HuBDNF.

These light scattering results eliminated the existence of dimers and the dimer-monomer transition model, consequently we focused our attention on further characterizing the peaks. In previous cases involving a two peak phenomena the early eluting

TABLE I
MOLECULAR WEIGHT CALCULATIONS OF BDNF
USING STANDARD PROTEINS

| Standard proteins | BDNF I | BDNF II |
|---------------------------------|--------|---------|
| LYS | 16 118 | 13 534 |
| RNase | 12 595 | 10 576 |
| OVA | 16 433 | 13 799 |
| BSA | 14 153 | 11 884 |
| Average | 14 825 | 12 448 |
| Standard deviation ^a | 1796 | 1508 |

^a $n = 4$.

peak corresponded to a native and/or a more folded conformation while the late eluting peak represented a denatured and/or a more unfolded conformation of the protein [13]. The conformational state of these molecules was studied by on-line and/or off-line analytical techniques [13,21,22].

Since r-HuBDNF interconverts at neutral pH, the activity cannot be determined on the time scale of chromatography and it cannot be used for determining whether the peaks correspond to the native and/or a more folded conformation or a denatured and/or a more unfolded conformation of the protein. In order to determine the conformational state peak I and II, we used on-line fluorescence spectroscopy at both fixed wavelengths and in the scanning mode.

On-line fluorescence spectroscopic peak analysis

Fluorescence of the eluents was monitored by setting the excitation wavelength at 276 nm and the emission wavelength to 385 nm. Fig. 6 displays the chromatogram of r-HuBDNF by RP-HPLC as monitored by UV (A) and fluorescence detection

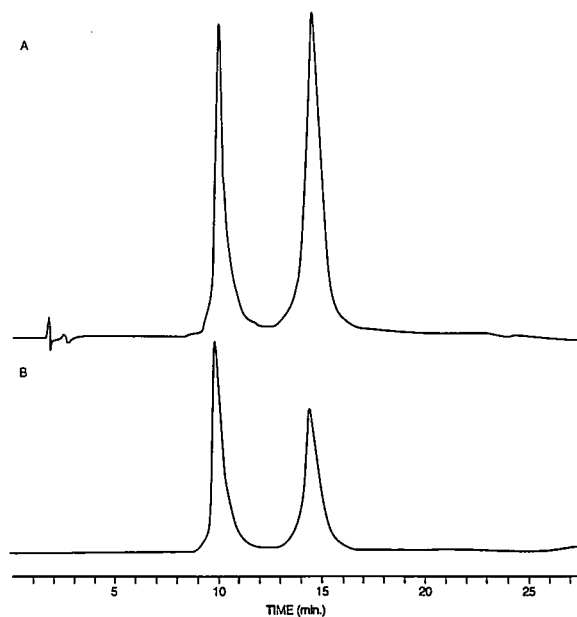


Fig. 6. Analysis of the conformational states of r-HuBDNF during RP-HPLC. (A) UV; (B) fluorescence (excitation wavelength 276 nm; emission wavelength 385 nm). Chromatographic conditions: see Fig. 5.

(B). It is apparent that the ratio of the two peaks (I/II) is about unity on the UV trace (A) while on the fluorescence trace (B) this ratio is much larger than one. This indicates that the fluorescence intensity is lower for the second peak than for the first peak. Decreased fluorescent intensity can occur when (a) the emission spectrum is altered, or (b) by solvent quenching. In order to answer the question, we utilized the detector's on-line spectrum acquisition capability and we took the fluorescence spectra at the apex of both peaks. The collected fluorescence spectra using 280 nm excitation revealed an about 10 nm red-shifted emission maximum for peak II, suggesting that this form is more unfolded than peak I. Similar fluorescence spectral shift was observed in acid induced denaturation of BDNF [23].

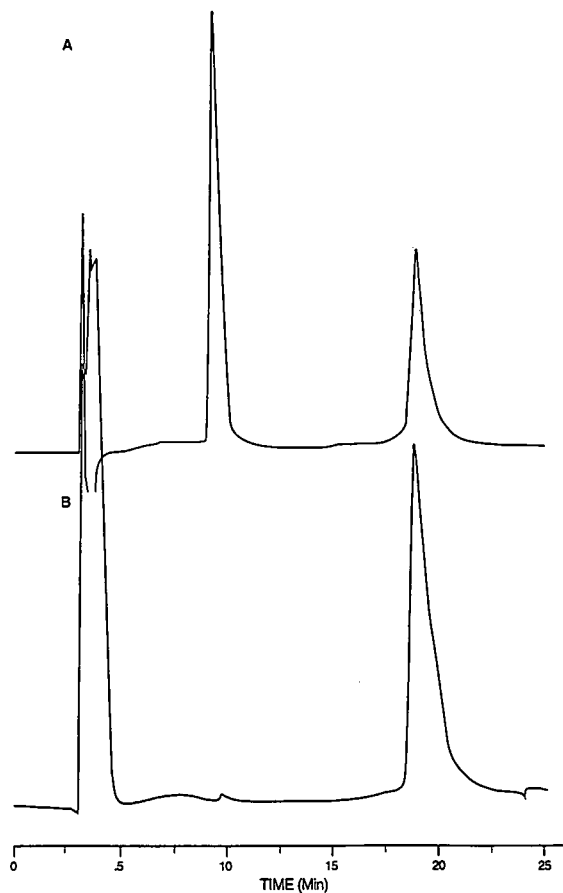


Fig. 7. Chromatogram of guanidine · HCl-denatured r-HuBDNF. (A) Standard r-HuBDNF; (B) guanidine · HCl-treated r-HuBDNF. Chromatographic conditions: see Fig. 1.

Such a red shift is indicative of a greater exposure of a tryptophan residue(s) to an aqueous environment, such as might occur by unfolding of the polypeptide chain. The fluorescence spectroscopic results are consistent with the hypothesis, that peak I represents a less unfolded and peak II a more unfolded BDNF structure.

Effect of guanidine · HCl on the BDNF peaks

Proteins incubated with guanidine · HCl most often lose all of their tertiary and secondary structure. As a further test of the nature of the peaks, we incubated an aliquot of peak II, which was collected and refolded in PBS, in 6 M guanidine · HCl, and then analyzed the sample with RP-HPLC. Fig. 7 displays the chromatograms of BDNF before (A) and after (B) guanidine · HCl treatment. After guanidine · HCl treatment, peak I disappeared from the chromatogram and only peak II was apparent. Collection of peak II, dialysis, lyophilization and resuspension in PBS, followed by a RP-HPLC analysis provided us with a chromatogram similar to our standard BDNF. This experiment confirms two observations: (a) that peak II must represent the denatured structure of r-HuBDNF; and (b) that the denaturation is reversible.

It is important to note that the guanidine · HCl-denatured species elute with the same retention time as the RP-HPLC denatured species, indicating that the final unfolded conformations attained by RP-HPLC alone or guanidine · HCl treatment followed by RP-HPLC are chromatographically identical.

CONCLUSIONS

The two peaks observed in the chromatogram are both the monomeric forms of the r-HuBDNF molecule. The first peak represents a folded form and the second later eluting peak is an unfolded form of the r-HuBDNF monomer. The first peak can be converted into the second by increasing the time the molecule spends on the column. Similar conversion was observed by increasing the temperature of chromatography [24].

In light of the various spectroscopic and biochemical evidences acquired during our work we can establish that the chromatographic behavior of r-HuBDNF under reversed-phase gradient elution can be traced to a conformational change occurring

in the molecule as a result of the chromatographic conditions. Similar chromatographic behavior has been observed previously with other proteins [12,13, 21]. Our observations are in agreement with those examples and serves as another case where the denatured forms of a protein under RP-HPLC conditions elute later than the native and/or folded structures.

r-HuBDNF exists as a dimer at physiological conditions, but under reversed-phase conditions only the monomeric form is present. These results indicate that the chromatographic process has two steps. In step one, the dimer breaks up as the molecule encounters the stationary phase. The dissociation happens rapidly, under RP-HPLC conditions. In step two, the unfolding of the molecule occurs. This second step has a half life, which is comparable with the time scale of chromatography allowing the visualization of both the folded and the unfolded conformers. A detailed analysis of the kinetics and thermodynamics of the observed conversion mechanism will be reported later [24].

ACKNOWLEDGEMENTS

Special thanks to G. Dollinger and R. Jones in helping to establish the 90°C light scattering method, to M. Haniu, C. Acklin, K. Stoney for peptide mapping and mass spectroscopy and to D. Patel for the activity assays, to T. Arakawa, L. Nahri for the BDNF solution denaturation data. Thanks are due to W. Kenney, J. Miller, E. Watson and T. Arakawa for helpful suggestions and review of the manuscript. The two fluorescence detectors were lent by Cole Scientific, Inc.

REFERENCES

- 1 R. Levi-Montalcini, *Ann. NY Acad. Sci.*, 55 (1952) 330.
- 2 R. H. Angeletti and R. A. Bradshaw, *Proc. Natl. Acad. Sci. USA*, 68 (1971) 2417.
- 3 Y.-A. Barde, *Neuron*, 2 (1989) 1525.
- 4 M. M. Hofer and Y.-A. Barde, *Nature (London)*, 331 (1988) 261.
- 5 J. Leibrock, F. Lottspeich, A. Hohn, M. Hofer, B. Hengerer, P. Masiakowski, H. Thoenen and Y.-A. Barde, *Nature (London)*, 341 (1989) 149.
- 6 H. Thoenen and Y.-A. Barde, *Physiol. Rev.*, 60 (1980) 1284.
- 7 H. Thoenen, C. Bandtlow and R. Heuman, *Rev. Physiol. Biochem. Pharmacol.*, 109 (1987) 145.
- 8 R. M. Lindsay, H. Thoenen and Y.-A. Barde, *Develop. Biol.*, 112 (1985) 319.

- 9 A. Hohn, J. Leibrock, K. Bailey and Y.-A. Barde, *Nature (London)*, 344 (1990) 339.
- 10 P. C. Maisonpierre, L. Belluscio, S. P. Squinto, H. Y. Ip, M. E. Furth, R. M. Lindsay and G. D. Yancopoulos, *Science (Washington, D.C.)*, 247 (1990) 1446.
- 11 F. Halböök, C. F. Ibañez and H. Persson, *Neuron*, 6 (1991) 845.
- 12 S. A. Cohen, S. Dong, K. Benedek and B. L. Karger, in I. M. Chaiken, M. Wilchek and I. Parikh (Editors), *Proceedings of the Fifth International Symposium on Affinity Chromatography and Biological Recognition*, Academic Press, New York, 1983, p. 479.
- 13 S. A. Cohen, K. P. Benedek, S. Dong, Y. Tapuhi and B. L. Karger, *Anal. Chem.*, 56 (1984) 217.
- 14 E. Watson and W. C. Kenney, *J. Chromatogr.*, 606 (1992) 165.
- 15 C. Acklin, K. Stoncy, R. Rosenfeld, J. M. Miller and M. Haniu. *Anal. Biochem.*, (1992) in press.
- 16 G. Dollinger, B. Cunico, M. Kunitani, D. Johnson and R. J. Jones, *J. Chromatogr.*, 592 (1992) 215.
- 17 U. K. Laemmli, *Nature (London)*, 227 (1970) 680.
- 18 K. Benedek, S. Dong and B. L. Karger, *J. Chromatogr.*, 317 (1984) 227.
- 19 R. Rosenfeld, G.-M. Wu and K. Benedek, unpublished results.
- 20 T. Takagi, *J. Chromatogr.*, 506 (1990) 409.
- 21 S.-L. Wu, K. Benedek and B. L. Karger, *J. Chromatogr.*, 359 (1986) 3.
- 22 P. Oroszlán, R. Blanco, X.-M. Lu, D. Yarmush and B. L. Karger, *J. Chromatogr.*, 500 (1990) 481.
- 23 L. Nahri, R. Rosenfeld, T. Arakawa and K. Benedek, in preparation.
- 24 K. Benedek, *J. Chromatogr.*, submitted for publication.

Immuno chromatographic analysis of proteins

Identification, characterization and purity determination

Alice Riggin and J. Richard Sportsman

Lilly Research Laboratories, Lilly Corporate Center, Indianapolis, IN 46285 (USA)

Fred E. Regnier

Department of Chemistry, Purdue University, West Lafayette, IN 47907 (USA)

ABSTRACT

Antibodies specific to a protein and its structural variants were immobilized on a high-performance Protein G column. This column recognized and selectively subtracted specific molecules from a sample. When a size-exclusion column was coupled with this high-performance affinity column, a comparison between the elution profile before and after the antibody immobilization was used to study antigen components present in the sample. Various human growth hormone structural variants and aggregates were studied using this approach. The technique is simple, fast and does not involve the usage of radioactive material.

INTRODUCTION

Immunoaffinity chromatography has been used widely both in the purification of macromolecules [1–3] and as an analytical tool for studying molecular interactions and protein structure [4–6]. Affinity chromatographic (AC) determinations of equilibrium and rate constants of solute–ligand interactants [8–10] through both frontal and zonal elution are some examples of analytical applications of the technique. Other examples are quantitative analysis of specific proteins [11–14] and the estimation of reaction rate constants [15,16].

Unfortunately, most proteins are so strongly retained by an immunoaffinity column that they must be denatured to effect their elution. Under these severe elution conditions, antibodies can lose specific-

ity and many proteins are irreversibly denatured. This paper introduces the approach of monitoring antigen components that are *not* retained by the affinity column. When antibodies specific to a protein and its structural variants are immobilized on an affinity column, this affinity column should recognize and selectively subtract specific molecules from the sample. Comparing the elution profiles before and after the antibody immobilization through a subtraction process may reveal antigen components present in the sample. Quantification of these components is achieved by measuring differences in peak areas.

Because of its great flexibility and ease of use, a short protein G column (30 × 2.1 mm I.D.) was used to immobilize antibodies. Affinity columns were prepared by immobilizing specific antibodies onto the protein G column as reported previously [13]. Although a size-exclusion column was used as the separation column in these studies, reversed-phase or ion-exchange columns can also be used.

Correspondence to: Dr. A. Riggin, Lilly Research Laboratories, Lilly Corporate Center, Indianapolis, IN 46285, USA.

The experiments reported in this paper were performed with a tandem column system consisting of an immunosorbent column directed against human growth hormone (hGH) and a size-exclusion column.

EXPERIMENTAL

Materials

Antibodies. Monoclonal antibodies to hGH (GHC101 and GHC072) were the same material described previously [12]. Rabbit antiserum to hGH (lot No. 184-15) was prepared by immunization techniques as previously described [17]. The serum was taken ten days after the third monthly booster injection.

Growth hormone and derivatives. Monomeric hGH (somatotropin, 22.1 kilodalton) of recombinant DNA origin was obtained from Lilly Research Labs. (Indianapolis, IN USA) and determined to be greater than 99% pure by size-exclusion chromatography (SEC) at Lilly [18]. The purity determined by reversed-phased HPLC was greater than 95%. Non-covalent hGH dimer was recovered from a pool of high-molecular-mass materials generated during the production of hGH and purified by SEC [19]. N-Terminal methionyl hGH (met-hGH) was prepared as described previously [20]. Methionyl-14 sulfoxide hGH was obtained by treating hGH with 3% hydrogen peroxide [21]. Desamido hGH, with the major deamination site at Asn-149 and the minor site at Asn-152, was produced by storage of hGH in ammonium bicarbonate (pH 9) for 72 h at 37°C [22]. An N-terminal methionyl, hGH variant,

molecular mass 20 kilodalton (20K met-hGH) was prepared by rDNA methods. Except for the N-terminal methionine residue, this material is identical to the natural 20 kilodalton hGH variant in which the 32–45 peptide fragment is omitted and the 1–31 segment is connected directly to the 46–191 segment. All the hGH derivatives described above were obtained from Lilly Research Labs.

Synthetic peptides. Homologous peptides of hGH, synthesized on a Beckman Model 990B automated synthesizer according to the Merrifield solid-phase method [23], were obtained from Lilly Research Labs. Peptide identities were confirmed by N-terminal sequence and total amino acid analysis. These peptides are 15 to 28 residues in length and are numbered according to the primary sequence of hGH. They are referred to as peptide 1–28, peptide 25–45, peptide 126–151, and peptide 171–191.

Other materials. Bovine serum albumin (BSA), Blue Dextran 2000, ferritin, aldolase, ovalbumin, chymotrypsinogen A and ribonuclease A are from the gel filtration calibration kits for protein molecular mass determination supplied by Pharmacia (Piscataway, NJ, USA). All other chemicals were analytical-reagent grade unless otherwise indicated. Reagent water was obtained from a Millipore Milli-Q water-purification system.

Apparatus

The chromatographic system used for this experiment is shown in Fig. 1. Valves V-1 and V-2 are two-position, six-port switching valves (Rheodyne, Model 7000, with pneumatic actuator). V-1 was coupled to the system as shown in the diagram so

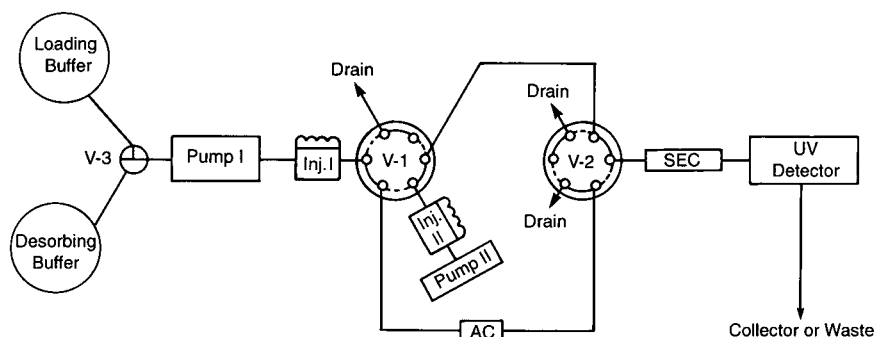


Fig. 1. Apparatus for Protein G AC-SEC tandem column immunochromatographic analysis. See text.

that either pump I or pump II can deliver mobile phase to the protein G affinity column (pore size 500 Å; 30 × 2.1 mm I.D., custom packed by Chromatochem, Missoula, MT, USA). V-2 was installed so that the protein G affinity column and an SEC column could be operated either in "column-tandem" mode (Fig. 1, connection of V-2 ports shown by broken line) or "column-independent" mode (Fig. 1, connection of V-2 ports shown by solid line). Either a GF-250 (DuPont, Zorbax Bioseries, 25 cm × 9.4 mm I.D.) or Ultraspherogel SEC3000 (Beckman, 30 cm × 7.5 mm I.D.) column was used in the SEC separations. Pump I (Beckman, Altex Model 110A) was used for antibody immobilization or regeneration of the protein G column. A simple switching "T" valve was installed at the solvent inlet of the pump to allow rapid switching between loading and desorbing buffers. Two Rheodyne (Model 7125) injection valves, equipped with a 20- μ l sample loop, were used. One was installed between pump I and V-1 for immobilization of antibodies. Another one was installed between pump II and V1 for sample introduction. Pump II (Spectra-Physics, SP8700XR, extended-range LC pump) was used for delivering the mobile phase to achieve the SEC separation.

The column eluate was monitored by a UV detector (Spectra-Physics SP8440XR). The detector output was interfaced with an HP1000 minicomputer where all data were collected, stored and processed using an in-house (Lilly Research Labs.) chromatographic software package.

Immobilization of antibodies onto the Protein G column

To immobilize antibodies onto the protein G column, V-1 was set at the pump I mode, and V-2 was set at the "column independent" mode. Tris-acetate buffer (50 mM, pH 7.4) was used as loading buffer. Antibody solutions were diluted to approximately 10 μ g/ml, and an aliquot of 20 μ l (about 200 μ g antibody) was injected via injector I onto the protein G column at a flow-rate of 0.5 ml/min for 5 min. Then the flow-rate was increased to 2 ml/min for 10 min to elute the unbound materials.

Regeneration of the Protein G column

To regenerate the protein G column, V-1 remained at the pump I mode, V-2 remained at the

"column independent" mode, and the column was eluted with 20% acetic acid at a flow-rate of 3 ml/min for 10 min to desorb any bound immunoglobulin G. Following acid-initiated desorption, the column was equilibrated with Tris-acetate buffer (50 mM, pH 7.4) for 15 min at 2 ml/min.

Protein G AC-SEC tandem column immunochromatographic procedure

The protein G column was regenerated using the procedure described above. Then, V-2 was switched to the "column-tandem" mode and V-1 was switched to allow pump II to deliver mobile phase onto the columns. After equilibrating the columns with Tris-acetate or ammonium hydrogencarbonate-acetate, 50 mM, pH 7.5 \pm 0.1, 20 μ l of sample were injected onto the protein G column via injector II, using a flow-rate of either 1.0 or 0.6 ml/min, depending on the experiment. The column eluent was monitored at 214 nm when ammonium hydrogencarbonate buffer was the mobile phase or at 280 nm when Tris-acetate buffer was the mobile phase. Antibody was then immobilized on the protein G column using the procedure described earlier. During antibody immobilization, the SEC column was equilibrated with appropriate mobile phase using pump II. After antibody was immobilized onto the protein G column, V-2 was again switched to the column-tandem mode and V-1 was switched to allow pump II to deliver mobile phase onto both columns. Another 20- μ l sample was injected onto the immunosorbent column and unretained solutes were eluted through the tandem column system. The chromatograms acquired before and after antibody immobilization were compared, and the difference obtained by subtracting each data point of the second chromatogram from the first were used to plot a difference chromatogram.

Antibody recognition of hGH

In an initial study of hGH recognition by anti-hGH mono- or polyclonal antibodies, samples were chromatographed on a Beckman Ultraspherogel SEC3000 SEC column (30 cm × 7.5 mm I.D.) and eluted with Tris-acetate buffer (50 mM, pH 7.4) at a flow-rate of 1 ml/min. Sample solution A was prepared by dissolving 1 mg each of BSA, hGH and ribonuclease A in mobile phase and adjusting the final volume to 1 ml. Sample solution B was pre-

pared by dissolving 1 mg each of BSA, hGH and chymotrypsinogen A in the mobile phase and adjusting the final volume to 1 ml. Sample solution A was analyzed by the immunochromatographic procedure as described above with 200 μg of immobilized GHC072 monoclonal antibody. Sample solution B was chromatographed on an immunoaffinity column containing approximately 200 μg of immobilized anti-hGH from a rabbit anti-serum (lot No. 184-15).

Binding study of hGH-related compounds

Stock solutions of hGH, met-hGH, desamido hGH, met-14-sulfoxide hGH, 20K met-hGH and hGH dimer were prepared by dissolving 1 mg of each protein in 1 ml Tris-acetate buffer (50 mM, pH 7.4) and stored refrigerated (5°C). Stock solutions of ferritin and cytidine were also prepared by dissolving 1 mg each in 1 ml of the above Tris-acetate buffer and stored in dark at 5°C. The synthetic peptide solutions were used directly.

Sample solutions of hGH, met-hGH, desamido hGH, met-14-sulfoxide hGH and hGH dimer were prepared by mixing 100 μl of each protein stock solution with 200 μl of ferritin and 20 μl of cytidine (used as high- and low-molecular-mass internal standards), and the final volume was adjusted to 1 ml with NH_4HCO_3 (50 mM, pH 7.6). A sample solution of 20K met-hGH was prepared similarly except cytidine was not added. Sample solutions of the peptides were prepared by mixing 20 μl of each stock solution with 20 μl of ferritin solution, and the final volume was adjusted to 100 μl with ammonium hydrogencarbonate buffer.

For the binding study of hGH-related compounds, a GF-250 column was selected for the SEC separation. Ammonium hydrogencarbonate-acetate buffer (50 mM, pH 7.6) was used as the mobile phase at flow-rates of both 0.6 ml/min and 1.0 ml/min.

The binding of hGH to both GHC072 and GHC101 monoclonal antibodies was examined. The immunoaffinity column was prepared by immobilizing 200 μg of either antibody onto the protein G column using the procedure described above.

Binding of hGH monomer and dimer

A test solution containing both hGH monomer and dimer was prepared by mixing 100 μl of both

the hGH monomer and dimer stock solutions with 200 μl of ferritin and 20 μl of the cytidine stock solutions and adjusting the final volume to 1 ml with the ammonium hydrogencarbonate buffer (50 mM, pH 7.6). This test solution was analyzed using the AC-SEC immunochromatographic procedure as previously described. The immunoaffinity column was prepared by the immobilization of approximately 300 μg of GHC072 or GHC101 antibody onto the protein G column.

A sample solution for further investigation of the competition of hGH monomer and dimer for binding to GHC072 antibody was prepared by adding the appropriate amount of hGH monomer and dimer stock solutions to ammonium hydrogencarbonate buffer (50 mM, pH 7.6) to a final concentration of 400 $\mu\text{g}/\text{ml}$ of each component. This mixture was analyzed using the AC-SEC immunochromatographic method at a flow-rate of 1 ml/min and a GHC072 immunoaffinity column with 100 μg of antibody. This experiment was then repeated, with less antigen and a lower flow-rate. The mixture of hGH monomer and dimer solution was diluted 1:2 with the mobile phase so that the final solution contained 200 $\mu\text{g}/\text{ml}$ each of hGH monomer and dimer. The AC-SEC immunochromatographic procedure was repeated with this diluted solution at a mobile phase flow-rate of 0.6 ml/min.

Band-broadening investigation

To investigate the possible band-broadening effect of the protein G column on the SEC separation, a test solution was injected via injector II onto the protein G column. V-2 was then switched to the "column independent" mode and V-1 was switched so that pump II was connected directly to the SEC column instead of the protein G column. Another 20- μl aliquot of the test solution was again injected onto the SEC column. The chromatograms obtained using the SEC column alone and the tandem protein G-SEC column were compared.

A test solution for the GF-250 column was prepared by mixing 100 μl each of the hGH monomer and dimer stock solutions, 200 μl of ferritin, and 20 μl of cytidine stock solutions; the final volume was adjusted to 1 ml with the ammonium hydrogencarbonate (50 mM, pH 7.6) mobile phase. The flow-rate was set at 0.6 ml/min and column eluent was monitored at 214 nm.

A test solution for the Ultraspherogel SEC3000 column was prepared by dissolving 1 mg of ovalbumin and ribonuclease A, 4 mg of aldolase, 0.4 mg of Blue Dextran 2000 and 0.5 mg of cytidine in 1 ml of Tris-acetate (50 mM, pH 7.4) mobile phase. The flow-rate was set at 1 ml/min and column eluent was monitored at 280 nm.

RESULTS AND DISCUSSION

Recognition of hGH by both mono- and polyclonal anti-hGH antibodies is demonstrated in Fig. 2. The hGH peak in Fig. 2A(a) disappeared [Fig. 2A(b)] when 200 μ g of GHC072 anti-hGH monoclonal antibody was immobilized on the protein G column. In contrast, the peak areas of BSA and ribonuclease A were not affected. The difference chromatogram (c) obtained by subtracting each data point of (b) from (a) re-created the hGH peak,

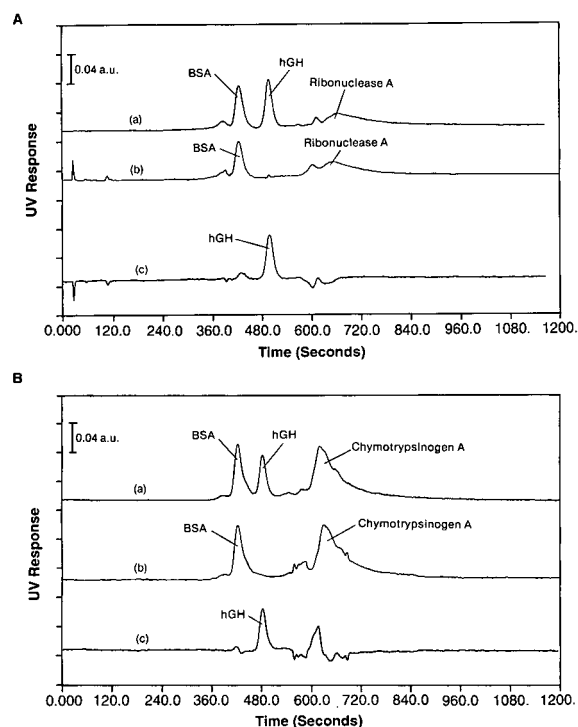


Fig. 2. Recognition of hGH by (A) GHC072 monoclonal antibody and (B) anti-hGH in rabbit anti serum, (a) before and (b) after immobilization of 200 μ g antibodies onto the Protein G column. The difference chromatogram (c) was obtained by subtracting each data point of (b) from (a). Experimental conditions are described in the text.

which was retained by the affinity column. The hGH peak area of (c) was 100.2% that of (a). Similar results are seen in Fig. 2B where the area of the regenerated hGH peak in (c) was 99.6% of that in (a). Fig. 2B also demonstrated that in a sample matrix containing hGH, BSA and chymotrypsinogen A, the anti-hGH in the rabbit anti-serum can selectively bind to hGH and allow non-specific components (BSA and chymotrypsinogen A) to elute unretained, as shown in trace (b). Coelution of antigen with impurities, with the peaks of interest, or a slight shift in retention times between chromatograms (a) and (c) could potentially generate false peaks in the difference chromatogram. Such an artifact peak with a retention time of 600 s is seen in trace (c). However, the hGH peak was correctly regenerated.

Results from a study on reactivity of hGH related compounds with anti-hGH monoclonal antibodies GHC072 and GHC101 are listed in Table I. hGH, met-hGH, desamido hGH, and met-14-sulfoxide hGH all bind to both GHC101 and GHC072 anti hGH monoclonal antibodies with equal affinity, except for 20K met-hGH and hGH dimer. Protein binding to the antibody was indicated by the disappearance of the protein peak in the chromatogram after antibody immobilization on the protein G col-

TABLE I

BINDING OF hGH, HOMOLOGOUS PEPTIDES OF hGH AND hGH DERIVATIVES TO MONOCLONAL ANTIBODIES TESTED BY AC-SEC IMMUNOCHROMATOGRAPHIC ANALYSIS

+ = Antibody binding; - = no significant binding; \pm = partial binding.

| Proteins/peptides | Monoclonal antibodies | |
|----------------------|-----------------------|--------|
| | GHC101 | GHC072 |
| hGH | + | + |
| hGH dimer | + | \pm |
| Desamide hGH | + | + |
| Met-hGH | + | + |
| 20K met-hGH | - | + |
| Met-14-sulfoxide hGH | + | + |
| Peptide 1-28 | - | - |
| 25-45 | - | - |
| 126-131 | - | - |
| 171-191 | - | - |

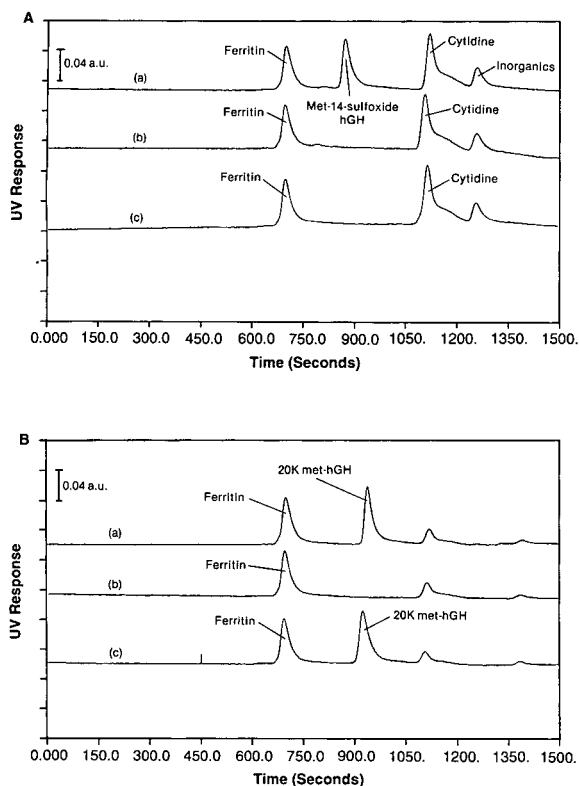


Fig. 3. Antibody binding of (A) met 14-sulfoxide hGH and (B) 20K met-hGH. AC-SEC chromatogram obtained (a) with no antibody immobilization on Protein G column, (b) with 200- μ g of GHC072, (c) with 200- μ g of GHC101 immobilized on the Protein G column. Experimental conditions are described in the text.

umn (Fig. 3A). Ferritin and cytidine were used as high and low molecular weight internal standards. 20K met-hGH binds to GHC072 antibody but does not bind to GHC101, as seen in Fig. 3B. The peak height ratio of 20K met-hGH to ferritin in trace (b) did not show significant change when the mobile phase flow-rate was changed from 1 ml/min to 0.6 ml/min. This indicates that the affinity of binding is sufficiently low that small changes in the flow-rate do not influence the binding of 20K methGH to GHC101. It is likely that the 32-45 peptide fragment that is omitted in this variant is important for the binding of GHC101 antibody. This is not too surprising because the residues 29-41 are thought to be solvent-exposed [24]. This conclusion is consistent with other studies [25-27].

It was found that 2 μ g each of hGH monomer

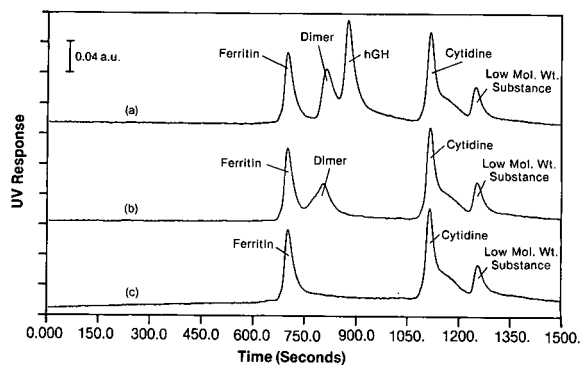


Fig. 4. Binding of 2 μ g each of hGH monomer and dimer to anti-hGH monoclonal antibodies. (a) Without antibody immobilization, (b) with 300 μ g GHC072 immobilized, (c) with 300 μ g GHC101 immobilized. Experimental conditions as described in the text.

and dimer bind very differently to GHC101 and GHC072 on the tandem AC-SEC immunochromatographic system. Fig. 4 demonstrates that both hGH dimer and monomer were retained (trace b) when 300 μ g of GHC101 was immobilized onto the protein G column. However, when 300 μ g of GHC072 was immobilized onto the protein G column, all the hGH monomer and only a portion of the dimer were retained. Trace (c) still exhibits a

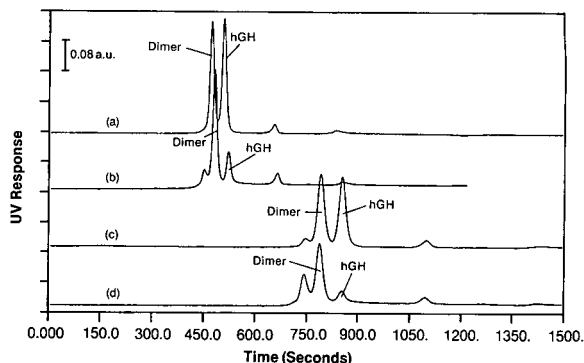


Fig. 5. Binding of hGH monomer and dimer to GHC072 monoclonal antibody. (a), (b): Sample containing 8 μ g each of hGH monomer and dimer, elution flow-rate is 1.0 ml/min; (a) without antibody, (b) with 100 μ g of GHC072 immobilized on Protein G column. (c), (d): Sample containing 4 μ g each of hGH, elution flow-rate is 0.6 ml/min; (c) without antibody, (d) with 200 μ g of GHC072 immobilized on Protein G column. Other experimental conditions as described in the text.

small peak of hGH dimer. Based on these AC–SEC immunochromatographic analysis, hGH dimer binds well to the GHC101 antibody but binds poorly to GHC072.

The relative binding of hGH monomer and dimer was further investigated by chromatographing a sample containing 8 μg each of hGH monomer and dimer on a protein G column with 100 μg of immobilized GHC072. Unbound material was chromatographed on an SEC column operated at a flow-rate of 1 ml/min. As shown in Fig. 5, only a portion of hGH dimer and monomer was retained by the affinity column (trace b). When the amount of hGH dimer and monomer was reduced to 4 μg each and the elution flow-rate was also reduced to 0.6 ml/min, there was still a difference in binding (trace d). Because the lower percentage of binding between GHC072 antibody and hGH dimer does not seem to be influenced by either the amount of antigen or the small change of the flow-rate, it is possible that the hGH dimer has more than one conformation and these conformations may have different affinities for GHC072.

None of the four synthetic peptides (1–28, 25–45, 126–131 or 171–191) tested showed any binding to either GHC072 or GHC101. In view of the fact that amino acids in the 25–45 region of hGH are involved in binding to GHC101, it is surprising that this peptide did not bind to the antibody. It is probable that the epitope for this antibody is either discontinuous or the binding of the antibody to hGH is sensitive to conformation [27].

The possibility of band-broadening introduced by the protein G column was investigated by comparing the chromatograms of the test solutions obtained using the SEC column alone to those obtained using protein G and the SEC column in tandem. Results of the investigation are shown in Fig. 6. As shown, the protein G column used in our experiments does exhibit a slight band-broadening effect but it should not affect the utility of the AC–SEC system. This effect can be further reduced if a shorter protein G column of a smaller diameter is used.

CONCLUSIONS

The objective of this research was to design a simple, fast, and economical approach for the study of

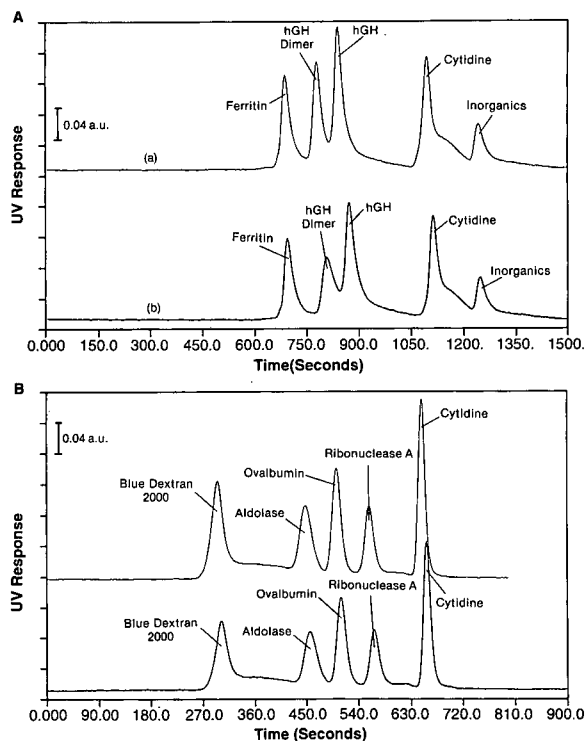


Fig. 6. Slight band-broadening introduced by Protein G column. (A) Protein G–GF250 system, at 0.6 ml/min flow-rate, (B) Protein G–Ulttraspherogel 3000 system, at 1.0 ml/min. (a) SEC column only, (b) Protein G–SEC tandem column.

molecular recognition in affinity chromatography. It is demonstrated in this paper that the tandem AC–SEC immunochromatographic technique can be used to rapidly characterize the interactions between antigen and antibodies. The work presented here also shows that protein G can be used to rapidly prepare an immunosorbent column that will interact specifically with antigens. The AC–SEC immunochromatographic system may be used as a powerful tool to differentiate between cross-reacting variants and the reactivity of antibodies for these variants.

REFERENCES

- 1 S. Josephson, M. Östling, S. Enfors, I. Persson, T. Moks, L. Abrahmsén, B. Österlöf, B. Nilsson and M. Uhlén, *Bio/technology*, 5 (1987) 379.
- 2 V. Planques, H. Pora and F. D. Menozzi, *J. Chromatogr.*, 539 (1991) 531.
- 3 S. Ohlson, L. Hasson, P. Larsson and K. Mosbach, *FEBS Lett.*, 93 (1978) 5.

- 4 D. Eilat and I. M. Chaiken, *Biochemistry*, 18 (1979) 790.
- 5 K. Kasai and Ishii, *J. Biochem.*, 77 (1975) 261.
- 6 I. M. Chaiken, *Anal. Biochem.*, 97 (1979) 1.
- 7 L. W. Nichol, A. G. Ogston, D. J. Winzor and W. H. Sawyer, *J. Biochem.*, 143 (1974) 435.
- 8 I. M. Chaiken, *J. Chromatogr.*, 376 (1986) 11.
- 9 D. J. Winzor, in P. D. G. Dean, W. S. Johnson and F. A. Middle (Editors), *Affinity Chromatography — A Practical Approach*, IRL Press, Washington, DC, 1987, p. 149.
- 10 H. E. Swaisgood and I. M. Chaiken, in I. M. Chaiken (Editor), *Analytical Affinity Chromatography*, CRC Press, Boca Raton, FL, 1987, pp. 65–116.
- 11 A. Riggin, F. E. Regnier and J. R. Sportsman, *Anal. Chem.*, 63 (1991) 468.
- 12 A. Riggin, F. E. Regnier and J. R. Sportsman, *Anal. Chim. Acta.*, 249 (1991) 185.
- 13 L. J. Janis, F. E. Regnier, *Anal. Chem.*, 61 (1989) 1901.
- 14 G. S. Blank and D. Vetterlein, *Anal. Biochem.*, 190 (1990) 317.
- 15 J. R. Sportsman, J. D. Liddl and G. S. Wilson, *Anal. Chem.*, 55 (1983) 771.
- 16 D. S. Hage, R. R. Walters and H. W. Hethcote, *Anal. Chem.*, 58 (1986) 274.
- 17 L. D. Taber, J. Apathy, A. Delong, and J. R. Sportsman, *J. Pharm. Sci.*, 76 (1987) 492.
- 18 R. M. Riggin, C. J. Shaar, G. K. Dorulla, D. S. Lefeber and D. J. Miner, *J. Chromatogr.*, 435 (1988) 307.
- 19 G. W. Becker, R. R. Bowsher, W. C. Mackeller, M. L. Poor, P. M. Tackitt and R. M. Riggin, *Biotechnol. Appl. Biochem.*, 9 (1987) 478.
- 20 D. V. Goeddel, H. L. Heynecker and T. Hozumi, *Nature (London)*, 281 (1979) 544.
- 21 G. W. Becker, P. M. Tackitt, W. W. Bromer, D. S. Lefeber and R. M. Riggin, *Biotechnol. Appl. Biochem.*, 10, (1988) 326.
- 22 A. C. Celniker, A. B. Chen, R. M. Wert and B. M. Sherman, *J. Clin. Endocrinol. Metab.*, 68 (1989) 469.
- 23 V. Roongta, *Biochemistry*, 28 (1989) 1048.
- 24 T. P. Hopp and K. R. Woods, *Proc. Natl. Acad. Sci. U.S.A.*, 78 (1981) 3824.
- 25 T. K. Surowy, R. M. Bartholomew and W. P. VanderLaan, *Mol. Immunol.*, 21 (1984) 345.
- 26 B. C. Cunningham, P. Jhurani, P. Ng and J. A. Wells, *Science (Washington, D.C.)*, 243 (1989) 1330.
- 27 L. D. Taber, *M. S. Thesis*, Indiana University School of Medicine, Indianapolis, IN, 1990.

Structural characterization of glycoprotein digests by microcolumn liquid chromatography–ionspray tandem mass spectrometry

Jinping Liu, Kevin J. Volk, Edward H. Kerns, Steven E. Klohr, Mike S. Lee and Ira E. Rosenberg

Bristol-Myers Squibb Pharmaceutical Research Institute, Wallingford, CT 06492 (USA)

ABSTRACT

An in-house modified microcolumn liquid chromatography (LC) system has been coupled to a PE-SCIEX API III triple-quadrupole mass spectrometer through an ionspray interface for the structural characterization of model glycoproteins, bovine ribonuclease B and human α_1 -acid glycoprotein. In conjunction with enzymatic digestion approaches using trypsin and peptide-N-glycosidase F, the feasibility of packed-capillary (250 μm I.D.) LC columns, coupled with ionspray mass spectrometry (MS) in a tandem format, have been assessed for glycopeptide mapping and structural determination. This configuration demonstrates a highly promising approach for the determination of glycosylation sites and the corresponding sequence structures of related tryptic fragments. A glycosylated tetrapeptide, Asn–Leu–Thr–Lys with carbohydrate moieties on Asn-34, was readily located for bovine ribonuclease B. Preliminary results using micro-LC–MS also show the identification of a class A carbohydrate attachment on a tryptic fragment of human α_1 -acid glycoprotein. The microheterogeneity of carbohydrate moieties can be quickly screened using this approach for either tryptic digests or the intact glycoprotein. These methods demonstrate potential applications for structural characterization of recombinant glycoproteins of pharmaceutical interest.

INTRODUCTION

Rapid advances in recombinant DNA techniques have stimulated great interest in proteins for novel therapeutic uses in the pharmaceutical industry. Glycoproteins are among the most attractive subjects because of their structural specificity and biological roles of oligosaccharides. During recent years, the fundamental understanding of biological functions of glycosylation of proteins has been explored. These include intracellular transport, the influences on the activity, stability, and solubility of the protein, antigenicity, molecular recognition, thermal stability, and the rate of proteolysis [1–5]. Structural characterization of glycoproteins, in-

cluding protein sequence information, carbohydrate compositions and the determination of glycosylation sites, presents a significant analytical challenge.

The detection and identification of glycoproteins have been traditionally accomplished using polyacrylamide gel electrophoresis followed by direct gel staining [6], membrane staining techniques [7–9] or lectin affinity chromatography [10–12]. Further structural characterization is often performed by chromatographic separation in conjunction with appropriate enzymatic methods. In recent years, anion-exchange chromatography with pulsed amperometric detection has been widely utilized for analysis of complex mixtures of oligosaccharides [13,14] and structural classification and microheterogeneity of carbohydrate moieties at specific attachment sites in glycoproteins while combined with fast atom bombardment mass spectrometry

Correspondence to: J. Liu, Bristol-Myers Squibb Pharmaceutical Research Institute, Wallingford, CT 06492, USA.

(FAB-MS) [15,16]. Reversed-phase high-performance liquid chromatography (RP-HPLC) has been well practiced for peptide mapping of protein digests and can often be adapted to map individual glycoforms of glycoproteins [16–18]. On-line LC-MS, especially with FAB-MS and electrospray MS, has received considerable attention in peptide mapping and subsequent structural characterization [15,19–22].

In any case, it is clear that the chemical or enzymatic cleavage of glycoproteins and subsequent separation and identification of the glycosylated peptide fragments is an important approach for the structural characterization of glycoproteins. Enzymatic and chemical digestion of glycoproteins usually generate complex mixtures of peptides, glycopeptides, and even oligosaccharides after the cleavage of carbohydrate side chains. Thus, a preliminary separation step with high resolution and high detection sensitivity and the feasibility of easy interfacing with a mass spectrometer is essential. Microcolumn liquid chromatography (micro-LC), especially using packed fused-silica capillaries of 50–320 μm I.D. has been a very successful technique for biological applications [23–25]. This technique uses the same separation method as conventional HPLC but with a miniaturized format and optimized instrumentation, providing very high mass sensitivity and excellent analytical resolution. The introduction of electrospray or ionspray (pneumatically assisted electrospray) interfaces for MS and the increased use of continuous flow (CF) FAB-MS have further stimulated the use of micro-LC to facilitate the on-line LC-MS configuration. The very low volumetric flow-rates (2–5 $\mu\text{l}/\text{min}$) attained with micro-LC techniques are well suited for either an electrospray or ionspray MS interface, or CF-FAB-MS for the conditions of potential high-sensitivity performance. There have been several reports which demonstrate the utility of these techniques for peptide mapping and protein characterization [26–29], however, techniques for the characterization of glycoproteins utilizing microcolumn separation techniques, especially coupled with MS, have not been well explored. This is partially due to the lack of instrumentation for performing micro-LC and also the structural complexity of glycoproteins.

In this paper, a micro-LC system in combination with tandem mass spectrometry (micro-LC-MS-

MS) is used for comparative glycopeptide mapping of model glycoprotein digests prior to, and after, proteolytic cleavages. This method has been applied to the determination of a glycosylation site and associated peptide structure of bovine ribonuclease B. Preliminary results for the partial determination of oligosaccharide attachment sites of a complex glycoprotein, human α_1 -acid glycoprotein, are also discussed.

EXPERIMENTAL

Materials

Protein sequencing-grade trifluoroacetic acid (TFA) (Sigma, St. Louis, MO, USA), UV-grade acetonitrile (J.T. Baker, Phillipsburg, NJ, USA) and HPLC-grade water (Fisher, Fair Lawn, NJ, USA) were used. Ribonuclease B (Type III-B, from bovine pancreas), α_1 -acid glycoprotein (human), L-1-tosylamide-2-phenylethyl chloromethyl ketone (TPCK)-treated trypsin, dithiothreitol (DTT), iodoacetamide, and ammonium bicarbonate were all purchased from Sigma. Peptide-N-glycosidase F (PNGase F) was obtained from Boehringer Mannheim (Indianapolis, IN, USA).

Reduction and S-carboxymethylation

The reduction and S-carboxymethylation of selected glycoproteins were performed prior to digestion. In this study, 500 μl of ribonuclease B (5 mg) dissolved in water were mixed with 500 μl of 0.5 M Tris-HCl buffer (pH 8.25) containing 2 mM EDTA and 6.0 M guanidine-HCl, and 100 μl of 0.4 M DTT. The mixed solution was incubated at 37°C for 3 h. A volume of 200 μl of 0.8 M iodoacetamide was then added and incubated for 1 h. A 3.5-mg sample of human α_1 -acid glycoprotein was treated in an identical manner. The samples were desalted overnight using Spectra/Por 6 membranes from Fisher and dried for further treatment.

Enzymatic digestion

The reduced and S-carboxymethylated ribonuclease B (RCM-ribonuclease B) (ca. 1 mg) and human α_1 -acid glycoprotein (ca. 0.8 mg) were digested with TPCK-trypsin in 0.1 M ammonium bicarbonate buffer (pH 8.00) with a substrate-enzyme ratio of 50:1 (w/w). The mixtures were incubated at 37°C for 24 h. After digestion, 100 μl of the tryptic digest

(approximate 10 nmol) was incubated with two units of peptide-N-glycosidase F (PNGase F) in 0.1 M ammonium bicarbonate (pH 8.30) containing 2 mM EDTA at 37°C for 24 h. The reaction mixtures were either directly used for chromatographic analysis or dried and stored in a freezer and redissolved in 0.1% TFA prior to use.

Microcolumn liquid chromatography

A Beckman System Gold conventional HPLC system was modified for performing micro-LC at low flow-rates. Solvent gradients were directly delivered into a micromixer obtained from Upchurch Scientific (Oak Harbor, WA, USA), at flow-rates of 0.2–0.4 ml/min. A precolumn splitting device was used to obtain appropriate output flow-rates (approximately 3 μ l/min) for packed capillary columns. The split ratio was easily regulated by adjusting the length of the restriction line (fused-silica capillary with 50 μ m I.D. and 361 μ m O.D.). The capillary columns with 250 μ m I.D. and 348 μ m O.D. were packed in-house with C₁₈, 5- μ m particles of 300 Å pore size, from Vydac (Hesperia, CA, USA) using an ISCO μ LC-500 pump. The columns were directly connected into a Valco micro-injector with 100 nl or 500 nl internal loops. The transfer line from column outlet consisted of fused-silica capillary with 50 μ m I.D. and 190 μ m O.D. on-line connected to UV detector and mass spectrometer. An ABI Model 785A UV detector (Applied Biosystem, Foster City, CA, USA) equipped with an Z-shape capillary flow cell obtained from LC Packings (San Francisco, CA, USA) was used in this study. The mobile phase used consisted of 0.1% TFA in water (solvent A) and solvent A–acetonitrile (20:80) with 0.1% TFA (solvent B). Solvent gradients (0%–60% solvent B over 120 min) were used for all separations.

Ionspray mass spectrometry

A PE-SCIEX (Thornhill, Ontario, Canada) API III triple-quadrupole mass spectrometer equipped with an ionspray interface was used on-line with the micro-LC system and UV detector described above. Micro-LC effluent was introduced directly into the ionspray source. Micro-LC–MS experiments were performed while scanning from m/z 300 to 1800 at a scan-rate of 4 s/scan. For the daughter MS–MS operation, the parent ions were selected in the first

quadrupole mass analyzer and transmitted into the second quadrupole (collision cell) with collision energy of 50 eV and argon collision gas thickness of $400 \cdot 10^{12}$ molecules/cm².

RESULTS AND DISCUSSION

Electrospray (or ionspray) MS has been increasingly used for determining molecular mass and structural analysis of peptides and proteins. Generally, multiple-charge states with a Gaussian distribution of relative intensities can be observed for the intact protein from which a single peak indicative of the molecular weight can be converted by deconvolution [30]. However, glycoprotein analysis appears to be more complicated. In the present study, we have selected bovine ribonuclease B, a glycoprotein with a single glycosylation site and high mannose content, as a model compound. Initial screening was performed directly by ionspray MS and the results are shown in Fig. 1. A deconvoluted mass spectrum was obtained for the intact glycoprotein without pretreatment as shown in Fig. 1A, exhibiting a pattern of microheterogeneity of glycosylation. It is known that structural heterogeneity of carbohydrate moieties attached on the peptide backbone of the protein frequently occurs in glycoproteins, especially for asparagine-linked glycoproteins [31,32]. This phenomenon was further noticed after the treatment with PNGase F, an enzyme which specifically cleaves N-linked carbohydrates between the di-N-acetylchitobiose unit and the asparagine residue of the polypeptide backbone. As shown in Fig. 1B, most glycosylated peaks disappear. The molecular mass of deglycosylated protein was found to be 13 692 which is consistent with the calculated value of 13 691 based on its known amino acid sequence. Actually, this peak was also observed in native glycoprotein, but can only be confirmed to be a deglycoform after the release of oligosaccharides. It could be due to the presence of ribonuclease A, a non-glycoprotein that has the same polypeptide backbone as ribonuclease B. Also noted was a component with an M_r of 13 895 corresponding to protein-GlcNAc. A possible explanation for this phenomenon is due to the enzymatic cleavage of carbohydrate moieties by Endo-F (Endo-b-N-acetylglucosaminidase F), an enzyme often co-existing with PNGase F, releasing a peptide at-

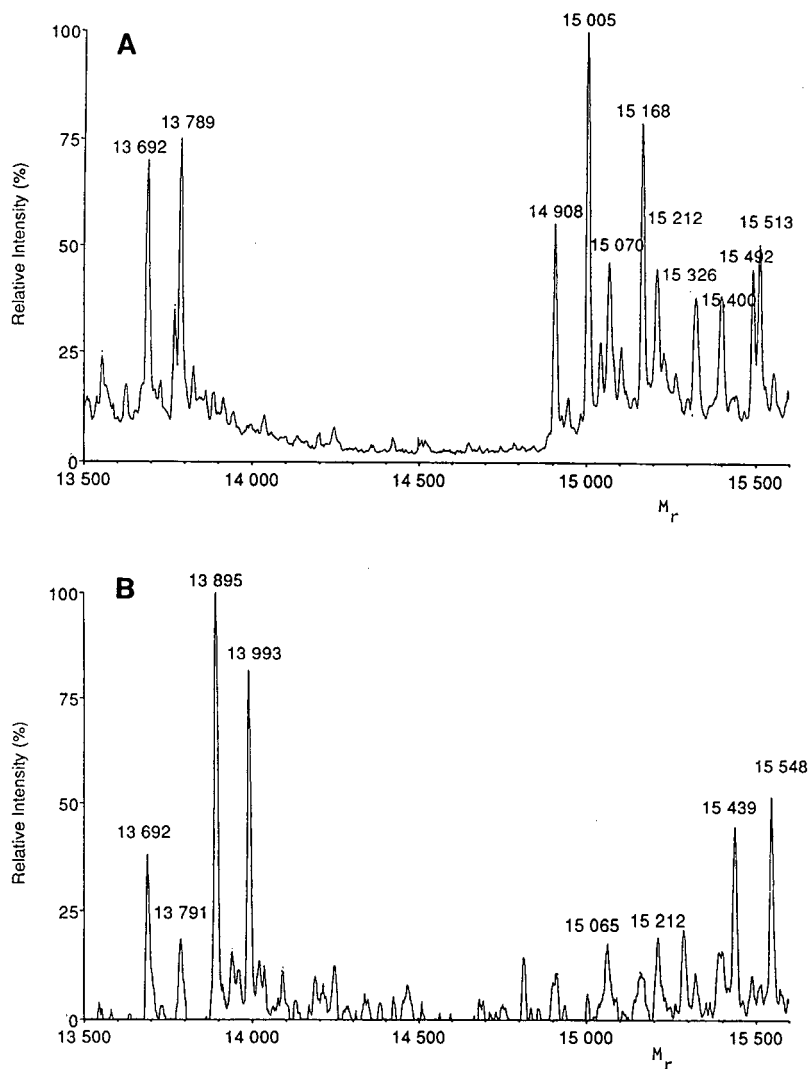


Fig. 1. Deconvoluted mass spectra of bovine ribonuclease B by ionspray-MS analysis. (A) Native protein; (B) PNGase F treated protein.

tached with one N-acetylglucosamine residue, peptide-GlcNAc, which is not itself a substrate for PNGase F [33]. Based on these studies, the carbohydrate content constitutes about 12% of the total molecular mass. This approach provides a method for quickly screening the microheterogeneity of oligosaccharide substructures of a glycoprotein and the determination of carbohydrate content. Table I lists possible glycoforms observed from these experiments in terms of diagnostic increments of M_r , 162 for a hexose residue and increments of M_r , 203 for N-acetylhexosamine residue.

Further structural analysis of glycoproteins generally requires fragmentation, either by chemical or enzymatic cleavage, and subsequent separation or isolation. Chromatographic isolation has been a traditional method for glycoprotein analysis, such as the use of lectin affinity chromatography. Peptide mapping is an attractive approach while utilized in conjunction with the appropriate enzymatic methods. By comparing peptide maps prior to, and after enzymatic cleavage, peptide fragments attached to oligosaccharides may be located and distinguished from non-glycosylated peptides. Mass spectrometry

TABLE I

HETEROGENEITY OF RIBONUCLEASE B GLYCOFORMS OBSERVED BY IONSpray-MS ANALYSIS

| Native protein | M_r | PNGase F-treated protein | M_r |
|---|--------|---|--------|
| Polypeptide chain | 13 692 | Polypeptide chain | 13 692 |
| Polypeptide adduct (phosphate) | 13 789 | Polypeptide adduct (phosphate) | 13 791 |
| Hex ₅ -(HexNAc) ₂ -polypeptide | 14 908 | HexNAc-polypeptide | 13 895 |
| Hex ₅ -(HexNAc) ₂ -(polypeptide + phosphate adduct) | 15 005 | HexNAc-(polypeptide + phosphate adduct) | 13 993 |
| Hex ₆ -(HexNAc) ₂ -polypeptide | 15 070 | | |
| Hex ₆ -(HexNAc) ₂ -(polypeptide + phosphate adduct) | 15 168 | | |
| Hex ₇ -(HexNAc) ₂ -(polypeptide + phosphate adduct) | 15 326 | | |
| Hex ₈ -(HexNAc) ₂ -(polypeptide + phosphate adduct) | 15 492 | | |

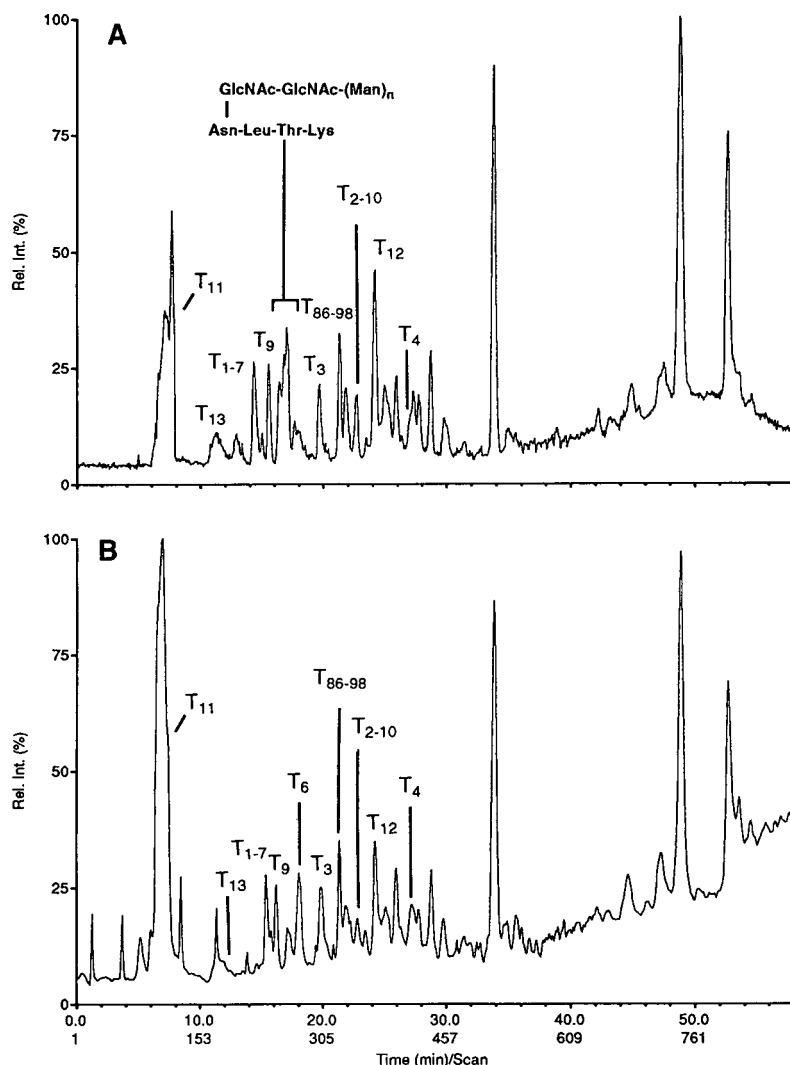


Fig. 2. Comparative peptide mapping of enzymatic digests of bovine ribonuclease B by micro-LC-ionspray MS. (A) TIC trace of digested RCM-glycoprotein with trypsin; (B) TIC trace of digested RCM-glycoprotein with trypsin and PNGase F. Capillary column: 33 cm \times 250 μ m I.D. (348 μ m O.D.) packed with C₁₈. Gradient conditions described in Experimental section. Approximate 52 picomol of digests were injected onto the column.

try, especially FAB-MS, has been utilized to determine the structure of oligosaccharides and the classification of glycosylation. However, an ionspray interface combined with micro-LC separation techniques is particularly attractive for mapping protein digests [34,35]. Fig. 2 shows the total ion current (TIC) MS chromatograms of enzymatic digests of bovine ribonuclease B. This glycoprotein was denatured, reduced, and *S*-carboxymethylated prior to enzymatic treatment. Trypsin was first used to digest the RCM-ribonuclease B, generating a mixture of peptides and glycopeptides. The fragments were separated and detected by micro-LC on-line with a UV detector and ionspray mass spectrometer. The tryptic map shown in Fig. 2A as the TIC profile, which correlates well with the UV absorbance trace, exhibits abundant signals that could be assigned to most of the expected normal peptide fragments (Fig. 2). Of particular interest is a unique broad peak between retention time 16 and 17.5 min which was determined to be related to the heterogeneity of glycoforms attached to a specific tryptic peptide. To establish the identity and the attachment of the carbohydrate substructure, tryptic fragments of ribo-

nuclease B were further reacted with PNGase F. After treatment with PNGase F, this particular broad peak disappeared and a new peak with a retention time of 18 min (T_6^*), which was absent in original tryptic map, was observed in the enzymatic digest (Fig. 2B). This new component corresponds to a peptide fragment with a molecular mass of 474.

A full scan mass spectrum (Fig. 3) averaging all the glycoforms of the glycosylated peptide, corresponding to the broad peak from 16 to 17.5 min (Fig. 2A), provides further detailed information for the confirmation of the presence of glycoforms attached on a single peptide. As shown in Fig. 3, a series of singly and doubly charged ions represent diagnostic increments of M_r 162 and 203 corresponding to hexose and GlcNAc substructures, respectively. The table inserted in Fig. 3 suggests the structures of the proposed glycopeptide with homogeneous components differing in the number of hexose units. For example, the arithmetic difference between the component of M_r 1691 (MH^+ at m/z 1692, MH_2^{2+} at m/z 846) and peptide substructure (M_r 474) is M_r 1217 which corresponds uniquely to a carbohydrate composition of five mannose and

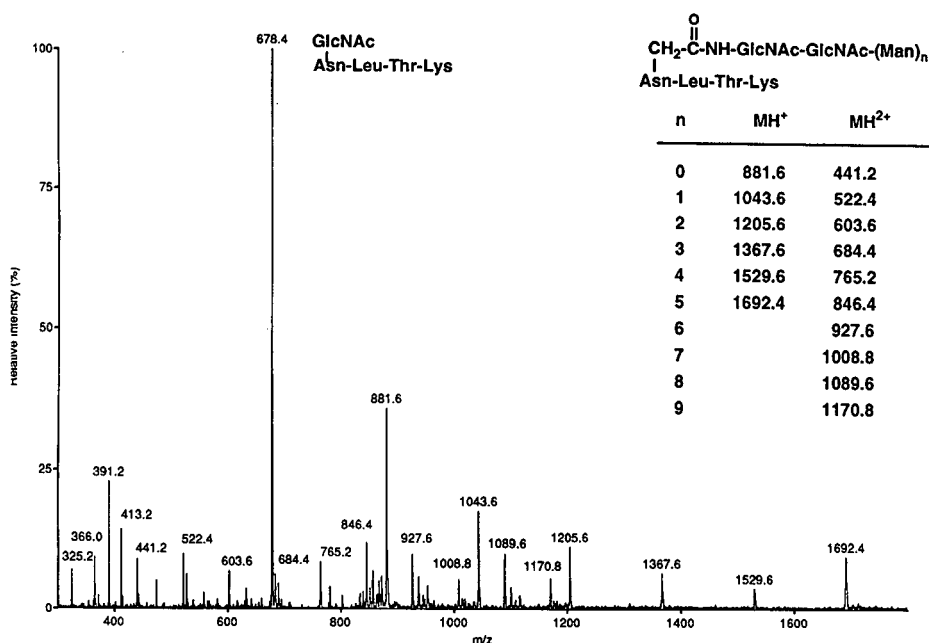


Fig. 3. Averaged full scan mass spectrum of glycoforms corresponding to the peaks indicated in Fig. 2A.

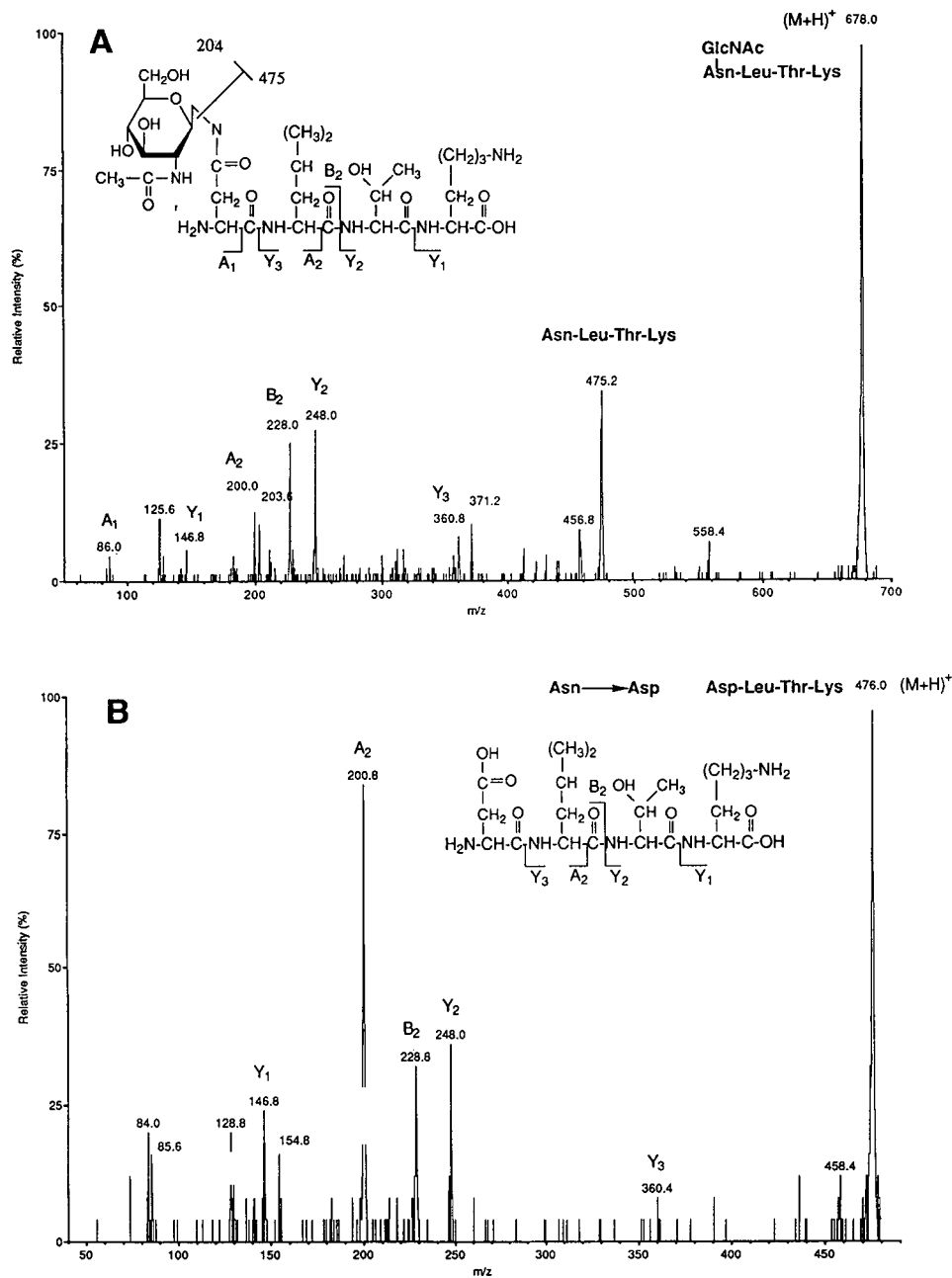


Fig. 4. Structural determination of a glycopeptide fragment from enzymatic digests of bovine ribonuclease B by micro-LC-MS-MS. (A) Daughter MS-MS spectrum of glycosylated peptide ion at m/z 678. (B) Daughter MS-MS spectrum of deglycosylated peptide ion at m/z 476.

two N-acetylglucosamine residues. Similarly, a mass difference of 1054 between M_r 1528 (MH^+ at m/z 1529, MH_2^+ at m/z 765) and the peptide confirms a sugar unit of four mannoses linked to two

N-acetylglucosamine residues. Additional carbohydrate units can be derived in a similar manner. The presence of an intense ion at m/z 678 in the full scan mass spectrum should be noted. As will be dis-

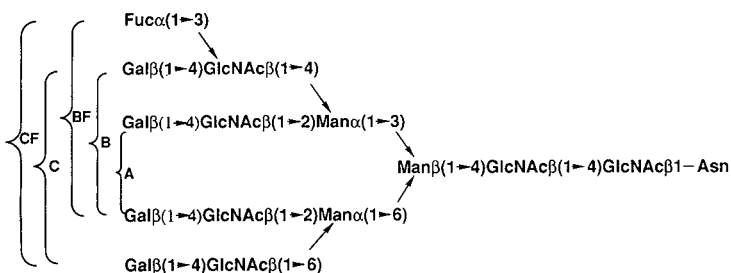


Fig. 5. Classes of carbohydrate moieties for human α_1 -acid glycoproteins [37].

cussed later, MS–MS experiments indicated that this ion corresponded to the tetrapeptide attached to a single N-acetylglucosamine residue. The presence of this glycoform is somewhat unusual since it was not observed in the original glycoprotein. It is most likely a mass spectrometric fragment ion formed during the ionization process. In conjunction with MS–MS studies, such fragmentation in the ion source facilitates the identification of the glycosylation site.

To confirm this structure and the carbohydrate attachment site, micro-LC–MS–MS experiments were performed prior to, and after the treatment of tryptic digest with PNGase F (Fig. 4). Fig. 4A shows a daughter MS–MS spectrum of the glycosylated fragment from the tryptic digest at m/z 678. The ion at m/z 475 represents the tetrapeptide substructure (Fig. 4A) due to the facile cleavage of N-linked sugar. A weak ion at m/z 204 corresponding to the N-acetylglucosamine residue fragment was also observed. The confirmation of this peptide sequence was based on typical Y-series fragment ions due to the fragmentation between peptide bonds of each amino acid as well as the A- and B-series ions. For example, Y_1 represents Lys at the C-terminus, Y_2 corresponds to the dipeptide fragment, Thr–Lys, and Y_3 corresponds to the tripeptide fragment, Leu–Thr–Lys. Amino acid residues from N-terminus were confirmed by A_1 , A_2 , and B_2 ions, indicating the presence of Asn, Asn–Leu, and Asn–Leu–Thr fragments, respectively.

After enzymatic cleavage of the sugar substructure by PNGase F, a new tryptic fragment, T_6^* , was observed. A daughter MS–MS spectrum of the deglycosylated fragment T_6^* (m/z 476) was obtained and is shown in Fig. 4B. The M_r of 475 and struc-

tural information obtained from the MS–MS spectrum are consistent with the conversion of asparagine into aspartic acid in the tetrapeptide after treatment by PNGase F [36]. This phenomenon was readily detected by ionspray MS and is an important piece of evidence for determining the site of carbohydrate attachment. From Fig. 4B, it is clear that the Y-series ions from the C-terminus of the deglycosylated peptide are the same as those found in glycosylated peptide. The observed M_r 1 increase for the A_2 and B_2 fragments from the N-terminus provides further evidence supporting the conversion of asparagine to aspartic acid. This information confirms that the carbohydrate is attached on the tryptic tetrapeptide, Asn–Leu–Thr–Lys, at the asparagine of position 34 in the polypeptide backbone of the glycoprotein.

We have applied this approach to a more complicated glycoprotein, human α_1 -acid glycoprotein, a protein consisting of a single polypeptide chain but with a relatively high carbohydrate content. Furthermore, these carbohydrates are N-linked oligosaccharides with complex degrees of branching and structural variability due to the microheterogeneity and they account for 45% of the total molecular mass of the protein. There are five classes of carbohydrate moieties reported [37] for this glycoprotein as shown in Fig. 5.

The major core is class A. Obviously, these branched oligosaccharides complicate the chromatographic separation as well as spectral interpretation. The preliminary results of this mapping strategy are shown in Fig. 6 which were obtained by treating the glycoprotein sequentially with trypsin and PNGase F. By comparing these two maps, it is apparent that fragment T_9 from the deglycosylated

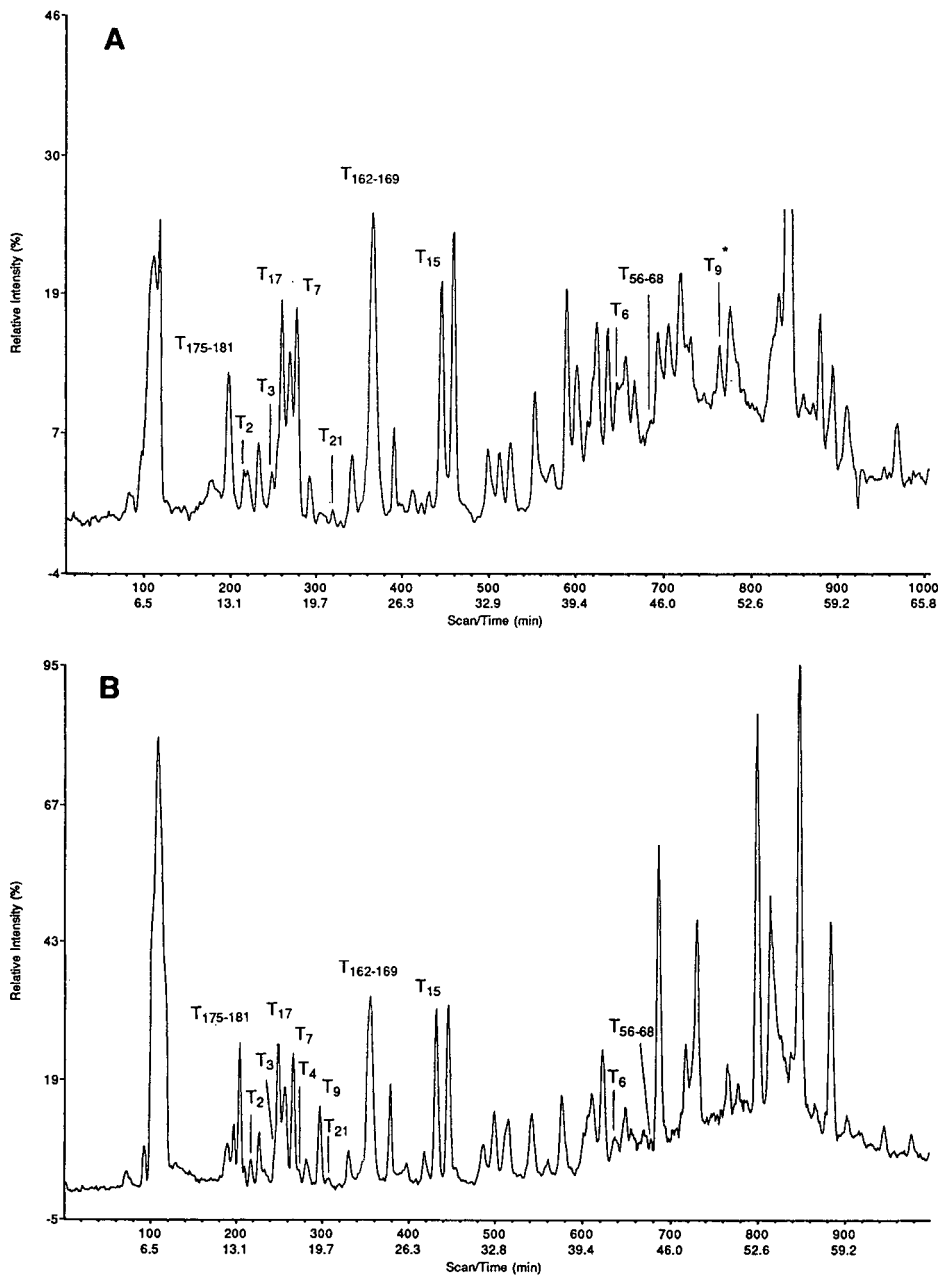


Fig. 6. Comparative peptide mapping of enzymatic digests of human α_1 -acid glycoprotein by micro-LC-ionspray-MS. (A) TIC trace of digested RCM-glycoprotein with trypsin; (B) TIC trace of digested RCM-glycoprotein with trypsin and PNGase F. Experimental conditions are the same as in Fig. 3.

digest (Fig. 6B) is unique since it was not observed in the glycosylated digest (Fig. 6A). In addition, a glycosylated peptide was located as T_9^* shown in Fig. 6A, which possibly corresponds to the pro-

posed carbohydrate structure based on the classification of the oligosaccharides demonstrated above. A full scan mass spectrum of the glycosylated tryptic fragment T_9^* was obtained and is shown in Fig.

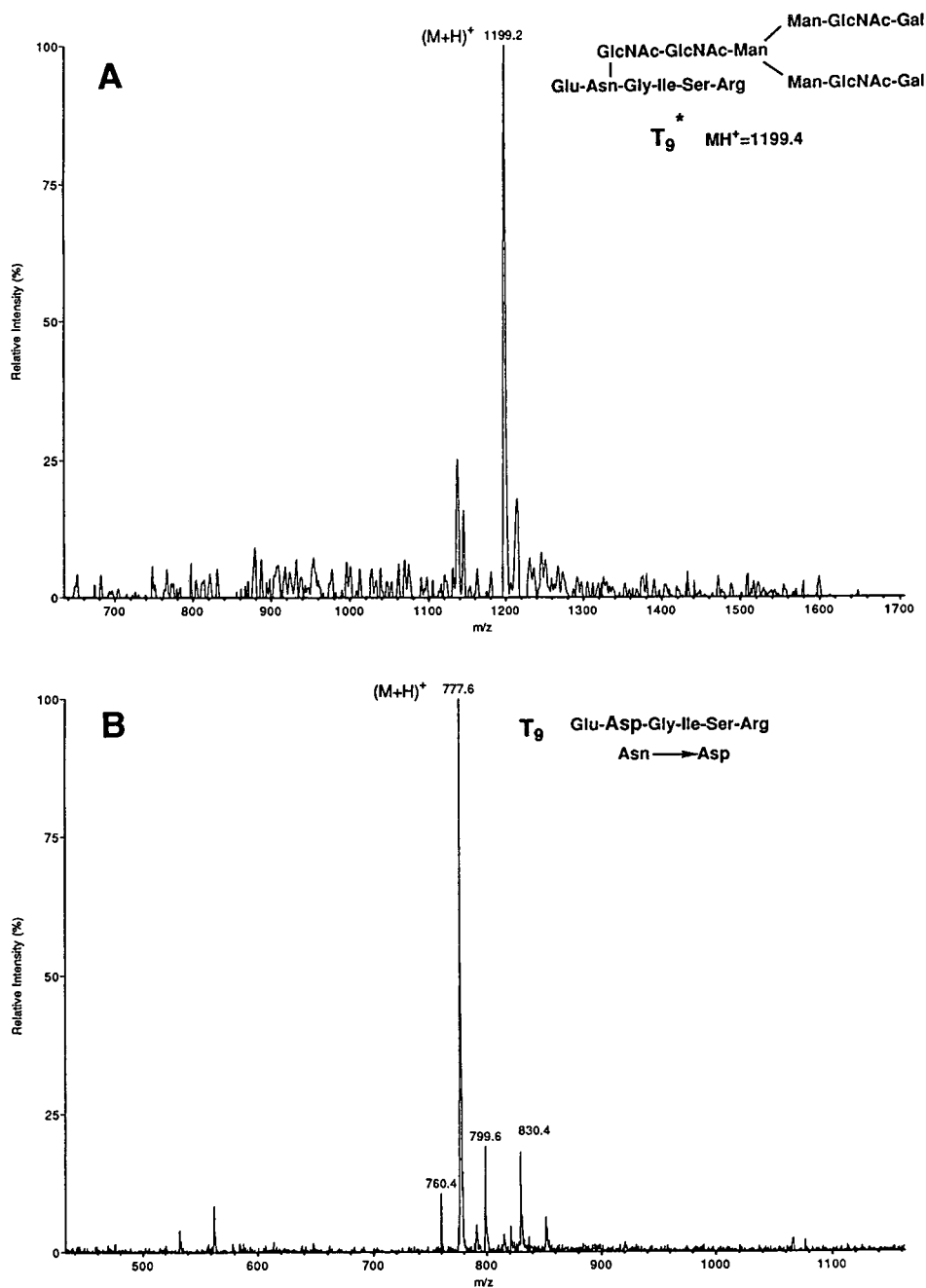


Fig. 7. Full scan mass spectra of a glycopeptide fragment from enzymatic digests of human α_1 -acid glycoprotein. (A) Glycosylated peptide; (B) deglycosylated peptide.

7A. A doubly charged ion (MH_2^+ 1199.2) was found to be related to the proposed glycopeptide that has molecular mass of 2396.8 (giving MH_2^+ 1199.4). Based on the known peptide sequence of

human α_1 -acid glycoprotein, the corresponding deglycosylated tryptic fragment could have a molecular mass of 775. The mass difference of M_r 1622 between the total molecular mass of glycosylated

peptide and the deglycosylated peptide agrees well with a class A carbohydrate chain. The full scan mass spectrum of deglycosylated fragment T₉ shown in Fig. 7B provides further evidence for this glycosylation. A singly charged ion (MH⁺) at *m/z* 777 was observed, *M_r* 1 more than the predicted peptide (MH⁺ at *m/z* 776) described above. This is consistent with studies on bovine ribonuclease B since enzymatic cleavage of the N-linked sugar unit by PNGase F results in conversion of asparagine to aspartic acid. Since this heavily glycosylated glycoprotein is highly branched, it appears that further studies utilizing highly efficient separations and the utilization of alternate enzyme combinations should be pursued in conjunction with micro-LC–MS–MS experiments for substructure determination and confirmation.

CONCLUSIONS

A strategy involving the use of micro-LC–MS–MS techniques has been shown to be capable of providing a highly sensitive method for peptide mapping of glycoproteins. In conjunction with appropriate enzymatic methods such as trypsin and PNGase F, high-resolution chromatographic separations of complex mixtures of peptides and glycopeptides provide valuable comparative maps for rapidly locating glycosylated peptide fragments.

Electrospray (or ionspray) ionization MS is an extremely attractive and novel technique for structural characterization of glycoproteins. Quick screening of the intact native glycoprotein by ion-spray-MS provides information of the microheterogeneity profile as well as the carbohydrate content. On-line coupling of micro-LC to MS is a very powerful configuration which permits rapid identification of enzymatically generated peptide and glycopeptide fragments present in the maps. Micro-LC–MS–MS techniques provide an extra dimension of information allowing for the characterization of peptide and glycopeptide substructures and the determination of carbohydrate attachment sites. The MS–MS fragmentation patterns of the tryptic fragments permits confirmation of carbohydrate attachments.

REFERENCES

- 1 T. W. Rademacher, R. B. Porekh and R. A. Dwek, *Annu. Rev. Biochem.*, 57 (1988) 785.
- 2 T. Feizi and R. A. Childs, *Trends Biol. Sci.*, 10 (1985) 24.
- 3 M. Fukada, *Biochim. Biophys. Acta*, 780 (1985) 780.
- 4 H. Schachter, *Clin. Biochem.*, 17 (1984) 3.
- 5 R. Kornfeld and S. Kornfeld, *Annu. Rev. Biochem.*, 45 (1976) 217.
- 6 G. Munoz, S. Marshall, M. Cabrera and A. Horvat, *Anal. Biochem.*, 170 (1988) 491.
- 7 K.-L. Hsi, L. Chen, D. H. Hawke, L. R. Zieske and P.-M. Yuan, *Anal. Biochem.*, 198 (1991) 238.
- 8 H. Ogawa, M. Ueno, H. Uchibori, I. Matsumoto and N. Seno, *Anal. Biochem.*, 190 (1990) 165.
- 9 S. Kitimato-Ochiati, Y. Katagiri and H. O. Chia, *Anal. Biochem.*, 147 (1985) 389.
- 10 E. D. Green and J. U. Baenziger, *Trends Biol. Sci.*, 14 (1989) 168.
- 11 R. K. Merkle and R. D. Cummings, *Methods Enzymol.*, 138 (1987) 232.
- 12 T. Osawa and T. Tsuji, *Annu. Rev. Biochem.*, 56 (1987) 21.
- 13 M. R. Hardy and R. R. Townsend, *Proc. Natl. Acad. Sci. U.S.A.*, 85 (1988) 3289.
- 14 L. J. Basa and M. W. Spellman, *J. Chromatogr.*, 499 (1990) 205.
- 15 J. R. Barr, K. R. Anumula, M. B. Vettese, P. B. Taylor and S. A. Carr, *Anal. Biochem.*, 192 (1991) 181.
- 16 M. W. Spellman, L. J. Basa, C. K. Leonard, J. A. Chakel, J. V. O'Connor, S. Wilson and H. Van Halbeek, *J. Biol. Chem.*, 264 (1989) 14100.
- 17 R. L. Garnick, N. J. Soll and P. A. Papa, *Anal. Chem.*, 60 (1988) 2546.
- 18 J. J. L'italien, *J. Chromatogr.*, 359 (1986) 213.
- 19 R. M. Caprioli, *Methods Enzymol.*, 193 (1990) 214.
- 20 M. A. Moseley, L. J. Deterding, J. S. M. Dewit, K. B. Tomer, R. T. Kennedy, N. Bragg and J. W. Jorgenson, *Anal. Chem.*, 61 (1989) 1577.
- 21 M. E. Hemling, G. D. Roberts, W. Johnson, S. A. Carr, *Biomed. Environ. Mass Spectrom.*, 19 (1990) 677.
- 22 S. A. Carr, M. E. Hemling, G. F. Wusserman, R. W. Sweet, K. Anumula, J. R. Barr, M. J. Huddleston and P. Taylor, *J. Biol. Chem.*, 264 (1989) 21286.
- 23 M. V. Novotny and D. Ishii (Editors), *Microcolumn Separations*, Elsevier, Amsterdam, 1985.
- 24 M. V. Novotny, *Science (Washington D.C.)*, 246 (1989) 51.
- 25 M. V. Novotny, *J. Microcol. Sep.*, 2 (1990) 7.
- 26 K. A. Cobb and M. V. Novotny, *Anal. Chem.*, 61 (1989) 2226.
- 27 M. Hail, S. Lewis, I. Jardine, J. Liu and M. V. Novotny, *J. Microcol. Sep.*, 2 (1990) 285.
- 28 L. J. Deterding, C. E. Parker, J. R. Perkins, M. A. Moseley, J. W. Jorgenson and K. B. Tomer, *J. Chromatogr.*, 554 (1991) 329.
- 29 E. C. Huang, T. Wachs, J. J. Conboy and J. D. Henion, *Anal. Chem.*, 62 (1990) 713A.
- 30 R. D. Smith, J. A. Loo, C. G. Edmonds, C. J. Barinaga and H. R. Udseth, *Anal. Chem.*, 62 (1990) 882.
- 31 R. Kornfeld and S. Kornfeld, *Annu. Rev. Biochem.*, 54 (1985) 631.

- 32 T. A. W. Koerner, J. H. Prestegard and R. K. Yu, *Methods Enzymol.*, 138 (1987) 38.
- 33 M. W. Spellman, *Anal. Chem.*, 62 (1990) 1714.
- 34 T. R. Covey, E. C. Hung and J. D. Henion, *Anal. Chem.*, 63 (1991) 1193.
- 35 V. Ling, A. W. Guzetta, E. Canova-Davis; J. T. Stults, W. S. Hancock, T. R. Covey and B. I. Shushan, *Anal. Chem.*, 63 (1991) 2909.
- 36 T. H. Plumer, J. H. Elder, S. Alexander, A. W. Phelan and A. L. Tarentino, *J. Biol. Chem.*, 259 (1984) 10700.
- 37 K. Schmid, J. P. Binette, L. Dorland, J. F. G. Vliegthart, B. Fournet and J. Montreuil, *Biochim. Biophys. Acta*, 581 (1979) 356.

High-performance liquid chromatography of tryptophan and other amino acids in hydrochloric acid hydrolysates

I. Molnár-Perl, M. Pintér-Szakács and M. Khalifa

Institute of Inorganic and Analytical Chemistry, L. Eötvös University, P.O. Box 32, H-1518 Budapest 112 (Hungary)

ABSTRACT

Tryptamine [3-(2-aminoethyl)indole] as an additive to 6 M HCl largely prevented the decomposition of tryptophan in proteins, and also in gas-phase hydrolysis, using a Pico-Tag Work Station, at 145°C for 4 h. This procedure proved to be excellent for amino acid analysis using conventional high-performance liquid chromatography with derivatization with phenyl isothiocyanate. The recovery of tryptophan from model solutions and from proteins was 80–98%. The results proved to be as good as any other obtained by the analysis of special alkaline or organic acid hydrolysates, most of which are suitable exclusively for the determination of tryptophan. The most important advantage of tryptamine was that it did not affect the quantitative recovery of other amino acids of proteins, as shown by the composition of lysozyme hydrolysates obtained in the absence and presence of various amounts of tryptamine. The reproducibility of the measurements was 3.7% (relative standard deviation) or less.

INTRODUCTION

It is well known that, under the common conditions of protein hydrolysis (6 M HCl, 100°C for 24 h or 145°C for 4 h), a considerable amount tryptophan is destroyed. A number of procedures have been published for the determination of tryptophan, including (i) the time-consuming and tedious alkaline hydrolyses suitable exclusively for tryptophan determination [1–10], (ii) organic acid [11–15], with the limitation that they are successful in total amino acid analysis by ion-exchange chromatography only [the non-volatile organic acids inhibit the derivatization of amino acids for both gas chromatography (GC) and high-performance liquid chromatography (HPLC)] and (iii) the common HCl hydrolyses with additives [16–23], such as thioglycolic acid [16,19], mercaptoethanesulphonic acid [17], ethanedithiol [18], mercaptoethanol [21], phenol [22] or tryptamine [20,23], which are expected to be the most promising for the subsequent simultane-

ous assay of amino acids, including tryptophan, in protein hydrolysates.

Recently, it has been found [22] that the addition of 1–3% of phenol to 6 M HCl acid largely (*ca.* 80% recovery) prevents the destruction of tryptophan in peptides and proteins during liquid-phase hydrolyses at 110, 145 and 160°C for 22 h, 4 h and 25 min, respectively. However, from gas-phase hydrolyses only 10–20% of tryptophan could be recovered even with 3% phenol containing 6 M HCl.

The aim of this work was (i) to study the inhibitory activity of [3-(2-aminoethyl)indole] (tryptamine) also in gas-phase hydrochloric acid hydrolysis and (ii) to demonstrate its utility in the determination of amino acids including tryptophan in hydrolysates as their phenylthiocarbamyl (PTC) derivatives by HPLC [24].

EXPERIMENTAL

Materials

Triethylamine (TEA), phenyl isothiocyanate (PITC), tryptamine, amino acids and proteins were obtained from Sigma (St. Louis, MO, USA) and

Correspondence to: I. Molnár-Perl, Institute of Inorganic and Analytical Chemistry, L. Eötvös University, P.O. Box 32, H-1518 Budapest 112, Hungary.

Serva (Heidelberg, Germany). HPLC-grade acetonitrile and methanol were purchased from Reanal (Budapest, Hungary). All other reagents were of the highest analytical purity. Hydrolysis and derivatization tubes were supplied with the Pico-Tag Work Station (Millipore–Waters, Chromatography Division, Milford, MA, USA).

Hydrolysis of proteins

Standard proteins (0.014–0.016 g, weighed with analytical accuracy) were dissolved in 10 cm³ of 0.1 M HCl. Standards of free amino acids (AA) in a mixture containing 5 μmol/cm³ of each were prepared in 0.1 M HCl. Tryptamine was dissolved in distilled water (2 μg/μl). Into a 50 × 6 mm tube, 5 μl of AA solution or 20 μl of standard protein solution were injected and various amounts of tryptamine were added (3.75–15 μl) and up to twelve tubes were placed in a vacuum vial. The vial was then attached to the Work Station manifold and the solvent removed under vacuum. After drying, the vacuum was released and 75 μl per tube of constant-boiling HCl were pipetted into the bottom of the vacuum vial. The vacuum vial was then re-attached to the manifold. First the vacuum valve was opened until it showed about 1–2 Torr (1 Torr = 133.322 Pa) and the HCl began to bubble (20–30 s). Thereafter, after closing the vacuum valve, the nitrogen valve was opened, purged for 30 s, and closed again. The vacuum–nitrogen cycles were repeated three times. After the last cycle, the vacuum valve was opened and the cap of the vial was closed under vacuum and put into the Pico-Tag Work Station oven (145°C for 4 h). After hydrolysis, the sample tubes were carefully removed from the vial and the HCl was wiped from the outside of each tube. The tubes were then transferred into a fresh reaction vial, attached to the manifold and evaporated to the constant minimum reading (*ca.* 65 mTorr). The hydrolysed samples were then ready for derivatization.

Derivatization of amino acids with PITC

A 5-μl volume of AA solution, used for comparison of the hydrolysed samples, was injected into 50 × 6 mm tubes and dried under vacuum. Hydrolysed AA (free amino acids) and hydrolysed proteins were redried by adding 10 μl of ethanol–water–TEA (2:2:1) to each tube. Thereafter to each redried sample 20 μl of derivatization reagent [etha-

nol–TEA–water–PITC (7:1:1:1)] were added and mixed by vortex mixing. Subsequently they were treated according to the Waters Pico-Tag Work Station manual.

The derivatized standards were dissolved in 600 μl and the hydrolysed and derivatized proteins in 300 μl of 0.05 M sodium acetate solution (pH 7.2). Thus, the 20-μl aliquots of AA solution contain 800–1000 pmol of each AA and the 20-μl protein samples represent, in total, 1.2–2.0 μg of AA.

Chromatography

The Liquochrom Model 2010 liquid chromatograph (Labor MIM, Budapest, Hungary) used consisted of two Liquopomp 312/1 solvent-delivery pumps and a Type OE-308 UV detector with a wavelength range of 195–440 nm. Samples were injected in 20-μl volumes using an injector supplied by Labor MIM. The columns (BST, Budapest, Hungary) were 150 mm × 4.00 mm with Hypersil ODS bonded phase (5 μm) (Shandon). Eluents were kept under a blanket of nitrogen. The solvent system consisted of two eluents: A = 0.05 M sodium acetate (pH = 7.2) and B = 0.1 M sodium acetate–acetonitrile–methanol (46:44:10) (mixed according to their volume ratios and titrated with glacial acetic acid or 50% sodium hydroxide to pH 7.2). A gradient which was optimized for the separation was from 0% to 100% B in 22 min. For 5 min a washing step with 100% B was applied, then after 100% A was applied for 2 min. After an additional elution for 5 min with solvent A, the system was ready for the next injection.

RESULTS AND DISCUSSION

Based on our earlier experience, *i.e.*, the facts that (i) tryptamine proved to be a powerful additive for the protection of tryptophan in classical HCl hydrolysis in the liquid phase [23] and (ii) gas-phase HCl hydrolysis in the Pico-Tag Work Station with subsequent determination of PTC-amino acids by HPLC can be regarded as one of the most promising methods in protein analysis [24], the extension of the inhibitory activity of tryptamine to gas-phase HCl hydrolyses seemed to be worthy of investigation.

The results of our studies on the effect of tryptamine on tryptophan measurement after HCl hy-

TABLE I

EFFECT OF AMOUNT OF TRYPTAMINE ON THE RECOVERY OF AMINO ACIDS IN MODEL SOLUTIONS (AA) BY HYDROLYSIS WITH 6 M HCl AT 145°C FOR 4 h IN THE GAS PHASE, MEASURED AS PTC-AMINO ACIDS BY HPLC

| No. | Amino acid | Detector responses: peak area (arbitrary units/pmol AA) ^a | | | | | Reproducibility data | | |
|-----|----------------|---|------------|-------------|-------------|-------------|----------------------|------|------------|
| | | Tryptamine added (μg per 70 μg AA) | | | | | Average | S.D. | R.S.D. (%) |
| | | 0 ^b | 0 | 7.5 | 15 | 30 | | | |
| 1 | Aspartic acid | 182 | 180 | 188 | 192 | 180 | 184 | 5.4 | 2.9 |
| 2 | Glutamic acid | 208 | 204 | 214 | 217 | 215 | 212 | 5.4 | 2.5 |
| 3 | Hydroxyproline | 207 | 203 | 209 | 214 | 207 | 208 | 4.0 | 1.9 |
| 4 | Serine | 160 | 150 | 151 | 161 | 162 | 157 | 5.8 | 3.7 |
| 5 | Glycine | 194 | 208 | 200 | 212 | 198 | 202 | 7.4 | 3.7 |
| 6 | Histidine | 170 | 178 | 177 | 183 | 175 | 177 | 4.7 | 2.7 |
| 7 | Threonine | 176 | 173 | 184 | 181 | 178 | 178 | 4.3 | 2.4 |
| 8 | Alanine | 200 | 199 | 211 | 211 | 212 | 207 | 6.5 | 3.1 |
| 9 | Proline | 245 | 240 | 236 | 246 | 240 | 241 | 4.1 | 1.7 |
| 10 | Arginine | 210 | 200 | 205 | 212 | 213 | 208 | 5.4 | 2.6 |
| 11 | Tyrosine | 193 | 191 | 202 | 203 | 195 | 197 | 4.8 | 2.5 |
| 12 | Valine | 207 | 205 | 200 | 204 | 212 | 208 | 6.0 | 2.9 |
| 13 | Methionine | 183 | 180 | 182 | 185 | 188 | 184 | 3.1 | 1.7 |
| 14 | Cyst(e)ine | 140 | 144 | 141 | 150 | 143 | 144 | 3.9 | 2.7 |
| 15 | Isoleucine | 192 | 184 | 182 | 190 | 188 | 187 | 4.2 | 2.2 |
| 16 | Leucine | 204 | 198 | 198 | 206 | 197 | 201 | 4.1 | 2.1 |
| 17 | Phenylalanine | 184 | 190 | 183 | 189 | 188 | 187 | 3.1 | 1.7 |
| 18 | Tryptophan | 198 (100) | 53 (27) | 151 (76) | 169 (85) | 188 (95) | | | |
| 19 | Lysine | 280 | 290 | 290 | 297 | 281 | 288 | 7.1 | 2.5 |

^a Single values represent the averages of six separate tests.^b Tests without hydrolysis; in parentheses, percentage of the theoretical values.

drolyses in the gas phase are presented in Tables I and II and Fig. 1.

Tryptamine (in the concentration range 15–30 μg per 70 μg of AA or 30 μg of protein) largely protects tryptophan from decomposition. In model solutions the inhibitory effect proved to be 80–95% (Table I) whereas with lysozyme 80% of the tryptophan content could be measured (Table II).

Applying 30 μg of tryptamine per 30–40 μg of α -chymotrypsin, bovine albumin and human albumin for their gas-phase hydrolysis by HCl, 76, 84 and 98% tryptophan contents were measured, respectively.

Regarding the effect of tryptamine on the other amino acids, it can be stated that their presence did not affect either the response values of the other components in model solutions (Table I) or the number of residues found in hydrolysates of lyso-

zyme (Table II, Fig. 1.) The repeatability for all other amino acids, besides tryptophan, obtained with model solutions or after hydrolyses performed with various amounts of tryptamine or without it proved to be good, *i.e.*, ($\leq 3.7\%$ (relative standard deviation) reproducibility data are given in Tables I and II.

These results are important with respect to the advantage of the use of tryptamine as an additive over phenol, even in liquid-phase hydrolysis. The presence of phenol seriously decreased the response of cystine [22]; on using 1–3% phenol-containing HCl for hydrolysis in model tests, the cystine response decreased to 40–50% of its original value.

Concerning the mechanism of the inhibitory effect of tryptamine (tryptamine being a decarboxylated tryptophan and present in a considerable excess over tryptophan), it is very likely that instead

TABLE II

EFFECT OF AMOUNT OF TRYPTAMINE ON THE RECOVERY OF AMINO ACIDS IN HYDROLYSATES OF LYSOZYME BY HYDROLYSIS WITH 6 M HCl AT 145°C FOR 4 h IN THE GAS PHASE, MEASURED AS PTC-AMINO ACIDS BY HPLC

| No. | Amino acid | Moles amino acid per mole protein ^a | | | | Reproducibility data | | | |
|-----|---------------|--|---|------|------|----------------------|---------|------|------------|
| | | Literature data | Tryptamine added (μg per 30 μg lysozyme) | | | | Average | S.D. | R.S.D. (%) |
| | | | 0 | 7.5 | 15 | 30 | | | |
| 1 | Aspartic acid | 20 | 19.7 | 19.8 | 19.5 | 19.6 | 19.6 | 0.14 | 0.7 |
| 2 | Glutamic acid | 5 | 5.1 | 5.1 | 5.1 | 5.0 | 5.1 | 0.06 | 1.2 |
| 4 | Serine | 8 | 8.2 | 8.0 | 7.8 | 8.0 | 8.0 | 0.16 | 2.0 |
| 5 | Glycine | 12 | 11.9 | 11.7 | 12.0 | 11.9 | 11.9 | 0.13 | 1.1 |
| 6 | Histidine | 1 | 1.09 | 1.09 | 1.01 | 1.08 | 1.05 | 0.04 | 3.5 |
| 7 | Threonine | 7 | 6.5 | 6.4 | 6.6 | 6.5 | 6.5 | 0.08 | 1.3 |
| 8 | Alanine | 12 | 11.9 | 12.0 | 12.0 | 12.1 | 12.0 | 0.08 | 0.7 |
| 9 | Proline | 2 | 2.04 | 2.04 | 2.11 | 2.08 | 2.08 | 0.04 | 1.8 |
| 10 | Arginine | 11 | 11.2 | 11.1 | 10.8 | 11.1 | 11.1 | 0.18 | 1.6 |
| 11 | Tyrosine | 3 | 2.95 | 3.15 | 3.20 | 3.11 | 3.13 | 0.11 | 3.6 |
| 12 | Valine | 6 | 6.1 | 6.0 | 6.0 | 6.0 | 6.0 | 0.05 | 1.0 |
| 13 | Methionine | 2 | 2.25 | 2.20 | 2.10 | 2.16 | 2.18 | 0.06 | 2.9 |
| 14 | Cyst(e)ine | 8 | 8.5 | 8.2 | 8.4 | 8.0 | 8.3 | 0.22 | 2.7 |
| 15 | Isoleucine | 6 | 6.2 | 6.2 | 6.0 | 6.1 | 6.1 | 0.10 | 1.6 |
| 16 | Leucine | 8 | 7.8 | 7.9 | 7.7 | 7.7 | 7.8 | 0.1 | 1.3 |
| 17 | Phenylalanine | 3 | 2.99 | 3.03 | 3.00 | 2.94 | 2.98 | 0.04 | 1.3 |
| 18 | Tryptophan | 6 | 0.6 | 3.4 | 4.8 | 4.8 | | | |
| | | | (10) | (57) | (80) | (80) | | | |
| 19 | Lysine | 6 | 6.0 | 6.3 | 6.2 | 6.1 | 6.2 | 0.14 | 2.3 |

^a As in Table I, literature data: [25].

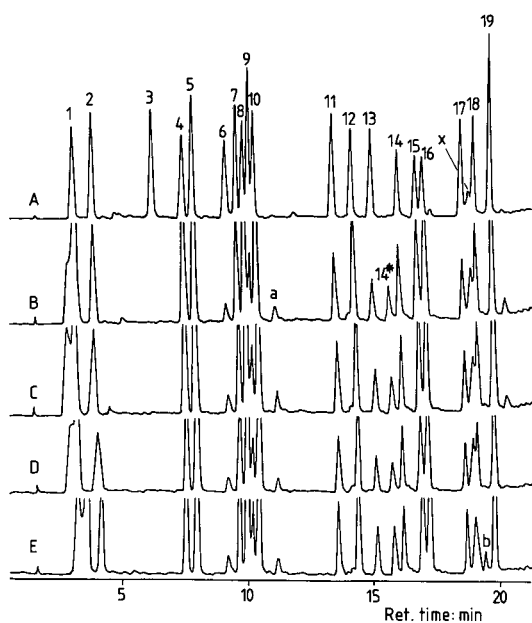


Fig. 1. Chromatograms of AA solution (A, detailed data in Table I: first column of data) and those of lysozyme hydrolysates (B-E, detailed data in Table II) obtained by HCl hydrolysis in the presence of (B) 30, (C) 15 and (D) 7.5 μg of tryptamine and (E) without additive. Peak identification as in Tables I and II; also, a = unknown component of lysozyme; b = decomposition product of tryptophan; x = reagent impurity: in AA solution (0.6 cm^3 volume) proved to be the half compared to those in lysozyme hydrolysates (0.3 cm^3 volume). 14* = Cystine separates into two peaks, as a result of racemization during hydrolysis. Note: aspartic acid in large amounts elutes as two peaks.

of tryptophan, tryptamine takes part in those undesirable interactions which lead to the decomposition of tryptophan.

In conclusion, tryptamine as an additive in gas-phase HCl hydrolysis, providing 76–98% recovery of tryptophan from a single hydrolysate with one injection together with other amino acids with 100% recovery, can be utilized as a powerful protocol in the rapid analysis of protein hydrolysates.

REFERENCES

- 1 J. C. Huet and J. C. Pernollet, *J. Chromatogr.*, 355 (1986) 451.
- 2 H. K. Nielsen and R. F. Hurrell, *J. Sci. Food Agric.*, 36 (1985) 893.
- 3 H. Sato, T. Seino, T. Kobayashi, A. Murai and Y. Yugar, *Agric. Biol. Chem.*, 48 (1984) 2961.
- 4 R. L. Levine, *J. Chromatogr.*, 236 (1982) 499.
- 5 P. J. Buttery and J. B. Soar, *J. Sci. Food Agric.*, 26 (1975) 1273.
- 6 A. P. Williams, D. Hewitt and P. J. Buttery, *J. Sci. Food Agric.*, 33 (1982) 860.
- 7 T. E. Hugli and S. Moore, *J. Biol. Chem.*, 247 (1972) 2828.
- 8 R. Know, G. O. Kohler, R. Palter and H. G. Walker, *Anal. Biochem.*, 36 (1970) 136.
- 9 E. L. Miller, *J. Sci. Food Agric.*, 18 (1967) 381.
- 10 J. R. Spies, *Anal. Chem.*, 39 (1967) 1412.
- 11 R. J. Simpson, M. R. Neuberger and T. Y. Liu, *J. Biol. Chem.*, 251 (1976) 1936.
- 12 T. Y. Liu and Y. H. Chang, *J. Biol. Chem.*, 246 (1971) 2842.
- 13 J. Gundel and E. Votisky, *Tagungsber. Akad. Landwirtschaftswiss. DDR*, 124 (1974) 59.
- 14 B. Penke, R. Ferenczi and K. Kovács, *Anal. Biochem.*, 60 (1974) 59.
- 15 R. J. Richard, M. R. Neuberger and T. Y. Liu, *J. Biol. Chem.*, 251 (1976) 1936.
- 16 R. B. Ashworth, *J. Assoc. Off. Anal. Chem.*, 70 (1987) 80.
- 17 M. L. G. Gardner, *Anal. Biochem.*, 141 (1984) 429.
- 18 P. Felker, *Anal. Biochem.*, 76 (1976) 192.
- 19 H. Matsubara and R. M. Sasaki, *Biochem. Biophys. Res. Commun.*, 35 (1969) 175.
- 20 L. C. Gruen and P. W. Nicholls, *Anal. Biochem.*, 47 (1972) 348.
- 21 L. T. Ng, A. Pascaud and M. Pascaud, *Anal. Biochem.*, 167 (1987) 47.
- 22 K. Muramoto and H. Kamiya, *Anal. Biochem.*, 189 (1990) 223.
- 23 V. Fábrián, M. P. Szakács and I. M. Perl, *J. Chromatogr.*, 520 (1990) 193.
- 24 M. Morvai, V. Fábrián and I. M. Perl, *J. Chromatogr.*, 600 (1992) 87.
- 25 R. L. Heinrikson and S. C. Meredith, *Anal. Biochem.*, 136 (1984) 65.

High-performance liquid chromatographic quantitation of phenylthiocarbamyl muramic acid and glucosamine from bacterial cell walls

Steven R. Hagen

Ribi ImmunoChem Research, Inc., 553 Old Corvallis Road, Hamilton, MT 59840 (USA)

ABSTRACT

A sensitive assay for the simultaneous determination of muramic acid and glucosamine from bacterial cell walls was developed. Cell wall skeleton (CWS) preparations were hydrolyzed with HCl to liberate free amino sugars, which were subsequently derivatized pre-column with phenylisothiocyanate. The phenylthiocarbamoyl (PTC) amino sugars were rapidly resolved by reversed-phase gradient HPLC and quantified with UV detection. With this assay, *Mycobacterium phlei* CWS samples were found to contain muramic acid levels comparable to those found with a specific enzymatic assay. However, a colorimetric total hexosamine assay gave values 20–30% higher than those obtained by the specific PTC amino sugar assay. The detection limit of each PTC amino sugar was 5 pmol.

INTRODUCTION

A unique feature of bacterial cell walls is their peptidoglycan component, which is composed of the amino sugars muramic acid (MA) and glucosamine (GlcN), and amino acids.

Since MA is unique to bacteria, the measurement of peptidoglycan amino sugars has relevance in several lines of research, including: bacterial cell wall biochemistry [1], cell wall immunomodulating and antitumor properties [2], and specific measurement of bacterial biomass and infection [3–5].

Peptidoglycan amino sugars have increasingly been quantified by chromatographic techniques, which potentially are more specific and sensitive than traditional colorimetric assays. GLC–MS has been successfully employed for the determination of bacterial cell wall MA [5–8]. HPLC analysis of MA and GlcN using pre-column derivatization reagents for amino acids, and hardware for amino acid anal-

ysis has resulted in low detection limits (10 pmol) and rapid sample preparation protocols [3,4,9].

This paper describes a more sensitive HPLC analysis of phenylthiocarbamyl (PTC) MA and GlcN after pre-column derivatization with phenylisothiocyanate (PITC), a widely employed reagent for amino acid analysis [10–12]. The method described involved a relatively simple sample preparation protocol and the detection limit for the PTC amino sugars was 5 pmol (signal-to-noise ratio of 3:1).

EXPERIMENTAL

Reagents

HPLC-grade acetonitrile (MeCN), methanol, sodium acetate trihydrate, water and reagent-grade concentrated hydrochloric acid were obtained from J. T. Baker (Phillipsburg, NJ, USA). HPLC-grade glacial acetic acid and phosphoric acid were obtained from Fisher Scientific (Pittsburgh, PA, USA). H amino acid standard (H-std), sequal grade PITC and HPLC-grade triethylamine (TEA) were obtained from Pierce (Rockford, IL, USA).

Correspondence to: Dr. S. R. Hagen, Ribi ImmunoChem Research, Inc., 553 Old Corvallis Road, Hamilton, MT 59840, USA.

L-Cysteic acid (CYA), D-glucosamine-HCl, muramic acid and disodium hydrogenphosphate were obtained from Sigma (St. Louis, MO, USA).

Sample hydrolysis

Cell wall skeleton (CWS) preparations (Ribi ImmunoChem Research, Hamilton, MT, USA; Nos. 014-104 to 014-107) were hydrolyzed *in vacuo* at 100°C for 12 to 42 h in 4 M HCl which contained 118.2 μmol CYA as an internal standard (2.00 mg CWS/ml acid solution).

Pre-column derivatization

Aliquots (100 μl) of sample hydrolysates in 50 \times 6 mm borosilicate glass tubes were dried to < 125 mTorr (1 Torr = 133.322 Pa) on a Picotag (Waters, Milford, MA, USA) vacuum station, then dried again after the addition of 20 μl of redry solution (methanol-water-TEA, 2:2:1). Finally, 20 μl of derivatizing solution (methanol-water-TEA-PITC, 7:1:1:1) was added to each tube, and the mixtures were held at atmospheric pressure for 5 min and then dried as stated above.

Calibration standard

Aliquots (20 μl) of a stock standard solution (which contained 591 μmol CYA, 928 μmol GlcN and 995 μmol MA) were subjected to the derivatization procedure as described above. Note: dry derivatized sample and standard preparations are stable for at least 3 weeks at -20°C.

Dilution prior to injection

Derivatized CWS and standard preparations were reconstituted in 100 μl of diluent (5 mM disodium hydrogenphosphate titrated to pH 7.5 with 5% phosphoric acid and mixed with MeCN; buffer: MeCN = 95:5, v/v). HPLC analyses of 10- μl aliquots of samples and 5-, 10-, 15- and 20- μl aliquots of calibration standards were conducted within 24 h after reconstitution with diluent.

Chromatography

Waters HPLC hardware was used: a WISP 700 autosampler, two 510 pumps, a Nova-pak 300 \times 3.9 mm stainless-steel 4 μm C₁₈ column (preceded by a 0.2- μm in-line filter) operated at 46°C inside a temperature control module, and a 440 spectrometer equipped with a 254-nm filter. The HPLC sys-

TABLE I

SOLVENT GRADIENT CONDITIONS USED FOR THE PTC AMINO SUGAR HPLC ANALYSES

| Time (min) | Flow (ml/min) | Percent eluent A | Percent eluent B | Curve type |
|------------|---------------|------------------|------------------|------------|
| 0.0 | 1.0 | 100.0 | 0.0 | — |
| 10.0 | 1.0 | 100.0 | 0.0 | — |
| 10.5 | 1.0 | 0.0 | 100.0 | Linear |
| 11.0 | 1.5 | 0.0 | 100.0 | — |
| 16.0 | 1.5 | 0.0 | 100.0 | — |
| 16.5 | 1.5 | 100.0 | 0.0 | Linear |
| 29.0 | 1.5 | 100.0 | 0.0 | — |
| 29.5 | 1.0 | 100.0 | 0.0 | — |

tem was controlled via a system interface module (SIM, Waters) by Maxima software (version 3.3, Waters) run in a NEC SX20 computer.

Eluents

The solvent system consisted of two eluents. Eluent A was an aqueous buffer of 0.05 M sodium acetate trihydrate, containing 0.1% (v/v) TEA and titrated to the desired pH (the range tested was pH 4.3 to 6.4) with glacial acetic acid; the buffer was mixed (v/v) with MeCN (the range tested was 3 to 6% MeCN). Eluent B, which was used solely as a column washing solvent, was MeCN-water (60:40, v/v). The solvent gradient utilized is displayed in Table I.

Quantitation

Chromatographic data were collected via the SIM and processed by the Maxima software. Injections of the calibration standard were used to prepare standard curves, and internal standard quantitation was used to calculate analyte concentrations.

Optimization of chromatographic conditions

The process was aided by preparing various H-std and calibration standard PTC derivatives as described above for the calibration standard preparation.

Standard addition experiments

CWS was treated as described above for samples, except that 4 M HCl spiked with GlcN (92.8 μmol),

MA (99.5 μmol) and CYA (118.2 μmol) was used. Recovery was evaluated by comparing peak areas of the spiked CWS samples to those of the non-spiked CWS samples.

Enzymatic MA and colorimetric total hexosamine assays

MA was measured in the CWS hydrolysates enzymatically as described by Tipper [13]. Total hexosamine was measured spectrophotometrically after CWS hydrolysis as described by Smith and Gilkerson [14].

RESULTS AND DISCUSSION

Chromatographic optimization was accomplished by starting with HPLC conditions similar to those employed for PTC amino acid analysis [10–12]. Specifically, standard and sample preparations were initially chromatographed on the Nova-Pak column using eluent A at pH 6.4 mixed 94:6 (v/v) with MeCN (gradient conditions as in Table I). Extensive interference was observed between the PTC amino sugars and amino acids. Therefore, the pH

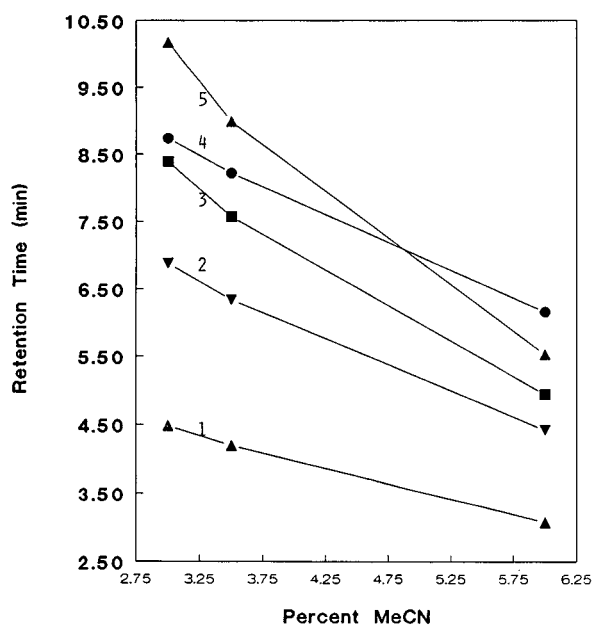


Fig. 1. The effects of eluent A MeCN content (percent, v/v) on the elution of PITC-derivatized CYA (1), MA (2), GlcN (4), aspartic acid (3) and glutamic acid (5).

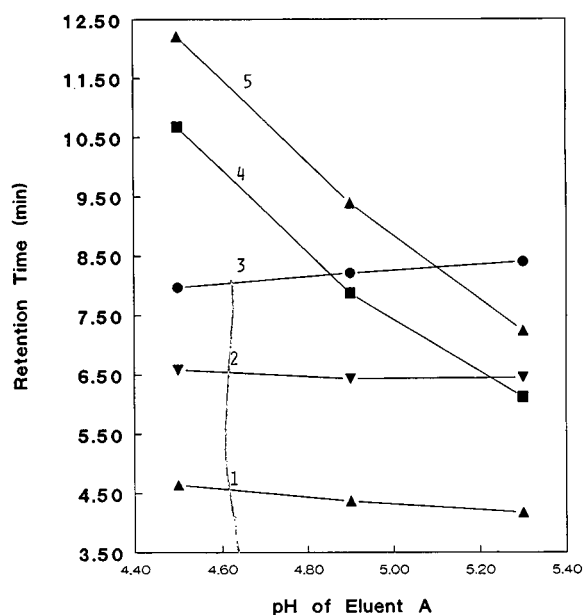


Fig. 2. The effects of eluent A pH on the elution of PITC-derivatized CYA (1), MA (2), GlcN (3), aspartic acid (4) and glutamic acid (5).

of eluent A was decreased incrementally until resolution of the major PTC amino sugar peaks was obtained in the pH range of 5.1–5.3. Further resolution was achieved by altering the MeCN content (between 3 and 6%, v/v) of eluent A (pH 5.1). The results of these tests indicated the optimal MeCN content to be 3.5% (v/v) (Fig. 1). Finally, the pH of eluent A with 3.5% (v/v) MeCN was decreased incrementally to pH 4.5 (Fig. 2). At a pH of 4.5 the internal standard (CYA) and major PTC amino sugar peaks eluted well before any possible interfering PTC amino acids, resulting in very rugged chromatographic conditions. Calibration standard and CWS analyses using eluent A adjusted to pH 4.5 and mixed 96.5:3.5 (v/v) with MeCN (10- μl injection volumes) are displayed in Fig. 3 (note the different y-axis scaling for each chromatogram).

An additional test of eluent A at pH 4.3 was made which revealed that at this pH the minor PTC amino sugar peaks in samples could be resolved. Major/minor peak area ratios for PTC MA and GlcN were identical in calibration standard and sample analyses under these conditions, suggesting that use of only the major peak areas for calibration

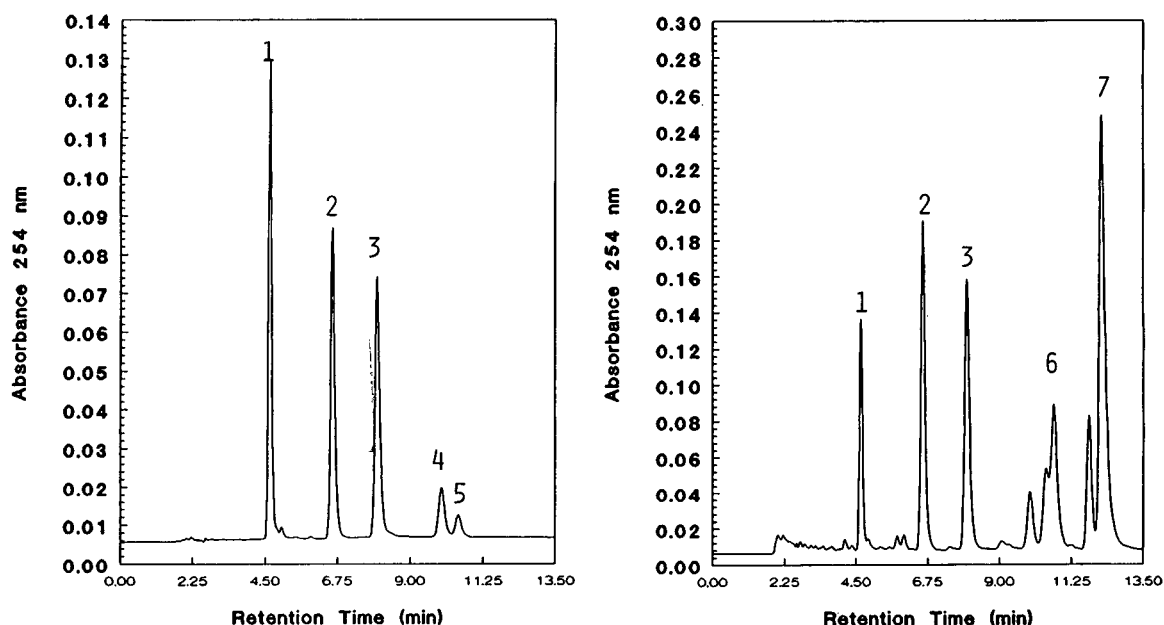


Fig. 3. Calibration standard (left) and CWS (right) chromatograms representing 10- μ l injections of reconstituted sample are shown. Note the differences in y -axis scaling for each chromatogram. 1 = CYA; 2,4 = MA; 3,5 = GlcN; 6 = aspartic acid; 7 = glutamic acid.

and quantitation was sufficient. Eluent A should not be adjusted below pH 4.5 for routine analyses, however, since resolution of MA and GlcN decreases as pH is lowered (Fig. 2).

After the chromatographic conditions were optimized, the duration of sample hydrolysis at 100°C resulting in maximal release of MA and GlcN was determined. Hydrolysis times from 12 to 42 h were tested twice, with comparable results indicating maximal release of MA (one-way analysis of variance, ANOVA $p = 0.0060$) after 30 h at 100°C and qual release of GlcN (ANOVA $p = 0.1085$) throughout (Fig. 4). In subsequent analyses of CWS, 30 h of hydrolysis at 100°C was used.

Day-to-day analytical variability was tested by preparing and analyzing samples independently four times. Variability in MA and GlcN response was low, with individual daily results having relative standard deviations (R.S.D.s) below 4% and the overall average R.S.D. below 6% (Table II).

CWS samples were spiked with standards in standard addition experiments to test for possible sample matrix effects on standard recovery. However, no matrix effects were observed, since the recoveries

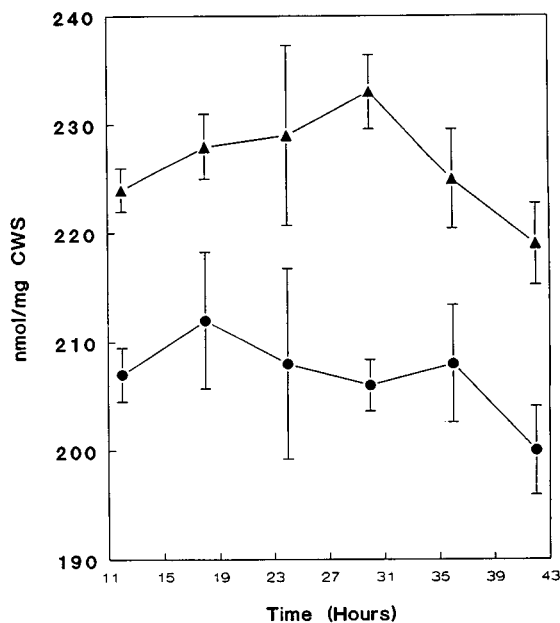


Fig. 4. The release of MA and GlcN from CWS as a function of heating time in 4 M HCl at 100°C is displayed. Each data point represents the mean of four samples, and the error bars represent one standard deviation of the mean. ▲ = Muramic acid; ● = glucosamine.

TABLE II

DAY-TO-DAY ANALYTICAL VARIABILITY OF THE PTC AMINO SUGAR ASSAY

One preparation of CWS (Ribi No. 014-107) was analyzed independently for MA and GlcN content on four separate dates. NA = Not applicable.

| Analysis date | Average MA (R.S.D., %) (nmol/mg CWS) | Average GlcN (R.S.D., %) (nmol/mg CWS) | <i>n</i> |
|-----------------|---|---|----------|
| March 30, 1992 | 238 (2.24) | 207 (3.44) | 4 |
| March 31, 1992 | 236 (1.88) | 235 (1.12) | 4 |
| April 3, 1992 | 252 (1.06) | 216 (1.69) | 4 |
| April 21, 1992 | 239 (0.63) | 226 (1.44) | 4 |
| Overall Average | 241 (3.02) | 221 (5.49) | NA |

of standards added to CWS samples (two times, independently) prior to acid hydrolysis approximated 100% (Table III).

The PTC amino sugar assay was compared to a specific enzymatic (lactate release) assay for MA [13]. Both assays yielded nearly identical results for MA content when four different CWS preparations were tested (Table IV). The total MA and GlcN content as determined by the PTC assay was also

compared to a colorimetric total hexosamine assay [14]. This experiment revealed 20–30% lower results for the PTC-based assay (Table IV).

The ratio of MA/GlcN was found to be 1.09 with the PTC amino sugar assay (using the overall average values from Table II), which is very close to the theoretical MA/GlcN ratio of 1.0 expected for bacterial CWS peptidoglycan. This ratio determined with the PTC assay and the agreement between the

TABLE III

AVERAGE PERCENT RECOVERIES OF MA AND GlcN ADDED TO SUBSAMPLES OF CWS (RIBI No. 014-107) DETERMINED INDEPENDENTLY TWO TIMES

| Analysis date | Recovery MA (R.S.D., %) | Recovery GlcN (R.S.D., %) | <i>n</i> |
|----------------|-------------------------|---------------------------|----------|
| March 31, 1992 | 102 (2.65) | 105 (3.11) | 4 |
| April 3, 1992 | 102 (2.01) | 102 (5.48) | 4 |

TABLE IV

SAMPLES FROM FOUR CWS PREPARATIONS ANALYZED AFTER ACID HYDROLYSIS WITH THREE ASSAYS [PTC AMINO SUGAR (PTC); ENZYMATIC MA (ENZ); COLORIMETRIC TOTAL HEXOSAMINE (TOT HEX)] IN ORDER TO COMPARE THEM

Values are listed as $\mu\text{mol/mg}$ CWS.

| CWS No. | MA (PTC) | MA (Enz) | MA + GlcN (PTC) | Tot Hex |
|---------|----------|----------|--------------------|---------|
| 014-104 | 0.20 | 0.24 | 0.38 | 0.60 |
| 014-105 | 0.23 | 0.23 | 0.45 | 0.62 |
| 014-106 | 0.25 | 0.23 | 0.49 | 0.58 |
| 014-107 | 0.24 | 0.22 | 0.46 | 0.57 |

MA values derived from the PTC and enzymatic methods suggest that the total hexosamine values from colorimetric assay were erroneously high, possibly due to sample matrix interferences.

The PTC amino sugar assay was more versatile than the enzymatic assay [13], and was shown to be superior to the colorimetric assay [14] owing to its greater specificity. The PTC assay exhibited a lower detection limit (5 pmol per injection vs. 10 pmol) than other published HPLC assays for CWS amino sugars [3,9], and a limit comparable to that of GLC–MS analysis [8]. The PTC assay described had the advantages of a relatively simple sample preparation protocol and very rugged chromatographic characteristics. Finally, in addition to pure bacterial CWS, this assay should be applicable to whole-cell amino sugar analysis:

REFERENCES

- 1 R. J. Doyle, J. Chaloupka and V. Vinter, *Microbiol. Rev.*, 52 (1988) 554.
- 2 J. Tomasic, L. Sesartic, S. A. Martin, Z. Valinger and B. Ladesic, *J. Chromatogr.*, 440 (1988) 405.
- 3 T. Mimura and D. Delmas, *J. Chromatogr.*, 280 (1983) 91.
- 4 L. Zelles, *Biol. Fertil. Soils*, 6 (1988) 125.
- 5 B. Christensson, J. Gilbert, A. Fox and S. L. Morgan, *Arthritis Rheum.*, 32 (1989) 1268.
- 6 A. Fox, J. H. Schwab and T. Cochran, *Infect. Immun.*, 29 (1980) 526.
- 7 A. Fox, J. C. Rogers, J. Gilbert, S. Morgan, C. H. Davis, S. Knight and P. B. Wyrick, *Infect. Immun.*, 58 (1990) 835.
- 8 A. Fox and K. Fox, *Infect. Immun.*, 59 (1991) 1202.
- 9 H. Takemoto, S. Hase and T. Ikenaka, *Anal. Biochem.*, 145 (1985) 245.
- 10 S. A. Cohen and D. J. Strydom, *Anal. Biochem.*, 174 (1988) 1.
- 11 S. R. Hagen, B. Frost and J. Augustin, *J. Assoc. Off. Anal. Chem.*, 72 (1989) 912.
- 12 S. R. Hagen, J. Augustin, E. Grings and P. Tassinari, *Food Chem.*, (1992) in press.
- 13 D. J. Tipper, *Biochemistry*, 60 (1968) 1441.
- 14 R. L. Smith and E. Gilkerson, *Anal. Biochem.*, 98 (1979) 478.

Detection of alkaloids in foods with a multi-detector high-performance liquid chromatographic system

Lorrie A. Lin

National Forensic Chemistry Center, US Food and Drug Administration, 1141 Central Parkway, Cincinnati, OH 45202 (USA)

ABSTRACT

A general screening method for alkaloid drugs in foods is described based on high-performance liquid chromatography with ultraviolet detection at three wavelengths, followed by fluorescence and electrochemical detectors in series. The chromatographic conditions include an ion-pairing reagent, which makes it possible to chromatograph acidic and basic drugs with one screen. Relative response ratios were determined from the peak areas of the alkaloids on the basis of all the detector signals. These ratios were used to create a "fingerprint" of the drugs and to predict the identity of an unknown component in a sample matrix. The fluorescence and electrochemical detectors allowed a detection limit for many of the alkaloids which would not be attainable with the ultraviolet detector alone. Typical detection limits with the electrochemical detector were 5–50 ng/ml and with the fluorescence detector 5–500 ng/ml, while the ultraviolet detector had detection limits of 1–20 µg/ml. The spiking concentrations in the relative response ratio experiments were approximately five times above the lowest detection limit. The extraction method investigated for orange juice yielded recoveries for most alkaloids of 80–100%. A stability study of ergot alkaloids in various food matrices demonstrated degradation, depending on the matrix, temperature, and duration of the experiment.

INTRODUCTION

The public food supply must be kept safe from accidental or purposeful contamination during product manufacturing and marketing. In several cases, contamination of a food product has caused serious illness or death to an unsuspecting consumer. Drugs are likely sources of contamination due to their ready availability. This paper focuses on the extraction of alkaloid drugs from orange juice as part of a screening method for alkaloids in foods. This work includes a study which evaluates the stability of ergot alkaloids in a variety of food matrices. The extracts are analyzed by a high-performance liquid chromatographic (HPLC) system which con-

sists of a UV detector that can detect three wavelengths simultaneously, a fluorescence detector, and an electrochemical detector. The use of multiple detectors has been shown to be effective in other forensic laboratories [1–5].

Determinations in which multi-detector systems are used can potentially generate chemical fingerprints of unknowns by using relative response ratios. This "fingerprint" identification is particularly applicable to drugs because most are amenable to UV, fluorescence, and/or electrochemical detection.

A problem which frequently occurs in a forensic laboratory is sample size limitation. In some cases there is only a small amount of sample to begin with and in other cases, several laboratories may have previously handled the sample, diminishing the amount of sample available. Generally, in order to get a conclusive identification of the sample, multiple analyses must be completed. One approach to decreasing the number of individual sample analy-

Correspondence to: Dr. L. A. Lin, National Forensic Chemistry Center, US Food and Drug Administration, 1141 Central Parkway, Cincinnati, OH 45202, USA.

ses and conserving sample is to have multiple detectors on line.

A drug data base has been developed on this system using relative response ratios of the three detectors. Using this method, it is possible to make an early prediction of the identity of an unknown component in a sample before confirmation by mass spectrometry can be completed. For example, a sample contains an unknown peak with a retention time equivalent to that for lysergic acid. However, unlike lysergic acid, the unknown does not demonstrate any electrochemical activity. Therefore, lysergic acid could be eliminated as a possible contaminant.

EXPERIMENTAL

Reagents

All of the alkaloids used in this study were obtained from Sigma. HPLC-grade methanol was obtained from J. T. Baker or equivalent. ACS-grade potassium phosphate monobasic was obtained from Fisher Scientific or equivalent. 1-Octanesulfonic acid was obtained from Sigma. ACS-grade potassium chloride was obtained from Fisher Scientific or equivalent. 85% ACS-grade phosphoric acid was obtained from Fisher Scientific or equivalent.

Standards

Stock standards were prepared in concentrations ranging from *ca.* 5000 to 20 000 $\mu\text{g}/\text{ml}$. The standards were prepared in an 80% methanol solution and the stock standards stored in the refrigerator. On the day of analysis a working standard was prepared by dilution of the stock standard solution with methanol.

Sample preparation

Sample matrices studied included orange juice, vegetable juice, milk, and a cola beverage. To prepare spikes, 2 ml of sample were placed in a polyethylene tube. The spiking solution, which consists of several alkaloids that produce a final concentration of 30–100 $\mu\text{g}/\text{ml}$ of each alkaloid in the sample, was added. In addition, method blanks were prepared that did not contain any spiking solution.

Preparation of orange juice and vegetable juice samples involved extraction using Analytichem C₁₈ solid-phase extraction (SPE) 1-ml cartridges using a

Supelco SPE vacuum manifold. To perform the extraction, 2 ml of 0.005 *M* 1-octanesulfonic acid (1-octanesulfonic acid allowed for better binding of the alkaloids to the SPE column) were added to 2 ml of juice, followed by vortex-mixing on high speed for 1 min. The SPE column was conditioned with 3 ml of methanol, followed by 3 ml of water. The column was not allowed to go to dryness after the methanol and water conditioning. The sample was applied to the SPE column (avoiding the column to go to dryness) and the column was washed with 3 ml of 10% methanol in water. The column was dried for 5 min after the methanol had washed through the column. The sample was eluted with 3 \times 1 ml of methanol and the column was dried for 2 min after the final methanol wash. The sample was filtered with 0.2- μm filters from Alltech Assoc. A 5- μl aliquot was injected onto the HPLC column.

Preparation of milk samples first involved precipitation of the proteins with HCl. To 2 ml of milk, 2 ml of 1 *M* HCl were added, followed by vortex-mixing on high speed for 1 min. The sample was centrifuged for 10 min. Then 1 ml of 0.005 *M* 1-octanesulfonic acid was added to the supernatant. Extraction was carried out as described above for the juices.

SPE was not necessary to clean up the cola sample. A 2-ml sample was mixed with 1 ml of methanol (1-octanesulfonic acid was not used as the sample was not eluted through an SPE column), followed by vortex-mixing, filtering, and injection of 5 μl of the sample onto the HPLC column.

Instrumentation

A Hewlett-Packard 1050 HPLC system was employed for these analyses. The 1050 included the 1050 autosampler, 1050 quaternary pumping system and the 1050 multiple-wavelength detector. Three signals can be collected from the multiple wavelength detector. The signals that were used for the analysis were 330, 280, and 254 nm. In addition to this detector, an HP 1045A programmable fluorescence detector and an HP 1049A programmable electrochemical detector were used. Each of these detectors were set with 1 V full-scale ranges at the factory and those ranges were not changed in this laboratory. The fluorescence detector was operated with an excitation wavelength of 254 nm and an emission wavelength of 408 nm. The slit width of

the excitation wavelength was 2 mm × 2 mm (equivalent to a 25-nm bandwidth) and the slit width of the emission wavelength was 4 mm × 4 mm (equivalent to a 50-nm bandwidth). The detector was set with a PMT gain of 12 and a response time of 6. The electrochemical detector was operated in the amperometric mode at a potential of 1.2 V versus an Ag/AgCl reference electrode with a glassy carbon working electrode. The electrochemical detector was equipped with a solvent thermostat that was maintained at 40°C.

The HPCL system was controlled by HP Chem Station Phoenix software. An HP Vectra 386/25 computer was employed. Since the software could not directly take the signals from the fluorescence and electrochemical detectors, an analog-to-digital converter was used for this purpose. The converter was an HP 35900. The data were printed by an HP Laser Jet III printer.

The column, obtained from Interaction Chemicals (pn 50838-1), was a C₁₈ 250 × 4.6 mm I.D., column, 5 μm particle size. A column heater was set at 30°C.

The mobile phase consisted of phosphate buffer, methanol, and 1-octanesulfonic acid as an ion-pairing reagent. To make 1 l of mobile phase, 2.0414 g of monobasic potassium phosphate (15 mM), 0.8112 g of 1-octanesulfonic acid (3.75 mM), and 0.5592 g of potassium chloride (7.5 mM) were added to 550 ml of methanol (55%) (potassium chloride was added to the mobile phase for the electrochemical detector which uses a solid-state Ag/AgCl reference electrode). Water, from a Millipore Milli-Q water purification system equipped with a final 0.22-μm filter, was added to get a final volume of 1 l. The solution was adjusted to pH 4.00 with a 10% solution of phosphoric acid using a Corning 245 pH meter, calibrated with pH 4.00 and pH 7.00 buffers (Fisher Scientific). Finally, the solution was filtered with 0.2-μm filters from Alltech Assoc. During the analysis, the mobile phase was continuous sparged with helium. The flow-rate was 1.0 ml/min.

RESULTS AND DISCUSSION

Relative response ratios

As indicated earlier, relative response ratios can yield a chemical fingerprint. Table I contains a list of alkaloids and their relative response ratios ob-

tained by employing UV detection at three wavelengths (330, 280, and 254 nm) and the signals from the fluorescence and electrochemical detectors. This table was developed by taking the smallest detector response and normalizing that to 1.0. The other detector responses were divided by the smallest detector response to obtain their normalized detector response. For instance, for a 2.5-μg/ml solution of LSD, the raw data counts were 5, 6, 9, 8771, and 93835 area counts for 280 nm, 330 nm, 254 nm, fluorescence, and electrochemical detection, respectively. Since 5 area counts is the smallest figure it was normalized to 1.0. All of the other detection signals were divided by 5 to yield their normalized detector responses. The raw data given above along with the detector settings given in the *Instrumentation* section could be used as a guide for other researchers to normalize their instruments and obtain a comparable table. Fig. 1 illustrates a fingerprint obtained after extraction from an orange juice matrix for morphine, codeine, eserine, and apomorphine using UV at 254 nm, fluorescence and electrochemical detection. The relative response ratios in the juice sample were not different from those of a standard. The retention times of the alkaloids studied are given in Table II.

The surface of the electrode in the electrochemical detector had to be carefully monitored. At the beginning of each experiment, a standard that consisted of 2.5 μg/ml of LSD and 10 μg/ml of ergotamine was injected. These compounds were chosen because they eluted early and late in the chromatogram. The area counts were maintained at least at 50 000 and 100 000 counts for LSD and ergotamine, respectively. If the counts dropped below these, the electrode surface was repolished with a kit obtained from Hewlett-Packard. The electrode surface was repolished every day while data for the relative response ratios were being obtained. Likewise, when an unknown sample is analyzed in this laboratory, the electrode surface is repolished.

This procedure has been used to identify strychnine in a real sample that was sent to this laboratory. The sample contained an unknown component that was not in the control. The unknown eluted at the same time as strychnine and its relative response ratios were the same as those for strychnine. The control was spiked with strychnine and the relative response ratios matched those in the sample. Mass

TABLE I

RELATIVE RESPONSE RATIOS (NORMALIZED DETECTOR RESPONSE RELATIVE TO SMALLEST DETECTOR RESPONSE)

Experimental conditions as described in the text. ND indicates that the compound was not detected.

| Compound | 280 nm | 330 nm | 254 nm | Florescence | Electrochemical |
|-------------------|--------|--------|--------|-------------|-----------------|
| Anabasine | 1.0 | ND | 30 | ND | 2299 |
| Apomorphine | 1.8 | ND | 1.0 | 29 | 1318 |
| Arecoline | ND | ND | 1.0 | ND | 20 881 |
| Atropine | ND | ND | 1.0 | ND | 149 |
| Berberine | 1.1 | ND | 1.0 | ND | 517 |
| Cocaine | 1.0 | ND | 1.3 | ND | 481 |
| Codeine | 1.0 | ND | 1.0 | 7 | 6050 |
| Colchicine | 1.0 | ND | 4.8 | ND | 775 |
| Dihydroergotamine | 3.1 | ND | 1.0 | 26 | 12 521 |
| Emetine | 8.9 | ND | 1.0 | 8 | 6732 |
| Ergocriptine | 1.0 | 1.6 | 4.1 | 1753 | 18 595 |
| Ergonovine | 1.0 | 1.4 | 3.0 | 453 | 54 652 |
| Ergotamine | 1.0 | 1.6 | 4.2 | 1881 | 29 863 |
| Eserine | 1.0 | ND | 8.6 | 99 | 4137 |
| Hydromorphone | 1.4 | ND | 1.0 | ND | 4173 |
| Lobeline | 1.0 | ND | 10 | ND | 462 |
| LSD | 1.0 | 1.2 | 1.8 | 1754 | 18 767 |
| Lysergic acid | 1.0 | 1.3 | 2.6 | 419 | 75 506 |
| Lysergol | 1.0 | 1.2 | 2.3 | 314 | 47 318 |
| Methylergonovine | 1.0 | 1.4 | 2.9 | 461 | 47 476 |
| Morphine | 1.4 | ND | 1.0 | 10 | 3581 |
| Nornicotine | 1.0 | ND | 3.6 | ND | 317 |
| Oxycodone | 1.3 | ND | 1.0 | ND | 3995 |
| Pentazocine | 9.3 | ND | 1.0 | ND | 21 641 |
| Scopolamine | ND | ND | 1.0 | ND | 5431 |
| Strychnine | 1.0 | ND | 3.6 | ND | 1275 |
| Yohimbine | 1.7 | ND | 1.0 | 82 | 918 |

spectrometry confirmed the unknown to be strychnine.

Orange juice extraction

Selected alkaloids were extracted from orange juice (Table III). The number of determinations in all cases was 7 with three method blanks. The blanks were averaged together and subtracted from the spikes should any matrix interference occur. To calculate the total number of analyses, however, 7 was multiplied by the number of detector signals that detected the alkaloid, *i.e.*, a solution of LSD in methanol was detected at all three UV wavelengths, and by the fluorescence and electrochemical detectors. Therefore, the actual number of determina-

tions for LSD was 35. However, a solution of strychnine in methanol was only detected by UV at 280 and 254 nm, and the electrochemical detector. Therefore, the actual number of determinations for strychnine is 21. Each of these determinations were averaged and the response was compared with that obtained for a standard in order to calculate the extraction efficiency for each alkaloid. The extraction efficiencies between detectors was comparable.

Ergot alkaloid matrix stability study

One of the concerns of this laboratory is an estimation of the stability of a poison in a particular product. This information may then be used to assess the inherent risk in a real product contamina-

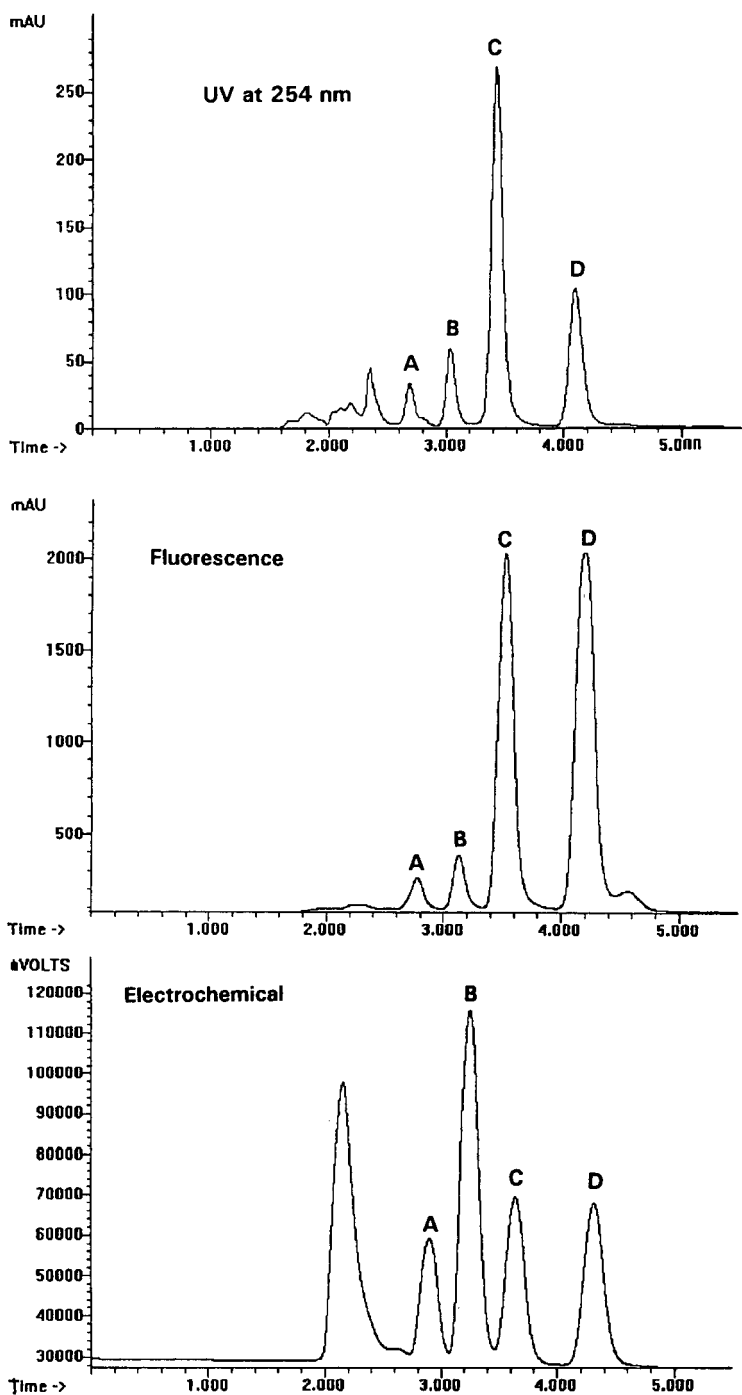


Fig. 1. Chromatograms of spiked orange juice samples. Conditions as described in the text. Peaks: A = morphine; B = codeine; C = eserine; D = apomorphine.

TABLE II
RETENTION TIMES OF ALKALOIDS

| Compound | Retention time (min) |
|-------------------|----------------------|
| Morphine | 2.8 |
| Arecoline | 2.9 |
| Hydromorphone | 3.0 |
| Nornicotine | 3.0 |
| Anabasine | 3.2 |
| Lysergic acid | 3.2 |
| Codeine | 3.3 |
| Oxycodone | 3.5 |
| Eserine | 3.8 |
| Ergonovine | 4.0 |
| Scopolamine | 4.2 |
| Lysergol | 4.3 |
| Apomorphine | 4.6 |
| Methylergonovine | 4.8 |
| Strychnine | 4.8 |
| Atropine | 5.0 |
| Colchicine | 5.5 |
| Cocaine | 7.3 |
| Yohimbine | 9.2 |
| LSD | 9.9 |
| Pentazocine | 10.2 |
| Berberine | 10.3 |
| Emetine | 12.5 |
| Lobeline | 14.8 |
| Ergotamine | 20.1 |
| Dihydroergotamine | 21.4 |
| Ergocriptine | 37.0 |

tion situation. The results of a study such as this are only definitive for the set of conditions used during the course of the study and may not apply to other sets of conditions. In this work, the stability of ergot alkaloids (lysergic acid, ergonovine, lysergol, methylergonovine, LSD, ergotamine, dihydroergotamine, and ergocriptine) was evaluated in orange juice, vegetable juice, milk, and a cola beverage under two different sets of storage conditions (with the exception of milk that was stored in only one condition). These matrices represented a fairly uniform or homogeneous sample matrix. The time period over which the stability was evaluated was two weeks.

Seven spiked samples and three blank drinks were analyzed on day 0 of the study. Seven spikes and three blanks that were refrigerated and seven spikes and three blanks that were stored at room

TABLE III
EXTRACTION OF SELECTED ALKALOIDS FROM ORANGE JUICE

Experimental conditions as described in the text.

| Compound | Spiking concentration ($\mu\text{g/ml}$) | Extraction efficiency ^a (%) |
|-------------------|--|--|
| Apomorphine | 10 | 68 |
| Arecoline | 200 | 94 |
| Codeine | 10 | 111 |
| Dihydroergotamine | 30 | 94 |
| Ergocriptine | 30 | 106 |
| Ergonovine | 5 | 100 |
| Ergotamine | 30 | 100 |
| Eserine | 10 | 100 |
| LSD | 0.125 | 84 |
| Lysergic acid | 5 | 98 |
| Lysergol | 5 | 101 |
| Methylergonovine | 5 | 100 |
| Morphine | 10 | 99 |
| Oxycodone | 10 | 98 |
| Scopolamine | 200 | 80 |
| Strychnine | 10 | 86 |

^a Efficiency = (sample area counts)/(standard area counts) (3/2) (100%); the equation contains the variable 3/2 because in all cases the initial sample volume was 2 ml and the final sample volume was 3 ml.

temperature were analyzed on day 7 (with the exception of milk, that was stored only at refrigerated temperatures). This was repeated on day 14. The samples stored at room temperature were left in the dark. A working standard containing the eight ergot alkaloids listed above at their spiking concentration levels (0.125 $\mu\text{g/ml}$ of LSD; 5 $\mu\text{g/ml}$ of lysergic acid, ergonovine, lysergol, and methylergonovine; and 30 $\mu\text{g/ml}$ of ergotamine, dihydroergotamine, and ergocriptine) was prepared on the first day of analysis. This standard was kept in the refrigerator during the experiment, and used as the standard on days 7 and 14. The percentage recovery from all five signals was determined. These recoveries were in good agreement with each other and were averaged. Tables IV-VII contain the stability study results in the orange juice, vegetable juice, milk, and cola beverage, respectively. The recoveries listed in the tables are the average of the five signals with the exception of dihydroergotamine in the cola beverage because it was not detected and

TABLE IV
PERCENT RECOVERIES OF ERGOT ALKALOIDS IN ORANGE JUICE

Experimental conditions as described in the text. ND indicates that the compound was not detected.

| Compound | Day 0 | Day 7/Refr. ^a | Day 7/RT ^b | Day 14/Refr. ^a | Day 14/RT ^b |
|-------------------|-------|--------------------------|-----------------------|---------------------------|------------------------|
| Dihydroergotamine | 94 | 68 | 64 | 88 | 51 |
| Ergocriptine | 106 | 68 | 80 | 121 | 91 |
| Ergonovine | 98 | 84 | 47 | 74 | 37 |
| Ergotamine | 100 | 70 | 80 | 111 | 79 |
| LSD | 84 | 61 | 86 | ND | ND |
| Lysergic acid | 100 | 94 | 88 | 91 | 72 |
| Lysergol | 101 | 96 | 85 | 93 | 76 |
| Methylergonovine | 100 | 92 | 85 | 89 | 76 |

^a Refrigerated temperature.

^b Room temperature.

TABLE V
PERCENT RECOVERIES OF ERGOT ALKALOIDS IN VEGETABLE JUICE

Experimental conditions as described in the text.

| Compound | Day 0 | Day7/Refr. ^a | Day 7/RT ^b | Day 14/Refr. ^a | Day 14/RT ^b |
|-------------------|-------|-------------------------|-----------------------|---------------------------|------------------------|
| Dihydroergotamine | 23 | 21 | 17 | 27 | 14 |
| Ergocriptine | 21 | 17 | 20 | 24 | 23 |
| Ergonovine | 42 | 27 | 36 | 43 | 55 |
| Ergotamine | 21 | 18 | 15 | 23 | 15 |
| LSD | 23 | 26 | 21 | 21 | 19 |
| Lysergic acid | 29 | 31 | 28 | 35 | 26 |
| Lysergol | 17 | 23 | 15 | 31 | 18 |
| Methylergonovine | 26 | 38 | 21 | 39 | 31 |

^a Refrigerated temperature.

^b Room temperature.

TABLE VI
PERCENT RECOVERIES OF ERGOT ALKALOIDS IN MILK

Experimental conditions as described in the text.

| Compound | Day 0 | Day 7 | Day 14 |
|-------------------|-------|-------|--------|
| Dihydroergotamine | 20 | 14 | 20 |
| Ergocriptine | 23 | 10 | 11 |
| Ergonovine | 30 | 29 | 34 |
| Ergotamine | 19 | 11 | 13 |
| LSD | 49 | 59 | 49 |
| Lysergic acid | 76 | 71 | 80 |
| Lysergol | 29 | 25 | 38 |
| Methylergonovine | 30 | 33 | 33 |

lysergic acid and lysergol in vegetable juice due to matrix interferences. Fluorescence and electrochemical chromatograms of vegetable juice, milk, and the cola beverage are presented in Figs. 2 and 3, respectively.

The recoveries in vegetable juice and milk are much poorer than those in the orange juice and cola beverage. One explanation for the poor recovery of alkaloids from the milk matrix could be the coprecipitation with the proteins. Also note that the recoveries appear to increase with time in the vegetable juice samples. This result is possibly due to a mold growth which occurred in these samples both at room temperature and under refrigeration. The sample preparation was sometimes difficult because

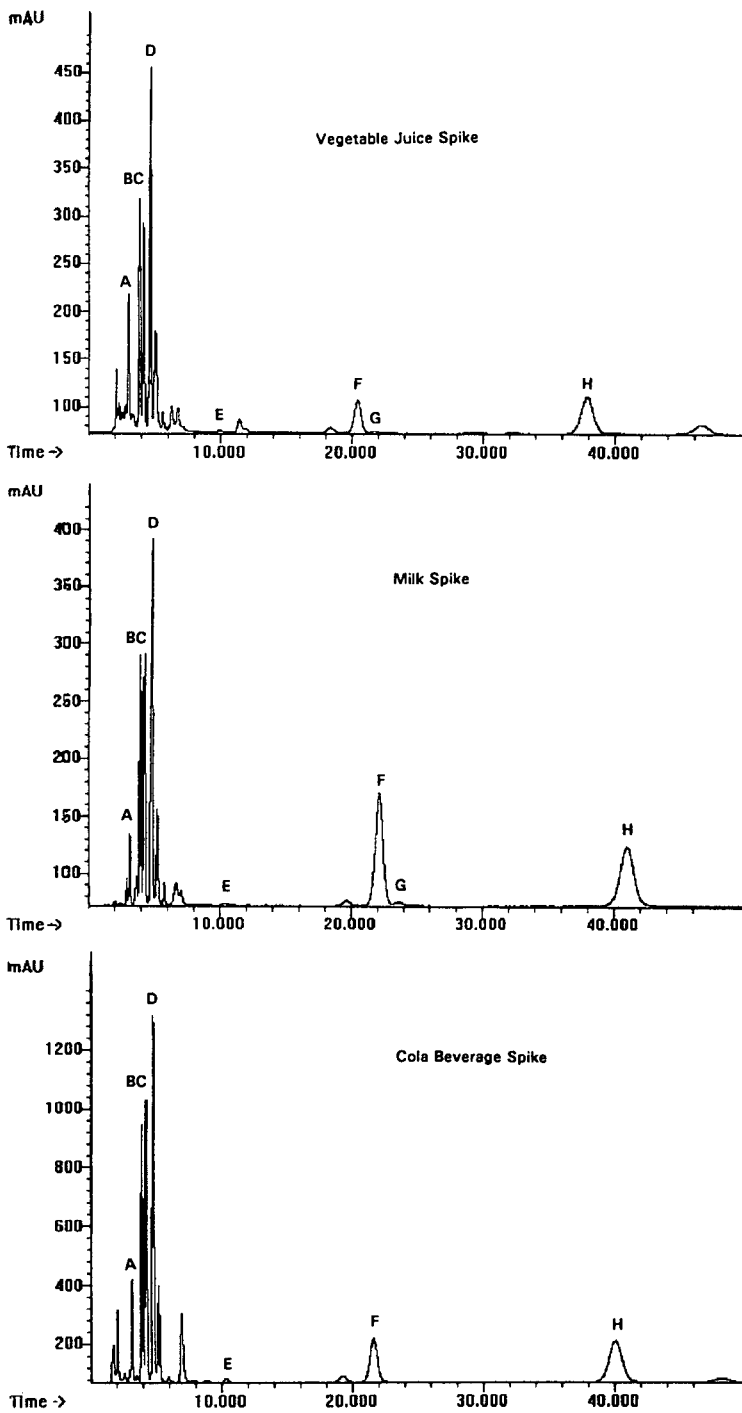


Fig. 2. Fluorescence chromatograms of ergot alkaloids in vegetable juice, milk, and a cola beverage. Peaks: A = lysergic acid; B = ergotamine; C = lysergol; D = methylergonovine; E = ergotamine; G = dihydroergotamine; H = ergocriptine.

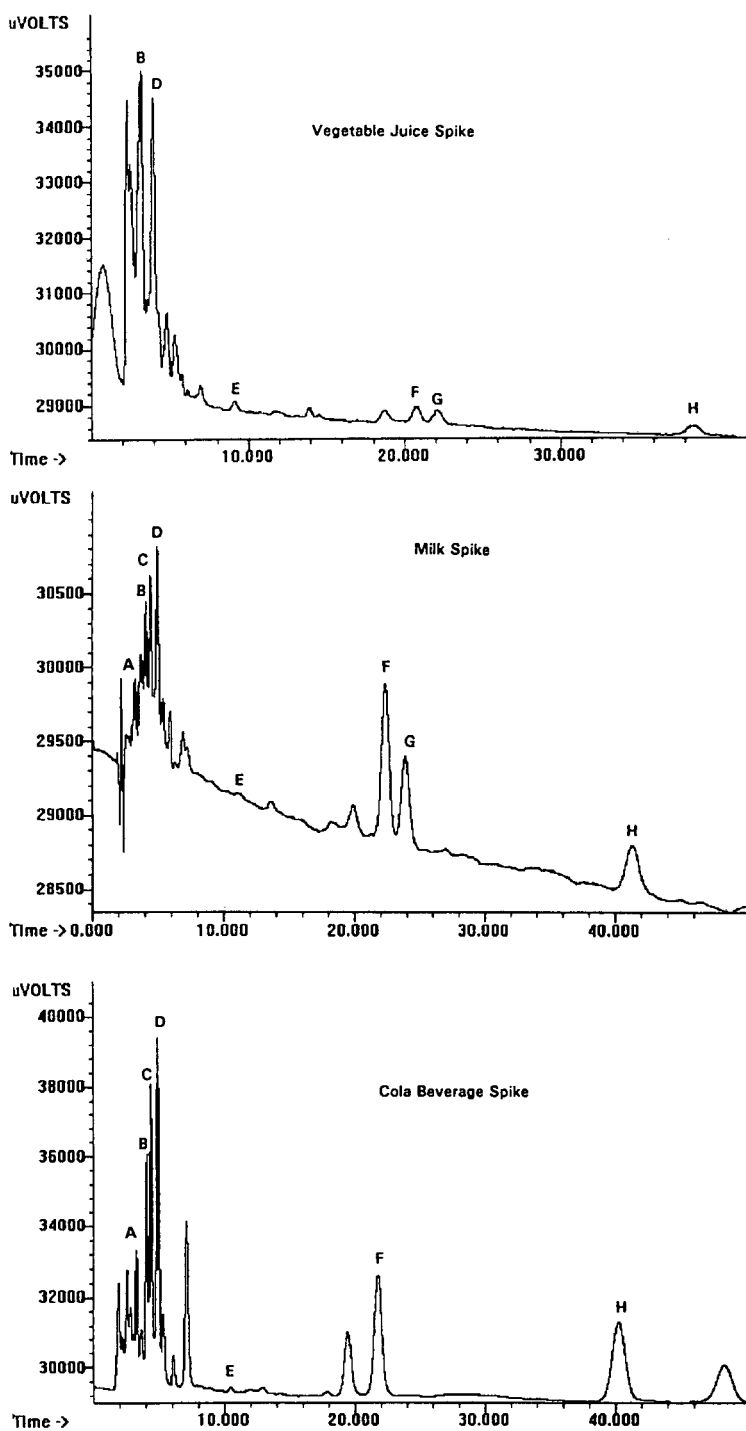


Fig. 3. Electrochemical chromatograms of ergot alkaloids in vegetable juice; milk, and a cola beverage. Peaks: A = lysergic acid; B = ergonovine; C = lysergol; D = methylergonovine; E = LSD; F = ergotamine, G = dihydroergotamine; H = ergocriptine.

TABLE VII

PERCENT RECOVERIES OF ERGOT ALKALOIDS IN COLA BEVERAGES

Experimental conditions as described in the text. ND indicates that the compound was not detected.

| Compound | Day 0 | Day 7/Refr. ^a | Day 7/RT ^b | Day 14/Refr. ^a | Day 14/RT ^b |
|-------------------|-------|--------------------------|-----------------------|---------------------------|------------------------|
| Dihydroergotamine | 45 | ND | ND | ND | ND |
| Ergocriptine | 64 | 64 | 52 | 69 | 46 |
| Ergonovine | 105 | 85 | 73 | 80 | 65 |
| Ergotamine | 39 | 30 | 25 | 39 | 25 |
| LSD | 113 | 78 | 57 | 78 | 57 |
| Lysergic acid | 105 | 87 | 58 | 89 | 67 |
| Lysergol | 103 | 87 | 65 | 88 | 66 |
| Methylergonovine | 101 | 87 | 62 | 80 | 63 |

^a Refrigerated temperature.

^b Room temperature.

not all of the mold could be scraped from the sample and this would hinder during the SPE step. Likewise, the recoveries increase for ergocriptine and ergotamine on day 14 in the orange juice. A matrix interference that could not be resolved from these alkaloids occurred on day 14 which made analyses difficult.

The remaining alkaloids either remained constant over the course of the experiment or slightly decreased with the exception of LSD in orange juice and dihydroergotamine in cola beverage. These components were not detected by the end of the study. It is believed that these components were completely metabolized in these matrices.

CONCLUSIONS

The general HPLC method is a good method for analyzing acidic and basic drugs due to the ion-pairing reagent in the mobile phase. This is demonstrated by the determination of lysergic acid and

lysergol during the same chromatographic run. By using multiple detectors, a chromatographic fingerprint of an unknown drug in a sample can be obtained. This method can be used for the analysis of extracts of drugs from food matrices. Although not all compounds can be detected by each detector or wavelength, it has been shown that each compound will be detected by at least one of the detectors.

Work is continuing in this area. Stability studies are being conducted in other matrices and other classes of drugs are being investigated.

REFERENCES

- 1 I. S. Lurie, *LC · GC*, 8 (1990) 454.
- 2 I. S. Lurie and S. M. Demchuk, *J. Liq. Chromatogr.*, 4 (1991) 337.
- 3 I. S. Lurie and S. M. Demchuk, *J. Liq. Chromatogr.*, 4 (1991) 357.
- 4 R. J. Flanagan and I. Jane, *J. Chromatogr.*, 323 (1985) 173.
- 5 I. Jane, A. KcKinnon and R. J. Flanagan, *J. Chromatogr.*, 323 (1985) 191.

Comparison of columns of chemically modified porous glass and silica in reversed-phase high-performance liquid chromatography of ginsenosides

Hideko Kanazawa, Yoshiko Nagata, Emi Kurosaki and Yoshikazu Matsushima

Kyoritsu College of Pharmacy, Shibakoen 1-5-30, Minato-ku, Tokyo 105 (Japan)

Nobuharu Takai

Institute of Industrial Science, University of Tokyo, Roppongi 7-22-1, Minato-ku, Tokyo 106 (Japan)

ABSTRACT

Reversed-phase high-performance liquid chromatograms of an extract of ginseng and mixtures of ginsenosides (ginseng saponins) on a number of columns of chemically modified porous glass (MPG, pore size 550 Å) and silica (pore size 80 and 300 Å) were compared. Although the retention behaviour of ginsenosides was similar on the columns examined, the capacity factors of ten ginsenosides on an octadecylsilyl-MPG (MPG-ODS) column were smaller than those on silica columns. It is concluded that the MPG-ODS column has a number of advantages over conventional silica-ODS columns for the chromatography of ginsenosides. These properties are attributable to the optimum pore size for the molecular size of the saponins on the one hand and to the narrow distribution range of the pore size on the other.

INTRODUCTION

Microporous glass (MPG) is a promising material as a packing in high-performance liquid chromatography (HPLC) owing to its high chemical resistance and its homogeneous and cylindrical pores. It is stable between pH 2 and 12. The distribution of the pore size is relatively narrow compared with silica [1]. Although chemically modified silicas are one of the most commonly used packing materials, their pore size distributions are broad and sometimes bimodal.

We have prepared octadecylsilyl porous glass (MPG-ODS) and used it as a packing in reversed-phase HPLC [2]. Columns of MPG-ODS have been

successfully used for the analytical and preparative HPLC of ginsenosides, saponins of ginseng [3–8]. Two water–acetonitrile mobile phases have been used for the isocratic elution of water-soluble panaxatriols and other less hydrophilic saponins. Recently, Petersen and Palmqvist [9] reported the HPLC of ginsenosides with a C₁₈ silica column. They used two-step gradient elution with water–acetonitrile for the simultaneous separation of six main ginsenosides. The retention times of ginsenosides on the MPG-ODS column were shorter than those on the octadecylsilylsilica (silica-ODS) columns. We have examined the chromatographic behaviour of the saponins and related compounds on a number of columns. This paper is concerned with a comparison of columns of chemically modified MPG and silica in the reversed-phase HPLC of ginsenosides and other substances.

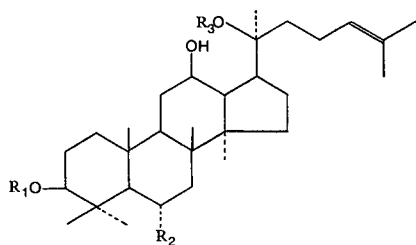
Correspondence to: Y. Matsushima, Kyoritsu College of Pharmacy, Shibakoen 1-5-30, Minato-ku, Tokyo 105, Japan.

EXPERIMENTAL

Materials

The MPG-ODS, silica-ODS (pore size 80 Å; particle size 5 μm) and silica-ODS (pore size 300 Å; particle size 5 μm) used were Hitachi gels 3161, 3156 and 3063, respectively. Other chemically modified packing materials of MPG and silica were prepared by methods analogous to that for MPG-ODS [2]. They were packed into a stainless-steel column (150 × 4.0 mm I.D.) by the slurry method. MPG (particle size 10 μm) was supplied by Ise Chemical Industries. Silica was Hitachi gel 3041.

Malonyl-ginsenosides were kindly supplied by Professor I. Kitagawa of the University of Osaka (Osaka, Japan). Standard samples of ginsenosides were obtained from Wako (Osaka, Japan) and those of estrogens were from Sigma (St. Louis, MO, USA). Acetonitrile for the mobile phase was of HPLC grade (Wako). Water was distilled and passed through a Milli-Q purification system (Millipore, Bedford, MA, USA). Other chemicals were of analytical-reagent grade.



| | R ₁ | R ₂ | R ₃ |
|-------------------------------------|--------------------------------------|------------------------|-------------------------|
| malonyl-ginsenoside Rb ₁ | Glc ² Glc ⁶ Ma | H | Glc ⁶ Glc |
| malonyl-ginsenoside Rb ₂ | Glc ² Glc ⁶ Ma | H | Glc ⁶ Ara(p) |
| malonyl-ginsenoside Rc | Glc ² Glc ⁶ Ma | H | Glc ⁶ Ara(f) |
| malonyl-ginsenoside Rd | Glc ² Glc ⁶ Ma | H | Glc |
| ginsenoside Rb ₁ | Glc ² Glc | H | Glc ⁶ Glc |
| ginsenoside Rb ₂ | Glc ² Glc | H | Glc ⁶ Ara(p) |
| ginsenoside Rc | Glc ² Glc | H | Glc ⁶ Ara(f) |
| ginsenoside Rd | Glc ² Glc | H | Glc |
| ginsenoside Re | H | O-Glc ² Rha | Glc |
| ginsenoside Rg ₁ | H | O-Glc | Glc |

HPLC conditions

The HPLC system consisted of a Tosoh Model CCPM prep pump, a UV-8010 monitor, an SC-8010 system controller and data processor and a PP-8010 recorder. The system was operated at room temperature. Predetermined volumes of an extract of ginseng, mixture of ginsenosides and estrogens were injected into the chromatograph. The flow-rate was 1 ml/min and the peaks were monitored at 203 nm.

For isocratic elution, mixtures of acetonitrile–50 mM KH₂PO₄ at several concentrations were used as the mobile phases. For the one-step separation of both panaxatriol- and panaxadiol-ginsenosides, a 30-min linear gradient elution from acetonitrile–50 mM KH₂PO₄ (15:85) to acetonitrile–50 mM KH₂PO₄ (50:50) was employed. The column void time was determined with sodium nitrite.

Sample preparation from ginseng

Ginseng was pulverized and extracted with 70% methanol at room temperature (20°C) for 30 min and the extract was filtered and evaporated. The residue was dissolved in water and applied to a Sep-Pak C₁₈ cartridge. After washing the column with water and 30% methanol, the sample was eluted with methanol and the eluate was evaporated to dryness under reduced pressure. The residue was dissolved in the eluent and injected into the HPLC system.

RESULTS AND DISCUSSION

The chromatograms of a ginseng extract on the columns of MPG-ODS, silica-ODS (pore size 80 Å) and silica-ODS (pore size 300 Å) with linear gradient elution are shown in Fig. 1. The content of malonyl-ginsenoside-Rd in the extract was too low to be detected in the chromatograms. Although the retention behaviours of the ginsenosides on both the MPG and silica columns were similar, the capacity factors of ten saponins were smaller on MPG than on silica columns. As shown in Fig. 2, the resolution between ginsenoside-Rg₁ and -Re on the MPG-ODS column was better than that on the silica-ODS column. At concentrations of acetonitrile lower than 30%, the two ginsenosides were so retained on the silica-ODS column that they were not eluted in 30 min.

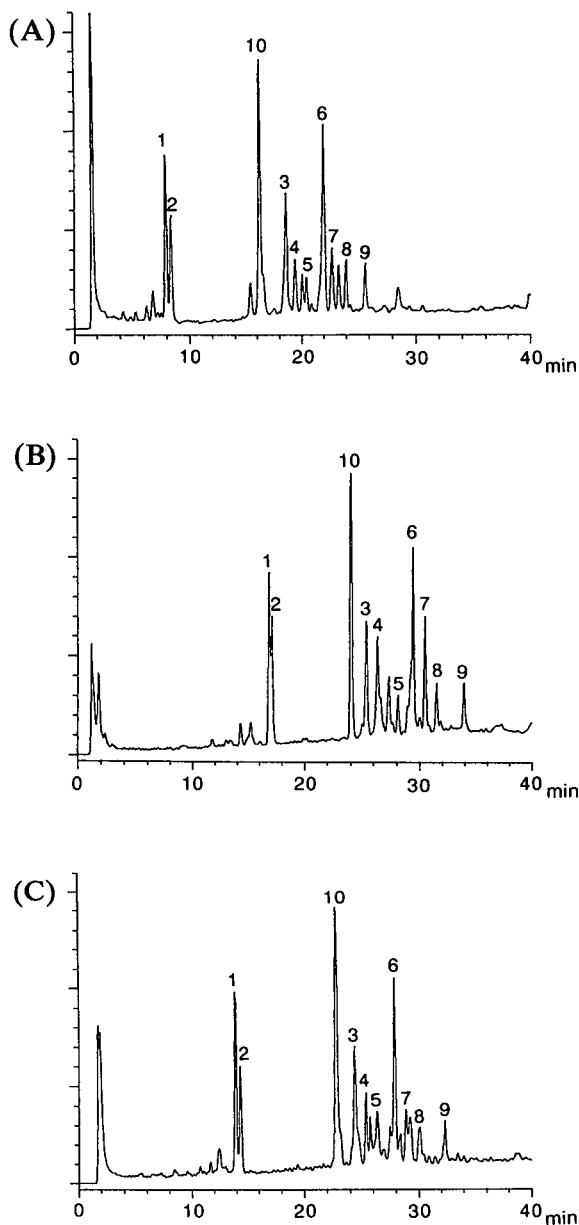


Fig. 1. Chromatograms of a ginseng extract on (A) MPG-ODS, (B) silica-ODS (80 Å) and (C) silica-ODS (300 Å) columns. Peaks: 1 = ginsenoside-Rg₁; 2 = ginsenoside-Re; 3 = malonyl-ginsenoside-Rb₁; 4 = malonyl-ginsenoside-Rc; 5 = malonyl-ginsenoside-Rb₂; 6 = ginsenoside-Rb₁; 7 = ginsenoside-Rc; 8 = ginsenoside-Rb₂; 9 = ginsenoside-Rd; 10 = ginsenoside-Ro (a pentacyclic terpenoid). Eluent, linear gradient from acetonitrile–50 mM KH₂PO₄ (15:85) to acetonitrile–50 mM KH₂PO₄ (50:50); flow-rate, 1.0 ml/min; detection, 203 nm.

The correlations of the capacity factors (k') of ginsenosides and estrogens on the MPG-ODS and silica-ODS (80 Å) columns were fairly good, as shown in Fig. 3. To obtain similar k' values for ginsenosides under isocratic conditions, the content of the organic solvent in the mobile phases was lower on the MPG-ODS than on the silica-ODS column. Under the common gradient conditions, ten ginsenosides and six estrogens were retained on silica-ODS to a greater extent than on MPG-ODS. These greater retentions may be attributed to the smaller size and ink-bottle shape of the pores of the silica gel.

The order of the elution of malonyl-ginsenoside-Rd and ginsenoside-Rb₁ was reversed on MPG-ODS and silica-ODS (80 Å). Under isocratic conditions, the same elution order of the two saponins was observed on MPG-ODS and silica-ODS (300 Å) (Fig. 4). The correlation of $\log k'$ of the ginsenosides and the estrogens on the MPG-ODS column were larger with silica-ODS (300 Å) than with silica-ODS (80 Å). These results suggest that a dominant factor of the retention order is the pore size. The $\log k'$ values of eight panaxadiol ginsenosides on the MPG-ODS column were plotted against the content of acetonitrile in the mobile phase, as shown in Fig. 5. Similar relationships were obtained with silica-ODS (300 Å), silica-ODS (80 Å) and silica-phenyl (80 Å) in the acetonitrile concentration range 27–30%. The order of the elution of the eight saponins did not change with variation in the concentration of acetonitrile in the range examined for the four columns.

MPG and silica (80 Å) were chemically modified with alkyl groups of chain lengths C₄, C₈ and C₁₂ and with a phenyl group. The chemically modified MPGs and silicas were packed into a stainless-steel column (150 × 4.0 mm I.D.). Mixtures of ginsenosides were chromatographed on the columns with gradient elution. The results are summarized in Fig. 6.

The elution order of malonyl-ginsenoside-Rd and ginsenoside-Rb₁ on MPG-phenyl and -C₄ and the silica (80 Å) columns was reversed on MPG-C₈, -C₁₂ and -ODS and silica-ODS (300 Å). Among the silica columns, the silica-ODS (300 Å) column achieved the shortest retention times of the ten saponins. The best resolution of ginsenoside-Rg₁ and

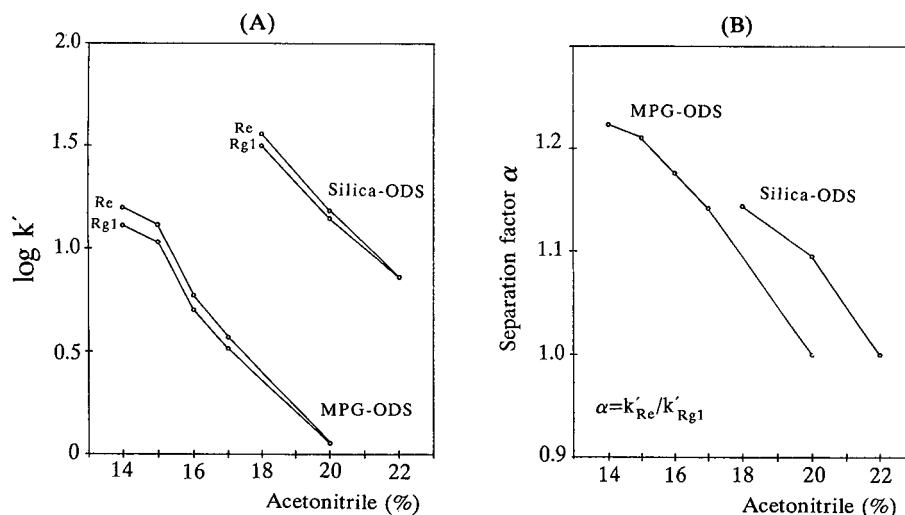


Fig. 2. Separation of ginsenoside- R_{g1} and - R_e on MPG-ODS and silica-ODS (80 Å) columns with isocratic elution. Mobile phase, acetonitrile–water.

- R_e was obtained on phenyl-modified MPG and silica.

Table I gives separation factors (α) of panaxadiol ginsenosides with isocratic elution on the MPG-ODS, silica-ODS (80 Å), silica-ODS (300 Å) and silica-phenyl (80 Å) columns. The resolutions be-

tween malonyl-ginsenoside- R_c and - R_{b2} (2–3) and between ginsenoside- R_c and - R_{b2} (6–7) were better on the MPG-ODS column than on the silica-ODS columns. Ginsenoside- R_c and - R_{b2} are isomers at the C-20-arabinose moiety, *i.e.*, the former is α -L-arabinofuranose whereas the latter is α -L-arabino-

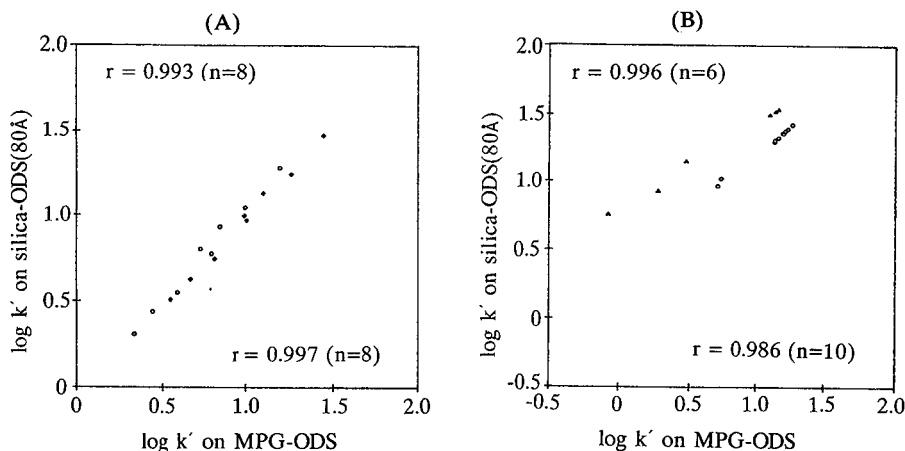


Fig. 3. Correlation of $\log k'$ values of ginsenosides and estrogens between MPG-ODS and silica-ODS (80 Å). (A) Isocratic elution; (B) gradient elution. Under isocratic conditions, the ratios of acetonitrile and 50 mM KH_2PO_4 for the MPG-ODS and silica-ODS (80 Å) columns were 25:75 and 30:70, respectively, for points (○), and 24:76 and 29:71, respectively, for points (◇). Ginsenoside- R_{g1} and - R_e were not separated under these conditions. Gradient conditions were the same as shown in Fig. 1. Symbol ○ represents the ten ginsenosides as numbered in Fig. 1 and Δ six estrogens, *viz.* estrone, estradiol, estriol, equiline, 17 β -estradiol-3-(β -D-glucuronide) and estriol-16 α (β -D-glucuronide).

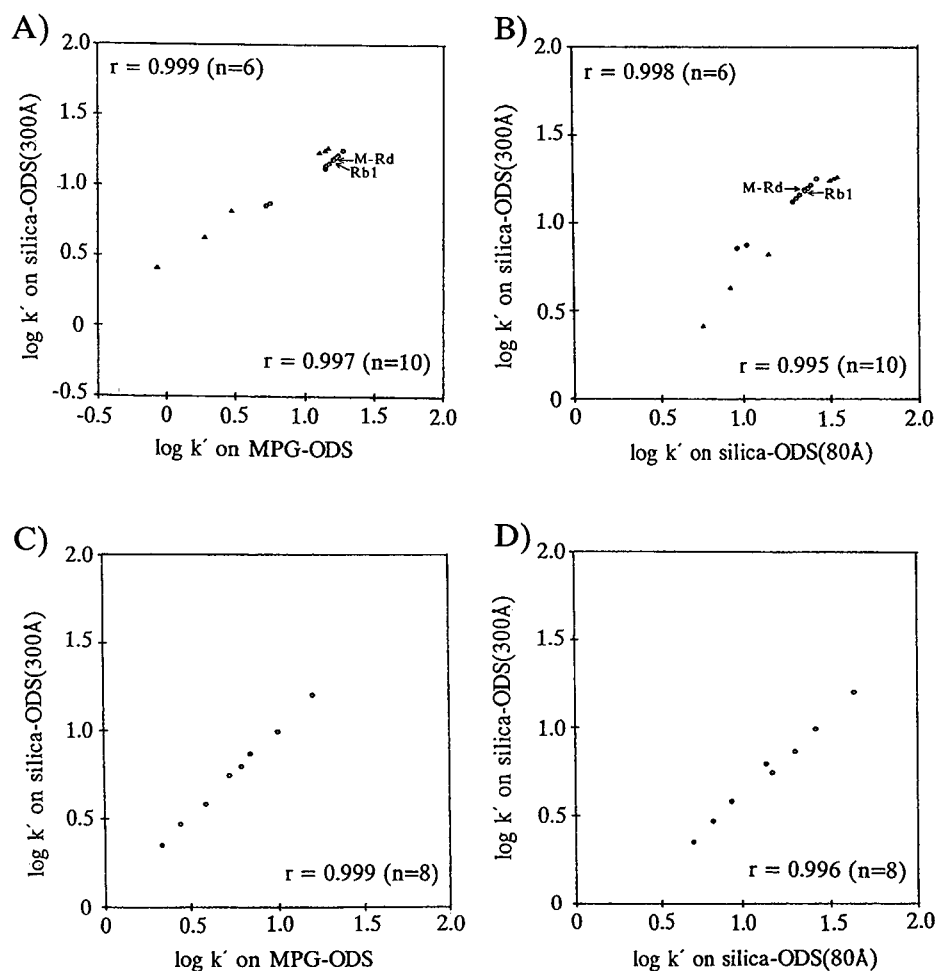


Fig. 4. Correlation of $\log k'$ values of ginsenosides and estrogens between MPG-ODS and silica-ODS (300 Å) columns and between silica-ODS (80 Å) and silica-ODS (300 Å) columns. (A) Correlations between MPG-ODS and silica-ODS (300 Å) with gradient elution; (B) correlation between silica-ODS (80 Å) and silica-ODS (300 Å) with gradient elution; (C) correlation between MPG-ODS and silica-ODS (300 Å) with isocratic elution; (D) correlation between silica-ODS (80 Å) and silica-ODS (300 Å) with isocratic elution. Under isocratic conditions, the ratios of acetonitrile and 50 mM KH_2PO_4 for MPG-ODS and silica-ODS columns were 25:75 and 28:72, respectively. Gradient conditions were the same as shown in Fig. 1. The symbol \circ represent the ten ginsenosides as numbered in Fig. 1 and \triangle the six estrogens listed in Fig. 3. M-Rd = malonyl-ginsenoside-Rd; Rb1 = ginsenoside-Rb₁.

pyranose. MPG-ODS achieved a better separation of the isomeric glycosides at C-20. The fact that the separation factors of the isomeric glycosides on silica-ODS columns (80 and 300 Å) were similar suggests that the pore size did not affect the separation of these isomeric glycosides.

ACKNOWLEDGEMENTS

This work was supported in part by the Science Research Promotion Fund of the Japan Private School Promotion Foundation and by Ise Chemical Industries. We thank Professor I. Kitagawa of the

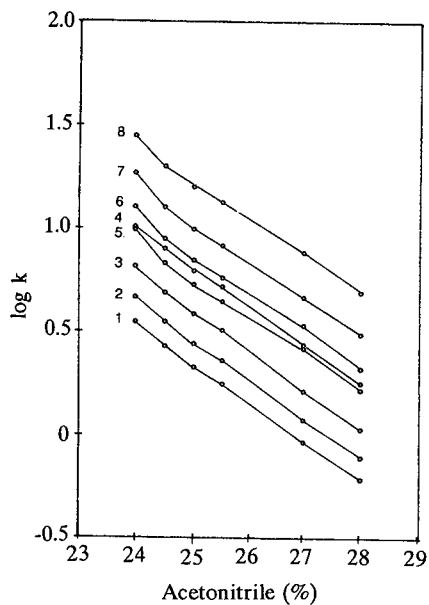


Fig. 5. Plots of $\log k'$ against the content of acetonitrile in the mobile phase. 1 = Malonyl-ginsenoside-Rb₁; 2 = malonyl-ginsenoside-Rc; 3 = malonyl-ginsenoside-Rb₂; 4 = malonyl-ginsenoside-Rd; 5 = ginsenoside-Rb₁; 6 = ginsenoside-Rc; 7 = ginsenoside-Rb₂; 8 = ginsenoside-Rd.

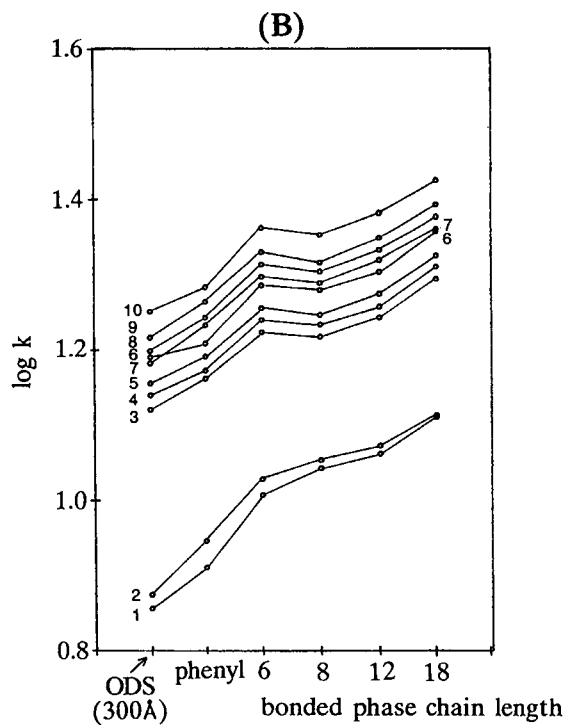
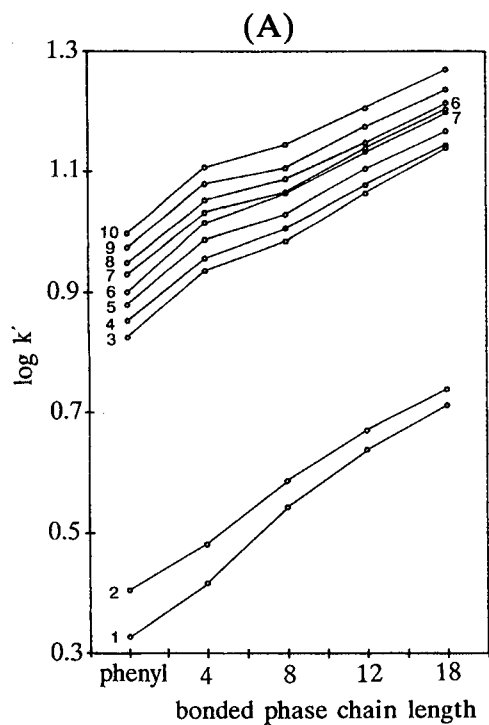


Fig. 6. Comparison of capacity factors of ginsenosides on chemically modified (A) MPG and (B) silica columns. 1 = Ginsenoside-Rg₁; 2 = ginsenoside-Re; 3 = malonyl-ginsenoside-Rb₁; 4 = malonyl-ginsenoside-Rc; 5 = malonyl-ginsenoside-Rb₂; 6 = malonyl-ginsenoside-Rd; 7 = ginsenoside-Rb₁; 8 = ginsenoside-Rc; 9 = ginsenoside-Rb₂; 10 = ginsenoside-Rd.

TABLE I

COMPARISON OF SEPARATION FACTORS (α)

HPLC conditions: eluent, for MPG-ODS, acetonitrile–50 mM KH_2PO_4 (25:75), for silica-ODS (80 Å), acetonitrile–50 mM KH_2PO_4 (30:70), for silica-ODS (300 Å), acetonitrile–50 mM KH_2PO_4 (28:72) and for silica-phenyl, acetonitrile–50 mM KH_2PO_4 (27:73); flow-rate, 1.0 ml/min; detection, 203 nm.

| Compounds separated ^a | Separation factor (α) | | | |
|----------------------------------|--------------------------------|-------------------|--------------------|---------------|
| | MPG-ODS | Silica-ODS (80 Å) | Silica-ODS (300 Å) | Silica-phenyl |
| 1–2 | 1.29 | 1.32 | 1.31 | 1.21 |
| 2–3 | 1.40 | 1.31 | 1.30 | 1.19 |
| 3–4 | 1.61 | 1.66 | 1.63 | 1.34 |
| 5–6 | 1.31 | 1.35 | 1.32 | 1.22 |
| 6–7 | 1.41 | 1.30 | 1.34 | 1.20 |
| 7–8 | 1.60 | 1.70 | 1.62 | 1.34 |

^a 1 = Malonyl-ginsenoside-Rb₁; 2 = malonyl-ginsenoside-Rc; 3 = malonyl-ginsenoside-Rb₂; 4 = malonyl-ginsenoside-Rd; 5 = ginsenoside-Rb₁; 6 = ginsenoside-Rc; 7 = ginsenoside-Rb₂; 8 = ginsenoside-Rd.

University of Osaka for the gift of the standard samples. The technical assistance of Yaeko Ida and Rika Uekama is gratefully acknowledged.

REFERENCES

- 1 N. Tanaka, K. Hashizume, M. Araki, H. Tsuchiya, A. Okuno, K. Iwaguchi, S. Ohnishi and N. Takai, *J. Chromatogr.*, 448 (1988) 95.
- 2 Y. Matsushima, Y. Nagata, K. Tagakusagi, M. Niyomura and N. Takai, *J. Chromatogr.*, 332 (1985) 265.
- 3 H. Kanazawa, Y. Nagata, Y. Matsushima, M. Tomoda and N. Takai, *Chromatographia*, 24 (1987) 517.
- 4 H. Kanazawa, Y. Nagata, Y. Matsushima, M. Tomoda and N. Takai, *Shoyakugaku Zasshi*, 43 (1989) 121.
- 5 N. Takai, H. Kanazawa, Y. Nagata, Y. Matsushima and N. Tomoda, *Seisan-kenkyu*, 41 (1989) 773.
- 6 H. Kanazawa, Y. Nagata, Y. Matsushima, M. Tomoda and N. Takai, *J. Chromatogr.*, 507 (1990) 327.
- 7 H. Kanazawa, Y. Nagata, Y. Matsushima, M. Tomoda and N. Takai, *Chem. Pharm. Bull.*, 38 (1990) 1630.
- 8 H. Kanazawa, Y. Nagata, Y. Matsushima, M. Tomoda and N. Takai, *J. Chromatogr.*, 537 (1991) 469.
- 9 T. G. Petersen and B. Palmqvist, *J. Chromatogr.*, 504 (1990) 139.

Carbohydrate analysis of fermentation broth by high-performance liquid chromatography utilizing solid-phase extraction

Robert G. Bell and Kevin L. Newman

A.L. Laboratories, 400 State Street, Chicago Heights, IL 60411 (USA)

ABSTRACT

Nutrient information concerning the specific needs in fermentation broth is crucial to the potency and production of an antibiotic. Nutrient analysis of carbohydrate metabolism by HPLC is hindered by an array of fermentation broth interferences. These interferences can be effectively removed by solid-phase extraction. The fermentation broth was diluted with an equal amount of water and vortexed. The sample mixture was eluted through an activated Acell QMA solid-phase cartridge. The resultant eluent was diluted with an equal amount of an acetonitrile-ethanol (75:25) mixture, vortexed and filtered. The sample extract was chromatographed on a YMC polyamine column using refractive index detection. The mobile phase consisted of acetonitrile-water (75:25) at a flow-rate of 1 ml/min. Under these conditions, glucose, fructose, sucrose and maltose were separated in less than 13 min with baseline resolution. This method is capable of monitoring the carbohydrate consumption and metabolism throughout the fermentation process.

INTRODUCTION

Nutrient information concerning the specific needs of microorganisms in fermentation broth is crucial to the potency and production of an antibiotic [1]. Two nutritional factors essential to microbial activity are a source of energy for cellular metabolic processes and a source of starting components for cellular synthesis. Carbohydrates are excellent sources of carbon, oxygen and hydrogen, and metabolic energy for many microorganisms. They are available as simple sugars or sugar polymers such as starch, dextrans, cellulose or hemicellulose. Since the biomass is typically 50% carbon on a dry weight basis, carbohydrates are frequently present in the media in concentrations higher than other nutrients and can account for about 20% of the total nutrient media [2].

The microbial environment is largely determined

by the composition of the growth media. The preferred media in an industrial fermentation setting is a complex or natural medium [3]. This media uses ingredients of natural origin and is not completely defined chemically. Although all carbohydrates have an empirical formula of $(\text{CH}_2\text{O})_n$, they are not equally available to microorganisms. In general, availability may be ranked as hexoses > disaccharides > pentoses > polysaccharides. Many microorganisms can grow well on a variety of carbohydrates, yet the yield of the product may be strongly dependent on the source. This is demonstrated by the microorganism *Cephalosporium acrimonium* in which glucose favors cell growth, galactose maximizes antibiotic concentration and sucrose optimizes antibiotic yield per cell [4]. Industrial fermentation broth contains a host of natural ingredients, such as soy and cottonseed flours, peanut and corn meals, molasses, starch, beef extract and lard oil, as well as the starting culture. It is crucial to the production and potency of an antibiotic to determine these nutritional characteristics before selecting a carbohydrate source for the cultivation of a specific

Correspondence to: R. G. Bell, Barre-National Inc., 7205 Windsor Boulevard, Baltimore, MD 21244-2654, USA (present address).

species. Determination of the carbohydrate needs of a microorganism is accomplished by monitoring the concentration of carbohydrates in the growth media during the microorganism lifetime. Through aerobic respiration, these starting materials undergo enzymatic and chemical degradation which result in numerous metabolic by-products which can interfere with chromatographic analysis. These fermentation broth matrix interferences can be effectively removed by the use of solid-phase extraction (SPE) enabling carbohydrate analysis of the broth by high-performance liquid chromatography (HPLC). SPE is a rapid and reproducible sample preparation technique that allows the SPE eluent to be injected immediately into the HPLC system without further preparation. The main advantages of SPE include small sample and solvent volumes, extended column life, shorter sample preparation times and better recovery levels [5,6]. This paper will describe the sample preparation technique and HPLC analysis for glucose, fructose, sucrose and maltose in fermentation broth.

EXPERIMENTAL

Materials

HPLC grade acetonitrile, ethanol, isopropyl alcohol and water (Burdick and Jackson, Muskegon, MI, USA) were used for extraction and chromatographic analysis. Biochemical reagent grade glucose, fructose, sucrose and maltose (J. T. Baker, Phillipsburg, NJ, USA) were used for standard and system suitability preparations. SPE cartridges were Acell Plus QMA Sep-Paks (Waters Assoc., Milford, MA, USA). Syringes (Becton Dickinson and Company, Rutherford, NJ, USA) were used for sample delivery into the SPE cartridges.

Chromatographic system

The chromatographic system was equipped with a constant flow, low pulse pump (Shimadzu LC-600, Kyoto, Japan) a refractive index detector (Shimadzu RID-6A), an autosampler (Shimadzu SIL-9A) and an integrator (Shimadzu CR-501). The separations were performed on a polyamine column [250 × 4.6 mm, I.D., 5 µm, (YMC, Morris Plains, NJ, USA)]. The detector and column were maintained at 35°C. The mobile phase consisted of acetonitrile–water (75:25, v/v) at a flow-rate of 1

ml/min. The mobile phase was filtered and degassed. The injection volume was 50 µl.

Sample preparation

SPE cartridges were previously wetted and activated by flushing the cartridge with 2–4 ml of methanol followed by 2–4 ml of water. Two ml of fermentation broth were mixed with an equal amount of water and rapidly agitated (vortex) for 1 min. The mixture was centrifuged for 5 min at 14 000 rpm (1600 g) using an ultracentrifuge (Eppendorf Centrifuge 5415C, Brinkman Instruments, Westbury, NY, USA). The resulting supernatant was transferred into a syringe with an activated SPE cartridge at its tip. The supernatant was slowly forced through the SPE cartridge at an approximate rate of 1 ml/min. The first milliliter that eluted was discarded. A volume of 1 ml of the eluent was accurately pipetted and added to 3 ml of a acetonitrile–ethanol (75:25, v/v) mixture and rapidly agitated (vortex) for 1 min. A precipitate was formed. The mixture was filtered through a 0.45-µm polypropylene filter disc. The resultant eluate was ready for HPLC analysis.

Standard and system suitability preparation

Standards were prepared from the individual sugars (glucose, fructose, sucrose and maltose) by dissolving an accurately weighed amount into a 100-ml volumetric flask and diluting with mobile phase. The concentration of the stock solutions of the sugars was 1 mg/ml. Dilutions were made accordingly. The system suitability solution contained the aforementioned sugars at approximate concentrations of 0.1 mg/ml.

Fermentation media

Defined media can be prepared by the procedure outlined by Vogel and Bonner [7] or Davis and Mingioli [8]. The end products of fermentation depends on the type of bacteria used and the nature of the fermentation media (*i.e.*, wine, beer, yogurt, yeast, antibiotics etc.)

Defined media [7] is prepared by dissolving 10 g of magnesium sulfate, 100 g citric acid, 500 g dipotassium hydrogenphosphate, 175 g ammonium sodium phosphate in 670 ml of water. This mixture represents the nutrient concentrate. Final medium is made by aseptically adding 1 ml of nutrient con-

centrate to 49 ml of a sterilized solution of 3% corn steep, 3% glucose, 4% soybean meal and 2% lard oil.

RESULTS AND DISCUSSION

The chromatographic procedure was validated for precision ($n = 6$) ($<2.0\%$), accuracy (99%), linearity (10^4), recovery (99%) minimum detectable quantity (10^{-8}) and minimum quantifiable quantity (10^{-7} g) for glucose, fructose, maltose and sucrose. Fig. 1a illustrates the ability of the chromatographic system to separate the sugars present in the system suitability mixture. Elution order is fructose ($t_R = 7.1$ min), glucose ($t_R = 8.5$ min), sucrose ($t_R = 10.9$ min) and maltose ($t_R = 12.5$ min). There is excellent resolution ($R_s > 1.25$) for the sugars examined. SPE recovery efficiencies were performed with the system suitability solution and spiked fermentation starting broth. Recoveries were greater than 99% (99.87% \pm 0.73% system suitability, 99.22% \pm 2.13% spiked broth). A calibration curve for the sugars is linear ($r > 0.999$) in the concentration range 0.001-1 mg/ml.

Fig. 1b-e depict fermentation chromatograms at fermentation times of 0, 6, 12 and 18 h. This chromatographic procedure is capable of identifying and quantifying these sugars during the fermentation cycle. The relative concentrations of these sugars can be plotted as a function of fermentation cycle time. The carbohydrate demands of the microorganism undergoing fermentation can be optimized by such plots by noting the metabolic consumption and production patterns of the various carbohydrates in relation to antibiotic production. At specific times during the fermentation process, carbohydrates can be spiked into the broth to enhance the growth or the production phases.

Fig. 2 compares extraction of SPE with an isopropyl alcohol liquid extraction at 5 and 17 h. (Isopropyl alcohol was chosen for its ability to extract the carbohydrates and precipitate the proteinaceous biomass simultaneously. An equal amount of isopropyl alcohol and fermentation broth were mixed and then shaken for 30 min in a wrist shaker. The mixture was centrifuged and filtered.) As illustrated in Fig. 2, SPE provides an excellent means of effectively removing the hydrophobic matrix interferences that exist in fermentation media. Compari-

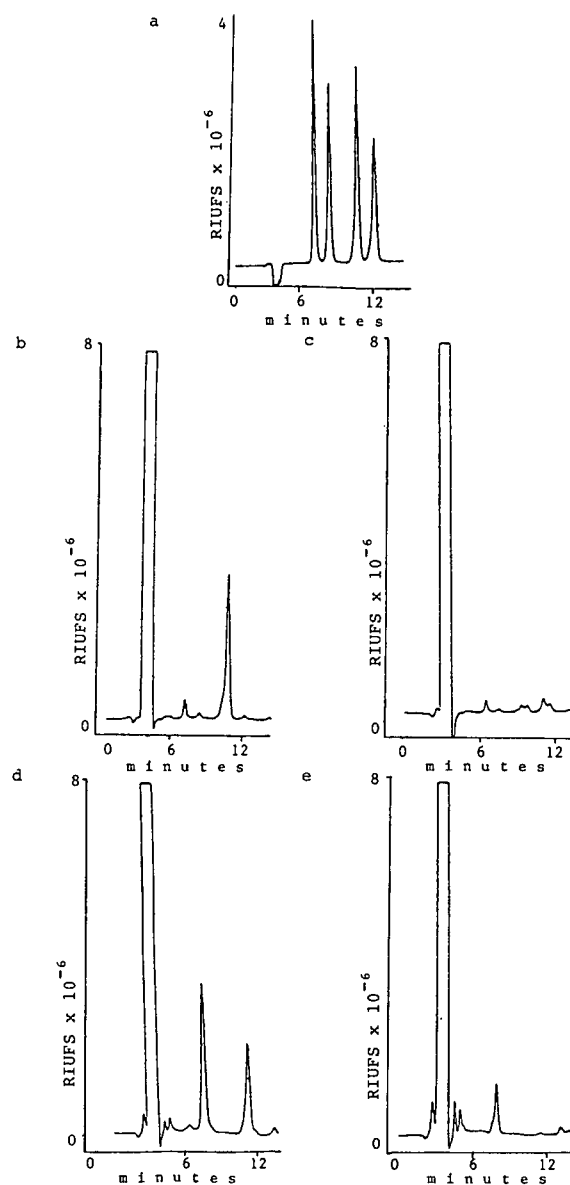


Fig. 1. Chromatograms of carbohydrate system suitability (a) and SPE extracts of fermentation broth (b-e) at 0, 6, 12 and 18 h of a fermentation cycle. Elution order: fructose ($t_R = 7.1$ min), glucose ($t_R = 8.5$ min), sucrose ($t_R = 10.9$ min), maltose ($t_R = 12.5$ min). RIUFS = Refractive index units full scale.

sons of the sample preparation techniques clearly demonstrates that SPE will minimize extraneous peaks and interferences and maintain baseline integrity better than solvent extraction. These hydrophobic interferences are due to the chemical and

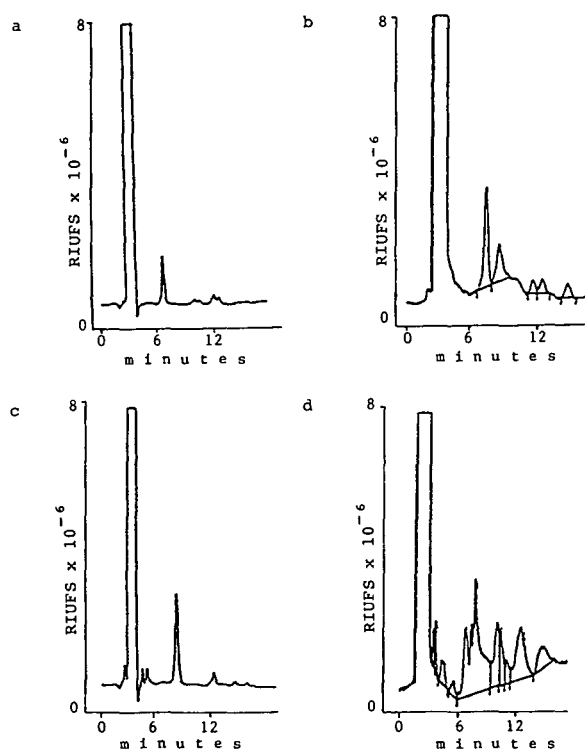


Fig. 2. Comparison chromatograms of SPE and isopropyl alcohol solvent extraction of fermentation broth. (a) and (c) are broth extracts at 5 and 17 h using SPE. (b) and (d) are broth extracts at 5 and 17 h using isopropyl alcohol liquid extraction.

enzymatic by-products of fermentation metabolism generally consisting of crude proteins and amino acids, waxes, sterols, phospholipids, pigments, vitamins, minerals, soluble gums and other related nutrients needed for fermentation. Eliminating these analytical interferences becomes increasingly important during the fermentation cycle. As aerobic respiration of the microorganism proceeds, the concentration of metabolic by-products increases and can interfere with identification and quantitation of the sugars as depicted in Fig. 2d. SPE provides other advantages for the chromatographic system. Column cleanup and maintenance is minimized as well as injector reproducibility and clogging.

Fermentation broth consistencies can vary from a watery consistency to a mud-like sludge. This is usually a function of the extent of fermentation and processing. Accuracy of this procedure is dependent upon proper sampling, dilution and resuspendability of the fermentation broth. Failure to perform

these may result in inadequate extraction, clumping and/or SPE overload.

This procedure will provide a rapid and accurate method for assessing carbohydrate needs and consumption patterns of microorganisms in fermentation media. This procedure can also discern other sugars, such as lactose, galactose, xylose, pyranose, inositol, and mannitol that may be required for other types of fermentation processes. Elucidation of these carbohydrate nutrient patterns will enable fermentation engineers to define their complex natural media, allowing adjustments to the broth using scientific judgement rather than inherited art. Identification of the metabolic processes and their nutrient needs will enhance the potency of industrial antibiotics production.

CONCLUSIONS

HPLC analysis of carbohydrates using SPE provides a rapid and reliable means in which to analyze individual sugars in fermentation media. SPE provides an excellent means to remove fermentation broth matrix interferences, allowing a clear interpretation of the chromatographic results. SPE provides several chromatographic advantages over traditional solvent extraction that result in less interferences, simultaneous elution and baseline shifting as well as maintaining column and chromatographic system integrity. The chromatographic assay is rugged and reliable allowing detection of carbohydrates in the fermentation extract throughout the microorganism's lifetime. This information can be used to optimize the microorganism's growth and subsequent antibiotic production in the fermentation broth since the simple sugars are the preferred carbon and energy source.

REFERENCES

- 1 R. G. Bell, *J. Chromatogr.*, 546 (1991) 251–257.
- 2 M. Frobisher, *Fundamentals of Microbiology*, Saunders, Philadelphia, PA, 8th ed., 1968, pp. 189–197.
- 3 L. E. Casida, *Industrial Microbiology*, Wiley, New York, 1968, pp. 230–242.
- 4 A. L. Demain, Y. M. Kennel and Y. Aharonwitz, in A. T. Bull, D. C. Ellwood and E. Ratledge (Editors), *Microbial Technology: Current State, Future Prospects*, Cambridge University Press, Cambridge, 1979, pp. 175–185.
- 5 R. Majors, *LC · GC*, 4 (1986) 972–984.
- 6 R. Majors, *LC · GC*, 7 (1989) 92–96.
- 7 J. Vogel and F. Bonner, *J. Biol. Chem.*, 218 (1956) 19.
- 8 B. Davis and F. Mingioli, *J. Bacteriol.*, 60 (1950) 17.

High-performance liquid chromatography with ion pairing and electrochemical detection for the determination of the stability of two forms of vitamin C

Kathryn M. De Antonis, Phyllis R. Brown and Zhen Yi

Department of Chemistry, University of Rhode Island, Kingston, RI 02881 (USA)

Paul D. Maugle

P.D.M. & Associates, Norwich, CT 06360 (USA)

ABSTRACT

An ion-pair method with sodium octanesulfonate and ethylenediaminetetraacetic acid was used for the analysis of extruded salmon and trout feeds for ethyl cellulose-coated L-ascorbic acid and one of its more stable analogues, dipotassium ascorbyl-2-sulfate dihydrate. For enhanced sensitivity electrochemical detection was used. The procedure used to extract the vitamin C from the feeds played a vital role in obtaining good recoveries. When the ascorbic acid was extruded manually, the recovery was poor. However, when a polytron homogenizer was employed, the vitamin C recoveries were greatly improved.

INTRODUCTION

Although most animals are able to synthesize their dietary requirements of vitamin C, certain types of fish cannot [1]. It is, therefore, imperative that these fish acquire vitamin C from their diet. Since unprotected vitamin C is unstable under ordinary conditions of light, temperature and moisture, protected forms of vitamin C must be developed and evaluated for use in vitamin-supplemented feeds.

Two protected forms of vitamin C, ethyl cellulose-coated L-ascorbic acid (C1) and dipotassium ascorbyl-2-sulfate dihydrate (C2), were analyzed by HPLC to determine their stability in manufactured feed matrices. These feeds were extruded trout feed, extruded salmon feed and moist salmon feed.

In order to evaluate effectively C1 and C2 in

feeds, good methods of analysis are required to identify and quantify these dosage forms. The important requirements for a reliable method are adequate sensitivity and recovery, and the ability of differentiate between the signal from the vitamin C and the matrix.

Vitamin C and its analogues in feeds and tissues have been analyzed by a variety of techniques. For example, Quadri *et al.* [2] used a spectrophotometric method to analyze C2 in pelleted fish feed, as did Soliman, *et al.* [3] who analyzed a variety of protected forms of vitamin C including C2. The stability of these preparations was observed during both feed manufacture and long-term storage. The analytical method used was adapted from the method of Roe [4]. De Antonis *et al.* [5] compared three HPLC methods for the analysis of C1 and C2 in shrimp tissues. Of these three methods, two used ion-pair chromatography and one used ion-exchange chromatography; all three used UV detection. Skelbaek *et al.* [6] analyzed two forms of vitamin C (not in-

Correspondence to: Dr. Phyllis R. Brown, Department of Chemistry, University of Rhode Island, Kingston, RI 02881, USA.

cluding C1 or C2) in pelleted fish feed both during and after manufacture. The analysis was done using reversed-phase HPLC with tetrahexylammonium bromide as an ion-pairing agent and UV detection at 243 nm. Schuep *et al.* [7] examined the stability of C2 in pelleted fish feed using reversed-phase HPLC with UV detection at 254 nm. Wang *et al.* [8] used ion-pair chromatography with tetrabutylammonium phosphate and electrochemical detection for vitamin C analysis. In the present work, C1 and C2 were analyzed with sodium octanesulfonate (SOS) as the ion-pairing agent and electrochemical detection for enhanced sensitivity.

Little is known about the stability of C2 during extrusion manufacturing, which is more rigorous than pelleting, and storage. This project was designed to examine the stability of C1 and C2 in feeds both during and after the manufacture process.

EXPERIMENTAL

Apparatus

Chromatographic analysis was performed using a Series 3B liquid chromatograph (Perkin-Elmer, Norwalk, CT, USA), a Model 625 autoinjector with a 20- μ l loop (Micromeritics, Norcross, GA, USA) and an LC-4B amperometric detector with a silver/silver chloride reference electrode and a glassy carbon working electrode (Perkin-Elmer). Peak heights were recorded with an Omniscribe strip-chart recorder (Houston Instruments, Austin, TX, USA), and peak areas were electronically integrated with a Model 3600 data station, using CHROM2 software (Perkin-Elmer). A reversed-phase Nucleosil C₁₈ column (I. Molnar, Berlin, Germany; 25 cm \times 4.6 mm I.D., 5- μ m particles) was used with a guard column packed with Sepalyte C₁₈ (25 μ m).

Chromatographic method

The column was a Nucleosil C₁₈ (I. Molnar; 25.0 cm \times 4.6 mm I.D.). The mobile phase was 500 ml of an aqueous solution containing 3.2812 g of sodium acetate, 0.0168 g of ethylenediaminetetraacetic acid (EDTA), 0.1082 g of SOS and 26.3 ml of methanol. The pH was adjusted to 4.0 with glacial acetic acid. The mobile phase was filtered through a 0.45- μ m filter prior to use. The flow-rate was 1.0 ml/min, and column was at room temperature. The electrochemical detector potential was varied from

0.70 to 0.95 V. The optimal potential value for C1 was 0.75 V and the optimal potential for C2 was 0.95 V.

Chemicals

Two commercially available forms of vitamin C were used as references, ethyl cellulose-coated L-ascorbic acid (C1) (97% pure, 3% ethyl cellulose) (Hoffman LaRoche, Nutley, NJ, USA) and dipotassium ascorbyl-2-sulfate dihydrate (C2) (97% pure, 48% ascorbic acid equivalence) (Pfizer, Specialty Chemicals Division, Groton, CT, USA).

The following chemicals, which were of reagent-grade quality, were used without further purification. EDTA and SOS were purchased from Sigma (St. Louis, MO, USA), glacial acetic acid and methanol from Fisher Scientific (Fairlawn, NJ, USA) sodium acetate from Matheson, Coleman, and Bell (Norwood, OH, USA) and dithiothreitol (DTT) from Eastman Kodak (Rochester, NY, USA).

Doubly distilled and deionized water was prepared on site and filtered through a 0.45- μ m filter (Millipore, Bedford, MA, USA) prior to use in the mobile phase.

Dry extruded feeds

Three one-ton batches of dry extruded trout feed and three one-ton batches of dry extruded salmon feed were manufactured by Archer Daniel Midland (Tuscalusa, AL, USA). The levels of C1 and C2 were different in the three batches of each feed. Three target treatment levels were made: (1) 250 mg/kg C2, (2) 350 mg/kg C2 and (3) 2200 mg/kg C1. These are further described as T1, T2 and T3 in the trout feed and S1, S2 and S3 in the salmon feed.

Twenty-five-pound samples of the six types of supplemented feeds (three treatment levels of trout feed and three treatment levels of salmon feed) were taken at three points in the manufacturing process. The first sample was taken immediately after supplementation, the second was taken at the die plate and the head of the extruder and the third was taken at the bagging operation after the feed was dried and cooled. In addition, baseline samples were taken prior to the addition of the vitamin C. The samples were frozen with dry ice and transported to the University of Rhode Island for storage and analysis.

Moist feeds

Duplicate batches of a soft moist salmon (33% moisture) containing the same ingredients as the extruded salmon feed were made at the University of Rhode Island's aquaculture facility using a Hobart (Toledo, OH, USA) laboratory-scale soft pelleting machine. The first batch was supplemented at a level of 1000 mg/kg C1, and the second batch was supplemented at a level of 350 mg/kg C2.

After cold pelleting, two samples of each feed were taken. One was immediately frozen (-70°C) using a bath of methanol and dry ice, and the other was stored at room temperature for 3 h prior to freezing. Samples of each feed were analyzed for C1 and C2 levels. In addition, the feeds were screened for pro-oxidants prior to their long-term stability evaluation.

In a separate study, C2 stability was examined in a commercial soft moist feed and its respective pre-manufacture mash provided by Conners Brothers (Blacks Harbor, New Brunswick, NJ, USA). The target potency of this batch was 250 mg/kg C2. The feed samples were received in a thawed state 3 days after manufacture and were stored at room temperature. Samples of the premanufacture mash and the finished feed were analyzed for C2 content five times in an 8-day period.

Standard preparation

Standard solutions for C1 and C2 in the concentration range 0.0001–0.01 mg/ml were analyzed. The solution were prepared in water.

Sample preparation

The vitamin C was extracted from the fish feeds using two techniques, a manual technique and a more rigorous technique which employed a polytron homogenizer.

In the manual extraction procedure, 0.5 g of the feed sample was ground to a fine powder with a mortar and pestle. The sample was then dissolved in 5 ml of a solution containing 6% metaphosphoric acid (mPA) (to precipitate the proteins [9]) and 0.2% DDT (for protection of sulfhydryl groups [10]) and vortexed for 2 min. The mixture was centrifuged at 3000 g for 3 min, and the supernatant was filtered through a 0.45- μm filter (Millipore). The filtrate was then diluted to 100 ml.

When the polytron was used, the feed sample was

ground and dissolved as previously described. The resulting solution was homogenized in three aliquots using the polytron. The supernatants from each aliquot were then pooled, diluted to 100 ml and filtered through 0.45- μm filters as previously described.

RESULTS AND DISCUSSION

Screening for pro-oxidants

There was no evidence of the presence of pro-oxidants which can accelerate the degradation of the ascorbic acid. The levels of moisture, lipid, protein, ash, fiber, calcium, potassium and phosphorus were determined. The levels were found to be very close to those measured in a typical commercial trout or salmon feed, indicating that these are appropriate batches of feed for this study.

Extraction procedure

The levels of C1 and C2 determined for the extruded feeds using the manual extraction procedure are significantly lower than the levels found using the Polytron. The ascorbic acid levels were determined using each of the extraction techniques for the samples taken after storage for 30 days at 25 and 40°C (Table I). The ascorbic acid was extracted from the feed more thoroughly using the polytron than the manual technique. In all cases there was an increase in ascorbic acid level when the polytron was employed.

Chromatographic method

Aqueous standard solutions containing C1 and C2 were analyzed. The retention times of C1 and C2 were approximately 3.5 and 4.5 min, respectively. The method exhibited good linearity for C1 and C2 in the concentration range 0.0001–0.01 mg/ml. The correlation coefficients for both dosage forms were 1.000 over two orders of magnitude.

The two forms of ascorbic acid were adequately separated from the feed matrix. All of the possible interfering peaks from the matrix were eluted after the ascorbic acid (see Figs. 1 and 2 for chromatograms of feeds containing C1 and C2).

Ascorbic acid stability

During manufacture, less than 5% of the C2 and greater than 98% of C1 was lost. These data in-

TABLE I
COMPARISON OF MANUAL AND POLYTRON SAMPLE PREPARATION

| Sample ^a | Dosage form | Target level (mg/g) | Level after 30 days (mg/g) | | | |
|---------------------|-------------|---------------------|----------------------------|--------|----------|--------|
| | | | 25°C | | 40°C | |
| | | | Polytron | Manual | Polytron | Manual |
| Trout: | | | | | | |
| T1 | C2 | 250 | 278 | 129 | 279 | 149 |
| T2 | C2 | 350 | 351 | 219 | 359 | 279 |
| Salmon: | | | | | | |
| S1 | C2 | 250 | 278 | 139 | 254 | 179 |
| S2 | C2 | 350 | 395 | 314 | 369 | 299 |

^a T3 and S3 were not monitored since the C1 levels were so low after manufacturing. T1 = trout feed with 250 mg/kg C2; T2 = trout feed with 350 mg/kg C2; T3 = trout feed with 2200 mg/kg C1; S1 = salmon feed with 250 mg/kg C2; S2 = salmon feed with 350 mg/kg C2; S3 = salmon feed with 2200 mg/kg C1.

dicates that C2 survived the rigorous extrusion manufacture process whereas the C1 did not (Table II).

The amount of C2 remaining in the extruded trout and salmon feeds was examined on a monthly basis for 6 months after manufacture. C1 was not monitored since there was an insignificant amount remaining after manufacture. After 6 months of storage, the extruded trout and salmon feeds retained 81-85% of the potency after manufacture which corresponds to 77-81% of the target poten-

cy. Due to inhomogeneity in the samples, the levels appear to increase with time at some points

In the soft moist feed 87% of the C2 survived cold pelleting, 85% remained after 3 h at room temperature, and 81% remained after 24 h at room temperature. Only 16% of C1 survived the cold pelleting. After 3 h at room temperature only 4.8% of C1 remained, and after 24 h at room temperature no C1 was detected.

In a separate study of C2 stability of the soft

TABLE II
ASCORBIC ACID LEVELS OBTAINED BY THE POLYTRON EXTRACTION TECHNIQUE

| Sample | Dosage form | Target level (mg/kg) | Level after supplementation (mg/kg) | Level at head of extruder (mg/kg) | Level after drying (mg/kg) | Percentage after manufacturing |
|---------|-------------|----------------------|-------------------------------------|-----------------------------------|----------------------------|--------------------------------|
| Trout: | | | | | | |
| T1 | C2 | 250 | 290 | N.M. ^a | 286 | 98.6 |
| T2 | C2 | 350 | 379 | N.M. | 363 | 95.8 |
| T3 | C1 | 2200 | 2240 | N.M. | 10 | 0.04 |
| Salmon: | | | | | | |
| S1 | C2 | 250 | 292 | N.M. | 283 | 96.9 |
| S2 | C2 | 350 | 399 | N.M. | 395 | 98.6 |
| S3 | C1 | 2200 | 2199 | N.M. | 40 | 1.83 |

^a N.M. = Not measured.

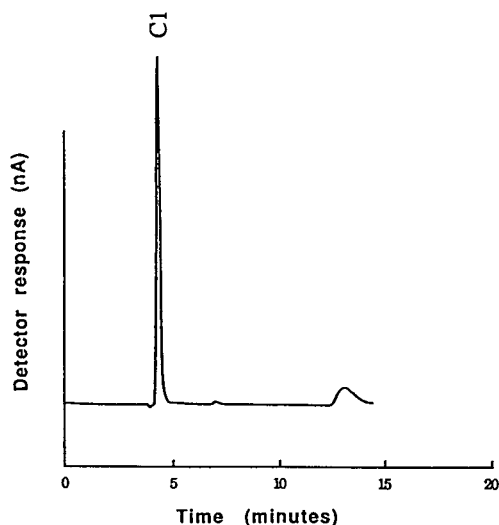


Fig. 1. Chromatogram obtained using a Nucleosil C_{18} column (I. Molnar; 25.0 × 4.6 mm I.D.). The mobile phase was 500 ml of an aqueous solution containing 3.2812 g of sodium acetate 0.0168 g of EDTA and 0.1082 g of SOS and 26.3 ml of methanol. The pH was adjusted to 4.0 with glacial acetic acid. The flow-rate was 1.0 ml/min, and the column was at room temperature. The electrochemical detector was set at 0.75 V, 200 nA full scale. The sample was a trout feed containing C1.

moist feed, samples of a commercial soft moist feed and its premanufacture mash were provided by Conners Brothers. When this feed was analyzed over an 8-day period, 78% of the C2 remained in the premanufacture mash after 2 weeks, and 66% remained in the feed after 2 weeks (Table III). The increase in C2 content from the premanufacture mash to the finished product is due to the loss of water in the feed.

TABLE III

C2 LEVEL OBTAINED IN MOIST FEED AND PREMANUFACTURE MASH FROM CONNERS BROTHERS

| Day | Premanufacture mash (mg/kg) | Feed ^a (mg/kg) |
|-----|-----------------------------|---------------------------|
| 0 | 223 | 300 |
| 2 | 211 | 270 |
| 4 | 198 | 205 |
| 6 | 185 | 201 |
| 8 | 176 | 199 |

^a Target amount is 250 mg/kg.

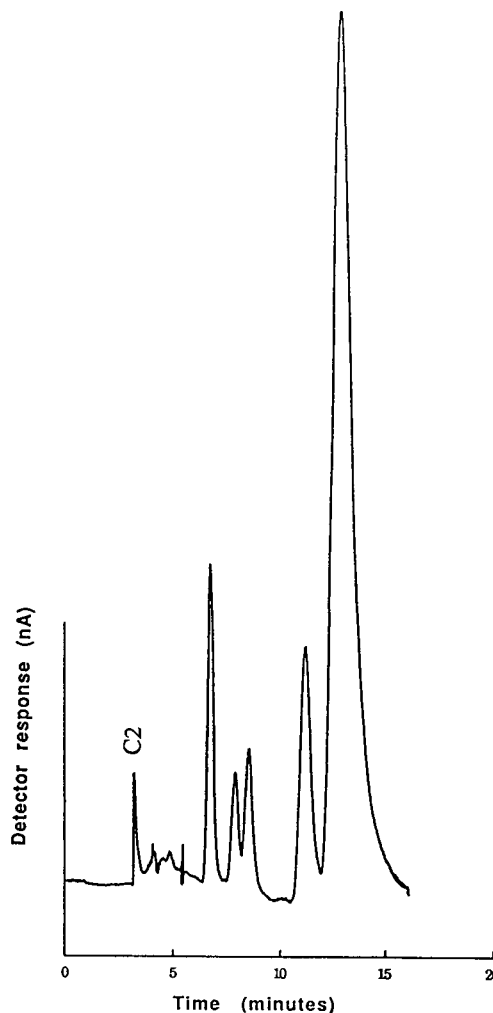


Fig. 2. Chromatogram obtained using a Nucleosil C_{18} column (I. Molnar; 25.0 cm × 4.6 mm I.D.). The mobile phase was 500 ml of an aqueous solution containing 3.2812 g of sodium acetate, 0.0168 g of EDTA and 0.1082 g of SOS, and 26.3 ml of methanol. The pH was adjusted to 4.0 with glacial acetic acid. The flow-rate was 1.0 ml/min, and the column was at room temperature. The electrochemical detector was set at 0.95 V, 20 nA full scale. The sample was a salmon feed containing C2.

CONCLUSION

The reversed phase HPLC system using ion pairing with SOS gives good linearity of C1 and C2 in the standard, and resolves the two forms of vitamin C from the feed matrix in the extract samples. The electrochemical detector gives adequate detection

for the ascorbic acid at the levels found in the feed matrices.

The extraction procedure greatly influenced the recovery of C1 and C2 from the dry extruded feeds. Data from samples extracted both with and without the homogenizer indicate that the homogenizer provides a more complete ascorbic acid extraction. In almost all cases, the homogenizer improved recovery of C1 and C2 from the feed, and the results are much more reproducible.

The data in this paper show that while almost none of the C1 activity remained after manufacture, greater than 95% of the C2 activity remained after manufacture, and less than 20% is lost during 6 months of storage at 40°C. In the most salmon feeds, 81% of C2 activity and none of the C1 activity was retained after 2 weeks of storage. Thus, C2 in commercial feeds is very stable during and after the manufacturing process of commercial feeds. Due to the instability of oils and vitamins other than vitamin C, commercial dry feeds are generally not stored for more than 90 days and soft moist feeds not longer than two weeks.

ACKNOWLEDGEMENTS

The authors wish to thank Archer Daniel Midland and Conners Brothers, Inc. for their assistance with this work. Partial support for this study was provided by Pfizer, Inc., Specialty Chemicals Division.

REFERENCES

- 1 B. W. Tucker and J. E. Halver, *Fish Physiol. Biochem.*, 2 (1986) 151.
- 2 S. F. Quadri, Y. T. Liang, P. A. Seib, C. W. Deyoe and R. C. Hosney, *J. Food Sci.*, 40 (1975) 837.
- 3 A. K. Soliman, K. Jauncey and R. J. Roberts, *Aquaculture*, 60 (1987) 73.
- 4 J. H. Roe, *The Vitamins*, Vol. VII, Academic Press, New York, 1967.
- 5 K. M. De Antonis, P. R. Brown and P. D. Maugle, *J. Liq. Chromatogr.*, 14 (1992) 2581.
- 6 T. Skelbaek, N. G. Anderson, M. Winning and S. Westergaard, *Aquaculture*, 84 (1990) 335.
- 7 W. Schuep, J. Marmet and W. Studer, *Aquaculture*, 79 (1989) 249.
- 8 X. Y. Wang, M. L. Liao, T. H. Hwa and P. A. Seib, *J. Assoc. Off. Anal. Chem.*, 71 (1988) 1158.
- 9 J. A. Albrecht and H. W. Schaefer, *J. Liq. Chromatogr.*, 13 (1990) 2633.
- 10 *The Merck Index*, Merck & Co., Rahway, NJ, 11th ed., 1989.

Estimation of the extent of lipid peroxidation in the ischemic and reperfused heart by monitoring lipid metabolic products with the aid of high-performance liquid chromatography

Gerald A. Cordis and Nilanjana Maulik

Cardiovascular Division, Department of Surgery, Surgical Research Center, University of Connecticut School of Medicine, Farmington, CT 06030 (USA)

Debasis Bagchi

Department of Pharmacy, Creighton University, Omaha, NE 68178 (USA)

Richard M. Engelman and Dipak K. Das

Cardiovascular Division, Department of Surgery, Surgical Research Center, University of Connecticut School of Medicine, Farmington, CT 06030 (USA)

ABSTRACT

Estimation of lipid peroxidation (LPO) through malonaldehyde (MDA) formation measured by assaying thiobarbituric acid reactive products remains the method of choice to study the development of oxidative stress to assess myocardial ischemic reperfusion injury. However, MDA estimation by this assay is non-specific and often gives erroneous results. In this report, we describe a method to estimate MDA, formaldehyde (FDA), acetaldehyde (ADA), and acetone, the degradation products of oxygen free radicals (OFR) and polyunsaturated fatty acids (PUFA), as presumptive markers for LPO. Isolated rat hearts were made ischemic for 30 min, followed by 60 min of reperfusion. The perfusates were collected, derivatized with 2,4-dinitrophenylhydrazine, and extracted with pentane. Aliquots of 25 μ l in acetonitrile were injected on a Beckman Ultrasphere C₁₈ (3 μ m) column. The products were eluted isocratically with a mobile phase containing acetonitrile–water–acetic acid (40:60:0.1, v/v/v). The peaks were identified by co-chromatography with the hydrazine derivatives of authentic standards. The retention times of MDA, FDA, ADA and acetone were 5.0, 6.3, 9.8 and 15.7 min, respectively. The results of our study indicated progressive increase in all four lipid metabolites with reperfusion time. Thus, our results demonstrate that the release of lipid metabolites from the isolated heart increased in response to oxidative stress. Since MDA, FDA, ADA, and acetone are the products of OFR–PUFA interactions, this method allows proper estimation of LPO to monitor the oxidative stress developed during the reperfusion of ischemic myocardium.

INTRODUCTION

The extent of lipid peroxidation in biological tissue and fluid is considered to be an important pa-

rameter for the identification of the oxidative stress developed under the pathophysiologic conditions [1,2]. Formation of malonaldehyde (MDA) is a widely recognized marker for lipid peroxidation [3], and the most commonly used method to estimate MDA formation is the spectrophotometric assay of the MDA following its reaction with thiobarbituric acid (TBA) [4,5]. Although this method is rapid and

Correspondence to: Dr. D. K. Das, Cardiovascular Division, Department of Surgery, University of Connecticut School of Medicine, Farmington, CT 06030-1110, USA.

relatively simple, the significance of the results is often blunted because of the incorrect interpretation of the results. The TBA-reactive products (often referred to as TBAR) as a measure for malonaldehyde formation in non-specific, because TBA not only forms a colored complex with malonaldehyde, but it also reacts with many other compounds including ribose, biliverdin, amino pyrimidines and sialic acid [6].

To overcome this problem a number of methods was developed to estimate MDA–TBA adducts using high-performance liquid chromatography (HPLC) [7,8]. Although these results are more reliable compared to the spectrophotometric methods of TBAR detection, this HPLC technique did not gain popularity because of the extremely complex nature of sample preparation and slowness of the technique.

In this report we describe a highly efficient technique to monitor the lipid peroxidation in biological tissue. It is well known that reperfusion of an ischemic tissue such as heart is associated with the formation of oxygen-derived free radicals which presumably attack the polyunsaturated fatty acids in the membrane phospholipids causing lipid peroxidation [9]. The extent of such lipid peroxidation was measured by estimating MDA and related lipid metabolic products after derivatizing with 2,4-dinitrophenylhydrazine (DNPH) using HPLC. Our results indicated this method to be extremely efficient and reliable to monitor the extent of lipid peroxidation in the ischemic reperfused myocardium as compared to any other available techniques.

EXPERIMENTAL

Materials

TBA and DNPH were obtained from Sigma (St. Louis, MO, USA). Malonaldehyde was purchased from Aldrich (Milwaukee, WI, USA), while formaldehyde, acetaldehyde, and acetone were from Sigma. DNPH standards were generated by derivatization of the pure compounds.

All organic solvents were of HPLC grade (Burdick & Jackson, Muskegon, MI, USA). Water was purified with a Milli-Q system. The mobile phase was filtered through a 0.22- μm nylon-66 solvent filter (Rainin Instrument, Woburn, MA, USA). All other chemicals were of analytical grade.

Methods

Isolated rat heart preparation. Sprague Dawley male rats of about 250 g body weight were anesthetized with intraperitoneal pentobarbital (80 mg per kg). Hearts were removed and quickly mounted on a noncirculating Langendorff perfusion apparatus as described previously [10]. Retrograde perfusion was established at a pressure of 100 cmH₂O ($9.8 \cdot 10^3$ Pa) with oxygenated normothermic Krebs–Henseleit bicarbonate (KHB) buffer containing 3% bovine serum albumin. Hearts were allowed to be equilibrated for 10 min at 37°C with noncirculating KHB buffer. The retrograde aortic flow was then terminated, and the heart was made ischemic for 30 min in physiological saline at 37°C. Reperfusion was then performed with the fresh KHB buffer for 60 min at normothermia. Perfusate samples were collected prior to ischemia (baseline), after ischemia and during the reperfusion for the estimation of MDA.

Assay for MDA as TBA-reactive materials. TBA-reactive materials were estimated by the well-established technique [11]. In short, 1 ml of the perfusate was mixed with 0.2 ml of 15% trichloroacetic acid, 1 ml of 0.75% TBA in 0.5% sodium acetate, and the mixture boiled for 15 min [11]. The red color of the TBA–MDA complex was read with a spectrophotometer using 535 nm wavelength.

Derivatization and extraction of lipid metabolites. The lipid metabolites extracted with the perfusate were derivatized using DNPH. For derivatization purpose, 310 mg of DNPH was dissolved in 100 ml of 2 M HCl, and 0.1 ml of this DNPH reagent (3.13 μmol) was added to 1.5 ml of the perfusate in a 20-ml screw-capped PTFE lined test tube. An aliquot of 0.5 ml of water was added to the tube, the contents were mixed by vortexing and then 10 ml of pentane was added to the mixture. The tubes were intermittently shaken for 30 min, and reactions were allowed to occur at room temperature. The organic phase was removed, and the aqueous phase was extracted with an additional 20 ml of pentane. The pentane extracts were combined, evaporated under a stream of nitrogen at 30°C, and reconstituted in 200 μl of acetonitrile. This filtered acetonitrile extract was directly injected onto the HPLC column.

HPLC procedure. A 25- μl volume of the filtered (0.2- μm Nylon-66 membrane filters in Microfilter-

fuge tubes from Rainin, Woburn, MA, USA) sample was injected onto a Beckman Ultrasphere ODS C₁₈ (3 μ m particle size, 7.5 cm \times 4.6 mm I.D.) column (Rainin, Woburn, MA, USA) in a Waters chromatograph (Milford, MA, USA) equipped with a Model 820 full control Maxima computer system, satellite Wisp Model 700 injector, Model 490 programmable multi-wavelength UV detector (4 channels), two Model 510 pumps, and a Bondapak C₁₈ Guard-Pak pre-column. The DNPH derivatives were detected at 307, 325 and 356 nm simultaneously with 3 channels of the M-490 detector at a flow-rate of 1 ml/min with an isocratic gradient of acetonitrile–water–acetic acid (40:60:0.1, v/v/v) for a total run time of 18 min. The column was washed with acetonitrile–acetic acid (100:0.1, v/v) before each day's work to remove any bound reagent.

Generation of standard curves. To make hydrazone standards, 30 ml of DNPH stock solution was allowed to react with an excess (1 to 3 nmol) of formaldehyde (FDA), acetaldehyde (ADA), MDA or acetone at room temperature. The precipitated hydrazones were filtered, dried, and recrystallized from methanol. Solutions containing 50 ng/ μ l of each of the four synthetic hydrazones were prepared and chromatographed as described above. The perfusion samples were spiked with the known amounts of each of the synthetic hydrazones to identify and confirm the presence of hydrazone derivatives of the lipid metabolites.

RESULTS

Separation and identification of lipid metabolites

The DNPH derivatives of authentic standards of FDA, ADA, MDA and acetone were separated using three different wavelengths: 307, 325 and 356 nm. MDA gives an absorption maximum at 307 nm whereas the absorption maximum for FDA, ADA and acetone is 356 nm. The retention times of MDA, FDA, ADA and acetone were 5, 6.3, 9.8 and 15.7 min, respectively, making a total run time of 18 min (Fig. 1).

Construction of calibration curve

With MAXIMA 820 software, calibration curves were produced and response factors were calculated for all the lipid metabolites. Ten different concen-

trations (10 pmol to 6.25 nmol) of each standard were injected and chromatographed as described previously. Various concentrations of each standard: (A) MDA, (B) FDA, (C) ADA, and (D) acetone were plotted against the peak area obtained. Standard curves were generated for all three wavelengths, 307, 325 and 356 nm.

The response factors were derived from the slope of each curve. Table I shows the values for the response factor, signal-to-noise (S/N) ratio, and the lowest limit of detection for each wavelength.

Quantitative estimation of lipid metabolites in the perfusate

Since reperfusion of ischemic myocardium is as-

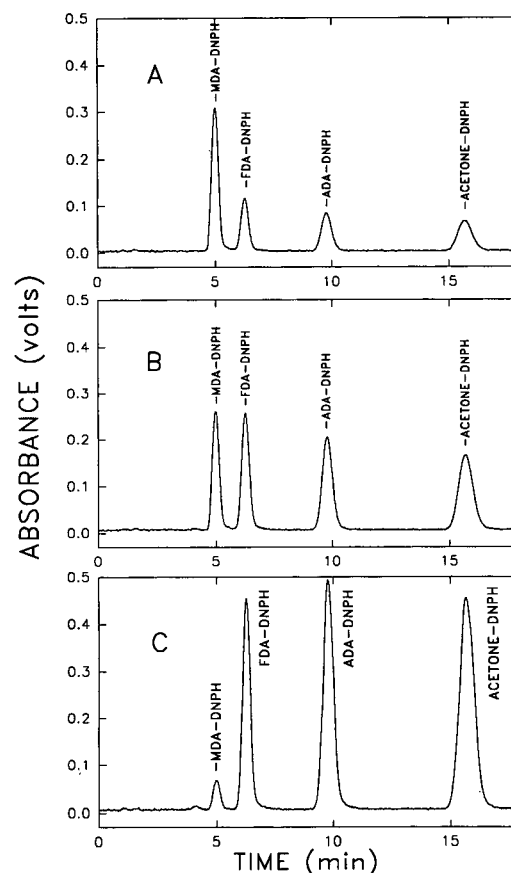


Fig. 1. Separation of MDA-DNPH, FDA-DNPH, ADA-DNPH, and acetone-DNPH standards by reversed-phase HPLC. Aliquots of 25 μ l of standard solutions containing 2 nmol of each DNPH standard were injected onto a C₁₈ column as described in *Methods* and the absorbance measured at three different wavelengths: (A) 307 nm; (B) 325 nm; (C) 356 nm.

TABLE I

RESPONSE FACTOR, r VALUE, LOWEST LIMIT OF DETECTION AND S/N RATIO FOR MDA, FDA, ADA AND ACETONE

| Standard | λ (nm) | Response factor ^a (10^{-7}) | r Value ^b | Lowest limit of detection (pmol) | S/N ratio |
|--------------|----------------|--|------------------------|----------------------------------|-------------|
| MDA-DNPH | 307 | 3.357057 | 0.9985 | 10 | 2.4 |
| MDA-DNPH | 325 | 4.045774 | 0.9981 | 30 | 2.7 |
| FDA-DNPH | 356 | 2.086545 | 0.9984 | 10 | 2.8 |
| FDA-DNPH | 325 | 3.752380 | 0.9982 | 30 | 2.7 |
| ADA-DNPH | 356 | 1.446131 | 0.9983 | 10 | 3.7 |
| ADA-DNPH | 325 | 3.534486 | 0.9987 | 30 | 4.0 |
| Acetone-DNPH | 356 | 1.125031 | 0.9984 | 10 | 3.9 |
| Acetone-DNPH | 325 | 3.195716 | 0.9982 | 30 | 3.1 |

^a Response factor equals the weight of the compound in the calibrating solution (nmol/injection) divided by the integrated peak area of the compound.

^b r Value is the correlation coefficient for a linear standard curve with a perfect correlation at 1.0000.

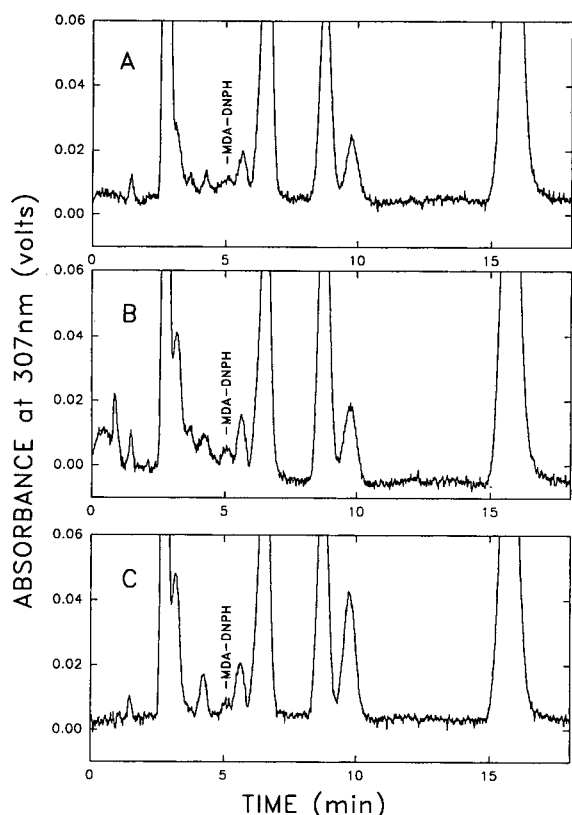


Fig. 2. Separation of MDA-DNPH in rat heart perfusates. Perfusates were collected, derivatized, extracted, and chromatographed as shown in Experimental. Absorbance was measured at 307 nm. (A) Baseline; (B) after 30 min of ischemia and 15 min of reperfusion; (C) after 30 min of ischemia and 60 min of reperfusion.

sociated with the production of lipid peroxidation products from the free radical-lipid interactions, we attempted to measure the lipid metabolites in the ischemic reperfused myocardium. The isolated rat hearts were subjected to 30 min of ischemia followed by 60 min of reperfusion. The perfusates obtained from the heart were processed as described in Methodology and the derivatized extracts were loaded onto the HPLC column equipped with programmable multi-wavelength UV detector. The results from (A) the baseline, (B) 15 min reperfusion, and (C) 60 min reperfusion heart perfusates are shown in Fig. 2 (307 nm), and Fig. 3 (356 nm). As shown in these Figs., the peaks for FDA, ADA, and acetone are already present in the baseline samples, and they increase progressively as the reperfusion progresses. MDA peak is barely present in the baseline sample, and it appears after the reperfusion and like other metabolite peaks, it increases as a function of the duration of reperfusion. The exact values are shown in Table II.

The identify of the peaks were confirmed by comparing the retention times with those of authentic standards. In addition, spiking with the standards was also performed [Fig. 4 (307 nm) and Fig. 5 (356 nm)]. Accuracy of the method was determined by standard addition technique. Addition of 50 pmol

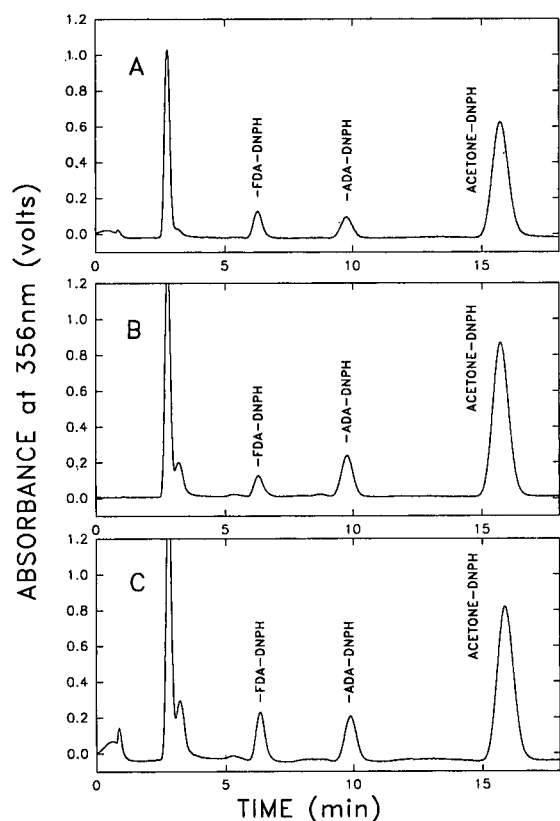


Fig. 3. Separation of FDA-DNPH, ADA-DNPH, and acetone-DNPH in rat heart perfusates under the same conditions as described in Fig. 2 except that the absorbance was measured at 356 nm. (A) Baseline; (B) after 30 min of ischemia and 15 min of reperfusion; (C) after 30 min of ischemia and 60 min of reperfusion.

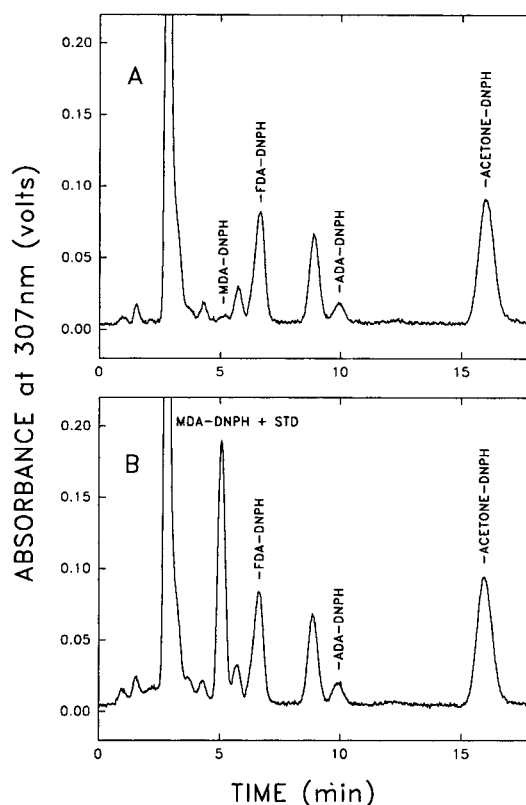


Fig. 4. Peak addition of MDA-DNPH to rat heart perfusate reperfused 15 min after 30 min of ischemia. Amounts of 0.33 nmol of MDA-DNPH standards were added to rat myocardial perfusate and chromatographed as shown in *Methods* and the absorbance measured at 307 nm. (A) Rat heart perfusate after 30 min of ischemia and 15 min of reperfusion; (B) same perfusate as in A with the addition of 0.33 nmol of MDA-DNPH standard.

TABLE II

ESTIMATION OF MDA-DNPH, FDA-DNPH, ADA-DNPH AND ACETONE-DNPH IN RAT HEART DURING ISCHEMIA AND REPERFUSION

| Time of reperfusion (min) | Amount \pm S.D. ($n = 6$) (nmol/ml perfusate) | | | | |
|---------------------------|---|-------------------|-------------------|-------------------|-----------------------|
| | MDA-TBA | MDA-DNPH (307 nm) | FDA-DNPH (356 nm) | ADA-DNPH (356 nm) | Acetone-DNPH (356 nm) |
| Baseline | 0.23 \pm 0.08 | 0.049 \pm 0.016 | 3.10 \pm 0.17 | 2.84 \pm 0.28 | 21.34 \pm 1.16 |
| 1 | 1.15 \pm 0.19 | 0.069 \pm 0.009 | 2.97 \pm 0.83 | 3.14 \pm 1.03 | 26.20 \pm 3.57 |
| 15 | 1.58 \pm 0.21 | 0.077 \pm 0.014 | 3.23 \pm 0.53 | 4.15 \pm 1.88 | 19.76 \pm 3.80 |
| 30 | 1.61 \pm 0.42 | 0.109 \pm 0.033 | 5.31 \pm 2.73 | 4.23 \pm 1.43 | 25.18 \pm 2.17 |
| 45 | 1.78 \pm 0.56 | 0.119 \pm 0.009 | 6.16 \pm 1.91 | 5.70 \pm 1.55 | 22.13 \pm 2.0 |
| 60 | 2.41 \pm 0.84 | 0.136 \pm 0.024 | 4.69 \pm 1.92 | 5.24 \pm 1.48 | 26.11 \pm 1.82 |

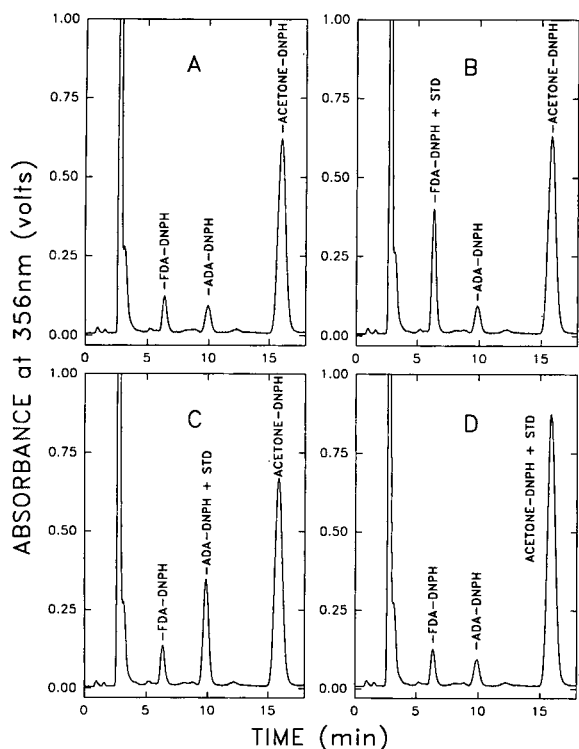


Fig. 5. Peak addition of DNPH standards to rat heart perfusate. Conditions were the same as described in Fig. 4, except that the absorbance was measured at 356 nm. (A) Rat heart perfusate after 15 min of reperfusion; (B) perfusate with the addition of 0.33 nmol of FDA-DNPH standard; (C) perfusate with the addition of 0.33 nmol of ADA-DNPH standard; and (D) perfusate with the addition of 0.33 nmol of acetone-DNPH standard.

TABLE III

ESTIMATION OF MDA AS TBA-REACTIVE PRODUCTS IN RAT HEART DURING ISCHEMIA AND REPERFUSION

| Time of reperfusion (min) | Amount of MDA \pm S.D. ($n = 6$) (nmol/ml perfusate) |
|---------------------------|--|
| Baseline | 0.23 \pm 0.08 |
| 1 | 1.15 \pm 0.19 |
| 15 | 1.58 \pm 0.21 |
| 30 | 1.61 \pm 0.42 |
| 45 | 1.78 \pm 0.56 |
| 60 | 2.41 \pm 0.84 |

of each of the standards were accurately reflected in the peak heights. Within-run and inter-run variations were 1 and 5%, respectively.

TBA-reactive materials

The same perfusate samples were also estimated by assaying the TBA-reactive materials. The values for TBA-reactive materials are shown in Table III. As expected these values were much higher compared to those obtained for MDAs from the corresponding myocardial perfusate samples.

DISCUSSION

Lipid peroxidation is a complex process in which polyunsaturated fatty acids are subjected to attack by the oxygen-derived free radicals resulting the formation of lipid hydroperoxides. In biological tissues these lipid hydroperoxides are broken down into variety of products including aldehydes and ketones [11]. A large variety of methods are available for the detection of lipid peroxidation products which include determination of diene conjugation [12], lipid hydroperoxides [13], chemiluminescence [14], hydroxy acids [15], ethane [16] and TBA-reactive materials [4,5]. Among these methods estimation of TBA reactive products is most popular and widely used to study the lipid peroxidation in biological samples. The success of the TBAR method depends on the accuracy of the determination of MDA content. However, as mentioned earlier, TBA reacts with many other compounds besides MDA, and as a result it often overestimates the MDA content and yields erroneous results. This method was subsequently modified to determine MDA-TBA complex by HPLC, but the slowness as well as the complexity of the procedure could not make it easily adaptable for the routine assay of MDA.

In this report we have described a method which can accurately estimate at least four different lipid breakdown products, MDA, FDA, ADA and acetone. In this method the carbonyls present in the myocardial tissue are converted into hydrazone derivatives by reacting with DNPH. This method was previously used to examine the lipid metabolites in the urine samples [17]. However, no attempt has ever been made to use this method to estimate the extent of lipid peroxidation under the pathophysi-

ological conditions in biological tissues such as heart. It has long been known that reperfusion of ischemic tissue produces oxygen free radicals, which subsequently attack the PUFA of the membrane lipids causing lipid peroxidation. Accurate estimation of the extent of lipid peroxidation is of utmost importance to monitor the development of oxidative stress in the ischemic reperfused tissue and to understand the pathophysiology of reperfusion injury. Our results indicate that DNPH method can be successfully used to estimate the lipid peroxidation in ischemic and reperfused heart.

Our results indicate that the values for TBA-reactive products are much higher compared to actual malonaldehyde values. This is not surprising, because TBA-reactive products estimates many other compounds besides MDA as mentioned earlier, thus overestimating the actual MDA values. MDA formation indeed occurs during the reperfusion of ischemic heart, but the amounts of MDA formed are very low.

ACKNOWLEDGEMENTS

This study was supported by Grants HL 22559 and HL 33889 from the US Public Health Service (National Institute of Health). We greatly appreciate the excellent secretarial assistance of Mrs. Laurie Amara.

REFERENCES

- 1 D. K. Das, R. M. Engelman, D. Flansaas, H. Otani, J. Roussou and R. H. Breyer, *Basic Res. Cardiol.*, 82 (1987) 36.
- 2 J. M. Petruska, S. H. Y. Wong, W. Sanderman and B. T. Mossman, *Free Rad. Biol. Med.*, 9 (1990) 51.
- 3 H. S. Lee and A. S. Csallany, *Lipids*, 22 (1987) 104.
- 4 T. F. Slater, *Methods Enzymol.*, 105 (1984) 283.
- 5 R. P. Bird and H. H. Draper, *Methods Enzymol.*, 105 (1984) 299.
- 6 J. M. C. Gutteridge and T. R. Tickner, *Anal. Biochem.*, 91 (1978) 250.
- 7 H. Esterbauer, J. Lang, S. Zadavec and T. F. Slater, *Methods Enzymol.*, 105 (1984) 319.
- 8 L. W. Yu, L. L. Latriano, S. Duncan, R. A. Hartwick and G. Witz, *Anal. Biochem.*, 156 (1986) 326.
- 9 X. Liu, R. Prasad, R. M. Engelman, R. M. Jones and D. K. Das, *Am. J. Physiol.*, 259 (1990) H1101.
- 10 H. Otani, R. Prasad, R. M. Jones and D. K. Das, *Am. J. Physiol.*, 257 (1989) H252.
- 11 H. Esterbauer, in D. C. H. Brien and T. F. Slater (Editors), *Free Radicals, Lipid Peroxidation and Cancer*, Academic Press, London, 1982, p. 101.
- 12 R. O. Recknagel and A. K. Ghosal, *Exp. Mol. Pathol.*, 5 (1966) 413.
- 13 W. A. Pryor and L. Castle, *Methods Enzymol.*, 105 (1984) 293.
- 14 J. R. Wright, R. C. Rumbaugh, H. D. Colby and P. R. Miles, *Arch. Biochem. Biophys.*, 192 (1979) 344.
- 15 J. Capdevila, L. J. Marnett, N. Chacos, R. A. Prough and R. W. Estabrook, *Proc. Natl. Acad. Sci. USA*, 79 (1982) 767.
- 16 C. Riely, G. Cohen and M. Lieberman, *Science, (Washington, D.C.)*, 183 (1974) 208.
- 17 M. A. Shara, P. H. Dickson, D. Bagchi and S. J. Stohs, *J. Chromatogr.*, 576 (1992) 221.

Size-exclusion chromatographic determination of β -glucan with postcolumn reaction detection

T. Suortti

Technical Research Centre of Finland, Food Research Laboratory, P.O. Box 203, SF-02151 Espoo (Finland)

ABSTRACT

Using the specific interaction of β -glucan with calcofluor dye as a detection method for size-exclusion chromatographic analysis, very simple direct extractions can be used for sample preparation. Either fluorescence or UV detection is employed. The calibration graphs are linear between 200 and 20 mg/l, although much more sensitive analyses are possible. The response remained independent of relative molecular mass in the range studied ($1.7 \cdot 10^6$ – $1.85 \cdot 10^5$). Results for barley and malt show good correlation with those obtained by flow-injection analysis using calcofluor.

INTRODUCTION

The major soluble component in barley and oat cell walls is (1 \rightarrow 3),(1 \rightarrow 4)- β -D-glucan. Most of the interest in oat β -glucan has been attributed to its possible role in lowering serum cholesterol levels [1]. It is also a good source of soluble fibre and in recent studies purified soluble fibre extract (oat gum) has been demonstrated to reduce postprandial glucose and insulin increases [2]. Jenkins *et al.* [3] have reported that a positive correlation exists between viscosity and the efficiency of soluble fibres in this reduction, hence oat gum with higher relative molecular mass components should be the preferred product.

On the other hand, in barley β -glucan is considered to be responsible for several problems in the brewing industry, including delayed filtration of wort and beer and gel precipitations in lagering. These problems are related not only to β -glucan content, but also to its relative molecular mass (M_r), especially in the concentration of the β -glucan fraction which is soluble in perchloric acid [4].

There are two widely used methods for β -glucan determination. One is based on the utilization of specific enzymes and the determination of released oligosaccharide or glucose [5]. The other is based on the specific interaction of β -glucan with calcofluor dye [6–8]. This interaction results in an increase in fluorescence intensity and also in a bathochromatic shift. The increase in fluorescence has been widely employed in flow-injection analysis (FIA) of β -glucan in beer and wort [9–12], and also in the determination of β -glucan fractions isolated by size-exclusion chromatography (SEC), both off-line [13–15] and recently for on-line post-column detection [16]. SEC of β -glucan has been studied by Vårum *et al.* [17], who showed that its structure is more rigid than that of dextran or pullulan, and hence their utilization as standards would result in severe overestimation of the relative molecular mass of β -glucan. Similar results were obtained also by Wood *et al.* [16].

The injection of highly viscous samples easily results in deformation of peak shapes and thus in erroneous results. This effect is most serious in SEC as dilution is less than in other chromatographic modes [18]. β -Glucan is one example of samples that have high viscosity and thus may easily result in erroneous results because of deformed peaks. We

Correspondence to: T. Suortti, Technical Research Centre of Finland, Food Research Laboratory, P.O. Box 203, SF-02151 Espoo, Finland.

encountered this effect in our initial experiments with a multi-angle laser light-scattering detector, where in some instances no change in molecular size could be seen with increasing elution volume. This effect could also be seen by the much improved peak shape on decreasing the sample concentration from 2000 to 200 mg/l [19]. This level is near the detection limit of the refractive index detector. β -Glucan samples are also easily contaminated by other polysaccharides, especially if more alkaline extraction conditions are used. Hence universal detection with a refractive index detector is by no means adequate without extensive cleaning of samples.

We have previously employed 50 mM sodium hydroxide solution as an SEC eluent for starch samples [20] and showed that the chromatographic conditions used give a linear calibration graph with pullulan standards in M_r range 853 000–5800 [21] and with a separation potential for much larger molecules. The employment of this elution system in connection with specific detection using calcofluor dye led us to a system for the determination of β -glucans in which aqueous buffers of any pH may be used for sample extraction followed by direct injection of the sample into the HPLC system. As we utilize the bathochromic shift that occurs on interaction of β -glucan with calcofluor, the method has a much lower background signal than the on-line postcolumn fluorimetric method utilizing only the increase in the fluorescence signal caused by the interaction of calcofluor with β -glucan. Hence our method works in the concentration range 200–20 mg/l and UV detection can also be used in addition to fluorimetric detection.

The good sensitivity also results in a sample/extractant ratio of 80–300, which in connection with the minimum sample treatment required results in high recoveries and reproducibility. Some results obtained with this method have been presented previously [22].

EXPERIMENTAL

Chemicals

Oat β -glucan standard compounds were isolated and their M_r were determined as $1.50 \cdot 10^6$ and $4.6 \cdot 10^5$ by measurement with a Malls detector (Dawn, Santa Barbara, CA, USA). Barley β -glucan with M_r

$= 1.85 \cdot 10^5$ was obtained from Biocon (Sydney, Australia). Wheat and rye arabinoxylans were obtained from Megazyme (Cork, Ireland), birch xylan from Roth (Karlsruhe, Germany) and calcofluor (Fluorescent Brightener 28) from Aldrich Chemie (Steinheim, Germany). The water used was distilled water passed through a Milli-Q purification system (Millipore, Bedford, MA, USA). All the other chemicals were of analytical-reagent grade. Milled barley and malt samples were obtained from the Biotechnical Laboratory of the Technical Research Centre of Finland and the oat bran samples were from our laboratory.

Equipment

The chromatographic system consisted of an M-590 pump, an M-715 automatic injector and μ Hydrogel 250 and 2000 columns in series in a column oven maintained at 65°C. Calcofluor solution (30 mg/l in 50 mM NaOH) was fed into the eluent by a reagent delivery module (RDM) at a flow-rate of 0.3 ml/min. For detection an M-490 fluorescence detector with $\lambda_{ex.} = 415$ nm and $\lambda_{em.} = 445$ nm at a sensitivity setting of $10 \times$ was employed, together with an M-991 diode-array detector monitoring at 415 nm. The instrument was controlled and data were handled by an M-820 Maxima workstation (all equipment from Millipore–Waters).

The eluent was 50 mM aqueous NaOH at a flow-rate of 0.5 ml/min and was continuously purged with helium.

Sample preparation

A 30-mg sample of milled barley or malt was mixed either with 20 ml of 50 mM NaOH solution (procedure A) or 20 ml of 50 mM sodium phosphate buffer (pH 11) (procedure B). A 300-mg sample of milled barley or malt was mixed with 20 ml of 1 M NaOH (procedure C), and a 100-mg sample was mixed with 18 ml of 50 mM perchloric acid (procedure D). All the samples were stirred overnight in a magnetic stirrer. The only sample preparation before injection of 50- μ l samples was dilution 1:10 with water of the samples prepared according to procedure C. Oat bran samples were prepared in a similar manner.

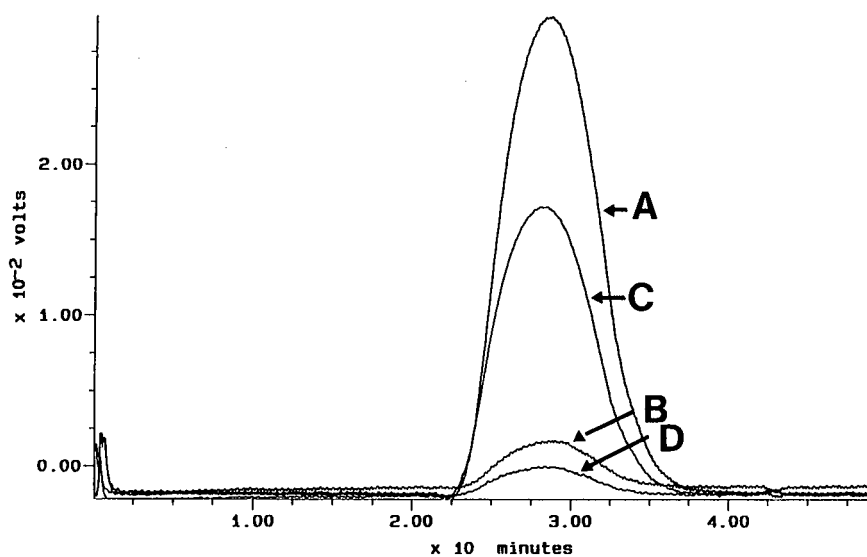


Fig. 1. SEC analysis of β -glucan standards containing 180 and 18 mg/l of β -glucan using (A and B) fluorescence detection and (C and D) UV detection. For other conditions, see text.

RESULTS AND DISCUSSION

The calibration graph based on the measurement of the area of the β -glucan peak was linear between β -glucan concentrations of 200 and 20 mg/l for both fluorescence and UV detection (Fig. 1). Both wavelengths chosen were optimum regarding the signal-to-noise ratio, which is mostly determined by the evenness of the flow of the calcofluor solution. At higher concentrations the calibration graph started to flatten because of too high a ratio of β -glucan to calcofluor. Attempts to increase the linear range by using more concentrated calcofluor solution resulted in a problem with the baseline. With lower concentrations the noise of the baseline started to affect the linearity, although as we are utilizing the bathochromic shift the background noise is less problematic than when working at lower wavelengths. The background signal may be reduced by diluting the calcofluor reagent and using a higher sensitivity setting of the fluorescence detector. Thus the detection limit may be reduced to 0.2 mg/l but the linearity of the calibration graph is inferior to that obtained in the concentration range 200–20 mg/l.

The relative standard deviations for the retention time of standards in a run lasting 70 h were 0.36% and 0.17% ($n = 8$), although the first value was

obtained for a broader peak, which may be the reason for the higher standard deviation.

The response for β -glucans in this relative molecular mass range remained independent of the latter. First the hydrolysed β -glucan sample having an estimated M_r of 30 000 showed a peak with a steeply dropping end, which indicates reduced interaction with calcofluor with small β -glucan molecules, as mentioned by Foldager and Jørgensen [13] and Manzanares *et al.* [15]. The addition of 0.1 M NaCl to increase the ionic strength of the calcofluor reagent, as suggested by Manzanares *et al.*, did not have any noticeable effect on the peak tailing, but this may be because our samples still had too high relative molecular masses to be affected by this phenomenon. Manzanares *et al.* [15] noticed this phenomenon already for β -glucans having $M_r < 200\,000$, but they calibrated their column with dextran so their relative molecular mass was erroneously high.

The relative standard deviation for eight standards run during a 70-h analysis series was 2.2%. A comparison between the β -glucan concentration calculated on the basis of the peak area in chromatograms from barley and malt samples prepared according to procedure B and with ordinary FIA using calcofluor is presented in Table I. As can be

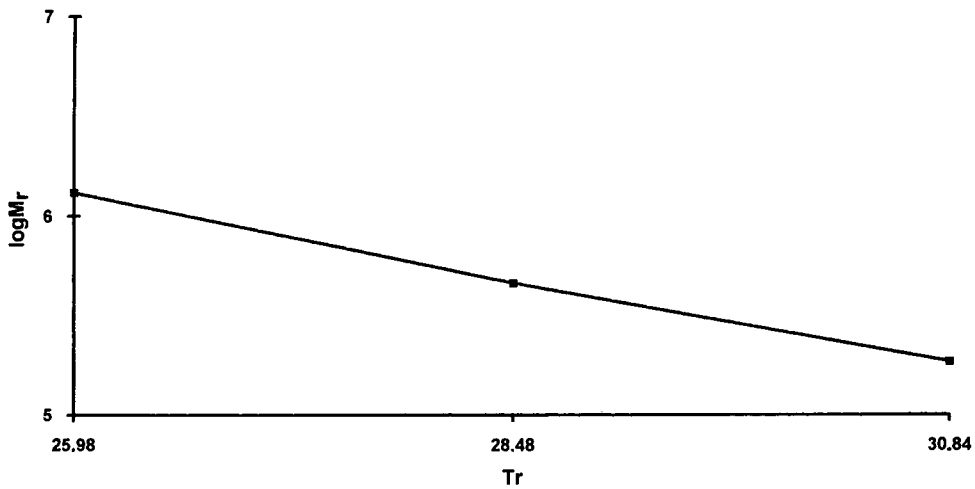


Fig. 2. SEC calibration plot. Tr in minutes.

seen, the results are very similar. The relative standard deviation for parallel samples was 2.3% with different extraction procedures. The β -glucan concentration obtained by procedure B varied from 19 to 47% in comparison with that obtained with procedure A. With procedure C the values varied from 77 to 94% and for procedure D, which measures

more the concentration of β -glucan that causes problems in beer manufacture, the values varied from 32 to 53%. As can be seen in Fig. 4, the relative molecular mass of these perchloric acid-soluble β -glucans is smaller than that in the fraction soluble in alkali. Figs. 3 and 4 also reveals that the relative molecular mass of β -glucan is not reduced during

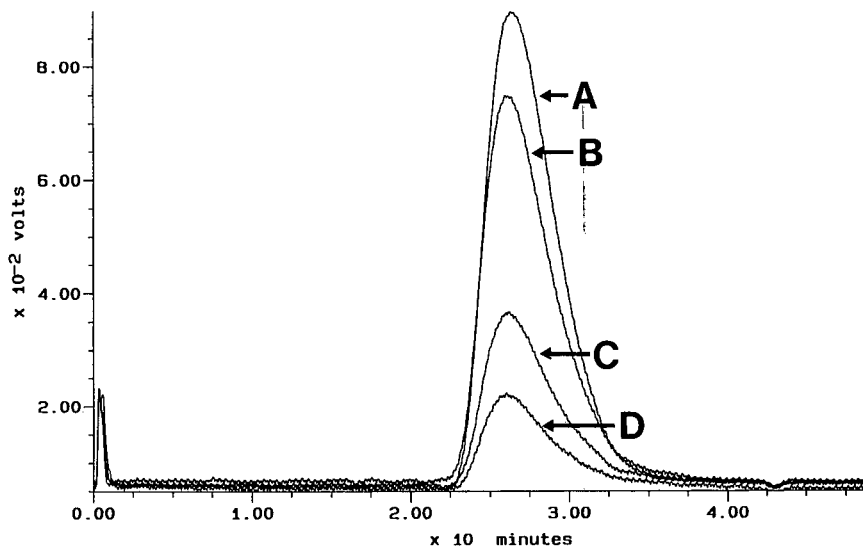


Fig. 3. Chromatogram of (A) Kymppi barley and (B-D) malts made from it during different stages of malting. Fluorescence detection. For other conditions, see text.

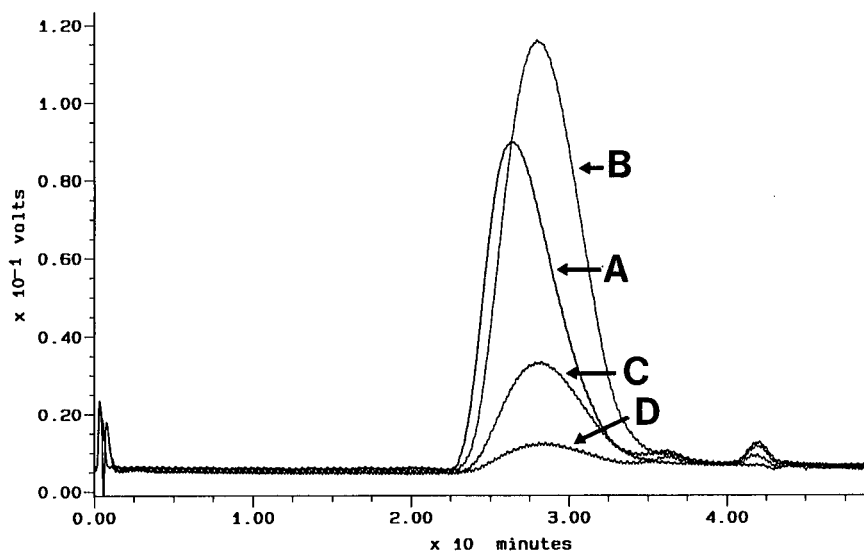


Fig. 4. Chromatogram of Kymppi barley with (A) alkaline extraction and (B) perchloric acid extraction. Chromatograms C and D are from perchloric acid extractions of malts made from Kymppi barley. Sample amounts for perchloric acid extractions were three times higher than for alkaline extraction.

malting, although the amount is reduced. The hydrolysis results in such small molecules that they are no longer stained by calcofluor.

For the oat bran, procedure A again gave the highest values, although the values from procedures

B and C ranged from 90 to 95%, which may reflect the easier accessibility to β -glucan in oat bran than in barley. The values for bran ranged from 55 to 47 g/kg.

Wood [8] has reported that calcofluor interacts with some other polysaccharides such as xylans. Some xylans and arabinoxylans were studied using the present chromatographic system but none of them showed any response in the relative molecular mass range considered.

The use of strongly alkaline solutions for extraction may also dissolve starch, so its possible effect was also studied. A 40-fold excess of starch in the β -glucan standard did not have any effect on the standard peak.

The method presented gives the possibility of studying the concentration and relative molecular mass of β -glucan in barley, malt and oat with minimum sample preparation and with good accuracy.

TABLE I

DETERMINATION OF β -GLUCAN CONCENTRATION BY THE CHROMATOGRAPHIC METHOD DESCRIBED AND BY THE FIA METHOD WITH CALCOFLUOR

| Sample | β -Glucan concentration (g/kg) | |
|---------------|--------------------------------------|-----|
| | SEC | FIA |
| <i>Barley</i> | | |
| Kymppi | 48 | 48 |
| HJA | 45 | 45 |
| Mut1460 | 24 | 24 |
| Mut737 | 31 | 35 |
| Minerva | 48 | 51 |
| Prisma | 34 | 32 |
| <i>Malt</i> | | |
| SH 16 | 33 | 38 |
| SH 17 | 17 | 17 |
| SH 18 | 8 | 9 |

ACKNOWLEDGEMENTS

The authors thanks Mrs. L. Öhrnberg for skilful technical assistance and S. Home for the barley and malt samples and FIA with calcofluor.

REFERENCES

- 1 J. W. Anderson, in F. M. Webster (Editor), *Oats, Chemistry and Technology*, American Association of Cereal Chemistry, St. Paul, MN, 1986, pp. 309–333.
- 2 P. J. Wood, J. T. Braate, F. W. Scott, D. Reidel and L. M. Poste, *J. Agric. Food Chem.*, 38 (1990) 753.
- 3 D. J. A. Jenkins, E. Bright-See, R. Gibson, R. G. Josse, D. Kritchevsky, R. D. Peterson and V. F. Rasper, *Report of the Expert Advisory Committee on Dietary Fiber*, Health Protection Branch, Health and Welfare Canada, Ottawa, 1978.
- 4 L. Narziss, E. Recheneder and M. J. Edney, *Brauwissenschaft*, 41 (1989) 277.
- 5 B. V. McLeary and M. Glennie-Holmes, *J. Inst. Brew.*, 91 (1985) 285.
- 6 P. J. Wood, *Ind Eng. Chem., Prod. Res. Dev.*, 19 (1980) 19.
- 7 P. J. Wood, *Carbohydr. Res.*, 85 (1980) 271.
- 8 P. J. Wood, *Carbohydr. Res.*, 102 (1982) 283.
- 9 K. G. Jørgensen, S. A. Jensen, P. Hartley and L. Munck, in *European Brewery Convention, Proceedings of the 20th Congress, Helsinki, 1985*, p. 403.
- 10 K. G. Jørgensen and S. Aastrup, in H. F. Linkems and J. Jackson (Editors), *Modern Methods of Plant Analysis, Vol. 7, Beer Analysis*, Springer, Heidelberg, 1986, pp. 88–108.
- 11 E. Mekis, G. Pintér and G. Béndek, *J. Inst. Brew.*, 93 (1987) 396.
- 12 J. M. Sendra, J. W. Carbonell, M. J. Gosalbes and V. Todo, *J. Inst. Brew.*, 95 (1989) 327.
- 13 L. Foldager and K. G. Jørgensen, *Carlsberg Res. Commun.*, 49 (1984) 525.
- 14 L. Narziss, E. Recheneder and M. J. Edney, *Brauwissenschaft*, 11 (1989) 430.
- 15 P. Manzanares, A. Navarro, J. M. Sendra and V. Carbonell, *J. Inst. Brew.*, 97 (1991) 101.
- 16 P. J. Wood, J. Weisz and W. Mahn, *Cereal Chem.*, 68 (1991) 530.
- 17 K. M. Vårum, A. Martinsen and O. Smidsrød, *Food Hydrocoll.*, 5 (1991) 363.
- 18 M. Czok, A. M. Katti and G. Guiochon, *J. Chromatogr.*, 546 (1991) 705.
- 19 T. Suortti, unpublished results.
- 20 T. Suortti and E. Pessa, *J. Chromatogr.*, 536 (1991) 251.
- 21 T. Suortti and E. Berthoft, *HPLC'91, Proceedings, San Francisco, October 1991*, in press.
- 22 K. Henrikson, O. Myllymäki, H. Vihinen and K. Poutanen, presented at *8th World Congress on Food Science and Technology, Toronto, Canada, September 29th–October 4th, 1991*.

Identification and determination of phenolic constituents in natural beverages and plant extracts by means of a coulometric electrode array system

Guido Achilli, Gian Piero Cellerino and Paul H. Gamache

ESA International, 45 Wiggins Avenue, Bedford, MA (USA)

GianVico Melzi d'Eril

Servizio di Analisi, Fondazione Mondino, Piazza Palestro 3, Pavia (Italy)

ABSTRACT

A general method for the evaluation of phenolic compounds in fermented beverages, fruit juices and plant extracts was developed using gradient HPLC and coulometric detection. In a single injection (10 μ l) it was possible to identify and determine 36 different molecules (flavonoids and simple and complex phenols), without sample extraction, purification or concentration, in several kinds of beers, red and white wines, lemon juice and soya, forsythia and tobacco extracts. The analytical performance of the method is reported. In addition to components already identified and described in the literature, a large number of other phenolic constituents were resolved. These other components may also be useful for the characterization of these beverages and extracts.

INTRODUCTION

Phenolic compounds are present in both plants and fruits and in their derived products such as wines, beers, juices and plant extracts. These compounds are very important in wines and beers as their bitterness and astringency contribute to taste. They also play a fundamental role in the ageing of wine as they act as natural preservatives. Some phenolic components are transferred from the barrel to the wine. This improves the taste or, as with distilled beverages such as brandy and whisky, generates the fundamental characteristics of the product.

Many researchers have made detailed studies of the characterization and determination of phenolic compounds. However, the great complexity of nat-

ural beverages has been a major obstacle to the identification of their constituents. In the last few years, in most of the work published on this topic high-performance liquid chromatography (HPLC) was used to separate the compounds, with different detection systems for determination of the separated compounds, *e.g.*, UV [1–5], electrochemical [6–8], photodiode array [9,10] and atomic absorption spectrometry [8]. Even though there have been numerous publications on this subject, only a relatively small number of phenolic compounds have been investigated at one time in each individual study.

This paper reports the separation and determination of 36 different compounds in a single run without sample extraction, purification or concentration. This was achieved using gradient reversed-phase HPLC and an array of sixteen coulometric electrodes for electrochemical detection.

Correspondence to: G. Achilli, Piazza Maggiolini 3, Parabiago, Milan, Italy.

EXPERIMENTAL

Chemicals

The mobile phase used in the gradient runs was purchased from ESA (Bedford, MA, USA). Mobile phase A was 34.7 μM sodium dodecyl sulphate (SDS)–0.1 M monobasic sodium phosphate–50 nM nitrilotriacetic acid–50% aqueous methanol (pH 3.45) and mobile phase B was 173 μM SDS–0.1 M monobasic sodium phosphate–50 nM nitrilotriacetic acid–50% aqueous methanol (pH 3.45). Solutions A and B were filtered through 0.2- μm PTFE lyophilic filters (Millipore, Bedford, MA, USA) and degassed by sonication under vacuum for 10 min prior to use.

The water used for the dilution of the standards and of the samples was purified with a Milli-Q R/O water purification system (Millipore).

Apparatus

A Coulochem electrode array system (CEAS) from ESA was used. The instrument consisted of a refrigerated autosampler capable of variable-volume injections with a 100- μl loop. A circulating bath was used to maintain sample vials between 0 and 4°C prior to analysis. Gradient operation was provided by two HPLC pumps capable of operating from 0.05 to 10 ml/min. The output of the pumps was connected to a dynamic gradient mixer. Solutes were separated on an HR 80 column (ESA) containing PTFE-lined ODS of 3- μm particle size (80 mm \times 4.6 mm I.D.). The detection system consisted of four cell packs in series, each pack containing four porous graphite working electrodes with associated palladium reference electrodes and platinum counter electrodes. The detector, column and a pulse damper were housed in a temperature-controlled compartment. Two additional pulse dampers were placed before the column and cell compartment. The autosampler, pumps, detectors, temperature-controlled box and all associated electronic circuitry were monitored and controlled by the CEAS software installed on a Model 386 computer equipped with a 80 Mbyte hard disk and a 1.2 Mbyte floppy disk drive. The computer was coupled to a high-resolution colour monitor with a "touch screen" interface and to a matrix graphic printer. The computer system also performed data storage, analysis and report generation. An appro-

priate software package was used for summary reports of the final data (Lotus 123).

Chromatographic method

A method capable of completely separating the 36 compounds chosen was developed. It consisted of a gradient where the organic modifier, pH and counter ion were altered during the run. The time line showing the gradient used in separation is presented in Fig. 1. The total flow-rate was 1.00 ml/min and the temperature compartment was maintained at 37°C. The sixteen detector potentials constituted a symmetric array: –250 mV at electrode 1 (to perform negative screening), 60 mV at electrode 2 with increments of 60 mV at each subsequent electrode until a value of 840 mV is reached at electrode 15, and –250 mV at electrode 16 (to verify possible generation of reversible components). The indicated potentials are referred to the solid-state palladium reference electrode built in the coulometric cells; their absolute value is about 250 mV lower than the corresponding potential measured by using an Ag/AgCl reference electrode.

Standard and sample preparation

All standards (Table I) were purchased from Sigma (St. Louis, MO, USA). The primary stock standard solutions were made by dissolving 10 mg of the component in 50% aqueous methanol. Individual secondary stock standard solutions were made by diluting each component of the primary solutions with deionized water in order to give a concentration of 1 $\mu\text{g}/\text{ml}$. These concentrates were then subdivided into 1-ml portions. They were stored at –30°C and thawed when necessary at 4°C. A 36-

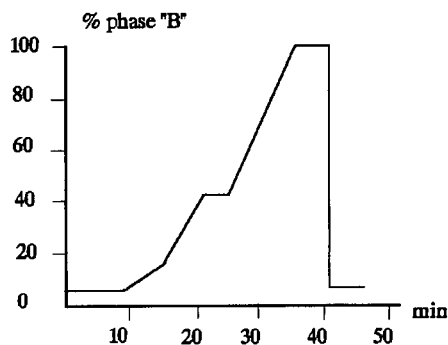


Fig. 1. Time line showing the gradient profile used in the method.

TABLE I

CHROMATOGRAPHIC AND ELECTROCHEMICAL CHARACTERISTICS OF THE EXTERNAL STANDARDS

| Identification No. | Name | Retention time (min) | Concentration (ng per 10 μ l) | Dominant potential (mV) | Within-run R.S.D. (%) | Between-run R.S.D. (%) |
|--------------------|--|----------------------|-----------------------------------|-------------------------|-----------------------|------------------------|
| 1 | Gallic acid | 3.25 | 3.75 | 60 | 1.20 | 2.20 |
| 2 | Tyrosine | 4.88 | 3.75 | 540 | 2.50 | 1.80 |
| 3 | Gentisic acid | 5.13 | 3.75 | 60 | 1.60 | 1.90 |
| 4 | Protocatechuic acid | 6.12 | 3.75 | 120 | 3.70 | 4.20 |
| 5 | 3,4-Dihydroxyphenylacetic acid (DOPAC) | 7.94 | 3.75 | 60 | 0.80 | 3.50 |
| 6 | Vanillyl alcohol | 10.54 | 3.75 | 300 | 0.70 | 2.50 |
| 7 | 4-Hydroxybenzoic acid (4-HBAC) | 10.77 | 1.87 | 720 | 1.60 | 5.20 |
| 8 | 4-Hydroxyphenylacetic acid (4-HPAC) | 13.32 | 3.75 | 540 | 1.80 | 3.40 |
| 9 | Salsolinol | 14.52 | 3.75 | 120 | 3.20 | 3.40 |
| 10 | Tyrosol | 15.27 | 3.75 | 600 | 2.80 | 2.60 |
| 11 | Esculin | 15.97 | 3.75 | 540 | 1.50 | 2.70 |
| 12 | Vanillic acid | 15.93 | 3.75 | 480 | 2.60 | 5.20 |
| 13 | Salicylic acid | 15.97 | 3.75 | 720 | 0.80 | 3.50 |
| 14 | Caffeic acid | 16.51 | 3.75 | 120 | 1.10 | 3.80 |
| 15 | Catechin | 16.58 | 3.75 | 480 | 2.50 | 2.20 |
| 16 | Esculetin | 17.14 | 3.75 | 180 | 2.40 | 4.40 |
| 17 | Tannic acid (1) | 17.47 | 56.20 | 120 | 3.20 | 4.80 |
| 18 | Chlorogenic acid | 17.98 | 3.75 | 120 | 2.50 | 3.80 |
| 19 | Vanillin | 18.17 | 3.75 | 480 | 1.10 | 4.30 |
| 20 | Syringic acid | 18.77 | 3.75 | 360 | 4.30 | 5.10 |
| 21 | Coniferyl alcohol | 20.78 | 3.75 | 300 | 3.80 | 3.70 |
| 22 | Syringaldehyde | 21.14 | 3.75 | 420 | 2.80 | 4.30 |
| 23 | <i>p</i> -Coumaric acid | 21.66 | 3.75 | 540 | 4.20 | 5.80 |
| 24 | <i>o</i> -Vanillin | 22.44 | 3.75 | 420 | 1.30 | 3.20 |
| 25 | Tanic acid (2) | 22.68 | 56.20 | 120 | 1.50 | 4.20 |
| 26 | Ferulic acid | 24.69 | 3.75 | 360 | 2.90 | 4.80 |
| 27 | Tannic acid (3) | 25.11 | 56.20 | 120 | 2.10 | 3.40 |
| 28 | Narigin | 28.71 | 7.50 | 660 | 3.80 | 5.50 |
| 29 | Hesperidin | 29.39 | 15.00 | 420 | 2.80 | 3.80 |
| 30 | Rutin (1) | 29.44 | 7.50 | 180 | 1.80 | 2.50 |
| 31 | Rutin (2) | 29.68 | 7.50 | 780 | 3.20 | 5.90 |
| 32 | Myricetin | 30.78 | 15.00 | 60 | 0.70 | 2.50 |
| 33 | Quercitrin (1) | 30.84 | 15.00 | 180 | 1.20 | 2.60 |
| 34 | Quercitrin (2) | 31.06 | 15.00 | 780 | 3.20 | 4.40 |
| 35 | Naringenin | 32.47 | 7.50 | 660 | 2.70 | 3.20 |
| 36 | Quercetin | 33.15 | 15.00 | 120 | 1.60 | 3.40 |
| 37 | Hesperetin (1) | 33.49 | 7.50 | 360 | 3.80 | 2.70 |
| 38 | Hesperetin (2) | 33.57 | 7.50 | 780 | 2.80 | 5.20 |
| 39 | Kaempferol | 35.71 | 11.20 | 180 | 1.90 | 3.40 |

component working standard solution was prepared by combining and diluting the aliquots of each of the secondary stock standard solutions to the concentrations given in Table I. The concentrations of the various components making up the working standard solutions were chosen in order to

have a good compromise with those found in the samples. Prior to injection all standard solutions were filtered through a 0.22- μ m membrane (Millipore). This method was used to measure the phenols present in four wines (Orvieto, Gewurtztraminer, Barbera, Barolo), three beers (Becks,

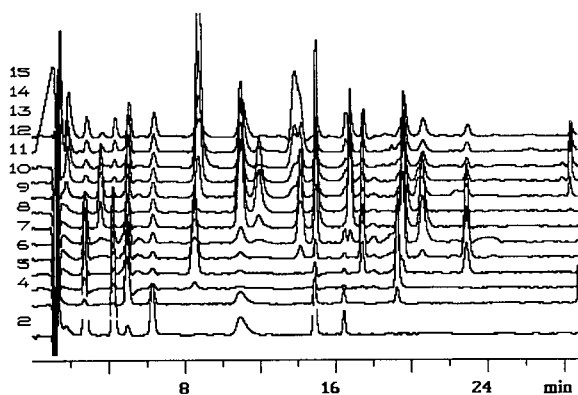


Fig. 2. Chromatogram of a 10- μ l sample containing the 36 standard components as external standard at the concentrations indicated in the Table I. Sensitivity full-scale, 0.5 μ A.

Groschs, Splugen), several lemon juices and three plant extracts. Soya, forsythia and tobacco extracts were obtained by digesting their respective beans (soya) or leaves (forsythia and tobacco) in methanol for 1 week. Prior to injection all samples were filtered through a 0.22- μ m membrane (Millipore) and immediately diluted 1:100 with filtered, deionized water.

Precision

To investigate the within-run precision, twenty sets of pure standards (at the concentrations given in Table II) were injected and analysed under the conditions described previously. Analysis of the same sample over a 10-day span (the sample was stored in aliquots at -20°C between assays) was used to measure the between-run precision.

RESULTS

The 36 standards are listed in Table I according to their retention times. Their injection concentrations, the within- and between-run precisions and their dominant potentials are also reported (the dominant potential is that electrode potential where the maximum signal occurs).

Confirmation of peak identification was carried out by spiking samples with the relevant standard. The peak identity confirmation was finally achieved by comparing the matching ratio (R) between a standard and the actual sample (R is the dominant channel/subdominant channel ratio [11]).

Fig. 2 shows the chromatogram of a 10- μ l sample containing the 36 components as external standard at the concentrations reported in Table I. The total analysis time was 36 min. Retention time reproducibility reported during the precision studies (carried out over a 10-day span) of each individual standard was found to be excellent (R.S.D. < 1.6%). This was due to the strict control of both the gradient profile and the column temperature. As a result, a double injection (with and without standard added) as suggested by Cartoni *et al.* [4] was avoided.

The reproducibility of the method was tested by repeated injections (twenty times) of a standard containing the concentration reported in Table I. The within-run concentration variability (R.S.D.) ranged from 0.70 to 4.30%. The between-run reproducibility was investigated by analysing the same standard solution over a 10-day span. The R.S.D. ranged from 1.80 to 5.90%. All but three standards were easily characterized as they had only one peak. The tannic acid standard, one of the three exceptions, produced three distinct peaks. All three peaks showed the same oxidation potential maximum but different absolute amounts. The components were identified as tannic acid 1, 2 and 3 according to their increasing retention times. The tannic acid 1–tannic acid 2–tannic acid 3 concentration ratio found was 1:17.5:36.5. No attempt was made to identify which structure corresponded to which peak. Similarly, hesperetin generated two peaks at two different retention times. In this instance the hesperetin 1–hesperetin 2 concentration ratio was 1:1.7. Quercitrin, the glucoside of the flavonol quercetin, contained two components in the standard. They had similar retention times but very distinct oxidation potentials with quercitrin 1 at 180 mV and quercitrin 2 at 780 mV. Although this can be interpreted as a single structure with two different oxidation maxima, the observation of a single peak with only one oxidation maximum in the samples suggests that the standard contained two distinct forms. The quercitrin 1–quercitrin 2 concentration ratio was 1:1.22.

The standard mixture was used to examine phenol levels in different kinds of wines, beers, lemon juices and plant extracts. Four distinct Italian wines were analysed: Orvieto, a white, dry, thin-bodied wine from Umbria; Gewürztraminer, a white, aromatic, rich-bodied wine from Alto Adige; Barbera,

TABLE II

CONCENTRATIONS OF THE COMPOUNDS IDENTIFIED IN THE DIFFERENT BEVERAGES AND EXTRACTS

| Compound | Concentration (mg/l of sample) | | | | | Concentration (mg per 100 g of dry material): plant extracts | | | |
|--|--------------------------------|----------------------|---------|----------|-----------------------------|---|-----------|-------|---------|
| | Wines | | | | Beer: Becks (Germany) | Fruit juice: lemon | Forsythia | Soya | Tobacco |
| | Orvieto | Gewürtz- traminer | Barbera | Barolo | | | | | |
| 4-HBAC | | | 1.8 | | | | 1.7 | | |
| 4-HPAC | 1.7 | | | 3.4 | 1.2 | | | | 4.5 |
| Caffeic acid | 17.6 | 6.5 | 2.1 | 45.7 | | | 4.4 | | |
| Catechin | 16.4 | 7.2 | | 47.7 | 5.4 | | 5.9 | | |
| Chlorogenic acid | 1.7 | 1.1 | 1.6 | 3.6 | | 5.8 | 1708.9 | | 211.3 |
| Coniferyl alcohol | | | 5.2 | | | | 3.1 | | |
| DOPAC | | | | | | | | | |
| Esculetin | | 1.4 | 5.6 | 1.1 | | | 20.3 | | |
| Esculin | | | | | | | 5.4 | | |
| Ferulic acid | 1.2 | 5.1 | 6.5 | 1.2 | 6.5 | | 2.5 | | |
| Gallic acid | 52.6 | 188.9 | 480.9 | 231.2 | | | | | |
| Gentisic acid | 5.0 | 14.6 | 7.5 | 2.9 | | | 0.6 | | |
| Hesperetin (1) | 3.2 | 3.1 | | 2.1 | | | 4095.1 | | |
| Hesperetin (2) | | | | | | | | | |
| Hesperidin | | 3.4 | 5.5 | 15.8 | | 1891.1 | 130.4 | 275.3 | |
| Kaempferol | | | | | 16.4 | | 4.5 | | |
| Myricetin | | | | | | | | 7.0 | |
| Naringenin | | | | | | | 48.5 | | |
| Naringin | | 16.4 | 22.0 | 53.5 | | | 11.8 | | |
| <i>o</i> -Vanillin | | | | 2.1 | 1.6 | | 0.7 | | |
| <i>p</i> -Coumaric acid | | | 2.0 | | | | 1.9 | | 7.5 |
| Protocatechuic acid | 14.2 | 14.1 | 61.1 | 26.7 | | | 4.4 | | 10.7 |
| Quercetin | | | | | | | 5.0 | | |
| Quercitrin (1) | | 6.1 | 5.9 | 3.2 | | | 6.0 | | |
| Quercitrin (2) | | | | | | | | | |
| Rutin (1) | | | 3.3 | | 1.8 | 24.5 | 1591.4 | | 506.0 |
| Rutin (2) | | | 17.3 | | | | | | |
| Salicylic acid | | | 22.6 | | | | | | |
| Salsolinol | | | 32.2 | | | | | | |
| Syringaldehyde | 6.1 | 23.8 | 86.7 | 35.3 | 0.7 | | 11.7 | | |
| Syringic acid | 1.6 | 1.2 | 0.7 | 25.2 | 0.5 | | 13.8 | | |
| Tannic acid (3) | 28.9 | | 138.5 | 62.4 | | | 211.6 | | |
| Tannic acid (2) | | | 327.0 | 145.5 | | | 102.0 | | |
| Tannic acid (1) | 4682.2 | 9332.2 | 4735.6 | 34 213.1 | | | 25.3 | | |
| Tyrosine | 73.5 | 237.3 | 64.5 | 3.6 | 54.8 | 36.2 | | 15.3 | 14.5 |
| Tyrosol | | 19.3 | 2.0 | | | | | | |
| Vanillic acid | 3.9 | 4.4 | 133.1 | 20.5 | 3.6 | | | | |
| Vanillin | 1.5 | 2.0 | 8.4 | 2.0 | | | 2.4 | | |
| Vanillyl alcohol | | | | | | | 1.3 | | |
| Sum of the measured phenolic compounds | 5911.3 | 10 888.1 | 7179.6 | 35 947.8 | 1093 | 2958 | 8121 | 398 | 137 |

a red, fresh, acidic, low tannin, medium-bodied wine from Piemonte; and Barolo, a red, tannic, high-bodied wine, aged 6 years in an oak barrel, from Piemonte.

After injecting the wine samples, many hundreds of peaks are obtained in addition to those generated by the compounds contained in the external standard. Such complexity of the natural matrix may

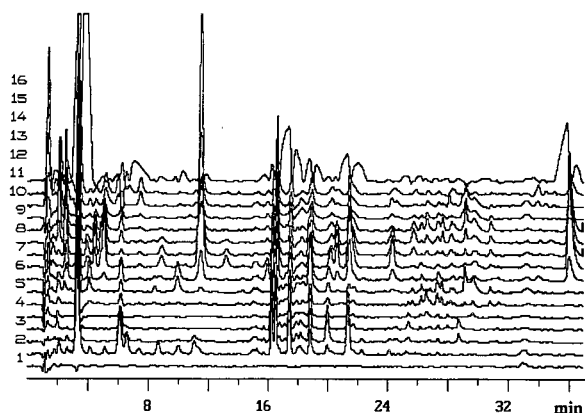


Fig. 3. Chromatogram of a 10- μ l Barolo wine sample showing the components found with the results presented in Table II. Dilution 1:100, filtered with a 0.22- μ m membrane. Sensitivity full-scale, 1 μ A.

cause problems in identifying and measuring the peaks of the external standard, which may be very close to or even overlap some peaks of the natural product. To investigate better the validity of the present separation for natural wines, we chose well differentiated varieties of wines. In no instance did the matrix effect represent a problem. We also focused our attention on three types of plants extracts which contain in high concentrations certain compounds. All three plants extracts and their major

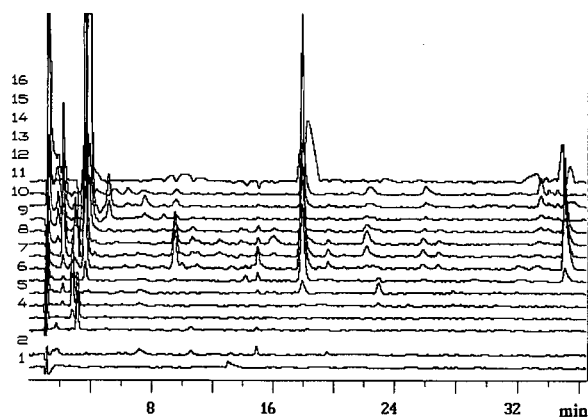


Fig. 4. Chromatogram of a 10- μ l beer sample (Becks) showing the components found with the results presented in Table II. Dilution 1:100, filtered with a 0.22- μ m membrane. Sensitivity full-scale, 1 μ A.

compounds are described in the Merck Index [12]. Hesperidin, a major component of lemon juices, and rutin, a major constituent of forsythia and tobacco leaves, are two examples.

Three different beers were also examined: German (Becks), Dutch (Groschs) and Italian (Splügen Double Malt). As they all presented similar data, only one is reported here. Lemon juices from different sources were also tested. The juice was produced by squeezing the fruit. The suspension after filtration was used. They also presented homogeneous data, hence only one is reported here. Lastly, methanol extracts of soya beans, forsythia leaves and tobacco leaves were analysed. The concentrations of the various components found in these samples are reported in Table II in alphabetical order.

The sixteen-channel chromatogram for one of the wine samples (Barolo) is shown in Fig. 3 and that for one of the beer samples (Becks) in Fig. 4.

DISCUSSION AND CONCLUSION

The use of the CEAS for the determination of neurochemicals in tissues and biological fluids has already been reported [13–15]. This type of separation and determination has been studied recently in the determination of 33 neurochemicals in the cerebrospinal fluid [11]. The coulometric efficiency of each element of the array allows a complete voltammetric resolution of analytes as a function of their reaction potential. Some peaks may be resolved by the detector even if they are unresolved when they leave the chromatographic column. In this study we have demonstrated that this technique can also be applied to phenolic compound in various natural beverages and plant extracts.

We separated 36 phenolic compounds in less than 36 min with this method. For the samples analysed here, we were able to measure 16–19 compounds in the white wine, 22–26 in the red wines, 10 in the beers, 4 in the lemon juices, 27 in the forsythia leaves, 3 in the soya beans and 6 in the tobacco leaves. The complexity of the matrix, in most instances showing hundreds of peaks, never interfered with the identification and determination of the compounds contained in the external standard.

In addition to those peaks which were measured, other peaks of electroactive molecules were found to be present in all the wine and beer samples. An

electrogenic components profile could therefore give a sort of fingerprint useful for characterizing the product.

In conclusion, we have demonstrated that by combining RP-HPLC with a highly selective array electrochemical detector it is possible to determine simultaneously large numbers of phenolic compounds in very different beverages and extracts. The reproducibility of the retention time coupled with the selectivity inherent to this detector allows measurements with high precision of a variety of different compound families in a single sample. The characterization among the various types of wines and their ageing in wooden barrels are possible subjects of future study.

REFERENCES

- 1 B. Y. Ong and C. W. Nagel, *J. Chromatogr.*, 157 (1978) 345.
- 2 I. McMurroughs, *J. Chromatogr.*, 218 (1981) 683.
- 3 F. Villeneuve, G. Abravanel, M. Moutonet and G. Alibert, *J. Chromatogr.*, 234 (1982) 131.
- 4 G. P. Cartoni, F. Coccioli, L. Pontelli and E. Quatrucci, *J. Chromatogr.*, 537 (1991) 93.
- 5 J. P. Goiffon, M. Brun and M. J. Bourrier, *J. Chromatogr.*, 537 (1991) 101.
- 6 D. A. Roston and P. T. Kissinger, *Anal. Chem.*, 53 (1981) 1695.
- 7 S. M. Lunte, *J. Chromatogr.*, 384 (1987) 371.
- 8 G. Weber, *Chromatographia*, 26 (1988) 133.
- 9 V. Hong and R. E. Wrolstad, *J. Agric. Food Chem.*, 38 (1990) 698.
- 10 V. Hong and R. E. Wrolstad, *J. Agric. Food Chem.*, 38 (1990) 708.
- 11 V. Rizzo, G. Melzi d'Eril, G. Achilli and G. Cellerino, *J. Chromatogr.*, 536 (1991) 229.
- 12 *The Merck Index*, Merck, Rahway, NJ, 11th ed., 1989.
- 13 W. R. Matson, P. G. Gamache, M. F. Beal and E. D. Bird, *Life Sci.*, 41 (1987) 905.
- 14 K. J. Swartz and W. R. Matson, *Anal. Biochem.*, 185 (1990) 363.
- 15 C. N. Svendsen and E. D. Bird, *Neurosci. Lett., Suppl.*, 35 (1989) 49.

CHROMSYMP. 2633

Supercritical fluid extraction of synthetic organochlorine compounds in submerged aquatic plants

Phillip R. McEachern and Gregory D. Foster

Department of Chemistry, George Mason University, Fairfax, VA 22030 (USA)

ABSTRACT

Supercritical carbon dioxide was used to extract nine synthetic organochlorine compounds (SOCs) from tissues of the aquatic plant *Hydrilla verticillata* in an off-line supercritical fluid extraction configuration. Lyophilized plant tissues (50 to 100 mg) were fortified with the SOC's at a level of 5 to 10 mg/kg and subjected to supercritical carbon dioxide extraction at 50°C and 38 MPa for 15 min. Mass recoveries of the SOC's amended to plant tissues averaged between 89 and 109%. When Florisil was present in the outlet end of the extraction vessel for the purpose of direct in-line clean-up during supercritical carbon dioxide extraction, mass recoveries of the amended SOC's were markedly lower for four of the nine analytes.

INTRODUCTION

During the past decade, the explosion in biomass of submerged aquatic vegetation (SAV) throughout the tidal freshwater reach of the Potomac river near Washington, DC, USA, particularly by the vascular plant *Hydrilla verticillata* Royle [1], has prompted interest in the role of SAV in influencing the environmental behaviour and biogeochemical cycling of synthetic organic compounds (SOC's) in the lower Potomac river aquatic food web. The collective SAV abundance in the Potomac river during the spring and summer growing seasons creates a sizable reservoir of plant lipids into which hydrophobic organic compounds may partition from contaminated water and sediments. To address this issue, it has become necessary to measure refractory organochlorine contaminants bioaccumulated in *Hydrilla* tissues.

The recent application of supercritical carbon dioxide extraction (SCDE) in trace analysis has been

reported for a wide variety of analytes and matrices – including volatile food and fragrance constituents [2–4], pesticides in soils and tissues [5–9], hydrocarbons in marine sediments [10], and air pollutants collected on polyurethane foam sorbents [11] – clearly demonstrating the benefits and usefulness of this extraction technique. The supercritical fluid state of matter has unique physical properties which are now being exploited in environmental trace analysis to lessen the need for using large amounts of subcritical organic solvents, such as dichloromethane. Supercritical fluids generally have low viscosities (e.g., 10^{-3} – 10^{-4} g/cm·s), moderate densities (e.g., 0.3–0.8 g/cm³), and high diffusivities (e.g., 10^{-3} – 10^{-4} cm²/s) enabling very efficient solubilization and mass transfer processes to rapidly isolate trace organics from solid matrices such as sediments, solid sorbents, and tissues. It was the overall intent of this study to assemble a laboratory-built SCDE apparatus and develop methods by which SOC's could be extracted from *Hydrilla* tissues in an off-line collection mode for subsequent analysis by using gas chromatography–electron-capture detection (GC–ECD).

Correspondence to: G. D. Foster, Department of Chemistry, George Mason University, Fairfax, VA 22030, USA.

EXPERIMENTAL

Plant sample preparation

Hydrilla verticillata specimens were collected with a rake, wrapped in clean aluminium foil, and frozen upon return to the laboratory until further processing. *Hydrilla* tissue was prepared for analysis by lyophilization in a VirTis Unitrap II freeze dryer (The VirTis Company, Gardiner, NY, USA) utilizing a dry ice/2-propanol slush as a pump oil fume trap to prevent sample contamination. The freeze dried sample was then dry homogenized in a Waring blender with a stainless-steel cup, transferred to a clean beaker, and placed in a desiccator until analysis. Care was taken when sub-sampling to obtain a consistent range of particle sizes when placing them into the SCDE extraction vessel. Plant tissue sample sizes ranged from 50 to 100 mg.

A 3-g portion of lyophilized, homogenized *Hydrilla* tissue was Soxhlet extracted with dichloromethane for 24 h to determine the percent weight of extractable lipids in the plant samples. The dichloromethane extract was subsequently evaporated to dryness and the residue, regarded as extractable lipids, was measured gravimetrically.

Apparatus

A schematic diagram of the SCDE setup is shown in Fig. 1. The supercritical state was attained and maintained through the use of a Perkin-Elmer Series 10 high-performance liquid chromatography pump (Perkin-Elmer, Norwalk, CT, USA) which had been modified for low-temperature liquid flow by the addition of a custom-designed pump-head heat exchanger according similar specifications reported by Simpson *et al.* [12] for supercritical fluid chromatography. Liquid carbon dioxide was pumped first (Fig. 1) through a 4-m section of 1/16 in. (1 in. = 2.54 cm) (O.D.) stainless-steel tubing (f) which itself was immersed in a constant-temperature water bath held at 50°C (e). Supercritical carbon dioxide then entered a flow-through pressure gauge [g; Alltech, Deerfield, IL, USA, 6000 p.s.i. (1 p.s.i. = 6894.76 Pa) full scale] in route to the extraction vessel (h), also positioned in the water bath. An SSI on/off valve (Alltech) followed the extraction vessel (i), to which was connected a low dead volume stainless-steel union fitted with an internal reducer (Suprex, Pittsburgh, PA, USA), 1/32 in. gland

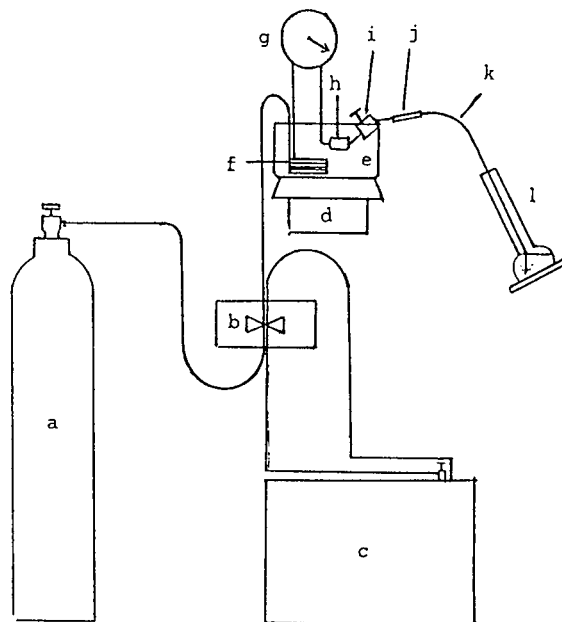


Fig. 1. Schematic diagram of apparatus used for supercritical carbon dioxide extraction: (a) CO₂ source; (b) CO₂ pump; (c) recirculating chiller for pump head cooling; (d) hot plate/stirrer; (e) large Pyrex crystallization dish; (f) heat exchange coil; (g) pressure gauge; (h) extraction vessel; (i) on/off valve; (j) low dead volume connector; (k) fused-silica restrictor; and (l) collection flask.

(Suprex), and 1/32 in. Vespel ferrule (Suprex); this arrangement was used to connect 20–22 μm (I.D.) fused-silica restrictor tubing (Polymicro Technologies, Phoenix, AZ, USA) to the SSI valve. The lengths of restrictors used were *ca.* 30–35 cm.

The extraction vessel (Fig. 2) was constructed by fitting a Swagelock low dead volume 1/16 in. to 1/4 in. stainless-steel reducing union to a Swagelock stainless-steel 1/16 in. to 1/4 in. fractional tube to fractional tube stub (Washington Valve and Fitting, Rockville, MD, USA). It was necessary to modify the vessel to utilize a 1/4 in. diameter, 0.062 in. thick, 0.5 μm porosity stainless-steel frit (Alltech) by grinding 1/8 in. from the fractional tube stub cylinder, giving an internal volume of about 0.31 ml.

Extraction and collection

The carbon dioxide used for SCDE was SFE grade and was acquired from Scott Specialty Gases

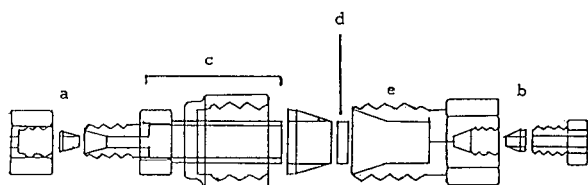


Fig. 2. Exploded view of supercritical fluid carbon dioxide extraction vessel: (a) inlet, stainless-steel 1/16 in. fractional tube and ferrules; (b) outlet, stainless-steel 1/16 in. male nut and ferrules; (c) Swagelock stainless-steel 1/16 in. fractional tube to 1/4 in. fractional tube stub; (d) 1/4 in. diameter, 0.5 μm pore size stainless-steel frit; and (e) Swagelock stainless-steel 1/4 in. to 1/16 in. low dead volume reducing union.

(Plumsteadville, PA, USA). During preliminary off-line SCDE, a pressure of 38 MPa (*ca.* 5500 p.s.i.) was maintained in the extraction vessel throughout the extraction cycle and extractions were performed in the dynamic mode. SCDE was performed for 15 min with a steady-state liquid carbon dioxide flow of 0.25 ml/min registered at the pump (corresponding to *ca.* 12 extraction vessel turnover volumes of equivalent liquid carbon dioxide).

Approximately 3 ml of *n*-hexane (Burdick & Jackson, Waukegan, WI, USA) was placed in a 5-ml volumetric flask (Fig. 1l) to collect the extracted analytes from decompressing carbon dioxide. The fused-silica restrictor (Fig. 1k) was immersed directly in the collection solvent and was held in place with the aid of a paper clip. Mirex was added as a surrogate standard to the flask prior to extraction to evaluate the retention of the analytes collected in *n*-hexane during carbon dioxide sparging. Holdup of analyte in the restrictor tube was evaluated (i) by performing SCDE using clean, empty extraction vessels immediately following a sample extraction with the same restrictor used in the sample extraction, and (ii) by analyzing *n*-hexane rinses of the restrictor tube after sample extractions. Isodrin was added to the solution after SCDE as an internal injection standard and contents in the collection flask were diluted to volume with *n*-hexane.

SCDE performance

The synthetic organochlorine compounds used to evaluate SCDE of *Hydrilla* tissue are shown in Table I along with their important physicochemical properties. Pure standards of each of these com-

TABLE I

ORGANOCHLORINE ANALYTES USED IN THIS STUDY AND THEIR IMPORTANT PHYSICOCHEMICAL PROPERTIES

| Analyte | $\text{p}S_{\text{w}}^{\text{a}}$ | $\log K_{\text{ow}}^{\text{b}}$ | Ref. ^c | GC peak No. ^d |
|-------------------------|-----------------------------------|---------------------------------|-------------------|--------------------------|
| Aldrin | 7.4 | na | 13 | 4 |
| α -Chlordane | 6.9 | 6.0 | 14 | 7 |
| γ -Chlordane | 6.9 | 6.0 | 14 | 6 |
| 4,4'-DDE | 7.5 | 5.7 | 14 | 8 |
| Dieldrin | 7.2 | 5.4 | 14 | 9 |
| γ -HCH (Lindane) | 6.3 | 3.8 | 14 | 3 |
| Hexachlorobenzene | 6.9 | 5.5 | 15 | 2 |
| Oxychlordane | na ^e | na | - | 5 |
| Pentachlorobenzene | 6.3 | 5.2 | 15 | 1 |

^a Inverse logarithm of molar water solubility.

^b Logarithm of *n*-octanol–water partition coefficient.

^c Physical property literature reference.

^d Gas chromatography peak reference number for Figs. 3 and 4.

^e na indicates parameter not available.

pounds along with isodrin and mirex were obtained from the U.S. EPA Pesticides and Industrial Chemicals Repository (Research Triangle Park, NC, USA) in neat form.

All general purpose glassware was scrupulously cleaned with nitric acid solution, rinsed in distilled water and burned overnight at 450°C, stored covered by burned aluminum foil, and rinsed repeatedly with hexane before use. Volumetric glassware was soaked in nitric acid solutions for 12 h, rinsed and sealed with foil, and hexane rinsed repeatedly prior to use. Granular anhydrous sodium sulfate (J. T. Baker, Hauppauge, NJ, USA) was used as the matrix for the initial optimization of SCDE conditions. Finely cut glass wool was placed within the extraction vessel along with Florisil sorbent and the sample for the evaluation of in-line clean-up. Sodium sulfate, Florisil, and glass wool were burned at 450°C overnight to remove any trace organic residues.

Initial optimization experiments involved spiking sodium sulfate housed in the extraction vessel with a hexane solution containing the nine analytes – the hexane was allowed to evaporate from the extraction vessel before SCDE was initiated – and sequentially extracting the sample over 15-min intervals, with the collection flask and solvent renewed at each interval, for a total of 60 min (4 fractions). In addi-

tion, SCDE of spiked sodium sulfate was performed under 23, 30 and 38 MPa pressure regimes.

Extraction performance involving actual samples of *Hydrilla* were performed in several stages. First, 50–100-mg samples of lyophilized *Hydrilla* tissue were loaded into the extraction vessel and SCDE was performed with and without the analytes amended to the sample. Secondly, Florisil was placed in the extraction vessel along with the tissue to minimize plant lipid carryover into the collection flask (*i.e.*, clean-up); the materials were loaded into the extraction vessel in the order of *Hydrilla*, glass wool (a neutral separator), and Florisil. Blanks were extracted with only glass wool and Florisil present. The analytes were amended to the samples at a concentration of 5–10 mg/kg per component. All SCDE experiments were performed either in triplicate or quadruplicate.

GC analysis

All GC analyses were performed on a Hewlett-Packard 5890 Series II gas chromatograph equipped with a ^{63}Ni electron-capture detector. The gas chromatograph was fitted with a 30 m \times 0.25 mm I.D., 0.25 μm film thickness, SE-54 fused-silica capillary column (Alltech). Samples were introduced into the gas chromatograph via the splitless mode of a split/splitless injector system. The GC injector and detector were maintained at 250 and 300°C, respectively. Helium was used as the carrier gas and its linear velocity through the column was 35 cm/s at 100°C, and 5% methane in argon was used as make up gas for the detector and its flow was maintained at 60 ml/min. Separations on the GC were temperature programmed with an initial temperature of 50°C (1 min hold), ramped from 50°C to 120 °C at a rate of 10°C per minute (with a 1-min hold at 120°C), then ramped again at a rate of 4°C per minute to 280°C (9.5 min final hold) for a total run time of 60 min. Analyte recoveries were obtained directly from auto-quantitation routines programmed in a Hewlett-Packard 3396 recording integrator.

RESULTS AND DISCUSSION

SCDE optimization

Extraction temperature was partially decided on by conforming to a temperature close to that com-

monly used in other SCDE experiments [16]. However, the most important factors in selecting the extraction temperature were based on the following considerations: (a) 50°C is safely above the 31°C critical temperature of carbon dioxide; (b) 50°C was a convenient temperature to use with the constant temperature water bath; and (c) it was desirable to keep the solubilization power of carbon dioxide at a maximum with working pressures less than 40 MPa by optimizing density. Although extraction temperature is known to be an important variable in SCDE, its effect on the target analyte recoveries was not studied in the experiments described herein.

Initial experiments involving SCDE of analyte-spiked anhydrous sodium sulfate demonstrated that recoveries were essentially independent of applied pressure. Therefore, 38 MPa was used subsequently in all SCDE experiments because it was known this pressure was well above any pressure-limited extraction condition, and this represented the highest density state for supercritical carbon dioxide (0.90 g/ml at 50°C and 38 MPa) that was feasible to use in the lab-built system.

Extraction of the target analytes from anhydrous sodium sulfate at 38 MPa and 50°C was essentially complete during the first 15 min as evidenced by Fig. 3. All of the analytes extracted during the second 15 min were present at levels below quantitative analysis. Because anhydrous sodium sulfate was considered to be an inert surface, the results obtained from the optimization experiments were thought to reflect the most ideal SCDE conditions from which a starting point for plant tissue analysis was derived.

SCDE of *Hydrilla* tissue

Efficient isolation of the target analyses amended to *Hydrilla* tissue was obtained after 15 min of extraction at 50°C and 38 MPa as shown in Fig. 4 and Table II. Less than 0.5% of the amended analytes were recovered during a second 15 min extraction of the same sample (see Fig. 4b). The third and fourth 15 min extraction intervals over the cumulative 60 min extraction showed similar chromatograms to that displayed in Fig. 4b. Chromatograms of blank extractions (with and without the presence of Florisil and glass wool) were nearly identical to the chromatogram shown in Fig. 4b, with the only exception from Fig. 4b being the absence of the

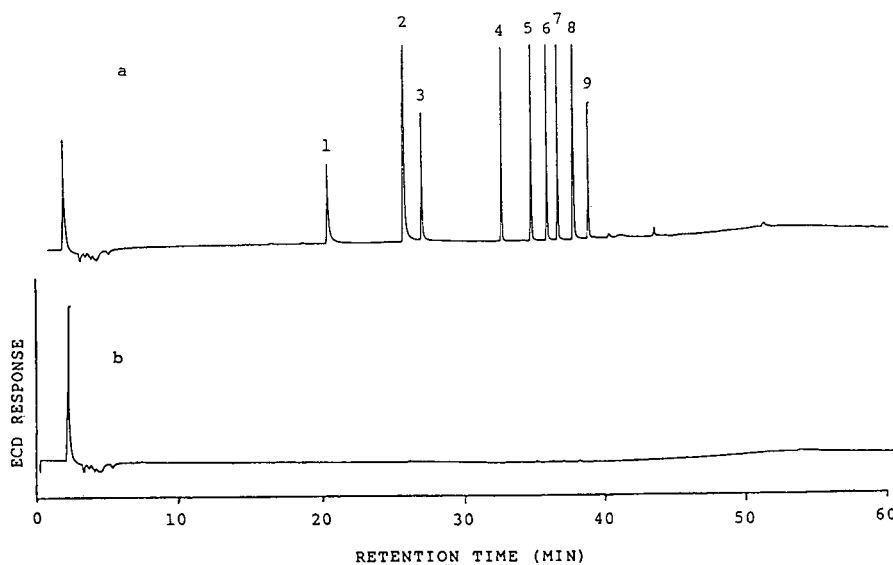


Fig. 3. Chromatograms showing optimization results from supercritical carbon dioxide extraction of analyte-amended (10 mg/kg per component) sodium sulfate: (a) first 15 min period of extraction; and (b) second 15 min period of extraction. GC peak designations are listed in Table I.

barely visible analyte peaks (isodrin and mirex excluded) in the blank chromatograms.

Recoveries of amended analytes in *Hydrilla* tissues are shown in Table II. Mean recoveries ranged

from 89% to 109% for SCDE carried out on amended *Hydrilla* tissue alone, and the R.S.D. values for the same extractions varied from 11.8 to 20.4%. Mirex recoveries were greater than 85% in

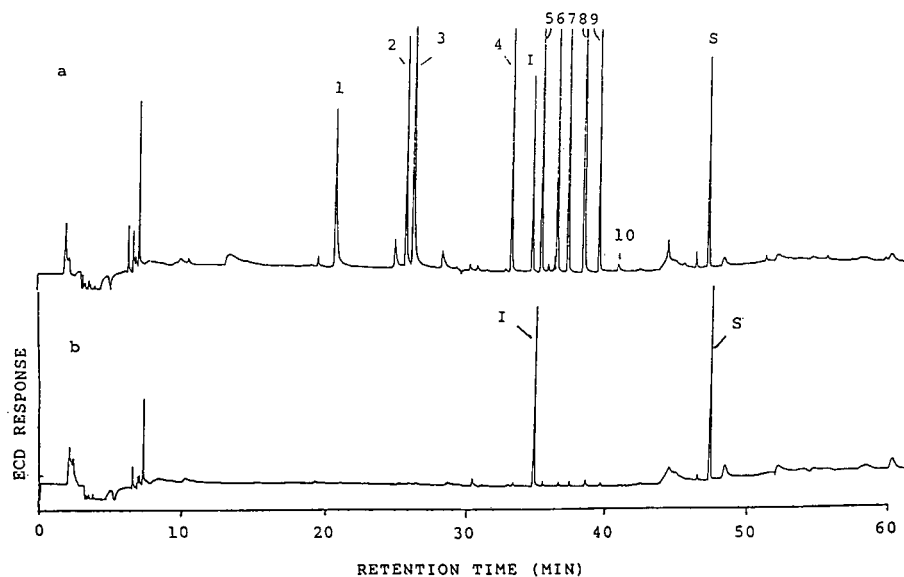


Fig. 4. Chromatograms showing supercritical carbon dioxide extraction of analyte-amended (10 mg/kg per component) *Hydrilla* tissue: (a) first 15 min period of extraction; and (b) second 15 min period of extraction. GC peak designations are listed in Table I. Isodrin internal standard (I) and mirex surrogate standard (S) peaks are also labeled in both chromatograms.

TABLE II

RECOVERIES OF ORGANOCHLORINE ANALYTES FROM HYDRILLA TISSUE USING OFF-LINE SUPERCRITICAL CARBON DIOXIDE EXTRACTION WITH AND WITHOUT FLORISIL SORBENT

| Analyte | <i>Hydrilla</i> alone ^a | | <i>Hydrilla</i> + glass wool + Florisil ^b | |
|-------------------------|------------------------------------|------------|--|------------|
| | Mean recovery (%) | R.S.D. (%) | Mean recovery (%) | R.S.D. (%) |
| Aldrin | 87.2 | 14.3 | 86.8 | 3.4 |
| α -Chlordane | 95.0 | 13.5 | 99.3 | 5.2 |
| γ -Chlordane | 98.6 | 11.8 | 101 | 6 |
| 4,4'-DDE | 89.8 | 12.9 | 73.0 | 19.3 |
| Dieldrin | 109 | 15 | 55.9 | 45.0 |
| γ -HCH (Lindane) | 90.9 | 20.4 | 67.0 | 7.5 |
| Hexachlorobenzene | 94.6 | 18.7 | 88.5 | 2.8 |
| Oxychlordane | 104 | 12 | 106 | 5 |
| Pentachlorobenzene | 101 | 14 | 86.7 | 5.4 |

^a $n = 4$.^b $n = 3$.

all of the experiments, indicating that the collection technique employed did not “purge out” the analytes isolated in *n*-hexane. Furthermore, there was no evidence of analyte holdup in the restrictor during a spiked tissue SCDE experiment.

Extractable lipids constitute a formidable interference problem in the conventional analysis of SOCs in tissues [17], and a lipid clean-up must usually be undertaken prior to GC–ECD analysis. The lipid content of lyophilized *Hydrilla verticillata* tissues was found to be 2.1% (w/w). Because it can be expected that lipids and other plant products will co-extract with the SOC analytes, a small amount of Florisil was incorporated into the extraction vessel in an attempt to fractionate interfering materials from the analytes during SCDE.

Substantial reductions in recoveries were observed for γ -hexachlorocyclohexane (HCH), 4,4'-DDE, dieldrin, and pentachlorobenzene when glass wool and Florisil were present in the extraction vessel (Table II), presumably due to the strong interaction of these analytes with the polar Florisil sorbent. Interestingly, the R.S.D. values for most of the analytes were consistently lower in samples with attending glass wool and sorbent with the exception of 4,4'-DDE and dieldrin. Dieldrin showed much lower recoveries and much higher variability in recoveries with Florisil present in the extraction vessel. None of the analyte physical properties shown

in Table I seem to correlate with the observed lower recovery effect. It has recently been stated, however, that supercritical fluid extraction efficiency is best correlated with the dipole moments of the supercritical fluids [18].

Florisil was selected in this study for in-line clean-up because this sorbent is used extensively for conventional column chromatography clean-up in pesticide analysis. Sorbents other than Florisil have yet to be evaluated in the SCDE of *Hydrilla* tissues. The in-line deployment of Florisil in SCDE would ideally minimize the need to conduct further clean-up in tissue analysis, substantially streamlining sample preparation procedures. In addition, in-line clean-up will be essential to the development of directly coupled SCDE–GC in the analysis of SOCs in tissues. It is important to note that one major observation concerning these particular samples was that the collected products from *Hydrilla* alone in the extraction vessel gave the *n*-hexane in the receiving flask a distinct yellow color, whereas those of *Hydrilla* with glass wool and Florisil in the extraction vessel showed a virtually no visible color in the collection solution. It is possible that the co-extraction of pigments or other natural plant substances may have accounted for the relatively higher R.S.D. values of the samples where Florisil and glass wool were not present, but further investigation was not attempted.

The SCDE procedure described herein would provide a detection limit of 0.5 mg/kg (estimated as an analyte response greater than three times the standard deviation of the baseline signal determined from replicate blank analyses) for the organochlorine analytes if it is used without any further modification. Unfortunately, this is well above 0.001 mg/kg detection limits that are typically available in more conventional tissue analysis methods [18]. Lowering detection limits for the SCDE technique to make it more applicable to field studies could, in fact, be accomplished in several ways, including (a) increasing the sample size, (b) concentrating the *n*-hexane collection solvent to a small volume, and (c) coupling SCDE with GC in an online (*i.e.*, directly coupled) configuration. It is strategy (a) and (b) above that is presently being pursued in developing a method for analyzing SOCs in *Hydrilla* tissues in our laboratory. The results of this study suggest that SCDE has the potential to replace subcritical solvents, when Soxhlet extraction is used for example, in the isolation of synthetic organochlorine contaminants from plant tissues.

ACKNOWLEDGEMENTS

Appreciation is extended to Ms. Jessica Hopple for field collections of *Hydrilla verticillata*. This research was supported by US Geological Survey, Department of the Interior, under USGS Agreement No. 14-08-0001-A0725.

The views and conclusions contained in this document are those of the authors and should not be interpreted necessarily representing the official pol-

icies, either express or implied, of the US Government.

REFERENCES

- 1 V. Carter and W. E. Webb, in E. Callender, V. Carter, D. C. Hahl, K. Hitt and B. I. Schultz (Editors), *A Water Quality Study of the Tidal Potomac River and Estuary-An Overview*, US Geological Water Supply Paper 2233, United States Government Printing Office, Washington, DC, 1984, p. 32.
- 2 S. B. Hawthorne, M. S. Kreiger and D. J. Miller, *Anal. Chem.*, 60 (1988) 472.
- 3 C. K. Huston and H. Ji, *J. Agric. Food Chem.*, 39 (1991) 1229.
- 4 J. W. Hill, H. H. Hill, Jr. and T. Maeda, *Anal. Chem.*, 63 (1991) 2152.
- 5 J. R. Wheeler and M. E. McNally, *J. Chromatogr. Sci.*, 27 (1989) 534.
- 6 V. Janda, G. Steenbeke and P. Sandra, *J. Chromatogr. Sci.*, 27 (1989) 200.
- 7 V. Lopez-Avila, N. S. Dodhiwala and W. F. Beckert, *J. Chromatogr. Sci.*, 28 (1990) 468.
- 8 J. M. Levy, R. A. Cavalier, T.N. Bosch, A. M. Rynaski and W. E. Huhak, *J. Chromatogr. Sci.*, 27 (1989) 341.
- 9 M. M. Schantz and S. N. Chesler, *J. Chromatogr.*, 363 (1986) 397.
- 10 S. B. Hawthorne, D. J. Miller and J. J. Langenfeld, *J. Chromatogr. Sci.*, 28 (1990) 2.
- 11 S. B. Hawthorne, M. S. Kreiger and D. J. Miller, *Anal. Chem.*, 61 (1989) 736.
- 12 R. C. Simpson, J. R. Gant and P. R. Brown, *J. Chromatogr.*, 371 (1986) 109.
- 13 E. E. Kenaga, *Ecotoxicol. Environ. Safety*, 4 (1980) 26.
- 14 D. Mackay, *Environ. Sci. Technol.*, 16 (1982) 274.
- 15 B. Oliver and A. J. Niimi, *Environ. Sci. Technol.*, 17 (1983) 287.
- 16 J. W. King, *J. Chromatogr. Sci.*, 27 (1989) 355.
- 17 T. Shan, *Multiresidue Analysis of Organohalogen Compounds in Tissues of Aquatic Organisms*, M. S. Thesis, George Mason University, Fairfax, VA 1992.
- 18 S. B. Hawthorne, J. J. Langenfeld, D. J. Miller and M. D. Burford, *Anal. Chem.*, 64 (1992) 1614.

CHROMSYMP. 2588

Separation of metallothionein isoforms by capillary zone electrophoresis

John H. Beattie

Division of Biochemical Sciences, Rowett Research Institute, Bucksburn, Aberdeen AB2 9SB (UK)

Mark P. Richards

USDA, Agricultural Research Service, Nonruminant Animal Nutrition Laboratory, Beltsville, MD 20705 (USA)

Ron Self

Division Services, Rowett Research Institute, Bucksburn, Aberdeen AB2 9SB (UK)

ABSTRACT

The potential of capillary zone electrophoresis (CZE) for the analysis of metallothionein (MT) isoforms was investigated. CZE was performed using two different systems, (1) a laboratory-constructed instrument with an ISCO UV detector and (2) a Waters Quanta 4000 system. Capillaries were of 75 μm I.D. \times ca. 1 m in length and loading times were up to 40 s by gravity or 4 s by electrokinetic migration at 30 kV. Samples were dissolved in 10 mM Tris-HCl buffer, pH 9.1, and electrophoresis was performed at 30 kV using a 50 mM Tris-HCl, pH 9.1 running buffer. Detection was by UV absorbance at 185 or 214 nm. Purified and semipurified MT samples were analysed for qualitative assessment of purity, relative isoform abundance and separation characteristics of MT from different species. As progress towards the development of a quantitative assay, the linearity of calibration curves and simple methods of sample preparation for analysis by CZE were investigated. Complete separation of a mixture of the two major MT isoforms was achieved in less than 5 min and the technique was found to be very useful for qualitative analysis of MT. Using a rabbit liver MT standard (500 $\mu\text{g}/\text{ml}^{-1}$), a linear relationship was found between the gravity load time and the integrated peak area. Standard calibration curves were also linear and the detection limit for both CZE instruments under our separation conditions was 1–10 μg MT ml^{-1} . The successful use of two solvent extraction procedures for tissue samples demonstrated the potential of CZE for routine quantitative analysis of MT.

INTRODUCTION

The unique chemical and physical properties of metallothionein (MT) and its suggested role in heavy metal metabolism and detoxification have been the subject of intense investigation ever since its initial discovery [1]. In most animal species, MT has 2 major isoforms (MT-1 and MT-2) which have a pI of between 3.9 and 4.6 and differences of charge

due to certain amino acid substitutions [2]. Both isoforms contain 33% cysteine residues with a highly conserved sequence. Transition metals such as Zn, Cd and Cu bind to MT through association with the cysteine thiol groups.

Early separation techniques involved lengthy chromatographic procedures in which MT quantification was indirect, based on measurement of the metal content of the protein [3]. Such techniques are insensitive and impracticable for the study of MT metabolism in some tissues including extracellular fluid matrices in which endogenous MT levels are low. Consequently, a number of different assays

Correspondence to: Dr. J. H. Beattie, Division of Biochemical Sciences, Rowett Research Institute, Bucksburn, Aberdeen AB2 9SB, UK.

have been developed which are more rapid and show improved sensitivity.

Immunological assays [radioimmunoassay (RIA) and enzyme linked immunosorbent assay (ELISA)] offer the highest level of detection sensitivity and are particularly useful for analysing MT present in low quantities such as in urine or plasma [4–6]. Complete crossreactivity of MT antibodies with MT from different species or even between the major isoforms of the protein in a single species is, however, questionable. Indeed, an assay has been developed specifically for the measurement of rat MT-1 [4].

Various metal-saturation assays have been published which depend on the displacement of metals bound to MT with a radioactive isotope of Hg, Cd or Ag [7–9]. These assays are of limited value since Hg and Cd will not displace Cu from MT [10] and the binding capacity for Ag is variable [11]. A more recent version of this assay uses ammonium tetrathiomolybdate to remove Cu from MT prior to saturation with ^{109}Cd [12].

A number of high-performance liquid chromatography (HPLC) techniques have been developed to isolate and quantify MT in tissue extracts. Suzuki [13] first developed an isolation procedure for MT which coupled size-exclusion HPLC with metal detection by atomic absorption spectrophotometry. Because this technique relies on a combination of size-exclusion and weak cationic exchange properties of the columns used, MT isoforms are not always completely resolved. Later, reversed-phase HPLC (RP-HPLC) techniques were developed which offer reasonably high detection sensitivity combined with the ability to resolve individual MT isoforms [14]. However, RP-HPLC requires the use of organic solvents and expensive columns.

Recently, CZE has been applied to the analysis of proteins and peptides [15,16] and is particularly suitable for the separation of low M_r molecules. MT is well suited to separation by CZE since it is a low M_r protein (*ca.* 6600 daltons, including metals) with, in most species, 2 major isoforms which differ in charge over a range of pH conditions. Separation of charged molecules is achieved in narrow-bore capillaries, usually less than 100 μm I.D., and up to 1 m in length, filled with an appropriate buffer solution. The molecules separate in an applied electric field according to their charge to mass ratio at the

selected pH. The advantages of CZE over other techniques include the speed of analysis (4–8 min for the separation of MT using the conditions described below), small sample requirements (1–100 nl), nanogram sensitivity, high resolution and improved discrimination. Our objectives were to assess the practicability of using CZE to separate MT isoforms for qualitative analysis and to develop a quantitative assay for routine analysis of MT isoforms in tissue and cell samples.

EXPERIMENTAL

Instrumentation and electrophoresis conditions

Two instruments were used to develop a method for the analysis for MT: a system constructed at the Rowett Institute which is described below and a Waters Quanta 4000 system with an autosampler and 6/12 well carousel (Millipore/Waters Chromatography Division, Watford, UK).

The laboratory-constructed capillary electrophoresis system was made by attaching a plastic box (150 mm \times 200 mm \times 70 mm deep) with a transparent hinged door, containing the anode and a retractable sample/electrolyte holder, to an ISCO CV⁴ variable wavelength (190–750 nm) UV-visible detector (ISCO, Lincoln, NE, USA). The cathode was placed outside the box immediately above an electrolyte vial holder on a retractable platform. The electrodes were constructed out of fine platinum tubing (PT007200, Goodfellow Metals, Cambridge, UK) and each end of a fused-silica, polyimide-coated capillary tube (94 cm \times 75 μm I.D.; Composite Metal Services, Worcester, UK) was threaded coaxially through an electrode until they were level. An optical window of about 1 cm length positioned about 20 cm from the cathode end was prepared by heating the polyimide tube coating with a flame and removing the charred material with acetone. The prepared tubing was carefully inserted into the flow cell cassette ensuring that the optical window was located in the light path of the detector. Absorbance was monitored at 214 nm.

The capillary tubing was filled with 50 mM Tris-HCl buffer, pH 9.1, under positive pressure applied at the appropriate end. A 2-ml bottle containing the same buffer was placed in position in the anode and cathode cell holders to submerge the ends of the capillary in electrolyte. When setting up the instru-

ment each day, the tube was conditioned by purging with 0.1 M KOH and then with electrolyte buffer. A potential of 30 kV was then applied across the capillary from a power supply (Brandenburg, alpha III) for a period of not less than 1 h to allow the system to stabilise. Each sample in 10 mM Tris-HCl buffer, pH 9.1, was loaded electrokinetically at 30 kV. Load time varied according to the sample concentration of MT but was usually no more than 4 s.

Using the Waters Quanta 4000 instrument and the same capillary dimensions described above, all samples were loaded under gravity for periods of up to 40 s (this being approximately equivalent to 4 s of electrokinetic loading). The capillary was conditioned with 0.1 M KOH at the start of each day and at intervals when required. Sample and electrolyte buffers were as described above and the conditions of electrophoresis were similar. The capillary was monitored for UV absorbance at 185 nm and data were collected and integrated by computer using a datalogging program.

Preparation of MT samples for electrophoresis

Purified rat liver Cd, ZnMT-1 and Cd, ZnMT-2 were gifts from Dr. Chiharu Toyama (National Institute for Environmental Studies, Tsukuba, Japan) and rabbit liver Cd, ZnMT isoforms were obtained from Sigma Chemical Company (Poole, UK). The isoform proteins from both species were used to demonstrate the application of CZE to the assessment of MT purity. In addition, rabbit MT-1 and MT-2 were used routinely for evaluating capillary condition and for investigating the potential of CZE for quantitative analysis of MT isoforms. In particular, the linearity of gravity loading time and MT concentration against integrated absorbance peak area was investigated using the Waters Quanta 4000 system. An attempt was also made to estimate the detection limit for MT.

Since CZE analysis of MT is very rapid, we investigated the value of measuring sequential fractions from a gel permeation column, thus adding a second analytical dimension to the chromatography profile. Using a Sephadex G-75 column (30 × 1.5 cm) equilibrated with 10 mM Tris-HCl, pH 8.6, and cytosol from a 50% tissue homogenate, sheep MT was separated from the liver of a single adult grey-face ewe which had been dosed orally with 500

mg Zn (as ZnSO₄ in saline-glycerol) and injected intraperitoneally (i.p.) with 2 mg Zn kg⁻¹ and then 4 mg Zn kg⁻¹ (ZnSO₄ in saline) on the following 2 days. The Zn concentration in each fraction was determined by atomic absorption spectrophotometry and individual fractions corresponding to the elution position of MT were analysed directly by CZE.

Direct analysis of tissue cytosols by CZE was found to be of little value for the quantification of MT (see Discussion below) and the use of gel permeation chromatography as an initial separation procedure was considered impracticable for routine analysis of MT. An attempt was therefore made to adapt and develop sample preparation techniques that would facilitate the rapid analysis of MT isoforms. Two methods were studied: an acetone precipitation technique and a method using acetonitrile to remove high *M_r* proteins. Liver homogenates (20% (w/v) in 10 mM Tris-HCl, pH 8.6, 0.25 M sucrose) were prepared from rats which had been injected i.p. with either saline or 3 mg Zn kg⁻¹ (ZnSO₄ in saline) for 4 consecutive days. CdCl₂ (25 μg Cd/ml cytosol) was added to the homogenates to stabilise MT before centrifugation at 105 000 g for 60 min. The addition of too much Cd at this stage can cause precipitation of MT. Aliquots were treated with acetone using the procedure of Hidalgo *et al.* [17]. The precipitated MT was reconstituted in 10 mM Tris-HCl buffer, pH 9.1, and subsequently analysed by CZE. Further ice-cold aliquots of cytosol were treated by the slow addition of cold acetonitrile, while vortexing, to a final concentration of 50% (v/v). The samples were left to stand at 4°C for 1 h before centrifugation at 1000 g for 15 min. The supernatants were analysed directly using CZE.

We were interested to investigate whether very small amounts of tissue could be used for analysis and so 8 mg replicate samples of liver from the saline- and Zn-injected rats were homogenised by sonication in 200 μl of 10 mM Tris-HCl buffer, pH 8.6. After centrifugation at 1000 g for 30 min (4°C), 150 μl of acetonitrile was slowly added, while vortexing, to an equal volume of the supernatant. The precipitate was removed by centrifugation at 1000 g for 15 min and the supernatant was analysed directly by CZE.

RESULTS

Purity analysis

Due to the high resolution of the CZE technique and the difference in charge between MT-1 and MT-2, the two isoforms of rat and rabbit liver MT showed complete separation (Figs. 1 and 2). When corrected for changes in the endo-osmotic front (EOF), there was no difference in the MT-1 and MT-2 separation characteristics between rat and rabbit. As expected from their negative charge at pH 9.1, both isoforms were detected after the EOF. The migration times for replicate electropherograms of purified MT-1 and MT-2 were consistently reproducible although some variation in migration times were noted when analysing tissue extracts. Marked improvements were made by re-conditioning the capillary with 0.1 M KOH between analyses, although this routine treatment was not found to be practicable with the laboratory constructed equipment where the capillary had to be purged manually.

In agreement with established knowledge concerning the charge differences between the isoforms, MT-2, which is more highly charged than MT-1, had the longest migration time (*ca.* 260 s compared to 230 s for MT-1; Fig. 1). The rat MT isoforms were found to be of high purity (>95%), although a very small component with a migration time intermediate to MT-1 and MT-2 was detected. However,

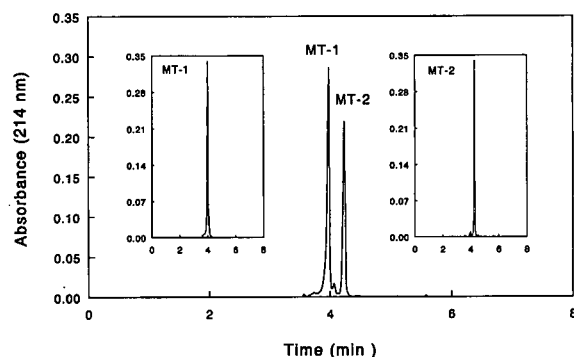


Fig. 1. Capillary zone electropherograms of rat liver MT and the individually purified MT-1 and MT-2 isoforms (inserts). Samples of MT (1.14 mg ml^{-1}), MT-1 (0.61 mg ml^{-1}) and MT-2 (0.53 mg ml^{-1}) were dissolved in 10 mM Tris-HCl buffer, pH 9.1, and loaded into the capillary by electrokinetic migration at 30 kV for 2 (MT) or 3 (MT-1 and MT-2) s. The running buffer was 50 mM Tris-HCl, pH 9.1, and the running voltage was 30 kV.

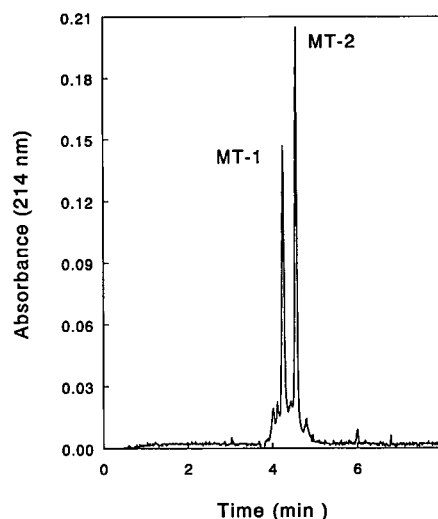


Fig. 2. Capillary zone electropherogram of rabbit liver MT (0.50 mg ml^{-1}) loaded by electrokinetic migration for 1 s. The buffers used to dissolve the sample and for running were the same as those described in the legend to Fig. 1.

the combined rabbit MT isoforms contained at least 4 small peaks in addition to the MT isoforms (Fig. 2). It is not clear whether these were contaminants or perhaps variant metalloforms of MT (*i.e.*, the same MT isoform with different metal composition). From absorbance peak area calculation, the relative proportion of MT-1 and MT-2 appeared to vary from lot-to-lot of the commercial rabbit protein but replicates from a single lot gave consistent results (data not shown).

Analysis of gel chromatography fractions

Most of the zinc from the sheep liver cytosol sample subjected to gel permeation column chromatography on Sephadex G-75 eluted, bound to MT, in fractions 12 through 17 inclusive and the CZE analyses of consecutive fractions are shown in Fig. 3. Fractions 13 to 17 show a prominent component which was found to have the same migration time as sheep MT-1 purified by ion-exchange chromatography. The migration time of MT-2 was also identified by CZE analysis of the purified isoform and it is clear that its cytosolic concentration was very much lower than that of MT-1. In contrast to MT-1 and MT-2, other contaminants clearly visible in fraction 12, were increasingly less conspicuous in

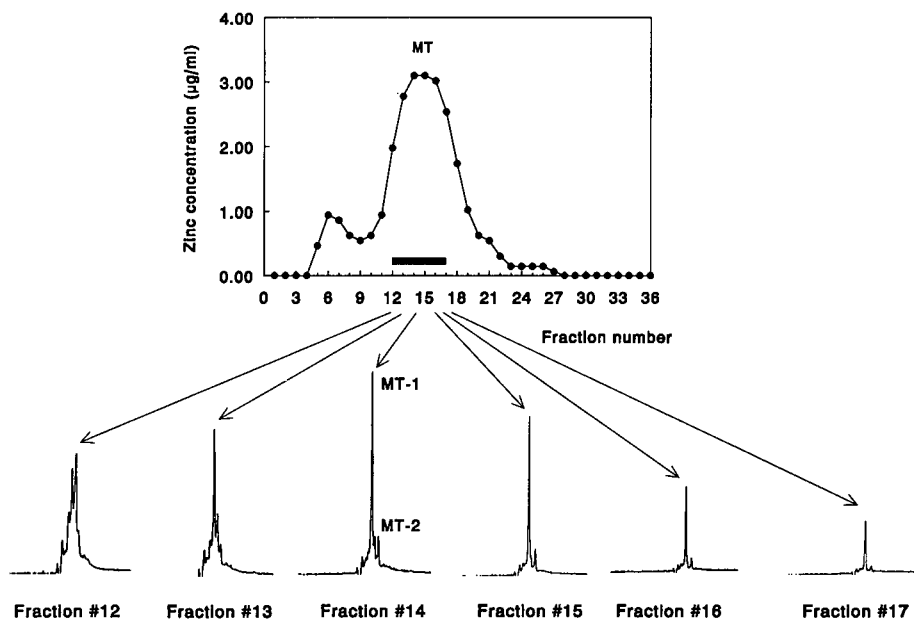


Fig. 3. A two-dimensional analysis of MT from a Zn-treated sheep. The first dimension (top panel) consisted of a gel permeation fractionation of cytosol on a column packed with Sephadex G-75 and eluted with 10 mM Tris-HCl, pH 8.6. The MT-containing column fractions (denoted by bar) were identified by an atomic absorption spectrophotometric analysis for Zn. These fractions (12–17) were then subjected directly to the second dimension analysis of CZE with loading by electrokinetic migration for 4 s at 30 kV and run in 50 mM Tris-HCl, pH 9.1, at 30 kV.

subsequent fractions. During purification of MT-1 and MT-2 on an anion-exchange column (Sephadex DEAE A-25), the appearance of some red coloration was noted in the MT-2 fraction. A sample was therefore desalted and concentrated on a Centri-con-3 molecular filtration unit (Amicon, UK) and analysed by CZE. The resulting electropherogram showed 3 components (Fig. 4a), the first of which had the same migration time as the purified sheep MT-1. In order to distinguish the remaining 2 components, the sample was re-analysed by CZE, this time monitoring absorbance at 414 nm. Since the ion-exchange fraction showed a small absorption maximum at 414 nm and MT does not absorb light at this wavelength, the resulting electropherogram clearly demonstrated that the second component (presumably haemoglobin) was the contaminating red protein (Fig. 4b).

Standard calibration

The relationship between gravity loading time of MT sample ($500 \mu\text{g ml}^{-1}$) and integrated absorbance peak area was found to be linear over the

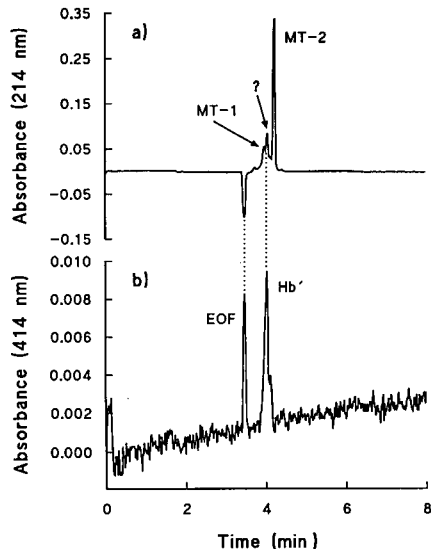


Fig. 4. (a) Capillary zone electropherogram of sheep liver MT-2 previously purified by anion-exchange chromatography and desalted by ultrafiltration. The lower panel (b) represents CZE of the same sample except that absorbance at 414 nm was monitored to detect the presence of a red protein contaminant (presumably haemoglobin, Hb). The endo-osmotic front (EOF) and contaminant MT-1 are also indicated.

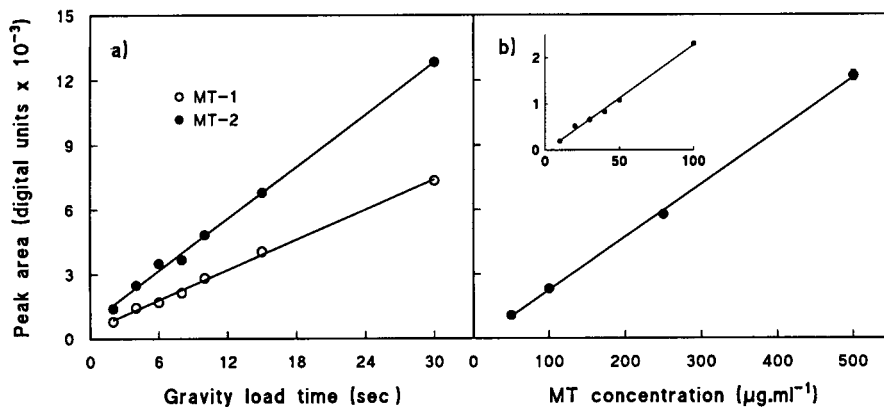


Fig. 5. Integrated peak areas of MT-1 and MT-2 isoforms from a rabbit liver MT sample (0.50 mg ml^{-1}) plotted as a function of (a) the gravity loading time or as a function of (b) the concentration of MT loaded into the capillary. A standard curve for the lower concentration range $10\text{--}100 \mu\text{g ml}^{-1}$ is also shown (insert). Each sample was dissolved in 10 mM Tris-HCl , pH 9.1, and run at 30 kV in 50 mM Tris-HCl , pH 9.1.

range of 2 to 30 s for both MT-1 and MT-2 (Fig. 5a). In addition, the ratio of MT-1:MT-2 remained constant over this range indicative of the fact that both isoforms loaded in the same proportion at each time. CZE of standard rabbit MT solutions also gave linear calibration lines across the entire concentration range ($10\text{--}500 \mu\text{g ml}^{-1}$ of MT-1 + MT-2) as can be seen in Fig. 5b. From linear regres-

sion of the data, the absolute limit of detection was estimated to be approximately $1 \mu\text{g ml}^{-1}$. Nevertheless, under our separating conditions, it would be appropriate to assume a working detection limit in the range $1\text{--}10 \mu\text{g ml}^{-1}$.

Analysis of MT in rat liver

Both MT isoforms were readily detected in the acetone-extracted hepatic cytosol samples from Zn-injected rats (Fig. 6). Relatively little contamination from other components was observed confirming the specificity of this preparation method for MT. MT-2 was clearly identifiable in the acetone extract from the livers of saline-injected (control) rats although the level of MT-1 was considerably lower.

The treatment of cytosol samples with acetonitrile was simple and rapid but could not remove all contaminants, particularly low M_r components. The isoforms were identified by standard additions of MT-1 and MT-2 to the acetonitrile-treated samples prior to re-analysis by CZE (Fig. 7). As with the acetone treatment, MT-2 was readily detected in the liver extract from saline-injected rats (Fig. 7a) but MT-1 was barely detectable. The presence of both isoforms in the liver extract from Zn-injected rats (Fig. 7d) confirmed the acetone treatment results.

MT was readily detected in the 8-mg liver samples from rats injected with Zn (Fig. 8). In agreement with the results for the 2 previous solvent ex-

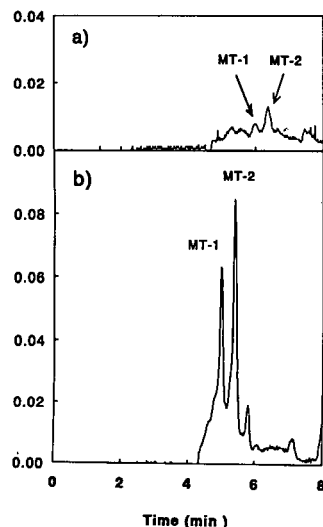


Fig. 6. Liver cytosol from control and zinc-injected rats was fractionated with acetone to enrich for MT and the 80% acetone insoluble pellet was redissolved in 1.0 ml of 10 mM Tris-HCl , pH 9.1, and subjected to CZE as described in the legend to Fig. 1.

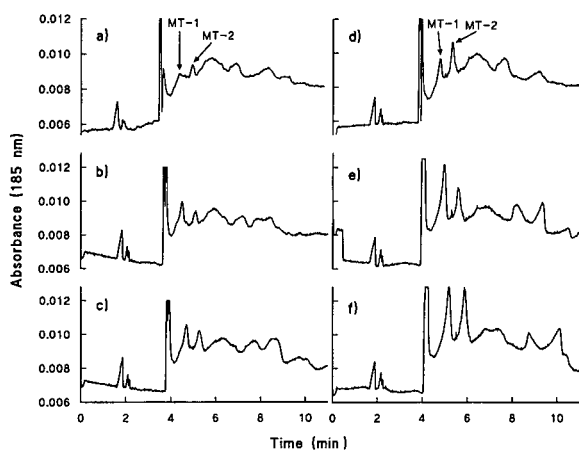


Fig. 7. Liver cytosol as described in the legend to Fig. 6 was treated with acetonitrile (50%, v/v) to remove contaminating proteins and the resulting supernatant after centrifugation was subjected to CZE. MT isoforms were detected in control cytosol (a) and in cytosol from Zn-injected rats (d). The identity of each isoform was confirmed by standard additions of MT-1 (b & e) and MT-2 (c & f) to the extract from Control and Zn-injected animals prior to CZE.

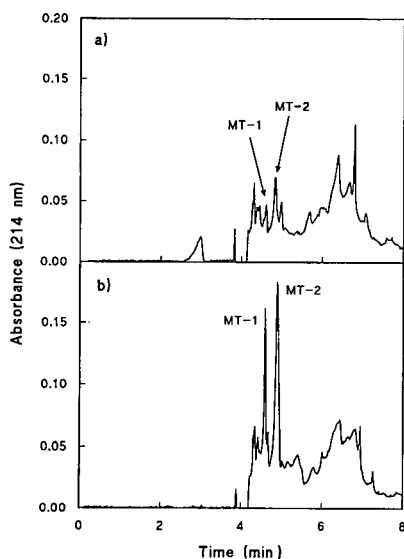


Fig. 8. Capillary electropherograms of acetonitrile-treated cytosol derived from a small (8 mg) sample of liver from (a) control and (b) zinc-injected rats. CZE was conducted as described in the legend to Fig. 1.

traction methods, considerably more MT-2 than MT-1 was detected in the liver of the saline-injected rats (Fig. 8a). A similar isoform ratio was also evident in the Zn-injected sample (Fig. 8b) and is consistent with co-ordinate induction of MT-1 and MT-2 isoforms by zinc.

DISCUSSION

The separation of the major MT isoforms by CZE was found to be simple, rapid and reproducible. In contrast to other electrophoresis techniques, CZE can be automated for batch analysis and would therefore be suitable for the routine analysis of MT-1 and MT-2 in large numbers of samples. The high resolution achieved is characteristic of this technique and was not seriously affected by increasing the sample load time up to at least 40 s (gravity) or 4 s (electrokinetic). The estimated detection limit concentration of 1–10 $\mu\text{g MT ml}^{-1}$ is high compared to, for example, immunological assays. However, since the volume of sample entering the capillary is usually < 100 nl, it is technically possible to analyse very small sample volumes (< 5 μl) repeatedly using positive or negative pressure loading techniques *e.g.* gravity. Thus very small quantities of MT can be extracted into a small volume to achieve an appropriate concentration for analysis by CZE. Consequently both MT-1 and MT-2 were readily determined from only 8 mg of liver using the acetonitrile preparation technique (Fig. 8). Further improvements in the sensitivity of analyses by CZE should accompany current advances in detector technology, particularly in the areas of electrochemical, mass spectrometry and laser-induced fluorescence detection.

The application of CZE to the qualitative analysis of MT isoforms has been discussed briefly [18] and the results would indicate that it is an invaluable technique for this purpose. For example, the commercially available rabbit liver MT samples consistently contain at least 4 components in addition to the 2 major MT isoforms. Monitoring the effluent from Sephadex G-75 column chromatography of Zn-induced sheep liver cytosol was valuable in determining the fractions of highest MT content and purity. Without any further chromatographic analysis, it was clear from the CZE data that the liver concentration of MT-1 was much higher than

that of MT-2 following injection of sheep with Zn. The preferential induction of MT-1 has been noted previously in sheep using traditional chromatographic methods of isoform separation [19]. Since there are 3 functional sheep MT-1 genes [20], we were interested to observe if the corresponding proteins could be resolved by CZE. However, only one peak for MT-1 was detected and it is unclear whether this contained unresolved components or whether only one MT-1 isoform had been induced. Considering the small number of amino acid substitutions [20,21] with relatively little or no change in the molecular weight or charge between MT-1 isoforms, it is perhaps not surprising that these proteins could not be resolved, if indeed they were present. It is also possible that the relative abundance of the MT-1 isoform compared to the MT-2 isoform reflects the combined contribution of different MT-1 isoforms unresolved by CZE. The power of CZE for checking MT purity might be further enhanced using an alternative method of analysis for multi-component identification such as CZE–mass spectrometry since modern mass spectrometers have the required mass resolution and sensitivity for this purpose. Alternatively, a different form of capillary electrophoresis might prove useful in the resolution of MT-1 isoforms, one that does not rely solely on differences in charge-to-mass ratio as CZE does. For example, micellar electrokinetic capillary chromatography (MECC) which resolves components partly on the basis of their hydrophobicity could be employed. Since all of the individual MT-1 isoforms from human liver samples are resolved with RP-HPLC [22], MECC may likely contribute added resolving capability to a separation of MT isoforms.

The linearity and reproducibility of the calibration curves for MT indicate that CZE is suited to the quantitative analysis of this protein. However, using the above described conditions of electrophoresis analysis of MT in a complex matrix such as liver cytosol was not possible due to the dominating presence of other proteins. Removal of these proteins by precipitation with solvents such as ethanol–chloroform and acetone has frequently been used in the purification procedure for MT [23,24]. Using rat cytosol as starting material, purification of MT for CZE analysis using acetone was successful but the method is relatively time consuming. Acetonitrile is

advantageous in that it provides reducing conditions and can be applied directly to the capillary column. Moreover, it has been demonstrated by radioimmunoassay, that the recovery of MT-1 from hepatocyte cytosol ($5 \cdot 10^6$ cells) treated with 50% acetonitrile was over 90% (unpublished data). The successful analysis of MT in 8-mg liver samples (Fig. 7) demonstrated the feasibility of using the acetonitrile preparation method with small amounts of tissue such as could be obtained by biopsy or from a single culture dish containing in the order of $5 \cdot 10^6$ hepatocytes. We therefore believe that acetonitrile extraction shows greatest potential for sample preparation prior to automated CZE analysis.

In conclusion, qualitative analysis of semi-purified or purified MT by CZE is of great value in the assessment of purity and the relative abundance of the two major MT isoforms. CZE also reveals information about differences in the charge to mass ratio of MT isoforms from different animal species. We have not as yet detected any difference in migration time of individual isoforms due to the type of bound metal but this area requires further investigation. Multiple isoforms of MT-1 in species such as sheep could not be resolved probably due to the relatively minor changes in charge to mass ratio associated with substitutions of individual amino acids. Standard calibration curves indicated linearity over an acceptable concentration range with an estimated detection limit of $1\text{--}10 \mu\text{g MT ml}^{-1}$. Prior removal of major protein contaminants by solvent precipitation offers a rapid method of preparing samples for CZE analysis. The use of acetonitrile is recommended for the preparation of small tissue or cell samples prior to quantification of MT by CZE.

REFERENCES

- 1 J. H. R. Kägi and B. L. Vallee, *J. Biol. Chem.*, 235 (1960) 3460.
- 2 J. H. R. Kägi and Y. Kojima (Editors), *Metallothionein II*, Birkhäuser Verlag, Basel, 1987, p. 31.
- 3 M. Vasák, *Methods Enzymol.*, 205 (1991) 41.
- 4 R. K. Mehra and I. Bremner, *Biochem. J.*, 213 (1983) 459.
- 5 J. S. Garvey, R. J. Vander Mallie and C. C. Chang, *Methods Enzymol.*, 84 (1984) 121.
- 6 A. Grider, K. J. Kao, P. A. Klein and R. J. Cousins, *J. Lab. Clin. Med.*, 113 (1989) 221.
- 7 J. K. Piotrowski, W. Bolanowska and A. Sapota, *Acta Biochim. Pol.*, 20 (1973) 207.

- 8 D. L. Eaton and B. F. Toal, *Toxicol. Appl. Pharmacol.*, 66 (1982) 134.
- 9 A. M. Scheuhammer and M. G. Cherian, *Toxicol. Appl. Pharmacol.*, 82 (1986) 417.
- 10 D. L. Eaton, *Toxicol. Appl. Pharmacol.*, 78 (1985) 158.
- 11 A. J. Zealazowski, Z. Gasyna and M. J. Stillman, *J. Biol. Chem.*, 264 (1989) 17 091.
- 12 D. Klein, R. Bartsch and K. Summer, *Anal. Biochem.*, 189 (1990) 35.
- 13 K. T. Suzuki, *Anal. Biochem.*, 102 (1980) 31.
- 14 M. P. Richards, *Methods Enzymol.*, 205 (1991) 217.
- 15 M. V. Novotny, K. A. Cobb and J. Liu, *Electrophoresis*, 11 (1990) 735.
- 16 P. D. Grossman, J. C. Colburn, H. H. Lauer, R. G. Nielsen, R. M. Riggan, G. S. Sittampalam and E. C. Rickard, *Anal. Chem.*, 61 (1989) 1186.
- 17 J. Hidalgo, M. Giralt, J. S. Garvey and A. Armario, *Am. J. Physiol.*, 254 (1988) E71.
- 18 M. P. Richards, J. H. Beattie and R. Self, *FASEB J.*, 6 (1992) A1093.
- 19 P. D. Whanger, *Methods Enzymol.*, 205 (1991) 358.
- 20 M. G. Peterson, F. Hannan and J. F. B. Mercer, *Eur. J. Biochem.*, 174 (1988) 417.
- 21 P. D. Whanger, S. Oh and J. T. Deagen, *J. Nutr.*, 111 (1981) 1207.
- 22 P. E. Hunziker and J. H. R. Kägi, *Biochem. J.*, 231 (1985) 375.
- 23 R. Bühler and J. H. R. Kägi, *FEBS Lett.*, 39 (1974) 229.
- 24 G. Roesijädi and B. A. Fowler, *Methods Enzymol.*, 205 (1991) 263.

Temperature-programmed capillary affinity gel electrophoresis for the sensitive base-specific separation of oligodeoxynucleotides

Yoshinobu Baba and Mitsutomo Tsuhako

Kobe Women's College of Pharmacy, Kitamachi, Motoyama, Higashinada-ku, Kobe 658 (Japan)

Tomohiro Sawa and Mitsuru Akashi

Department of Applied Chemistry and Chemical Engineering, Faculty of Engineering, Kagoshima University, Korimoto, Kagoshima 890 (Japan)

ABSTRACT

High-performance base-specific separations of oligodeoxynucleotides were performed by temperature-programmed capillary affinity gel electrophoresis (CAGE), in which poly(9-vinyladenine) (PVAd) was utilized as an affinity ligand. The migration behaviour of oligodeoxynucleotides was investigated at different capillary temperatures. The migration time and resolution of oligodeoxyadenylic acids, which do not interact with PVAd, decrease with increase in temperature as in capillary gel electrophoretic separation. The migration behaviour of oligothymidylic acids, which interact with PVAd, is manipulated by varying the capillary temperature, which leads to changes in the dissociation process of specific hydrogen bonding between oligothymidylic acids and PVAd. The implementation of temperature-programmed CAGE was illustrated by the selective and sensitive base recognition of oligodeoxynucleotides with efficiencies as high as several times 10^6 plates per metre.

INTRODUCTION

Capillary gel electrophoresis (CGE) [1] is rapidly becoming an important tool for the separation of single- and double-stranded polynucleotides (DNA and RNA). Extremely high-resolution and high-speed separations could be performed by CGE. However, CGE is not applicable to the sequence-specific separation of polynucleotides, such as sequence isomer separations, as the separation by CGE is based on a molecular sieving effect. Development of new CGE columns with special selectivity extends the versatility of CGE, as in HPLC.

Recently we developed capillary affinity gel electrophoresis (CAGE) as an alternative format of

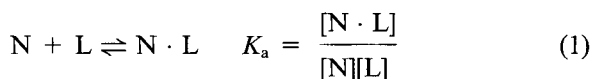
CGE, incorporating an affinity ligand within a polyacrylamide gel matrix, for the specific base recognition of oligodeoxynucleotides [2–5]. The incorporation of an affinity ligand within a gel can be used to manipulate the selectivity of CGE separations. CAGE using poly(9-vinyladenine) (PVAd) as an affinity ligand was effective for the selective separation of oligothymidylic acids from a mixture of oligodeoxynucleotides [2–4]. Additionally, CAGE separated completely the sequence isomers of hexadeoxynucleotide (TTTATT, TTTTAT and TTTTAA) [5], which could not be separated by CGE [5]. PVAd has been shown to form *in vitro* the complex with the complementary strand of polynucleotide by complementary hydrogen bonding [6,7] and to be an excellent affinity ligand [8–10] for high-performance affinity chromatography and affinity gel electrophoresis. The selectivity and efficiency of

Correspondence to: Y. Baba, Kobe Women's College of Pharmacy, Kitamachi, Motoyama, Higashinada-ku, Kobe 658, Japan.

base-specific separations by CAGE were strongly affected by several parameters, such as the size of PVAd, capillary temperature and concentrations of PVAd and urea [2–4]. In this study, the effect of temperature on the migration behaviour of oligodeoxynucleotides was investigated in CAGE separations. It is demonstrated that temperature-programmed CAGE is effective for the high-performance base-specific separation of oligodeoxynucleotides.

THEORY

The migration time, t , of an oligodeoxynucleotide in CAGE in the presence of the interaction (eqn. 1) of oligodeoxynucleotides (N) and affinity ligands (L) is expressed as eqn. 2 [2]:



$$t = t_0(1 + K_a[L]_t) \quad (2)$$

where t_0 is the migration time of oligodeoxynucleotide in the absence of affinity ligand, K_a is the apparent association constant between oligodeoxynucleotide and an affinity ligand (L) and $[L]_t$ is the total L concentration. Temperature affects two parameters in eqn. 2, viz., t_0 and K_a . The relationship between temperature and t_0 was formulated by Guttman and Cooke [11] as follows:

$$t_0 = l \cdot 6\pi r \eta / EQ$$

$$\eta = C_1 \exp(E_a/RT)$$

$$\ln t_0 = \ln(l \cdot \text{constant}/EQ) + E_a/RT \quad (3)$$

where l is the effective length of the capillary up to the detection point, η is the viscosity of the surrounding gel–buffer medium, r is the root mean square radius of the polynucleotide, C_1 is a constant, E is the applied field, Q is the net charge of polynucleotides, E_a is the activation energy for the viscous flow, R is the universal gas constant and T is the absolute temperature. The effect of temperature on K_a was expressed as

$$\ln K_a = -\Delta G/RT$$

^a C = g N,N'-methylamide + g Bis per 10

where ΔG is the free energy change in the equilibrium of eqn. 1.

EXPERIMENTAL

Chemicals

Unless stated otherwise, chemicals were of analytical-reagent or electrophoretic grade from Wako (Osaka, Japan). Oligodeoxyadenylic acids, pdA_{12–18}, and oligothymidylic acids, pdT_{12–18}, were obtained from Pharmacia (Uppsala, Sweden). The pdT₁₅ sample was chemically synthesized using a Applied Biosystems (ABI, Foster City, CA, USA) Model 391 DNA synthesizer. Samples were diluted to 2.5 units per 500 μ l with distilled water and stored at -18°C until used. PVAd was prepared by the method reported previously [2,6,7]. The PVAd sample thus obtained had a relative molecular mass ranging from 10 000 to 30 000.

Capillary electrophoresis

An ABI Model 270A capillary electrophoresis system was used for the CAGE separations. Polyimide-coated fused-silica capillaries (375 μ m O.D. and 100 μ m I.D.) (GL Sciences, Tokyo, Japan) were used, with an effective length of 22 cm and a total length of 42 cm. The buffer was a mixture of 0.1 M Tris and 0.1 M boric acid with 7 M urea (pH 8.6) for the preparation of the gel-filled capillaries and as the running buffer. Capillaries filled with polyacrylamide–PVAd conjugated gel (8% T, 5% C and 0.05–0.1% PVAd)^a were prepared by the method reported previously [2,12–14]. The percentage of PVAd was calculated by the equation 100 PVAd(g)/[acrylamide(g) + Bis(g) + PVAd(g)]. Gel-filled capillaries were mounted in the ABI Model 270A system and run with buffer solution at 9 kV (214 V/cm). Samples were electrophoretically injected into the capillary by applying a voltage of 5 kV for 0.1–1 s. The temperature of the agitated air surrounding the capillary was maintained constant within $\pm 0.1^\circ\text{C}$. Oligonucleotides were detected at 260 nm.

RESULTS AND DISCUSSION

arations of oligodeoxynucleotides. Oligothymidylic acids were selectively separated from a mixture of oligodeoxynucleotides by using CAGE utilizing PVAd as follows. In CGE separations, each oligodeoxynucleotide with the same chain length and difference base composition would elute with almost the same electrophoretic mobility [2]. On the other hand, the mobility of oligothymidylic acids shows strong retardation due to its specific interaction with PVAd, whereas the mobilities of other oligodeoxynucleotides that cannot interact with PVAd are unchanged. A difference in the mobilities results in the specific recognition of oligothymidylic acids over other oligodeoxynucleotides.

Effect of temperature in the capillary affinity gel electrophoretic separations

Figs. 1 and 2 compare the separations of the pdA_{12–18} and the pdT_{12–18} mixture by CAGE at different temperatures. It can be seen in Fig. 1 that

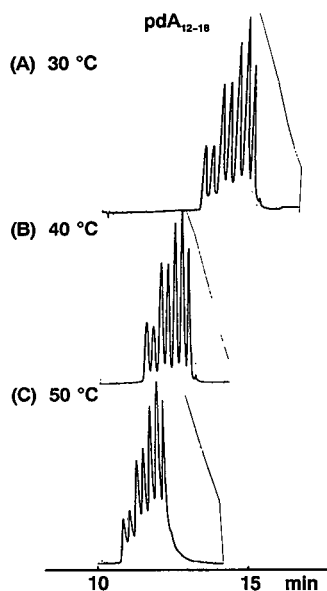


Fig. 1. Separation of pdA_{12–18} by CAGE at (A) 30, (B) 40 and (C) 50°C. Capillary, 100 μm I.D., 375 μm O.D., total length 42 cm, effective length 22 cm. Running buffer, 0.1 M Tris–borate and 7 M urea (pH 8.6). Gel contained 8% T, 5% C and 0.05% PVAd with a relative molecular mass range of 10 000–30 000. Field, 214 V/cm; current, 9 μA ; injection, 5 kV for 1 s; detection, 260 nm.

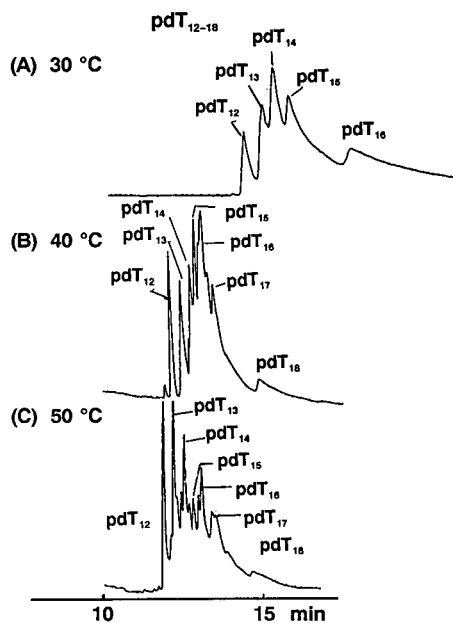


Fig. 2. Separation of pdT_{12–18} by CAGE at (A) 30, (B) 40 and (C) 50°C. Conditions as in Fig. 1.

the migration time and resolution of pdA_{12–18} decrease as the temperature increases. The results in Fig. 1 were comparable to the effect of temperature on the migration time of pdA_{12–18} in CGE without an affinity ligand [15]. This suggests that a decrease in the migration time of pdA_{12–18} is mainly caused by a decrease in the viscosity of the surrounding gel–buffer with an increase in temperature as expressed in eqn. 3 [11]. The effect of temperature on K_a in eqn. 4 is not taken into account in this instance, because the interaction of pdA_{12–18} with PVAd is negligible.

The effect of temperature on the electropherogram of pdT_{12–18} as shown in Fig. 2 was different from that in CGE, which was similar to the results in Fig. 1 [15]. The migration time of pdT_{12–18} was more affected by temperature than that of pdA_{12–18}, as shown in Fig. 1. In addition, some band broadening was observed at lower temperature. This indicates that temperature affects not only the viscosity process in eqn. 3, but also the association process expressed as eqn. 4. As the affinity ligand would bind tightly to pdT_{12–18} by hydrogen bonding at lower temperature, band broadening increased as temperature decreased. Dissociation of hydrogen bonding, which occurred at elevat-

ed temperature, resulted in a decrease in the association constant, K_a , in eqn. 4. Therefore, the migration times at 40 and 50°C (Fig. 2B and C) were almost comparable to those in CGE [15]. Some peaks that appeared in Fig. 2B and C in addition to the peaks for pdT₁₂₋₁₈ would correspond to the peaks for dephosphorylated oligodeoxythymidylic acids.

We tried the base-specific separation of pdT₁₂₋₁₈ from a mixture of oligodeoxynucleotides by using isothermal CAGE as shown in Fig. 3. Oligothymidylic acids were selectively separated from the mixture at 30°C, but the resolution of pdT₁₂₋₁₈ decreased considerably as shown in Fig. 3A. The base selectivity of pdT₁₂₋₁₈ over pdA₁₂₋₁₈ was significantly diminished above 40°C (Fig. 3B). Consequently, sensitive base-specific separation was not be achieved by using isothermal CAGE. We next turned to the use of temperature-programmed CAGE for high-performance specific base recognition.

High-performance base-specific separation by temperature-programmed CAGE

As in chromatographic methods [16], the main purpose of using temperature programming in CAGE is to improve the speed and/or the efficiency

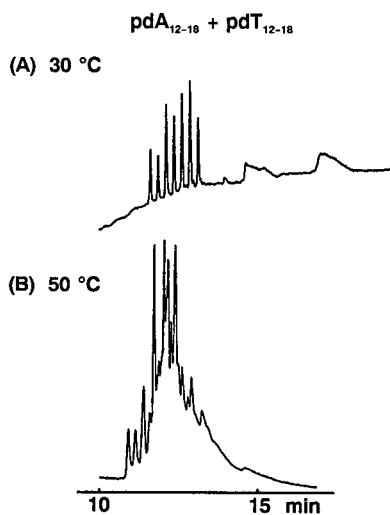


Fig. 3. Separation of a mixture of pdA₁₂₋₁₈ and pdT₁₂₋₁₈ by capillary affinity gel electrophoresis at (A) 30 and (B) 50°C. Conditions as in Fig. 1.

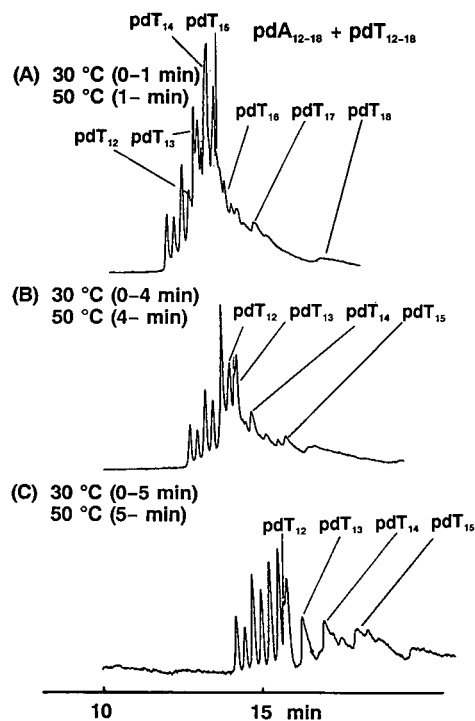


Fig. 4. Influence of temperature programming on the separation of a mixture of pdA₁₂₋₁₈ and pdT₁₂₋₁₈: (A) 30°C for 1 min, then step to 50°C; (B) 30°C for 4 min, then step to 50°C; (C) 30°C for 5 min, then step to 50°C. Conditions as in Fig. 1.

of a separation. Fig. 4 demonstrates the effect of temperature programming on the electrophoretic behaviour of a mixture of pdA₁₂₋₁₈ and pdT₁₂₋₁₈ in CAGE. CAGE was initially performed at 30°C. After an appropriate time as shown in Fig. 4, the temperature was elevated to 50°C. The temperature programming was actually performed as a gradient in which the temperature was gradually increased from 30 to 50°C during a *ca.* 3-min interval during electrophoresis rather than as stepwise changes. An attempt to improve the resolution by temperature programming in Fig. 4A was not successful. The base-specific separation can be further improved by employing temperature programming with a longer period at the initial temperature during electrophoresis, as shown in Fig. 4B and C. The migration time of pdT₁₂₋₁₆ in Fig. 4C decreased substantially in comparison with isothermal CAGE at 30°C in Figs. 2A and 3A. In addition, temperature programming resulted in sharper bands compared with

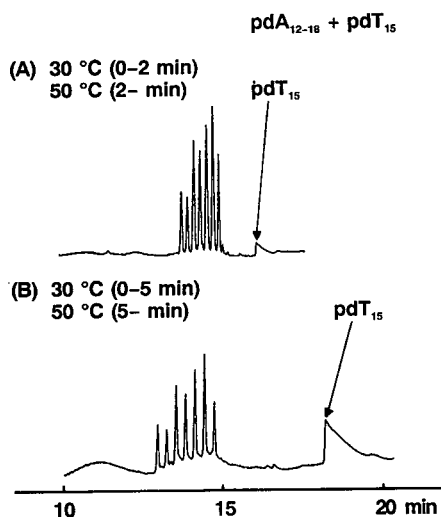


Fig. 5. Influence of temperature programming on the separation of a mixture of pdA_{12-18} and pdT_{15} : (A) 30°C for 2 min, then step to 50°C; (B) 30°C for 5 min, then step to 50°C. Gel contained 8% T, 5% C and 0.1% PVAd with a relative molecular mass range of 10 000–30 000. Other conditions as in Fig. 1.

isothermal conditions. The pdT_{13-16} bands were separated completely from pdA_{12-18} , but the pdT_{12} band partially overlapped that of pdA_{18} . The pdT_{14-16} bands were severely broadened owing to the strong interaction with PVAd. A relatively simple mixture of oligodeoxynucleotides was next separated by temperature programming to show the performance of the base-specific separation by CAGE.

Fig. 5 demonstrates that the base-specific separation of a mixture of pdA_{12-18} and pdT_{15} was achieved using CAGE with temperature programming, which was similar to that in Fig. 4, whereas that without an affinity ligand did not [2]. However, the pdT_{15} band was severely broadened and the efficiency of CAGE was not improved, probably owing to the strong interaction of pdT_{15} with PVAd. An increase in the initial temperature of the programme would be effective in achieving high-efficiency recognition of pdT_{15} .

Fig. 6 shows the effect of elevating the initial temperature on the efficiency of the base-specific separation of a mixture of pdA_{12-18} and pdT_{15} . An attempt to reduce the band broadening by raising

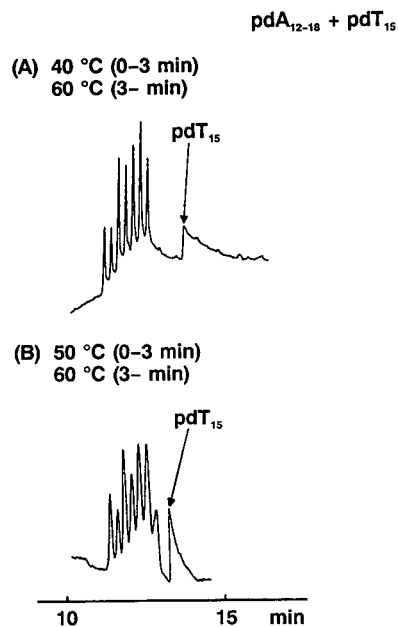


Fig. 6. Influence of initial temperature on the separation of a mixture of pdA_{12-18} and pdT_{15} : (A) 40°C for 3 min, then step to 60°C; (B) 50°C for 3 min, then step to 60°C. Other conditions as in Fig. 4.

the initial temperature to 40°C was not totally successful, although the analysis time was shortened (see Fig. 6A). The band broadening was further diminished by employing an initial temperature of 50°C, as shown in Fig. 6B. The plate number of pdT_{15} was $1 \cdot 10^5$ – $3 \cdot 10^6$ per metre in Fig. 6B. This value was slightly reduced compared with that obtained by CGE [2], but much higher (by several tens of thousands) than that achieved by high-performance affinity chromatography [16]. The results in Fig. 6 clearly demonstrate that the resolving power and separation speed of temperature-programmed CAGE in base-specific separation compare favourably with those of high-performance affinity chromatography [16].

In conclusion, temperature programming was found to be effective for manipulating the selectivity and improving the speed and the efficiency of CAGE, and for achieving sensitive and high-resolution base-specific separations of oligodeoxynucleotides. This method will allow its application to the complex mixture of DNA, where inadequate separation is obtained in isothermal CAGE experiments.

ACKNOWLEDGEMENTS

The authors gratefully acknowledge support for this research by a travel grant from the Ichikizaki Fund for Young Chemists. This work was partially supported by a Grant-in-Aid for Scientific Research No. 04771913 from the Ministry of Education, Science and Culture, Japan.

REFERENCES

- 1 Y. Baba and M. Tsuchioka, *Trends Anal. Chem.*, 11 (1992) 280, and references cited therein.
- 2 Y. Baba, M. Tsuchioka, T. Sawa, E. Yashima and M. Akashi, *Anal. Chem.*, 64 (1992) 1920.
- 3 T. Sawa, E. Yashima, M. Akashi, Y. Baba and M. Tsuchioka, *J. High Resolut. Chromatogr.*, 15 (1992) in press.
- 4 T. Sawa, M. Akashi, Y. Baba and M. Tsuchioka, unpublished results.
- 5 M. Akashi, T. Sawa, Y. Baba and M. Tsuchioka, *J. High Resolut. Chromatogr.*, 15 (1992) 625.
- 6 M. Akashi, H. Iwasaki, N. Miyauchi, T. Sato, J. Sunamoto and K. Takemoto, *J. Bioactive Compatible Polym.*, 4 (1989) 124.
- 7 E. Yashima, T. Tajima, N. Miyauchi and M. Akashi, *Biopolymers*, 32 (1992) 811.
- 8 M. Akashi, M. Yamaguchi, H. Miyata, M. Hayashi, E. Yashima and N. Miyauchi, *Chem. Lett.*, (1988) 1093.
- 9 E. Yashima, T. Shiiba, T. Sawa, N. Miyauchi and M. Akashi, *J. Chromatogr.*, 603 (1992) 111.
- 10 E. Yashima, N. Suehiro, M. Akashi and N. Miyauchi, *Chem. Lett.*, (1990) 1113.
- 11 A. Guttman and N. Cooke, *J. Chromatogr.*, 559 (1991) 285.
- 12 Y. Baba, T. Matsuura, K. Wakamoto, Y. Morita, Y. Nishitsu and M. Tsuchioka, *Anal. Chem.*, 64 (1992) 1221.
- 13 Y. Baba, T. Matsuura, K. Wakamoto and M. Tsuchioka, *Chem. Lett.*, (1991) 371.
- 14 Y. Baba, T. Matsuura, K. Wakamoto and M. Tsuchioka, *J. Chromatogr.*, 558 (1991) 273.
- 15 Y. Baba, Y. Morita, Y. Nishitsu, and M. Tsuchioka, unpublished results.
- 16 T. A. Goss, T. Bard, and H. W. Jarret, *J. Chromatogr.*, 508 (1990) 279.

Determination of ten β -blockers in urine by micellar electrokinetic capillary chromatography

P. Lukkari, H. Sirén, M. Pantsar and M.-L. Riekkola

Department of Chemistry, Analytical Chemistry Division, University of Helsinki, P.O. Box 6 (Vuorikatu 20), SF-00014 Helsinki (Finland)

ABSTRACT

β -Adrenergic blocking agents are of therapeutic value in the treatment of migraine and various cardiovascular disorders (angina pectoris, cardiac arrhythmia, hypertension). Owing to their sedative effect, they are also used as doping agents in sport. A characteristic feature of β -blockers is the alkanolamine side-chain terminating in a secondary amino group. The pK_a values vary from 9.2 to 9.8. Because some β -blockers are hydrophilic and some lipophilic, simultaneous determination is difficult. In this work, a method based on micellar electrokinetic capillary chromatography (MECC) was developed for the separation and determination of β -blockers. The 0.08 M phosphate buffer (pH 7.0) solution contained 10 mM N-cetyl-N,N,N-trimethylammonium bromide (CTAB). Ten parent β -blockers in human urine could be separated in a single run and determined quantitatively by the internal standard (2,6-dimethylphenol) method. Neither endogenous compounds in urine nor caffeine and its metabolites interfered with the analysis. The clean-up procedure for urine consisted of a simple filtration through 0.5- μ m PTFE membranes. The MECC method exhibited good repeatability and a linear range of 25–150 μ g/ml. The method was applied to determination of oxprenolol in real samples.

INTRODUCTION

The determination of drugs in biological fluids is growing in importance owing to the need to understand better the biochemical effects of drugs and the continuing development of more selective and effective drugs.

Methods for the screening and identification of β -blockers have been studied over several decades. TLC, HPLC and high-resolution GC-MS [1,2] are the conventional approaches after the drugs have been isolated from the matrices. Although these methods meet the demands of selectivity and sensitivity, the character of β -blockers complicates the necessary preparation of biological fluids for their determination. Some β -blockers are lipophilic and others hydrophilic. In addition, their relatively high pK_a values (9.2–9.8), caused by hydrogen bonding

between the free electron pair on the nitrogen atom of the terminal amino group and the hydrogen atom of the β -hydroxyl group, complicate their adsorption and extraction. At physiological pH (pH 7.4), β -blockers exist as single cations [3], which permits their separation and determination by methods based on ion-pair and micellar formations.

Capillary zone electrophoresis (CZE) has developed rapidly since Jorgenson and Lukacs [4,5] first realized the advantages of using narrow-bore (I.D. < 100 μ m) silica capillaries. In CZE, charged particles can be separated on the basis of differences in their electrophoretic mobilities (μ_{ep}). Electroosmotic flow (EOF), which occurs in an electrolyte-filled capillary under an electric field, has a flat flow profile and mobility μ_{eo} ; normally $\mu_{eo} > \mu_{ep}$. This effect forces all solutes (anionic, cationic and neutral) to migrate towards the cathode end of the capillary. Even anionic compounds are carried to the cathode as the EOF is much stronger than the μ_{ep} of the charged particles. Under the influence of EOF, neutral particles migrate together at the velocity of the electrolyte.

Correspondence to: M.-L. Riekkola, Department of Chemistry, Analytical Chemistry Division, University of Helsinki, P.O. Box 6 (Vuorikatu 20), SF-00100 Helsinki, Finland.

Micellar electrokinetic capillary chromatography (MECC), which is an adaptation of CZE, was described by Terabe *et al.* in 1984 [6]. In MECC, an ionic surfactant added to the electrolyte facilitates the separation of neutral particles, something that is not achieved by CZE. Although MECC is useful for the separation of electrically neutral compounds, it is also effective for separating ionic compounds, which, because of their similar electrophoretic mobilities, are not adequately resolved by CZE [7,8]. It is thought that chromatographic distribution principles are involved in MECC. Also, MECC has been used in drug analyses [9–12].

In this paper we present an MECC method for the determination of ten parent β -blockers. The separation mechanism is based on the differential partitioning of analytes between an electroosmotically purged aqueous 0.08 M phosphate buffer phase and an electrophoretically retained cetyltrimethylammonium (10 mM) micellar pseudo-phase. With this method the ten parent β -blockers (spiked) in urine were separated during a single run, after sample preparation consisting only of filtration of the urine. The linear concentration ranges were studied for eventual application of the method to real samples obtained after oral administration of the drug. In addition, the possible interference of caffeine was investigated.

EXPERIMENTAL

Apparatus

MECC was performed in a 68 cm \times 50 μ m I.D. fused-silica capillary tube (White Associates, Pittsburgh, PA, USA) where 600 mm was the effective length for separation. A Waters Quanta 4000 capillary electrophoresis system (Millipore, Waters Chromatography Division, Milford, MA, USA) was employed. Detection was at 214 nm. All experiments were done at ambient temperature. Injections were made hydrostatically for 30 s and the running voltage was -26 kV at the injector end. The data (peak height) were collected with an HP 3392A integrator and the identification of oxprenolol and its hydroxy-substituted metabolites was performed with GC-MS using a Hewlett-Packard (Avondale, PA, USA) Model 5890A gas chromatograph and a Hewlett-Packard Model 5989A single-stage quadrupole mass spectrometer.

Materials

The β -blockers studied were acebutolol hydrochloride, alprenolol hydrochloride, atenolol, labetalol hydrochloride, (\pm)-metoprolol (+)-tartrate, nadolol, oxprenolol hydrochloride, pindolol, (*S*)-(-)-propranolol hydrochloride and timolol maleate, all from Sigma (St. Louis, MO, USA). 2,6-Dimethylphenol (internal standard), sodium dihydrogenphosphate monohydrate, disodium hydrogenphosphate dihydrate and N-cetyl-N,N,N-trimethylammonium bromide (CTAB) were obtained from Merck (Darmstadt, Germany) and were used as received. Other reagents used in the development of the method were of analytical-reagent grade and were used as received. Distilled water was purified through a Water-I system from Gelman Sciences (Ann Arbor, MI, USA). All the micellar buffer solutions were filtered through 0.45- μ m membrane filters (Millipore, Molsheim, France) and degassed before use. Samples and other solutions were filtered through Millex filters of 0.5- μ m pore size (Nihon Millipore, Yonezawa, Japan).

Procedure

To ensure reproducible separations, before each injection the capillary was purged for 2 min with the buffer solution.

Preparation of spiked human urine samples

A human urine pool was diluted with water (1:2) and the mixture was spiked with a solution containing an accurately measured amount of each β -blocker. The urine samples were filtered through filters of 0.5- μ m pore size and then analysed.

RESULTS

Optimization of MECC conditions

A standard solution of the ten β -blockers was prepared for optimization of the MECC conditions in the absence of the matrix. The elution order of the compounds was studied by individual spiking, but all ten β -blockers were always included in the solution. A pH of 7.0 produced by phosphate salts was chosen for the eluent on the basis of past experience in the analysis of β -blockers by ion-pair liquid chromatography.

The parameters investigated were the concentrations of phosphate and the micelle former, CTAB.

which normally is used as the ion-pair former in HPLC, and the applied voltage. Phosphate concentrations from 0.05 to 0.15 M and CTAB concentrations of 5, 8, 10, 12 and 15 mM were studied. On the basis of their simultaneous effect on the resolution, we chose concentrations of 0.08 M phosphate buffer and 10 mM CTAB. Under these buffer and micellar conditions the best value for the voltage was –26 kV. The analysis could thus be performed and almost a baseline separation achieved with the lowest current of the apparatus.

Choice of internal standard

An internal standard was required for quantitative MECC analysis because the ambient temperature and the temperature in the sample space influence the migration times. The negative temperature effect could have been reduced if our CZE equipment had included a temperature control unit.

A suitable internal standard was not easily found as two main requirements had to be met: it had to resemble the structure of the β -blockers, *i.e.*, it had to have at least either a hydroxyl or an amino group, and it had to migrate in the middle of the drug zone. 2,6-Dimethylphenol, met both of these criteria and was chosen as the internal standard (ISTD). Its resolution from drugs migrating nearby was complete. A further advantage of 2,6-dimethylphenol is that it is unlikely to be found in the human body. Diphenylamine and probenecid were also evaluated as internal standards but were found to be unsuitable, the former because it did not absorb well enough at 214 nm and the latter because it migrated together with timolol and atenolol.

Samples and technique

The samples were prepared by adding various amounts of the standard mixture to human urine diluted with water (1:2). The internal standard was added. The only preparation applied to the samples was filtration. A blank pooled urine sample obtained from people drinking coffee or tea, but not smoking and not using drugs, was prepared simultaneously, without internal standard addition.

As can be seen in Fig. 1, neither endogenous compounds in urine nor caffeine and its metabolites interfered with the analysis as they migrated to the detector within 5 min. After their migration was complete, all ten β -blockers and the internal stan-

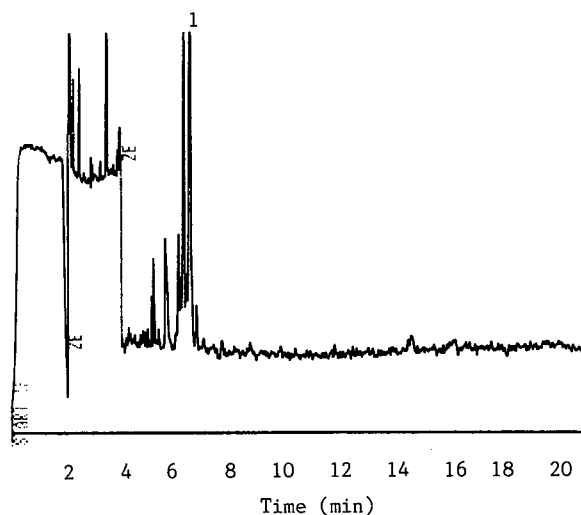


Fig. 1. Electropherogram of blank human urine sample in 0.08 M sodium phosphate buffer containing 10 mM CTAB. Capillary, 68 cm \times 50 μ m I.D.; pH, 7.0; hydrodynamic injection mode, 30 s at 10 cm height; detection, UV at 214 nm; applied voltage, –26 kV; temperature, ambient. In the electropherogram caffeine migrates in zone 1.

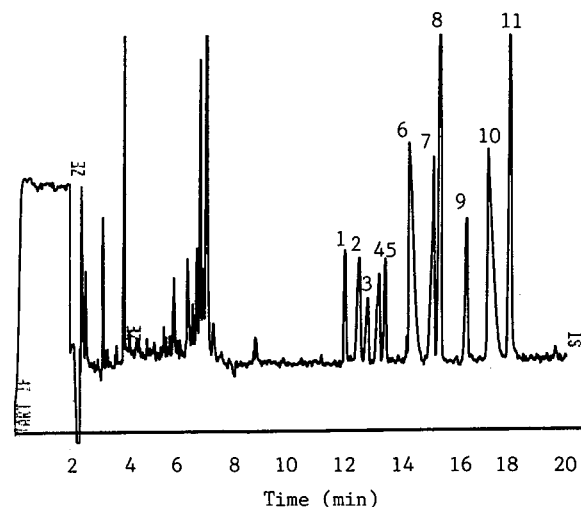


Fig. 2. Electropherogram of a human urine sample in 0.08 M sodium phosphate buffer with 10 mM CTAB. Capillary, 68 cm \times 50 μ m I.D.; pH, 7.0; hydrodynamic injection mode, 30 s at 10 cm height; detection, UV at 214 nm; applied voltage, –26 kV; temperature, ambient. The concentrations of the β -blockers were 75 μ g/ml, except for timolol and 2,6-dimethylphenol (150 μ g/ml). Elution order and relative retention times of the solutes: 1 = acebutolol (0.84); 2 = nadolol (0.87); 3 = timolol (0.90); 4 = atenolol (0.92); 5 = metoprolol (0.94); 6 = 2,6-dimethylphenol (1.00) (internal standard); 7 = oxprenolol (1.06); 8 = pindolol (1.08); 9 = alprenolol (1.15); 10 = labetalol (1.20); 11 = propranolol (1.26).

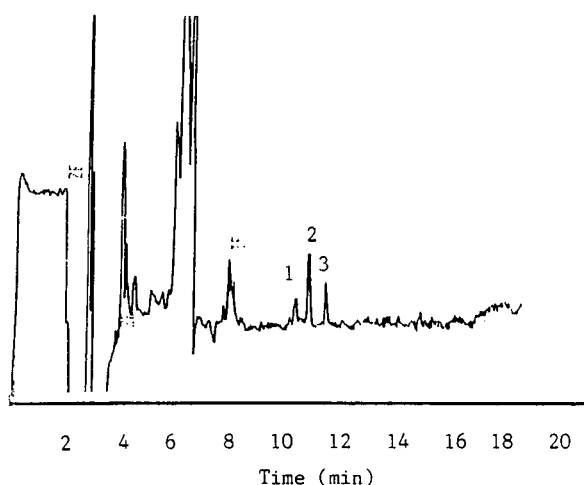


Fig. 3. Electropherogram of a real human urine sample after eightfold concentration by solid-phase extraction in 0.08 M sodium phosphate buffer with 10 mM CTAB. Capillary, 58 cm \times 50 μ m I.D.; pH, 7.0; hydrodynamic injection mode, 60 s at 10 cm height; detection, UV at 214 nm; applied voltage, -26 kV; temperature, ambient. Peaks: 1 and 2 = hydroxy-substituted metabolites of oxprenolol; 3 = oxprenolol. The urine was taken 0–4 h after administration.

dard were eluted with high efficiency and resolution (Fig. 2) within 20 min. As can be seen in Fig. 1, the zone in which the β -blockers migrated was entirely free from other drugs and compounds.

The described method was also applied to the screening β -blockers in real samples. Oxprenolol and its two hydroxy-substituted metabolites were separated after eightfold concentration in less than 12 min from a human urine sample (Fig. 3). The compounds were identified using GC-MS.

The elution order of the drugs was determined by adding them one by one to a standard solution and was found to be acebutolol, nadolol, timolol, atenolol, metoprolol, 2,6-dimethylphenol, oxprenolol, pindolol, alprenolol, labetalol and propranolol. The detector responses of the drugs differed widely when their UV absorption was measured at 214 nm (one of the constant wavelengths in the apparatus). They absorb more strongly in the wavelength range 220–230 nm and the availability of this range would improve the determination.

Repeatability

Repeatability of the injections, which took 30 s at

TABLE I

REPEATABILITY OF INJECTION AT THE LEVEL OF 150 μ g/ml (TIMOLOL 300 μ g/ml)

Analyses were performed using 150 μ g/ml of 2,6-dimethylphenol as the internal standard. χ is the mean ($n = 6$) of (peak height of compound)/(peak height of internal standard), S.D. the standard deviation and R.S.D. the relative standard deviation.

| Compound | χ | S.D. | R.S.D. (%) |
|-------------|--------|------|------------|
| Acebutolol | 1.23 | 0.03 | 2.4 |
| Nadolol | 0.93 | 0.02 | 2.6 |
| Timolol | 0.24 | 0.02 | 8.2 |
| Atenolol | 0.68 | 0.01 | 2.0 |
| Metoprolol | 0.72 | 0.03 | 4.2 |
| Oxprenolol | 0.64 | 0.02 | 2.5 |
| Pindolol | 3.65 | 0.07 | 2.0 |
| Alprenolol | 0.99 | 0.03 | 2.6 |
| Labetalol | 1.35 | 0.04 | 2.7 |
| Propranolol | 4.18 | 0.09 | 2.2 |

a height of 10 cm, was studied at concentrations of 150 μ g/ml, except for timolol, which was studied at 300 μ g/ml. 2,6-Dimethylphenol (150 μ g/ml) was added to ensure the repeatability of the injections. The relative standard deviations varied from 2.0 to 8.2% ($n = 6$) (Table I). These relatively high values are probably due to the hydrodynamic injection technique and the strong matrix effect.

The repeatability of the method was studied at two concentration levels, 25 and 150 μ g/ml (50 and 300 μ g/ml for timolol). The relative standard devia-

TABLE II

REPEATABILITY OF THE METHOD AT THE LEVEL OF 25 μ g/ml (TIMOLOL 50 μ g/ml)

Details as in Table I, except $n = 5$.

| Compound | χ | S.D. | R.S.D. (%) |
|-------------|--------|------|------------|
| Acebutolol | 0.34 | 0.01 | 2.8 |
| Nadolol | 0.35 | 0.02 | 5.6 |
| Timolol | 0.12 | 0.01 | 7.0 |
| Atenolol | 0.23 | 0.01 | 2.0 |
| Metoprolol | 0.25 | 0.01 | 5.1 |
| Oxprenolol | 0.23 | 0.01 | 3.8 |
| Pindolol | 0.67 | 0.04 | 6.3 |
| Alprenolol | 0.31 | 0.02 | 5.0 |
| Labetalol | 0.57 | 0.01 | 2.4 |
| Propranolol | 1.18 | 0.08 | 6.7 |

TABLE III
REPEATABILITY OF THE METHOD AT THE LEVEL OF
150 $\mu\text{g/ml}$ (TIMOLOL 300 $\mu\text{g/ml}$)

Details as in Table I.

| Compound | χ | S.D. | R.S.D. (%) |
|-------------|--------|------|------------|
| Acebutolol | 0.88 | 0.02 | 2.7 |
| Nadolol | 0.82 | 0.03 | 4.1 |
| Timolol | 0.31 | 0.01 | 2.7 |
| Atenolol | 0.60 | 0.02 | 3.2 |
| Metoprolol | 0.64 | 0.02 | 3.8 |
| Oxprenolol | 0.61 | 0.02 | 3.8 |
| Pindolol | 2.01 | 0.07 | 3.4 |
| Alprenolol | 0.86 | 0.03 | 3.8 |
| Labetalol | 1.26 | 0.04 | 3.3 |
| Propranolol | 3.67 | 0.11 | 2.9 |

tions varied from 2.0 to 7.0% ($n = 5$) at the 25 $\mu\text{g/ml}$ (timolol 50 $\mu\text{g/ml}$) level and from 2.7 to 4.1% ($n = 6$) at the 150 $\mu\text{g/ml}$ (timolol 300 $\mu\text{g/ml}$) level (Tables II and III). The repeatability can be considered to be satisfactory.

Linearity

The linearity range for the compounds in human urine was 25–150 $\mu\text{g/ml}$, except for timolol, for

TABLE IV
LINEARITY OF THE METHOD IN THE RANGE 25–150
 $\mu\text{g/ml}$ (TIMOLOL 50–300 $\mu\text{g/ml}$)

Analyses were performed using 150 $\mu\text{g/ml}$ of 2,6-dimethylphenol as the internal standard. The concentrations of β -blockers in the determination of the linear range were 25, 50, 75, 100 and 150 $\mu\text{g/ml}$ (for timolol 50, 100, 150, 200 and 300 $\mu\text{g/ml}$). r is the correlation coefficient. The equation for the straight line is $y = bx + a$, where a is the intercept on the y -axis and b is the slope. The β -blockers were eluted in the order listed.

| Compound | r | a | b |
|-------------|-------|------|------|
| Acebutolol | 0.998 | 2.00 | 0.01 |
| Nadolol | 0.994 | 0.14 | 0.01 |
| Timolol | 0.997 | 0.05 | 0.02 |
| Atenolol | 0.994 | 0.09 | 0.01 |
| Metoprolol | 0.992 | 0.06 | 0.01 |
| Oxprenolol | 0.996 | 0.05 | 0.01 |
| Pindolol | 0.999 | 0.07 | 0.02 |
| Alprenolol | 0.998 | 0.06 | 0.01 |
| Labetalol | 0.998 | 0.33 | 0.01 |
| Propranolol | 1.000 | 0.12 | 0.03 |

which it was 50–300 $\mu\text{g/ml}$. At concentrations higher than 150 $\mu\text{g/ml}$, (for timolol higher than 300 $\mu\text{g/ml}$) the calibration graphs were parabolic. The correlation coefficients of the straight lines ranged from 0.992 to 1.000 (Table IV).

Detection limits

The detection limits for the drugs were calculated from electropherograms obtained using human urine spiked with the ten β -blockers. The detection limits were 10 $\mu\text{g/ml}$ for all compounds except timolol, for which it was 20 $\mu\text{g/ml}$, with a signal-to-noise ratio of 3. This meant that, for detection at 214 nm, the concentration of the drugs in samples had to be at the $\mu\text{g/ml}$ level before injection.

CONCLUSIONS

The described MECC method was successful for the simultaneous determination of acebutolol, nadolol, timolol, atenolol, metoprolol, oxprenolol, pindolol, alprenolol, labetalol and propranolol added to human urine. Under the conditions applied, the ten β -blockers can be separated with high efficiency and resolution in less than 20 min. The repeatability is good when the sample contains an internal standard such as 2,6-dimethylphenol. Also, this MECC method is suitable for the determination of β -blockers in real urine samples. The sample preparation method for isolation of the drugs is extremely simple and, unlike normal clean-up methods such as liquid-liquid and solid-phase extraction, it is not time consuming. Complicated clean-up techniques limit the number of routine analyses that a laboratory can handle, and transfer of extracts, evaporation and other procedures are likely to result in sample losses through adsorption.

The MECC method is highly practical as the samples do not require more than a simple filtration before injection. The use of GC- and LC-electron-capture detection and GC-MS techniques requires derivatization of analytes, which makes screening very expensive. Chromatographic separation is nevertheless commonly used for pindolol, propranolol, alprenolol, oxprenolol, practolol and timolol [13]. In some of the methods another β -blocker is used as an internal standard on the basis that patients are unlikely to be using two of the drugs together. In published methods, only a few drugs are deter-

mined simultaneously [14], which makes those methods unsuitable for screening.

The detection limits achieved were 10 $\mu\text{g/ml}$ for all the β -blockers except timolol (20 $\mu\text{g/ml}$). In comparison, the detection limit for atenolol is as low as 2 ng/ml using HPLC with fluorescence detection [15]. However, the detection limits are at the $\mu\text{g/ml}$ level for atenolol, metoprolol and labetalol in HPLC analysis with UV detection. Injection volumes can be very low with MECC, which should make it possible to preconcentrate the sample without taking larger volumes of the sample to the clean-up stage.

The MECC method offers an alternative to current methods for the screening of β -adrenoceptor antagonists. The poor sensitivity, the main disadvantage of the method as it now exists, might be overcome by preconcentration of the drugs. The effect of preconcentration, and of other pretreatment methods such as hydrolysis, will be studied and developed further.

REFERENCES

- 1 P. Lillsunde and T. Korte, *J. Anal. Toxicol.*, 15 (1991) 71.
- 2 M. Ahnoff, M. Ervik, P.-O. Lagerström, B.-A. Persson and J. Vessman, *J. Chromatogr.*, 340 (1985) 73.
- 3 M. Laxer, A. C. Capomacchia and G. E. Hardee, *Talanta*, 28 (1981) 973.
- 4 J. W. Jorgenson and K. D. Lukacs, *Anal. Chem.*, 53 (1981) 1298.
- 5 J. W. Jorgenson and K. D. Lukacs, *J. Chromatogr.*, 218 (1981) 209.
- 6 S. Terabe, K. Otsuka, K. Ichiakva, A. Tsuchiya and T. Ando, *Anal. Chem.*, 56 (1984) 111.
- 7 A. S. Cohen, S. Terabe, J. A. Smith and B. L. Karger, *Anal. Chem.*, 59 (1987) 1021.
- 8 H. Nishi, N. Tsumagari, K. Kakimoto and S. Terabe, *J. Chromatogr.*, 465 (1989) 331.
- 9 W. Thormann, P. Meier, C. Marcolli and F. Binder, *J. Chromatogr.*, 545 (1991) 445.
- 10 W. Thormann, A. Minger, S. Molteni, J. Caslavská and P. Gebauer, *J. Chromatogr.*, 593 (1992) 275.
- 11 P. Wernly and W. Thormann, *Anal. Chem.*, 63 (1991) 2878.
- 12 P. Lukkari, J. Jumppanen, K. Jinno, H. Elo and M.-L. Riekkola, *J. Pharm. Biomed. Anal.*, 10 (1992) 561.
- 13 Y.-G. Yee, P. Rubin and T. F. Blaschke, *J. Chromatogr.*, 171 (1979) 357.
- 14 P. M. Harrison, A. M. Tonkin and A. J. McLean, *J. Chromatogr.*, 339 (1985) 429.
- 15 D.-S. Lho, J.-K. Hong, H.-K. Peak, J. A. Lee and J. Park, *J. Anal. Toxicol.*, 14 (1990) 429.

Voltage programming in capillary zone electrophoresis

Huan-Tsung Chang and Edward S. Yeung

Ames Laboratory—US Department of Energy and Department of Chemistry, Iowa State University, Ames, IA 50011 (USA)

ABSTRACT

Temperature is an important factor in capillary zone electrophoresis since it affects the viscosity and the pH of the buffer solution. In this study, a capillary tube with a large radius (130 μm I.D.) and filled with buffer at a high ionic strength is used to generate substantial joule heat within the capillary tube to force a significant increase in temperature, in turn to decrease the viscosity and to change the pH of the buffer solution. From a study of the degree of dissociation of analytes at different voltages, we show that voltage-induced pH change is significant in 0.1 *M* tris(hydroxyamino)methane (THAM) but not in 0.025 *M* hydrogencarbonate buffer system. A step change in voltage from 15 to 25 kV is implemented to generate a pH gradient in the THAM buffer solution. The results show that the method is useful for separating phenols which cannot be separated at a fixed voltage.

INTRODUCTION

Temperature [1,2] is an important parameter in capillary zone electrophoresis [CZE] since it affects not only the flow through convection, but also ionization of the analyte and the capillary surface, the viscosity and the pH of the buffer solution. The effects are smaller than 0.5% per degree for all these terms except for viscosity which has a 2% per degree change. In CZE, temperature control is often used to provide efficient heat removal [3,4]. Manipulation of chemical equilibria such as metal chelation and micelle partitioning [5,6] within the capillary tube through temperature control has also been proposed.

pH is also an important factor to determine selectivity in CZE since it will affect the dissociation of analytes and ionization of the capillary surface, which in turn changes the electrophoretic mobility of charged analyte and the electroosmotic flow coefficient [7,8]. pH gradients have been used to improve the separation process. Boček and co-workers [9,10] used a two-buffer system to force the mi-

gration of varying ratios of two ions into the capillary during separation. Although pH change as a function of temperature is insignificant for most buffers, it is possible to generate a substantial pH change if a buffer system with a large temperature (*T*) coefficient (dpH/dT) is used. Whang and Yeung [11] demonstrated the effect of temperature-induced pH change on the separation of dyes. In their study, tris (hydroxyamino)methane (THAM) buffer which has a large temperature coefficient is used to generate a pH gradient via controlling the temperature of the column.

Joule heat is evolved when electrical current passes through the capillary tube. This is usually not desirable because it will distort the zone distribution. However, it is possible to increase the temperature significantly by using a high concentration of buffer, running at a high voltage and using a capillary tube with a large radius [12]. One can then dramatically decrease the viscosity and change the pH of the buffer. As viscosity decreases, the electrophoretic mobility and electroosmotic flow coefficient will increase. Thus, shorter separation time and better resolution may be achieved. Altering the pH further modifies the selectivity for components such as weak acids and bases.

In this paper, the effect of Joule heat on CZE is

Correspondence to: Dr. E. S. Yeung, Ames Laboratory—US Department of Energy and Department of Chemistry, Iowa State University, Ames, IA 50011, USA.

examined. THAM (with large dpH/dT) and hydrogencarbonate (with small dpH/dT) are used to study the effect of voltage-induced pH change on the separation of phenols. We also show the implementation of a step change in voltage from 15 to 25 kV to generate a pH gradient for separating phenols in 0.1 M THAM buffer system.

THEORY

Separation in CZE is dependent on the electroosmotic flow coefficient and the electrophoretic mobility. Careful consideration of the factors that affect these parameters is important to obtaining good separations. Eqn. 1 [13] can be used to relate the decrease in electroosmotic flow coefficient, m_{eo} , to the increase in viscosity

$$m_{\text{eo}} = \varepsilon \zeta_c / 4\pi\eta \quad (1)$$

where ε is the dielectric constant, ζ_c is the ζ potential at the slipping plane and η is the bulk viscosity. Electrophoretic mobility, m_{ep} , can be given by [14]

$$m_{\text{ep}} = \varepsilon \zeta_a / 6\pi\eta \quad (2)$$

where ζ_a is the ζ potential of the analyte. Eqns. 1 and 2 show that both the electroosmotic flow coefficient and the electrophoretic mobility increase when the viscosity of the buffer decreases. In order to force fast flow, low viscosity of the buffer is needed. Temperature is an important factor in determining the viscosity of the buffer solution. They are related by

$$1/\eta = A e^{-B/T} \quad (3)$$

where A and B are constants related to the medium. From eqn. 3, fast flow will be achieved at high temperatures.

Since the effective electrophoretic mobility, m_{eff} , is proportional to the fraction of free ion of the analyte, Tiselius (see ref. 15) derived the equation

$$m_{\text{eff}} = \sum \alpha_i m_{\text{ep}} \quad (4)$$

where α_i is the degree of dissociation and m_{ep} is the absolute mobility of the i th ionic form of a molecule. To relate the effective electrophoretic mobility, degree of dissociation for a monovalent ion and viscosity of the bulk solution, eqn. 4 can be combined with eqn. 2 to give

$$m_{\text{eff}} = \alpha_i \varepsilon \zeta_a / 4\pi\eta \quad (5)$$

In order to simplify the problem for estimating the changing mobilities of an analyte ζ_a is assumed to be constant at different voltages. The ratio of mobilities at different conditions i and j is then

$$(m_{\text{eff}i}/m_{\text{eff}j}) = (\alpha_i/\alpha_j)(\eta_j/\eta_i) \quad (6)$$

In this study, η_i/η_j can be calculated from the m_{ep} of benzoic acid at different voltages since it is completely dissociated over the range of pH used.

Since the temperature of the capillary tube is an important factor in establishing the viscosity, pH of the buffer, and the degree of dissociation of the analyte, it is important to know the temperature of capillary tube. It can be estimated by eqn. 7 [16]

$$T = 1820/[\ln(m_{\text{eo}1}) - \ln(m_{\text{eo}2}) + 6.11] \quad (7)$$

where $m_{\text{eo}1}$ and $m_{\text{eo}2}$ are the electroosmotic flow coefficient at 298 K and T K. Therefore, T can be determined by measuring $m_{\text{eo}1}$ at a low voltage where we assume little heat is generated, and then measuring $m_{\text{eo}2}$ at a high voltage. As soon as the temperature of capillary tube is determined, the pH of the buffer can be calculated from the temperature coefficient of the buffer. Then, α can be estimated from eqn. 8

$$\alpha = K_a/(K_a + [\text{H}^+]) \quad (8)$$

where K_a is the dissociation constant of the analyte.

EXPERIMENTAL

A commercial electrophoresis instrument (Isco Model 3850, Lincoln, NE, USA) was used for all electrophoretic experiments. The fused-silica capillary (Polymicro Technologies, Phoenix, AZ, USA) was 55 cm \times 130 μm I.D. At 35 cm from the injection end, the polyimide coating was burned off to form the detection window. A digitizer (Data Translation Model DT 2802, Palo Alto, CA, USA) and a computer (PC/AT, IBM, Boca Raton, FL, USA) were used to collect and store all of the data.

All chemicals were of reagent grade and were obtained from Aldrich (Milwaukee, WI, USA), except that THAM and sodium hydrogencarbonate were from Fisher (Fair Lawn, NJ, USA). Buffer solutions were adjusted by HCl and NaOH to pH 8.5. The injected concentration of each analyte is $2 \cdot 10^{-4}$ M, except that mesityl oxide is present at $2 \cdot 10^{-3}$ M. Mesityl oxide was used to measure the electroosmotic flow coefficient. Benzoic acid was

TABLE I
THE EFFECT OF TEMPERATURE ON pH OF 0.1 M THAM AND 0.025 M HYDROGENCARBONATE BUFFER SOLUTIONS

| Temperature (°C) | pH | |
|------------------|------|-------------------------------|
| | THAM | HCO ₃ ⁻ |
| 30 | 8.44 | 8.56 |
| 40 | 8.29 | 8.60 |
| 50 | 8.06 | 8.64 |
| 60 | 7.92 | 8.73 |
| 70 | 7.77 | 8.79 |
| 80 | 7.70 | 8.87 |

used as the other marker to estimate the change of electrophoretic mobility as a function of the change in viscosity. The sample solution was raised to 10 cm high for hydrodynamic injection from the anodic end of the capillary for 8 s.

RESULTS AND DISCUSSION

In order to demonstrate the effect of voltage-induced pH change within the capillary tube on the electrophoretic mobilities of analytes, two electrophoresis buffers which have different temperature coefficients are chosen. THAM with a large temperature coefficient and hydrogencarbonate with a small temperature coefficient are suitable buffers in our study. From Table I, which lists actual experi-

mental measurements in our laboratory, the pH of THAM buffer at different temperatures can be estimated from the following equations

$$\text{pH}_2 = \text{pH}_1 - 0.023 (T_2 - T_1) \quad 40\text{--}50^\circ\text{C} \quad (9)$$

$$\text{pH}_2 = \text{pH}_1 - 0.007 (T_2 - T_1) \quad 70\text{--}80^\circ\text{C} \quad (10)$$

$$\text{pH}_2 = \text{pH}_1 - 0.015 (T_2 - T_1) \quad 30\text{--}40 \text{ and } 50\text{--}70^\circ\text{C} \quad (11)$$

On the other hand, pH of the hydrogencarbonate buffer increases as temperature increases. The pH of bicarbonate buffer at different temperatures can be calculated from eqns. 12 and 13

$$\text{pH}_2 = \text{pH}_1 + 0.004 (T_2 - T_1) \quad 30\text{--}50^\circ\text{C} \quad (12)$$

$$\text{pH}_2 = \text{pH}_1 + 0.007 (T_2 - T_1) \quad 50\text{--}80^\circ\text{C} \quad (13)$$

The decrease in the viscosity of the buffer is significant as can be seen from the dramatic change in electroosmotic flow coefficient in both systems as the voltage changes from 10 to 25 kV. From Tables II and III, the fractional changes in electroosmotic flow coefficient and the electrophoretic mobility between 10 and 25 kV based on the two markers, mesityl oxide (neutral) and benzoic acid (completely dissociated), are 2.1 and 2.2 for THAM and 2.0 and 2.0 for hydrogencarbonate buffers, respectively. The results show that our markers are well suited for predicting the change of m_{eo} and m_{ep} due to the change in viscosity of the buffer solution. Also this shows that the dissociation effect of these two markers can be neglected in the range of voltage-induced pH change in this work. Based on the m_{eo}

TABLE II
ELECTROOSMOTIC FLOW COEFFICIENT (m_{eo}) AND ELECTROPHORETIC MOBILITIES (m_{ep}) OF ANALYTES IN 0.1 M THAM BUFFER SOLUTION AT DIFFERENT VOLTAGES

Units are in $10^{-4} \text{ cm V}^{-1} \text{ s}^{-1}$. 1 = Mesityl oxide; 2 = 4-chlorophenol; 3 = 3-chlorophenol; 4 = 2-chlorophenol; 5 = 3-nitrophenol; 6 = 2,4-dichlorophenol; 7 = 3-methyl-4-nitrophenol; 8 = 4-nitrophenol; 9 = 2-nitrophenol; 10 = benzoic acid.

| Voltage (kV) | m_{eo} | | m_{ep} | | | | | | | |
|--------------|----------|-----|----------|-----|-----|-----|-----|-----|-----|-----|
| | 1 | 2 | 3 | 4 | 5 | 6 | 7 | 8 | 9 | 10 |
| 10 | -4.5 | 0.4 | 0.8 | 1.7 | 1.8 | 2.2 | 2.5 | 2.8 | 2.8 | 2.9 |
| 15 | -5.2 | 0.3 | 0.7 | 1.7 | 1.8 | 2.4 | 2.9 | 3.3 | 3.3 | 3.4 |
| 20 | -6.7 | 0.3 | 0.7 | 1.7 | 2.0 | 2.8 | 3.6 | 4.1 | 4.1 | 4.4 |
| 25 | -9.5 | 0.2 | 0.7 | 1.3 | 1.8 | 2.7 | 4.4 | 5.1 | 5.3 | 6.3 |

TABLE III

ELECTROSMOTIC FLOW COEFFICIENT (m_{eo}) AND ELECTROPHORETIC MOBILITIES (m_{ep}) OF ANALYTES IN 0.025 M HYDROGENCARBONATE BUFFER SOLUTION AT DIFFERENT VOLTAGESUnits are in 10^{-4} cm V^{-1} s $^{-1}$. 1–10 represent the same analytes as those in Table II.

| Voltage (kV) | m_{eo} | | m_{ep} | | | | | | | |
|--------------|----------|-----|----------|-----|-----|-----|-----|-----|-----|-----|
| | 1 | 2 | 3 | 4 | 5 | 6 | 7 | 8 | 9 | 10 |
| 10 | -5.0 | 0.8 | 1.3 | 2.2 | 2.3 | 2.5 | 2.7 | 3.0 | 3.0 | 3.0 |
| 15 | -6.0 | 1.0 | 1.6 | 2.6 | 2.7 | 2.9 | 3.2 | 3.5 | 3.5 | 3.5 |
| 20 | -7.7 | 1.3 | 1.6 | 2.6 | 2.7 | 2.9 | 3.2 | 3.5 | 3.5 | 3.5 |
| 25 | -9.9 | 1.8 | 3.1 | 4.5 | 4.8 | 5.0 | 5.5 | 6.0 | 6.0 | 6.0 |

values obtained (mesityl oxide), one can calculate the temperature of the liquid at the various operating voltages by using eqn. 7. This is shown in Table IV.

TABLE IV

THE CALCULATED TEMPERATURE AND pH OF 0.1 M THAM AND 0.025 M HYDROGENCARBONATE BUFFER SOLUTIONS AT DIFFERENT VOLTAGES

| Voltage | THAM | | HCO_3^- | |
|---------|------------------|------|------------------|------|
| | Temperature (°C) | pH | Temperature (°C) | pH |
| 10 | 32 | 8.41 | 28 | 8.54 |
| 15 | 40 | 8.29 | 37 | 8.59 |
| 20 | 54 | 8.00 | 51 | 8.65 |
| 25 | 76 | 7.73 | 66 | 8.77 |

Since the electrophoretic mobility of an analyte depends on the fraction of its free ion, the degree of dissociation should be determined. It is a function of pH as expressed in eqn. 8. Hence, in order to illustrate the effect of voltage-induced pH change, it is important to know the degree of dissociation of the analytes at different voltages. Based on the results shown in Tables II and III, the ratio of the degree of dissociation of analytes at different voltages can be calculated from eqn. 6. The results are shown in Tables V and VI. From Table V, it is obvious that the pH of THAM buffer decreases when the voltage increases since the ratio decreases. The results of observed and calculated values agree each other, which means that the trend of pH change we estimated is correct. The ratios decrease in the THAM system while they increase a little in the hy-

TABLE V

COMPARISON OF THE OBSERVED AND CALCULATED RATIOS OF THE FRACTIONAL DISSOCIATION (α) OF ANALYTES IN 0.1 M THAM BUFFER SOLUTION AT DIFFERENT VOLTAGES1 = α_{15}/α_{10} ; 2 = α_{20}/α_{10} ; 3 = α_{25}/α_{10} ; the subscript refers to kV operating voltage.

| Analytes | Observed | | | Calculated | | |
|------------------------|----------|------|------|------------|------|------|
| | 1 | 2 | 3 | 1 | 2 | 3 |
| 2-Nitrophenol | 1.01 | 0.97 | 0.87 | 1.01 | 0.95 | 0.86 |
| 4-Nitrophenol | 1.01 | 0.97 | 0.84 | 1.01 | 0.95 | 0.85 |
| 3-Methyl-4-nitrophenol | 0.99 | 0.95 | 0.81 | 1.01 | 0.95 | 0.85 |
| 2,4-Dichlorophenol | 0.93 | 0.84 | 0.56 | 1.03 | 0.81 | 0.59 |
| 3-Nitrophenol | 0.85 | 0.73 | 0.46 | 1.06 | 0.72 | 0.46 |
| 2-Chlorophenol | 1.12 | 0.86 | 0.46 | 1.07 | 0.68 | 0.41 |
| 3-Chlorophenol | 1.19 | 0.92 | 0.46 | 1.10 | 0.61 | 0.34 |
| 4-Chlorophenol | 0.64 | 0.49 | 0.23 | 1.11 | 0.59 | 0.32 |

TABLE VI

COMPARISON OF THE OBSERVED AND CALCULATED RATIOS OF THE FRACTIONAL DISSOCIATION (α) OF ANALYTES IN 0.025 M HYDROGENCARBONATE BUFFER SOLUTION AT DIFFERENT VOLTAGES1 = $\alpha_{1.5}/\alpha_{1.0}$; 2 = $\alpha_{2.0}/\alpha_{1.0}$; 3 = $\alpha_{2.5}/\alpha_{1.0}$; the subscript refers to kV operating voltage.

| Analytes | Observed | | | Calculated | | |
|------------------------|----------|------|------|------------|------|------|
| | 1 | 2 | 3 | 1 | 2 | 3 |
| 2-Nitrophenol | 1.00 | 0.96 | 1.00 | 1.00 | 1.01 | 1.02 |
| 4-Nitrophenol | 1.00 | 0.96 | 1.00 | 1.00 | 1.01 | 1.02 |
| 3-Methyl-4-nitrophenol | 1.02 | 0.97 | 1.02 | 1.00 | 1.01 | 1.02 |
| 2,4-Dichlorophenol | 0.99 | 0.94 | 1.00 | 1.02 | 1.04 | 1.08 |
| 3-Nitrophenol | 1.01 | 0.97 | 1.02 | 1.04 | 1.09 | 1.17 |
| 2-Chlorophenol | 1.01 | 0.96 | 1.02 | 1.05 | 1.12 | 1.24 |
| 3-Chlorophenol | 1.05 | 1.03 | 1.19 | 1.09 | 1.20 | 1.45 |
| 4-Chlorophenol | 1.07 | 1.04 | 1.13 | 1.11 | 1.24 | 1.56 |

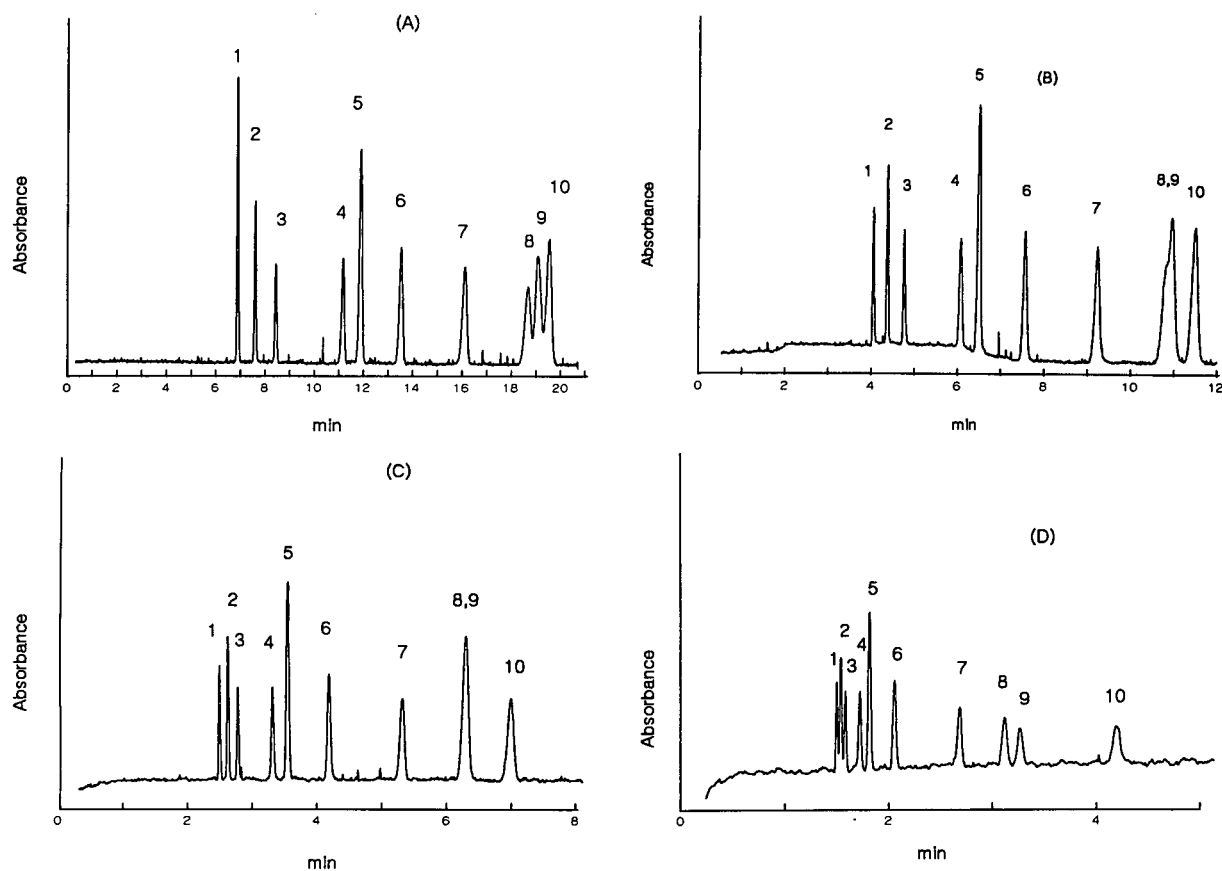


Fig. 1. Separation of analytes in pH 8.5, 0.1 M THAM buffer solution at different voltages. Column: 130 μm I.D. \times 360 μm O.D. \times 55 cm total length (35 cm effective length). Detection wavelength = 218 nm. (A) 10 kV, (B) 15 kV, (C) 20 kV, (D) 25 kV. Peaks: 1 = mesityl oxide; 2 = 4-chlorophenol; 3 = 3-chlorophenol; 4 = 2-chlorophenol; 5 = 3-nitrophenol; 6 = 2,4-dichlorophenol; 7 = 3-methyl-4-nitrophenol; 8 = 4-nitrophenol; 9 = 2-nitrophenol; 10 = benzoic acid.

drogencarbonate system as the voltage increases. It is worth noting that the ratio changes significantly in the THAM buffer, implying that large voltage-induced pH changes can be obtained in the THAM buffer.

A group of phenolic compounds which have pK_a ranging from 7 to 9.5 are selected to demonstrate the separation improvement due to voltage-induced pH change. The effect of voltage-induced pH change on the separation of phenols can be shown in Figs. 1 and 2 for constant voltage operation. In the THAM system, 2-nitrophenol ($pK_a = 7.15$) and 4-nitrophenol ($pK_a = 7.17$) cannot be separated at the lower voltages while they can be separated at 25 kV. The result also agrees with our estimation of the pH of the buffer system in Table IV because the change in the degree of dissociation of an analyte is

more significant when the pH is near its pK_a . The other advantage is that electroosmotic flow increases as viscosity decreases, speeding up the separation. However, resolution among the first three analytes became worse at the high voltage.

In the hydrogencarbonate system, benzoic acid, 2-nitrophenol and 4-nitrophenol, which all have low pK_a values, cannot be completely separated. This is due to the insignificant increase in pH in the hydrogencarbonate buffer as voltage increases. Comparison of the result of separation ability in these two buffer systems again supports our conclusion that there is a higher voltage-induced pH change in the THAM buffer than in the bicarbonate buffer.

As discussed in the introduction, pH gradient is a well known method to improve the separation abil-

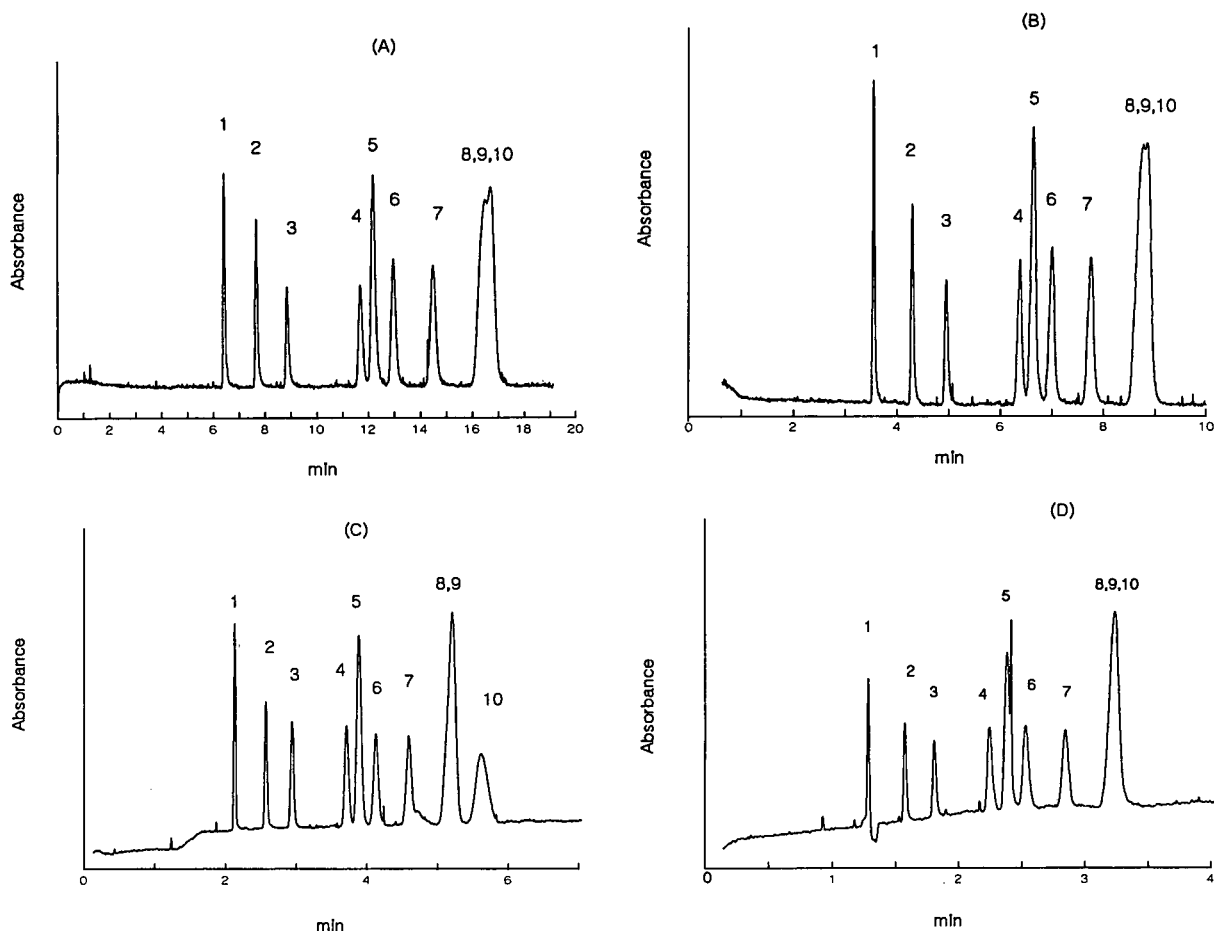


Fig. 2. Separation of analytes in pH 8.5, 0.025 M hydrogencarbonate buffer solution at different voltages. Other conditions as in Fig. 1.

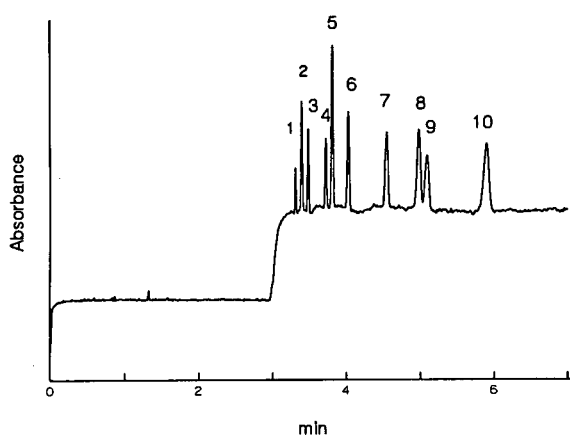


Fig. 3. The effect of voltage-induced pH program on the separation of phenols in pH 8.5, 0.1 M THAM buffer solution.

ity in CZE. To demonstrate the possibility of pH gradient generated via a step change in voltage, we use Fig. 3 as an example. Voltage programming starts from 15 kV for 3 min, then jumps to 25 kV for the remainder of the run. All analytes can be separated in 6 min with little overlap. There is a baseline shift due to the temperature change, as has been reported earlier [11]. From this result, we can conclude that voltage programming is advantageous for certain CE separations. As in the case of pH programming [9–11], groups of analytes that cannot be separated at any single pH can thus be resolved.

In summary, we have demonstrated the use of Joule heat to increase the temperature of the buffer during CZE separation. The resulting increase in temperature is able to generate a noticeable voltage-induced pH change and a change of the viscosity of 0.1 M THAM buffer to alter selectivity. Implementation is best in large-diameter capillaries, with high operating voltage, and at high buffer concentrations. In fact, efficient cooling of the capillary, *e.g.* in certain commercial CE instruments, is counterproductive in this mode of operation. There is the possibility that high Joule heating can reduce the

efficiency of the separation. However, for the systems studied here, degradation in efficiency was not observed. The use of voltage programming is in general simpler than the use of temperature programming [11]. The recycle time is also shorter since only the capillary and not the coolant needs to be returned to the initial temperature before the start of the next run.

ACKNOWLEDGEMENTS

Ames Laboratory is operated for the US Department of Energy by Iowa State University under contract No. W-7405-Eng-82. This work was supported by the Director of Energy Research, Office of Basic Energy Sciences and Office of Health and Environmental Research.

REFERENCES

- 1 S. Hjertén, *Electrophoresis*, 11 (1990) 665.
- 2 G. O. Roberts, P. H. Rhodes and R. S. Snyder, *J. Chromatogr.*, 480 (1989) 35.
- 3 E. Grushka, R. M. McCormick and J. J. Kirkland, *Anal. Chem.*, 61 (1989) 241.
- 4 Y. Kurosu, K. Hibi, T. Sasaki and M. Saito, *J. High Resolut. Chromatogr.*, 14 (1991) 200.
- 5 S. Terabe, K. Otsuka and T. Ando, *Anal. Chem.*, 61 (1989) 251.
- 6 A. S. Cohen, S. Terabe, J. A. Smith and B. L. Karger, *Anal. Chem.*, 59 (1987) 1021.
- 7 D. L. Middleton and W. J. Lambert, *Anal. Chem.*, 62 (1990) 1585.
- 8 S. Wren, *J. Microcol. Sep.*, 3 (1991) 147.
- 9 P. Gebaur, M. Deml, J. Pospichal and P. Boček, *Electrophoresis*, 11 (1990) 724.
- 10 M. Deml, J. Pospichal, J. Sudor and P. Boček, *J. Chromatogr.*, 470 (1989) 43.
- 11 C. W. Whang and E. S. Yeung, *Anal. Chem.*, 64 (1992) 502.
- 12 S. Hjertén, *Chromatogr. Rev.*, 9 (1967) 122.
- 13 C. L. Rice and R. Whitehead, *J. Phys. Chem.*, 69 (1965) 4017.
- 14 J. Th. G. Overbeek and P. H. Wiersema, in M. Bier (Editor), *Electrophoresis—Theory, Methods and Application*, Vol. 2, Academic Press, New York, 1967, p. 9.
- 15 F. M. Everaerts, J. L. Beckers and Th. P. E. M. Verheggen, *Isotachopheresis—Theory, Instrumentation and Applications*, Elsevier, Amsterdam, New York, 1976, pp. 27–40.
- 16 K. Salmon, R. L. Chien and D. Burgi, *J. Liq. Chromatogr.*, 14 (1991) 847.

Fundamental and practical aspects of coupled capillaries for the control of electroosmotic flow in capillary zone electrophoresis of proteins

Wassim Nashabeh and Ziad El Rassi

Department of Chemistry, Oklahoma State University, Stillwater, OK 74078-0447 (USA)

ABSTRACT

This article represents an extension to a new approach, which was introduced very recently by our laboratory, for the control of the magnitude of electroosmotic flow in capillary zone electrophoresis. In this new approach, short fused-silica capillaries having different ζ potentials were coupled in series, and the amount of the electroosmotic flow was conveniently varied by changing the lengths of the individual capillary segments. The different coupled capillary systems evaluated in this study comprised various combinations of untreated fused-silica capillaries and polyether-coated capillaries having various electroosmotic flow characteristics. A general equation relating the average electroosmotic flow velocity in the coupled capillaries to the intrinsic electroosmotic velocity of the connected segments and their corresponding lengths has been derived and verified experimentally. The rate of the electroosmotic flow in a given system of coupled capillaries could be tuned over a range bordered by the lowest and highest intrinsic flow-rates of the connected capillary segments. In addition, a system of coupled capillaries that permitted a stepwise change in the rate of the electroosmotic flow during analysis was introduced and evaluated. These elution schemes were useful in the rapid separation of oppositely charged proteins in a single electrophoretic run and in the rapid analytical determination of the various components of heterogeneous proteins.

INTRODUCTION

In capillary zone electrophoresis (CZE), the observed migration behavior of charged species is determined by the electroosmotic flow (EOF) of the bulk solution inside the capillary and the electrophoretic mobilities of the analytes. While separation in CZE is based on differences in the electrophoretic mobilities of the analytes, the amount of time the solutes spend in the capillary is affected by the direction and magnitude of the EOF, which contribute to the migration of all analytes to the same extent regardless of their charges. While a relatively low level of electroosmotic flow is advantageous for the separation of closely related positively or negatively charged species, the analysis of basic, neutral and acidic solutes in a single electrophoretic run

would require a relatively strong electroosmotic flow velocity.

Recently, Lee and co-workers [1,2] demonstrated that the direction and velocity of the EOF can be changed by the application of an external electric potential across a buffer-filled sheath capillary surrounding the separation capillary. More recently, Hayes and Ewing [3] proposed the use of a radial voltage with capillaries having an external film of conductive polymer for the control of EOF in CZE. However, the control of the electroosmotic flow by virtue of electronic means, *i.e.*, application of an external electric field, is only effective at low pH or with the use of surface modified capillaries whereby the concentration of the ionized surface groups are quite low and thus can be overcome by the electrostatic charges induced by the external potential.

Very recently, we have introduced a new electrophoretic system for the control of EOF in CZE. In this system, two capillaries having different wall ζ

Correspondence to: Dr. Z. El Rassi, Department of Chemistry, Oklahoma State University, Stillwater, OK 74078-0447 USA.

potential were coupled in series beyond the detection point [4]. When fused-silica capillaries with polyether coatings were connected to untreated fused-silica capillary tubes, the average electroosmotic flow velocity throughout the tandem capillary system was found to be a linear function of the fractional length of the individual connected capillary segments. This enabled the tuning of the rate of EOF independently of the applied voltage within the upper and lower limits of the intrinsic electroosmotic mobilities in the individual connected capillaries. The tandem operation allowed the rapid analysis of acidic proteins that would repulse electrostatically from the negatively charged fused-silica surface.

The aim of the present article is to investigate the potentials of other coupled capillary systems in the control of EOF and to extend the utility of the new approach to the rapid analysis of oppositely charged proteins in a single electrophoretic run with minimum solute-wall interaction. This was accomplished by connecting in series fused-silica capillaries of different intrinsic electroosmotic flow characteristics whose inner surfaces were either naked or modified with polyether chains of various length. Such coupling has reduced the analysis time of model proteins by a factor of 2 on the average. In addition, a configuration of coupled capillaries which allowed a stepwise increase in the electroosmotic flow during analysis was introduced. This elution scheme permitted a 3-fold decrease in the analysis time of model proteins without sacrificing the high separation efficiencies that can be achieved with surface-modified capillaries.

EXPERIMENTAL

Apparatus

The instrument for capillary electrophoresis used in this study was assembled in-house from commercially available components, and resembled that reported earlier [4,5]. It comprised two high-voltage power supplies of positive and negative polarity Models MJ30P400 and MJ30N400, respectively, from Glassman High Voltage (Whitehouse Station, NJ, USA) and a Linear (Reno, NV, USA) Model 200 UV-VIS variable wavelength detector equipped with a cell for on-column capillary detection. The electropherograms were recorded with a Shimadzu

TABLE I
PROTEINS USED IN THIS STUDY

| Proteins | M_r | pI |
|--------------------------|--------|------|
| Lysozyme | 14 100 | 11.0 |
| Ribonuclease A | 13 700 | 9.40 |
| Carbonic anhydrase | 31 000 | 6.20 |
| α -Lactalbumin | 14 200 | 4.80 |
| β -Lactoglobulin A | 35 000 | 5.23 |
| Albumin, egg | 45 000 | 4.63 |

computing integrator Model C-R6A (Columbia, MD, USA) equipped with a floppy disk drive and a cathode-ray tube (CRT) monitor.

Reagents and materials

Lysozyme from chicken egg white, ribonuclease A from bovine pancreas, carbonic anhydrase from bovine erythrocytes, α -lactalbumin and β -lactoglobulin A from bovine milk and albumin from chicken egg were purchased from Sigma (St. Louis, MO, USA). Table I compiles the molecular weights (M_r) and isoelectric points (pI) of these proteins. Reagent grade sodium phosphate monobasic, hydrochloric acid, sodium hydroxide and HPLC grade methanol were obtained from Fisher Scientific (Pittsburgh, PA, USA). Phenol which was used as an inert tracer for measuring the electroosmotic flow (EOF) was obtained from J. T. Baker (Phillipsburg NJ, USA).

Capillary columns

Polyimide-coated fused-silica capillary columns of 50 μm I.D. and 365 μm O.D. were obtained from Polymicro Technology (Phoenix, AZ, USA). Both untreated and coated capillaries were used in this study. The coated capillaries were modified in-house with surface-bound hydroxylated polyether chains of various length according to previously described procedures [6]. The capillary coding I-200 and F-2000 is used to denote capillaries with interlocked coatings having polyethylene glycol 200 chains and capillaries having fuzzy coatings with polyethylene glycol 2000 moieties, respectively.

Other procedures

The capillary segments of the tandem capillary systems were connected butt-to-butt using PTFE tubes the inner diameter of which matched the outer

diameter of the connected capillary columns. In all cases the connection was made beyond the detection point. While the length of the individual capillaries having different surface characteristics was varied to span a wide range of fractional length, the total length of the coupled capillaries was kept constant at 80 cm with a detection window at 30 cm from the inlet reservoir. It has to be noted that in all experiments, the background electrolyte was 0.1 M sodium phosphate, pH 6.50. Solute introduction was by hydrodynamic flow (*i.e.*, by gravity flow) at a differential height of 5 cm between the electrolyte reservoirs for 10 s. The detection wavelength was set at 210 nm for sensing the various proteins as well as the inert tracer.

To ensure reproducible separations the capillary column was flushed successively with fresh buffer, water, methanol, water, and again running buffer. In addition, the running electrolyte was renewed after each run and the capillary was allowed to equilibrate with the new buffer for 10 min before each injection.

RESULTS AND DISCUSSION

Control of electroosmotic flow by coupled capillaries

We have previously shown [4] that for a system of n coupled capillaries having the same inner diameter but differing in their ζ potentials, the average electroosmotic mobility, μ_{eo} , across the tandem system is a weighted average of the intrinsic or local electroosmotic mobilities in the individual connected segments as follows [4]:

$$\mu_{eo} = \frac{\sum_{i=1}^n \mu_{eo,i} l_i}{l_t} \quad (1)$$

where l_i is the length of the individual capillary segment, i , l_t is the total length of the connected capillaries and $\mu_{eo,i}$ is the intrinsic electroosmotic mobility in each capillary segment, i , measured on a separate length l_i . Eqn. 1 can be rearranged as a linear function of the fractional length of a given capillary segment, i , in the tandem capillaries as in eqn. 2.

where j and k are random variables. It follows then that the average electroosmotic flow or bulk flow across the tandem capillary system can be in principle controlled to any desired value bordered by the lowest and highest intrinsic electroosmotic mobilities in the individual capillaries.

Due to the differences between the intrinsic electroosmotic flows in the connected segments and the uniform bulk flow across the tandem capillary system, a compensating hydrostatic pressure would develop. Consequently, a change from a plug flow profile to a laminar or poiseuille profile would result. As the difference between the intrinsic electroosmotic flow and the bulk flow increases, the laminar flow profile would become more pronounced. Although a purely pressure driven laminar flow is known to introduce band broadening, it has been shown recently that the superposition of poiseuille flow on an electroosmotic flow may not necessarily deteriorate the separation efficiencies [7]. In addition, under conditions whereby the pressure driven flow opposes the bulk flow, the electrokinetic dispersion coefficient may be even reduced [7]. A detailed treatment concerning the effects of superposed laminar and electroosmotic flow profiles on electrokinetic dispersion in CZE can be found in ref. 7.

Eqn. 2 was verified experimentally by measuring the EOF in 3 different tandem capillary systems, *i.e.*, F-2000 \rightarrow I-200, F-2000 \rightarrow untreated and I-200 \rightarrow untreated, using phenol as the inert tracer. The results are shown in Fig. 1 by plots of the electroosmotic mobility *versus* the fractional length of the capillary segment having the highest intrinsic EOF. This will be the untreated capillary segment in the F-2000 \rightarrow untreated and I-200 \rightarrow untreated tandem capillaries, and I-200 capillary in the F-2000 \rightarrow I-200 coupled capillaries (see legend of Fig. 1 for details). As expected, the EOF changed linearly with the fractional length of the coupled capillaries and fitted quite well to eqn. 2 with correlation coefficients of 0.997 on average. The data points in Fig. 1 show clearly that the EOF can be changed in a predictable manner by varying the length of the connected capillary segment(s). The slope of these curves,

$$\mu_{eo} = \left(\mu_{eo,i} - \sum_{j=1; j \neq i}^n \mu_{eo,j} \right) \frac{l_i}{l_t} + \sum_{j=1; j \neq i}^n \mu_{eo,j} \left[1 - \frac{\sum_{k=1; k \neq i, j}^n l_k}{l_t} \right] \quad (2)$$

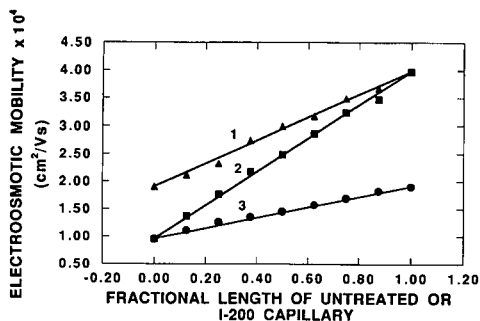


Fig. 1. Plots of the electroosmotic mobility *versus* the fractional length of the untreated capillary segment in (1) and (2) or *versus* the fractional length of the I-200 capillary segment in (3). (1) I-200 → untreated; (2) F-2000 → untreated; (3) F-2000 → I-200 tandem capillaries, 30 cm (to the detection point), 80 cm (total length) \times 50 μ m I.D.; running voltage, 20 kV; background electrolyte, 0.1 M sodium phosphate solution, pH 6.50. Inert tracer, phenol.

$\mu_{eo,i} - \sum_{j=1; j \neq i}^n \mu_{eo,j}$, is indicative of the range over

which the EOF can be varied. The greater the slope, the wider is the range of variation. For instance, and at the voltage of the experiments of Fig. 1, the F-2000 → untreated coupled capillaries with the highest slope allowed the tuning of the EOF to any value between 28 and 115 nl/min, while with the F-2000 → I-200 tandem capillary system the change in the EOF was limited to the interval 28 to 58 nl/min.

Evaluation of the F-2000 → I-200 coupled capillaries with proteins

An important feature of coupled capillaries is their ability to adjust the analysis time to suit a particular separation problem. To realize this attractive advantage, the tandem system should meet three major criteria: (i) solute–wall interactions must be absent, (ii) the coupled capillaries should not introduce band broadening and (iii) the connected capillary segments should allow the tuning of the EOF over a wide range to accommodate the electrophoresis of a broad range of analytes.

Although, our initial studies with the I-200 → untreated capillaries showed promise in the rapid and efficient analysis of acidic proteins [4], this system was not suitable for the simultaneous separation of both acidic and basic proteins. In fact, as the basic

proteins entered the untreated segment of the I-200 → untreated tandem system, the EOF started to decrease during the electrophoretic run due to solute adsorption on the inner surface of the capillary, and concomitant decrease in the magnitude of the negative ζ potential of the capillary wall. This phenomenon drastically delayed and in some instances inhibited the elution of the later eluting acidic proteins.

A better approach that would enable the analysis of oppositely charged species in the absence of solute–wall interactions is the use of the F-2000 → I-200 coupled capillaries. The polyether chains of these coated capillaries have been shown effective in minimizing solute–wall interaction [6]. Furthermore, due to the difference in the length and the way in which the polyether chains are attached to the capillary inner surface, the F-2000 and I-200 capillaries possess different levels of electroosmotic flow [6]. Therefore, their coupling would allow the tuning of the EOF so that oppositely charged solutes could be analyzed in a single electrophoretic run with high separation efficiencies.

The feasibility of the F-2000 → I-200 tandem capillaries in the rapid analysis of biopolymers was demonstrated by using a mixture of 5 model proteins the pI values of which ranged from 4.8 to 11.0 (see Table I). Fig. 2a depicts a typical electropherogram of this protein mixture performed on an F-2000 capillary at an applied voltage of 20 kV using 0.1 M sodium phosphate solution, pH 6.50, as the running electrolyte. Due to the low electroosmotic flow obtained with the F-2000 capillary (*ca.* 28 nl/min), carbonic anhydrase was eluted after *ca.* 65 min while the elution of α -lactalbumin would require 235 min as calculated from the EOF and the electrophoretic mobility of this solute. On the other hand, β -lactoglobulin A, having an electrophoretic mobility greater in magnitude and opposite in direction to the electroosmotic flow, would leave the F-2000 capillary and enter the inlet buffer reservoir after introducing the sample by gravity-driven flow. Although high separation efficiencies could be achieved, the F-2000 capillary can be only used for the analysis of basic and moderately acidic solutes. Fig. 2b and c illustrates the electropherograms of the same protein mixture performed on the F-2000 → I-200 coupled capillaries with 0.25 and 0.5 fractional length of the I-200 capillary segment, respectively, under other-

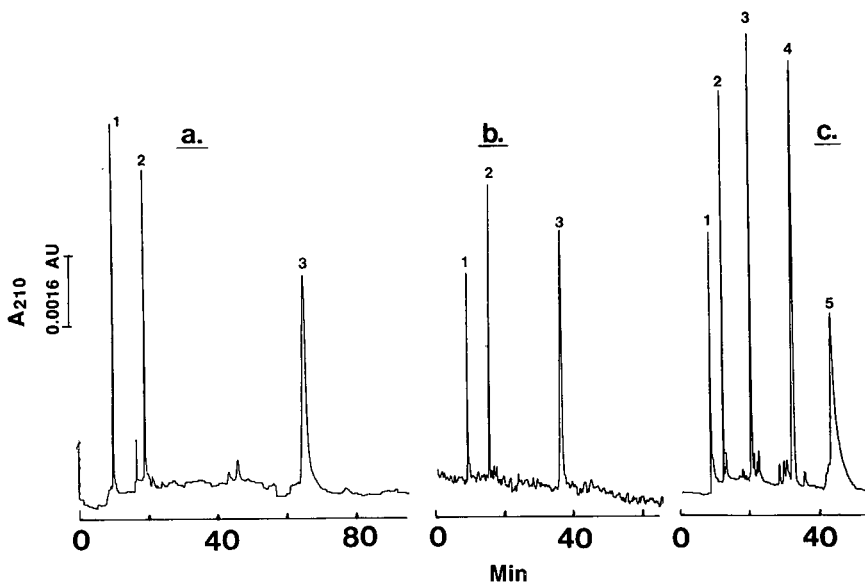


Fig. 2. Typical electropherograms of proteins obtained on F-2000 coated capillary in (a) and on tandem F-2000 → I-200 capillaries with 0.25 and 0.5 fractional length of the I-200 capillary segment in (b) and (c), respectively. Proteins: 1 = lysozyme; 2 = ribonuclease A; 3 = carbonic anhydrase; 4 = α -lactalbumin; 5 = β -lactoglobulin A. All other conditions are as in Fig. 1.

wise identical conditions as in Fig. 2a. It can be seen from these electropherograms that the analysis time of the model proteins decreased as the fractional length of the I-200 capillary increased. At 0.5 fractional length of the I-200 capillary, the EOF generated (43 nl/min) by the tandem capillaries was enough to bring about the analysis of all 5 proteins within 50 min.

Fig. 3 illustrates typical plots of the overall and electrophoretic mobilities of two proteins as well as plots of the electroosmotic mobility *versus* the fractional length of the I-200 capillary segment in F-2000 → I-200 coupled capillaries. In both cases, the electrophoretic mobility of the two test proteins remained practically unchanged while the overall and electroosmotic mobilities increased linearly and paralleled each other. This observation indicates that the variation in the analysis time of the model proteins is solely due to the change in the EOF, and no significant interaction between the proteins and the inner surface proper of the capillaries was present.

The effect of the tandem system on the bandwidth of the separated proteins was also investigated. Table II summarizes the plate height obtained with three model proteins at each fractional length stud-

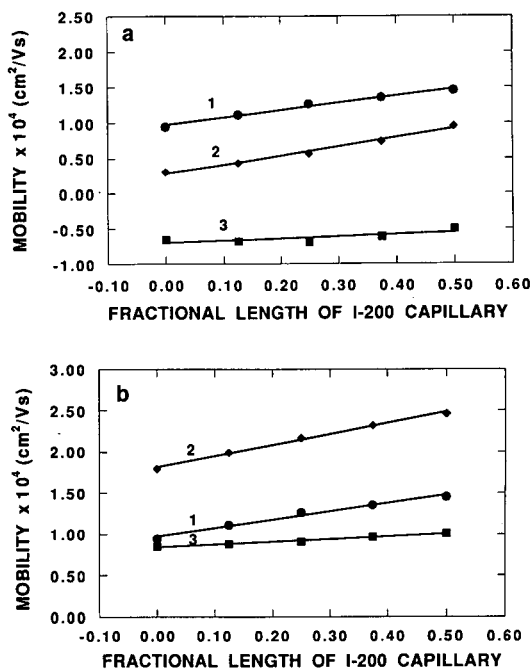


Fig. 3. Plots of overall (2) and electrophoretic (3) mobilities of (a) carbonic anhydrase and (b) lysozyme as well as plots of the electroosmotic (1) mobility of phenol *versus* the fractional length of the I-200 capillary segment in the F-2000 → I-200 tandem system. All other conditions are as in Fig. 1.

TABLE II
VALUES OF PLATE HEIGHT (H) MEASURED FROM
SELECTED PROTEIN PEAKS

| Protein | H (μm) | | | | |
|-----------------------------------|--|-------|------|-------|------|
| | Fractional length of I-200 capillary in the F-2000 \rightarrow I-200 system | | | | |
| | 0.00 | 0.125 | 0.25 | 0.375 | 0.50 |
| Lysozyme | 7.05 | 6.12 | 6.70 | 7.59 | 7.50 |
| Ribonuclease A | 3.50 | 4.10 | 5.00 | 5.80 | 6.67 |
| Carbonic anhydrase | 20.4 | 18.8 | 15.2 | 16.5 | 19.2 |
| Average plate height ^a | 10.3 | 9.67 | 8.97 | 9.96 | 11.1 |

^a Average plate height was calculated for all three proteins at each fractional length. Conditions are as in Fig. 2.

ied. It can be seen from Table II that while the average plate height of the three model proteins remained almost the same, the analysis time decreased by a factor of *ca.* 2.0 at 0.5 fractional length of each of the connected capillaries. It is believed that shortening the residence time of the separated analytes has decreased the amount of molecular diffusion, and subsequently may have compensated for band broadening caused by the laminar flow profile.

Analysis of ovalbumin

Ovalbumin, the major protein constituent of egg white, is a heterogeneous protein due to the variation in its phosphate content [8]. About 75% of this protein possesses two phosphate groups per molecule of the protein, and is designated A_1 . The remaining ovalbumin consists largely of another component, A_2 , having only one phosphate group per molecule. In addition, small amounts of phosphate-free component, A_3 , are also present. Obviously, when ovalbumin is analyzed by electrophoresis it shows different bands [9].

Therefore, ovalbumin was a good example to evaluate the effect of the magnitude of EOF as far as the quality of the analytical information generated during CZE separation is concerned. In other words, the goal was to determine whether there would be a loss in the analytical information when the speed of separation is increased. On this basis

two tandem capillary systems of moderate and relatively high EOF were evaluated. As demonstrated in Fig. 1, F-2000 \rightarrow I-200 offers a tunable flow over a moderate range whereas F-2000 \rightarrow untreated allows a higher EOF to be realized. Fig. 4a and b represents typical electropherograms of ovalbumin performed on the F-2000 \rightarrow I-200 and F-2000 \rightarrow untreated tandem capillaries, respectively. Similarly to previous observations in free-boundary electrophoresis [9], this protein showed different electrophoretic components due to the variation in its phosphorous content. Comparison of Fig. 4a and b reveals that both electropherograms clearly show all the differently phosphorylated components of ovalbumin; the only difference is that the analysis time on the F-2000 \rightarrow untreated system was decreased by a factor of *ca.* 4.0. Thus, while drastically decreasing the analysis time, the analytical information remained almost the same when going from low to high EOF by the use of coupled capillaries.

Rapid separation of proteins by stepwise increase in the EOF

The analysis time of oppositely charged proteins was further decreased by increasing the EOF during the electrophoretic run. This was carried out by switching manually from one tandem capillary system of relatively low EOF to another set of coupled capillaries of higher EOF, see Fig. 5. At the beginning of the run, the tandem system consisted of three capillary segments connected in series and containing F-2000, I-200 and untreated capillary at

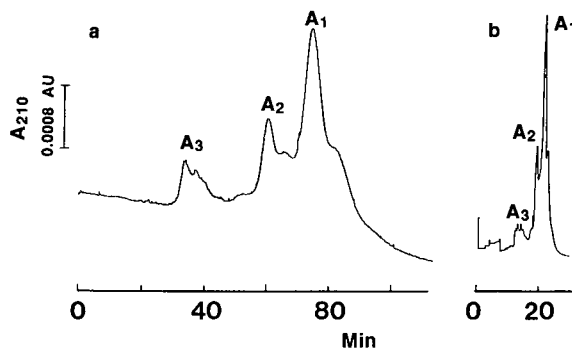


Fig. 4. Typical electropherograms of ovalbumin obtained on (a) F-2000 \rightarrow I-200 and (b) F-2000 \rightarrow untreated at 0.5 fractional length of the I-200 and untreated capillary, respectively. All other conditions are as in Fig. 1.

0.5, 0.25 and 0.25 fractional lengths, respectively. Thereafter, a stepwise increase in EOF was carried out by connecting in series F-2000 and untreated capillary at 0.5 fractional length each. In both tandem capillary systems, the F-2000 capillary having the most inert surface toward proteins, was selected as the separation capillary. Under these conditions, the EOF was increased stepwise from 58.2 to 72.5 nl/min. Fig. 5 is a typical electropherogram of the five model proteins using the stepwise increase in the EOF. The arrow in Fig. 5 indicates the time at which the stepwise increase in EOF was performed. It should be noted that the voltage was turned off at the time the first set of coupled capillaries was disconnected and replaced by the untreated capillary segment. This manual operation required less than 20 s.

As can be seen in Fig. 1, a relatively high level of EOF can only be achieved with the incorporation of an untreated capillary segment in the tandem capillaries. But, no basic solute should come into direct contact with the inner surface of the untreated fused-silica capillary to avoid solute–wall interactions, and in turn the unpredictable change in the level and polarity of EOF. For this reason, the length of the I-200 segment in the first set of coupled capillaries was adjusted to trap all the basic proteins as they elute from the fuzzy capillary after being separated and detected. Thus, while the I-200 segment provided the shielding from wall interaction, its presence in conjunction with the untreated segment afforded a moderate EOF. Once all basic solutes entered the I-200 capillary, a stepwise increase in EOF was performed whereby both the I-200 and untreated capillaries were disconnected and replaced by one untreated segment at 0.5 fractional length to speed the net migration of the acidic solutes.

The above elution schemes involving two-step coupled capillaries yielded an increase in the EOF by a factor of 1.35 in I and 1.69 in II (see Fig. 5), when compared to the F-2000 → I-200 tandem capillary system at 0.5 fractional length of the I-200 capillary segment in Fig. 2c. Furthermore, comparison of Figs. 2a and 5 reveals that the average plate height for lysozyme, ribonuclease A and carbonic anhydrase increased slightly from 10.3 to 12.5 μm , a factor of 1.2, while the migration time for these proteins decreased by factors of 1.9, 2.4 and 4.7, respectively. The slight increase in the plate height

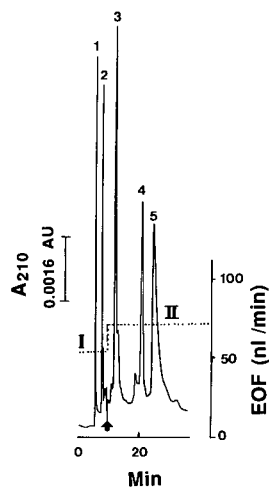


Fig. 5. Rapid capillary zone electrophoresis of proteins with stepwise increase in the electroosmotic flow. I, initial flow: F-2000 → I-200 → untreated coupled capillaries at 0.5, 0.25 and 0.25 fractional length of the F-2000, I-200 and untreated capillaries, respectively. II: F-2000 → untreated capillaries at 0.5 fractional length each. All other conditions are as in Fig. 1. The arrow is to indicate the time at which the stepwise increase in EOF occurred.

may be attributed to the presence of a more pronounced laminar flow as a result of the large difference between the bulk flow and the intrinsic EOF in the F-2000 capillary segment.

To develop this concept further and permit the realization of several stepwise increases in the EOF during analysis, a multiple capillary device which will allow the switching between several coupled capillary systems having different electroosmotic flow characteristics is under development [10].

The two-step tandem capillaries provided the rapid analysis of proteins at relatively moderate applied voltage. To obtain nearly the same EOF (*i.e.*, 65.0 nl/min) with the F-2000 capillary as with the two-step coupled capillaries, the F-2000 capillary had to be operated at an applied voltage of 28 kV whereby the current was relatively high (155 μA). Fig. 6 illustrates a typical electropherogram of the protein mixture obtained at high voltage with F-2000 capillary. As can be seen in Fig. 6, with the exception of ribonuclease A the proteins underwent severe sample degradation. The peak of β -lactoglobulin A disappeared, lysozyme eluted as a tailing peak and only short peaks were observed for

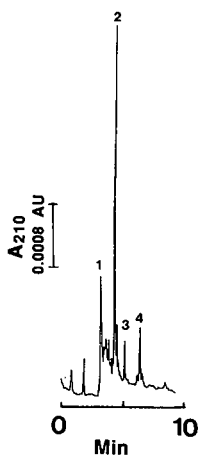


Fig. 6. Electropherogram of model proteins on fuzzy 2000-coated capillary at an applied voltage of 28 kV. All other conditions are as in Fig. 2a.

carbonic anhydrase and α -lactalbumin. These observations may be attributed to system overheating [11,12] and/or to the binding of the proteins to the coating proper by hydrophobic interactions at elevated temperatures due to heat-induced conformational changes as previously shown in liquid chromatography [13,14]. Very recently, it has been shown that capillary temperature can dramatically affect the electrophoretic patterns of proteins in CZE via the reduction of the structural metal in metalloproteins and by inducing conformational changes [15].

ACKNOWLEDGEMENTS

The financial supports from the Dean Incentive Program, College of Arts and Sciences at Oklahoma State University and from the Oklahoma Water Resources Research Institute are greatly appreciated.

REFERENCES

- 1 C. S. Lee, W. C. Blanchard and C.-T. Wu, *Anal. Chem.*, 62 (1990) 1550.
- 2 C. S. Lee, D. McManigill, C.-T. Wu and B. Patel, *Anal. Chem.*, 63 (1991) 1519.
- 3 M. A. Hayes and A. G. Ewing, *Anal. Chem.*, 64 (1992) 512.
- 4 W. Nashabeh and Z. El Rassi, *J. High Resolut. Chromatogr.*, 15 (1992) 289.
- 5 W. Nashabeh and Z. El Rassi, *J. Chromatogr.*, 596 (1992) 251.
- 6 W. Nashabeh and Z. El Rassi, *J. Chromatogr.*, 559 (1991) 367.
- 7 R. Datta and V. R. Kotamarthi, *AIChE Journal*, 36 (1990) 916.
- 8 A. Gottschalk and E. R. B. Graham, in H. Neurath (Editor), *The Proteins: Composition, Structure and Function*, Vol. IV, Academic Press, New York, 1966, pp. 113-115.
- 9 G. E. Perlmann, *J. Gen. Physiol.*, 35 (1952) 711.
- 10 W. Nashabeh, J. T. Smith and Z. El Rassi, *Electrophoresis*, submitted for publication.
- 11 K. A. Cobb, V. Dolnik and M. Novotny, *Anal. Chem.*, 62 (1990) 2478.
- 12 J. S. Green and J. W. Jorgenson, *J. Chromatogr.*, 478 (1989) 63.
- 13 S. Hjertén, *J. Chromatogr.*, 87 (1973) 325.
- 14 Z. El Rassi, A. L. Lee and Cs. Horváth, in J. A. Asenjo (Editor), *Separation Processes in Biotechnology*, Marcel Dekker, New York, 1990, p. 477.
- 15 R. S. Rush, A. S. Cohen and B. L. Karger, *Anal. Chem.*, 63 (1991) 1346.

Determination of sulphonamides in pharmaceuticals by capillary electrophoresis

C. L. Ng, H. K. Lee and S. F. Y. Li

Department of Chemistry, National University of Singapore, Kent Ridge, Singapore 0511 (Singapore)

ABSTRACT

A mixture of seven sulphonamides was separated using capillary electrophoresis with β -cyclodextrin as modifier. The separation was carried out with on-column UV detection at 210 nm. The effects of the pH of the electrophoretic media and β -cyclodextrin concentration on the selectivity and migration times of the sulphonamides were investigated. In addition, the migration behaviour of this group of compounds was examined. This technique was then applied to the determination of sulphonamides in pharmaceuticals.

INTRODUCTION

Sulphonamide drugs are used for the treatment of susceptible bacterial infections, such as those related to the respiratory, digestive and urinary tracts. This group of compounds has been analysed successfully by thin-layer chromatography [1] and high-performance liquid chromatography (HPLC) using isocratic and gradient elution [2–5], but these methods are time consuming [2–3]. Interest in sulphonamides mainly lies in the determination of residues in animal tissues. However, sulphonamides can be toxic when they are used at therapeutic doses [6]. Pharmaceutical assays on these drugs have also been published [7]. As sulphonamides are mostly polar compounds, capillary electrophoresis (CE) might be expected to be a good alternative for their analysis.

CE has become popular in recent years mainly because of its ability to separate charged and neutral species with high efficiency. Micellar electrokinetic chromatography (MEKC), one of the modes of CE, involves the use of surfactant solutions such

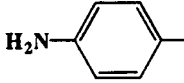
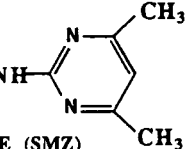
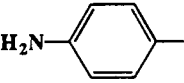
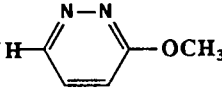
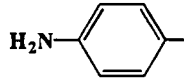
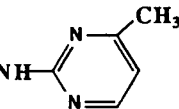
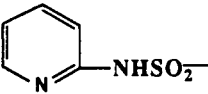
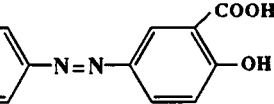
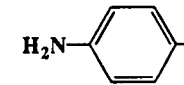
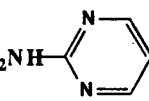
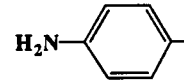
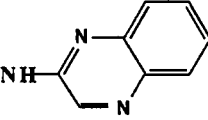
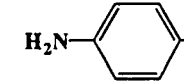
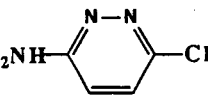
as sodium dodecyl sulphate (SDS). Selectivity in MEKC separations can be enhanced by adding modifiers to the system. The introduction of cyclodextrin into the micellar solution has been reported to provide additional selectivity for chiral separations via host–guest-type complexation [8]. To date, CE has been successfully employed in analyses of environmental pollutants [9,10], biological compounds [11,12] and pharmaceutical products [13,14].

In this work, the separation of seven sulphonamides using capillary zone electrophoresis (CZE) with β -cyclodextrin (β -CD) as modifier was examined. This technique was applied to the determination of sulphonamides in commercial drug tablets. In addition, the effects of pH and β -CD concentrations on the migration behaviour of the sulphonamides in the system are discussed.

EXPERIMENTAL

Experiments were conducted on a laboratory-built CE system. A Spellman (Plainview, NY, USA) Model RM15P10KD power supply capable of delivering up to 15 kV was used. A fused-silica capillary tube of 50 μ m I.D. (Polymicro Technologies, Phoenix, AZ, USA) and 50 cm effective length with an optically transparent coating was employed. A

Correspondence to: S. F. Y. Li, Department of Chemistry, National University of Singapore, Kent Ridge, Singapore 0511, Singapore.

| R | R' | pKa |
|---|---|------|
|  |  | 7.5 |
| SULFAMETHAZINE (SMZ) | | |
|  |  | NA** |
| SULFAMETHOXYPYRIDAZINE (SMP) | | |
|  |  | 7.0 |
| SULFAMERAZINE (SM) | | |
|  |  | NA |
| SULFASALAZINE (SS) | | |
|  |  | 6.4 |
| SULFADIAZINE (SD) | | |
|  |  | 5.5 |
| SULFAQUINOXALINE (SQX) | | |
|  |  | NA |
| SULFACHLOROPYRIDAZINE (SCP) | | |

** : NOT AVAILABLE

Fig. 1. Structures of sulphonamides, their abbreviations and some pK_a values. The pK_a value refers to the ionization of the hydrogen attached to N-1.

Shimadzu (Kyoto, Japan) Model SPD-6A UV spectrophotometric detector was used for the detection of peaks. Chromatographic data were collected and analysed using a Shimadzu Chromatopac C-R6A data processor.

The pH of the buffer solutions used in the CE system was adjusted by mixing appropriate portions of sodium dihydrogenphosphate and sodium tetraborate solutions. β -Cyclodextrin was purchased from Fluka (Buchs, Switzerland). The seven sulphonamide standards used were purchased from Sigma (St. Louis, MO, USA). The structures of the seven sulphonamides, their abbreviations and some of the pK_a values are shown in Fig. 1. The sulphonamide standards were dissolved in HPLC-grade methanol (BDH, Poole, UK), each at a concentration of 1000 $\mu\text{g/ml}$.

Sample solutions were introduced manually. One end of the capillary was placed in a sample vial containing the sample solution and the sample was introduced by siphoning from the sample solution at a height of 9 cm higher than the electrophoretic solution in which the other end of the tube was immersed. The injection time was about 4 s. Each injection was estimated to be 1 nl.

Sample preparations

The method for the extraction of sulphonamides from pharmaceuticals is as follows. The sample was first ground into powder in a mortar, 100 mg of the powder were accurately weighed into a 100-ml volumetric flask, 75 ml of 0.025 *M* NaOH solution were added and the solution was shaken for 30 min. The solution was then diluted to volume with 0.025 *M* NaOH, mixed and filtered. The solution was then diluted to half its concentration with 0.025 *M* NaOH solution before injection into the CE system for analysis.

For the determination of the percentage recovery of the extraction procedure, 100 mg of standard sulphonamide were weighed into a 100-ml volumetric flask. Then the extraction procedure described was followed. A 50-ml volume of 0.025 *M* NaOH solution was used to dilute the solution before injection into the system.

RESULTS AND DISCUSSION

Preliminary experiments were conducted at a

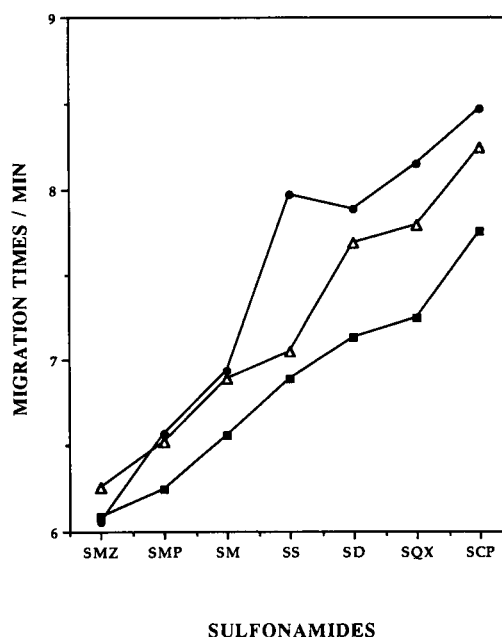


Fig. 2. Variation of migration times of sulphonamides with β -CD concentration. \bullet = 0; Δ = 5; \blacksquare = 10 mM β -CD. Electrophoretic medium, 0.05 *M* phosphate–0.05 *M* borate buffer (pH 7); separation tube, 50 cm \times 50 μm I.D. fused-silica capillary; voltage, 15 kV; detection wavelength, 210 nm.

constant pH of 7 and varying the concentration of β -CD at 0, 5 and 10 mM. The effect of the concentration of β -CD on the migration times of the sulphonamides is shown in Fig. 2. As can be seen, there is a decrease in the migration times of the solutes with increase in β -CD concentration. This could be attributed to the fact that with an increase in β -CD concentration, the solutes would have a higher probability of being incorporated into the neutral cavity of β -CD. Terabe *et al.* [15] successfully separated neutral polycyclic aromatic hydrocarbons (PAHs) using cyclodextrin-modified micellar electrokinetic chromatography. These compounds have at least two benzene rings that can be effectively incorporated into the cavity of CD, which consequently resulted in separation. The same could be said of the sulphonamides. These compounds have at least one benzene ring each and a heterocyclic ring in their structures, as shown in Fig. 1, which could easily be incorporated into the cavity of β -CD. In addition, Fig. 2 shows that the migration order does not change with increase in β -CD concentration. This indicates that the addition of β -CD

to the electrophoretic medium does not significantly affect the overall ionization state of the sulphonamides. Nevertheless, the resolution between the peaks was observed to improve with higher concentrations of β -CD because of the increase in the formation of inclusion complexes.

This observation of decreasing migration times of the sulphonamides with increase in β -CD concentration is in contrast to the observations of Fanali [16], who found that the migration times increased with increase in β -CD concentration for chiral compounds. This is not surprising because at this pH (7), some of the sulphonamides would be partially ionized or totally deprotonated, depending on their pK_a values (given in Fig. 1). The partially ionized solutes (SMZ and SM, $pK_a \geq 7$) were also found to elute earlier than solutes that were totally ionised ($pK_a < 7$). As the experiments were conducted at a constant pH, we would expect the change in the electroosmotic flow velocity with increase in β -CD concentration to be minimal. In the absence of β -CD, the partially negatively charged sulphonamides would be experiencing an electrophoretic pull towards the positive electrode. These partially ionized solutes would be incorporated into the β -CD on addition of β -CD, which is moving at a speed equal to the electroosmotic velocity. Under CE conditions, the neutral β -CD would travel faster than the anionic solutes towards the cathode. In addition, inclusion complexation of the solutes with β -CD would increase with increase in β -CD concentration. Hence the electrophoretic pull towards the anode would be diminished. Subsequently, an increase in the apparent velocity and thus a decrease in the migration times for the neutral or partially ionized compounds was observed. The migration times for the anionic solutes was also observed to decrease even though there was no effective complexation, as incorporation of the negatively charged compounds into the neutral β -CD cavity would be hindered. The observed shorter migration time of the negatively charged sulphonamides could be attributed to hydrogen bonding between the OH groups on the glucose ring of β -CD and the nitrogen moiety of the sulphonamides. As a result, the anions would be dragged along with the β -CD towards the negative electrode. Consequently, a decrease in migration times was observed for the sulphonamides with increase in β -CD concentration.

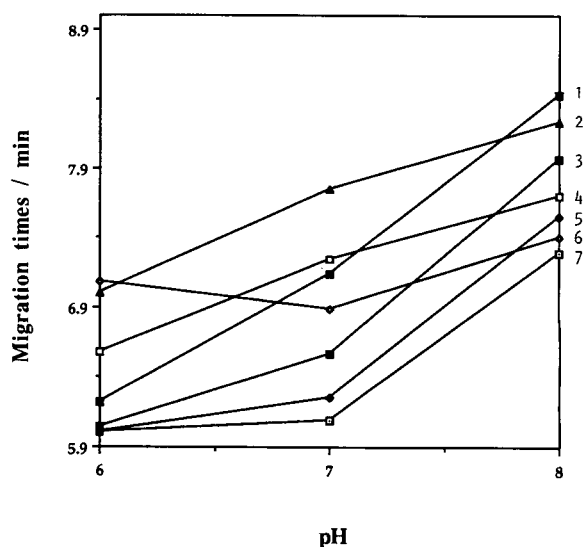


Fig. 3. Variation of migration times of sulphonamides with pH of the buffer. Electrophoretic medium, 0.05 M phosphate–0.05 M borate buffer–10 mM β -CD; separation tube, 50 cm \times 50 μ m I.D. fused-silica capillary; voltage, 15 kV; detection wavelength, 210 nm. 1 = SD; 2 = SCP; 3 = SM; 4 = SQX; 5 = SMP; 6 = SS; 7 = SMZ.

The effect of pH on the migration behaviour of sulphonamides was also investigated. Experiments were carried out at different pH values at a constant β -CD concentration of 10 mM. The effect of pH on the migration times of the sulphonamides is illustrated in Fig. 3. There is a general increase in migration times of the analytes with increase in pH. From the structures of the sulphonamides, it was noted that they can act as weak acids in dilute alkaline solutions or weak bases in dilute acidic solutions. Therefore, at high pH (8), the sulphonamides tend to be deprotonated at N-1, the nitrogen bonded next to the sulphur moiety. Consequently, these compounds would be negatively charged at this pH and would not be effectively incorporated into the neutral cavity of the β -CD. Instead, they would experience a stronger attractive pull towards the anode. It is known that electroosmotic flow velocity increases with increase in pH [17]. In the present instance, as the increase in electroosmotic flow is less than the electrophoretic velocity of the analytes, the overall effect is a net decrease in the apparent velocity, which accounts for the increase in migration times of the sulphonamides. It was found that at a pH of 7 and with 10 mM β -CD, satis-

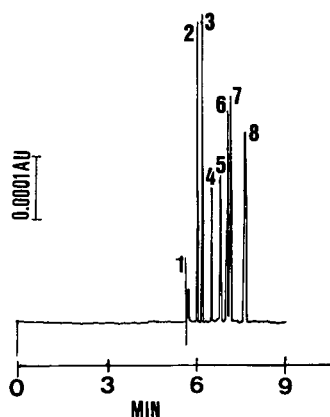


Fig. 4. Electropherogram of the seven sulphonamides. Electrophoretic medium, 0.05 M phosphate–0.05 M borate buffer (pH 7)–10 mM β -CD; separation tube, 50 cm \times 50 μ m I.D. fused-silica capillary; voltage, 15 kV; detection wavelength, 210 nm. Peaks: 1 = MeOH; 2 = SMZ; 3 = SMP; 4 = SM; 5 = SS; 6 = SD; 7 = SQX; 8 = SCP.

factory separation for the group of seven sulphonamides was achieved. A typical electropherogram is shown in Fig. 4. It was observed that there was no general trend in the migration orders of the sulphonamides. It is not possible to explain the trend solely by considering the structures alone because the R and R' substituents vary in shape, sizes and polarity in this instance. However, it was found that the migration order could be related to the pK_a values, *i.e.*, compounds with higher pK_a values (higher than the pH of the buffer) would migrate faster than those with pK_a values less than the pH of the electrophoretic medium.

TABLE I

SULPHONAMIDES INVESTIGATED, CORRELATION COEFFICIENTS AND DETECTION LIMITS OBTAINED AT A SIGNAL-TO-NOISE RATIO OF 2

| Sulphonamide ^a | Correlation coefficient, <i>r</i> | Detection limit (pg) |
|---------------------------|-----------------------------------|----------------------|
| SMZ | 0.97674 | 18 |
| SMP | 0.9667 | 19 |
| SM | 0.9907 | 26 |
| SS | 0.9937 | 43 |
| SD | 0.9986 | 31 |
| SQX | 0.9838 | 25 |
| SCP | 0.9969 | 25 |

^a See Fig. 1 for full names.

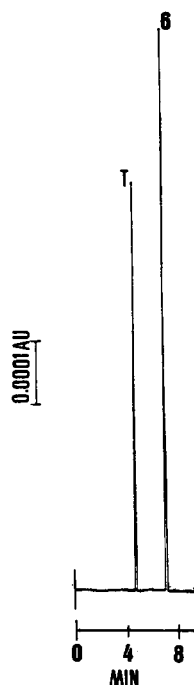


Fig. 5. Electropherogram of the extracted sample in 150 ml of 0.025 M NaOH. Electrophoretic conditions as in Fig. 4. Peaks: T = trimethoprim; 6 = SD.

Determination of sulphonamides in pharmaceuticals

Once a satisfactory separation had been obtained, the technique was applied to the determination of sulphonamides in pharmaceuticals. Linear calibration graphs in the range 100–1000 μ g/ml were obtained for the seven sulphonamides. Low detection limits in the picogram range was obtained. The correlation coefficient, *r*, and the detection limits at a signal-to-noise ratio of 2 are given in Table I.

Combination drug formulations in the form of tablets or suspensions containing sulphonamides are most frequently used to administer oral doses to human patients. In this investigation, drug tablets containing the active component (sulphadiazine) and trimethoprim (inhibitors of folic acid synthetase) were used. Good linearity was obtained between the amount injected and peak area. The recovery using the extraction method [18] was found to be $85.97 \pm 0.03\%$. A typical electropherogram of the extracted samples is shown in Fig. 5. For two sulphadiazine–trimethoprim tablets with an indicated content of 0.410 g, the amounts found, based in a

recovery of 85.97%, were 0.412 ± 0.0051 and 0.407 ± 0.0048 g (mean \pm S.D., $n = 4$). Hence the amount was within the limits of 95–100% of the amount indicated. The results obtained suggested that CE is a useful method for the routine determination of sulphonamides in pharmaceuticals.

ACKNOWLEDGEMENT

The authors thank the National University of Singapore for financial assistance.

REFERENCES

- 1 G. J. Reimer and A. Suarez, *J. Chromatogr.*, 555 (1991) 315.
- 2 R. F. Cross, *J. Chromatogr.*, 478 (1989) 422.
- 3 M. M. L. Aerts, W. M. J. Beek and U. A. Th. Brinkman, *J. Chromatogr.*, 435 (1988) 97.
- 4 A. R. Long, C. R. Short and S. A. Barker, *J. Chromatogr.*, 502 (1990) 87.
- 5 M. Patthy, *J. Chromatogr.*, 275 (1983) 115.
- 6 W. E. Lloyd and H. D. Mercer, in J. H. Steele and G. W. Beran (Editors), *CRC Handbook Series of Zoonoses, Section D: Antibiotics, Sulfonamides, and Public Health*, Vol. 1, CRC Press, Boca Raton, FL, 1984, p. 217.
- 7 H. Umagat, P. F. McGarry and R. J. Tscherne, *J. Pharm. Sci.*, 68 (1979) 922.
- 8 S. Fanali, *J. Chromatogr.*, 474 (1989) 441.
- 9 C. P. Ong, C. L. Ng, N. C. Chong, H. K. Lee and S. F. Y. Li, *J. Chromatogr.*, 516 (1990) 263.
- 10 Y. F. Yik, C. L. Ng, C. P. Ong, S. B. Khoo, H. K. Lee and S. F. Y. Li, *Bull. Singapore Natl. Inst. Chem.*, 18 (1990) 91.
- 11 D. E. Burton, M. J. Sepaniak and M. P. Maskarinec, *Chromatographia*, 21 (1986) 583.
- 12 K. Otsuka, S. Terabe and T. Ando, *J. Chromatogr.*, 348 (1985) 39.
- 13 S. Fujiwara and S. Honda, *Anal. Chem.*, 59 (1987) 2772.
- 14 H. Nishi, N. Tsumagari, T. Nakimoto and S. Terabe, *J. Chromatogr.*, 477 (1989) 259.
- 15 S. Terabe, Y. Miyashita, O. Shibata, E. R. Barnhart, L. R. Alexander, D. G. Patterson, B. L. Karger, K. Hosoya and N. Tanaka, *J. Chromatogr.*, 516 (1990) 23.
- 16 S. Fanali, *J. Chromatogr.*, 545 (1991) 437.
- 17 K. Otsuka and S. Terabe, *J. Microcol. Sep.*, 1 (1989) 150.
- 18 *US Pharmacopeia National Formulary*, Pharmacopeial Convention, Rockville, MD, 16th ed, United States 1985, p. 989.

Capillary sodium dodecyl sulfate gel electrophoresis of proteins

Andr s Guttman, Judith A. Nolan and Nelson Cooke

Beckman Instruments, Inc., Fullerton, CA 92634 (USA)

ABSTRACT

In recent years, there has been considerable activity in the separation and characterization of protein molecules by sodium dodecylsulfate (SDS) gel electrophoresis with particular interest in using this technique to separate on the basis of size and to estimate molecular mass. In this paper we report a new improved and automated electrophoretic method in the form of high-performance capillary SDS gel electrophoresis. Rapid separations of protein molecules in the molecular mass range of 20 000–200 000 daltons were demonstrated with excellent linearity and intra- and inter-day reproducibility of the migration time. Monomer–dimer forms of the recombinant human ciliary neurotrophic factor were examined by the use of this method under reducing and non-reducing conditions.

INTRODUCTION

Electrophoresis in polyacrylamide or other gels containing ionic detergents, such as sodium dodecyl sulfate (SDS), has proven to be a powerful tool for the size separation of protein molecules, the estimation of their molecular mass and assessment of their purity [1]. In the presence of reducing agents such as mercaptoethanol, the detergent (SDS) dissociates proteins into their constituent subunits and binds to the polypeptide chains, so that similar charge-to-mass ratios of the proteins are obtained [2]. In gel electrophoresis, the polymer network structure creates a sieving effect so that separation can be performed based on the size of the molecules [3]. An approximately linear relationship is obtained if the logarithm of the molecular mass of standard polypeptide chains are plotted against their electrophoretic mobilities [4]. The method is reliable and reproducible in the molecular mass range of 20 000–200 000 daltons generally within 10% of those obtained by other techniques [2]. Prior to the applica-

tion of the sample to the gel, the proteins are denatured by heat treatment in the presence of a thiol-reducing agent such as β -mercaptoethanol or dithiothreitol. Rod or slab gels of a variety of cross-linked polyacrylamides were conventionally used as sieving matrices to separate these polypeptide chains according to their molecular masses [5].

In the past several years capillary gel electrophoresis has been successfully utilized for the size separation and purity assessment of synthetic oligonucleotide probes and primers [6] and polymerase chain reaction (PCR) products [7]. Early attempts to apply capillary gel electrophoresis for protein separation by SDS polyacrylamide gel electrophoresis (PAGE) have involved highly concentrated cross-linked polyacrylamide as sieving medium [8]. Later, others employed lower-concentration cross-linked polyacrylamide [9] and linear polyacrylamide in the capillary as sieving material [10]. Recently, Karger's group [11] introduced non-polyacrylamide-type, low-viscosity branched polymers such as dextrans with excellent UV transparency at 214 nm to obtain size separation with enhanced detectability.

In this paper we report the use of a non-polyacrylamide-based, hydrophilic linear polymer

Correspondence to: Dr. A. Guttman, Beckman Instruments, Inc., Fullerton, CA 92634, USA.

network for capillary SDS gel electrophoresis of proteins. This polymer network is advantageous in that capillary gels are easily prepared and are easily replaceable if necessary. Examples are shown of the usefulness of this system in the demonstration of dimer formation of the recombinant human ciliary neurotrophic factor.

EXPERIMENTAL

Apparatus

In all these studies, the P/ACE System 2100 capillary electrophoresis apparatus (Beckman Instruments, Fullerton, CA, USA) was used in reversed polarity mode (cathode on the injection side). The separations were monitored on-column at 214 nm. The temperature of the gel-filled capillary columns was controlled at 20°C by the liquid cooling system of the P/ACE instrument. The electropherograms were acquired and stored on an Everex 386/33 computer. Molecular masses of the protein samples were estimated by using the Molecular Weight Determination Option of the System Gold software package (Beckman Instruments).

Procedures

In all the capillary electrophoresis experiments the eCAP SDS-200 (Beckman Instruments) capillary electrophoresis size separation kit for SDS proteins was used. In this kit the sieving matrix is a low-viscosity gel formulation which is not bonded to the capillary wall. This permits replacement of the gel-buffer system in the coated capillary column by means of the pressure rinse operation mode of the P/ACE apparatus (*i.e.*, replaceable gel). It is important to note, that a coated capillary column should be used in these experiments to eliminate the electroosmotic flow and minimize adsorption of proteins on the inner surface of the column. The 47 cm long (40 cm to the detector) and 0.1 mm I.D. coated eCAP SDS-200 fused-silica capillary column (Beckman Instruments) was washed with 1 M HCl after each run. In some specific applications a longer or a shorter column may be required to extend a useful range and/or to shorten the analysis time. The samples were injected by pressure (typically: 30–60 s, 0.5 p.s.i.) into the replaceable gel-filled capillary column.

The slab gel experiments were performed on

SDS-PAGE (10% polyacrylamide) according to the procedure of Laemmli [12] applying 30 V/cm constant field on a Bio-Rad Mini-Protean II dual-slab cell system (Bio-Rad Labs, Richmond, CA, USA). The separated bands were visualized by Commassie Brilliant Blue R250 staining [13].

Chemicals

The high-molecular-mass SDS protein test mixture (29 000–205 000 daltons) and the lysozyme were purchased from Sigma (St. Louis, MO, USA). Before injection, the samples were diluted to 0.2–2 mg/ml with the eCAP SDS-200 sample buffer (final concentration: 60 mM Tris-HCl, 1% SDS, pH 6.6) and were boiled in a water bath for 5 min after adding 2.5% β -mercaptoethanol as reducing agent and 0.005% Orange G as internal standard. The samples were stored at –20°C or freshly used. All buffer and gel solutions were filtered through a 1.2 μ m pore size filter (Schleicher and Schuell, Keene, NH, USA) and carefully vacuum-degassed.

RESULTS AND DISCUSSION

Fig. 1 shows the complete separation of a mixture of six proteins (size range 29 000–205 000 daltons) in only 22 min. The inset in Fig. 1 shows the polyacrylamide slab gel trace of the same protein test mixture. Detected amounts for the two systems were 120 ng total protein on the SDS-200 column and 10 μ g total protein on the slab gel. The differences in relative migration times and relative migration distances for the two techniques are explained by the use of different sieving polymer matrices. A linear relationship between the logarithm of molecular mass and mobility were found in both instances. The relative standard deviation (R.S.D.) in capillary gel electrophoresis (CGE) gave high linearity for the range of 20 000–200 000 daltons (R.S.D._{CGE} = 0.995%) versus the slab gel (R.S.D._{SLAB} = 0.986%, data not shown). The calibration curve can be used for molecular mass estimation of unknown proteins with 10% accuracy. As can be observed, well resolved peaks are obtained for each component; however, some peaks seem to be broader than others. It is postulated that this phenomenon is caused by small differences in the complexation of SDS with the different protein molecules [1–3]. Table I is a comparison of the individual steps and

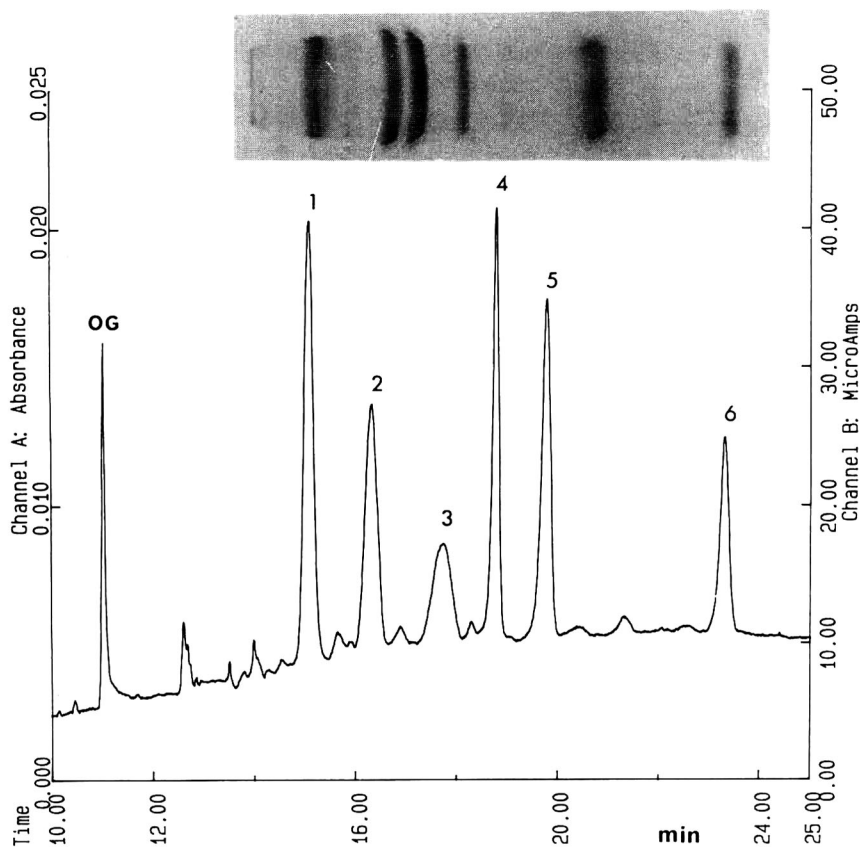


Fig. 1. Capillary SDS gel electrophoresis of six proteins on an eCAP SDS-200 capillary. Inset: SDS-PAGE pattern of the same sample mixture. Peaks: 1 = carbonic anhydrase (molecular mass, M_r 29 000); 2 = ovalbumin (M_r 45 000); 3 = bovine serum albumin (M_r 66 000); 4 = phosphorylase B (M_r 97 400); 5 = β -galactosidase (M_r 116 000); 6 = myosin (M_r 205 000). A tracking dye Orange G (OG) was added to the sample. Conditions: injected amount, 100 ng protein; detection, 214 nm; run temperature, 20°C; applied electric field, 300 V/cm; current, 25–30 μ A.

TABLE I
COMPARISON OF eCAP SDS-200 AND SDS-PAGE ANALYSIS

| Step | Time (min) | |
|--------------------|--------------|-----------------------------|
| | eCap SDS-200 | SDS-PAGE |
| Gel preparation | 6 | 80 |
| Sample preparation | 10 | 10 |
| Gel run time | 25 | 35 |
| Staining | — | 90 |
| Destaining | — | 720 |
| Drying | — | 720 (without dryer) |
| Quantitation | 2 | 20 (densitometer) |
| Total | 43 | 1675 (for sixteen lanes) |

required time for both the traditional slab SDS-PAGE system and eCAP SDS-200 techniques. These data clearly show that even in an optimal case running sixteen different samples on the slab gel system, the automated capillary electrophoresis system is less time-consuming. It is important to note that capillary SDS gel electrophoresis is more easily quantitated (data is shown later) while in slab gel electrophoresis the frequently used visualization dye Coomassie Brilliant Blue R250 does not bind in a stoichiometric fashion for all proteins, making quantitative interpretation difficult [14]. It is important to note, that with the inclusion of an internal standard (Orange G) for each sample it is unnecessary to bracket samples with standard runs. The existing sieving phenomena in capillary SDS gel

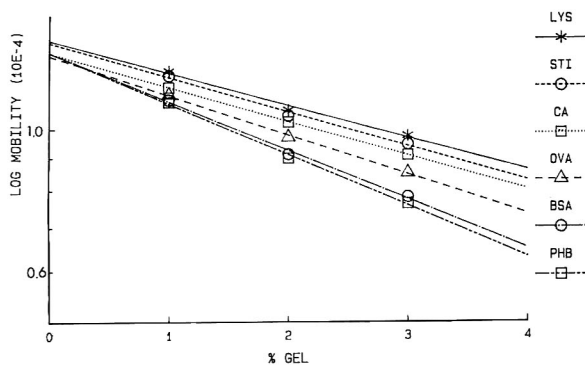


Fig. 2. Ferguson plot of logarithm mobility versus percent gel concentration for six proteins. LYS = lysozyme; STI = soybean trypsin inhibitor; CA = carbonic anhydrase; OVA = ovalbumin; BSA = bovine serum albumin; PHB = phosphorylase B.

electrophoresis was demonstrated by the Ferguson method [15]. As Fig. 2 shows, the plots of log mobility versus % (w/v) gel (Ferguson plots) were linear (R.S.D. = 0.995) with an intercept at 0% gel concentration which represents approximately the free solution mobility of the SDS-protein complex. Other variables such as polymer molecular mass, degree of polymer branching and column temperature will also affect the separation [16].

Using the pressure injection mode of this capillary electrophoresis system the injected amount is *ca.* 1 nl/s for this particular capillary and gel-buffer system based on the migration velocity of the internal standard using the low-pressure rinse (injection pressure) mode [17]. As an example, the amount for phosphorylase B (molecular mass 97 400 daltons) detected on column is 10^{-9} g (10^{-14} mol). The peak area was a linear function of the injected amount for lysozyme over a range of 10 μ g/ml ($7 \cdot 10^{-7}$ M) to 1 mg/ml with R.S.D. = 0.999. Identical volumes of samples with different protein concentration were injected in this experiments. The capillary column was washed with 1 M HCl after each run to remove absorbed proteins, if any, from the capillary wall.

Initial characterization of the capillary SDS gel electrophoresis technique involved the determination of reproducibility for migration time. The R.S.D. of the uncorrected migration times for eighteen runs of the standard proteins range from 0.4 to 0.8%. These data represent a capillary and buffer that was cycled for 100 runs (intra- and inter-day variability) by altering nine replicate injections of the high-molecular-mass Sigma standard and nine replicate injections of untreated calf serum diluted

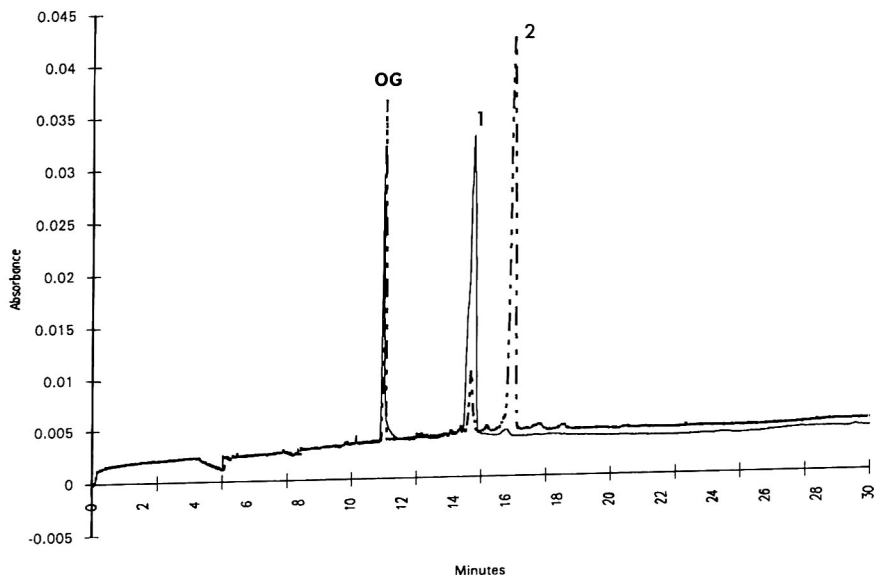


Fig. 3. Capillary SDS gel electrophoretic separation of the reduced (monomer, solid line) and unreduced (dimer, dotted line) proprietary protein, referred to as SFP. Conditions are the same as in Fig. 1.

1:50 with water. The good reproducibility of the results may be attributed to the direct visualization of the proteins during the separation and the ability to replace the polymer network with a rinsing step after each run. If a particulate sample was applied to the gel, or a sample containing a contaminant too large to be analyzed in the standard run time, the replacement of the low-viscosity gel alleviates any damage to the gel that would have occurred in a non-replaceable system.

As an example, the issue of disulfide bond formation for a proprietary protein, referred to as SFP, was addressed. The quantity of dimerization of the product was analyzed by preparing two samples, with and without disulfide reduction (Fig. 3). The larger peak (peak 2) in the run under non-reducing conditions (dotted line) is a dimer of a predicted molecular mass of 46 000 daltons. Upon addition of β -mercaptoethanol to the sample, the peak moved to the location of the monomer (molecular mass 23 000 daltons, peak 1, solid line). The two peaks were verified by molecular mass estimation. Predicted masses for the monomer and dimer were 21 700 and 51 000 daltons, respectively, in good agreement with the known values.

ACKNOWLEDGEMENT

The authors gratefully acknowledge Professor Barry L. Karger for his stimulating discussions.

REFERENCES

- 1 A. T. Andrews, *Electrophoresis*, Clarendon Press, Oxford, 2nd ed., 1986.
- 2 K. Weber and M. Osborn, *J. Biol. Chem.*, 244 (1969) 4406.
- 3 B. D. Hames and D. Rickwood (Editors), *Gel Electrophoresis of Proteins*, IRL, Washington, DC, 1983.
- 4 J. A. Reynolds and C. Tanford, *Proc. Natl. Acad. Sci. USA*, 66 (1970) 1002.
- 5 A. Chrambach, *The Practice of Quantitative Gel Electrophoresis* VCH, Deerfield Beach, FL, 1985.
- 6 A. Guttman, A. S. Cohen, D. H. Heiger and B. L. Karger, *Anal. Chem.*, 62 (1990) 137.
- 7 H. E. Schwartz, K. J. Ulfelder, F. J. Sunzeri, F. J. Busch and R. G. Brownlee, *J. Chromatogr.*, 559 (1991) 267.
- 8 A. S. Cohen and B. L. Karger, *J. Chromatogr.*, 397 (1987) 409.
- 9 K. Tsuji, *J. Chromatogr.*, 550 (1991) 823.
- 10 A. Widhalm, C. Schwer, D. Blass and E. Kenndler, *J. Chromatogr.*, 546 (1991) 446.
- 11 B. L. Karger, presented at the 4th International Symposium on HPLC, Amsterdam, Feb. 9–13, 1992, LW-1.
- 12 U. K. Laemmli, *Nature*, 227 (1970) 680.
- 13 D. Freifelder, *Physical Biochemistry*; W.H. Freeman, New York, 2nd ed., 1982.
- 14 S. Fazekas de St. Groth, R. G. Webster and A. Datyner, *Biochim. Biophys. Acta*, 71 (1963) 377.
- 15 K. A. Ferguson, *Metab. Clin. Exp.*, 13 (1964) 985.
- 16 A. Guttman, J. Horvath and N. Cooke, presented at the 6th Symposium, Protein Society, San Diego, July 25–29, 1992, PT-78.
- 17 J. Harbough, M. Collette and H. E. Schwartz, *Technical Bulletin*, TBIC-103, Beckman Instruments, Fullerton, CA, 1990.

Prediction of the migration behavior of organic acids in micellar electrokinetic chromatography

Scott C. Smith[☆] and Morteza G. Khaledi

Department of Chemistry, North Carolina State University, Box 8204, Raleigh, NC 27695-8204 (USA)

ABSTRACT

The migration behavior of an homologous series of phenols in micellar electrokinetic chromatography is quantitatively presented. This model describes mobility in terms of fundamental physical and chemical constants of each solute (acid dissociation constant K_a , micelle binding constant K^m), the pH of the buffer, and the micelle concentration ($[M]$) in the buffer. The model was used to predict the mobility of each solute over a two-dimensional pH/ $[M]$ space. Predicted and actual electropherograms show the usefulness of this technique.

INTRODUCTION

In any separation technique it is desirable to have the option of manipulating a variety of parameters in order to affect and subsequently control the quality of a separation. In high-performance capillary electrophoresis (HPCE), the urgency for controlling migration and selectivity has been lessened because of the high efficiency of the technique. There are cases, however, in which manipulation of the separation selectivity parameters is needed [1–9]. Until recently, however, little work has been performed in the areas of prediction of migration behavior and subsequent optimization of the separation.

Recently, models that describe the migration behavior of solutes have been developed [10]. These models describe migration in terms of fundamental physical and chemical parameters of the solutes: pK_a , micelle–water binding constant, and (for acidic

or anionic solutes) the mobility of the anionic solute in the absence of micelles. A model was used to correctly predict the migration behavior and optimize the capillary zone electrophoretic (CZE) separation of halogenated phenols in aqueous buffer through manipulation of buffer pH [11]. However, CZE separation of solutes with similar pK_a values was inadequate.

The inclusion of a second chemical equilibrium, namely the solute association equilibrium with micelles, is discussed in this paper. The results of the prediction of migration behavior in micellar electrokinetic capillary chromatography (MECC) using the mathematical models are presented.

EXPERIMENTAL

The experimental apparatus and calculations have been presented in detail previously [11], and follow the work of Jorgenson and Lukacs [12]. The experimental reagent differs only by the inclusion of sodium dodecyl sulfate (SDS; Fisher Scientific, Raleigh, NC, USA) as the surfactant and Sudan III (Aldrich, Milwaukee, WI, USA) as the marker for the elution of the micelles injected with the sample. The procedure differs only by the alteration of the pH range to 8–12.

Correspondence to: Dr. M. G. Khaledi, Department of Chemistry, North Carolina State University, Box 8204, Raleigh, NC 27695-8204, USA.

[☆] Present address: Magellan Laboratories Incorporated, P.O. Box 13341, Research Triangle Park, NC 27709, USA.

RESULTS AND DISCUSSION

The mobility of an acidic solute in MECC can be described by the following model [10]:

$$\mu = \frac{\mu_{\text{HA}} + \mu_{\text{A}^-}(K_{\text{a,app}}/[\text{H}^+])}{1 + (K_{\text{a,app}}/[\text{H}^+])} \quad (1)$$

where μ is the total mobility of the solute, μ_{HA} is the mobility of the neutral form of the solute, μ_{A^-} is the mobility of the anionic form, and $K_{\text{a,app}}$ is the apparent acid dissociation constant in micellar media. The mobilities of the neutral and anionic forms of the solute are defined as follows:

$$\mu_{\text{HA}} = \frac{K_{\text{HA}}^{\text{m}} [\text{M}] \mu_{\text{mc}}}{1 + K_{\text{HA}}^{\text{m}} [\text{M}]} \quad (2)$$

and

$$\mu_{\text{A}^-} = \frac{\mu_{\text{A}^{\text{aq}}} + K_{\text{A}^-}^{\text{m}} [\text{M}] \mu_{\text{mc}}}{1 + K_{\text{A}^-}^{\text{m}} [\text{M}]} \quad (3)$$

where K^{m} is the binding constant of the solute form to micelles, $[\text{M}]$ is the concentration of surfactant present as micelles, μ_{mc} is the mobility of the micelles, and $\mu_{\text{A}^{\text{aq}}}$ is the mobility of the anionic form in the absence of micelles. The concentration of surfactant present as micelles is the total surfactant concentration ($[\text{S}]$) minus the critical micelle concentration (CMC).

Eqn. 1 predicts a sigmoidal behavior for the variation of mobility as a function of pH. At low pH values ($\leq \text{p}K_{\text{a,app}} - 2$) the acid is uncharged and mobility is a result of binding with the mobile micelles as described in eqn. 2. Conversely, at high pH ($\geq \text{p}K_{\text{a,app}} + 2$) the acid is fully charged and the mobility is a combination of two factors: the binding with the mobile micelles and the mobility in the absence of micelles, as described in eqn. 3.

Using these three equations, the mobility of a solute is described in terms of fundamental physical and chemical constants characteristic of each solute. By knowing the values of these constants, the mobility of the solute can be predicted for any pH and micelle concentration.

By measuring mobility over a pH range that is within $\text{p}K_{\text{a,app}} \pm 2$, the unknown parameters ($\text{p}K_{\text{a,app}}$, μ_{A^-} and μ_{HA}) can be determined using weighted non-linear (WNLIN) regression. WNLIN regression is an iterative algorithm that estimates the

values of the unknown parameters in order to minimize the error in the fit.

If $\text{p}K_{\text{a,app}}$ is known, it is possible to determine μ_{A^-} and μ_{HA} without WNLIN regression by measuring the mobility at $\text{pH} = \text{p}K_{\text{a,app}} - 2$ (for μ_{HA}) and $\text{pH} = \text{p}K_{\text{a,app}} + 2$ (for μ_{A^-}).

Calculation of $K_{\text{A}^-}^{\text{m}}$ and K_{HA}^{m}

The migration factor k' of the charged and the neutral solute species can be calculated from μ_{A^-} and μ_{HA} :

$$k'_{\text{HA}} = \frac{\mu_{\text{HA}}}{\mu_{\text{mc}} - \mu_{\text{HA}}} \quad (4)$$

and

$$k'_{\text{A}^-} = \frac{\mu_{\text{A}^-} - \mu_{\text{A}^{\text{aq}}}}{\mu_{\text{mc}} - \mu_{\text{A}^-}} \quad (5)$$

Terabe and co-workers [13,14] pointed out the relationship between k' and K^{m} :

$$k' = (P^{\text{m}}V)/([\text{S}] - \text{CMC}) \quad (6)$$

where P^{m} is the water–micelle partition coefficient and V is the molar volume of the micelles. (The term $P^{\text{m}}V$ is shown in Appendix 1 of this paper to be equal to K^{m} .) Therefore, K^{m} is the slope when k' is graphed as a function of surfactant concentration. In all, there are two ways to calculate $K_{\text{A}^-}^{\text{m}}$ and K_{HA}^{m} : first, by using WNLIN estimates of $\text{p}K_{\text{a,app}}$, μ_{A^-} and μ_{HA} in eqns. 2 and 3; and second, by plotting k' as a function of $[\text{SDS}]$ according to eqn. 6.

Most of the experiments were designed to generate data for use with WNLIN regression. This WNLIN data set was collected at nine pH values (8–12, 0.5 increments) and two surfactant concentrations (20 and 80 mM). (Since the variation of mobility as a function of pH is sigmoidal but the variation with surfactant concentration is linear, more pH data are required for reliable operation of WNLIN regression.) These data were used in the first method described above, and were used in the prediction of migration behavior that will be discussed later. In order to test the second method, a separate set of data more appropriate for the linear form of eqn. 6 was collected at two pH values (8 and 12) and four surfactant concentrations (20, 40, 60 and 80 mM).

The $K_{\text{A}^-}^{\text{m}}$ and K_{HA}^{m} values calculated from the two

TABLE I

COMPARISON OF MICELLE BINDING CONSTANTS K_{HA}^m AND $K_{A^-}^m$

| | | 4-Propyl-phenol | 4-Methyl-phenol | 4-Ethyl-phenol | 4-Isopropyl-phenol | Phenol |
|--------------------|--------------------|-----------------|-----------------|----------------|--------------------|--------|
| Set 1 ^a | K_{HA}^m | 11.1 | 30.1 | 74.6 | 155.4 | 200.6 |
| | σK_{HA}^m | 0.7 | 0.6 | 2.9 | 28.6 | 27.1 |
| | $K_{A^-}^m$ | -0.74 | 2.8 | 13.1 | 26.0 | 45.8 |
| | $\sigma K_{A^-}^m$ | 1.10 | 1.2 | 6.2 | 21.2 | 79.2 |
| Set 2 ^b | K_{HA}^m | 8.09 | 21.47 | 51.03 | 105.90 | 137.70 |
| | σK_{HA}^m | 0.77 | 0.95 | 1.23 | 1.64 | 1.87 |
| | $K_{A^-}^m$ | 2.82 | 8.60 | 18.29 | 30.52 | 38.12 |
| | $\sigma K_{A^-}^m$ | 0.95 | 0.90 | 1.00 | 1.31 | 1.44 |

^a Based on WNLIN estimates of μ_{A^-} and μ_{HA} from data taken at nine pH and two [SDS] values, using eqn. 1.

^b Based on linear regression of data taken at pH 8 and 12 and 20, 40, 60 and 80 mM SDS using eqn. 6.

data sets are presented in Table I for phenol and four alkylphenols. Both sets show the same trend of an increase in K^m with hydrophobicity of the phenol substituent. When $\ln K^m$ is plotted as a function of the number of substituent carbons on the phenol, as shown in Fig. 1, all sets show the expected linear behavior.

Fig. 2 shows k' as a function of [SDS] for the five solutes at low pH, where the solutes are neutral. According to eqn. 6, the x -intercept is the CMC. In Fig. 2, the value of 4 mM appears to be valid. Fig. 3 is the same as Fig. 2 except at high pH, where the

solutes are charged. Note that the correlation of the data to the linear regression fit is equally as good in Figs. 2 and 3; however, the x -intercept in Fig. 3 for four of the five solutes is in the range -20 to -22 mM. Of course, negative concentration has no physical meaning, but cannot be dismissed on the basis of misinterpreted data or faulty calculations.

Prediction of mobility

After determining estimates of $pK_{a,app}$, μ_{A^-} and μ_{HA} by WNLIN regression, eqns. 2, 3 and 4 can be used to predict mobility over the entire pH/SDS

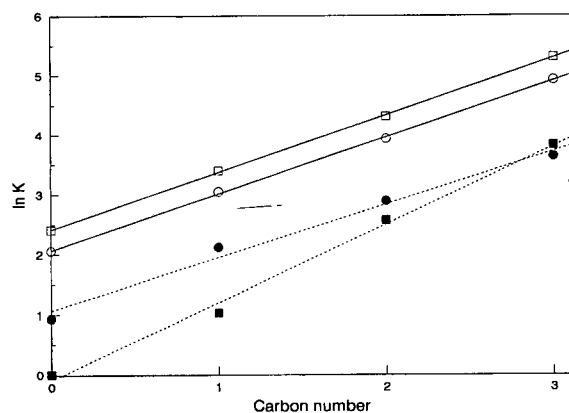


Fig. 1. Relationship between $\ln K_{HA}^m$ (—) and $\ln K_{A^-}^m$ (---) and the number of carbons in the phenol substituent for set 1 (\square and \blacksquare) and set 2 (\circ and \bullet).

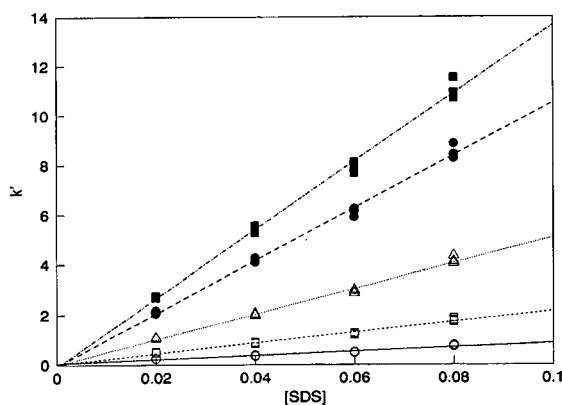


Fig. 2. k' as a function of SDS concentration at pH 8 for the neutral forms of phenol (\circ), 4-methylphenol (\square), 4-ethylphenol (\triangle), 4-isopropylphenol (\bullet) and 4-propylphenol (\blacksquare).

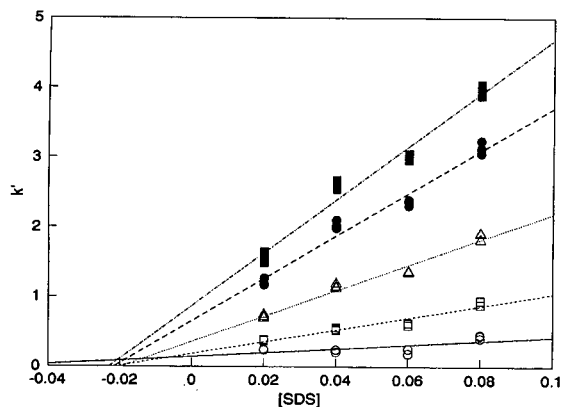


Fig. 3. k' as a function of SDS concentration at pH 12 for the anionic forms of phenol (○), 4-methylphenol (□), 4-ethylphenol (△), 4-isopropylphenol (●) and 4-propylphenol (■).

space. Figs. 4 and 5 show the mobility surface for two hypothetical components. The component represented in Fig. 4 strongly interacts with micelles in its neutral form ($K_{HA}^m = 220$) and moderately in its anionic form ($K_A^m = 1$). This component is typical of phenols such as the propylphenols and the di-, tri- and pentachlorophenols. The shape of the sigmoidal curve along the pH axis is generally unchanged as a function of [SDS], and the increase in [SDS] slightly increases mobility. Greatest mobility occurs at pH 8

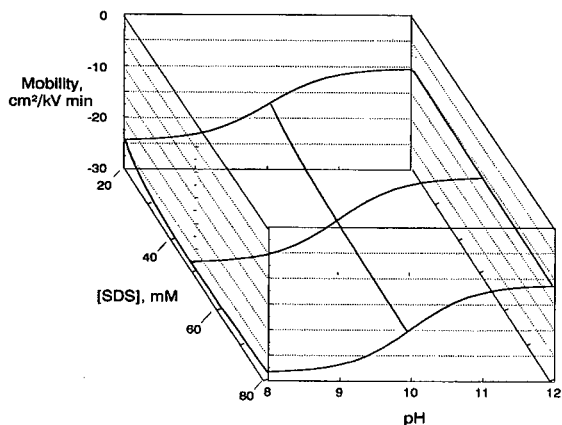


Fig. 4. Variation of mobility as a function of both pH and [SDS] for a hypothetical solute, based on the following values: $K_{HA}^m = 220$; $K_A^m = 0.8$; $\mu_{A^-} = -11$; $\mu_{HA} = -27.5$; $\mu_{aq} = -10$ and $\mu_{mc} = -30$.

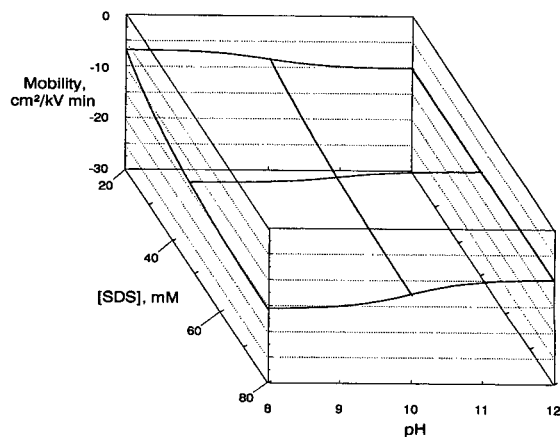


Fig. 5. Variation of mobility as a function of both pH and [SDS] for a hypothetical solute, based on the following values: $K_{HA}^m = 14$; $K_A^m = 0.002$; $\mu_{A^-} = -10.25$; $\mu_{HA} = -12.5$; $\mu_{aq} = -10$ and $\mu_{mc} = -30$.

and [SDS] = 80 mM, which is expected since this point is where the fraction of the neutral form of the solute and the concentration of micelles are the greatest.

The contrast to the strongly interacting component in Fig. 4 is the weakly interacting component in Fig. 5. The degree of interaction with micelles of the neutral ($K_{HA}^m = 14$) and anionic ($K_A^m = 0.002$) forms are representative of phenols such as methyl- and ethylphenol and fluoro-, chloro- and bromophenol. The mobility at high pH is constant over the entire [SDS] range, typical of anionic solutes that interact poorly with micelles.

The shape of the sigmoidal curve along the pH axis changes considerably as a function of [SDS], illustrating the importance of [SDS] on whether the mobility of the neutral form of the solute is greater or less than the anionic form.

The mobilities of the alkylphenols were predicted using the values of $pK_{a,app}$, μ_{A^-} and μ_{HA} estimated by WNLIN. As shown in Table II, $pK_{a,app}$ as estimated by WNLIN did not exhibit consistent behavior as a function of micelle concentration. To account for this variation, an estimate of $pK_{a,app}$ was made by extrapolating between the values measured at 20 and 80 mM.

Mobility predictions were made at six pH/SDS locations: 8.0/20, 8.8/20, 9.5/20, 9.9/63, 9.5/77 and 10.1/77. The first three points were selected for their importance in the separation optimization, which

TABLE II

pK_a VALUES OF PHENOL AND FOUR ALKYLPHENOLS, AS ESTIMATED BY WEIGHTED NON-LINEAR REGRESSION, AT 0, 20 AND 80 mM SDS

| | pK_a | | | |
|-------------------|---------|----------|-----------|-----------|
| | Ref. 16 | 0 mM SDS | 20 mM SDS | 80 mM SDS |
| Phenol | 9.99 | 9.98 | 9.65 | 9.66 |
| 4-Methylphenol | 10.26 | 10.29 | 9.94 | 10.46 |
| 4-Ethylphenol | | 10.22 | 9.19 | 10.19 |
| 4-Isopropylphenol | 10.28 | 10.37 | 9.84 | 10.31 |
| 4-Propylphenol | | 10.33 | 10.24 | 10.27 |

will be discussed later. The last three hold no particular significance. The correlation between actual and predicted mobilities are presented in Fig. 6. From linear regression, the slope of the best fit of the data (1.013) is very close to the slope expected from perfect correlation (1.000); also, the high correlation coefficient ($r^2 = 0.998$) indicates the usefulness of eqn. 1 as a model of mobility.

The pH range selected in this study was well suited for the alkylphenols since it covered the range of $pK_a \pm 2$. If data are not collected within the $pK_a \pm 2$ range the estimates will become inaccurate. An

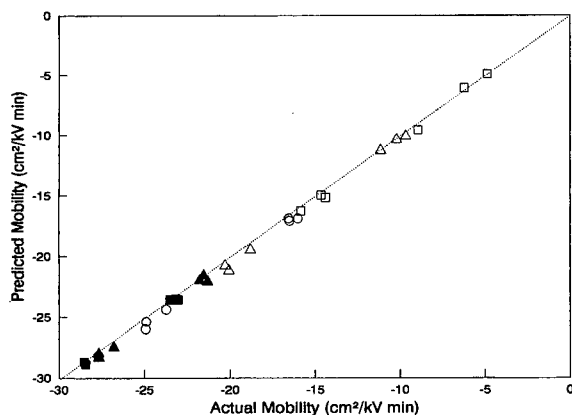


Fig. 6. Correlation between predicted and actual mobilities of phenol (□), 4-methylphenol (△), 4-ethylphenol (○), 4-isopropylphenol (▲) and 4-propylphenol (■) at the six pH/SDS locations described in the text. The line represents the ideal case of 1:1 correlation.

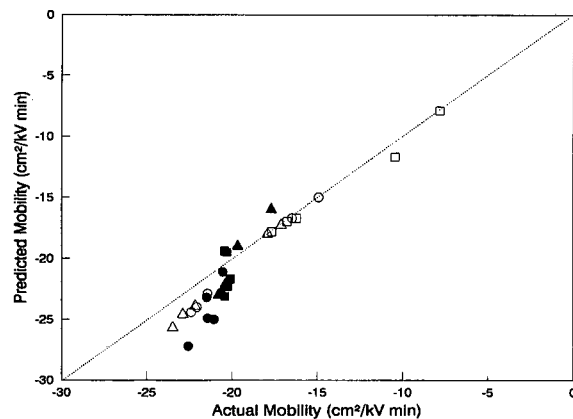


Fig. 7. Correlation between predicted and actual mobilities of 4-fluorophenol (□), 4-bromophenol (△), 4-chlorophenol (○), 2-chlorophenol (▲), 2,5-dichlorophenol (■) and 3,5-dichlorophenol (●) at the six pH/SDS locations described in the text. The line represents the ideal case of 1:1 correlation.

example of this is illustrated in Fig. 7, which is the correlation between predicted and actual mobilities for a set of halogen-substituted phenols. Reasonable correlation exists for 4-fluorophenol, which has a $pK_{a,app}$ of approximately 9.5. As the $pK_{a,app}$ for the solutes shifts away from the center of the pH range studied (pH 10), the correlation becomes increasingly worse. The lowest correlations are for 2,5- and 3,5-dichlorophenol, which have $pK_{a,app}$ values of approximately 7.7 and 8.8, respectively.

Optimization of separations: a preliminary study

In the optimization of separations in CZE, the resolution between the worst resolved peak pair was used as the criterion [11]. Resolution, in its simplest form, is described by refs. 12 and 15:

$$R = \frac{N^{1/2}}{4} \left(\frac{\mu_2 - \mu_1}{\mu_{avg} + \mu_{eo}} \right) \quad (7)$$

where N is the separation efficiency, μ_{avg} is the average mobility of the solutes, and μ_{eo} is the electroosmotic mobility. Resolution is directly proportional to the difference in the mobilities of two solutes ($\mu_2 - \mu_1$). For this preliminary study, this term was used as the optimization criterion.

The minimum $\mu_2 - \mu_1$ over the pH/SDS space is presented in Fig. 8 for the alkylphenol mixture. The optimum separation is at pH 9.4 and 21 mM SDS. Experiments were performed at pH 9.5 and 20 mM

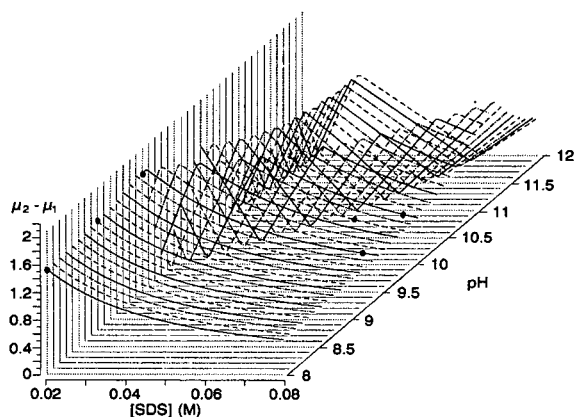
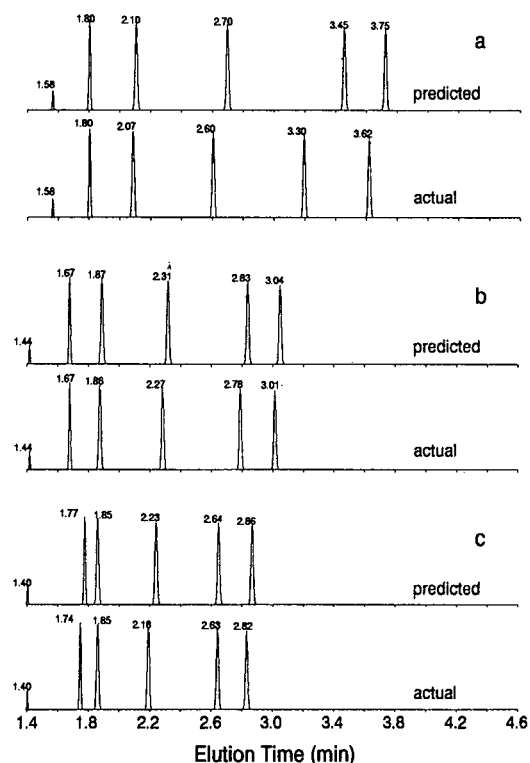


Fig. 8. Smallest difference in mobility between peak pairs as a function of both pH and [SDS]. The circles indicate the pH/SDS locations where confirmatory experiments were performed.



SDS, as mentioned previously, in addition to two other points at 20 mM SDS and three in a featureless region at higher SDS concentration. These points are highlighted in Fig. 8.

The actual and predicted electropherograms at each of the six pH/SDS locations are reconstructed from the elution times in Fig. 9a–f. There is excellent agreement at the predicted optimum and at a location near the optimum (Fig. 9b and c). Some of the difference between predicted and actual elution times is most likely due to the extreme sensitivity of the predicted elution time on the value selected as t_0 . For example, if the t_0 in Fig. 9a were 1.56 rather than 1.58, the elution times would be 1.77, 2.06, 2.64, 3.35 and 3.63 min, respectively.

Propagation of error in predicting mobility

In all, seven terms are used in the prediction of mobility: pH, [SDS], $pK_{a,app}$, μ_{HA} , μ_{A^-} , μ_{mc} and μ_{aq} . The mobility terms are used to first estimate $K_{A^-}^m$ and K_{HA}^m , which are then used in the prediction of

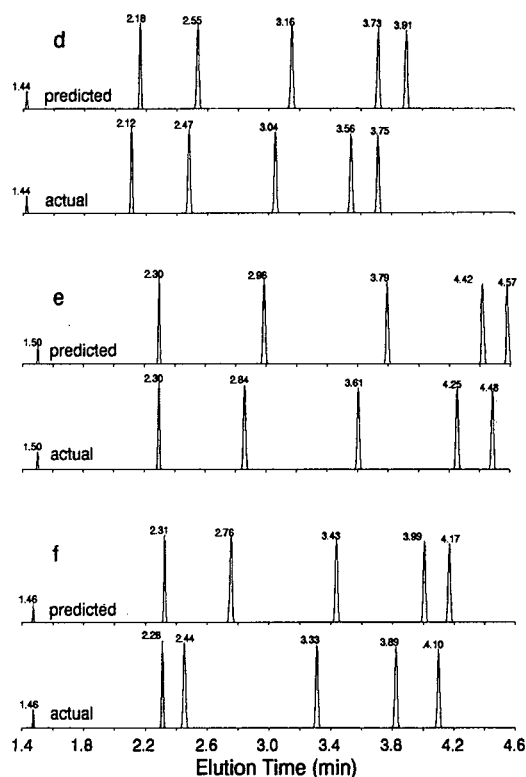


Fig. 9. Predicted and actual elution times at the six pH/SDS locations: (a) 8.0/20; (b) 8.8/20; (c) 9.5/20; (d) 9.9/63; (e) 9.5/77 and (f) 10.1/77. Electropherograms were reconstructed from elution time data.

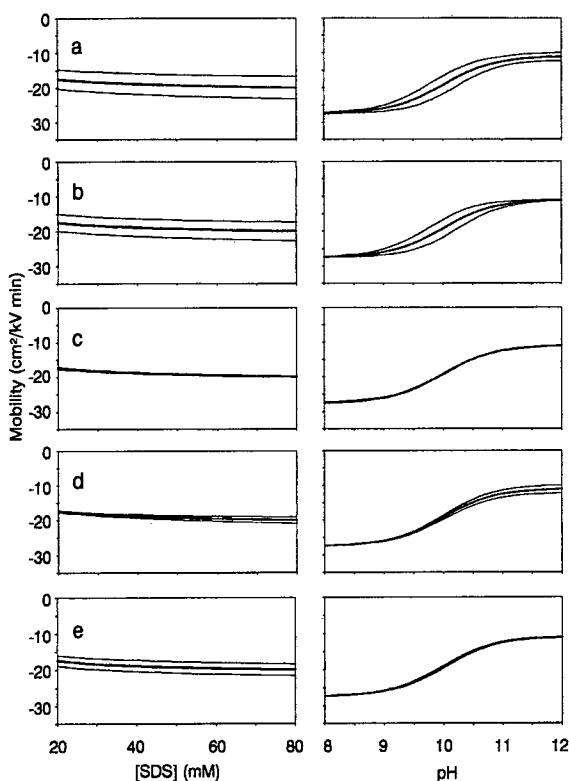


Fig. 10. Total propagated error and individual contributions of five terms to the total error for the hypothetical solute presented in Fig. 4. Each graph presents the mobility (thick line) and the error envelope (thin lines) as a function of either [SDS] at pH 10 (left column) or as a function of pH at 50 mM SDS. For this solute, the error associated with each contributing term are as follows: (a) total propagated error; (b) $\sigma pK_a = 0.4$; (c) $\sigma K_{HA}^m = 13$; (d) $\sigma K_A^m = 1.28$ and (e) $\sigma pH = 0.02$.

mobility. The total propagated error for the strongly interacting hypothetical solute illustrated in Fig. 4 and the contribution to the total error from five each of these terms is presented in Fig. 10a-e. (The contributions of $\sigma[SDS]$, $\sigma\mu_{mc}$ and $\sigma\mu_{aq}$ are negligible.) The graphs on the left were calculated at pH 10; those on the right were calculated at 50 mM SDS.

In general, the total error is very small at low pH but rapidly increases to a near-constant level at the pK_a of the hypothetical compound. In Fig. 9, the agreement between predicted and actual elution times became worse with increasing surfactant concentration. This suggests that the main contribution to the error is from K_A^m , since it increases with both

pH and [SDS] and since it, along with $pK_{a,app}$, are the largest contributors to the total error.

The total error in the prediction of mobility will also impact on the level of confidence in the prediction of elution order. This problem was addressed in the work with optimization in CZE [11]. The level of confidence in the ability to predict elution order is proportional to the difference in the predicted mobilities of the solutes and inversely proportional to the error associated with the predicted mobilities, as shown in eqn. 8:

$$t = \frac{n^{1/2}(\mu_1 - \mu_2)}{(\sigma_1^2 + \sigma_2^2)^{1/2}} \quad (8)$$

where t is the t -distribution value, μ_1 and μ_2 are the average mobilities of solutes 1 and 2, σ_1 and σ_2 are the standard deviations of the mobilities of solutes 1 and 2, and n_1 and n_2 are the number of measurements. This relationship assumes $n_1 = n_2$.

In conclusion, two chemical equilibria characteristic of each solute, pK_a and K^m , can be easily exploited by adjusting the pH and [SDS] of the buffer for the purpose of migration prediction and optimization of the separation. The migration behavior of solutes can be predicted on the basis of a few experiments.

ACKNOWLEDGEMENTS

The authors gratefully acknowledge a research grant from the National Institutes of Health (FIRST Award, GM 38738). The authors also gratefully acknowledge the use of the loan of the SP-4200 integrator from Burroughs Wellcome Company. The authors also acknowledge Joost K. Strasters for assistance in the preparation of some of the figures.

APPENDIX

Relationship between binding constant and partition coefficient

It has been reported [17,18] that the relationship between the binding constant K^m and the partition coefficient P^m is:

$$K = (P - 1) V \quad (A1)$$

where V is the volume occupied by one mole of surfactant present as micelles. Use of this equation has resulted in conflicting results in early derivation

of the models used for this and previous studies. The conflicts were resolved upon re-derivation of eqn. A1, as follows.

Given:

$$P = \frac{\text{concentration of solute in micellar phase}}{\text{concentration of solute in aqueous phase}} = \frac{[S]_m}{[S]_w} = \frac{n_{s,m}/v_m}{n_{s,w}/v_w} = \frac{n_{s,m}v_w}{n_{s,w}v_m}$$

and

$$K = \frac{\text{concentration of solute-micelle complex}}{(\text{concentration of solute in aqueous phase})(\text{concentration of micelles in aqueous phase})}$$

$$= \frac{[S-M]_w}{[S]_w[M]_w} = \frac{n_{s-m}/v_w}{(n_{s,w}/v_w)(n_m/v_w)} = \frac{n_{s-m}}{n_{s,w}n_m/v_w} = \frac{n_{s-m}v_w}{n_{s,w}n_m}$$

Assuming one solute molecule binds with or partitions with one micelle, the number of solute molecules in micelles must also be the number of solute-micelle complexes and $n_{s,m} = n_{s-m}$. Combining the above equations yields

$$K = P \frac{v_m}{n_m}$$

Given that V = molar volume of surfactant = v_m/n_m ,

$$K = PV \quad (\text{A2})$$

REFERENCES

- 1 A. S. Cohen, S. Terabe, J. A. Smith and B. L. Karger, *Anal. Chem.*, 59 (1987) 1021–1027.
- 2 S. Honda, S. Iwase, A. Makino and S. Fujiwara, *Anal. Biochem.*, 176 (1989) 72–77.
- 3 P. Gozel, E. Gassman, H. Michelson and R. N. Zare, *Anal. Chem.*, 59 (1987) 44–49.
- 4 S. Fujiwara and S. Honda, *Anal. Chem.*, 59 (1987) 487–490.
- 5 I. Jelinek, J. Dohnal, J. Snopek and E. Smolkova-Keulemansova, *J. Chromatogr.*, 435 (1988) 496–500.
- 6 I. Jelinek, J. Snopek and E. Smolkova-Keulemansova, *J. Chromatogr.*, 405 (1987) 379–384.
- 7 S. Fanali, *J. Chromatogr.*, 474 (1989) 441–446.
- 8 A. Guttman, A. Paulus, A. S. Cohen, N. Grinberg and B. L. Karger, *J. Chromatogr.*, 448 (1988) 41–53.
- 9 S. Terabe, H. Ozaki, K. Otsuka and T. Ando, *J. Chromatogr.*, 332 (1985) 211–217.
- 10 M. G. Khaledi, S. C. Smith and J. K. Strasters, *Anal. Chem.*, 63 (1991) 1820–1830.
- 11 S. C. Smith and M. G. Khaledi, *Anal. Chem.*, submitted for publication.
- 12 J. W. Jorgenson and K. D. Lucacs, *Anal. Chem.*, 53 (1981) 1298.
- 13 S. Terabe, K. Otsuka and T. Ando, *Anal. Chem.*, 57 (1985) 834–841.
- 14 S. Terabe, K. Otsuka, K. Ichikawa, A. Tsushiya and T. Ando, *Anal. Chem.*, 56 (1984) 111.
- 15 J. C. Giddings, *Sep. Sci.*, 4 (1969) 181–189.
- 16 W. Schultz, G. W. Riggan and S. K. Wesley, in K. L. Kaiser (Editor), *QSAR in Environmental Toxicology*, Vol. II, Reidel Publishing Co., New York, 1987, p. 333.
- 17 I. V. Berezin, K. Martinek and A. K. Yatsiminski, *Russ. Chem. Rev.*, 42 (1973) 778.
- 18 W. H. Hinze, in W. L. Hinze and D. W. Armstrong (Editors), *Ordered Media in Chemical Separations (ACS Symposium Series, Vol. 342)*, American Chemical Society, Washington, DC, 1987, p. 17.

Polymer- and surfactant-coated capillaries for isoelectric focusing

Xian-Wei Yao and Fred E. Regnier

Department of Chemistry, Purdue University, West Lafayette, IN 47907 (USA)

ABSTRACT

This paper reports a method for deactivation of fused-silica capillaries to be used in capillary isoelectric focusing (cIEF). Deactivation was achieved by adsorbing either a surfactant or hydrophilic polymer to alkylsilane-derivatized capillaries. The surfactant PF-108 and methyl cellulose reduced electro-osmotic flow (EOF) 20 to 30 fold in comparison to underivatized capillaries. Although EOF was reduced sufficiently to allow focusing to permit separations to be completed before proteins were swept through the capillary, there was adequate flow to obviate the need for a separate mobilization step. This reduces the complexity of cIEF and increases reproducibility. Based on resolution of hemoglobin variants, proteins that varied 0.03 pH units in isoelectric point were resolvable. This is equivalent to the highest resolution achieved in conventional slab and tube gel isoelectric focusing.

INTRODUCTION

Fused silica is widely used to fabricate the 10–100 μm I.D. capillaries used in capillary electrophoresis. The principal disadvantage of fused-silica capillaries in the electrophoresis and isoelectric focusing of proteins is that they tenaciously adsorb cationic species and show strong electro-osmotically driven flow [1]. These properties of fused silica arise from silanol ionization above pH 4.0 to produce a negatively charged surface. Whereas solute adsorption diminishes recovery and limits the analytical utility of data obtained from the separation, electro-osmosis compromises separation efficiency by sweeping the ampholyte and sample components out of the system before focusing is complete.

This problem has been addressed in several ways. One has been to adsorb methyl cellulose directly to the surface of the capillary [2,3]. The function of adsorbed methyl cellulose is to (1) physically exclude proteins from contact with the charged capil-

lary and (2) greatly increase the viscosity of the double layer adjacent to the silica surface. Although separations approaching those of conventional acrylamide gel-based systems have been achieved with capillaries coated in this manner, the longevity and shielding properties of this coating have not been established. A second approach is to covalently bond a polymer, such as polyacrylamide, to the capillary wall [4]. The function of the polymer layer and the separations that may be obtained with these capillaries are similar to those of the adsorbed polymer layer. The problem with coatings that contain ester and amide linkages is that they slowly hydrolyze, limiting capillary life [5].

Isoelectric focusing (IEF), as a separation technique in a capillary electrophoretic system may be divided into three steps. The first is creation of the pH gradient. This is achieved by focusing an ‘ampholyte’ solution containing a large number of ampholytic species, each with a different *pI*. When there are a large number of ampholyte species and the difference in their *pI* is small, a continuous pH gradient is formed. The second step is the introduction and focusing of sample components. Because this step is similar to step one, they are often com-

Correspondence to: F. E. Regnier, Department of Chemistry, Purdue University, West Lafayette, IN 47907, USA.

bined. The time required to focus both ampholyte and sample components depends on the slope of the pH gradient and the applied potential. These initial steps of isoelectric focusing are common to all IEF systems. It is the third step, mobilization, that is unique to capillary isoelectric focusing (cIEF). Mobilization refers to the process of adding an ionic species to the system which triggers the focused ampholyte and proteins to be transported past the detector. It has been the practice in cIEF to carry out focusing and mobilization in discrete steps [6].

This paper reports an alternative approach to surface deactivation that allows (c)IEF to be carried out either in the manner described above or to combine all of the steps into a single operation. The essential elements of this approach are to control both protein adsorption and the magnitude of electro-osmotic flow (EOF) through the adsorption of selected polymers and surfactants to octadecylsilane-derivatized capillaries.

EXPERIMENTAL

Chemicals

IEF markers (hemoglobin C, S, F and A) were a gift from Isolab (Akron, OH, USA). Methyl celluloses (MC), polyvinyl alcohol (PVA), polyvinyl pyrrolidone (PVP), Brij 35, mesityl oxide, toluene and octadecyltrichlorosilane were purchased from Aldrich (Milwaukee, WI, USA). PF108 was a gift from BASF (Parsippany, NJ, USA). Pharmalyte (pH 3–10) was purchased from Pharmacia (Piscataway, NJ, USA).

Instrumentation

cIEF was performed on a component system. A Spellman Model FHR 30P 60/EI (Spellman, Plainview, NY, USA) power supply was used to apply the electric field across the capillary. On-line detection was performed by mounting the surfactant-coated octadecylsilanederivatized capillary (either 50 μm I.D. or 25 μm I.D.) on a 254 nm UV absorbance detector (Bio-analytical System, West Lafayette, IN, USA). The detector signal was recorded with an OmniScribe recorder (Houston Instrument, Austin, TX, USA). High-voltage components of the system were placed in a Lucite cabinet with a safety interlock.

Capillary coating

The coating procedure was applied by a modification of the Town's procedure [7]. Fused-silica capillaries were first treated with 1.0 M NaOH for 30 min. They were then washed with deionized water and methanol, respectively, for 30 min each. The capillaries (25 μm I.D. or 50 μm I.D.) were placed in a GC oven at 90°C for 2 h with a nitrogen carrier stream at 400 kPa to evaporate the residual methanol. Octadecyltrichlorosilane with 50% toluene was then pushed through the capillaries by pressure. The capillaries were placed in the oven at 90°C for 6 h with new solution continuously being pushed through the capillaries. After 6 h of silylation, the residual octadecyltrichlorosilane and toluene were removed from the capillaries by pressure. The capillaries were then washed with methanol for 20 min and then with deionized water for 30 min. Surfactant solutions were pushed continuously through the capillaries for 6 h to complete the coating process.

cIEF process

The protein sample mixture was prepared by mixing the protein solution and Pharmalyte (pH 3–10) at a final ampholyte concentration of 1 to 2%. In the loading step, the capillary was filled with the sample mixture by positive pressure. The two ends of the capillary were placed into 10 mM phosphoric acid anolyte and 20 mM sodium hydroxide catholyte, respectively. Focusing was started by applying approximately 500 V/cm to the loaded capillary. The current dropped gradually to a constant "residual" value. This residual current, which is not zero because of EOF in the capillary, indicates the end of focusing.

Cathodic mobilization [6] and EOF mobilization [8] were both used to drive the formed pH gradient with the focused protein zones to the detector window. EOF mobilization utilized EOF in the capillary as the driving force. It combines the focusing and mobilization steps to simplify the operation of cIEF and eliminate possible error. EOF mobilization was employed for the separations reported in this paper. After each run, the capillary was flushed with the surfactant solution for a few minutes.

Capillaries of 25 μm I.D. have been found to have advantages over larger I.D. capillaries. Heat dissipation is more efficient due to the increased sur-

face area-to-volume ratio of smaller capillaries. Therefore higher voltage could be applied to achieve separations more rapidly.

RESULTS AND DISCUSSION

Surface modification

Surface modification to control both adsorption and electro-osmotic flow is an essential element of capillary isoelectric focusing. It has been established [7] that surfactants adsorbed to the surface of octadecylsilane-derivatized capillaries effectively control the protein adsorption problem while reducing EOF. These studies also suggested that the degree of reduction in EOF was proportional to the size of the hydrophilic portion of the surfactant. This led to the hypothesis in this work that EOF in a capillary could be adjusted to any desired value through the use of adsorbed surfactants and polymers of various size. It was further hypothesized that amphiphilic copolymers or oligomers containing both hydrophobic and hydrophilic monomers would adsorb to an octadecylsilane-derivatized surface in such a manner that hydrophobic groups would accumulate at the capillary surface and hydrophilic groups would be turned outward toward the aqueous phase. It was expected that these adsorbed coatings would shield the octadecylsilane surface from contact with proteins as they do in chromatographic applications [9].

These hypotheses were tested using octadecylsilane-derivatized capillaries to which one of the following surfactants or polymers had been adsorbed; Brij 35 surfactant, PF-108 surfactant, methyl cellulose, polyvinyl alcohol, or polyvinyl pyrrolidone. Coatings were applied by passing several hundred column volumes of a 0.4% polymer/surfactant solution through the alkylsilane-derivatized capillary. Subsequent separations were carried out using buffers containing 0.4% of the surfactant or polymer. It is seen in Fig. 1 that there is approximately a six-fold difference in EOF between the Brij 35 surfactant and methyl cellulose 4000 cP (MC-4000) coated capillaries. The EOF of the MC-4000- and PF-108-coated capillary was approximately 1/20 to 1/30 that of a native fused-silica capillary, depending on the pH at which the measurements are made. Prior work shows that this reduction in EOF may be attributed to two effects [7]. The first is due to

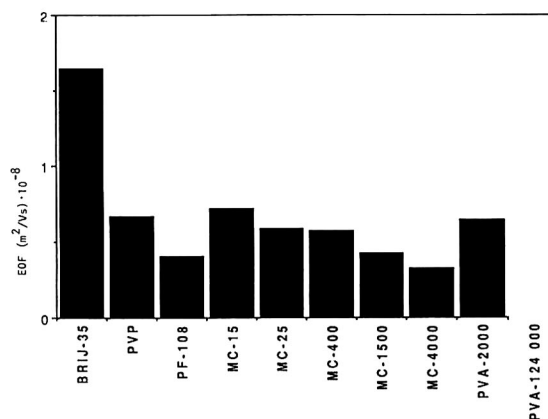


Fig. 1. Electro-osmotic flow of various polymer- and surfactant-coated octadecylsilane (C_{18}) derivatized capillaries. Experimental conditions of CZE: 50 μ m I.D. 120 cm separation length and 30 cm total length capillaries were employed to measure the retention time of the neutral marker (mesityl oxide) at pH 6 under 9 kV.

silylation of the capillary wall. Organosilane derivatization reduces the number of surface silanols and reduces the ζ potential which drives EOF. The second is due to the adsorbed polymer increasing the local viscosity at the capillary surface.

Adsorption of polymers at surfaces is generally thought to be by a loop-and-train mechanism [10]. As the molecular weight of the polymer becomes larger, the adsorbed coating becomes thicker and more viscous. Coating thickness is also proportional to the concentration of the coating solution [10]. This should cause the EOF of a coated capillary to decrease inversely with the molecular weight and concentration of polymer in the coating solution.

TABLE I

THE EFFECT OF POLYMER CONCENTRATIONS ON EOF

Experimental conditions: a PVA-2000-coated octadecylsilane-derivatized capillary, 75 μ m I.D., 30/20 cm in length, pH 6 phosphate buffer, under 9 kV.

| PVA in buffer (%) | PVA in capillary (%) | Retention of mesityl oxide (min) |
|-------------------|----------------------|----------------------------------|
| 0 | 0 | 9 |
| 0.4 | 0 | 14 |
| 0.4 | 0.4 | 18 |
| 0.4 | 4 | 24 |

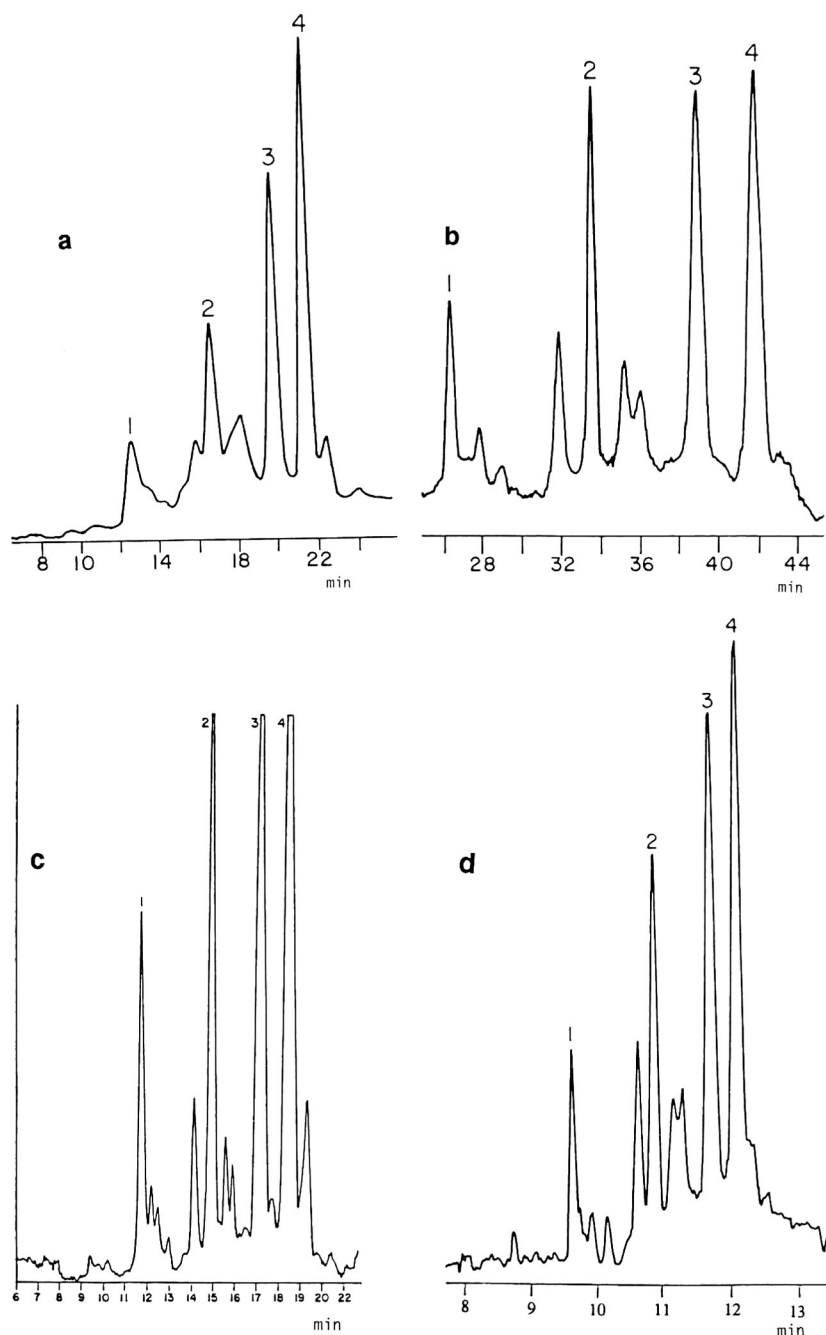


Fig. 2. Electropherograms of Hb variants separated by (a) a methyl cellulose (15 cP)-coated octadecylsilane-derivatized (MC-15 + C₁₈) capillary (25 μ m I.D. with 16 cm separation length and 20 cm total length); (b) a methyl cellulose (25 cP)-coated octadecylsilane-derivatized (MC-25 + C₁₈) capillary (25 μ m I.D. with 16 cm separation length and 20 cm total length); (c) a methyl cellulose (4000 cP)-coated octadecylsilane-derivatized capillary (25 μ m I.D. with 12 cm separation length and 16 cm total length); (d) a polyvinyl alcohol) 124 000-coated octadecylsilane-derivatized (PVA-124 000 + C₁₈) capillary (25 μ m I.D. with 11 cm separation length and 16 cm total length). Sample solutions: 1 mg/ml Hb in 1–2% ampholyte with a 0.2% polymer additive. Voltage: 500 V/cm. EOF mobilizations were employed without interrupting the experiments. The major peaks 1, 2, 3 and 4 are HbC, HbS, HbF and HbA, respectively.

As expected, EOF was inversely related to molecular weight of the coating polymer in both the case of methyl cellulose- and polyvinyl alcohol-coated capillaries (Fig. 1). However, less than a two-fold change in EOF was achieved by a large variation in polymer molecular weight. To achieve large differences in EOF, it is seen that different polymers must be used.

The impact of polymer concentration on EOF is seen in Table I. Columns initially coated with a 0.4% solution of PVA were further treated with 10 column volumes of either 0, 0.4 or 4% PVA. These capillaries were then operated with a buffer solution containing either 0 or 0.4% PVA. A capillary treated and operated with 0.4% PVA served as the control. The mesityl oxide transport time in the control system was 18 min. It is seen that pretreatment with 4% PVA increased the transport time to 24 min. The clear implication is that a thicker coating resulted from exposing the column to a higher concentration of polymer. In contrast, it is seen that pretreatment and operation with buffers that contain no polymer substantially reduced the transport time of the neutral marker. This behavior implies that PVA adsorption on an octadecylsilane-derivatized surface is very dynamic, readjusting rapidly with variations of polymer concentrations in the buffer.

EOF is perceived as a negative phenomenon in cIEF that causes protein mixtures to be swept past the detector before they are fully separated. Systems with no EOF are also limited in that a post-focusing mobilizer must be added to transport solutes to the detector [6]. An alternative to these two extremes would be to use a polymer-coated capillary in which EOF was adjusted to allow both complete focusing and transport simultaneously.

Evaluation of coated capillaries

The human hemoglobin (Hb) variants (C, S, F and A) have been widely used in the evaluation of isoelectric focusing systems. Literature values [11] for the isoelectric points of these proteins are as follows; HbC = 7.42, HbS = 7.20, HbF = 7.05, and HbA = 6.98. [It should be noted that the *pI* of these proteins in a separation system could be slightly different than these values.] These variants were readily separated in all of the methyl cellulose and polyvinyl alcohol-coated capillaries (Fig. 2).

Based on the resolution of the hemoglobin F and A pair, proteins that vary as little as 0.03 pH units in isoelectric point can be baseline resolved. Partial resolution can probably be achieved between proteins that vary 0.01 *pI* units.

The quality of these isoelectric focusing separations was evaluated in several ways. Visual inspection of the electropherograms shows that the best resolution was achieved with the MC-25-coated column. One is left with the clear impression that the coatings play a role in resolution, as will be shown below. The type of coating also contributes to analysis time because mobilization is achieved by EOF. By selecting from the series of polymers and surfactants in Fig. 1, it is possible to control both resolution and analysis time.

Other measures of the quality and resolution of an isoelectric focusing system are the linearity and slope of the pH gradient, *i.e.* $d(\text{pH})/d(\text{length})$. The more linear the pH gradient and the smaller the slope, the better the resolution of the system. Unfortunately it is not possible to measure pH directly in a capillary. Instead, it is necessary to determine the gradient from the elution time of standards. A plot of pH *versus* time is seen for a series of columns in Fig. 3. Slopes for these curves (m_t), linearity (R), and the standard deviation of data points is seen in Table II. The linearity is quite good, ranging from 0.995 to 1.000.

The most widely used method of specifying resolution in isoelectric focusing is in terms of the difference in *pI* of adjacent peaks, *i.e.* their resolution is defined as being equal to 1. If we assume that (i) the pH gradient is linear, (ii) these adjacent bands are of equal width, and (iii) the solutes are similar in diffusion coefficient, then

$$R_s = (t_2 - t_1)/0.5(\Delta t_2 + \Delta t_1) \quad (1)$$

where t_2 and t_1 are the elution times and Δt_2 and Δt_1 are the peak widths of proteins 2 and 1, respectively. Based on the assumptions that the peaks are of equal width and $R_s = 1$, this equation reduces to

$$\Delta t_2 = t_2 - t_1 \quad (2)$$

Since peak width may also be defined in terms of standard deviation where $\Delta t = 4\sigma$, then

$$4\sigma_2 = t_2 - t_1 \quad (3)$$

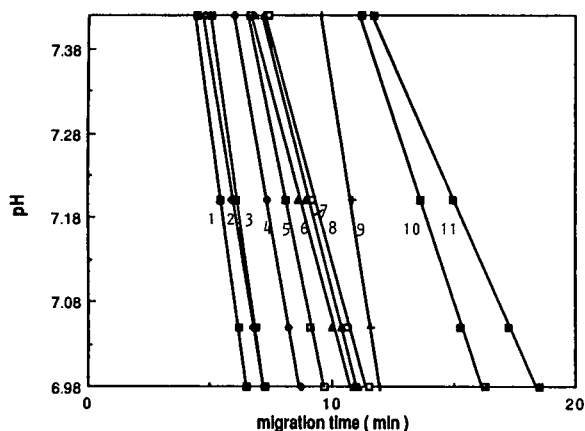


Fig. 3. The calibration curves of the separated Hb variant zones in a linear pH gradient by the coated capillaries. Experimental conditions of cIEF: 25 μm I.D. coated capillaries with 10–15 cm separation length and 14–20 cm total length. Sample solutions: 1 mg/ml Hb in 1–2% ampholyte with a 0.2% polymer additive. Voltage: 500 V/cm. EOF mobilizations were employed without interrupting the experiments. 1–5 = MC-15; 6–8 = MC-25; 10, 11 = MC-4000 and 9 = PVA 124 000.

According to Fig. 3, it is seen that

$$\text{pH} = m_i(t) + b \quad (4)$$

Substituting eqn. 4 in eqn. 3, it may be shown that

$$4 \sigma_2 = d(\text{pH})/m_i \quad (5)$$

where $d(\text{pH})$ is the difference in the pH between the peak maxima of the two solutes. But this difference in pH is the difference in the isoelectric point of the two proteins, therefore,

$$4 \sigma_2 = d(\text{pI})/m_i \quad (6)$$

A more exact description of resolution is given by the equation

$$\Delta pI = 3[D(m_i)/E(-du/\text{pH})]^{1/2} \quad (7)$$

TABLE II

ANALYSIS OF THE RESOLUTION AND LINEARITY OF THE VARIOUS COATED CAPILLARIES

| Coatings | n | mean of R^2 | S.D. | m.r. ΔpI^a | slope $m_i(\Delta \text{pH}/\Delta t)$ |
|------------------------|-----|---------------|--------|--------------------|--|
| C_{18} + MC-15 | 5 | 0.997 | 0.0010 | 0.050 | -0.1001 |
| C_{18} + MC-25 | 3 | 0.995 | 0.0015 | 0.029 | -0.0287 |
| C_{18} + MC-4000 | 2 | 0.998 | 0.0007 | 0.039 | -0.0648 |
| C_{18} + PVA-124 000 | 1 | 1.000 | — | 0.046 | -0.1815 |

^a m.r. ΔpI stands for the minimum resolvable ΔpI .

where D is the diffusion coefficient of the analyte, E is the applied field strength in V/cm, m_i is the slope of the pH vs. time calibration curve, and $-du/\text{pH}$ is the change in mobility with pH [12]. The problem with eqn. 7 is that it is difficult to obtain D and $-du/\text{pH}$ for many solutes. Eqn. 6 is more tractable experimentally. Although the assumptions made in deriving resolution eqn. 6 may not be valid in many cases, it is probably suitable for evaluating coating quality where the same analytes are used in all cases under nearly identical conditions. The impact of coating chemistry on resolution in terms of ΔpI is shown in Table II. The MC-25-coated capillary had more than twice the resolution of any other capillary. However, it also took the longest to achieve a separation. Resolution appears to be compromised in very rapid separations.

The effect of ampholyte concentration on resolution

Increasing the ampholyte concentration from 0.8 to 2% increased resolution (ΔpI values according to eqn. 6 are 0.054 and 0.038, respectively) (Fig. 4). It is thought that this was due to an increase in the buffer capacity and viscosity of the more concentrated ampholyte. Data to support this viscosity hypothesis will be provided below.

The impact of viscosity on resolution

According to eqn. 7, the diffusion coefficient (D) of a protein is directly proportional to ΔpI . This suggests that increasing the viscosity of the ampholyte to reduce D would enhance resolution. This was found to be true when 2% glycerol was used to increase viscosity (Fig. 5). However, it should be noted that elution time is substantially longer in the case of the separation with 2% glycerol. This means that the rate of electro-osmotic pumping was reduced with the higher viscosity ampholyte. Because

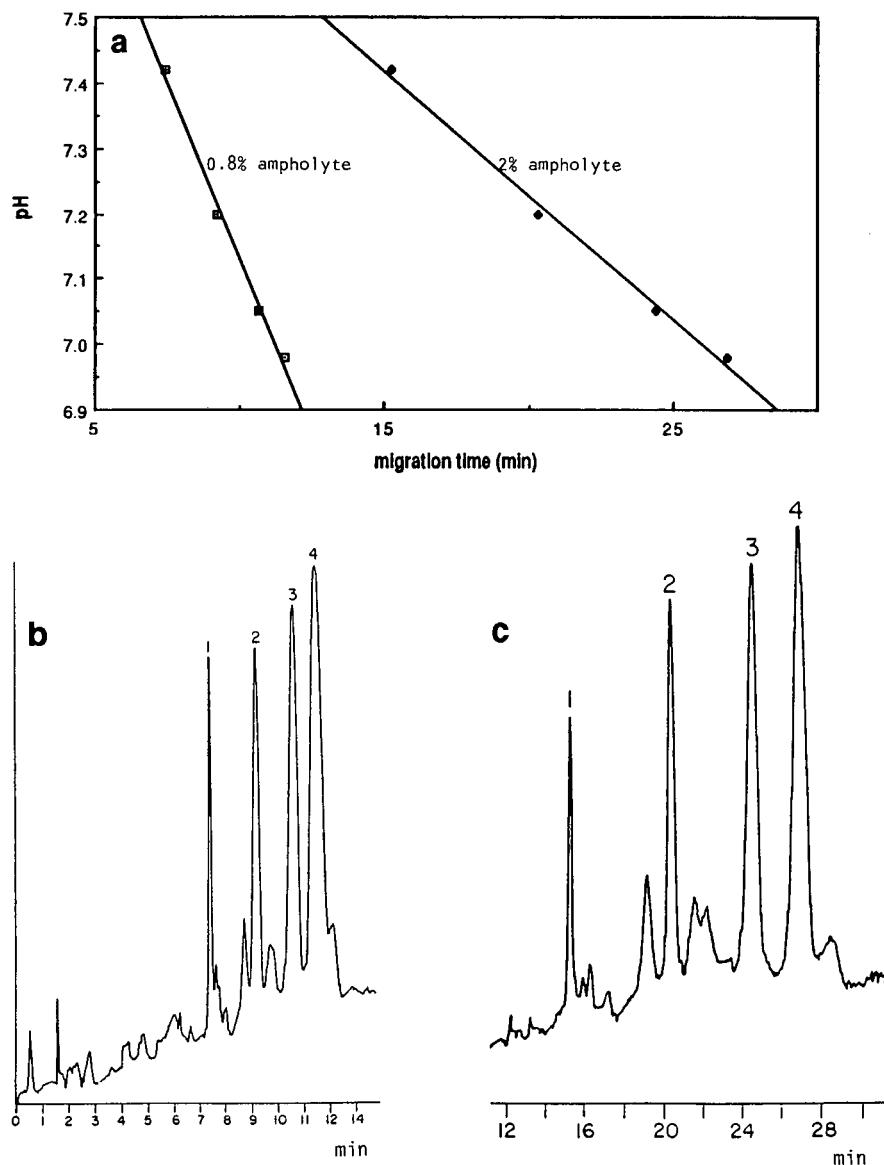


Fig. 4. The effect of the ampholyte concentration on resolution. (a) The effect on the calibration curves of the separated Hb variant zones. (b,c) Electropherogram comparison. (b) 0.8% ampholyte; (c) 2% ampholyte. cIEF conditions: A MC-25-coated capillary, 25 μm I.D. with 14 cm separation length and 18 cm total length. Sample solutions: 1 mg/ml Hb in (a) 0.8 and (b) 2.0% ampholyte with a 0.2% polymer additive. Voltage: 500 V/cm. EOF mobilizations were employed without interrupting the experiments. The major peaks 1, 2, 3 and 4 are HbC, HbS, HbF and HbA, respectively.

focusing and elution were achieved in 5–8 min, it could be that more complete focusing was achieved in the column with the lower electro-osmotic flow, *i.e.* the column with the 2% glycerol additive. Focusing at still higher viscosity proved negative (data not shown). This was attributed to the fact that fo-

cusing was achieved at 500 V/cm and too high viscosity causes overheating.

Reproducibility

Reproducibility between runs and batches was examined in the separation of hemoglobin variants.

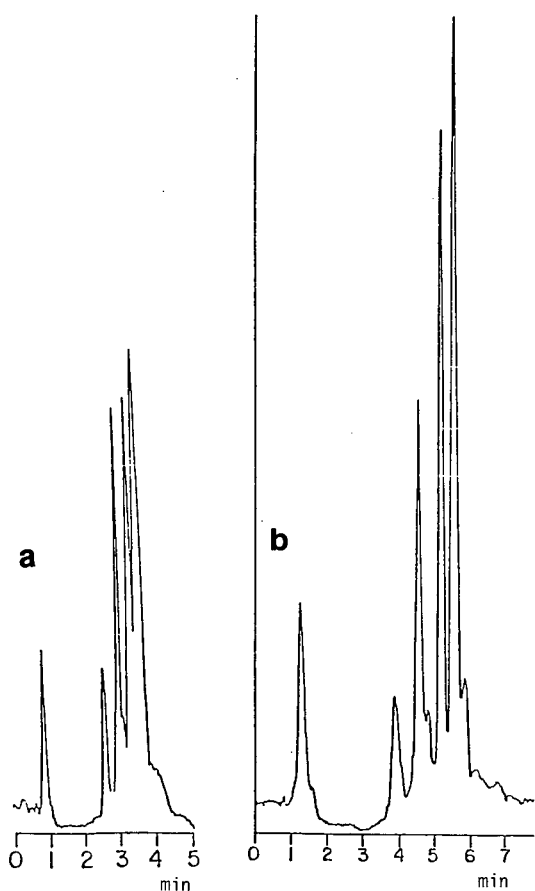


Fig. 5. Viscosity effects: (a) without glycerol, (b) with 2% glycerol. cIEF conditions: A MC-25-coated capillary, 25 μm I.D. with 10 cm separation length and 14 cm total length. Sample solutions: 1 mg/ml Hb in 0.2% ampholyte with a 0.2% polymer additive. Voltage: 500 V/cm. EOF mobilizations were employed without interrupting the experiments. The major peaks 1, 2, 3 and 4 are HbC, HbS, HbF and HbA, respectively.

A run to run comparison in a fast separation is shown in Fig. 6. Batch to batch comparisons were made with two different preparations of MC-25-coated capillaries. The coefficients of linearity for the two plots were 0.988 and 1.000 with an R.S.D. of 0.007. Resolution of the individual preparations computed from the peak width of hemoglobin F was 0.029 and 0.039 ΔpI .

CONCLUSIONS

It may be concluded that both surfactants and

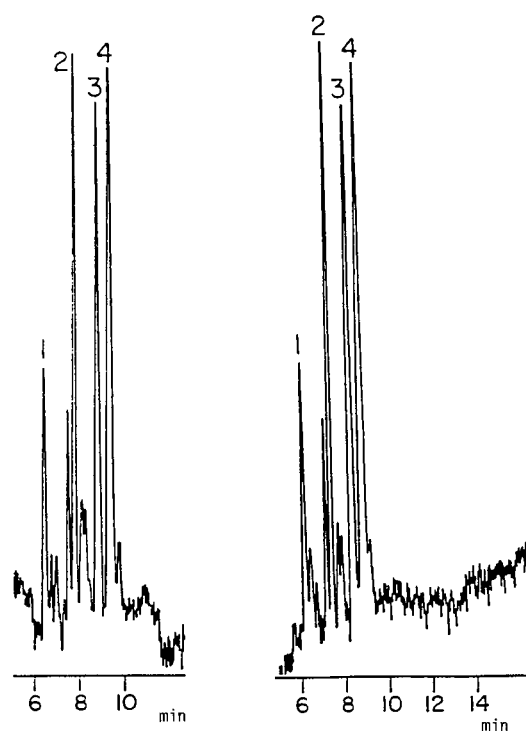


Fig. 6. Electropherograms of the two consecutive cIEF experiments. CIEF conditions: A MC-15-coated capillary, 25 μm I.D. with 10 cm separation length and 14 cm total length. Sample solutions: 1 mg/ml Hb in 1-2% ampholyte with a 0.2% polymer additive. Voltage: 500 V/cm. EOF mobilizations were employed without interrupting the experiments. The major peaks 1, 2, 3 and 4 are HbC, HbS, HbF and HbA, respectively.

hydrophilic polymers adsorbed to octadecylsilane-derivatized capillaries can effectively control electro-osmotic flow and the adsorption of proteins at the internal surface of fused-silica columns. Higher-molecular-weight polymers were more effective than low-molecular-weight surfactants in controlling electro-osmotic flow. Through control of electro-osmotic flow it was possible to combine the focusing and mobilization steps. Under ideal conditions the resolution of this capillary isoelectric focusing system approached that of conventional slab and tube gel systems. Moreover, separations were achieved in less than an hour in all cases.

ACKNOWLEDGEMENT

The authors gratefully acknowledge support

from the National Institute of Health (NIH grant number 35421).

REFERENCES

- 1 S. Hjerten, *J. Chromatogr.*, 347 (1985) 191.
- 2 S. Hjerten, *J. Chromatogr. Rev.*, 9 (1967) 122.
- 3 B. J. Herren, S. G. Shafer, J. V. Alstine, J. M. Harris and R. S. Snyder, *J. Colloid Interface Sci.*, 115 (1987) 46.
- 4 S. Hjerten, *J. Chromatogr.*, 347 (1985) 191.
- 5 K. Cobb, V. Dolnik and M. Novotny, *Anal. Chem.*, 62 (1990) 2478.
- 6 S. Hjerten and M.-D. Zhu, *J. Chromatogr.*, 346 (1985) 265.
- 7 J. K. Town and F. E. Regnier, *Anal. Chem.*, 63 (1991) 1126.
- 8 J. R. Mazzeo and I. S. Krull, *Anal. Chem.*, 63 (1991) 2852.
- 9 C. R. Desilets, M. A. Rounds and F. E. Regnier, *J. Chromatogr.*, 544 (1991) 25.
- 10 A. J. Alpert and F. E. Regnier, *J. Chromatogr.*, 185 (1979) 375.
- 11 *Data from the supplier*, Isolab, Akron, OH.
- 12 B. L. Karger, A. S. Cohen and A. Guttman, *J. Chromatogr.*, 492 (1989) 585.

Capillary electrophoresis of glycoconjugates in alkaline media

Morgan Stefansson and Douglas Westerlund

Department of Analytical Pharmaceutical Chemistry, Uppsala University, Biomedical Centre, S-751 23 Uppsala (Sweden)

ABSTRACT

Glycoconjugates were separated by capillary electrophoresis at alkaline pH and the migration order was investigated using different complex-forming agents in the electrolyte. Addition of cationic micelles, formed by cetrinide hydroxide, made the separation of anomers and element analogues possible. Boric acid gave the highest selectivity but the peak efficiency was slightly lower owing to slow kinetics of the complexation mechanism. Although the background electrolyte had very high pH values, no indications of instability of the fused-silica capillary or the analytes were observed under the separation conditions used.

INTRODUCTION

Carbohydrates pose separation and detection problems because of the large number of similar structures available and the inherent lack of chromophores and fluorescence properties. Extensive efforts have been made to separate carbohydrates, including the use of TLC, GC, LC, gel permeation, supercritical fluid and ion-exchange chromatography and electrophoresis [1]. In CE, solutes separate according to differences in electric charge and molecular size. For carbohydrates, this has been performed by derivatization [2,3] when charge and UV- or fluorescent-active groups were introduced into the solutes, thus enhancing the detection possibilities. Ionization of the solutes has also been achieved at alkaline pH [4] and by complex formation with borate [5,6] or alkaline earth metal ions [7].

Carbohydrates are weak acids [8] and partly charged at $\text{pH} \geq 12$. They can be separated depending on differences in their pK_a values, molec-

ular size or complexation with species present in the electrolyte.

The aim of this study was to compare the selectivities obtained by the use of different separation modes at alkaline pH, including micellar electrokinetic capillary chromatography (MECC) with a cationic detergent, complexation with borate and with a cationic polymer. 4-Nitro- (4-NP), 4-amino- (4-AP) and phenyl-substituted carbohydrates (glycosides) were used as model substances for on-line UV detection. Separations of glycoconjugates including element analogues and nucleosides are presented.

EXPERIMENTAL

Equipment

The capillary electrophoresis system used was a Model 3140 and a Model 3850 (ISCO, Lincoln, NE, USA), both equipped with a $67 \text{ cm} \times 50 \mu\text{m}$ I.D. fused-silica capillary (Polymicro Technologies, Phoenix, AZ, USA). The polyimide coating was burned off 26 cm from the cathode end of the capillary to form the observation window for on-line UV absorption detection. Electropherograms from the ISCO Model 3850 were recorded with a Kipp & Zonen BD 40 recorder. Different polarity modes

Correspondence to: M. Stefansson, Department of Analytical Pharmaceutical Chemistry, Uppsala University, Biomedical Centre, S-751 23 Uppsala, Sweden.

were used depending on the direction of the electroosmotic flow. Sample solutions diluted with water were introduced into the tube by gravity flow by raising one end of the tube 5 cm higher than the level of the opposite electrode solution for about 10 s. Analyses were carried out at ± 7 kV (-7 kV was used in the cetrimide and polybrene systems) and 27°C . Water obtained with a Milli-Q purification system (Millipore) was used to prepare all solutions.

Capillary conditioning

A new capillary was flushed with 1 M NaOH for 2 h, 0.1 M HCl for 30 min and 0.1 M NaOH for 30 min before the running buffer was introduced into the tube. Finally, the system was equilibrated by a pre-run for 10–15 min before analysis. The capillary was stored in running buffer overnight and rinsed with 0.1 M NaOH every morning and after changing the running buffer.

Chemicals

All test solutes except hexadecyltrimethylammonium (CTA) bromide (Fluka, Buchs, Switzerland) were obtained from Sigma (St. Louis, MO, USA). CTA bromide was converted into the corresponding hydroxide by shaking with silver oxide and extraction with dichloromethane. Any remaining bromide was tested for by adding silver nitrate in nitric acid to the solution. The concentration of CTA hydroxide was determined by titration with hydrochloric acid and phenolphthalein as indicator. Sodium hydroxide solutions were prepared from 1 M Titrisol solution (Merck, Darmstadt, Germany) and all hydroxide solutions were kept in plastic bottles.

RESULTS AND DISCUSSION

Effect of pH

Carbohydrates are weak acids with $\text{p}K_a$ values in the range 12–14, becoming increasingly charged with increasing hydroxide concentration, *i.e.*, pH. The linear relationship between the electroosmotic velocity, μ_{eo} , and the inverse square root of the ionic strength (data not shown: *cf.*, ref. 9) indicated that the performance of the capillary was compatible with the strong alkaline conditions used in this study. The influence of pH on the relative migration for 4-NP conjugates compared with water as a

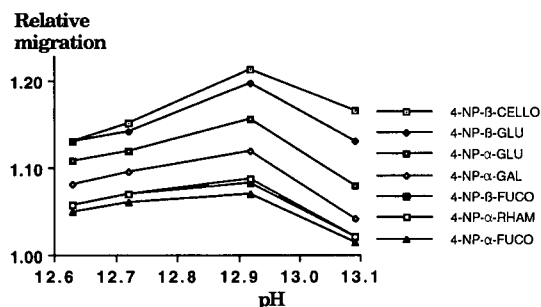


Fig. 1. Variation of the relative migration of seven 4-NP conjugates with pH. The electrolyte was $0.5\text{ M Na}_3\text{PO}_4$ in NaOH . UV detection at 300 nm.

marker for the electroosmosis is shown in Fig. 1. The degree of solute ionization, at a specific pH, depends on the $\text{p}K_a$ values of the sugars and pH is therefore an important parameter in the regulation of the selectivity. Generally, the selectivity increased with increasing hydroxide concentration and a separation of five glycoconjugates at pH 13.09 is shown in Fig. 2. The high current ($\leq 70\ \mu\text{A}$) will give rise to temperature effects and was the limiting factor for further increases in pH. The migration times for the

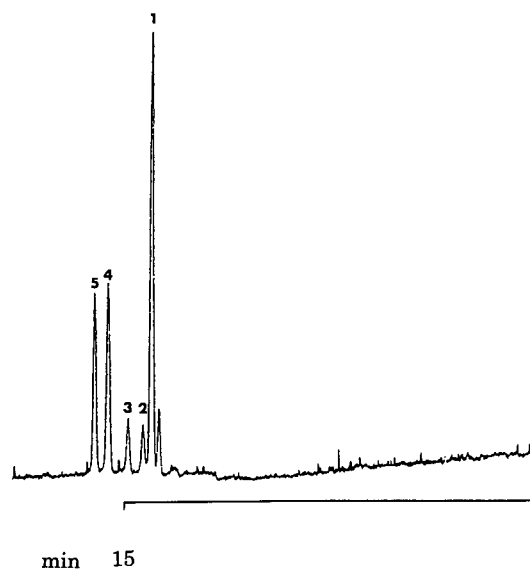


Fig. 2. Electropherogram of the separation of five 4-NP conjugates with 0.1 M NaOH in $0.05\text{ M Na}_3\text{PO}_4$. Peaks: 1 = 4-NP- α -L- and 4-NP- β -L-fucosides and 4NP- α -L-rhamnoside; 2 = 4-NP- α -D-galactoside; 3 = 4-NP- α -D-glucoside; 4 = 4-NP- α -D-mannoside; 5 = 4-NP- β -D-cellobioside. UV detection at 267 nm; 0.01 a.u.f.s.

TABLE I

ADDITION OF ORGANIC MODIFIERS

Capillary: see Experimental. Electrolyte: 0.1 M NaOH (A) and organic modifier (MeOH = methanol and ACN = acetonitrile). Solute: 4-nitrophenyl- β -D-cellobioside.

| Parameter | Electrolyte | | | |
|--|----------------------|----------------------|----------------------|----------------------|
| | A | A + 10% MeOH | A + 30% MeOH | A + 30% ACN |
| Electroosmotic flow (cm ² /V · s) | $5.69 \cdot 10^{-4}$ | $3.88 \cdot 10^{-4}$ | $1.61 \cdot 10^{-4}$ | $2.71 \cdot 10^{-4}$ |
| Number of theoretical plates | 110 000 | 75 000 | 36 000 | 55 000 |
| Current (μ A) | 61 | 48 | 32 | 40 |

related phenyl-conjugates increased in the order $-\beta$ -D-galactoside = $-\alpha$ -D-mannoside < $-\alpha$ -D-glucoside = $-\beta$ -D-glucoside < $-\beta$ -D-glucuronide.

Although very high pH values were used throughout this study, no detrimental effects on the separation system could be observed. The same fused-silica capillary was used for more than 1 month and showed the same performance. No indications of degradation of the analytes were found under the conditions used during the separations.

Effect of organic modifiers

Uncharged organic modifiers added to the electrolyte have been shown to decrease the electroosmotic mobility [10–13]. The exact mechanism is not fully understood, but a decrease in the zeta potential, changes in the dielectric properties of the Stern layer and effects on surface charge generation and adsorption of ions in the compact layer are believed to account for this effect [14].

A decrease in the electroosmotic velocity, apparent number of theoretical plates and current was observed (Table I) on addition of methanol or acetonitrile to the buffer, the former giving the largest decreases in the electrophoretic parameters. Further, these changes were proportional to the decrease in the current.

Cationic micellar electrokinetic capillary chromatography

At high pH, the anionically charged carbohydrates can distribute to a micellar pseudo-phase present in the electrolyte. Possible mechanisms are ion-pair distribution to the micelle or ion exchange with the micellar charges. Both principles suggest

that other anions present in the electrolyte will compete with the solute for distribution to the limited number of micelles. The cationically charged and hydrophobic detergent CTA hydroxide was investigated for this purpose (the critical micelle concentration is 0.9 mM [15]).

The electroosmotic flow was reversed by the addition of CTA to the electrolyte and, hence, the polarity of the electric field was reversed. The reversal has been claimed [16] to be due to adsorption of CTA to the negatively charged silica wall, thus creating a positively charged layer where the electroosmosis is generated by the migration of hydroxide ions towards the anode.

The influence of CTA concentration on the relative migration (compared with water as a marker for electroosmosis) for five phenyl glycosides (Fig. 3) showed that all solutes distributed to the micelles but to different extents. When CTA was added as its bromide salt at 40 mM, the relative migration decreased by 30–40%, expressing the competition from bromide for distribution to the cationically

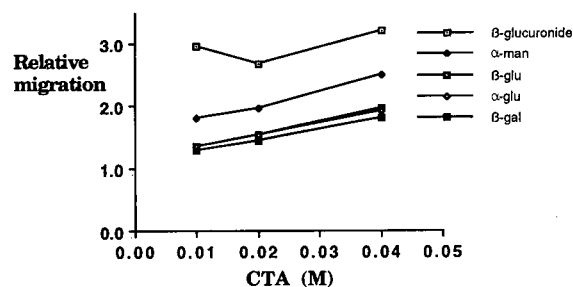


Fig. 3. Variation of the relative migration with CTA concentration at a constant hydroxide concentration (0.1 M).

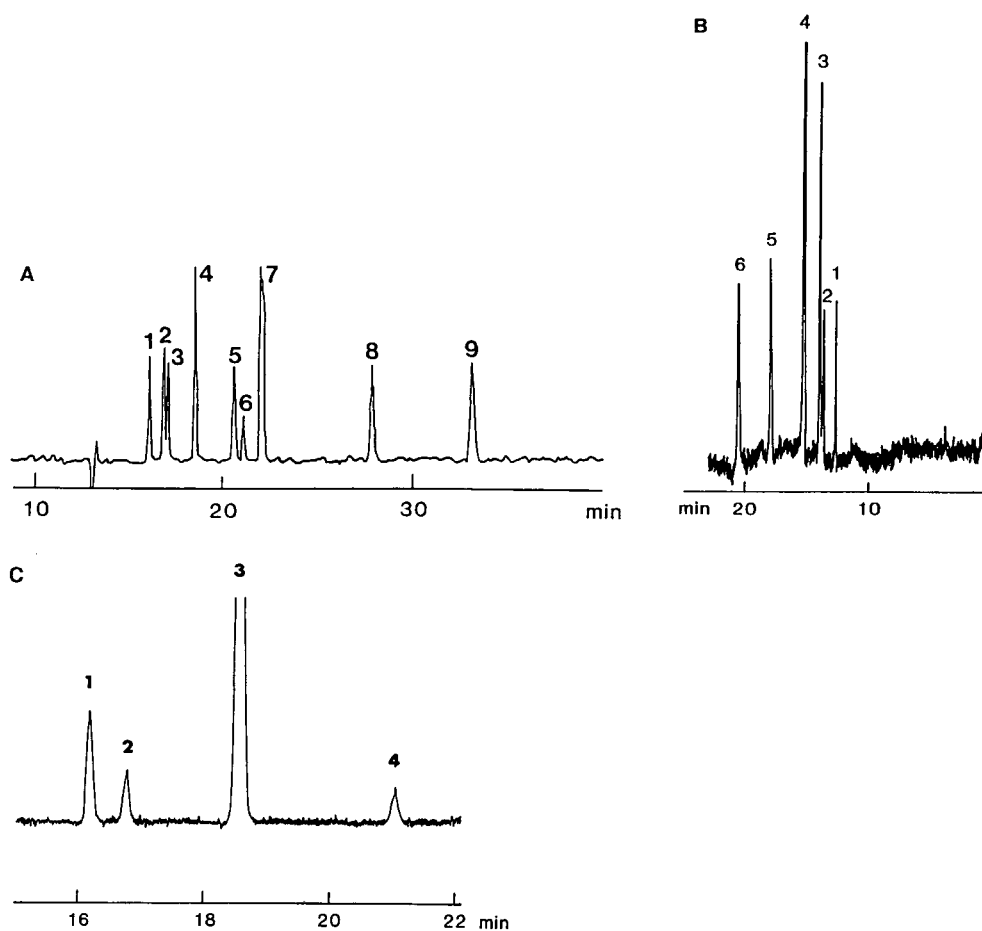


Fig. 4. Separation of (A) glyconjugates, (B) nucleosides and (C) element analogues. (A) 1 = 4-AP-thio- β -D-galactoside; 2 = 4-AP-thio- β -D-glucoside; 3 = 4-AP-thio- β -L-fucoside; 4 = 4-AP-N-acetylthio- β -D-glucosaminide; 5 = phenyl- β -D-galactoside; 6 = 4-AP-thio- β -D-xyloside; 7 = phenyl- α - and - β -D-glucosides; 8 = phenyl- α -D-mannoside; 9 = phenyl- β -D-glucuronide. 0.01 a.u.f.s. (B) 1 = uridine; 2 = cytidine; 3 = adenosine; 4 = thymidine; 5 = guanosine; 6 = inosine. 0.005 a.u.f.s. (C) 1 = 4-AP- β -D-xyloside; 2 = 4-AP- β -L-fucoside; 3 = 4-AP- β -L-thiofucoside; 4 = 4-AP-thio- β -D-xyloside. 0.01 a.u.f.s. Electrolyte: 40 mM CTA in 0.1 M hydroxide. UV detection at 267 nm.

charged micelles. The relative migration increased with increasing CTA concentration, *i.e.*, micelle concentration, but the electroosmotic velocity was almost constant. The separations of nine glycoconjugates and six nucleosides (riboside derivatives), using 40 mM CTA hydroxide in 60 mM sodium hydroxide as electrolyte, is displayed in Fig. 4A and B. This system could also be used in the separation of element analogues (Fig. 4C) where the oxygen atoms in the ring (peaks 1 and 4) and in the glycosidic bond (peaks 2 and 3) have been replaced with a sulphur atom. When a capillary from another batch

was used the differences in migration times were *ca.* 7%.

Electrolyte stability

Because of the high pH in the electrolyte, carbon dioxide is taken up, forming carbonate. This resulted in a gradual decrease in the electroosmotic velocity due to an increase in the ionic strength. Further, the selectivity decreased with increasing carbonate concentration and the separation of phenyl- α -D-glucose and phenyl- β -D-glucose (see Fig. 4A) was lost after about 2 h. This was probably due to com-

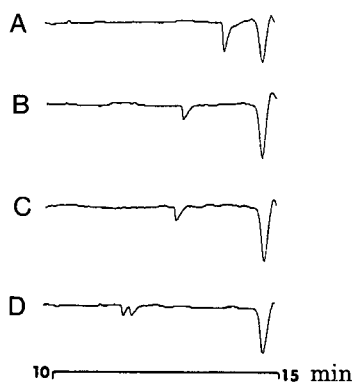


Fig. 5. Separation and indirect detection at 292 nm of (A) raffinose, (B) melibiose, (C) cellobiose and (D) galactosamine and glucosamine. The migration time of the system peak was 14.7 min. Electrolyte: 1.0 mM dimethylprotriptylin iodide in 40 mM CTA and 0.1 M hydroxide. 0.01 a.u.f.s.

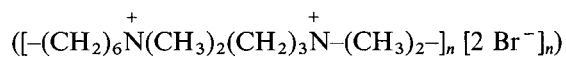
petition from the divalent carbonate anion for distribution to the micelles as the separation was restored when a newly prepared buffer was introduced.

Indirect UV detection

Indirect detection has been used for many years [17] and the theoretical background has been described [18]. In this study, 1.0 mM dimethylprotriptyline (DMP) iodide was added to 40 mM CTA hydroxide in 60 mM NaOH. Electropherograms from injections of amino sugars and di-, tri- and tetrasaccharides are shown in Fig. 5. The responses were low and the detection limits were in the picomole range. The relative migrations increased with increasing size of the sugars but all solutes migrated faster than the electroosmotic flow, indicating no or very little interaction with the micelles. The migrations were unstable in this system and there was a pronounced degradation of DMP in the strongly alkaline solution.

Polymeric cation

Cationic polymers such as polybrene with the general structure



have been used in the ion-exchange electrokinetic chromatography of acids [19]. Both polymer and

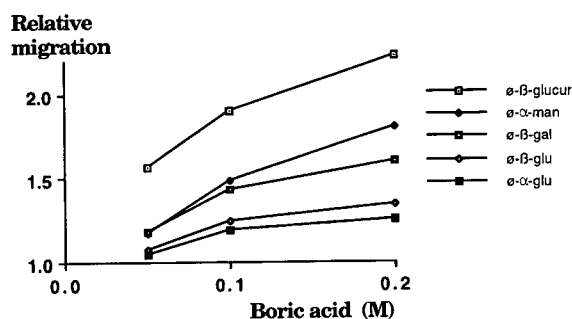


Fig. 6. Relative migration *versus* borate concentration. Electrolyte: sodium hydroxide and borate (pH 11.2); UV detection at 267 nm.

solute molecules are dragged along with the electroosmosis, but their electrophoretic mobilities are in opposite directions. Accordingly, anions can be separated based on differences in electrophoretic mobility and ion-pair formation constants with the cationic polymer. The electroosmotic flow was reversed, indicating that polybrene is adsorbed on the silica wall. Compared with the MECC system there was a change in the migration order for the phenyl glycosides, this being $-\beta$ -D-glucuronide, $-\beta$ -D-glucoside, $-\beta$ -D-galactoside and $-\alpha$ -D-mannoside. The relative migration times for the solutes were close to 1, except for the glucuronide, indicating poor ion-pair formation with polybrene. This was probably due to the high concentration of bromide present in the system competing for ion-pair formation with the polymer and, preferably, the corresponding hydroxide salt should be used in order to minimize this effect.

Boric acid

Borate has long been used as a complexing agent for carbohydrates and polyols. In this study, borate was included for comparison regarding selectivity. The relative migration times (Fig. 6) increased with increasing borate concentration as the degree of complex formation increased. The migration order (Fig. 7) was different to those with the other systems, thus offering further possibilities for carbohydrate separations. The lower peak efficiencies ($N \approx 65\,000$) due to slow kinetics of the borate complexation were offset by the gain in the selectivity. Borate can complex to more than one polyol molecule and, in an attempt to increase the selectivity

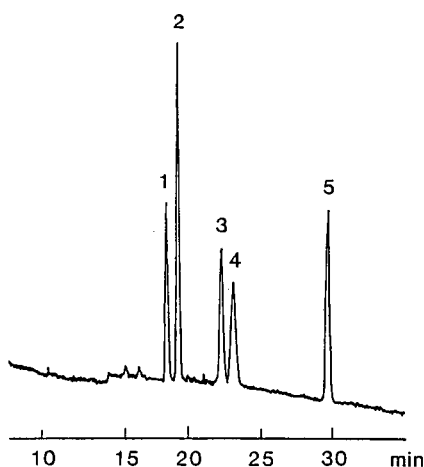


Fig. 7. Separation of phenyl conjugates as borate complexes. Peaks: 1 = phenyl- α -D-glucoside; 2 = phenyl- β -D-glucoside; 3 = phenyl- β -D-galactoside; 4 = phenyl- α -D-mannoside; 5 = phenyl- β -D-glucuronide. Electrolyte: 0.1 M boric acid in 0.1 M NaOH at pH 11.2. UV detection at 267 nm; 0.01 a.u.f.s.

further, mannitol (a polyol giving strong complexes with borate) was added to the electrolyte. The aim was to investigate the selectivity of the complexation between the borate–mannitol complex and the glycoconjugates. Extremely broad peaks were obtained, however, for the galactose and mannose derivatives ($N \approx 400$), probably owing to even slower complexation kinetics.

CONCLUSIONS

Glycoconjugates were separated as anions using highly alkaline buffer solutions. The selectivities were governed by the pK_a value and the size of the glycoconjugate and by electrolyte additives. A change in the migration order was obtained by addition of a cationic detergent to the buffer, owing to

differences between the solutes in distribution to the micelles. Further shifts in migration order could be obtained by addition of a polymeric cation or borate as complex-forming agents in the electrolyte. The study demonstrated that there are several ways to control selectivity and, hence, the separation of glycoconjugates by the addition of complex-forming agents to the electrolyte.

REFERENCES

- 1 S. C. Churms, *J. Chromatogr.*, 500 (1990) 555–583.
- 2 J. Liu, O. Shirota and M. Novotny, *Anal. Chem.*, 63 (1991) 413–417.
- 3 J. Liu, O. Shirota and M. Novotny, *J. Chromatogr.*, 559 (1991) 223–235.
- 4 T. W. Garner and E. S. Yeung, *J. Chromatogr.*, 515 (1990) 639–644.
- 5 S. Honda, S. Iwase, A. Makino and S. Fujiwara, *Anal. Biochem.*, 176 (1989) 72–77.
- 6 S. Hofstetter-Kuhn, A. Paulus, E. Gassman and H. M. Widmer, *Anal. Chem.*, 63 (1991) 1541–1547.
- 7 S. Honda, K. Yamamoto, S. Suzuki, M. Ueda and K. Kakehi, *J. Chromatogr.*, 588 (1991) 327–333.
- 8 J. A. Rendleman, Jr., *Adv. Chem. Ser.*, 117 (1973) 51–69.
- 9 A. J. Bard and L. R. Faulkner, *Electrochemical Methods. Fundamentals and Applications*, Wiley, New York, 1980.
- 10 S. Fujiwara and S. Honda, *Anal. Chem.*, 59 (1987) 487–490.
- 11 J. Liu, K. Cobb and M. Novotny, *J. Chromatogr.*, 468 (1988) 55–65.
- 12 K. Salomon, D. S. Burgi and J. C. Helmer, *J. Chromatogr.*, 559 (1991) 69–80.
- 13 C. Schwer and E. Kenndler, *Anal. Chem.*, 63 (1991) 1801–1807.
- 14 J. W. Jorgenson and K. D. Lukacs, *Anal. Chem.*, 53 (1981) 1298–1302.
- 15 P. Mukerjee and K. H. Mysels, *Nat. Stand. Ref. Data Ser.*, Nat. Bur. Stand., Washington, DC, 20 234 (1971).
- 16 K. Otsuka, S. Terabe and T. Ando, *J. Chromatogr.*, 332 (1985) 219–226.
- 17 S. Hjertén, *Chromatogr. Rev.*, 9 (1976) 122–219.
- 18 H. Poppe, *J. Chromatogr.*, 506 (1990) 45–60.
- 19 S. Terabe and T. Isemura, *J. Chromatogr.*, 515 (1990) 667–676.

Observation of flow profiles in electroosmosis in a rectangular capillary[☆]

Takao Tsuda and Masakazu Ikedo

Department of Applied Chemistry, Nagoya Institute of Technology, Gokiso, Showa, Nagoya 466 (Japan)

Glenn Jones, Rajeev Dadoo and Richard N. Zare

Department of Chemistry, Stanford University, Stanford, CA 94305 (USA)

ABSTRACT

The flow profile of electroosmosis in capillary electrophoresis was studied by using a dye and a rectangular capillary. The movement of the dye is observed with a microscope–video system, and then advances per unit time are measured from the recorded video tapes. The medium at the central portion moves like a plug flow, and the zone front at the edges are ahead of the central portion. The flow profile in a capillary column with a circular cross-section is proposed. The flow profiles of ionic solutes are also discussed.

INTRODUCTION

The flow profile in electroosmosis has been discussed under the conditions of electroosmotically driven open-tubular liquid chromatography [1–7], capillary zone electrophoresis (CZE) [8–13] and electroosmotically driven electrochromatography [14]. The flow profile in electroosmosis is different from the parabolic laminar velocity profile of pressurized flow. The former flow profile is much flatter than the latter. Thus very narrow peaks are obtained in electroosmotically driven liquid chromatography (ELC) and CZE. In early experiments, Pretorius *et al.* [1] and Tsuda *et al.* [3] obtained 10 and 30 times less band broadening in ELC than expected with pressurized flow. There have been sev-

eral studies of flow profiles in electroosmosis [1,3,10,11]. Pretorius *et al.* [1] suggested that the profile is flat except in the region of a diffuse electric double layer near the column inner wall, where the flow profile is a quadratic velocity profile owing to the friction experienced by the viscous liquid flowing by the wall. Jorgenson and Lukas [8] assumed that the zone broadening in CZE is only generated by axial molecular diffusion of a solute and a medium. Tsuda *et al.* [3] found that it was difficult to explain the experimental results just from the axial molecular diffusion, and proposed that the flow profile might be a combined form of plug and Poiseuille flow. Guiochon and co-workers [10,11] also assumed that the electroosmotic flow profile is an expression of a combination of plug and Poiseuille flow, proposed an equation and calculated the contribution of each to the real electroosmotic flow profile by using experimental data.

For the analysis of zone broadening under pressurized flow conditions, Taylor [15] used a method in which a coloured solution was introduced continuously into a narrow capillary tube at several different velocities. The concentration of the coloured

Correspondence to: T. Tsuda, Department of Applied Chemistry, Nagoya Institute of Technology, Gokiso, Showa, Nagoya 466, Japan.

[☆] Part of this paper was presented at the 2nd International Symposium on High Performance Capillary Electrophoresis, San Francisco, CA, January 24–26th 1990, and the 15th International Meeting on Column Liquid Chromatography, Basle, June 3rd–7th, 1991.

solute at each axial point of the tube was measured after the zone front had travelled past the centre part of the capillary tube. He proposed equations for the zone broadening in which diffusion coefficients, flow velocity, column radius and time are included and also a general equation for band broadening in a capillary tube.

In this work, we used a similar method in which a fluorescent solution is continuously introduced into a capillary column, with the front profile being observed by through a microscope charge coupled device (CCD) camera–video cathode ray tube (CRT) system. A rectangular capillary tube [16], which has been used for CZE, is used because the flat sides cause fewer distortions in the observed zone front than do the more common round walls.

EXPERIMENTAL

Rectangular capillaries ($1\text{ mm} \times 50\text{ }\mu\text{m}$) were purchased from Wilmad Glass (Buena, NJ, USA). A high-voltage power supply (0–30 kV with a reversible polarity output) is used (Hipotronics, Inc., Brewster, NY, USA). For the study of electroosmotic flow profiles, the applied voltage on a rectangular capillary (164 mm long) and electric current were 1.59 kV (97 V/cm) and $0.12\text{ }\mu\text{A}$, respectively, for the experiments using pure methanol as a medium and Rhodamine 590–methanol solution as a sample zone. For the study of zone front of ionic molecules, 5 mM phosphate buffer (pH 6.8) as a medium and a rectangular capillary 300 mm long were used. The current through the capillary was monitored as a potential drop across a $64\text{ k}\Omega$ resistor on the ground side of the circuit. A schematic diagram of the instrument used for the observation and recording of the zone front is shown in Fig. 1. The rectangular capillary was placed on *XY* stage-1 under a Nikon (Tokyo, Japan) SMZ-2T stereoscope equipped with a Sony (Park Ridge, NJ, USA), DXC-101 color video CCD camera, VHS video recorder (National, Tokyo, Japan) and CRT (Sony). The zone front was kept under the microscope by adjusting the capillary position with *XY* stage-1.

Syringes (A and B in Fig. 1) made of polyethylene were used as reservoirs, with electrodes set inside them. The medium or sample solution can be kept inside the syringe without closing the outlet part

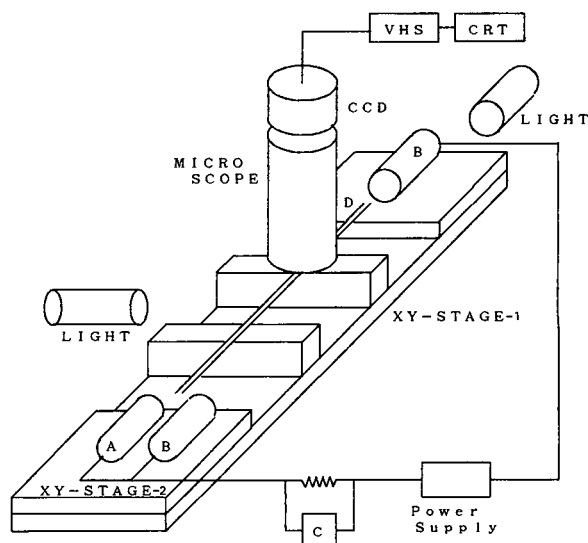


Fig. 1. Schematic diagram of the instrument for visual observation of zone front. A and B are reservoirs of the medium and coloured sample solution, respectively. Each reservoir has its own platinum electrode. Current is measured at C. D is a rectangular capillary, $1\text{ mm} \times 50\text{ }\mu\text{m}$ and 1.64 m long. Light is focused on the zone front, which is kept under a microscope by adjusting *XY* stage-1.

used for connection of a needle, which permits the rectangular capillary to be inserted through this orifice.

The operational procedure for the introduction of the sample solution is as follows. When one of the ends of the empty rectangular capillary is inserted into reservoir B, the medium in the reservoir is introduced into the capillary via capillary action. Then the other end is inserted into another reservoir B. Subsequently, the end of rectangular capillary is inserted into the outlet of the syringe containing sample solution (reservoir A in Fig. 1) with gentle and smooth motion of *XY* stage-2. This procedure is very important for producing a sharp zone front. Then a voltage is applied. Immediately after the application of the voltage, the coloured solution travels into the rectangular capillary and its zone front is followed under the microscope system by continuous or stepwise operation of *XY* stage-1.

The sample solution was continuously introduced into the rectangular capillary in a similar fashion to frontal analysis in chromatography [17]. With the dye zone front illuminated using two lens-

es fed by two fibre-optic cables from a light source (150-W halogen lamp; Cole-Parmer Instrument, Chicago, IL, USA), the fluorescent image of the front was recorded.

Rhodamine 590, sulphorhodamine 640 and disodium fluorescein were purchased from Exciton Chemical (Dayton, OH, USA) and used as received.

RESULTS AND DISCUSSION

Electroosmotic flow in capillary tubing is generated under a potential gradient in various media, such as water, with electrolytes, pure methanol, acetonitrile, methanol–hexane [3], methanol–benzene [1] or mixtures of water and organic solvents [18]. The flow-rate of electroosmosis under unit potential gradient is dependent on the dielectric constant and viscosity of the medium, the amount of positive or negative surface charge on the inner wall and the diffuse double layer [3,9,13,19]. Linear flow velocities of electroosmosis under a unit potential gradient of methanol and acetonitrile are half and twice that of distilled water, respectively [3]. Electropherograms obtained using organic and aqueous organic media show almost same resolutions compared with those obtained using water or water with electrolyte [4,18]. Therefore, we consider that the use of methanol as a medium for the study of electroosmotic flow profile will give a general answer. As methanol has high solubility for dyes, it is convenient for observation of zone front movements.

Rhodamine 590 in methanol is assumed to be neutral, hence the behaviour of the zone of Rhodamine 590 solution corresponds directly to the behaviour of electroosmosis, *i.e.*, the zone front shows the flow profile of electroosmosis.

For the observation of the electroosmotic flow profile, we selected a rectangular capillary with height 50 μm , width 1 mm and length 164 mm, where these dimensions are defined as the *Z*, *Y* and *X* axes, respectively. The rectangular capillary is positioned so that the microscope images the *XY* surface of the capillary.

The use of a rectangular capillary for the observation of flow profiles in electroosmosis has several advantages. The flow velocity in electroosmosis is dependent on the amount of charge on the wall [13]. The medium in a rectangular capillary is surrounded by two sets of parallel plates, namely two *XY*

plates and two *XZ* plates. At the centre part of the *Y* axis of the rectangular capillary the medium is affected mainly by the two parallel *XY* plates. The medium near the *XZ* plates is affected by both the two 1-mm parallel plates (*XY*) and the 50- μm plate (*XZ*). Therefore, the geometric difference between the edge and centre of the 1-mm plate makes the effect of the wall on the flow profile apparent. The difference in flow at the edge of the 1-mm width (*y* axis) *versus* the centre would be caused by the effect of the 50- μm plate (*XZ*), because the effect of charges on the 1-mm plate and its diffuse double layer would influence the flow profile equally at all parts of the *XY* plate.

When we inject continuously a dye–methanol solution into the rectangular capillary and force it with a pressurized flow by lifting up one of the ends of the rectangular capillary, we can observe a typical Poiseuille flow profile at its zone front. Under a potential gradient and keeping both ends of the capillary at the same level, we obtain completely different flow profiles from Poiseuille flow, as shown in Fig. 2.

The current is very stable during the run, *i.e.*, there is only a small difference in conductivity between pure methanol and 10^{-4} M Rhodamine–methanol solution. If there had been a considerable conductivity difference between them, a molecule entering the pure methanol zone from the zone front of Rhodamine–methanol would travel with higher velocity than those remaining in the sample zone, because the potential gradient in the pure methanol would be higher than that in Rhodamine–methanol zone. Diffusion of the zone front would result. A gradient of the concentration of Rhodamine the range of in the zone front along the *X* axis was not observed visually, and was not found in computerized images obtained from the recorded video tape.

Zone fronts of Rhodamine 590 in methanol solution are shown in Fig. 2. The period between the pictures is 1 s. The advance of the zone front between two pictures can be measured from photographs by matching the positions of the stationary marks on the rectangular capillary. The zone front shown in Fig. 2 is flat at the centre with small bends at both ends of the 1-mm axis, namely near the 50- μm plates. The travelling of the zone front recorded on video tape was analysed by computer

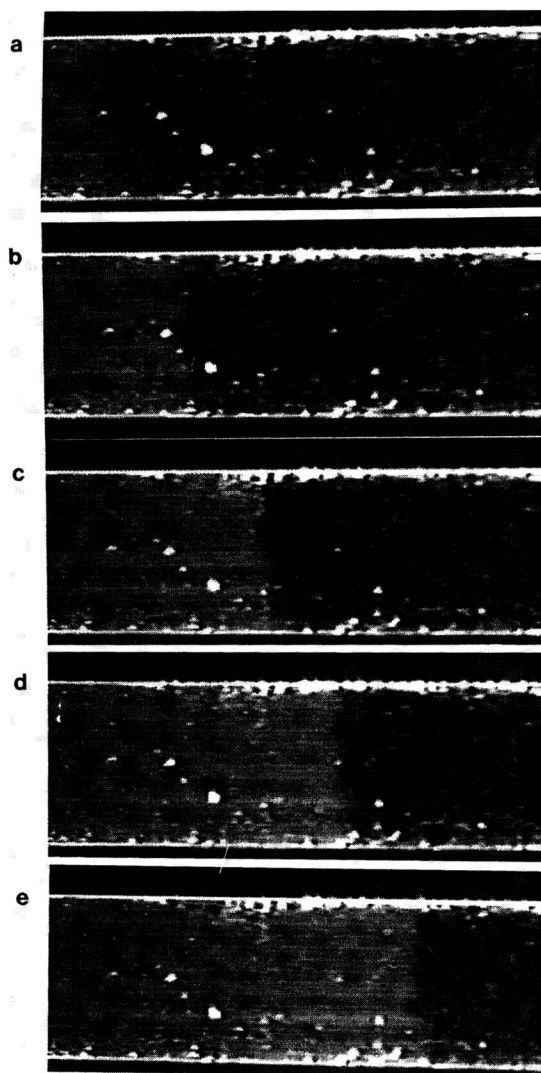


Fig. 2. Photographs of zone front of electroosmotic flow. Coloured sample solution: 0.1 mM Rhodamine 590 in methanol. Applied voltage and current, 1.59 kV and 0.12 μ A, respectively. The period between photographs is 1 s. The five photographs a–e are a series.

software. The result obtained is the image of the advancing zone front, shown in Fig. 3. The four images of advances in Fig. 3 are over successive 4-s spans, and the 1-mm axis is divided into seventeen sections. Both edges in the X -dimension of the image correspond to zone fronts.

The advances of the zone front along the X axis are summarized numerically in Table I. The average

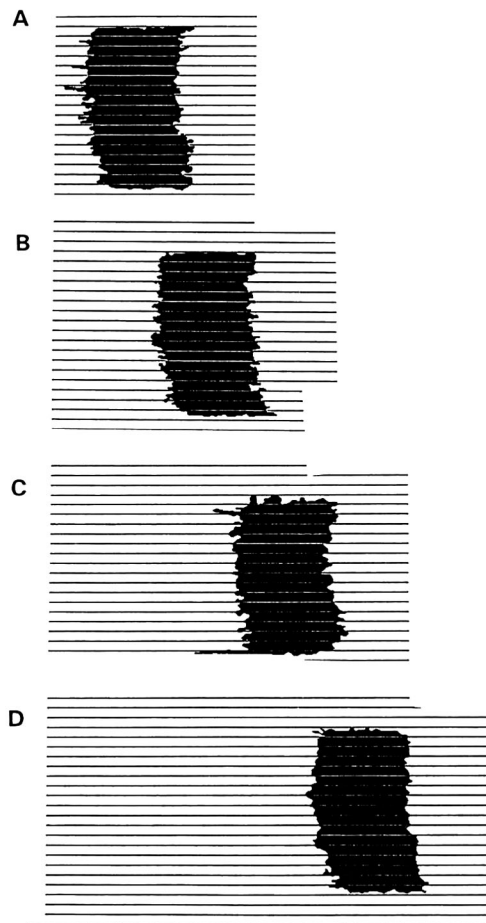


Fig. 3. Computed images of zone front on the X axis over a 1-s span. The four images A–D are a series. Each image shows advances in the X axis over 1 s. The two ends of an image on the X axis correspond to zone fronts of 1 s apart.

numbers at each Y section are similar. The flow profile is plug-like in the centre part of the capillary from sections 1 to 15. Unfortunately, the numerical values of the advances at sections 0 and 16 are not stable enough to estimate.

To examine the profile in the vicinity of the 50- μ m plate, we focused the movement of the zone front with high magnification. One of the photographs obtained is shown in Fig. 4. The zone front at the near wall, namely near to 0 or 16 of the Y -axis, is further ahead (larger value of the X -axis) than the position of the zone front at the central portion.

It is concluded that at the central portion the ad-

TABLE I

ADVANCES OF THE ZONE FRONT ALONG THE X AXIS OVER A 1-s PERIOD AT Y SECTION

Mean of average value and its standard deviation are 7.69 and 0.12, respectively. The one unit of X-axis: 57.8 μm .

| No. of Y section | Experiment No. | | | | Average value |
|------------------|----------------|-----|-----|-----|---------------|
| | 1 | 2 | 3 | 4 | |
| 0 | — | 8.3 | — | 7.5 | — |
| 1 | 7.8 | 7.6 | 8.0 | 7.0 | 7.6 |
| 2 | 7.2 | 8.3 | 7.6 | 7.2 | 7.58 |
| 3 | 8.0 | 6.9 | 8.4 | 7.8 | 7.78 |
| 4 | 8.1 | 7.8 | 8.0 | 7.1 | 7.75 |
| 5 | 8.0 | 8.3 | 6.7 | 8.5 | 7.88 |
| 6 | 7.6 | 8.0 | 7.4 | 7.8 | 7.7 |
| 7 | 7.0 | 8.2 | 7.8 | 7.4 | 7.63 |
| 8 | 7.7 | 8.0 | 6.5 | 8.5 | 7.68 |
| 9 | 8.1 | 8.1 | 7.4 | 7.6 | 7.8 |
| 10 | 7.5 | 8.4 | 8.0 | 7.5 | 7.85 |
| 11 | 8.0 | 7.7 | 7.6 | 7.7 | 7.75 |
| 12 | 7.4 | 7.6 | 8.5 | 7.0 | 7.63 |
| 13 | 7.8 | 7.5 | 8.2 | 7.5 | 7.75 |
| 14 | 6.8 | 8.0 | 8.3 | 6.9 | 7.5 |
| 15 | 6.0 | 8.6 | 7.6 | 7.7 | 7.48 |
| 16 | — | 8.0 | — | — | — |

vances are similar in Fig. 2 and 3 and Table I, and the zone fronts at the edges of the 1-mm axis in Figs. 2 and 4 are ahead compared with the centre part. This phenomenon was observed in every experiment which we recorded.

We therefore suggest the following: the edge portion of the zone front advances at the very initial period, immediately after application of voltage on the rectangular capillary following the smooth operation of changing the reservoir from A to B. From then on the zone will maintain equal speeds at

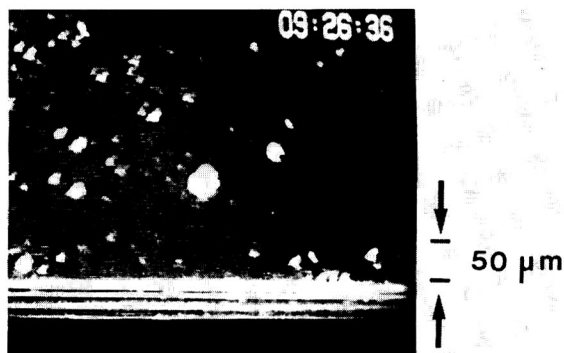


Fig. 4. Zone front near the 50- μm plate. Experimental conditions as in Fig. 2.

every point along the Y-axis. To our knowledge, this is the first time that the zone front pattern in electroosmosis has been directly observed. The centred part is behind edges. This finding is unique. The flow profile observed is very different from the suggestion of Pretorius *et al.* [1].

There is some possibility that capillary action of the dye-methanol solution into the rectangular capillary and/or adsorption of the solute on the inner wall during the operation of the introduction of the dye solution may occur, and they affect the zone front profile. The capillary action is very strong when a liquid is introduced into the empty rectangular capillary, but it might be negligible when a dye-methanol solution is introduced into the capillary filled with methanol and its concentration is low enough. Concerning the adsorption of the dye on the inner wall, it may be very weak or non-existent, because the washing out of the dye-methanol

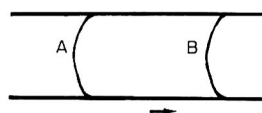


Fig. 5. Proposed zone front in a capillary column with circular cross-section of 100–50 μm I.D.

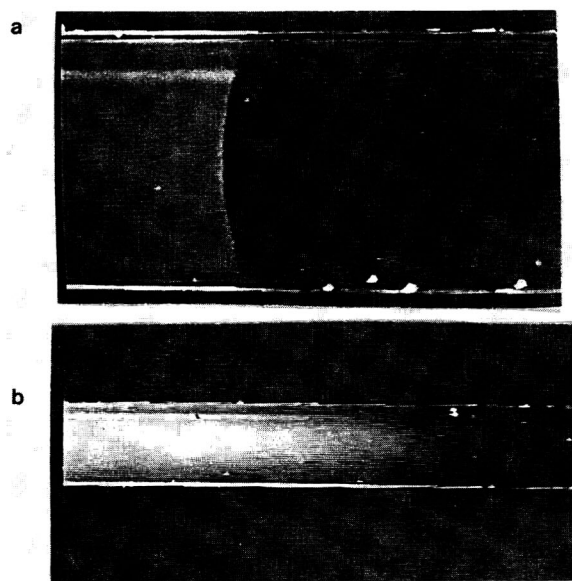


Fig. 6. Photographs of zone front of ionic solutes. (a) 0.05 mM Rhodamine 590 and (b) 0.1 mM disodium fluorescein in 5 mM phosphate buffer as ionic solutes. Applied voltage, 10 kV. A rectangular capillary (1 mm \times 50 μ m and 30 cm long) was used.

solution from the rectangular capillary with pure methanol was performed very easily. If there is some adsorption, the concentration at the region very near the XZ plate will decrease after the short period of development and it will result as the zone front at the edge will be behind to its central part. We did not observe this phenomenon. Also in the process of development the zone front at the edge is more advanced compared with the central part. Therefore, we conclude that there is not much effect of capillary action and adsorption during the operation of the introduction and the development of the zone.

The zone front in a capillary column with a circular cross-section of 100–50 μ m I.D. will be different from the zone front shown in Fig. 2, because the geometrical dimension is different from the rectangular capillary used, especially the length of central portion. From the present experimental results, we propose the zone front profile in a 100–50 μ m I.D. capillary column with circular cross-section as shown in Fig. 5. The central portion of the zone front is retarded compared with the edges, as with a rectangular capillary.

Flow profile of ionic solutes in aqueous solution

We consider that Rhodamine 590 in methanol is neutral, and its zone profile corresponds to that of electroosmosis. However, in 5 mM phosphate buffer (pH 6.8) with 5% ethylene glycol, Rhodamine 590 should have one positive charge and disodium fluorescein two negative charges. The zone front of these two ionic solutes in buffer solution is shown in Fig. 6. The negatively charged ionic solute has an electrostatic repulsion with the surface charge on the inner wall in its vicinity, and the positively charged ionic solute has an attraction with the wall. The zone fronts of both ionic solutes are different from those of neutral solutes. The difference is particularly pronounced at both ends of the 1-mm axis (Y) of the rectangular capillary. The zone front at both ends of the Y axis moves forward or back owing to the positive or negative charge of the solute, respectively. Therefore, the zone front profile might be induced from electrostatic forces between ionic solutes and the charge on the surface of the inner wall under a potential gradient. The zone front of ionic solutes is not flat.

The advances per unit period at each Y axis are nearly equal as in electroosmosis, even though the zone front observed is not flat. More quantitative measurements of these advances at each Y section are in progress. The zone fronts of ionic dyes are dependent on their charges. The front zone profiles in electroosmosis and with ionic dyes each have a specific pattern. These findings are not explained by the general equation proposed for electroosmosis [9,19]. Although the diffuse double layer and the amount of surface charges on the inner wall are important factors, they might not have the power to affect molecules over a distance of several micrometres. The change in the nature of the medium under a potential gradient may be a key factor. Further experiments are planned to find the relationship between flow profiles and physical parameters.

ACKNOWLEDGEMENTS

We thank Pias Comp. (Tokyo, Japan) for the analysis of flow patterns. T.T. thanks the Ministry of Education, Japan, for the support of his leave. Beckman Instruments provided financial support for this research.

REFERENCES

- 1 V. Pretorius, B. J. Hopkins and J. D. Schieke, *J. Chromatogr.*, 99 (1974) 23–30.
- 2 J. W. Jorgenson, K. D. Lukacs, *J. Chromatogr.*, 218 (1981) 209.
- 3 T. Tsuda, K. Nomura and G. Nakagawa, *J. Chromatogr.*, 248 (1982) 241–247.
- 4 T. Tsuda, *Nippon Kagaku Kaishi*, (1986) 937–942; *C.A.*, 105 (1986) 126484r.
- 5 W. D. Pfeffer and E. S. Yeung, *Anal. Chem.*, 62 (1990) 2178–2182.
- 6 J. H. Knox and I. H. Grant, *Chromatographia*, 32 (1991) 317–328.
- 7 H. Yamamoto, J. Baumann and F. Erni, *J. Chromatogr.*, 593 (1992) 313–319.
- 8 J. W. Jorgenson and K. D. Lukacs, *Anal. Chem.*, 53 (1981) 1298–1302.
- 9 T. Tsuda, K. Nomura and G. Nakagawa, *J. Chromatogr.*, 264 (1983) 385–392.
- 10 M. Martin and G. Guiochon, *Anal. Chem.*, 56 (1984) 614–620.
- 11 M. Martin, G. Guiochon, Y. Walbroehl and J. W. Jorgenson, *Anal. Chem.*, 56 (1984) 614–620.
- 12 X. Huang, J. Lukey, M. L. Gordon and R. N. Zare, *Anal. Chem.*, 61 (1989) 766–770.
- 13 T. Tsuda, *J. Liq. Chromatogr.*, 12 (1989) 2501–2514.
- 14 W. D. Pfeffer and E. S. Yeung, *J. Chromatogr.*, 557 (1991) 125–136.
- 15 G. Taylor, *Proc. R. Soc. London, Ser. A*, 219 (1953) 186.
- 16 T. Tsuda, J. V. Sweedler and R. N. Zare, *Anal. Chem.*, 62 (1990) 2149.
- 17 A. B. Littlewood, *Gas Chromatography*, Academic Press, New York, 1970.
- 18 S. Fujiwara and S. Honda, *Anal. Chem.*, 59 (1987) 487–490.
- 19 S. Hjertén, *Chromatogr. Rev.* 9 (1967) 122–219.

On-line sample preconcentration on a packed-inlet capillary for improving the sensitivity of capillary electrophoretic analysis of pharmaceuticals

Michael E. Swartz and Michael Merion

Millipore Waters Chromatography, 34 Maple Street, Milford, MA 01757 (USA)

ABSTRACT

An on-line preconcentration method is reported that improves the sensitivity of capillary electrophoretic analyses by at least two orders of magnitude. The method uses a concentrator capillary with a 75 μm I.D. and a 1-mm length packed bed at the inlet end that can concentrate samples using the principles of liquid chromatography. Using low-molecular-mass pharmaceutical standards as examples, the parameters used in developing a preconcentration sensitivity enhancement method were optimized. The optimized method was then used to evaluate the quantitative aspects of capillaries of this type, including run to run and capillary to capillary reproducibility, linearity, and efficiency and resolution. In addition, the analysis of a urine sample spiked with doxepin at the 500 ppb level is reported.

INTRODUCTION

One of the most important issues facing the technology of capillary electrophoresis (CE) is sensitivity. In general, when compared with other analytical techniques such as liquid chromatography (LC), CE is a less sensitive technique. This difference lies primarily in two areas. The first is detector path length. In LC the path length of the detector cell is generally between 5 and 10 mm. However, in CE, since detection is performed on-column, the path length of the detector flow cell is determined by the internal diameter of the capillary, resulting in a detector cell path length that is about 100 times less than that of LC. Because absorbance is related to path length in a linear fashion according to Beer's law, sensitivity greatly suffers. The second difference is the ability to analyze low concentration samples. In LC, large volumes of a sample at a low concentration can be loaded and concentrated at the head of a column. Sample is later eluted with a

gradient giving greatly enhanced sensitivity. However, in CE, the application of large sample volumes results in broader peaks and diminishing resolution.

Several approaches to improving the sensitivity of CE analyses have been devised. The use of different detection schemes such as fluorescence [1], and electrochemistry [2] have been reported that enhance sensitivity for compounds that are amenable to these types of selective detection. Extended path-length detector cells [3–5] have also been employed, however they provide only a 5–15 fold sensitivity enhancement, while compromising resolution and efficiency. Isotachophoretic sample loading (stacking) and field amplification have also been employed as on column concentration methods [6–8], however most of this work has been limited to low-molecular-mass organic acids or inorganic species. Guzman *et al.* [9] reported the use of both multiple capillaries arranged in bundles, and the use of concentrator capillaries containing an antibody covalently bound to a solid support material to increase sample loading, and hence sensitivity. This off-line method resulted in poor recovery, however, and no reproducibility or quantitative information was re-

Correspondence to: M. E. Swartz, Millipore Waters Chromatography, 34 Maple Street, Milford, MA 01757, USA.

ported. In addition, capillaries of this type are not currently commercially available. This work describes the use of on-line preconcentration capillaries that improve the sensitivity of capillary electrophoretic analyses of some common pharmaceuticals by utilizing the principles of reversed-phase LC, first reported in 1990 for the analysis of peptides [10]. There are several advantages to this technique as opposed to off-line preconcentration. These include the ability to automate the assay, leading to better reproducibility, as well as the ability to address sample limited situations. Off-line preconcentration techniques can also add significant levels of impurities. It is for this reason that ion chromatographic trace enrichment is almost exclusively performed on-line. Using on-line concentration capillaries, we have been able to extend the detection limits over two orders of magnitude lower than those obtained with conventional capillaries without compromising resolution, efficiency, or reproducibility and quantitative capabilities.

EXPERIMENTAL

Chemicals

Doxepin and propranolol (Fig. 1) were purchased from Sigma (St. Louis, MO, USA), citric acid and citric acid trisodium salt dihydrate from Aldrich (Milwaukee, WI, USA), and LC-grade acetonitrile (ACN) and methanol from J. T. Baker (Phillipsburgh, NJ, USA). All were obtained in the highest purity available and used without further purification. Run buffers were prepared with Milli-Q water (Millipore, Marlborough, MA, USA) using the appropriate proportions of 0.025 M concentrations of citric acid and the sodium salt to a pH of 4.0. Eluent buffers were prepared by the addition of the appropriate amount of ACN to the run buffer. Both run and eluent buffers were filtered and degassed under vacuum daily. Sep-Pak C₁₈ cartridges were obtained from Millipore.

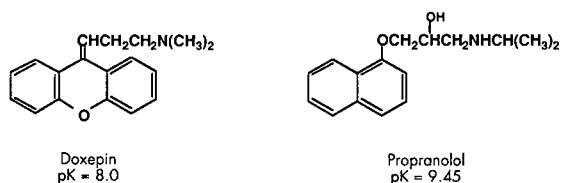


Fig. 1. Structure of doxepin and propranolol test compounds.

Capillary electrophoresis system

A Waters Quanta 4000 capillary electrophoresis system was used throughout (Millipore Waters Chromatography, Marlboro, MA, USA). Separations were performed using both standard capillaries (60 cm × 75 μm I.D.), and concentrator capillaries as described below. All analyses were performed with UV detection at 214 nm, electromigration injections of 5 kV, and an applied voltage of 250 V/cm. Data was collected and processed on a Model 845 chromatography data workstation (Millipore) at 10 points per second. The data workstation system suitability software was used to calculate reproducibility.

Concentrator capillaries

Concentrator capillaries were obtained from Millipore. These commercially available capillaries consist of a 1.0 mm packed bed of a polymeric reversed-phase chromatographic packing material at the injection end of the capillary, held in place with a glass frit on both ends. Capillaries were equilibrated prior to use by a manual purge of neat ACN using a syringe. This insured adequate wetting of the packing material. This was followed by an instrument purge of ACN for 15 min, water for 15 min, and run buffer for 15 min. Under continuous use this equilibration procedure was replaced with a between run instrument purge of run buffer only. The capillaries were stored in ACN when not in use. Samples were concentrated using these capillaries by performing an electromigration sample injection varying in time from 20 s to over 16 min in length. The sample was retained by the packing material, while the sample solution gradually filled the capillary. Following the injection, the capillary was purged, refilling it with the separation buffer. The sample was eluted from the packing using an injection of a small volume of an aqueous ACN mixture, again using electromigration. From this point the electrophoretic separation proceeded in a normal fashion.

Sample preparation

Standards were prepared in Milli-Q water at the 1.0 mg/ml level and diluted with water to the desired concentrations. Spiked urine samples were prepared by adding 1.0 ml 5.0 ppm doxepin in water to 9.0 ml urine filtered prior to use with a Millex-HA

filter (Millipore). Sample preparation was performed by loading the entire 10-ml spiked urine sample onto a prepared C₁₈ Sep-Pak cartridge, and washing the cartridge with a two-step procedure first with water, followed by methanol–water (60:40). The doxepin was eluted from the cartridge in a 10-ml fraction of methanol–water (75:25), which was collected, concentrated by drying, and reconstituted to 1.0 ml with water, and injected.

RESULTS AND DISCUSSION

Method development

At low pH, both doxepin and propranolol (Fig. 1) are positively charged and can be separated by conventional free zone CE using a standard capillary as shown in Fig. 4a. Lower pH values were evaluated, and while providing increased resolution, a significant decrease in the electroosmotic flow (EOF) is obtained. This results in poor sample loading using the electrokinetic injection mode employed with the concentrator capillary. During this stage of research, doxepin alone was used to develop the concentrator capillary elution conditions as outlined below. The method development consisted of determining the ACN concentrations and elution time necessary to elute the sample from the packing once concentrated. As a starting point, an arbitrary figure of three times the packed bed volume was used as an eluent volume. This was determined by measuring the EOF velocity, accomplished by measuring the time for a neutral compound (ACN sol-

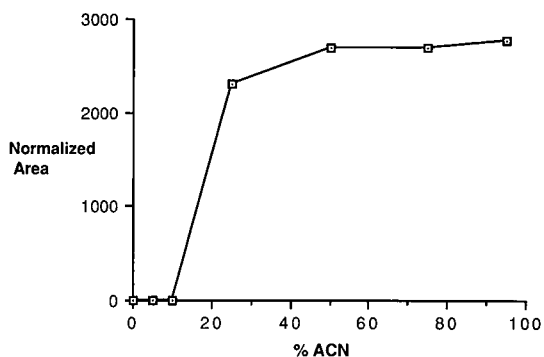


Fig. 2. Plot of normalized area versus %ACN used in eluent. Conditions as described in experimental. A 1.0-ppm solution of doxepin was injected with a 5-min concentration step and a 12-s elution both at 5 kV. Normalized area is area/migration time.

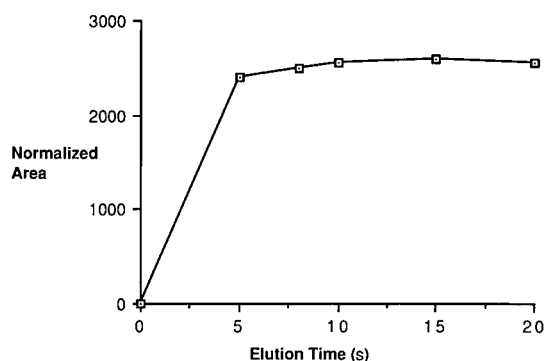


Fig. 3. Plot of normalized area versus elution time in s. Conditions as described in Experimental. A 1.0-ppm solution of doxepin was injected with a 5-min concentration step at 5 kV. A 75% solution of ACN in run buffer was used as eluent.

vent) to migrate the length of the capillary according to the formula:

$$V = L/N_t$$

where V = EOF velocity in mm/s; N_t = migration time of ACN in s; L = length of capillary in mm. Using this formula, the EOF velocity was found to be 0.253 mm/s. The reciprocal of velocity, 3.95 s/mm, indicates that for a 1.0-mm packed bed, an elution time of 12 s should be used.

Next, the effect of different eluent ACN concentrations were measured as a way of assessing the recovery of doxepin from the packing. Since different concentrations of ACN in the eluent can affect the background current and subsequently affect the migration time, and hence the area, areas normalized for migration time were calculated and plotted versus the percent ACN in the eluent. This graph is presented in Fig. 2. As can be seen, ACN concentrations in excess of 50% result in a plateau in the normalized area. These data, in conjunction with subsequent blank injections, offers proof that 100% recovery is obtained using ACN concentrations in electrolyte above 50%.

Next, elution time was varied to determine if the 12-s injection of eluent is sufficient. As seen in Fig. 3, after 10 s a plateau in the normalized area is reached that, in combination with subsequent blank injections, again indicates 100% recovery. All additional work was therefore carried out at eluent ACN concentrations above 50%, with elution times exceeding 10 seconds.

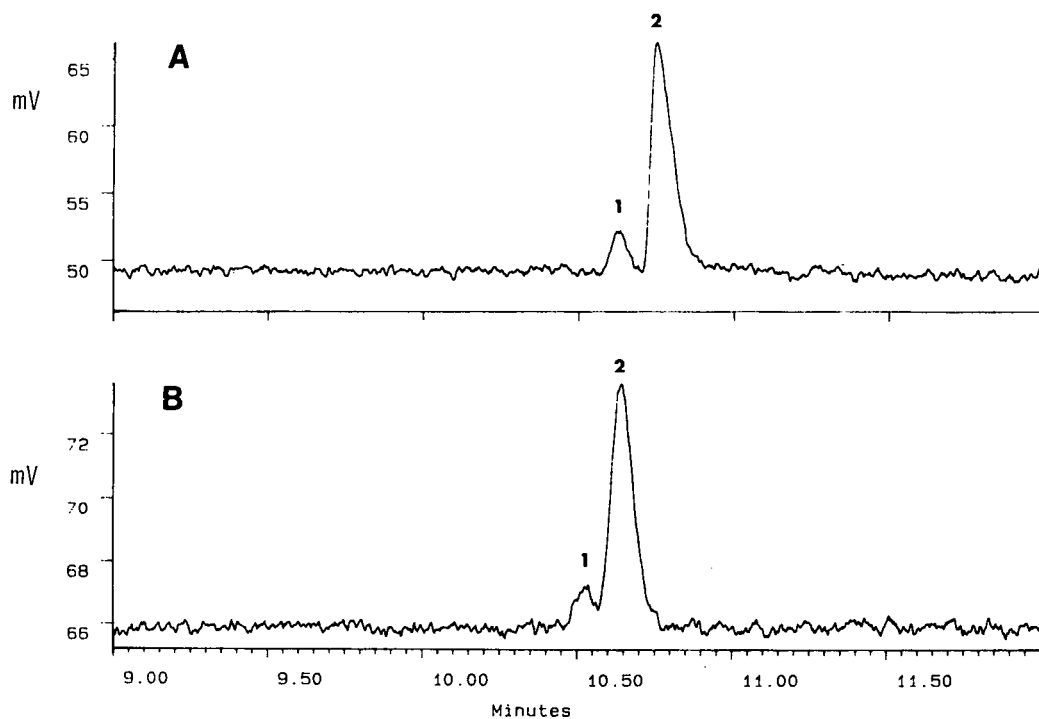


Fig. 4. Comparison electropherogram of (A) standard capillary and (B) concentrator capillary. Conditions as described in Experimental. Peaks: 1 = doxepin, 2 = propranolol. For (A) a 10-s electromigration injection at 5 kV was used. Peaks represent doxepin and propranolol concentrations of 10 (signal-to-noise ratio of 3) and 60 ppm respectively. For (B) a 16.7-min concentration step and a 15-s elution step both at 5 kV was used, with an eluent concentration of 75% ACN in run buffer. Peaks represent doxepin and propranolol concentrations of 100 (signal-to noise ratio of 3) and 600 ppb respectively.

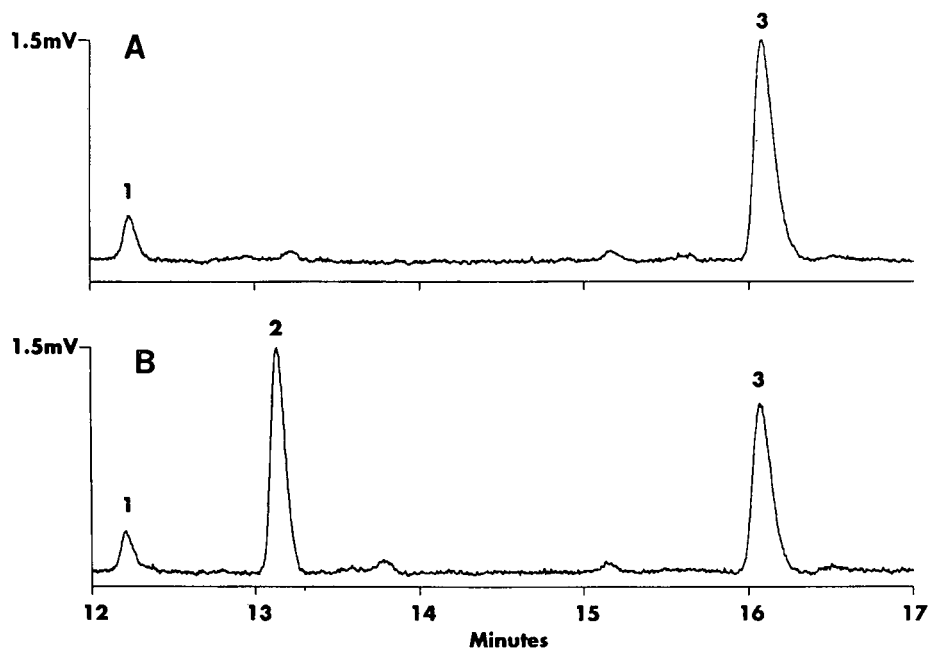


Fig. 5. Comparison electropherogram of (A) urine blank, and (B) urine spiked with doxepin at the 0.5 ppm level. Conditions are identical to those reported in Fig. 4B. Peaks: 1 = unknown, 2 = doxepin, 3 = unknown.

TABLE I
CONCENTRATOR CAPILLARY REPRODUCIBILITY

Conditions as reported in Fig. 4B. A 1.0-ppm solution of doxepin was used.

| | R.S.D. (%) | |
|------------------------------------|----------------|------|
| | Migration time | Area |
| Run to run ($n = 5$) | 1.74 | 1.90 |
| Capillary to capillary ($n = 3$) | 7.87 | 4.18 |

Sensitivity enhancement

To determine the sensitivity enhancement that the concentrator capillary provides, a head to head comparison under identical separation conditions was made between a standard capillary and a concentrator capillary. The results are presented in Fig. 4. This comparison shows that under these conditions, the concentrator capillary can provide up to two orders of magnitude improvement in sensitivity as measured by the signal to noise ratio. The slight differences in migration times between the two capillaries is a result of batch to batch differences in capillary stock (see Reproducibility below).

Spiked urine sample

Following sample preparation, a urine blank and a spiked urine sample were run under identical conditions with the results shown in Fig. 5. Using the concentrator capillary a peak for doxepin at the 0.5 ppm level can easily be seen. This level is well into the therapeutic range for most small molecule pharmaceuticals and given the signal-to-noise level, could be easily quantitated. This level would be below the detection limits of a standard capillary using conventional CE techniques.

Concentrator capillary reproducibility

Both run to run ($n = 5$) and capillary to capillary ($n = 3$) reproducibility are presented in Table I. The relative standard deviation (R.S.D.) for both migration time and peak area are less than 2.0% for the run to run experiment which is typical of conventional CE techniques [11]. The R.S.D.s are higher for the capillary to capillary experiment reflecting the differences in lots of stock capillary material. From the authors' experience this error is similar to that obtained from lot to lot of standard capillaries.

Concentrator capillary linearity

Linearity was evaluated over three orders of magnitude from 10 ppb to 10 ppm. Excellent linearity with a correlation coefficient of 1.00 was obtained over the entire range. Above 10 ppm, a plateau was reached indicating detector photomultiplier saturation under the injection conditions employed. The solution to detector saturation is to inject less at higher ppm levels, and this is done by decreasing the concentration time. Decreasing the concentration time at higher concentrations can extend the linear range another two orders of magnitude. Therefore, under these conditions, using a combination of concentration times, linearity over five orders of magnitude, from 10 ppb to 1000 ppm can be obtained.

CONCLUSIONS

The use of concentrator capillaries of this type to perform on-line preconcentration improves the sensitivity of CE analyses by at least two orders of magnitude into the low ppb range. Run to run and capillary to capillary reproducibility, as well as linearity, is sufficient to allow quantitative use of these types of capillaries in the pharmaceutical laboratory. In conjunction with other CE techniques such as low wavelength detection and isotachophoretic sample loading, concentrator capillaries of this type may help to overcome the sensitivity limitations of CE to extend the range of applications to therapeutic drug monitoring.

REFERENCES

- 1 R. A. Wallingford and A. G. Ewing, *Adv. Chromatogr.*, 29 (1989) 1.
- 2 R. A. Wallingford and A. G. Ewing, *Anal. Chem.*, 59 (1987) 1762.
- 3 T. Tsuda, J. V. Sweedler and R. N. Zare, *Anal. Chem.*, 62 (1990) 2149.
- 4 J.-P. Chervet, M. Ursem, J. P. Salzman and R. W. Vannoort, *J. High Resolut. Chromatogr.*, 12 (1989) 278.
- 5 G. B. Gordon, *US Pat.*, 5 061 361, October 29 (1991).
- 6 F. E. P. Mikkers, F. M. Everaerts and Th. P. E. M. Verheggenh, *J. Chromatogr.*, 169 (1979) 1.
- 7 R. L. Chien and D. S. Burgi, *Anal. Chem.*, 64(8) (1992) 489A.
- 8 P. Jandik and W. R. Jones, *J. Chromatogr.*, 546 (1991) 431.
- 9 N. A. Guzman, M. A. Trebilcock and J. P. Advis, *J. Liq. Chromatogr.*, 14 (1991) 997.
- 10 M. Merion, R. H. Aebersold and M. Fuchs, presented at the *Conference on Capillary Electrophoresis, Frederick, MD, October 1990*, Abstract No. 7.
- 11 M. E. Swartz, *J. Liq. Chromatogr.*, 14(5) (1991) 923.

Screening of β -blockers in human serum by ion-pair chromatography and their identification as methyl or acetyl derivatives by gas chromatography–mass spectrometry

H. Sirén, M. Saarinen, S. Hainari, P. Lukkari and M.-L. Riekkola

Department of Chemistry, Analytical Chemistry Division, University of Helsinki, Vuorikatu 20, SF-00100 Helsinki (Finland)

ABSTRACT

A simultaneous screening method for atenolol, acebutolol, metoprolol, oxprenolol, alprenolol and propranolol by ion-pair chromatography with a column-switching technique was developed. The serum samples were purified using either liquid–liquid extraction or solid-phase extraction methods. The pretreatment of the samples consisted of hydrolysis and protein precipitation. The drug separation was on either octadecylsilica or polymer-based alkyl column material. Binary eluent mixtures containing methanol and a buffer solution with a quaternary ammonium salt as an ion-pair former were used. Detection of the compounds in liquid chromatographic analysis was based on ultraviolet spectra. The effects of methanol, two buffers and the ion-pair former on the retention of the compounds were studied. The determination limits ranged from nanograms to micrograms in the ion-pair chromatographic method, depending on the drug studied. Identification was based on the mass spectra or, if necessary, on selected-ion monitoring spectra of either the methylated or the acetylated compounds obtained by means of gas chromatography–electron impact or negative chemical ionization mass spectrometry. The detection limits for the identified compounds were in the picogram range. The matrix effect was strong, and this resulted in determination limits in the nanogram range with the scan method.

INTRODUCTION

β -Adrenoceptor blocking drugs are of therapeutic value in the treatment of various cardiovascular disorders, such as angina pectoris, cardiac arrhythmia and hypertension. They are so sensitive that even a small oral dose of the drug gives sufficient blockade [1]. Because of the sedative effect of the β -blockers they are also misused as doping agents in some sports [2,3].

β -Blockers are exceptionally toxic and most of them possess a narrow therapeutic range; the difference between the lowest therapeutic and highest tolerable doses is small. Their unusually low concentrations in human blood makes their analysis diffi-

cult. In addition, the half-lives ($t_{1/2}$) of these drugs in serum or plasma are only a few hours, except for alprenolol [1]. They therefore require a sensitive and rapid screening method. Special problems can arise during screening of biological fluids, such as urine or serum, because low concentrations of the drugs or their metabolites have to be determined in these matrices, which contain high concentrations of other endogenous compounds or proteins.

Polar β -blockers have previously been analysed by reversed-phase high-performance liquid chromatography (RP-HPLC) using ultraviolet (UV) or highly specific fluorescence detectors [4]. As separation of ionic compounds in RP-HPLC is based on their weakly acidic or basic functional groups, ion-pair chromatographic (IPC) methods can be used for analyses for these drugs by adding organic compounds to the eluent to form ion pairs with oppositely charged sample molecules. In analyses for

Correspondence to: H. Sirén, Department of Chemistry, Analytical Chemistry Division, University of Helsinki, Vuorikatu 20, SF-00100, Helsinki, Finland.

these drugs either the negative or positive charge must be masked by the counter-ion and the other suppressed by choosing an appropriate pH. The presence of a basic amino group in an analyte often leads to long retention times. Control of the mobile phase pH and/or addition of amines to the mobile phase are frequently used cures for peak tailing [5,6].

Often liquid–liquid extraction (LLE) is used to clean up and separate drugs from the matrices. The choice of the solvent in LLE plays no significant role because all the usual organic solvent have been proved to be suitable. The pretreatment of the sample has sometimes included back-extraction of the drugs into the aqueous solution, which is considered to be a good procedure for cleaning up the organic material.

LLE has been found to be an inadequate clean-up procedure as far as very lipophilic compounds in plasma are concerned. Therefore, the use of solid-phase extraction (SPE) as a clean-up procedure has increased in analyses for both hydrophilic and hydrophobic compounds. Moreover, especially the recovery of β -blockers, like that of many other drugs, is better with SPE than LLE, which further expanded the use of the technique for their purification.

Gas chromatography–mass spectrometry (GC–MS) is both a primary and a confirmation technique in analyses for β -blockers [7]. The drugs are first extracted by LLE from urine before derivatization of their polar functional groups. In human doping analysis, and also in horse doping, blood samples may increase the reliability of the results if serum is to be used in the case where no good method for screening exists or more precision is demanded for reliable results.

In this paper we present a method for simultaneously screening the β -blockers atenolol, acebutolol, metoprolol, oxprenolol, alprenolol and propranolol in human serum by ion-pair chromatography with UV detection and their confirmed identification as their methyl and acetyl derivatives by GC–MS. Ion-pair chromatographic analyses were carried out using either acetate or phosphate buffers containing N-cetyl-N,N,N-trimethylammonium bromide (CTAB). The technique was based on ion-pair formation of the drugs with CTAB. After injection the compounds were adsorbed on the column material,

and both the water-soluble and non-ion-pair-forming compounds were eluted using pure water as the mobile phase for 1 min to waste.

Using biphenylamine as an internal standard (I.S.), we found the method to be suitable for pharmacokinetic studies and investigated the possible interference of caffeine and five other β -blockers, namely sotalol, nadolol, timolol, pindolol and labetalol. The separation of the enantiomers of these pharmaceuticals was not studied owing to the selection of the column materials and to their unknown stabilities in the presence of the chiral compounds in the eluent.

Our main aim was to obtain information for micellar electrokinetic capillary chromatography (MECC) of the parent β -blockers using CTAB as the micelle and to have a reference technique for HPLC for the determination of these drugs in biological fluids [8]. Hence the metabolites were not screened by HPLC. In addition, the UV spectra of the ion-paired metabolites were not known. However, in identification by GC–MS the metabolites were registered and identified, because reference data were available in our system library and in the literature [9].

EXPERIMENTAL

Apparatus

Liquid chromatography. The liquid chromatograph was a Hewlett-Packard Model 1090 instrument equipped with a Model 1040A diode-array detector, a computer, a disc drive unit, an integrator, a printer and a plotter (Hewlett-Packard, Avondale, PA, USA). The columns used were Hypersil C₁₈ (10 and 100 × 4.6 mm I.D., 5 μ m), Shiseido SG-120 (polymer-based C₁₈) (150 × 4.6 I.D., 5 μ m), HP Guard C₁₈ (5 × 4.6 mm I.D., 5 μ m), Hibar[®] Li-Chrosorb RP-18 (Merck) (250 × 4.6 mm I.D., 10 μ m) and Asahipak C8P-50 (Asahipak) (150 × 4.6 mm I.D., 5 μ m). Detection was at 230, 260 and 280 nm with a 10-nm wavelength width. The reference wavelength was at 500 nm. After injection the compounds were adsorbed on the column material, and both the water-soluble and non-ion-pair-forming compounds were eluted to waste for 1 min by column switching using pure water as the mobile phase. The samples were separated at ambient temperature (22–26°C).

Gas chromatography–mass spectrometry. A Hewlett-Packard Model 5989A single-stage quadrupole mass spectrometer was used with electron impact (EI, 70 eV) or negative chemical ionization (NCI). A Hewlett-Packard Model 5890A gas chromatograph, an HP 98785A monitor, an HP 6000 330S digital data storage, an HP 9000 345 data system and an HP LaserJet III printer were used for analysis, data storage and reporting. The carrier gas (helium) was purified with a Supelco high-capacity carrier gas purifier (Supelco, Bellefonte, PA, USA).

The compounds were separated on an HP ULTRA-1 high-performance GC column (12.5 m × 0.20 mm I.D., 0.33 μm). The temperature was programmed from 125 to 310°C at 15 and 10°C/min. The temperatures of the injector, transfer line, source and quadrupole were 260, 280, 270 and 120°C, respectively. The carrier gas was helium (1.0 or 1.5 ml/min at 150°C) and the CI reagent gas was methane. Injection was done by the solvent flush method (1 or 2 μl with solvent plug) with methanol–toluene (4:96, v/v) as solvent. The full-scan mass spectra of the β-blockers were scanned from 40 to 650 u at a rate of 0.96 ms/u. When necessary selective ion-monitoring technique (SIM) was also used with at least six main fragments obtained from the scan spectra of the derivatized parent compounds.

Materials and reagents

The β-blockers used were acebutolol hydrochloride, alprenolol hydrochloride, atenolol, labetalol hydrochloride, (±)-metoprolol (+)-tartrate, nadolol, oxprenolol hydrochloride, pindolol, (S)-(-)-propranolol hydrochloride, timolol maleate and anhydrous caffeine (Sigma, St. Louis, MO, USA).

The tablets taken by volunteers were 100 mg of alprenolol (Aptin N, Hässle), 25 mg of propranolol (Propral, Medipolar), 40 mg of oxprenolol (Trasicor, Ciba), 100 mg of acebutolol (Espesil, Orion), 50 mg of metoprolol (Seloken, Astra) and 50 mg of atenolol (Tenoblock, Leiras). The doses were given once to the volunteers so that another drug was not taken before the urine taken from the volunteer was equal to the drug-free urine. The β-blockers were administered after overnight fasting. Serum samples were separated by centrifugation and stored frozen in PTFE tubes until analysed.

The high-purity solvents and analytical-reagent grade reagents were as follows: glycine, NaOH,

CH₂Cl₂, propanol, methanol (LiChrosolv), Na₂SO₄, H₂SO₄, zinc sulphate, diethyl ether, glacial acetic acid, sodium acetate, NaH₂PO₄, Na₂HPO₄, pyridine, biphenylamine, N-cetyl-N,N,N-trimethylamine bromide (CTAB), potassium carbonate, acetic anhydride, methyl iodide, potassium hydrogenphthalate and disodium tetraborate decahydrate (Merck, Darmstadt, Germany), acetone and toluene (Rathburn, glass distilled) and N,N-dimethyloctylamine (DMOA, 95%, Aldrich) and distilled, ionized water (Water I-system, Gelman Sciences, Ann Arbor, MI, USA). β-Glucuronidase (EC 3.2.1.31) Type H-1 from *Helix pomatia* (416 800 units/g), stored at –20°C (Sigma), was used for enzymatic hydrolysis.

The pH of the buffer solutions used in mobile phase was adjusted using a Jenway 3030 pH meter and electrode (Jenway, Felsted, UK) containing 4 M KCl in saturated AgCl. Calibration was made with potassium dihydrogenphthalate (0.050 M, pH 4.00) and sodium tetraborate (0.010 M, pH 9.81) buffer solutions.

Ultrasonication was performed with Eurosonic 44 (Oriola, Prolab). The blood samples were centrifuged at 1000 g with a Heraus Christ Medifuge. Sartorius Minisart NML sterile filter units (0.45 μm; Sartorius, Göttingen, Germany) and Millex filters of 0.5-μm pore size from Millipore (Nihon Millipore, Yonezawa, Japan) were used for filtration of the samples. The eluents containing CTAB were filtered through 0.45-μm membranes (Millipore, Mosheim, France) and degassed with helium before use.

Preparation of standard solutions

Stock standard solutions of the respective drugs (1 mg/ml) were prepared in methanol. Calibration standards for biological fluids were made by adding each standard solution to the blank biological medium.

Pretreatment of blood

The respective β-blockers were administered to two volunteers who were coffee or tea drinkers, non-smokers or non-drug-users in the morning after overnight fasting. Blood samples from the volunteers were collected in 5- and 10-ml VT-050PZX Venoject tubes with a silicone coating (Terumo Europe, Belgium) 2 and 3 h after administration of the

drugs. They were kept at ambient temperature (22–26°C) for 1 h, after which they were centrifuged for 10 min at 1000 g (3000 rpm). The incubation of the serum samples was carried out with Type H-1 enzymes at 60°C for 1 h or overnight at ambient temperature.

Spiked serum sample preparation

The MIX6 sample solution, which was a mixture of six β -blockers, was made by adding 500 μ l of each stock solution (see *Preparation of standard solutions*) to 900 μ l of serum [hydrolysed, proteins precipitated and eluted through Supelclean LC-18 3 ml-SPE tubes (Supelco)]. The working concentration was 2.56 μ g in 20 μ l (loop volume 20 μ l).

Pretreatment of the serum samples by liquid-liquid extraction

Method I. A 50- μ l volume of the I.S. (1 mg/ml), 50 μ l of glycine buffer (0.5 M, pH 12), 50 μ l of NaOH (2 M), 1 ml of saturated NaCl solution and 4 ml of mixture containing CH₂Cl₂ and propanol (3:97, v/v) were mixed with 3 ml of serum. The mixture was shaken mechanically for 10 min. After centrifugation for 5 min at 2000 g, the organic layer was separated, dried with Na₂SO₄ for 10 min and further centrifuged for 5 min. The organic phase was then filtered and analysed by LC [10].

Method II. A 50- μ l volume of the I.S., 0.1 ml of NaOH (0.2 M) and 6 ml of CH₂Cl₂ were mixed with 3 ml of serum. The mixture was shaken mechanically for 10 min and centrifuged for 10 min at 2000 g. The organic layer was then separated and added to 0.1 ml of sulphuric acid (0.025 M). After shaking for 1 min and centrifugation for 5 min, the organic phase was separated and analysed by LC [11].

Method III. A 50- μ l volume of the I.S. (1 mg/ml), 0.5 ml of zinc sulphate (0.70 M), 0.5 ml of DMOA (0.5 mM) and 0.5 ml of NaOH (1.0 M) were mixed with 3 ml of serum, shaken mechanically and centrifuged. The water phase was filtered and analysed by LC [12].

Method IV. A 50- μ l volume of the I.S., 0.5 ml of NaOH (5 M), 2 ml of diethyl ether and 3 g of Na₂SO₄ were mixed with 3 ml of serum. The mixture was shaken mechanically for 10 min and centrifuged for 5 min. The diethyl ether layer was separated and evaporated off. The residue was dis-

solved in 2 ml of methanol-water (1:1, v/v) and analysed by LC.

Solid-phase extraction

SPE columns were regenerated with methanol and distilled, deionized water. The samples were adsorbed on the C₁₈ phase, washed with 1 ml of water, dried in vacuum and eluted with 2 ml of water-methanol (10:90, v/v). In screening runs the sample volume was 2 ml, but in quantitative studies the volume was reduced to 600 μ l by evaporation of the solvent.

Preparation of the buffers

The buffers used in LC separation were made from 0.1 M sodium acetate by decreasing the pH to 6.0 with both 50% and 1% glacial acetic acid, and 0.1 M sodium dihydrogenphosphate and 0.1 M disodium hydrogenphosphate (pH 7.0). After adjusting the pH to 6.0 or 7.0, 9 mM of N-cetyl-N,N,N-trimethylammonium bromide were added into the buffer. The pH values of the solutions were not changed by the addition.

HPLC gradients

The β -blockers were eluted with two solvent gradient methods. With the acetate buffer the methanol gradient was increased from 4% at rate of 6% per 2 min to 10%, at 20% per 4 min to 30% and finally at 30% per 6 min to 60%. When the LC separation was made using phosphate buffer, the methanol gradient started from 30%, which was maintained for 4 min. It was then increased at a rate of 5% per 4 min to 50% and finally at 10% per 2 min to 60%.

Derivatization for GC-MS

Methylation. After the SPE treatment the methanol extract was evaporated in a heating block under nitrogen. A 1.5-g amount of K₂CO₃, 200 μ l of acetone and 50 μ l of CH₃I were added to the dry residue. The resulting solution was incubated at 60°C for 60 min before the acetone was evaporated under nitrogen, after which the residue was dissolved in 100 μ l of methanol-toluene (4:96, v/v). GC-MS was carried out on the derivatives contained in the methanol-toluene mixture by injecting 2 μ l of the solution.

Acetylation. After the SPE clean-up the extract

was evaporated under nitrogen as described in the methylation process. The residue was dissolved in 150 μ l of acetic anhydride–pyridine (2:3, v/v) and incubated at 80°C for 60 min before being analysed by GC–MS.

RESULTS

Chromatographic separation in LC

In the absence of the ion-pair reagent, CTAB, the compounds were eluted in one zone without peak

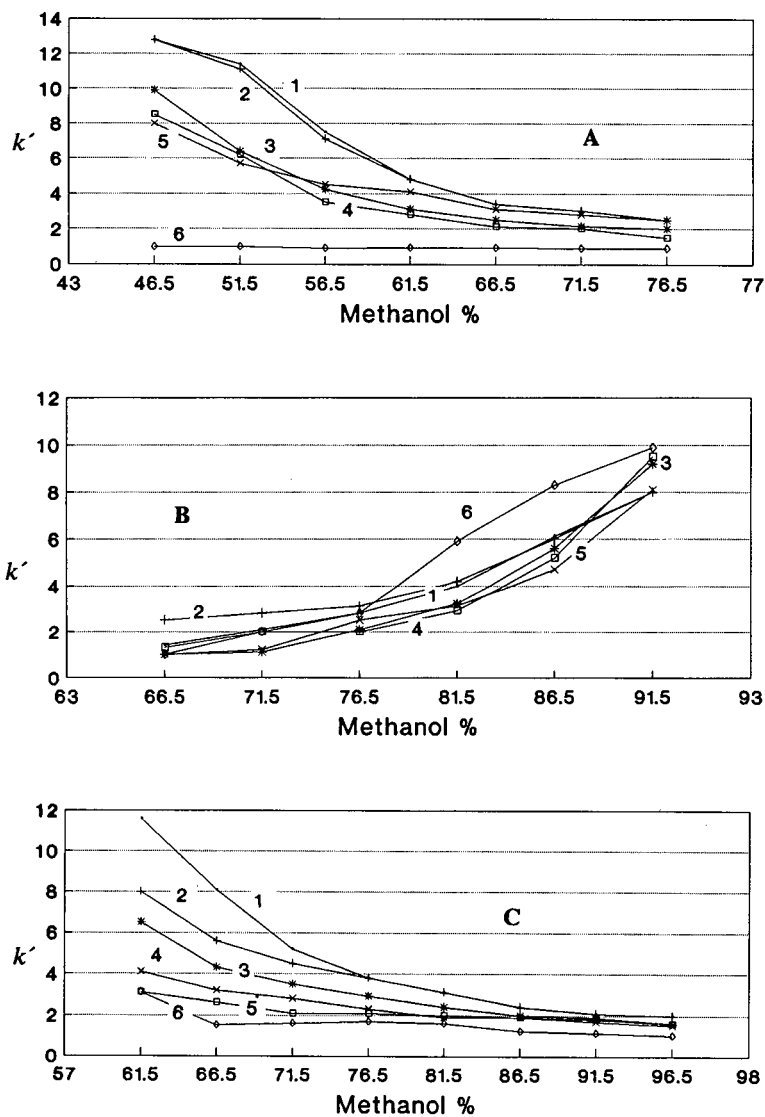


Fig. 1. Effect of methanol content on the retention of β -blockers in ion-pair chromatography. (1) Alprenolol, (2) propranolol, (3) oxprenolol, (4) acebutolol, (5) metoprolol and (6) atenolol. UV detection at 230 nm. Column, Shiseido SG-120; ion-pair former, CTAB. Mobile phases: (A) phosphate buffer without CTAB; (B) CTAB without buffer; (C) acetate buffer without CTAB. Flow-rate 0.7 ml/min.

TABLE I
RELATIVE RETENTION TIMES OF THE COMPOUNDS STUDIED

LC conditions: Asahipak C8P-50 column; eluent; acetate buffer containing CTAB and methanol; gradient elution; detection at 260 nm. GC-MS conditions as described under Experimental. Flow-rate of the carrier gas, 1.5 ml/min.

| Compound | Relative retention time | | |
|----------------------|---------------------------|----------------------------|----------------------------|
| | HPLC, ion-paired drugs | GC-MS, methylated drugs | GC-MS, acetylated drugs |
| Atenolol | 0.205 | 2.97 | 3.02 |
| Sotalol | 0.211 | — | — |
| Caffeine | 0.377 | 1.51 | 1.43 |
| Nadolol | 0.395 | 2.88 | — |
| Metoprolol | 0.527 | 2.56 | 3.04 |
| Timolol | 0.562 | 2.86 | — |
| Acebutolol | 0.608 | 3.84 | 2.90 |
| Pindolol | 0.665 | 2.71 | — |
| Oxprenolol | 0.692 | 1.93 | 2.71 |
| Alprenolol | 0.926 | 1.74 | 2.69 |
| Propranolol | 0.854 | 2.51 | 3.21 |
| Labetalol | 0.976 | 4.26 | — |
| Biphenylamine (I.S.) | 1.00 | 1.00 | 1.00 |

resolution, making it impossible to analyse for all six β -blockers simultaneously. It was known that the members of the β -blocker group were difficult to separate under reversed-phase conditions on modified phases in the pH range 1.5–7.5 [13]. Therefore,

we had to optimize the chromatographic conditions. The eluent composition has a clear effect on the resolution of the ion pairs, as can be seen in Fig. 1 and in the chromatograms in Figs. 2 and 3. Fig. 1 shows the capacity factors of the β -blockers to de-

TABLE II
NUMBER OF EFFECTIVE THEORETICAL PLATES, k' , α AND R FOR β -BLOCKERS SPIKED IN SERUM
 $\lambda = 260$ nm. Column: Asahipak C8P-50. Gradient elution (see Experimental).

| Compound ^a | Matrix ^b | k' | N (plates per metre) | α | R^c |
|-----------------------|---------------------|------------------|------------------------|-----------------|------------------|
| 1 | a | 4.76 \pm 0.23 | 3800 \pm 800 | 2.85 \pm 0.06 | 13.42 \pm 0.71 |
| | b | 4.24 \pm 0.09 | 4900 \pm 100 | 1.91 \pm 0.03 | 3.10 \pm 0.15 |
| 2 | a | 13.58 \pm 0.53 | 9700 \pm 800 | 1.15 \pm 0.01 | 2.96 \pm 0.40 |
| | b | 8.38 \pm 0.27 | 6900 \pm 1000 | 1.07 \pm 0.03 | 0.51 \pm 0.12 |
| 3 | a | 15.66 \pm 0.46 | 2000 \pm 2600 | 1.14 \pm 0.00 | 3.28 \pm 0.19 |
| | b | 8.43 \pm 0.15 | 6200 \pm 600 | 1.76 \pm 0.09 | 3.62 \pm 0.41 |
| 4 | a | 17.89 \pm 0.52 | 24 000 \pm 2000 | 1.24 \pm 0.01 | 6.88 \pm 0.28 |
| | b | 14.89 \pm 0.51 | 6700 \pm 800 | 1.50 \pm 0.04 | 3.51 \pm 0.29 |
| 5 | a | 22.14 \pm 0.61 | 57 000 \pm 13 800 | 1.09 \pm 0.01 | 3.51 \pm 0.35 |
| | b | 21.78 \pm 0.20 | 37 800 \pm 4100 | 1.25 \pm 0.02 | 6.79 \pm 0.85 |
| 6 | a | 24.10 \pm 0.74 | 68 800 \pm 10 000 | 1.07 \pm 0.02 | 3.27 \pm 0.35 |
| | b | 27.96 \pm 0.30 | 40 900 \pm 4700 | 1.07 \pm 0.01 | 1.39 \pm 0.12 |
| I.S. | a | 25.73 \pm 1.04 | 69 600 \pm 7600 | | |
| | b | 28.72 \pm 0.78 | 65 400 \pm 5400 | | |

^a Compounds: 1 = atenolol; 2 = metoprolol; 3 = acebutolol; 4 = oxprenolol; 5 = propranolol; 6 = alprenolol.

^b a = Acetate buffer eluent; b = phosphate buffer eluent.

^c R = Resolution.

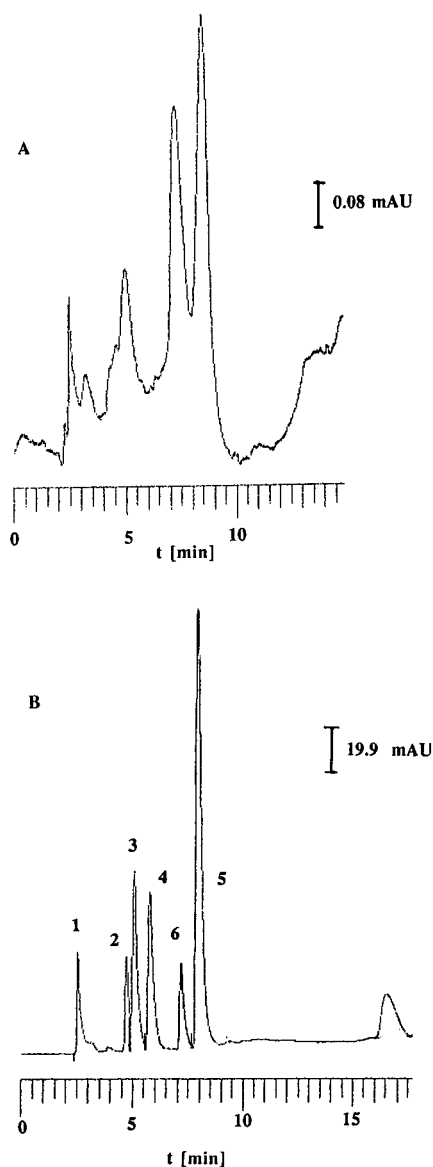


Fig. 2. HPLC of the separation of β -blockers with the ion-pair technique. (A) Blank human serum sample; (B) with six β -blockers added to human serum sample. Gradient elution (see Experimental). Compounds: 1 = atenolol; 2 = acebutolol; 3 = metoprolol; 4 = oxprenolol; 5 = propranolol; 6 = alprenolol. Eluent, phosphate buffer–methanol containing 9 mM CTAB; detection wavelength, 260 nm.

crease with increasing methanol concentration of the eluent when CTAB was not used. However, when no buffers were used, *i.e.*, phosphate or acetate ions were not present, the capacity factors in-

creased with increasing methanol concentration. When both the buffer and the ion-pair former were in the mobile phase the use of methanol led to the same trend as in buffer solutions of pH 6.0 and 7.0.

Biphenylamine was chosen as the internal standard, because it eluted at the end of the drug zone and therefore did not interfere with the separation of the β -blockers. The elution order of all the drugs analysed when the acetate buffer with CTAB and methanol was used is given in Table I. The hydrophilic compounds were eluted first: atenolol, acebutolol, metoprolol, oxprenolol, alprenolol and propranolol. The elution order of acebutolol and metoprolol and also that of alprenolol and propranolol changed and the pressure in the HPLC system increased considerably when the acetate buffer was changed to phosphate. The number of effective theoretical plates for the β -blockers spiked in serum were higher with the acetate than the phosphate buffer (Table II). As can be seen from the standard deviations, the methanol gradient elution is a valid method to separate these six β -blockers from each other.

According to this study, the best column materials for the separation of the six β -blockers were Hibar C₁₈ and Asahipak C8P-50 materials. Fig. 2 shows chromatograms obtained from the SPE-treated blank and with β -blocker-spiked human serum samples. The peaks eluted within 10 min because of the methanol gradient. Fig. 3 shows the liquid chromatograms obtained from the real serum samples taken from the volunteers. Fig. 3A–C show that baseline resolution is not achieved when small drug concentrations are to be determined. However, with normally treated patients the parent compounds can be easily identified from profile chromatograms (Fig. 3D and E) 3 h after oral administration.

It became evident that all the extraction methods were tedious and lacked high and reproducible absolute extraction efficiencies. Table III shows the recovery ratios obtained with the LLE techniques (I–IV) using the two eluent buffers. The recovery ratios of propranolol were very poor for each method and could not be improved by changing the buffer. These results suggest that selective extraction eluents should be used for each drug. In contrast to LLE, SPE gave high recovery ratios in all instances. Therefore, we preferred SPE to LLE in further studies.

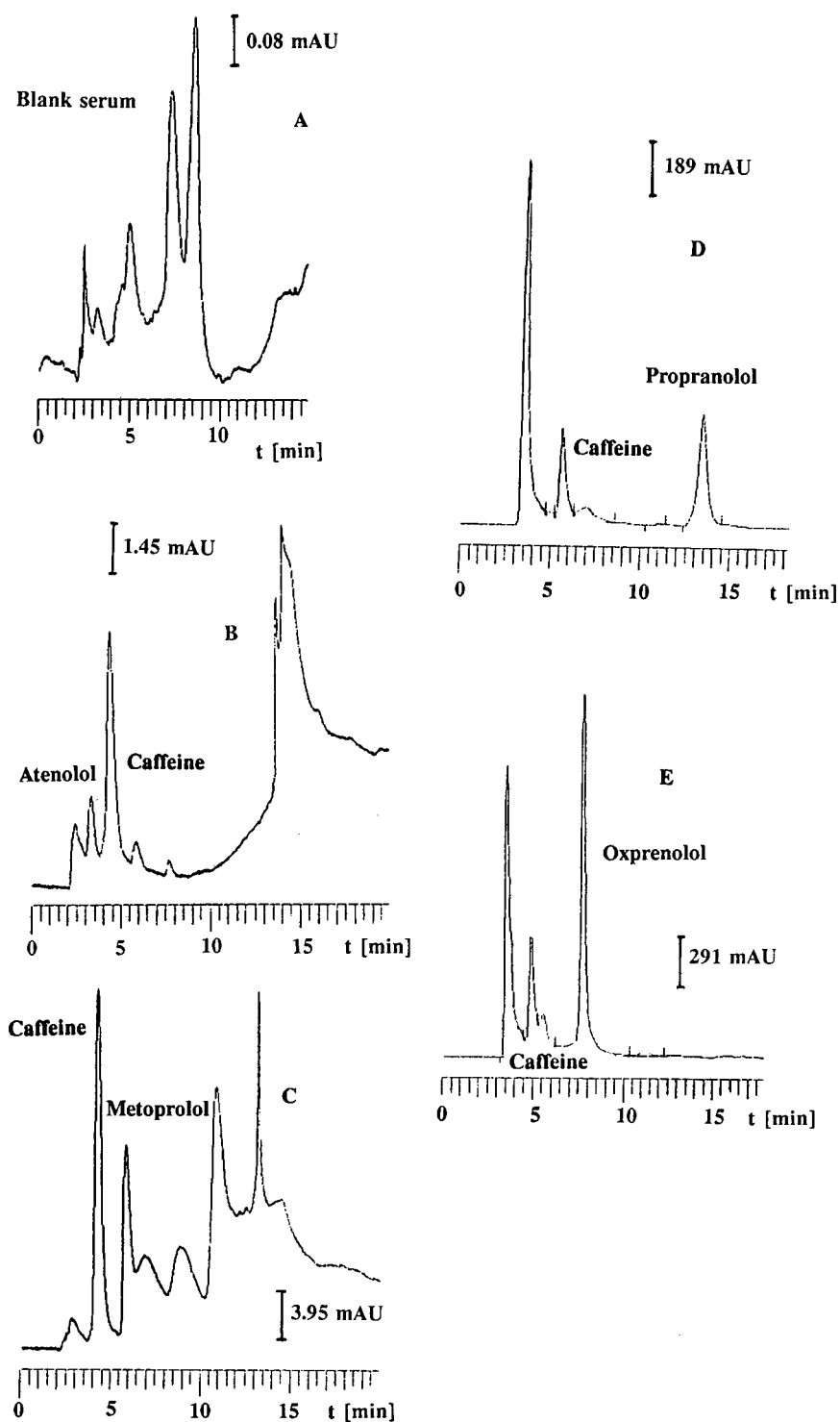


Fig. 3. Liquid chromatograms obtained from (A) blank serum and from 1-ml human serum samples taken 3 h after administration of (B) atenolol and (C) metoprolol and from 3-ml serum samples taken 3 h after administration of (D) propranolol and (E) oxprenolol. Column, Asahipak C8P-50. Gradient flow with methanol (1 ml/min). Conditions as in Table I.

TABLE III
RECOVERIES WITH LLE ONLY USING BUFFER AND METHANOL IN THE ELUENT

The recoveries were calculated against the internal standard, which was added to the matrix before SPE clean-up. Eluents in HPLC separation were without CTAB: (a) acetate buffer and methanol and (b) phosphate buffer and methanol. Column, Hypersil C₁₈.

| Compound | Eluent | I | II | III | IV | SPE |
|-------------|--------|-----|-----|-----|-----|-----|
| Propranolol | a | 7 | 11 | 15 | 8 | 78 |
| | b | 9 | 14 | 15 | 5 | 52 |
| Metoprolol | a | 12 | 7 | 4 | 21 | 86 |
| | b | 78 | — | 11 | 86 | 63 |
| Oxprenolol | a | 11 | 47 | 39 | 68 | 81 |
| | b | 16 | — | 9 | 86 | 76 |
| Acebutolol | a | 100 | — | 11 | 43 | 65 |
| | b | 50 | — | 10 | 27 | 67 |
| Alprenolol | a | 47 | 100 | 9 | 33 | 65 |
| | b | 18 | — | 10 | 68 | 66 |
| Atenolol | a | — | 100 | 33 | 100 | 87 |
| | b | 21 | 89 | — | 98 | 81 |

The liquid chromatograms of real serum samples showed that the concentrations of the β -blockers after oral administration are very low in human serum. Although possible co-eluting and interfering compounds could be removed from the biological

fluid, the volume of the samples had to be fairly large (1–3 ml) when no preconcentration was done. Fig. 3 shows the chromatograms obtained from 1- and 3-ml serum samples 3 h after oral administration of the tablet (see Experimental).

Accuracy and reproducibility in LC

The accuracy and reproducibility of the results for drug-free serum samples spiked with the β -blockers were determined by comparing the peak-height ratios of 128 $\mu\text{g}/\text{ml}$ of the drugs to the I.S. with those obtained for aqueous solutions containing similar concentrations of drugs and the I.S.

The sensitivity limits of the drugs at 260 nm are given in Table IV. The calibration graph was obtained by plotting the ratio of the peak area of the drug to that of the I.S. The linearity of the plot of concentration of the drugs *versus* peak area from the detection limit (signal-to-noise ratio = 3) to 128.2 $\mu\text{g}/\text{ml}$ in serum was tested. The results are given in Table IV. Calibration was carried out using the MIX6-spiked serum sample.

GC-MS

A poor GC response of β -blockers, attributed to the interaction of hydroxy and amine groups with the column materials, was observed. Derivatization was carried out to improve their GC analyses. Fur-

TABLE IV
DETERMINATION LIMITS AND LINEARITY OF THE ION-PAIR CHROMATOGRAPHIC METHOD FROM DETERMINATION LIMIT to 128.2 $\mu\text{g}/\text{ml}$.

Eluent, acetate-methanol gradient (see Experimental); detection at 260 nm; ion-pair former, CTAB; column, Asahipak C8P-50. The concentrations of the β -blockers in the determined linear range were the determination limits, 27.8, 47.6, 83.3 and 128.2 $\mu\text{g}/\text{ml}$. r is the correlation coefficient. The equation for the straight line was $y = bx + a$, where a is the intercept of the ordinate and b is the slope. The elution order was as in Table I.

| Compound | Determination limit ^a (ng/ml) | a^b | b^b | r^b |
|-------------|--|-------------|-----------|-------------|
| Atenolol | 630 | 12.58/9.59 | 5.08/0.27 | 0.982/0.987 |
| Metoprolol | 580 | 24.19/23.00 | 4.93/0.20 | 0.987/0.994 |
| Acebutolol | 500 | 23.13/24.57 | 4.22/0.21 | 0.992/0.991 |
| Oxprenolol | 350 | 21.27/22.40 | 2.64/0.12 | 0.997/0.997 |
| Alprenolol | 670 | 20.66/23.30 | 3.65/0.19 | 0.998/0.999 |
| Propranolol | 100 | 18.60/23.10 | 0.71/0.03 | 0.993/0.997 |

^a Signal-to-noise ratio = 3.

^b First values calculated from peak heights; second values calculated from peak areas.

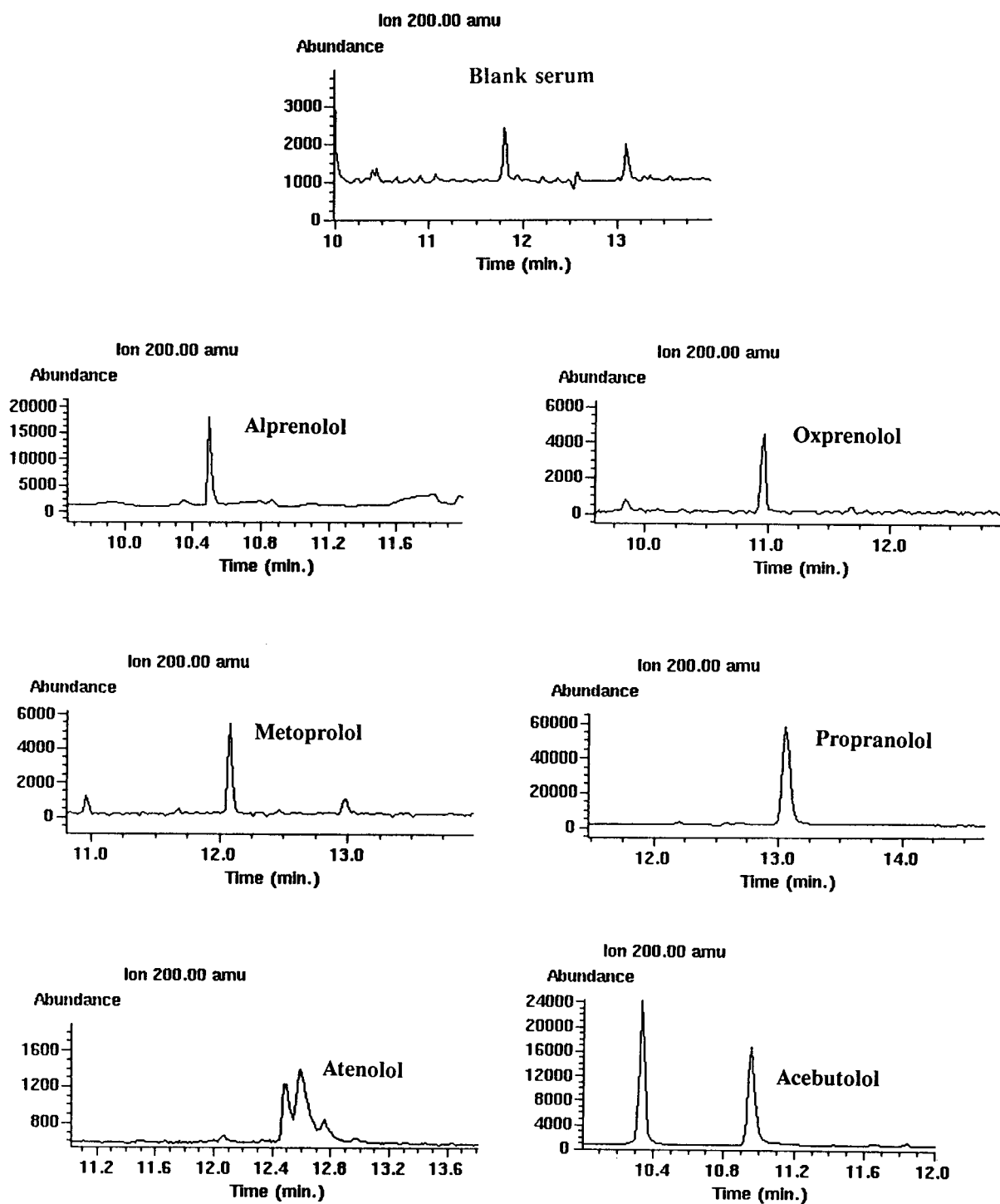


Fig. 4. Selected ion chromatograms of acetylated serum samples obtained by GC–EI–MS. Conditions as described under Experimental.

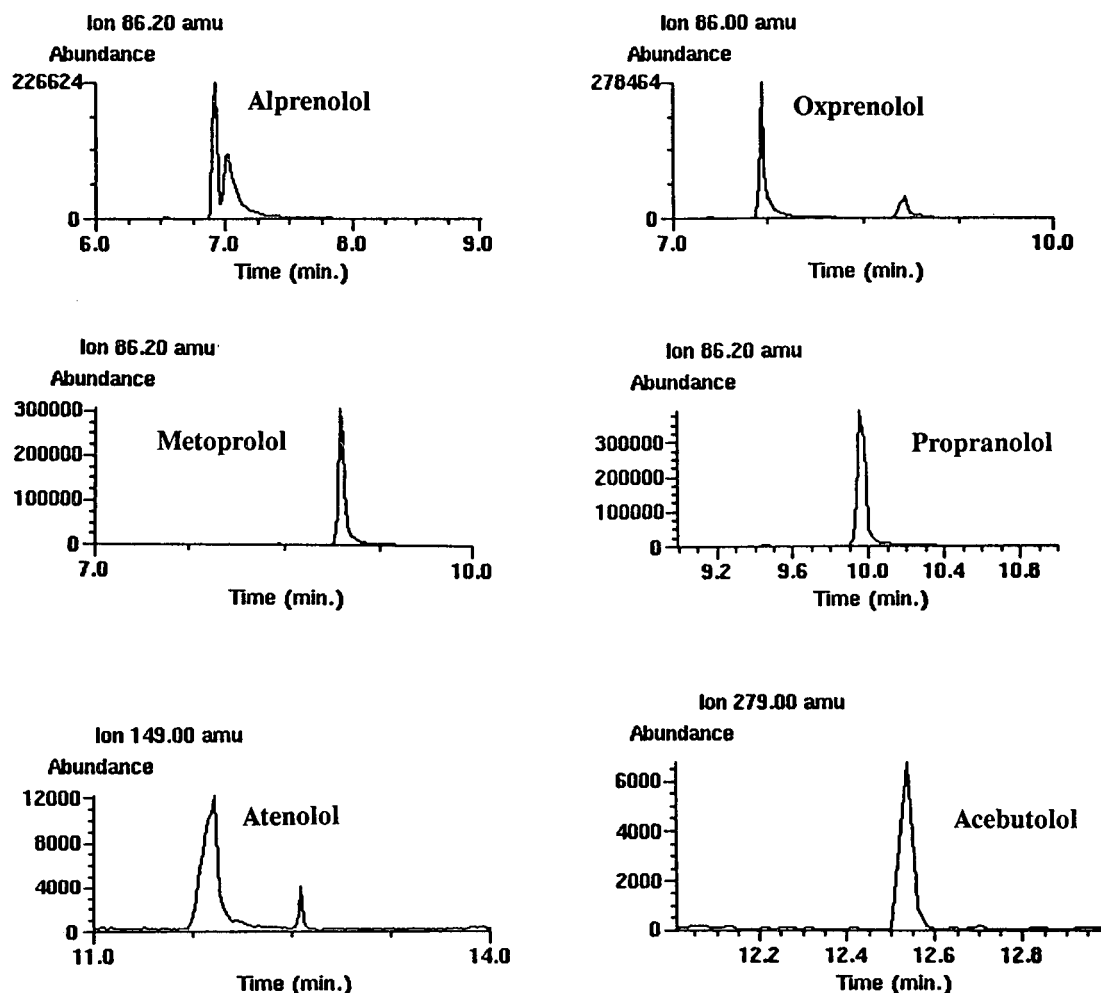


Fig. 5. Selected ion chromatograms of methylated serum samples obtained by GC–negative-ion-CI-MS. Run conditions as described under Experimental.

ther, typical fragments from derivatized oxypropylamine chain help in the identification of the compounds in the overall mass spectra.

All the methylated and acetylated β -blockers in the serum samples from volunteers who had taken the pharmaceuticals were identified. Identification of the acetylated and methylated β -blockers was not complicated because only one product resulted from the incubation. The retention times of the derivatized β -blockers relative to the I.S. are given in Table I.

The most intense fragment ions observed from the methylated β -blockers were at m/z 149, 167, 71, 86, 91 and 107 and from the acetylated oxypropyl-

amine chain at m/z 72, 98, 140, 158 and 200. Lower detection limits were obtained by methylation than by acetylation in with alprenolol, atenolol, metoprolol and oxprenolol. In addition, the detection limits for acebutolol and propranolol were very low when they were acetylated and subjected to GC–EI-MS. The selective ion chromatograms of acetyl derivatives of the drugs are shown in Fig. 4, where they are compared with the chromatogram of the blank serum sample and those of the methyl derivatives in Fig. 5. Tables IV and V show the detection and determination limits for the studied β -blockers. The concentrations of the drugs in the serum samples taken from the volunteers are given in Table VI.

TABLE V
DETECTION LIMITS FOR THE β -BLOCKERS IN GC-MS ANALYSES

Data taken from SIM chromatogram (ions as in Figs. 4 and 5) obtained from scan analyses. Detection limits (LOD) calculated from the equation $LOD = (V_{inj} \cdot 3 \cdot \%E)/(peak\text{-}peak\ S/N)$, where $\%E = [(peak\ area\ of\ extracted\ drug\ in\ serum\ sample)/(peak\ area\ of\ non\text{-}extracted\ drug)] \cdot V_{extr} \cdot 100\%$. V_{extr} = extracted volume. Recoveries were determined from the mean of six replicates taken from each drug. S/N = signal-to-noise ratio.

| Compound | Detection limit (ng) | |
|-------------|----------------------|-------------------|
| | Acetyl derivative | Methyl derivative |
| Acebutolol | 26 (EI) | 127 (EI) |
| | 42 (NCI) | 615 (NCI) |
| Alprenolol | 124 (EI) | 25 (EI) |
| | 103 (NCI) | 36 (NCI) |
| Atenolol | 111 (EI) | 81 (EI) |
| | 105 (NCI) | 67 (NCI) |
| Metoprolol | 21 (EI) | 3.1 (EI) |
| | 50 (NCI) | 27 (NCI) |
| Oxprenolol | 58 (EI) | 51 (EI) |
| | 34 (NCI) | 32 (NCI) |
| Propranolol | 21 (EI) | 87 (EI) |
| | 37 (NCI) | 56 (NCI) |

DISCUSSION

The ion-pair chromatographic screening and GC-MS identification methods described are useful for the determination of atenolol, acebutolol, metoprolol, oxprenolol, alprenolol and propranolol. However, the main metabolites were not screened in

HPLC, because the UV spectra of the ion-paired compounds were not known. In addition, the clean-up techniques were not optimized for their extraction. Further, in SPE clean-up we should have used another ion-pair former compound in order to obtain better recoveries.

Details of the partition behaviour of drugs in extraction experiments are usually not given. Depending on the drugs being studied, it is possible to obtain high recovery ratios, accuracy and reproducibility by suitable adjustment and estimation of extraction parameters such as the solvent, volume ratio of the phases and the concentration of the base versus the ion pair.

The required pretreatment of the sample depends largely on the selectivity of the detection. Clean-up procedures such as back-extraction or extraction from a basic solution may be needed with less selective detectors. The use of troublesome or time-consuming clean-up methods considerably decreases the number of analyses that can be made in a laboratory. In addition, transfer of the extracts, evaporation steps and all other measurements may cause adsorption or losses of the sample. One way to overcome these problems is to use the column-switching technique in HPLC, where the dilute sample is injected into a precolumn. After washing with water the sample is easily transferred into the analytical column with the eluent. β -Blockers are usually eluted quantitatively. By optimizing the HPLC eluent conditions the parent compounds could be eluted within 10 min. The HPLC method permits analyses of six β -blockers in a single serum extract

TABLE VI
DETERMINATION LIMITS FOR REAL SAMPLES AND CONCENTRATIONS OF DRUGS IN SERUM 3 h AFTER ADMINISTRATION

GC-EI-MS studies.

| Compound | Determination limit (ng) | | Concentration of drug in serum (ng/ml) |
|-------------|--------------------------|-------------------|--|
| | Acetyl derivative | Methyl derivative | |
| Acebutolol | 1.8 | 7.1 | 780 |
| Alprenolol | 0.6 | 7.6 | 120 |
| Atenolol | 3.2 | 5.3 | 330 |
| Metoprolol | 6.3 | 7.3 | 230 |
| Oxprenolol | 3.0 | 3.2 | 290 |
| Propranolol | 1.5 | 5.4 | 350 |

with high specificity. The retention order of the compounds was changed when phosphate was changed to acetate buffer and the pH was decreased.

The separation of the enantiomers of the pharmaceuticals was not studied owing to the separation of the column material and to the unknown stabilities in the presence of chiral compounds in the mobile phase during the gradient elution.

ACKNOWLEDGEMENTS

We are grateful to Kirsi Lumme, Anu Ennelin, Mari Pantsar and Mikko Koskinen for their assistance during these studies.

REFERENCES

- 1 J. E. F. Reynolds (Editor), *Martindale, The Extra Pharmacopoeia*. Pharmaceutical Press, London, 29th ed., 1989.
- 2 J. Park, S. Park, D. Lho, H. P. Choo, B. Chung, C. Yoon, H. Min and M. J. Choi, *J. Anal. Toxicol.*, 14 (1990) 66.
- 3 D.-S. Lho, H.-S. Shin, B.-K. Kang and J. Park, *J. Anal. Toxicol.*, 14 (1990) 73.
- 4 M. Ahnoff, M. Ervik, P.-O. Lagerström, B.-A. Persson and J. Vessman, *J. Chromatogr.*, 340 (1985) 73.
- 5 B. A. Bidlingmeyer, *J. Chromatogr. Sci.*, 18 (1980) 525.
- 6 W. H. Pirkle and J. A. Burke, III, *J. Chromatogr.*, 557 (1991) 173.
- 7 D.-S. Lho, J.-K. Hong, H.-K. Paek, J.-A. Lee and J. Park, *J. Anal. Toxicol.*, 14 (1990) 77.
- 8 P. Lukkari, H. Sirén, M. Pantsar and M.-L. Riekkola, *J. Chromatogr.*, 632 (1993) 143.
- 9 H. Maurer and K. Pflieger, *J. Chromatogr.*, 382 (1986) 147.
- 10 M. T. Rossell, A. M. Vermeulen and F. M. Belpaire, *J. Chromatogr.*, 568 (1991) 239.
- 11 C.-D. Fan, H. Zhao and M. S. S. Chow, *J. Chromatogr.*, 570 (1991) 217.
- 12 M. Johansson, *Acta Univ. Ups., Abstr. Uppsala Diss. Fac. Pharm.*, 42 (1988) 1–49.
- 13 E. Owino, B. J. Clasck and A. F. Fell, *J. Chromatogr. Sci.*, 29 (1991) 450.

Isoelectric focusing field-flow fractionation and capillary isoelectric focusing with electroosmotic zone displacement

Two approaches to protein analysis in flowing streams

Josef Chmelík

Institute of Analytical Chemistry, Czechoslovak Academy of Sciences, CS-611 42 Brno (Czechoslovakia)

Wolfgang Thormann

Department of Clinical Pharmacology, University of Berne, Murtenstrasse 35, CH-3010 Berne (Switzerland)

ABSTRACT

A comparison of the separation of three proteins by two focusing methods in flowing streams, isoelectric focusing field-flow fractionation (IEF_f) in a trapezoidal cross-section channel and capillary isoelectric focusing with electroosmotic zone displacement (cIEF) in an uncoated, open-tubular fused-silica capillary, is presented. In IEF_f a hydrodynamic flow with a characteristic flow velocity profile as well as an electric force field and a chemical equilibrium (pH) gradient arranged perpendicular to the direction of flow are employed for separation. cIEF uses an electrokinetic plug flow with the separating electrical and chemical fields parallel to its direction. Protein zones are monitored by conventional detectors developed for liquid chromatography and capillary electrophoresis respectively. With current instruments, separation by cIEF is shown to be characterized by higher efficiency and resolution than separation in IEF_f. However, the latter method operates at much lower voltages and is simpler to apply for micropreparative purposes. The time intervals required for separation and analysis in the two methods are comparable.

INTRODUCTION

In isoelectric focusing (IEF), sample constituents are sorted in order of their isoelectric points in an equilibrium gradient. Proteins and other amphoteric compounds are separated in a pH gradient provided that their isoelectric points are different. Good resolution is favoured by both a low diffusion coefficient and a high mobility slope at the isoelectric point, conditions which are well satisfied by all proteins. A high electric field strength and a shallow pH gradient further enhance resolution. Depending on instrumental parameters, a resolving power of

the order of 0.01 pH unit is typically achievable. Traditionally, IEF has been carried out in gels, requiring tedious, time-consuming preparation and protein staining procedures [1]. Compared with HPLC, the common practice of gel IEF is slow, labour intensive, prone to relatively poor reproducibility, difficult to quantitate and not accessible to simple automation. Therefore, in the past few years considerable attention has been focused on protein isoelectric focusing in capillaries [2–26].

First, free fluid focusing with the electric field parallel to the column axis was studied in capillaries of rectangular cross-section [2–6], in tubular glass capillaries [7–9], in PTFE capillaries [5,10,11] or in coated, open-tubular fused-silica capillaries of very small inner diameter (I.D.) [12–16]. These approaches operated with minimized electroosmosis

Correspondence to: Dr. Josef Chmelík, Institute of Analytical Chemistry, Czechoslovak Academy of Sciences, Veveří 97, CS-611 42 Brno, Czechoslovakia.

in which stationary steady-state zone patterns were established. Zone detection occurred either by the use of array detection [2,3,5,6] or by UV absorption measurement towards the column end which required that after focusing the proteins had to be mobilized and swept past a stationary detector [7–16]. Essentially two approaches for mobilization were studied. First electrophoretic mobilization was achieved through power interruption after focusing and replacement of one of the two electrode buffers prior to reapplication of current [7–15]. The second method consisted in the use of hydrodynamic flow which was applied after focusing was attained and without interruption of the current flow [7,16].

In a second series of studies it was discovered that small amounts of a neutral polymer [hydroxypropyl-methylcellulose (HPMC) or methylcellulose] added to the buffer allowed IEF analyses of proteins to be performed in untreated, open-tubular fused-silica capillaries, *i.e.*, in the presence of an electroosmotic flow along the separation axis [17–19]. In this approach the electroosmotic flow displaced the developing zone pattern towards and across the point of detection and made mobilization after focusing unnecessary. The added polymer provided a dynamic coating of the capillary surface which reduced both the protein–wall interactions and the electroosmotic flow. This, in addition to the plug flow characteristics of electroosmosis, were important prerequisites for low sample dispersion and therefore for efficient focusing.

In a third approach, focusing was investigated in a flowing stream with the electric force field being perpendicular to the column axis and flow. This method, termed isoelectric focusing field-flow fractionation (IEF₄), was experimentally introduced by Chmelik *et al.* [20] in a trapezoidal cross-section channel and by Thormann *et al.* [21] in a rectangular cross-section channel. The latter group named this technique electrical hyperlayer field-flow fractionation, following the terminology of Giddings [22]. So far, the formation of the pH gradient in a thin channel [23], IEF₄ of a low-molecular-mass substance [24] and a high-molecular-mass compound [25] and the separation of three proteins [26] in a trapezoidal cross-section channel have been carefully studied.

This paper is devoted to the elucidation of the differences, similarities, advantages and disadvan-

tages of the two focusing methods in flowing streams, *viz.*, IEF₄ and capillary isoelectric focusing with electroosmotic zone displacement (cIEF).

EXPERIMENTAL

Chemicals

All chemicals were of analytical-reagent grade. Cytochrome *c* from horse heart (CYTC; M_r 12 384, pI 9.3) and HPMC were obtained from Sigma (St. Louis, MO, USA), ferritin from horse spleen (FER; M_r 450 000, pI 4.2–4.5) and equine myoglobin from skeletal muscle (MYO; M_r 17 800, pI 6.8–7.0) from Serva (Heidelberg, Germany) and Ampholine (pH 3.5–10) from Pharmacia–LKB (Bromma, Sweden).

Instrumentation and experimental conditions

For IEF₄ the experimental set-up was described in detail elsewhere and the experimental conditions used were selected on the basis of previous measurements [25,26]. The length of the trapezoidal cross-section channel was 25 cm, the height was 0.5 cm and the lengths of the two opposite walls of the trapezoid were 0.45 and 0.95 mm (volume 0.875 ml). PLGC ultrafiltration membranes (Millipore, Bedford, MA, USA) separated the focusing channel from the electrode compartments. Proteins were dissolved in 2% (w/v) carrier ampholyte solution and introduced with a four-port valve (featuring a 5- μ l sample loop) through a capillary inlet placed 2 cm downstream from the carrier ampholyte inlet. The concentrations of CYTC, MYO and FER were 17, 17 and 1 μ M, respectively. Sample injection occurred over a period of 4 min using a Model 355 syringe pump (Sage Instruments, Cambridge, MA, USA). A Model 2150 HPLC pump (LKB, Bromma, Sweden) was employed to pump the carrier ampholyte solution at a pump rate of 10 μ l/min during sampling and the subsequent 10-min relaxation period. The flow-rate was increased to 40 μ l/min during elution. Eluting zones were monitored with a Model 2158 Uvicord SD (LKB, Bromma, Sweden) photometric detector at 405 nm and a Model 2210 recorder (LKB). A Model 2297 Macrodrive 5 power supply (LKB) was used to apply up to 10 V (maximum current 100 mA). The electric field was applied during the entire experiment, including sample injection. A Vario Perpex two-channel peristaltic pump (H. J.

Guldener, Zurich, Switzerland) was used to pump solutions of acetic acid and sodium hydroxide (50 mM each) through the anodic and cathodic electrode chambers respectively (pump rate 250 $\mu\text{l}/\text{min}$ each). The carrier ampholyte and sample solutions were degassed by vacuum and filtered through 0.2- μm Nalgene (25 mm diameter) disposable syringe filters (Nalge, Rochester, NY, USA).

A laboratory-made instrument was employed for cIEF [19]. It featured a 75 μm I.D. fused-silica capillary of about 90 cm length (Polymicro Technologies, Phoenix, AZ, USA) together with a UVIS 206 PHD fast-scanning multi-wavelength detector and a No. 9550-0155 capillary detector cell (both from Linear Instruments, Reno, NV, USA). The effective separation distance was about 70 cm between the anodic capillary end and the detection window. No cooling of the capillary was provided. Two 50-ml plastic bottles served as electrode vessels, containing 10 mM phosphoric acid (anolyte) and 20 mM NaOH with 0.1% HPMC (catholyte). Current was applied at a constant voltage (20 kV) with a Model HCN 14-20000 power supply (FUG Elektronik, Rosenheim, Germany). A VacTorr 150 vacuum pump (CGA/Precision Scientific, Chicago, IL, USA) was used to rinse the capillary. New capillaries were first rinsed with 1 M NaOH (20 min) and then 0.1 M NaOH containing 0.3% HPMC (10 min). The latter solution was also used to condition the capillary at the beginning of a series of experiments (10-min wash). Before each run the capillary was cleaned with catholyte for at least 10 min. Sample proteins were dissolved in 2.5% Ampholine solution without the addition of HPMC. The concentrations of CYTC, MYO and FER were 4.8, 3.4 and 0.1 μM , respectively. Sample application occurred manually via gravity through lifting the capillary end (dipped into the sample vial) to a height of 65 cm for 6 min.

RESULTS AND DISCUSSION

Before turning to the comparison of the experimental results, basic differences and similarities of the methods of interest and the performance of the experiments are considered. IEF₄ and cIEF differ fundamentally in two respects, the orientation of the electric field with respect to column axis and flow, and the shape of the velocity profile. In IEF₄ the force field is applied perpendicularly to the column

axis and hydrodynamic flow with a characteristic flow profile being employed for elution. The shape of the flow velocity profile, which is determined by the geometry of the separation channel [27], is a prerequisite for sequential elution of the separated compounds (Figs. 1A and 2). In cIEF the electric field is parallel to the column axis and an electroosmotic flow with a plug profile is utilized solely for the displacement of the entire zone structure towards and across the detector (Fig. 1A).

In addition to the electric field and pH gradient used in IEF, IEF₄ employs the flow of the liquid carrier through a thin separation channel as a third factor affecting separation. Amphoteric solutes are transported via isoelectric focusing to the equilibrium positions, where these compounds possess no net overall charge, and narrow focused solute zones with nearly Gaussian concentration distributions are formed. Provided that solutes exhibit different isoelectric points, they focus in different positions across the separation channel (Fig. 2B). Unequal flow velocities cause differential migration of focused solutes along the channel, *i.e.*, their longitudinal separation (Fig. 2C). Owing to the dimensions of the channel a high electric field strength can be

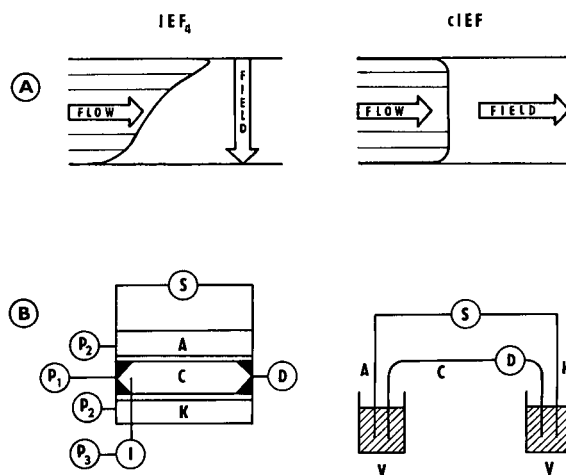


Fig. 1. IEF₄ in the trapezoidal cross-section channel and IEF with electroosmotic zone displacement with (A) orientation of electric field and flow, as well as the characteristic flow velocity profiles, and (B) schematic representations of the experimental set-ups. A = Anode; K = cathode; C = channel or capillary; D = detector; I = injection port; P₁ = carrier ampholyte pump; P₂ = electrolyte pumps; P₃ = sample pump; S = power supply; V = electrolyte vessel.

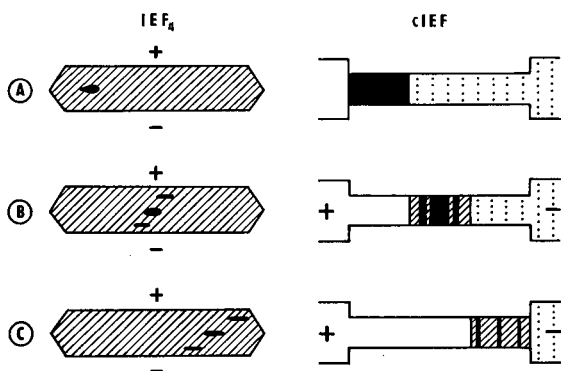


Fig. 2. Separation in IEF₄ and cIEF with (A) sample application, (B) focusing and (C) elution. Proteins are represented by the black areas, carrier ampholytes by the hatched areas and catholyte and anolyte in cIEF by the dotted and white areas, respectively. The directions of both hydrodynamic (IEF₄) and electroosmotic (cIEF) flows are from left to right.

applied with a fairly small voltage, this keeping Joule heating at a low level. IEF₄ is an elution technique, its instrumental set-up being similar to that of HPLC [20,21]. The IEF₄ procedure consists of three phases, sample injection, relaxation and elution. Typically each phase is executed at a different carrier flow-rate. The experimental conditions for the successful performance of an IEF₄ experiment in the trapezoidal cross-section channel of 0.875-ml volume have been reported in other papers [25,26]. It was found that (i) the sample has to be injected under applied electric power into the centre of a slowly flowing stream (10 μ l/min), (ii) the relaxation time, *i.e.*, the time period necessary for formation of a focused zone, should be of the order of 10 min with no or minimal flow only and (iii) the efficiency decreases with increasing flow-rate of the carrier ampholyte solution. A fractogram depicting the separation of FER, MYO and CYTC is presented in Fig. 3A.

cIEF is performed in an uncoated, open-tubular fused-silica capillary of typically 75 μ m I.D. The experimental arrangement used in this work is depicted schematically in Figs. 1B and 2. An experiment proceeds as follows. First the entire capillary is filled with the catholyte containing a neutral polymer. Sample composed of carrier ampholytes and proteins is introduced at the anodic capillary end and is occupying 5–30% of the effective capillary length (Fig. 2A). After power application two

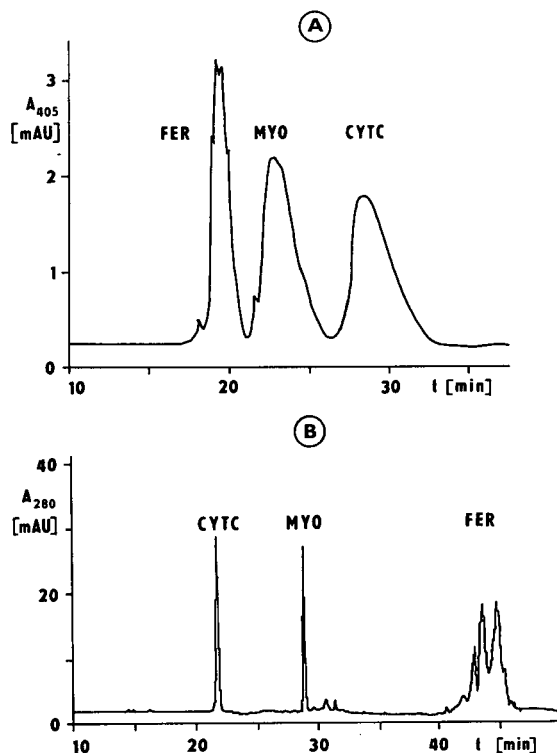


Fig. 3. Separation of CYTC, MYO and FER by (A) IEF₄ in a trapezoidal cross-section channel of 25 cm length (volume 0.875 ml) and (B) cIEF using a fused-silica capillary of 75 μ m I.D. and 90 cm total length (volume 4 μ l). The detection wavelength (detector positions) were 405 nm (off-column) and 280 nm (on-column), respectively. The power levels applied were about 1 and 0.1 W, respectively, values which were previously found to guarantee safe operation (refs. 26 and 19, respectively). For experimental details, see text.

electrokinetic effects occur simultaneously (Fig. 2B), the formation of a longitudinal pH gradient and the separation of proteins (isoelectric focusing), and, owing to the negative surface charge of untreated fused silica, the displacement of the entire pattern towards the cathode (electroosmosis). Basic proteins, such as CYTC, reach the detector prior to neutral and acidic proteins, as is seen with the example shown in Fig. 3B. This experiment, performed in a capillary of 4- μ l volume, was executed with a lower (about 18-, 25- and 50-fold for CYTC, MYO and FER, respectively) amount of protein compared to that employed in IEF₄ (Fig. 3A). The protein load per unit of column volume, however, was higher in the cIEF experiment.

From the experimental results for the two methods (Fig. 3), it is apparent that the three proteins are eluted in reverse order. In IEF₄, FER has the lowest and CYTC the highest elution time, and MYO elutes between them. This observation agrees well with theory because with the configuration employed (anode at the wider side of the channel) CYTC is expected to focus in the narrower part of the channel where elution is slow, MYO somewhere in the centre and FER towards the wider part where elution is fast. In cIEF the order of elution is determined by the electroosmotic flow, which is in the direction of the cathode. Therefore, the compound with the highest isoelectric point reaches the detector first and the elution order is according to decreasing isoelectric points. Hence, in the experiments presented, the sequence in cIEF has to be the opposite to that in IEF₄. It is important to add that reversal of the polarity in IEF₄ together with an exchange of the electrode buffers would simply reverse the elution order of the proteins in that method. This, however, does not apply to cIEF.

Comparison of the traces in Fig. 3 further reveals that both the efficiency (peak width) and resolution are much higher in cIEF. Separation of the three proteins is essentially achieved in both approaches. By *pI* discrimination as employed in IEF₄ and cIEF, CYTC is a single-component protein. The fractogram and electropherogram are both characterized by a single peak. However, differences are observed with MYO and FER, proteins which contain several components with different *pI* values. MYO contains minor compounds which are more acidic than the main protein. These are well resolved in cIEF and detected as a significant shoulder or unresolved peak in IEF₄. FER is a more complex protein containing many isoforms of different *pI*, up to six being detected by cIEF, whereas the fractogram showing several shoulders only.

In both methods, the resolution is dependent on the slope of the pH gradient and the power applied. Increased resolution is obtained by making the equilibrium gradient shallower and/or the electric field larger. In IEF₄ different experimental parameters, including the time interval of sample loading and the choice and concentration of the electrolytes in the electrode compartments, also have an influence on resolution. For example, with 10-min sample loading, the resolution for FER was higher than

that obtained with a 4-min time interval shown in Fig. 3A (data not shown). The efficiency in IEF₄ is dependent on the relaxation process and the elution flow-rate, whereas in cIEF the efficiency is strongly influenced by the temporal behaviour of the electroosmotic flow.

From a theoretical point of view, IEF₄ in a trapezoidal cross-section channel is not as efficient as IEF₄ in a rectangular cross-section channel of high aspect ratio [28]. However, results obtained so far in the latter configuration have not confirmed the theoretical expectations [21]. Technical and material problems encountered in the construction of the rectangular cross-section channel are believed to be the reason for this. It appears to be very difficult to place narrowly (a few tenths of 1 mm) two flat membranes which define the ribbon-like channel. Further, establishment of the lateral pH gradient is hampered by the non-ideal behaviour of the membranes under current flow. Further efforts will have to be devoted to exploit new materials for the construction of a more efficient channel of rectangular cross-section. cIEF as described here and elsewhere [19] is different to the cIEF approach reported by Mazzeo and Krull [17,18]. They used a configuration in which the column is initially completely filled with the sample, requiring the further addition of a strong base to the sample in order to be able to detect basic proteins [10,15]. Because of the relatively short initial sample zone in our fully dynamic approach, this disadvantage is not encountered. It should be added that the dynamics of cIEF in the presence of electroosmotic zone displacement are not yet fully understood. Further investigations using both experimental studies and theoretical descriptions of the underlying processes will provide further insight into this methodology and will lead to the complete elucidation of the analytical capabilities of cIEF.

ACKNOWLEDGEMENT

This work was partly sponsored by the Swiss National Science Foundation.

REFERENCES

- 1 P. G. Righetti, *Isoelectric Focusing: Theory, Methodology and Applications*, Elsevier, Amsterdam, 1983.

- 2 W. Thormann, R. A. Mosher and M. Bier, *J. Chromatogr.*, 351 (1986) 17.
- 3 W. Thormann, N. B. Egen, R. A. Mosher and M. Bier, *J. Biochem. Biophys. Methods*, 11 (1985) 287.
- 4 W. Thormann, A. Tsai, J. P. Michaud, R. A. Mosher and M. Bier, *J. Chromatogr.*, 389 (1987) 75.
- 5 R. A. Mosher, W. Thormann and M. Bier, *J. Chromatogr.*, 436 (1988) 191.
- 6 R. A. Mosher, W. Thormann, R. Kuhn and H. Wagner, *J. Chromatogr.*, 478 (1989) 39.
- 7 S. Hjertén and M. Zhu, *J. Chromatogr.*, 346 (1985) 265.
- 8 S. Hjertén, J. L. Liao and K. Yao, *J. Chromatogr.*, 387 (1987) 127.
- 9 S. Hjertén, K. Elenbring, F. Kilår, J. Liao, J. C. Chen, C. J. Siebert and M. Zhu, *J. Chromatogr.*, 403 (1987) 47.
- 10 M. A. Firestone and W. Thormann, *J. Chromatogr.*, 436 (1988) 309.
- 11 W. Thormann and M. A. Firestone, in J. C. Janson and L. Riden (Editors), *Protein Purification*, VCH, Weinheim, 1989, pp. 469–492.
- 12 F. Kilår and S. Hjertén, *Electrophoresis*, 10 (1989) 23.
- 13 F. Kilår and S. Hjertén, *J. Chromatogr.*, 480 (1989) 351.
- 14 M. Zhu, D. L. Hansen, S. Burd and F. Gannon, *J. Chromatogr.*, 480 (1989) 311.
- 15 M. Zhu, R. Rodriguez and T. Wehr, *J. Chromatogr.*, 559 (1991) 479.
- 16 S. Chen and J. E. Wiktorowicz, *Anal. Biochem.*, submitted for publication.
- 17 J. R. Mazzeo and I. S. Krull, *Anal. Chem.*, 63 (1991) 2852.
- 18 J. R. Mazzeo and I. S. Krull, *J. Microcol. Sep.*, 4 (1992) 29.
- 19 W. Thormann, J. Caslavská, S. Molteni and J. Chmelik, *J. Chromatogr.*, 589 (1992) 321.
- 20 J. Chmelik, M. Deml and J. Janca, *Anal. Chem.*, 61 (1989) 912.
- 21 W. Thormann, M. A. Firestone, M. L. Dietz, T. Cecconie and R. A. Mosher, *J. Chromatogr.*, 461 (1989) 95.
- 22 J. C. Giddings, *Sep. Sci. Technol.*, 18 (1983) 765.
- 23 J. Chmelik, *J. Chromatogr.*, 539 (1991) 111.
- 24 J. Chmelik, *J. Chromatogr.*, 545 (1991) 349.
- 25 J. Chmelik and W. Thormann, *J. Chromatogr.*, 600 (1992) 297.
- 26 J. Chmelik and W. Thormann, *J. Chromatogr.*, 600 (1992) 305.
- 27 J. Pazourek and J. Chmelik, *J. Chromatogr.*, 593 (1992) 357.
- 28 J. Janča and J. Chmelik, *Anal. Chem.*, 56 (1984) 2481.

Author Index Vols. 631 and 632

- Abbas, A. A. and Shelly, D. C.
Axial illumination of fused-silica capillaries. Investigation of fluorescence and refractive index detection 631(1993)133
- Achilli, G., Cellerino, G. P., Gamache, P. H. and Melzi d'Eril, G. V.
Identification and determination of phenolic constituents in natural beverages and plant extracts by means of a coulometric electrode array system 632(1993)111
- Afeyan, N., see Varady, L. 631(1993)107
- Aguilar, M. I., see Wilce, M. C. J. 632(1993)11
- Akashi, M., see Baba, Y. 632(1993)137
- Aoki, F., see Ôi, N. 631(1993)177
- Baba, Y., Tshako, M., Sawa, T. and Akashi, M.
Temperature-programmed capillary affinity gel electrophoresis for the sensitive base-specific separation of oligodeoxynucleotides 632(1993)137
- Bagchi, D., see Cordis, G. A. 632(1993)97
- Bal, F., see Josić, D. 632(1993)1
- Balmér, K., Lagerström, P.-O., Larsson, S. and Persson, B.-A.
Direct chiral separation of almokalant on Chiralcel OD and Chiralpak AD for liquid chromatographic assay of biological samples 631(1993)191
- Beattie, J. H., Richards, M. P. and Self, R.
Separation of metallothionein isoforms by capillary zone electrophoresis 632(1993)127
- Bell, R. G. and Newman, K. L.
Carbohydrate analysis of fermentation broth by high-performance liquid chromatography utilizing solid-phase extraction 632(1993)87
- Benedek, K., see Rosenfeld, R. 632(1993)29
- Berry, D. L., see Zoutendam, P. H. 631(1993)221
- Bliesner, D. M. and Sentell, K. B.
Deuterium nuclear magnetic resonance spectroscopy as a probe for reversed-phase liquid chromatographic bonded phase solvation: methanol and acetonitrile mobile phase components 631(1993)23
- Boppana, V. K., see Miller-Stein, C. 631(1993)233
- Boppana, V. K., Miller-Stein, C. and Rhodes, G. R.
Normal-phase high-performance liquid chromatographic determination of epristeride, a prostatic steroid 5 α -reductase enzyme inhibitor, in human plasma 631(1993)251
- Boppana, V. K., see Simpson, R. C. 631(1993)227
- Brown, B. L., see Geiser, F. O. 631(1993)1
- Brown, P. R., see De Antonis, K. M. 632(1993)91
- Carkuff, D. W., see Zoutendam, P. H. 631(1993)221
- Carreras, D., see Imaz, C. 631(1993)201
- Cellerino, G. P., see Achilli, G. 632(1993)111
- Chang, H.-T. and Yeung, E. S.
Voltage programming in capillary zone electrophoresis 632(1993)149
- Chlenov, M. A., Kandyba, E. I., Nagornaya, L. V., Orlova, I. L. and Volgin, Y. V.
High-performance liquid chromatography of human glycoprotein hormones 631(1993)261
- Chmelik, J. and Thormann, W.
Isoelectric focusing field-flow fractionation and capillary isoelectric focusing with electroosmotic zone displacement. Two approaches to protein analysis in flowing streams 632(1993)229
- Coenegracht, P. M. J., Metting, H. J., Van Loo, E. M., Snoeijs, G. J. and Doornbos, D. A.
Peak tracking with a neural network for spectral recognition 631(1993)145
- Cook, S. E., see Varady, L. 631(1993)107
- Cooke, N., see Guttman, A. 632(1993)171
- Cordis, G. A., Maulik, N., Bagchi, D., Engelman, R. M. and Das, D. K.
Estimation of the extent of lipid peroxidation in the ischemic and reperfused heart by monitoring lipid metabolic products with the aid of high-performance liquid chromatography 632(1993)97
- Cortes, R., see Imaz, C. 631(1993)201
- Cserhádi, T., see Forgács, E. 631(1993)207
- Dadoo, R., see Tsuda, T. 632(1993)201
- Das, D. K., see Cordis, G. A. 632(1993)97
- Dasari, G., Prince, I. and Hearn, M. T. W.
High-performance liquid chromatography of amino acids, peptides and proteins. CXXIV. Physical characterisation of fluidized-bed behaviour of chromatographic packing materials 631(1993)115
- De Antonis, K. M., Brown, P. R., Yi, Z. and Maugle, P. D.
High-performance liquid chromatography with ion pairing and electrochemical detection for the determination of the stability of two forms of vitamin C 632(1993)91
- Doornbos, D. A., see Coenegracht, P. M. J. 631(1993)145
- Dorsey, J. G., see Hsieh, M.-M. 631(1993)63
- El Rassi, Z., see Nashabeh, W. 632(1993)157
- El Rassi, Z., see Yu, J. 631(1993)91
- Engelman, R. M., see Cordis, G. A. 632(1993)97
- Excoffer, J.-L., Joseph, M., Robinson, J. J. and Sheehan, T. L.
Faster quantitative evaluation of high-performance liquid chromatography-ultraviolet diode-array data by multicomponent analysis 631(1993)15
- Forgács, E., Valkó, K., Cserhádi, T. and Magyar, K.
Porous graphitized carbon and octadecylsilica columns in the separation of some monoamine oxidase inhibitory drugs 631(1993)207
- Foster, G. D., see McEachern, P. R. 632(1993)119
- Fox, A. R. and McLoughlin, D. A.
Rapid, sensitive high-performance liquid chromatographic method for the quantification of promethazine in human serum with electrochemical detection 631(1993)255
- Fujima, H., see Haginaka, J. 631(1993)183
- Gamache, P. H., see Achilli, G. 632(1993)111
- Geiser, F. O., Golt, C., Kung, Jr., L., Justice, J. D. and Brown, B. L.
Chromatographic method verification by means of three-dimensional, multivariate visualization 631(1993)1

- Giese, R. W., see Saha, M. 631(1993)161
 Golt, C., see Geiser, F. O. 631(1993)1
 Guiochon, G., see Seidel-Morgenstern, A. 631(1993)37
 Guttman, A., Nolan, J. A. and Cooke, N.
 Capillary sodium dodecyl sulfate gel electrophoresis of proteins 632(1993)171
 Hagen, S. R.
 High-performance liquid chromatographic quantitation of phenylthiocarbamyl muramic acid and glucosamine from bacterial cell walls 632(1993)63
 Haginaka, J., Murashima, T., Seyama, C., Fujima, H. and Wada, H.
 Retention and enantioselective properties of racemic compounds on modified ovomucoid columns. II.
 Reaction with glyceraldehyde, formaldehyde and glutaric anhydride 631(1993)183
 Hainari, S., see Sirén, H. 632(1993)215
 Hearn, M. T. W., see Dasari, G. 631(1993)115
 Hearn, M. T. W., see Wilce, M. C. J. 632(1993)11
 Hermansson, I., see Hermansson, J. 631(1993)79
 Hermansson, J., Hermansson, I. and Nordin, J.
 Characterization of a Chiral-AGP capillary column coupled to a micro sample-enrichment system with UV and electrospray mass spectrometric detection 631(1993)79
 Hsieh, M.-M. and Dorsey, J. G.
 Accurate determination of log k'_w in reversed-phase liquid chromatography. Implications for quantitative structure-retention relationships 631(1993)63
 Huang, C.-Y., see Wen, K.-C. 631(1993)241
 Hwang, B. Y.-H., see Miller-Stein, C. 631(1993)233
 Hwang, B. Y.-H., see Simpson, R. C. 631(1993)227
 Ikedo, M., see Tsuda, T. 632(1993)201
 Imaz, C., Carreras, D., Navajas, R., Rodriguez, C., Rodriguez, A. F., Maynar, J. and Cortes, R.
 Determination of ephedrine in urine by high-performance liquid chromatography 631(1993)201
 Jones, G., see Tsuda, T. 632(1993)201
 Joseph, M., see Excoffier, J.-L. 631(1993)15
 Josić, D., Bal, F. and Schwinn, H.
 Isolation of plasma proteins from the clotting cascade by heparin affinity chromatography 632(1993)1
 Justice, J. D., see Geiser, F. O. 631(1993)1
 Kanazawa, H., Nagata, Y., Kuroski, E., Matsushima, Y. and Takai, N.
 Comparison of columns of chemically modified porous glass and silica in reversed-phase high-performance liquid chromatography of ginsenosides 632(1993)79
 Kanazawa, H., Nagata, Y., Matsushima, Y., Takai, N., Uchiyama, H., Nishimura, R. and Takeuchi, A.
 Liquid chromatography-mass spectrometry for the determination of medetomidine and other anaesthetics in plasma 631(1993)215
 Kandyba, E. I., see Chlenov, M. A. 631(1993)261
 Keating, K. M., Rogers, B. L., Weber, L., Morgenstern, J. P., Klapper, D. G. and Kuo, M.
 Immunoaffinity chromatography of recombinant *Amb a 1* in the presence of a denaturing agent 631(1993)269
 Kerns, E. H., see Liu, J. 632(1993)45
 Khaledi, M. G., see Kord, A. S. 631(1993)125
 Khaledi, M. G., see Smith, S. C. 632(1993)177
 Khalifa, M., see Molnár-Perl, I. 632(1993)57
 Kitahara, H., see Ōi, N. 631(1993)177
 Klapper, D. G., see Keating, K. M. 631(1993)269
 Klohr, S. E., see Liu, J. 632(1993)45
 Knock, S. L., see Kurosky, A. 631(1993)281
 Kord, A. S. and Khaledi, M. G.
 Selectivity of organic solvents in micellar liquid chromatography of amino acids and peptides 631(1993)125
 Kresin, L., see Kunitani, M. 632(1993)19
 Kung, Jr., L., see Geiser, F. O. 631(1993)1
 Kunitani, M. and Kresin, L.
 High-performance liquid chromatographic analysis of carbohydrate mass composition in glycoproteins 632(1993)19
 Kuo, M., see Keating, K. M. 631(1993)269
 Kuroski, E., see Kanazawa, H. 632(1993)79
 Kurosky, A., Miller, B. T. and Knock, S. L.
 Kinetic analysis of biotinylation of specific residues of peptides by high-performance liquid chromatography 631(1993)281
 Lagerström, P.-O., see Balmér, K. 631(1993)191
 Larsson, S., see Balmér, K. 631(1993)191
 Lee, H. K., see Ng, C. L. 632(1993)165
 Lee, M. S., see Liu, J. 632(1993)45
 Li, S. F. Y., see Ng, C. L. 632(1993)165
 Lin, J.-Y., see Yang, M.-H. 631(1993)165
 Lin, L. A.
 Detection of alkaloids in foods with a multi-detector high-performance liquid chromatographic system 632(1993)69
 Liu, J., Volk, K. J., Kerns, E. H., Klohr, S. E., Lee, M. S. and Rosenberg, I. E.
 Structural characterization of glycoprotein digests by microcolumn liquid chromatography-ionspray tandem mass spectrometry 632(1993)45
 Lu, F.-L., see Wen, K.-C. 631(1993)241
 Lukkari, P., see Sirén, H. 632(1993)215
 Lukkari, P., Sirén, H., Panssar, M. and Riekkola, M.-L.
 Determination of ten β -blockers in urine by micellar electrokinetic capillary chromatography 632(1993)143
 Magyar, K., see Forgács, E. 631(1993)207
 Matsushima, Y., see Kanazawa, H. 631(1993)215
 Matsushima, Y., see Kanazawa, H. 632(1993)79
 Maugle, P. D., see De Antonis, K. M. 632(1993)91
 Maulik, N., see Cordis, G. A. 632(1993)97
 Maynar, J., see Imaz, C. 631(1993)201
 McEachern, P. R. and Foster, G. D.
 Supercritical fluid extraction of synthetic organochlorine compounds in submerged aquatic plants 632(1993)119
 McLoughlin, D. A., see Fox, A. R. 631(1993)255
 McNally, J. J., see Shaw, C. J. 631(1993)173
 Melzi d'Eril, G.V., see Achilli, G. 632(1993)111
 Merion, M., see Swartz, M. E. 632(1993)209
 Metting, H. J., see Conegracht, P. M. J. 631(1993)145
 Miller, B. T., see Kurosky, A. 631(1993)281
 Miller-Stein, C., see Boppana, V. K. 631(1993)251

- Miller-Stein, C., Hwang, B. Y.-H., Rhodes, G. R. and Boppana, V. K.
Column-switching high-performance liquid chromatographic method for the determination of SK&F 106203 in human plasma after fluorescence derivatization with 9-anthryldiazomethane 631(1993)233
- Molnár-Perl, I., Pintér-Szakács, M. and Khalifa, M.
High-performance liquid chromatography of tryptophan and other amino acids in hydrochloric acid hydrolysates 632(1993)57
- Monkarsh, S. P., Russoman, E. A. and Roy, S. K.
Separation of interleukins by a preparative chromatofocusing-like method 631(1993)277
- Morgenstern, J. P., see Keating, K. M. 631(1993)269
- Mu, N., see Varady, L. 631(1993)107
- Murashima, T., see Haginaka, J. 631(1993)183
- Nagata, Y., see Kanazawa, H. 631(1993)215
- Nagata, Y., see Kanazawa, H. 632(1993)79
- Nagornaya, L. V., see Chlenov, M. A. 631(1993)261
- Nashabeh, W. and El Rassi, Z.
Fundamental and practical aspects of coupled capillaries for the control of electroosmotic flow in capillary zone electrophoresis of proteins 632(1993)157
- Navajas, R., see Imaz, C. 631(1993)201
- Newman, K. L., see Bell, R. G. 632(1993)87
- Ng, C. L., Lee, H. K. and Li, S. F. Y.
Determination of sulphonamides in pharmaceuticals by capillary electrophoresis 632(1993)165
- Nishimura, R., see Kanazawa, H. 631(1993)215
- Nolan, J. A., see Guttman, A. 632(1993)171
- Nordin, J., see Hermansson, J. 631(1993)79
- Ôi, N., Kitahara, H. and Aoki, F.
Enantiomer separation by high-performance liquid chromatography with copper(II) complexes of Schiff bases as chiral stationary phases 631(1993)177
- Orlova, I. L., see Chlenov, M. A. 631(1993)261
- Pantsar, M., see Lukkari, P. 632(1993)143
- Park, S. A., see Shaw, C. J. 631(1993)173
- Persson, B.-A., see Balmér, K. 631(1993)191
- Pintér-Szakács, M., see Molnár-Perl, I. 632(1993)57
- Press, J. B., see Shaw, C. J. 631(1993)173
- Prince, I., see Dasari, G. 631(1993)115
- Regnier, F. E., see Riggan, A. 632(1993)37
- Regnier, F. E., see Varady, L. 631(1993)107
- Regnier, F. E., see Yao, X.-W. 632(1993)185
- Rhodes, G. R., see Boppana, V. K. 631(1993)251
- Rhodes, G. R., see Miller-Stein, C. 631(1993)233
- Rhodes, G. R., see Simpson, R. C. 631(1993)227
- Richards, M. P., see Beattie, J. H. 632(1993)127
- Riekkola, M.-L., see Lukkari, P. 632(1993)143
- Riekkola, M.-L., see Sirén, H. 632(1993)215
- Riggan, A., Sportsman, J. R. and Regnier, F. E.
Immunochemical analysis of proteins.
Identification, characterization and purity determination 632(1993)37
- Robinson, J. J., see Excoffier, J.-L. 631(1993)15
- Rodriguez, A. F., see Imaz, C. 631(1993)201
- Rodriguez, C., see Imaz, C. 631(1993)201
- Rogers, B. L., see Keating, K. M. 631(1993)269
- Rosenberg, I. E., see Liu, J. 632(1993)45
- Rosenfeld, R. and Benedek, K.
Conformational changes of brain-derived neurotrophic factor during reversed-phase high-performance liquid chromatography 632(1993)29
- Roy, S. K., see Monkarsh, S. P. 631(1993)277
- Russoman, E. A., see Monkarsh, S. P. 631(1993)277
- Saarinen, M., see Sirén, H. 632(1993)215
- Saha, M. and Giese, R. W.
Primary contribution of the injector to carryover of a trace analyte in high-performance liquid chromatography 631(1993)161
- Sanfilippo, P. J., see Shaw, C. J. 631(1993)173
- Sawa, T., see Baba, Y. 632(1993)137
- Schwinn, H., see Josić, D. 632(1993)1
- Seidel-Morgenstern, A. and Guiochon, G.
Thermodynamics of the adsorption of Tröger's base enantiomers from ethanol on cellulose triacetate 631(1993)37
- Self, R., see Beattie, J. H. 632(1993)127
- Sentell, K. B., see Bliesner, D. M. 631(1993)23
- Seyama, C., see Haginaka, J. 631(1993)183
- Shaw, C. J., Sanfilippo, P. J., McNally, J. J., Park, S. A. and Press, J. B.
Analytical and preparative high-performance liquid chromatographic separation of thienopyran enantiomers 631(1993)173
- Sheehan, T. L., see Excoffier, J.-L. 631(1993)15
- Shelly, D. C., see Abbas, A. A. 631(1993)133
- Simpson, R. C., Boppana, V. K., Hwang, B. Y.-H. and Rhodes, G. R.
Determination of oxiracetam in human plasma by reversed-phase high-performance liquid chromatography with fluorimetric detection 631(1993)227
- Sirén, H., see Lukkari, P. 632(1993)143
- Sirén, H., Saarinen, M., Hainari, S., Lukkari, P. and Riekkola, M.-L.
Screening of β -blockers in human serum by ion-pair chromatography and their identification as methyl or acetyl derivatives by gas chromatography-mass spectrometry 632(1993)215
- Slégel, P., see Valkó, K. 631(1993)49
- Smith, S. C. and Khaledi, M. G.
Prediction of the migration behavior of organic acids in micellar electrokinetic chromatography 632(1993)177
- Snoeijer, G. J., see Coenegracht, P. M. J. 631(1993)145
- Sportsman, J. R., see Riggan, A. 632(1993)37
- Stefansson, M. and Westerlund, D.
Capillary electrophoresis of glycoconjugates in alkaline media 632(1993)195
- Suortti, T.
Size-exclusion chromatographic determination of β -glucan with postcolumn reaction detection 632(1993)105
- Swartz, M. E. and Merion, M.
On-line sample preconcentration on a packed-inlet capillary for improving the sensitivity of capillary electrophoretic analysis of pharmaceuticals 632(1993)209
- Takai, N., see Kanazawa, H. 631(1993)215

- Takai, N., see Kanazawa, H. 632(1993)79
- Takeuchi, A., see Kanazawa, H. 631(1993)215
- Thormann, W., see Chmelík, J. 632(1993)229
- Tsuda, T., Ikedo, M., Jones, G., Dadoo, R. and Zare, R. N.
Observation of flow profiles in electroosmosis in a
rectangular capillary 632(1993)201
- Tsuhako, M., see Baba, Y. 632(1993)137
- Turujman, S. A.
Rapid direct resolution of the stereoisomers of all-*trans*
astaxanthin on a Pirkle covalent L-leucine column
631(1993)197
- Uchiyama, H., see Kanazawa, H. 631(1993)215
- Valkó, K., see Forgács, E. 631(1993)207
- Valkó, K. and Slégel, P.
New chromatographic hydrophobicity index (ϕ_0) based
on the slope and the intercept of the log k' versus organic
phase concentration plot 631(1993)49
- Van Loo, E. M., see Coenegracht, P. M. J. 631(1993)145
- Varady, L., Mu, N., Yang, Y.-B., Cook, S. E., Afeyan, N. and
Regnier, F. E.
Fimbriated stationary phases for proteins 631(1993)107
- Volgin, Y. V., see Chlenov, M. A. 631(1993)261
- Volk, K. J., see Liu, J. 632(1993)45
- Wada, H., see Haginaka, J. 631(1993)183
- Weber, L., see Keating, K. M. 631(1993)269
- Wen, K.-C., Huang, C.-Y. and Lu, F.-L.
Determination of baicalin and puerarin in traditional
Chinese medicinal preparations by high-performance
liquid chromatography. 631(1993)241
- Westerlund, D., see Stefansson, M. 632(1993)195
- Wilce, M. C. J., Aguilar, M. I. and Hearn, M. T. W.
High-performance liquid chromatography of amino acids,
peptides and proteins. CXXII. Application of
experimentally derived retention coefficients to the
prediction of peptide retention times: studies with
myohemerythrin 632(1993)11
- Yang, M.-H. and Lin, J.-Y.
N-Arylcarbamoyl derivatives of amino acids as chiral
stationary phases for optical resolution by high-
performance liquid chromatography 631(1993)165
- Yang, Y.-B., see Varady, L. 631(1993)107
- Yao, X.-W. and Regnier, F. E.
Polymer- and surfactant-coated capillaries for isoelectric
focusing 632(1993)185
- Yeung, E. S., see Chang, H.-T. 632(1993)149
- Yi, Z., see De Antonis, K. M. 632(1993)91
- Yu, J. and El Rassi, Z.
Reversed-phase liquid chromatography with
microspherical octadecyl-zirconia bonded stationary
phases 631(1993)91
- Zare, R. N., see Tsuda, T. 632(1993)201
- Zoutendam, P. H., Berry, D. L. and Carkuff, D. W.
Reversed-phase high-performance liquid chromatographic
of the cardiac glycoside LNF-209 with refractive index
detection 631(1993)221

Liquid Chromatography in Biomedical Analysis

edited by T. Hanai

Journal of Chromatography Library, Volume 50

This book presents a guide for the analysis of biomedically important compounds using modern liquid chromatographic techniques. After a brief summary of basic liquid chromatographic methods and optimization strategies, the main part of the book focuses on the various classes of biomedically important compounds: amino acids, catecholamines, carbohydrates, fatty acids, nucleotides, porphyrins, prostaglandins and steroid hormones. The different chapters discuss specialized techniques pertaining to each class of compounds, such as sample pretreatment, pre- and post-column derivatization, detection and quantification.

Contents:

1. Liquid chromatography in biomedical analysis: basic approach (C.K. Lim).
 2. Optimization of liquid chromatography for biomedically important compounds (T. Hanai).
 3. Amino acids (Y. Ishida).
 4. Bile acids (J. Goto and T. Nambara).
 5. Carbohydrates (S. Honda).
 6. Catecholamines (K. Mori).
 7. Fatty acids (T. Hirai).
 8. Nucleotides (C.K. Lim).
 9. Porphyrins (C.K. Lim).
 10. Prostaglandins (T. Hirai).
 11. Steroid hormones (T. Hirai).
 12. Miscellaneous (T. Hanai).
- Subject Index.

1991 xii + 296 pages
Price: US \$ 169.00 / Dfl. 270.00
ISBN 0-444-87451-8

*"...essential reading for
biomedical analysts."*
The Analyst

*"...highly recommended for
pharmaceutical-industry
laboratories that carry out
pharmacokinetic and
drug-metabolism studies."*
LC-GC



ELSEVIER
SCIENCE PUBLISHERS

"This book will be valuable for anyone involved in liquid chromatography. It is timely and highlights throughout the techniques that are most successful. This is not so much a book to put on the shelf of the specialist for reference purposes, but instead it is a book which is meant to be read by the general reader to obtain perspective and insights into this general area."

**Trends in Analytical
Chemistry**

ORDER INFORMATION

For USA and Canada
**ELSEVIER SCIENCE
PUBLISHERS**
Judy Weislogel
P.O. Box 945
Madison Square Station,
New York, NY 10160-0757
Tel: (212) 989 5800
Fax: (212) 633 3880

In all other countries

**ELSEVIER SCIENCE
PUBLISHERS**
P.O. Box 211
1000 AE Amsterdam
The Netherlands
Tel: (+31-20) 5803 753
Fax: (+31-20) 5803 705

US\$ prices are valid only for the USA & Canada and are subject to exchange rate fluctuations; in all other countries the Dutch guilder price (Dfl.) is definitive. Customers in the European Community should add the appropriate VAT rate applicable in their country to the price(s). Books are sent post-free if prepaid.

Capillary Electrophoresis

Principles, Practice and Applications

by S.F.Y. LI, National University of Singapore, Singapore

Journal of Chromatography Library Volume 52

Capillary Electrophoresis (CE) has had a very significant impact on the field of analytical chemistry in recent years as the technique is capable of very high resolution separations, requiring only small amounts of samples and reagents. Furthermore, it can be readily adapted to automatic sample handling and real time data processing. Many new methodologies based on CE have been reported. Rapid, reproducible separations of extremely small amounts of chemicals and biochemicals, including peptides, proteins, nucleotides, DNA, enantiomers, carbohydrates, vitamins, inorganic ions, pharmaceuticals and environmental pollutants have been demonstrated. A wide range of applications have been developed in greatly diverse fields, such as chemical, biotechnological, environmental and pharmaceutical analysis.

This book covers all aspects of CE, from the principles and technical aspects to the most important applications. It is intended to meet the growing need for a thorough and balanced treatment of CE. The book will serve as a comprehensive reference work and can also be used as a textbook for advanced undergraduate and graduate courses. Both the experienced analyst and the newcomer will find the text useful.

Contents:

- 1. Introduction.** Historical Background. Overview of High Performance CE. Principles of Separations. Comparison with Other Separation Techniques.
- 2. Sample Injection Methods.**

Introduction. Electrokinetic Injection. Hydrodynamic Injection. Electric Sample Splitter. Split Flow Syringe Injection System. Rotary Type Injector. Freeze Plug Injection. Sampling Device with Feeder. Microinjectors. Optical Gating. **3. Detection Techniques.** Introduction. UV-Visible Absorbance Detectors. Photodiode Array Detectors. Fluorescence Detectors. Laser-based Thermo-optical and Refractive Index Detectors. Indirect Detection. Conductivity Detection. Electrochemical Detection. Mass Spectrometric Detection. **4. Column Technology.** Uncoated Capillary Columns. Coated Columns. Gel-filled Columns. Packed Columns. Combining Packed and Open-Tubular Column. **5. Electrophoretic Media.** Electrophoretic Buffer Systems. Micellar Electrokinetic Capillary Chromatography. Inclusion Pseudophases. Metal-complexing Pseudophases. Other Types of Electrophoretic Media. **6. Special Systems and Methods.** Buffer Programming. Fraction Collection. Hyphenated Techniques. Field Effect Electroosmosis. Systematic Optimization of Separation. **7. Applications of CE.** Biomolecules. Pharmaceutical and Clinical Analysis. Inorganic Ions. Hydrocarbons. Foods and Drinks. Environmental Pollutants. Carbohydrates. Toxins. Polymers

and Particles. Natural Products. Fuel. Metal Chelates. Industrial Waste Water. Explosives. Miscellaneous Applications. **8. Recent Advances and Prospect for Growth.** Recent Reviews in CE. Advances in Injection Techniques. Novel Detection Techniques. Advances in Column Technology. Progress on Electrolyte Systems. New Systems and Methods. Additional Applications Based on CE. Future Trends. **References. Index.**

1992 xxvi + 586 pages
Price: US\$ 247.00 / Dfl. 395.00
ISBN 0-444-89433-0

"Everything seems to be there, any detection system you have ever dreamed of, any capillary coating, enough electrolyte systems to saturate your wits, and more..."

"...by far the most thorough and comprehensive book in the field yet to appear."

P.G. Righetti, Milan

ORDER INFORMATION

For USA and Canada
ELSEVIER SCIENCE PUBLISHERS

Judy Weislogel
P.O. Box 945
Madison Square Station,
New York, NY 10160-0757
Tel: (212) 989 5800
Fax: (212) 633 3880

In all other countries

ELSEVIER SCIENCE PUBLISHERS

P.O. Box 211
1000 AE Amsterdam
The Netherlands
Tel: (+31-20) 5803 753
Fax: (+31-20) 5803 705

US\$ prices are valid only for the USA & Canada and are subject to exchange rate fluctuations; in all other countries the Dutch guilder



ELSEVIER
SCIENCE PUBLISHERS

PUBLICATION SCHEDULE FOR THE 1993 SUBSCRIPTION

Journal of Chromatography and Journal of Chromatography, Biomedical Applications

| MONTH | O 1992 | N 1992 | D 1992 | J | F | |
|-----------------------------------|-----------------------|----------------|-----------------------------|----------------------------------|--|---|
| Journal of Chromatography | 623/1 623/2 624 | 625/1 625/2 | 626/1 626/2 627/1 + 2 | 628/1 628/2 629/1 629/2 | 630/1 + 2 631/1 + 2 632/1 + 2 633/1 + 2 | The publication schedule for further issues will be published later |
| Cumulative Indexes, Vols. 601-650 | | | | | | |
| Bibliography Section | | | | | | |
| Biomedical Applications | | | | 612/1 | 612/2 | |

INFORMATION FOR AUTHORS

(Detailed *Instructions to Authors* were published in Vol. 609, pp. 439-445. A free reprint can be obtained by application to the publisher, Elsevier Science Publishers B.V., P.O. Box 330, 1000 AH Amsterdam, The Netherlands.)

Types of Contributions. The following types of papers are published in the *Journal of Chromatography* and the section on *Biomedical Applications*: Regular research papers (Full-length papers), Review articles, Short Communications and Discussions. Short Communications are usually descriptions of short investigations, or they can report minor technical improvements of previously published procedures; they reflect the same quality of research as Full-length papers, but should preferably not exceed five printed pages. Discussions (one or two pages) should explain, amplify, correct or otherwise comment substantively upon an article recently published in the journal. For Review articles, see inside front cover under Submission of Papers.

Submission. Every paper must be accompanied by a letter from the senior author, stating that he/she is submitting the paper for publication in the *Journal of Chromatography*.

Manuscripts. Manuscripts should be typed in **double spacing** on consecutively numbered pages of uniform size. The manuscript should be preceded by a sheet of manuscript paper carrying the title of the paper and the name and full postal address of the person to whom the proofs are to be sent. As a rule, papers should be divided into sections, headed by a caption (*e.g.*, Abstract, Introduction, Experimental, Results, Discussion, etc.). All illustrations, photographs, tables, etc., should be on separate sheets.

Abstract. All articles should have an abstract of 50-100 words which clearly and briefly indicates what is new, different and significant. No references should be given.

Introduction. Every paper must have a concise introduction mentioning what has been done before on the topic described, and stating clearly what is new in the paper now submitted.

Illustrations. The figures should be submitted in a form suitable for reproduction, drawn in Indian ink on drawing or tracing paper. Each illustration should have a legend, all the *legends* being typed (with double spacing) together on a *separate sheet*. If structures are given in the text, the original drawings should be supplied. Coloured illustrations are reproduced at the author's expense, the cost being determined by the number of pages and by the number of colours needed. The written permission of the author and publisher must be obtained for the use of any figure already published. Its source must be indicated in the legend.

References. References should be numbered in the order in which they are cited in the text, and listed in numerical sequence on a separate sheet at the end of the article. Please check a recent issue for the layout of the reference list. Abbreviations for the titles of journals should follow the system used by *Chemical Abstracts*. Articles not yet published should be given as "in press" (journal should be specified), "submitted for publication" (journal should be specified), "in preparation" or "personal communication".

Dispatch. Before sending the manuscript to the Editor please check that the envelope contains four copies of the paper complete with references, legends and figures. One of the sets of figures must be the originals suitable for direct reproduction. Please also ensure that permission to publish has been obtained from your institute.

Proofs. One set of proofs will be sent to the author to be carefully checked for printer's errors. Corrections must be restricted to instances in which the proof is at variance with the manuscript. "Extra corrections" will be inserted at the author's expense.

Reprints. Fifty reprints will be supplied free of charge. Additional reprints can be ordered by the authors. An order form containing price quotations will be sent to the authors together with the proofs of their article.

Advertisements. The Editors of the journal accept no responsibility for the contents of the advertisements. Advertisement rates are available on request. Advertising orders and enquiries can be sent to the Advertising Manager, Elsevier Science Publishers B.V., Advertising Department, P.O. Box 211, 1000 AE Amsterdam, Netherlands; courier shipments to: Van de Sande Bakhuizenstraat 4, 1061 AG Amsterdam, Netherlands; Tel. (+31-20) 515 3220/515 3222, Telefax (+31-20) 6833 041, Telex 16479 els vi nl. UK: T. G. Scott & Son Ltd., Tim Blake, Portland House, 21 Narborough Road, Cosby, Leics. LE9 5TA, UK; Tel. (+44-533) 753 333, Telefax (+44-533) 750 522. USA and Canada: Weston Media Associates, Daniel S. Lipner, P.O. Box 1110, Greens Farms, CT 06436-1110, USA; Tel. (+1-203) 261 2500, Telefax (+1-203) 261 0101.

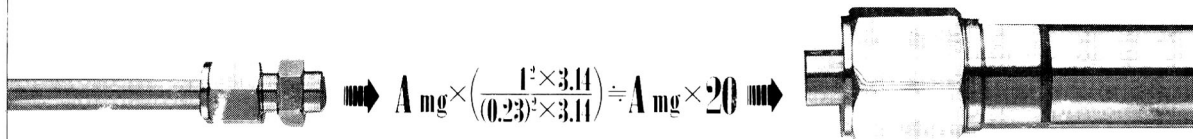
For Superior Chiral Separation

From Analytical to Semi-preparative column

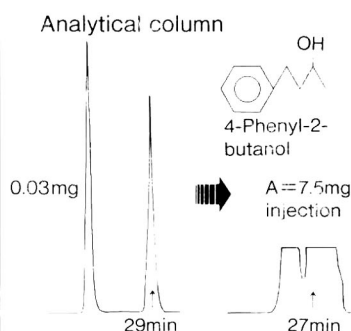
HPLC column output is directly proportional to cross section.

- Analytical column
0.46cm ϕ \times 25cm

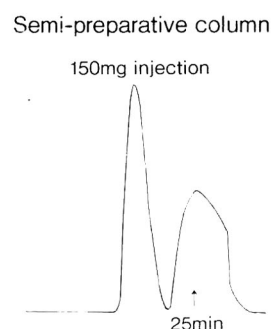
- Semi-preparative column
2cm ϕ \times 25cm



A = maximum sample amount of Analytical column



| CHIRALCEL OD | column | CHIRALCEL OD |
|--------------------------------|------------------|---------------------------|
| 0.46cm ϕ \times 25cm | column size | 2cm ϕ \times 25cm |
| 10 μ m | Particle size | 10 μ m |
| Hexane/IPA (9:1) | eluent | Hexane/IPA (9:1) |
| 0.3ml/min. | flow rate | 6ml/min. |
| UV 254 nm | detection | UV 254 nm |
| max 0.03mg \rightarrow 7.5mg | injection amount | 7.5mg \times 20 = 150mg |



Standard Available Column

- CHIRALPAK /CHIRALCEL[®] (Particle size 10 μ m)

| | I. D. | Length |
|-------------------------|---------------|--------|
| Analytical column | 0.46cm ϕ | 25cm |
| Pre-column | 0.46cm ϕ | 5cm |
| Semi-preparative column | 1cm ϕ | 25cm |
| | 2cm ϕ | 25cm |

- CROWNPAK[™] (Particle size 5 μ m)

| | I. D. | Length |
|-------------------|--------------|--------|
| Analytical column | 0.4cm ϕ | 15cm |
| Pre-column | 0.4cm ϕ | 1cm |

CHIRAL TECHNOLOGIES, INC.

730 SPRINGDALE DRIVE
DRAWER I
EXTON, PA 19341
Phone: 215-594-2100
Fax: 215-594-2325

DAICEL (EUROPA) GmbH

Oststr. 22
4000 Düsseldorf 1, Germany
Phone: 49/211/369848
Telex: (41) 8588042 DCEL D
Fax: 49/211/364429

DAICEL CHEMICAL INDUSTRIES, LTD.

8-1, Kasumigaseki 3-chome, Chiyoda-ku, Tokyo 100, Japan
Phone: 81-3-3507-3151 Fax: 81-3-3507-3193

CHIRALCEL, CHIRALPAK and CROWNPAK are trademarks of DAICEL CHEMICAL IND., LTD.